1993

A Characterization Of The Fast Pyrolysis Of Cellulose And Wood Biomass

Robert George Graham

A CHARACTERIZATION OF THE FAST PYROLYSIS OF CELLULOSE AND WOOD BIOMASS

by

Robert G. Graham

Department of Chemical Engineering

Submitted in partial fulfilment
of the requirements for the degree of
Doctor of Philosophy

Faculty of Graduate Studies
The University of Western Ontario
London, Ontario
February 1993

TABLE OF CONTENTS (cont'd)

ABSTRACT

The science of ***biomass*** fast pyrolysis is relatively young and incomplete. To date, there has been no systematic attempt to define fast pyrolysis in terms of chemistry, product distribution, kinetics, heat transfer requirements, and requisite process conditions. Neither has there been any experimental work which tracks the reaction progress as a function of both temperature and residence time. Furthermore, the literature provides a fragmented and often contradictory view of the nature of fast pyrolysis.

This thesis provides a coherent picture of the fast pyrolysis of cellulose and wood via an extensive literature review and systematic research. The literature review is an essential element of the thesis. It is not an uncritical summary, but is an interpretive integration of published knowledge. As such, it provides a comprehensive structure for the characterization of biomass fast pyrolysis.

The literature review suggests that fast pyrolysis reactions consist of biomass activation followed by primary fragmentation and secondary vapour-phase cracking; the secondary cracking reactions are the focus of the thesis experimental work. This work was carried out predominantly in the Ultrapyrolysis plant at the University of Western Ontario, and to a lesser degree in the RTP plant at Ensyn Technologies Inc.

Both reactor systems provide extremely rapid heat transfer to biomass combined with precise control of short residence times. In order to prove the integrity and reliability of the hardware, initial work involved the rapid pyrolysis of a model compound (ethane) and a comparison of the use of both gaseous and solid particulate heat transfer media. The cornerstone work involved the systematic characterization of the product distribution of secondary cracking reactions as a function of temperature and residence time. The ranges of temperatures and residence times under investigation were 650 to 900 °C and 30 ms to 1 s, respectively. The data from this work was used to generate rate equations for the secondary reactions of cellulose and wood fast pyrolysis. Finally, a cooperative study was conducted with the University of Waterloo to compare cellulose fast pyrolysis results from two independent reactor systems. The joint study exhibited excellent agreement and congruity over a broad range of pyrolysis temperatures.

ACKNOWLEDGEMENTS

To God, The Source of all knowledge

To His Son, Who makes that knowledge personal

To my dear wife and best friend, Lolita, who makes every day worth living

To my parents, who have given me a priceless heritage

To Dr. Bergougnou, who teaches beyond the borders of engineering, and who has continually encouraged me along this long and winding thesis road

To my colleagues, co-workers and friends, particularly Barry Freel, John Hazlett and Apostolos Vogiatzis who contributed profoundly to the success of my thesis work.

TABLE OF CONTENTS

TABLE OF CONTENTS (cont'd)

LIST OF TABLES

LIST OF TABLES (cont'd)

LIST OF TABLES (cont'd)

LIST OF FIGURES

LIST OF FIGURES (cont'd)

LIST OF FIGURES (cont'd)

LIST OF APPENDICES

NOMENCLATURE

A	pre-exponential constant (s^{-1})
Atm	atmosphere
B/T	benzene and toluene products
BENZ.	benzene
cm	centimeter
C	elemental carbon
C_1	one-carbon hydrocarbons
C_o	concentration at time "0"
C_t	concentration at time "t"
CH_4	methane
C_2+	hydrocarbons with two or more carbon atoms
C_2H_2	acetylene
C_2H_4	ethylene
C_2H_6	ethane
C_3+	hydrocarbons with three or more carbon atoms
C_3H_6	propylene
C_4	four-carbon hydrocarbons
C_5	five-carbon hydrocarbons
C_6	six-carbon hydrocarbons
CO	carbon monoxide
CO_2	carbon dioxide
°C	degrees centigrade (Celsius)
D_p	mean particle size
DP	degree of polymerization (avge. number of monomers)
E_a	activation energy (kJ/mole)
g	gram
g	gravitational constant (9.81 m/s^2).
GC	gas chromatograph
GLC	gas/liquid chromatograph
h	height of mercury column (m)
H	elemental hydrogen
H_2	hydrogen
ID	inside diameter
k	Arrhenius rate constant (s^{-1})
k_c	rate constant for char-producing reactions
k_{cr}	rate constant for cracking reactions
kg	kilogram
k_i	rate constant for activation (initiation)
k_v	rate constant for volatile-producing reactions
kmol	kilogram mole
kJ	kilojoule
kW	kilowatt
°K	degrees Kelvin

NOMENCLATURE (cont'd)

l	litre
m	meter
mm	millimeter
mol	gram mole
ms	millisecond
MJ	megajoule
Nm^3	normal cubic meter (0°C and 1 Atm)
MPa	megaPascal
NSB	National Standards Bureau
MW	molecular weight
N	elemental nitrogen
N_2	molecular nitrogen
NREL	National Renewable Energy Laboratory
O	elemental oxygen
P	pressure (Pa)
P_i	prompt gas yield of total gas or gas component "i"
Pa	Pascal
PC	personal computer
R	universal gas constant (0.008314 kJ/mole-°K)
RTP	Rapid Thermal Processing
s	second
S	elemental sulphur
SERI	Solar Energy Research Institute
t	time or residence time
$t_{1/2}$	half life
t_o	zero residence time
T	temperature (°C or °K)
TGA	thermo-gravimetric analyzer
tonne	metric tonne (1000 kg)
μm	micrometer or micron
UP	ultrapyrolysis
USWG	U.S. Water Gallon
U.W.O.	University of Western Ontario
V	mass yield at residence time "t"
V^*	maximum attainable yield at temperature "T"
W	mass of reactant or product
W_A	mass of activated biomass (cellulose)
W_C	mass of char product
W_{cell}	mass of cellulose
W_G	mass of gas product
W_V	mass of volatiles
WTM	wet test meter

1.0 INTRODUCTION

Rapid, flash or fast pyrolysis had its roots in fossil fuel processing, and was investigated in order to generate optimum yields of high-value products from relatively low-value feed materials. The process is characterized by extremely rapid feedstock heating rates, very short processing times, and fast product quenching or cooling. The products are typically fuels and chemicals which are kinetically determined and therefore not predicted by equilibrium.

Severe limitations existed in the ability of fundamental researchers to theoretically predict the nature of principal products from fossil fuels, let alone their yields. These limitations occurred for a number reasons. First, petroleum, petroleum derivatives and coal are complex nonhomogeneous mixtures of chemicals. Second, the chemistry is non-equilibrium and a variety of tools based on thermodynamic principles are therefore not available for modelling studies. Finally, complex free-radical chemistry can play an important role in fast pyrolysis processes.

Systematic studies were therefore initiated to methodically explore the quality and yields of fast pyrolysis products from fossil fuels as a function of temperature, residence time, catalysis and reaction atmosphere (inert, reducing or oxidative). Out of these studies, a broad data base was assembled which characterized conversion to liquid fuels and

chemicals. Experimental results confirmed that rapid thermal reactions typically result in the production of primary chemicals or "chemical intermediates" which are very reactive. High reactivity is generally an index of an economic value which is higher than that associated with secondary products (typical of slow pyrolysis and some conventional cracking processes).

The work in rapid fossil fuel processing was maturing in the late 1970's when the cost of conventional energy supplies was comparatively high, and was expected to dramatically increase. The energy cost projections, security of supply considerations and reliance on imports incubated an abrupt interest in alternative fuels. Biomass, particularly lignocellulosics (wood and plant residues), was of particular interest because of its relative abundance. As a result, several public and private projects were initiated worldwide to investigate efficient biomass conversion. Initially, the majority of bioenergy research was carried out in support of processes which were currently or historically in commercial use. In particular, combustion, slow pyrolysis and gasification were the subjects of many investigations. Nevertheless, a few researchers began to consider that the rapid pyrolysis research which was showing potential for fossil fuel feedstocks should also be applied to biomass materials.

It was in this atmosphere of renewed interest in biomass conversion and the publication of promising results evident in fossil fuel fast pyrolysis research, that the present study of

the rapid pyrolysis of biomass was initiated in 1978 at the University of Western Ontario. The first task was to develop an experimental apparatus which could rapidly heat the feedstock and allow precise control of residence times over a reasonable temperature range. Hot particulate solids were selected to carry and rapidly transfer heat to the biomass feedstock and the residence time control was achieved using an entrained-bed (transport) reactor. These two features were integrated into the U.W.O. "Ultrapyrolysis" reactor system known as a thermal vortical contactor or "thermovortactor".

Cellulose was selected as the principal feedstock in the study for two reasons:

- it is the predominant component of most biomass materials
- there is an abundance of literature available dealing with its properties, and its conversion via slow pyrolysis

Wood, the most abundant natural biomass resource, was also a candidate feedstock to be processed if time permitted.

As was the case for fossil fuel research, the fast pyrolysis of biomass is chemically complex and practically impossible to model from first principles. The yield and quality of non-equilibrium products must be determined by routine, methodical experimental analysis. As a direct result of an exhaustive review of coal and biomass pyrolysis literature (Chapter 2), the effects of reactor residence time and temperature were identified as the principal experimental variables. Their effects on product quality and yield were a primary objective of the thesis research.

The work was initially designed to characterize only the production of gaseous products, particularly petrochemical gases (olefins), synthesis gas (CO and H_2) and fuel gas. However, it was inevitable that an investigation of the non-gaseous products would be pursued in a perfunctory manner.

Although a characterization of gaseous products has remained as the principal object throughout the investigation, a remarkable lack of solid char production was observed as the work proceeded. This confirmed that char was not a significant primary product as has been recently accepted. The low char yield was also being confirmed in parallel work by other fast pyrolysis researchers. Furthermore, preliminary results demonstrated that very high primary liquid yields were evident at lower temperatures and very short residence times. These primary liquid oils were radically different from the viscous, secondary tars produced by traditional slow pyrolysis. Only a minor attempt was made to determine the composition of these liquids and to shed light on the mechanism of fast pyrolysis.

The fast pyrolysis work was conducted in three distinct systems. The majority of experiments were carried out in the Ultrapyrolysis entrained-bed system at the University of Western Ontario. Selected trials were undertaken in the Rapid Thermal Processing RTP-1 recirculating transported-bed system at Ensyn Technologies Inc. in Ottawa, and a joint-study was completed in cooperation with the University of Waterloo in the Waterloo Fluidized Bed Fast Pyrolysis (WFFP) pilot plant.

This thesis is organized to first acquaint the reader with slow and fast pyrolysis, and then to present the actual experimental study. A thorough review of the literature, including definitions of terms, proposed chemical pathways and kinetics, heat transfer effects, background research, and process development, is given in the following chapter. This review provides a foundation for the experimental work which follows. The remainder of the thesis consists of the experimental program and includes research objectives, equipment, procedure, results, modelling, discussion and conclusions.

To the best of the authors knowledge, this thesis presents the only systematic study of effect of temperature and reactor residence time on the fast pyrolysis of cellulose and wood. In addition, an empirical model has been generated from the data to effectively assist in reactor scale-up and product yield selection. The model accurately predicts the yields of total gas, principal gas components and total liquid yields for a specified temperature and residence time.

During the course of the thesis research, more than forty papers have been published in journals, books, and conference proceedings. These are listed in Appendix 1.0. In addition, the Ultrapyrolysis research program has led to the development of a fast pyrolysis process, Rapid Thermal Processing (RTP), which has become the central technology of a private company. As a result, the commercial production of chemicals and fuels from biomass via fast pyrolysis is a reality [31,83,84].

2.0 LITERATURE REVIEW

The discussion in the following paragraphs is a consequence of an extensive overview of biomass thermochemical conversion. It is more than a simple uncritical review, and implicitly embodies an interpretation and integration of the subject matter to provide a solid foundation and context for the experimental thesis work. This overview includes a brief characterization of biomass, a definition of pyrolysis and thermochemical conversion terms, and an explanation of fast pyrolysis within the framework of conventional pyrolysis and other thermochemical processes. The potential benefits of successful commercialization of fast pyrolysis are also briefly highlighted.

Considerably more attention is then devoted to a review of mechanisms, chemical pathways and kinetics of biomass pyrolysis. This includes a characterization of the initial reactions associated with primary pyrolysis of the feedstock, and important primary and secondary vapour-phase reactions. A discussion of heating rate and heat transfer phenomena is given which includes references to work conducted by the author during this thesis work and other published literature. Finally, a summary of current and past fast pyrolysis initiatives, including both fundamental bench-scale research and process development work is presented. Fundamental work is typically concerned with characterizing product distributions, mechanisms and kinetics, while process development is concerned with eventual scale-up to commercial applications (i.e., engineering).

2.1 BIOMASS CHARACTERIZATION

In its broadest sense for thermochemical conversion applications, biomass includes all organic material that has been recently derived from living plants or animals. As such, biomass is renewable, and includes wood and wood residues, forest residuals, agricultural materials, food industry byproducts, components of municipal solid waste, pulp residues, newsprint, corrugate, animal manures, sewage sludge, etc. The term "recently" excludes fossil fuel feedstocks, but provides for the possible inclusion of peat.

A more narrow definition is one which occurs very frequently in the bioenergy community and throughout the biomass conversion literature. This definition includes only that organic material which is derived from plants, particularly trees (wood) and agricultural food crops. These are the most abundant biomass materials by far and are known collectively as "lignocellulosics"; a term derived from the two most important constituents of wood and plant materials, lignin and cellulose. Lignocellulosic feedstocks are the focus of this thesis.

Cellulose, the principal cell wall component in many biomass materials, is a polymer of anhydroglucose units ($C_6H_{10}O_5$) connected to each other by ether-type linkages known as glycosidic bonds. It is characterized by an orderly crystalline structure (Figure 1) and constitutes 40 to 50% by mass of most dry woods. Aside from the secondary hydrogen bonds and Van der Waals forces between the cellulosic strands, the weakest bonds within the chain are the C-O glycosidic linkages [2,90,177,190].

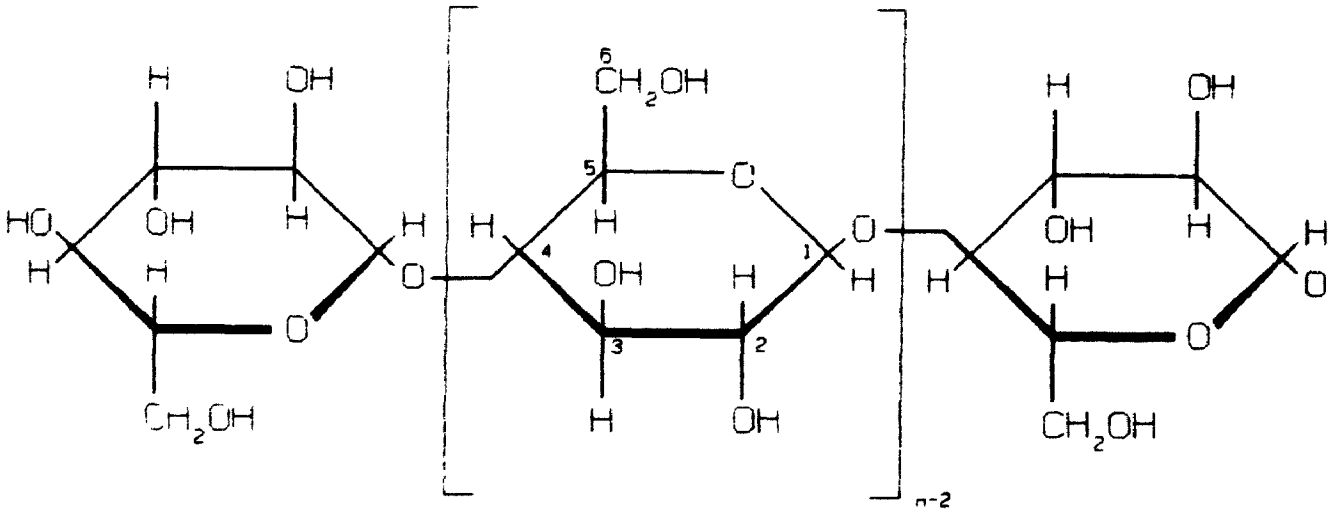

Figure 1. The Cellulose Molecule [11]

All other polymeric polysaccharides in biomass tissues are known collectively as hemicellulose, and constitute between 25 and 35% of the dry mass of most woods. Hemicellulose is a complex heteropolymer which exhibits a branched molecular structure and whose composition varies significantly. It normally contains 2 to 4 different simple sugar units [2,90,177, 206] including D-xylose, D-mannose, D-glucose, D-galactose, or L-arabinose. There are two principal hemicelluloses found in hardwoods, acetyl-methylglucurono-xylan (Figure 2) and glucomannan. The xylan is clearly predominant, and typically constitutes 20-30% of extractive-free hardwoods.

The third major biomass component, lignin, is an extremely complex non-carbohydrate polymer based primarily on the phenylpropane unit, and constitutes between 15 and 30% by mass of most wood species [2,90,138,177]. It acts as a cementing agent for the cellulose and hemicellulose fibres, and is composed of phenylpropane monomer groups which form the polymer by linkages involving the aromatic rings and various functional groups. The phenylpropane monomers are exclusively guaiacyl-propane units in coniferyl woods, while deciduous wood lignin consists of both guaiacyl- and syringyl-propane units (Figure 3.)

2.2 PYROLYSIS AND THERMOCHEMICAL CONVERSION

Biomass can be converted to fuels and chemicals by a number of thermochemical and biochemical processes. Biochemical conversion is beyond the scope of this thesis. Thermochemical

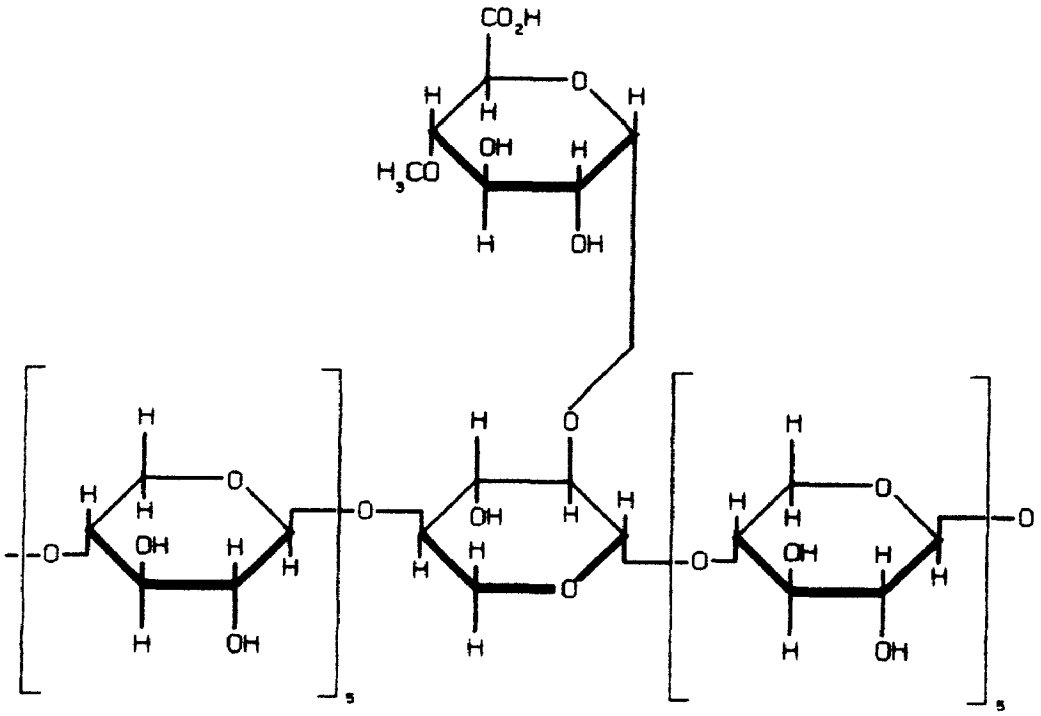

Figure 2. O-Acetyl-4-O-Methylglucurono-Xylan Hemicellulose Structure [177]

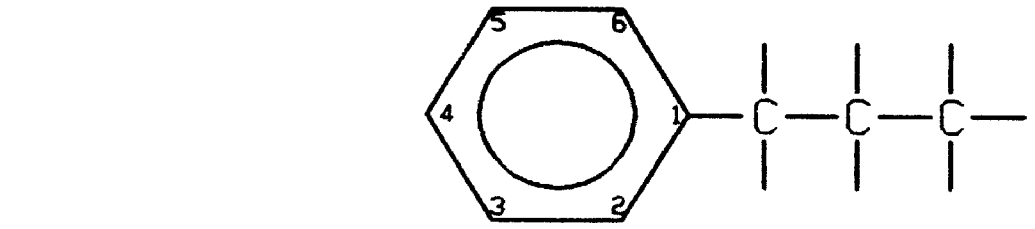

Phenylpropane

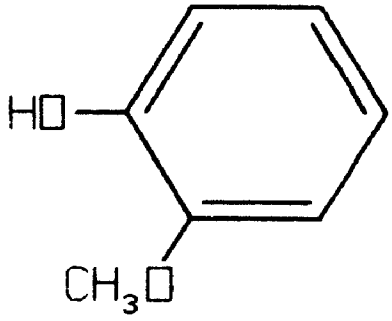

Guaiacyl

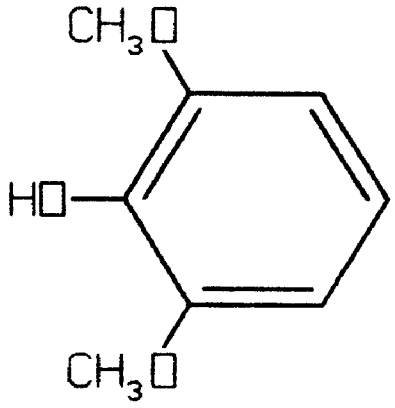

Syringyl

Figure 3. Representative Lignin Component Structures [11]

processes typically include combustion, gasification, hydrogenation and pyrolysis. Combustion involves the addition of air such that the amount of oxygen is equal to or greater than the amount required for complete oxidation of the feed material. Gasification in its broadest sense refers to any thermal process, whether oxidative or not, which converts organic material to a product which is primarily a combustible gas. Depending on its quality, the gas may be used directly as a fuel gas or as a synthesis gas. More commonly, gasification refers to an oxidative thermal process which uses air or oxygen in amounts which are sub-stoichiometric for complete combustion. The combustion of a relatively small fraction of the feed provides process heat to convert the balance into a combustible gas. Hydrogenation is a high-pressure liquefaction process which converts biomass to a liquid product at moderate temperatures (200-400°C) in the presence of hydrogen and a catalyst. An accelerated decrease in interest in biomass hydrogenation has recently occurred because the relatively high cost of pressurized processes and hydrogen does not result in a significantly proportional increase in the value of the product.

Pyrolysis may be defined in its broadest sense as the thermal decomposition of organic matter occurring with the complete absence of air or oxygen in the reactor system [3,10, 29,30,31,33,64,79,80,97,108,117,145,149,151,177,178,179,181, 187,193,194,195]. Some researchers would consider oxygen-deficient (i.e., less air or oxygen than is required stoichio-

metrically for complete combustion) thermal decomposition to be a true pyrolysis process as long as the primary products are liquid or solid [3,10,31,50,52,79,149,177,194]. As defined previously, when the primary products of the oxygen-deficient decomposition are gases, the process is known as gasification [30,31,42,79,149,151,177,219]. In this thesis, only those thermal processes which completely exclude air or oxygen in the reaction zone will be considered to be truly pyrolytic.

2.3 PYROLYSIS AND FAST PYROLYSIS

Pyrolysis, pyrolytic gasification, flash pyrolysis, and fast (rapid) pyrolysis are terms which frequently appear in the biomass and coal conversion literature. Conventional "slow" pyrolysis is typically characterized by a low feedstock heating rate (<10°C/s), low temperatures (<350°C) and relatively long gas and solids residence times (i.e. >5 s for the gas, while solids residence times can be minutes, hours or days). Tar and char are the principal products arising from the slow devolatilization of the feedstock and the secondary coking and polymerization or recombination reactions which are allowed to occur after primary pyrolysis has taken place [29,30,31,52,58,79,80, 108,151,177,178,179,181,187,194].

Pyrolytic gasification is a relatively obscure term applied to any pyrolysis process, whether fast or slow, which excludes oxygen or air and gives a non-condensible synthesis gas or medium-energy fuel gas (10 to 20 MJ/Nm^3) as the primary product.

In this process, tar and char are viewed as undesirable by-products [59,79,80,142,149,203,208,209].

In the context of biomass conversion, flash pyrolysis originally referred, with some exceptions, to a rapid heating rate process (10 to 10,000°C/s) occurring at moderate temperatures (typically 400 to 600°C) whose liquid "oil" products were maximized at the expense of char and gas [9,22,42, 43,45,65,105,106,155,201]. Vapour residence times were normally less than 2 s [79,80,88,145,169,170,171,177,178,194]. Fast pyrolysis was differentiated from flash pyrolysis in the biomass literature primarily with respect to temperature, vapour residence times, and end-product. Extremely high heating rates (ie. 1000-10,000°C/s), high temperatures (greater than 600°C), and short vapour residence times (less than 0.5 s) were identified as the primary conditions required to maximize the production of high-quality gases (i.e., olefins and other hydrocarbons) at the expense of char and condensible liquids [40,41,47,53,75,76,79,80,90,108,118,119,130,131,149,150, 51,177, 178,194,212].

It is important to note that the distinction between the terms fast, flash and rapid pyrolysis has largely disappeared over the past 5 or 6 years. Currently, these terms are used interchangeably to describe any thermal or thermo-catalytic conversion process which is characterized by rapid heating rates, short residence times, fast product quench and the exclusion of air or oxygen from the reaction zone [26,29,30,31,

39,83,84,101,140,141,146,152,153,154,174,175,176]. With respect to fossil fuel feedstocks, only the term "flash" has been consistently used in the literature to identify rapid pyrolysis processes [36,61,62,63,69,80,178,191,200,202,205,210,211].

Recent research has more fully characterized the chemical mechanisms of pyrolysis, and fast pyrolysis can now be distinguished from slow pyrolysis in terms of the chemical mechanisms and kinetics, and the interrelated effects of temperature and heating rate. These are addressed individually in subsequent sections, and are integrated in Section 2.10.

In the meantime, fast pyrolysis can be characterized in terms of three basic criteria which must be satisfied for the production of high yields of value-added products, including olefins, hydrocarbons, light primary liquids or other primary chemicals [2,4,8,22,26,29,30,31,42,47,52,53,55,77,78,79,80,81, 86,90,109,124,125,127,131,150,152,153,174,175,178,190,194]:

1. High heat transfer rates to the carbonaceous feedstock causing heat-up rates on the scale of tens of thousands of degrees celsius per second.

2. Moderate to high reactor temperatures (i.e., between 450 and 1100°C).

3. Short vapour residence times (i.e., less than 800 ms), normally achieved by rapid quenching of the reaction products.

2.4 POTENTIAL COMMERCIAL VALUE OF BIOMASS FAST PYROLYSIS

The development of a successful fast pyrolysis technology for biomass would, under certain circumstances, offer products and a process with some of the best features of conventional

biomass thermochemical conversion without many of the associated disadvantages [2,11,29,30,31,52,53,75,79,80,81,107,109,115,127, 151,177,178]. A detailed comparison of fast pyrolysis with other thermochemical conversion technologies, including combustion, air and oxygen gasification, liquefaction and slow pyrolysis, has been given by the author elsewhere [80]. By way of summary, the beneficial features of fast pyrolysis are as follows [2,3,8,9,15,29,30,31,53,57,58,65,75,78,79,80,81,94,105, 107,125,127,133,141,144,150,151,155,171,173,176,178,194,220]:

1. The process can be operated as a biomass "refinery", analogous to a petroleum refinery, where value-added products are used for specialty and commodity chemicals (eg. petrochemicals), and low-value products are used as fuels.

2. Fast pyrolysis is more selective in terms of final product distribution. For example, high yields of olefinic/petrochemical gases, specialty chemicals, or light liquid fuels can be produced in a single reactor system with the minimal production of char or heavy tars, by varying temperature and residence time.

3. In the case of fuel production, fast pyrolysis can produce high yields of a <u>liquid</u> fuel which is readily stored and transported. In this fashion, the fuel production process (i.e., biomass conversion technology) can be decoupled from the end-use (ie. fuel conversion technology). In other words, fuel production does not have to directly correspond to fuel demand as is typically the case with gasification and combustion.

4. For the production of a gas for chemical synthesis, fast pyrolysis is more efficient. For example, a particular biomass may be selectively depolymerized to suitable monomers instead of being fully degraded to syngas (CO/H_2)

5. Typically, any "fast" conversion processes tends to have the general economic advantage which is associated with a high capacity per unit volume of reactor.

6. No costly requirements for pure oxygen, hydrogen or high-pressure.

2.5 PYROLYTIC PATHWAYS AND CHEMICAL MECHANISMS

The current interest in fast pyrolysis and its potential for producing high-quality fuels, chemicals, petrochemicals and synthesis gas from biomass is largely because of the fundamental mechanistic research performed during the past three decades by Byrne [35], Broido [33], Kilzer and Broido [97], Bradbury [28], Shafizadeh [179-190], Soltes [193,194,195], Arsenau [16,17], Piskorz and co-workers [139,141,176], Diebold [48,52,55,178], and Antal [2-15,101,128]. Other researchers have also made a significant contribution to the understanding of certain fundamental aspects of pyrolysis [34,44,68,108,117-123,148,152,159, 167,168,178,199,203,221].

The majority of early biomass pyrolysis mechanistic studies were initiated primarily in conjunction with applied fire-retardant research, and generally focused on cellulose as the model biomass feedstock [11,17,21,34,35,97,179,181]. This research was undertaken before *rapid* pyrolysis was distinctly defined and therefore before the dramatic effect of heating rate was clearly identified. In spite of this, it is remarkable to note the following as reported by Byrne [35]:

1. The existence of at least two competing primary pyrolysis reactions was speculated on, and experimentally confirmed, by 1956.

2. Levoglucosan was widely recognized as a principal primary pyrolysis product in the 1950's.

3. The term "flash pyrolysis" was used early as early as 1961 to identify high intensity thermal decomposition of biomass. The principal products were identified as "volatiles" and included carbon oxides, water and carbonyls (aldehydes and ketones).

4. By 1966, the importance of carbonyl compounds, particularly hydroxyacetaldehyde (glycoaldehyde), in primary pyrolysis reaction pathways was recognized and detailed mechanisms for their formation were proposed.

Madorsky, as reviewed in Byrne [35], Kilzer and Broido [33,97], Byrne [35], Bradbury [28] and Shafizadeh [179-190] are clearly the pivotal researchers who have provided the foundation for our modern understanding of biomass (cellulose) pyrolysis mechanisms. Arsenau [16,17], Soltes [193,195] and Antal [2-15, 128] have confirmed much of this early work using more modern analytical techniques. Diebold [55,178] has made a significant contribution by integrating the results of early studies with more recent fast pyrolysis work. In effect, he has bridged the gap between the old and the new. Piskorz and co-workers (139-141,146,169-176), Antal [2-15,28], Richards [159] and Evans [68] have recently made a significant contribution to the refinement of our current understanding of primary pyrolysis mechanisms and fast pyrolysis mechanisms.

It appears that Madorsky, as reviewed in Byrne [35], first proposed two modes of cellulose pyrolysis which either preserved the hexose units by depolymerization, or destroyed the rings and chains by dehydration and condensation to char. Levoglucosan was identified as a typical intermediate when depolymerization occurred. Kilzer and Broido [97] expanded on this basic premise of Madorsky, and first formulated a simple mechanism which explained cellulose pyrolysis in terms of two competing primary reactions (Figure 4). The low temperature pathway was thought to predominate at temperatures which are less than 280°C, and

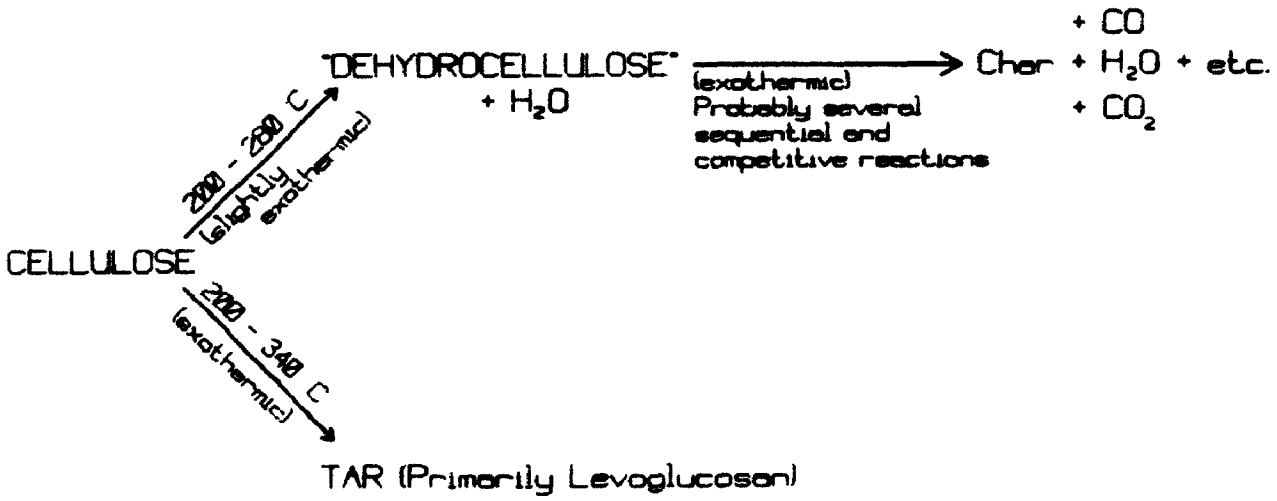

Figure 4. Primary Cellulose Pyrolysis Mechanism: Kilzer and Broido [97]

results in the production of water and "dehydrocellulose" via dehydration of cellulose. The structure of dehydrocellulose was not specifically identified, but was thought to involve a tetrahydro-5-hydroxymethylfurfural system. Dehydrocellulose quickly decomposes by fragmentation to char, CO, CO_2, and water "by sequential dehydration and decarboxylation reactions" [55].

The proposed high-temperature pathway, dominating at temperatures above 300°C, involves a depolymerization or "unzipping" of the cellulose polymer to form a volatile tar, primarily levoglucosan. Levoglucosan is an isomer of the cellulose monomer. Diebold [55] summarizes the mechanism as a chain cleavage followed by a subsequent rearrangement of the anhydroglucose monomers (intermediates) to levoglucosan.

Byrne [35] accepted the general hypotheses of Madorsky and Kilzer and Broido, and then tried to actually identify specific chemical intermediates in the competing pathways using the relatively new tool (at that time) of gas-liquid chromatography (GLC). In his work, a number of anhydrosugar intermediates, including several anhydrogluco-pyranose structures, were identified in the high-temperature depolymerization pathway leading to levoglucosan formation.

Byrne also proposes a mechanism for volatile, carbonyl compound formation which he assumes, in error, to reflect the low-temperature pathway proposed by Kilzer and Broido. A close examination of his original paper reveals that the experiments dealing with carbonyl formation were actually conducted at

420°C. Recent research, reviewed in subsequent sections, has confirmed that the carbonyl-forming fragmentation reactions compete with the anhydrosugar-forming depolymerization reactions at elevated temperatures. Byrne assumed in a general sense that the carbonyl compounds underwent condensation reactions with water elimination to develop ethylenic crosslinks between carbon chains, ultimately resulting in the production of carbon rich char, water and carbon oxides. However, his specific detailed mechanism stops at the evolution carbonyl compounds, and the ultimate formation of char from these chemical species is an unsubstantiated assumption. Nevertheless, Byrne did confirm the presence of 19 carbonyl compounds and correctly determined that hydroxyacetaldehyde (glycoaldehyde) and glyoxal were the most important and abundant intermediates. He also correctly reported that anhydrosugars and carbonyl compounds were produced by competing, not sequential, reactions. This was largely ignored and forgotten in the literature until very recently.

Covering four decades, the laboratory of Shafizadeh at the University of Montana consistently produced large volumes of high quality work on cellulose pyrolysis mechanisms [179-190]. Routinely in his literature, Shafizadeh periodically proposed three principal competing pathways (Figure 5) for the primary pyrolysis of cellulosics. In effect, he agreed with the earlier "two-pathway" work of Madorsky and Byrne, but proposed a third primary route whose characterization required significant revision by subsequent researchers. According to his model,

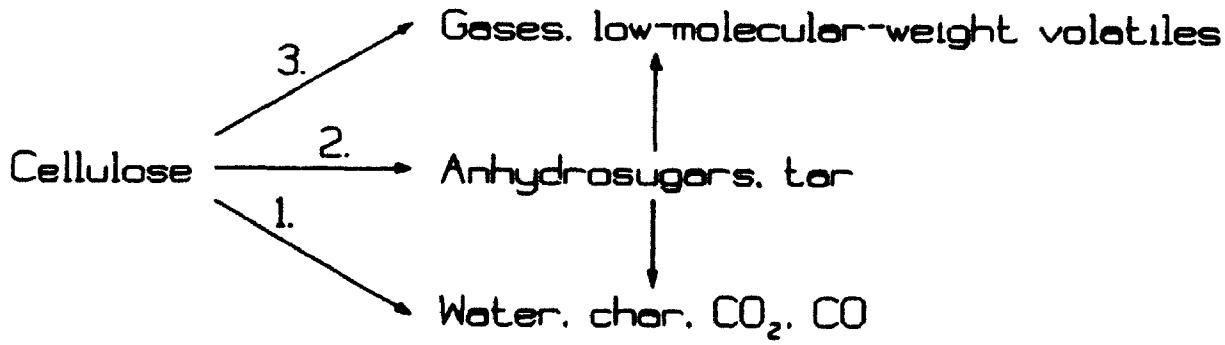

Figure 5. Primary Cellulose Pyrolysis Mechanism: Shafizadeh [188]

pyrolysis at temperatures below 280°C (Pathway 1 in Figure 5) favours the production of char, water, CO_2 and CO via dehydration. Depolymerization via cleavage of the glycosidic bond, transglycosolation and rearrangement to anhydrosugars (the most important being levoglucosan) is favoured at temperatures between 300 and 500°C (Pathway 2 in Figure 5). Finally, Shafizadeh reports that for high heating rates "flash pyrolysis at still high temperatures (above 500°C) results in ... a mixture of low-molecular gaseous or volatile products" (Pathway 3 in Figure 5). The volatiles and gases are produced by fission, dehydration, disproportionation, decarboxylation and decarbonylation, and are identified principally as carbonyls (including glyoxal, hydroxyacetaldehyde and furaldehyde), carboxyls, olefins and carbon oxides [188]. Very detailed mechanisms and chemical intermediates are proposed by Shafizadeh et al. but their full review is beyond the scope of this thesis.

As early as 1968, Shafizadeh [179] clearly demonstrated that acid washing of the cellulose feed and acid catalysis enhanced the formation of levoglucosan, while alkaline catalysis favoured fission reactions leading to the production of carbonyl compounds. Furthermore, Shafizadeh clearly recognized, although did not fully understand, the importance of heating rate and the nature of the biomass feedstock (composition, impurities, morphology, DP) on the pyrolytic mechanism. Antal [11,12,13] recognizes these considerations in his attempts to reconcile diverse pyrolysis mechanistic and kinetic investigations.

It is important to note that Shafizadeh typically described only two of the primary pyrolysis pathways (namely 1 and 2 in Figure 5) in most of his publications. As stated above, the third route was nevertheless occasionally identified [179,188]. This relatively infrequent consideration is likely because Shafizadeh was not fully convinced that the third pathway was in fact a competing reaction. He hints that his personal conviction was that the low molecular mass volatiles were produced from the anhydrosugars (via the 2nd mechanism), but concedes that there is no experimental evidence to suggest primary production from direct fragmentation of the cellulosic ring [188].

The integrated results of recent research, particularly by Piskorz and coworkers [139,141,146,176], Elliott [in 139], Evans [68], Antal [11], and Richards [159], have confirmed that the third pathway is in fact a primary competitive pyrolytic mechanism [159]. The existence of hydroxyacetaldehyde as a primary intermediate product, as proposed by earlier researchers [35,188], has also been confirmed. Piskorz, Richards and Evans have gone further than simply confirming previous propositions, and have enhanced Shafizadeh's three-pathway model of primary pyrolysis. When Shafizadeh did address all three of the different product distributions produced from the three parallel competing reaction mechanisms, he was unclear with respect to the nature of the third mechanism which led to the formation of "volatiles" and gases. After confirming the existence of a

third primary pathway, Piskorz, Richards and Evans identified it as one which favours the direct production of carbonyls via ring cleavage. Shafizadeh no doubt saw evidence of this mechanism from kinetic studies, but the volatiles and gases which he identified were likely secondary decomposition products derived from the anhydrosugars at elevated temperatures, or were produced by the fragmentation pathway which was significant but not dominant at his experimental conditions. He had proposed in a detailed mechanism that carbonyls, including hydroxy-acetaldehyde, were likely formed by secondary decomposition of anhydrosugars which were produced via the second primary pyrolysis pathway. This was initially accepted by Piskorz [139] but then rejected [141,176] after a landmark study conducted by Richards [159]. Piskorz and Evans clearly showed that anhydrosugars can be selected and optimized directly at the expense of carbonyls, and also confirmed the conditions to select one pathway over the other. The net result is that we now have a relatively simple yet elegant model of primary pyrolysis which has become broadly accepted. This model provides a basis to relate and integrate the results from a broad range of biomass pyrolysis studies, both fast and slow, and is summarized in Figure 6. It is important to note that an initial "activation" step, common to all of the three subsequent primary steps, is shown in Figure 6, but has not been included in the above discussion. The existence of this step was inferred from kinetic studies which are reviewed in Section 2.7.

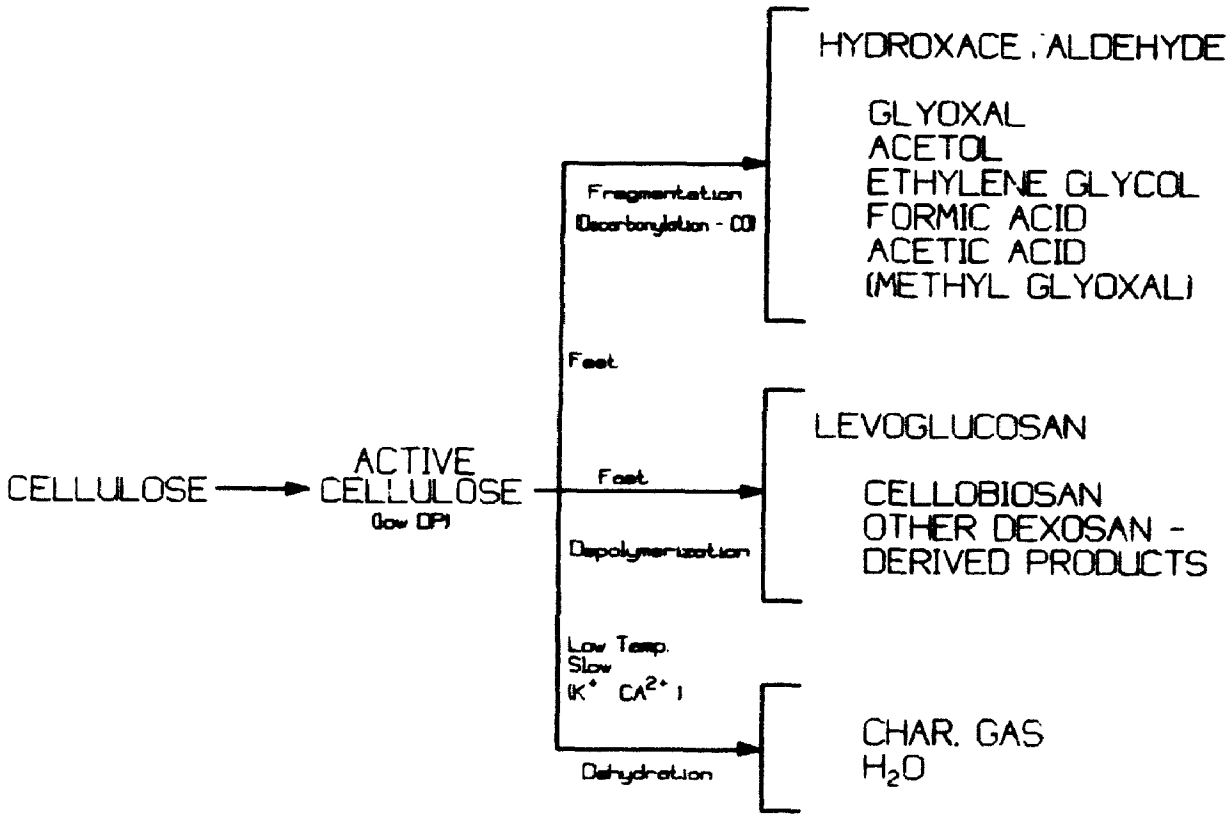

Figure 6. Modified Scott Model [176]

In this most recent model, it is clear that cellulosic biomass can be converted to the following generic products via three competing primary pyrolysis reactions:

1. Dehydration/Condensation products (char, H_2O, gas and tar).
2. Depolymerization products (primarily anhydrosugars).
3. Fragmentation products (carbonyls, acids and alcohols).

The first reaction pathway is heterolytic and dominates at low pyrolytic temperatures (for example, <280°C). The "tar" is extremely viscous, and can be viewed as a product which is intermediate between the solid biomass feedstock and solid char product. It is reduced to char, gases, and water once the dehydration and condensation reactions go to completion. The second and third pathways are homolytic and predominate at elevated temperatures (>350°C) under fast pyrolysis conditions. Cellulose depolymerization leads to the production of anhydrosugars, principally levoglucosan. Piskorz [141] suggests that glucose, fructose and cellobiosan (from which formaldehyde is derived) are also significant depolymerization products. Ring fragmentation, dehydration and decarbonylation reactions, result primarily in the production of hydroxyacetaldehyde, other carbonyls, and organic acids and alcohols.

The selection of fragmentation over depolymerization is affected by the presence of cationic substances, biomass morphology and the degree of polymerization or "DP" [11,13,141, 179]. In very small quantities (<0.5%), cationic substances (particularly alkali or alkaline earth cations) will favour

fragmentation by apparently retarding depolymerization [141]. These substances are normally associated with "natural" cellulose and other biomass materials, and can be readily removed with a mild acid wash [11,141,179]. The depolymerization reactions are therefore favoured when cations are removed from, or absent in, the biomass feed material. Arsenau [16,17] correctly reported that as early as 1951, it was known that alkali salts resulted in diminished levoglucosan yields. He incorrectly speculated, albeit without experimental evidence and without knowledge of a third primary pathway, that these cations favoured the production of dehydrocellulose by catalyzing the first (low-temperature) primary pyrolysis route.

The morphology (crystallinity and DP) also affect the pathway selection, although to a lesser degree than the presence of cations [11,141,178,187,190]. A low DP and reduced crystallinity exposes more end sites and thus favours depolymerization.

There is convincing evidence that temperature, as well as the presence of cations and biomass morphology, greatly affects selection of the two homolytic pathways. Otherwise, it is very difficult to fully reconcile the earlier mechanistic studies of Byrne, Broido, Kilzer, Shafizadeh, Bradbury and Arsenau with the recent work of Piskorz, Evans and Richards. For example, it is clear that many of these earlier experiments (conducted at temperatures between 280 and 330°C) used untreated cellulosic biomass which had its inherent cationic composition preserved. In spite of this, significant amounts of levoglucosan were

produced. After acid-washing of the same feedstock at the same temperature, Shafizadeh noted that yields of levoglucosan and other anhydrosugars could be *further* increased [11,141,179]. Furthermore, the particular importance of carbonyl compounds (including hydroxyacetaldehyde) which was first noted by Byrne, had been largely forgotten, and in subsequent studies little attention was given to the analyses and quantification of these chemical species. Where primary carbonyls were measured and found to be present in significant quantities, it was often incorrectly assumed that they were formed by secondary cracking of the anhydrosugars at elevated temperatures.

The pyrolysis experiments of Piskorz, Richards and Evans were conducted in the temperature range of 350 to 600°C. In these mechanistic studies, the importance of hydroxyacetaldehyde was recognized *a priori*, and therefore appropriate analyses and quantification techniques were employed. As noted earlier, carbonyl compounds, particularly hydroxyacetaldehyde, were typically among the principal products, unless acid-washing of the biomass material occurred. However, using untreated Avicel cellulose and keeping the residence time constant, Piskorz [141] observed that hydroxyacetaldehyde yield decreased from a maximum at about 600°C to a minimum at about 400°C, with a corresponding increase in levoglucosan yield reaching a maximum at 400°C. This evidence suggests that the depolymerization pathway must predominate between 300 and 450°C while fragmentation predominates at temperatures exceeding 450°C.

2.6 FAST PYROLYSIS PATHWAYS AND MECHANISMS

In Section 2.3, fast pyrolysis was defined in terms of the *process* conditions which must be met in order to yield a defined set of generic fast pyrolysis products. The following discussion on fast pyrolysis mechanisms combined with the previous discussion on *general* pyrolysis mechanisms (Section 2.5) will now permit *fast* pyrolysis to be defined in terms of the chemical pathways which are followed. As will become apparent, fast pyrolysis can consist of both primary and secondary chemical reactions. Primary reactions involve the production of secondary chemical species (primary products) *directly* from the biomass feedstock (or via an activated primary intermediate) while the subsequent secondary reactions involve the chemical reactions of the primary products to form secondary products.

2.6.1 Primary Fast Pyrolysis Reactions

Given the general definition of a primary reaction, the three primary pyrolysis reactions which follow "activation" (Section 2.5 and Figure 6) are the only candidates to be considered as primary fast pyrolysis reactions. The low-temperature pathway is typical of slow pyrolysis and by definition does not conform to the general characterization of fast pyrolysis (Section 2.3) as a rapid process which produces value-added products, either liquid or gaseous. The low-temperature dehydration pathway can therefore be immediately eliminated from further consideration. Although the rationale

is less obvious, the depolymerization pathway (Figure 6) can also be eliminated for the following reasons:

1. It appears that this pathway can be pursued without the stringent heat transfer, temperature and residence time requirements which are typical of fast pyrolysis processes.

2. The principal product, levoglucosan, is not currently deemed to be a commercial value-added product. There is no evidence that any unique value-added secondary products arise from levoglucosan, which cannot be produced more effectively by the ring fragmentation mechanism.

The above rationale does not suggest that the depolymerization pathway does not have any potential commercial value. What is being stated is that this pathway does not seem to fall within the functional definition of rapid pyrolysis at the present time. As more mechanistic research is pursued and chemical mechanisms are better understood, perhaps the depolymerization will be redefined in terms of fast pyrolysis.

What follows from this process of elimination, is that primary fast pyrolysis consists of cellulose activation, common to all cellulose pyrolysis processes, followed by non-random fragmentation of the ring structure. The "activated" cellulose in the primary pathway is a slightly depolymerized material (either a "plastic" or a liquid depending on the temperature), which exhibits minimal weight loss [11,28,55]. Antal [13] and Kothari [101] suggest that the primary fast pyrolysis pathway should be simply termed "vaporization". What is implicit in this primary pathway is that char is not a requisite primary product from cellulose (as was once held), and therefore should be noticeably absent in the spectrum of true fast pyrolysis

products. This has been confirmed in many cellulose fast pyrolysis studies [2,4,8,10,11,33,34,42,46,53,55,64,65,79,81, 90,97,105,108,112,117,124,125,127,131,145,150,151,155,169,170, 179,181,187,193].

2.6.2 Secondary Fast pyrolysis Reactions

It is not a simple task to identify the numerous secondary pyrolysis reactions which follow primary pyrolysis. These reactions are extremely complex, and have been addressed in a large volume of research which has been published over the past 40 years. Often the results are contradictory and difficult to reconcile. The secondary reactions associated with low-temperature dehydration and higher-temperature depolymerization pathways have been dealt with in great detail in studies by Byrne [35], Broido and Kilzer [33,97], Arsenau [16,17], Bradbury [28], Shafizadeh [179-190], Soltes [194,195] and Antal [11,13]. A review is beyond the scope of this thesis since these two primary pyrolytic pathways do not occur within the context of true *fast* pyrolysis conditions. The reader is referred particularly to Shafizadeh [188] and Antal [11].

Secondary fast pyrolysis reactions are those which follow the primary fragmentation pathway as described in Section 2.5 (Figure 6). Since the science of fast pyrolysis is very young, very little is known about the precise nature of *primary* fast pyrolysis. Consequently, very little is known about *secondary* fast pyrolysis reaction mechanisms. Indeed, one of the central objectives of the experimental component of this thesis is to

empirically characterize the secondary fast pyrolysis reactions. One means of providing a foundation for the experimental work is to identify the array of *possible* secondary reactions, as suggested from related thermochemical conversion studies, and then to determine the likelihood of their occurrence under fast pyrolysis conditions. Six general secondary reactions are known to be significant in conventional thermal processes, and must be therefore be evaluated with respect to their possible significance in fast pyrolysis processes. These reactions include cracking, reforming, recombination/repolymerization, the water-gas shift, the Boudouard reaction and the carbon-steam reaction.

The thermal decomposition or vapour phase pyrolysis of heavy hydrocarbons and organic compounds to smaller fragments is known as cracking. During the course of this endothermic, generic reaction pathway, C-C, C-H, and C-O bonds are broken and rearranged resulting in shorter carbon chains, ring cleavage, the production of H_2, CO and CO_2, and the formation of unsaturated compounds (eg. olefins). Although it has not been fully characterized with respect to its specific role in biomass pyrolysis mechanisms, vapour-phase cracking has been generally recognized as the single most important class of secondary reactions occurring under conditions of fast pyrolysis [5,11,13, 14,42,55,80,90,93,110,147,178,185]. Preliminary studies suggest that it occurs on a time scale of tens of milliseconds at temperatures exceeding 700°C [2,4,5,8,11,13,14,32,54,55,71,90, 110,122,123,130,131,136,137,147,152,164,178,194,218]. As with

any cracking process, the final product distribution will depend largely on residence time and temperature, but also on pressure and catalysis. High yields of valuable carbonyl and hydrocarbon intermediates, which are not predicted by chemical equilibrium, can be realized. Graham and coworkers, during the course of this thesis work (see references in Appendix 1), researchers at M.I.T. [86,90,108,130,131,136,137], Diebold [48-58] and Antal [8,11,12,13,14,15] have concluded that the major products of the initial cracking of primary fast pyrolysis vapours are carbon monoxide, carbon dioxide, methane, hydrogen and ethylene and other olefins at temperatures between 700 and 1000°C.

Other hydrocarbons are also formed but are rapidly cracked at these temperatures, and persist only in small quantities. Carbon dioxide, carbon monoxide, methane, water, and perhaps some ethylene are thought to be byproducts of primary fast pyrolysis, and persist throughout secondary reaction conditions. As stated above, CO_2, CO, CH_4 and a minor amount of water are also secondary reaction products. Antal [14] further speculates that a fixed fraction of carbon atoms in the volatiles appear to be dedicated to CO formation at temperatures above 600°C. The promotion of decarboxylation and dehydration reactions would favour olefin production and would be accompanied by a decrease in CO formation and an increase in CO_2 evolution. Antal [14] reports, however, that the role of decarboxylation is decreased as the temperature is increased, and that some means must be found to access those carbon atoms dedicated to CO formation if

a dramatic increase in ethylene yields is to be realized. Antal [11,13,14], Diebold [55] and others [156,157] also stress the importance of free-radical chemistry in the cracking mechanisms, something which is well recognized in petroleum cracking reactions [18,37,67,72,96,111,116,135,158,196,197,198, 204].

Reforming is a very broad class of thermal or catalytic endothermic reactions of hydrocarbons in the presence of hydrogen or steam at elevated pressures (2-7 MPa) which results in isomerization, hydrogenation and eventual fragmentation to light hydrocarbon and hydrogen free-radicals. Thermal and steam reforming, typically carried out in the temperature range of 540-800°C and at pressures between 3.5 and 7.0 MPa, resembles cracking in the sense that molecular size is reduced, but produce a vastly different product distribution (while releasing heat in the process). Catalytic reforming is carried out in the temperature range of 450 to 550 °C and at pressures between 2 and 3 MPa. It is characterized by molecular restructuring (ie. aromatization, cyclization and isomerization) as opposed to molecular size reduction. Some of the thermal and steam reforming reactions were at one time assumed to occur at a significant level in the pyrolysis vapour phase [2,4,91,147, 218]. However, it has now been clearly demonstrated that at the temperatures, residence times, and relatively low pressures characterized by fast pyrolysis, reforming is completely eclipsed by the dominance of the cracking reactions [8,11,13,14, 15,55,65,91,137,218].

Recombination or repolymerization reactions are typically tar- and char-forming secondary reactions which are most likely to occur in the **condensed phase** under conditions of reduced temperatures and long residence times (via the dehydration primary pathway). However, recombination of primary **vapour-phase** products by condensation can also form stable secondary tar. This is favoured by long vapour residence times, moderate temperatures (200 to 500°C) and high partial pressures [178]. These conditions allow the primary molecules to be in close proximity for significant periods of time in the condensed phase and permit frequent collisions to occur in the vapour phase. Extended reaction times at moderate temperatures result in the formation of char, water, CO and CO_2 from secondary tars. Under true fast pyrolysis conditions, recombination reactions are not likely to occur. However, if heat transfer is limited for any reason (i.e., improper reactor operation or large biomass particles) or if the primary fast pyrolysis vapours are exposed to high pressures, polymerization and condensation with the resultant formation of tar and char may occur.

The water-gas shift is the reversible reaction of steam with carbon monoxide to produce hydrogen and carbon dioxide. This exothermic reaction is considerably faster than the reactions of carbon-steam and carbon-carbon dioxide [27,46,100, 110,147,218], and under some circumstances may contribute to the final product distribution in fast pyrolysis processes [110,218]. The vapour phase temperature and nature of the

carrier gas (i.e., steam, carbon dioxide, recycle gas, etc.), will determine the direction and extent of the reaction. In the absence of an appropriate shift catalyst such as iron or nickel, the forward step (i.e., the production of hydrogen and carbon dioxide from steam and carbon monoxide) is faster than the reverse step at temperatures below 810°C [218]. Over the entire fast pyrolysis temperature range an approach to equilibrium clearly favours the production of steam and carbon monoxide at the expense of hydrogen and carbon dioxide [85].

The carbon-steam and carbon-carbon dioxide (Boudouard) reactions are similar with respect to rate, mechanism and degree of endothermicity. The former is the reaction of carbon with steam to produce hydrogen and carbon monoxide, proceeds at a negligible rate below 830°C, and is thought to play a minor role in fast pyrolysis due to its relatively slow kinetics (i.e., compared to primary pyrolysis and cracking) at temperatures exceeding 830°C [2,8,14,54, 87,91,147,218]. Nandi [129] reports the kinetics on a minute time scale in the temperature range of 630-930°C, and Hallen [87] concludes that only by catalysis can the carbon-steam reaction participate significantly in any pyrolysis process.

The Boudouard reaction which is that of carbon with carbon dioxide to produce carbon monoxide, is hardly detectable below 850°C and is also thought to play only a minor role in fast pyrolysis [2,5,14,27,60,110,218]. Edrich [60] reports that its rate may be up to 100 times slower than that of primary

pyrolysis at temperatures approaching 1100°C. In his initial work, Antal [5] treated biomass as a carbon source for the Boudouard or steam reactions but quickly recognized the predominance of the cracking phenomenon.

It is apparent from the discussion of the possible secondary reactions that, aside from the water-gas shift at temperatures greater than 810°C, steam is a relatively inert participant in fast pyrolysis processes. The majority of researchers have in fact confirmed that under typical fast pyrolysis conditions, steam acts primarily as a diluent to prevent secondary polymerization and promote cracking in the vapour phase [5,6,14,26,38,54,91]. This is consistent with petroleum cracking practice where steam is added as an inert to enhance the yield of olefins [38].

It is apparent that secondary fast pyrolysis consists primarily of cracking reactions with some evidence to suggest that the water-gas shift may play a significant, though not dominant, role at temperatures above 810°C. Purely mechanistic studies should therefore occupy themselves with the pyrolysis or cracking of those primary products which are derived from the fragmentation primary pathway (i.e., carbonyls, acids and organic alcohols), if the specific chemical pathways of secondary fast pyrolysis are to be identified. The fast pyrolysis of model compounds, including hydroxyacetaldehyde, would certainly be of great utility.

It is important to note that the characterization of secondary fast pyrolysis has been greatly simplified in this discussion. Most of the *possible generic* reactions have been evaluated, leaving "cracking" as the principal characteristic secondary fast pyrolysis reaction. However, cracking is not a simple single reaction pathway or mechanism. It is in itself a very complex set of reactions which include bond breaking and formation, ultimately towards reduced average molecular mass, both by conventional thermolysis and free-radical mechanisms. As is the case with petroleum feedstocks, the cracking of complex organic chemicals and polymeric substances, including biomass, can only be empirically modelled at this time. This type of modelling, as applied to lignocellulosic biomass, is a principal thesis objective.

2.6.3 Overall Fast Pyrolysis Pathways

Diebold, who was initially interested in the production of olefinic gases from biomass, is apparently the first researcher to attempt to identify fast pyrolysis reaction mechanisms within the framework of general pyrolysis reactions. In 1980, he assembled pyrolysis experts who consensually proposed a global biomass pyrolysis model [178], as illustrated in Figure 7. This model was remarkable for its time and has remained substantially correct. Certainly, important improvements and refinements have been made for specific biomass feedstocks such as cellulose, particularly with respect to the identification of specific predominant chemical intermediates (Refer to Section 2.5).

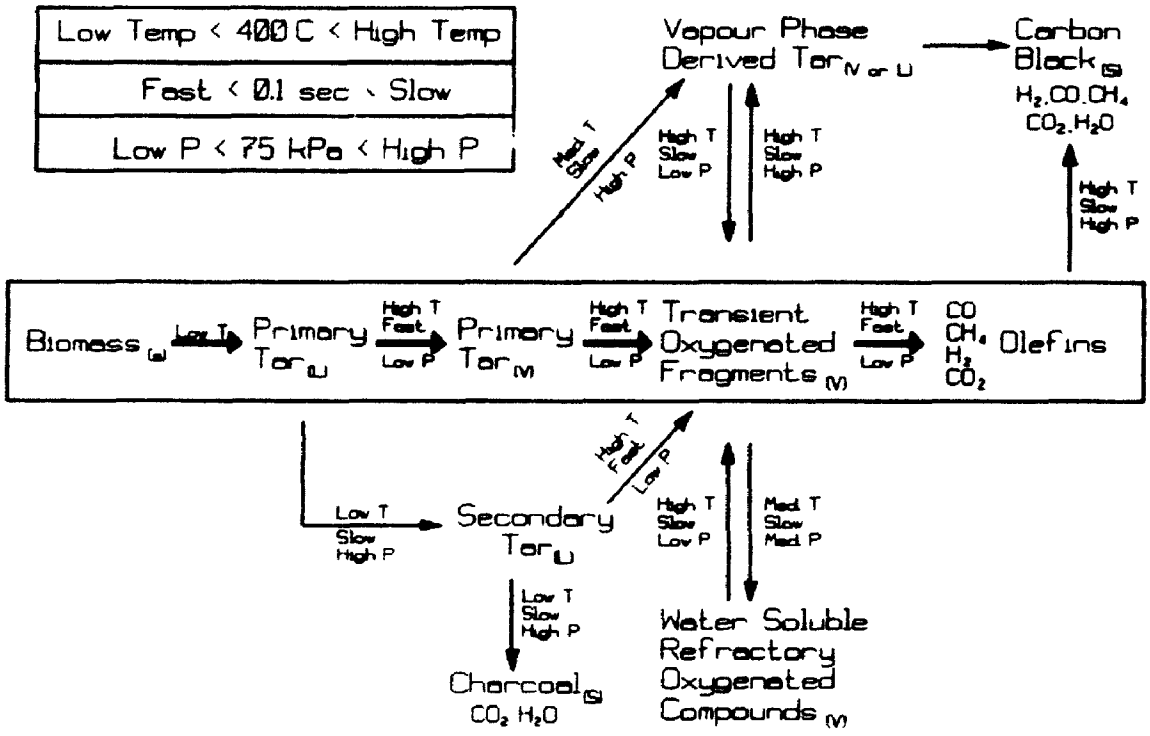

Figure 7. Diebold Model [55]

A fast pyrolytic pathway which clearly favours the production of olefins and other gases in non-equilibrium compositions is illustrated in Figure 7. Initially, a primary liquid (termed perhaps incorrectly as primary "tar") is formed at the surface of the reacting solid. Once this primary liquid is formed on the biomass surface, moderate to high temperatures (i.e. >400°C), high heating rates, and low vapour partial pressures will promote olefin formation (and that of other low-molecular mass gases in non-equilibrium compositions) by the following reaction sequence [178]:

1. Primary liquids are vaporized from the liquid-solid surface. This precludes the formation of stable secondary tars by recombination (repolymerization). Vaporization is essentially complete at about 500°C [13,101].

2. The vaporized primary liquids are thermally cracked to produce transient oxygenated fragments. These fragments (now known to be carbonyls, organic acids and alcohols, and depolymerized lignin) can form equilibrium mixtures of pyroligneous acids (i.e., acetaldehyde, methanol, furan, acetic acid, acetone, etc.) and vapour phase-derived tar by recombination under non fast pyrolysis conditions.

3. The transient oxygenated fragments are thermally cracked to yield olefins, other hydrocarbons, carbon oxides and hydrogen.

Extended reaction times will allow the olefins and related products to react in the vapour phase and form particulate carbon (carbon black) and permanent, low-molecular mass, equilibrium gases. Therefore, to preserve the olefins, the pyrolysis pathway must be interrupted by rapid quenching of the intermediates before equilibrium can occur [178].

The principal sequential reactions in the overall fast pyrolysis pathway have become apparent from a review of the available literature (Sections 2.5 and 2.6), an analysis of the possible generic chemical reactions and the consensus of pyrolysis experts. **Mechanistically, fast pyrolysis consists of activation, fragmentation and cracking.** Preservation of valuable fast pyrolysis gaseous or liquid products will occur if product quenching occurs before vapour-phase cracking is allowed to proceed to any appreciable extent.

Fast pyrolysis has now been defined in terms of the requirements for process conditions (temperature, residence time and pressure) and the selected chemical pathway. What remains to complete the definition is a characterization in terms of heat transfer requirements, and the techniques and equipment which can actually achieve fast pyrolysis in the laboratory and in commercial applications. However, before this characterization is completed, a brief review of pyrolysis kinetics is given in order to provide a foundation for the kinetics component of the experimental thesis work.

2.7 KINETIC STUDIES

2.7.1 Primary Pyrolysis Kinetics

The global kinetics of conventional and primary rapid pyrolysis are well documented by Antal [4,6,8,9,11,13,14,15], Bradbury [28], Shafizadeh [28,179,187,189,190], Broido [33], Arsenau [17], and others [1,19,21,32,34,46,55,60,93,95,103,110,

129,147,148,152,160,174,175,177,178,207,208,212,222]. However, because of the complexity of the degradation pathway, the historical kinetic research has typically dealt with the rate of solid biomass *disappearance* (i.e., volatilization or devolatilization rate) rather than the rate of *formation* of primary, secondary and equilibrium products [6,14,86,90,108,145,190]. More recently, fast pyrolysis conversion techniques, advanced analytical procedures and the understanding of reaction pathways have improved to the point where the primary and secondary reaction kinetics of fast pyrolysis are beginning to be quantified in terms of product formation. Bergougnou and Graham [Appendix 1], Diebold [55] and researchers at M.I.T. [86,90,108, 130,131,136,137] have contributed in this area.

Numerous kinetic investigations of the primary pyrolysis of biomass have been conducted over the past four decades with apparently very little agreement [1,4,6,8,9,11,13,14,19,21,28, 32,33,34,46,55,60,93,95,103,110,129,147,148,152,160,161,174,175, 177,178,187,189,190,207,208,212,222]. Quite often, researchers were unaware of the basic primary pathways and failed to appreciate the significance of heating rate (and its role in determining whether fast or slow pyrolysis reactions would occur). Furthermore, they seldom recognized the importance of the feedstock quality (i.e., morphology, DP, inorganic composition, impurities, etc.). The work of Bradbury [28] has endured with broad acceptance, and is therefore the focus of this discussion. Antal [11,13] has certainly made a large

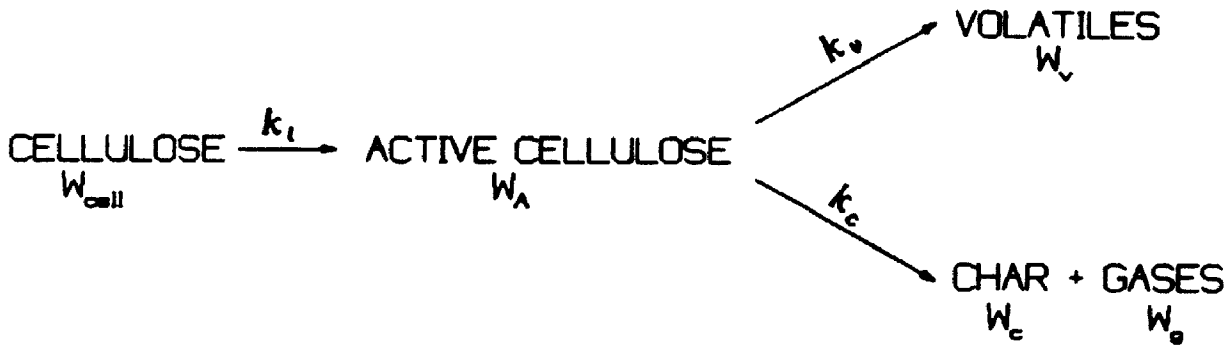

Figure 8. Bradbury Kinetic Model [28]

contribution by reconciling diverse biomass pyrolysis kinetic studies (including his own earlier work) to the findings of Bradbury.

As discussed in the previous section, the three-pathway primary pyrolysis model is relatively recent, and requires further mechanistic and kinetic experimental work. Consequently, the earlier two-pathway primary mechanism of Kilzer and Broido (Figure 4) has served as a model for most kinetic studies. Bradbury [28], working in the laboratory of Shafizadeh, carried out kinetic studies using this model, and in the process discovered a primary activation step which precedes the three primary pathways (Figure 6) which are now known to occur. Bradbury's model, given in Figure 8, assumes that cellulose pyrolysis can be described by a simple three reaction pathway. The first reaction is a first-order initiation step leading to the formation of "active cellulose". The exact nature of this intermediate is not known, but Diebold [55] reports that it has a much lower degree of polymerization than the initial cellulose feedstock, and is considered to be in a liquid or "plastic" state. The activation step is followed by two competitive first-order reactions, one yielding volatiles (volatilization) and the other char and a gaseous fraction (dehydration). The latter is favoured at lower temperatures, and the kinetic equations are given as follows:

$$\frac{-d(W_{CELL})}{dt} = k_1[W_{CELL}] \quad (1)$$

$$\frac{d(W_A)}{dt} = k_1[W_{CELL}] - (k_v+k_c)[W_A] \quad (2)$$

$$\frac{d(W_C)}{dt} = 0.35k_c[W_{CELL}] \quad (3)$$

Where,

$$k_1 = 2.80 \times 10^{19}\, e^{-[(243/RT)]} s^{-1} \quad (4)$$

$$k_v = 3.17 \times 10^{14}\, e^{-[(198/RT)]} s^{-1} \quad (5)$$

$$k_c = 1.32 \times 10^{10}\, e^{-[(151/RT)]} s^{-1} \quad (6)$$

Note: The Arrhenius kinetic parameters are given as,

$$k = A\, e^{-[Ea/RT]} \quad (7)$$

k = rate constant (s^{-1})
A = pre-exponential constant (s^{-1})
Ea = activation energy (kJ/mole)
R = universal gas constant (0.008314 kJ/mole-K)
T = absolute reaction temperature (K)

The constant "0.35" in equation (3) represents an empirically-determined char fraction.

Diebold [55 and as referenced in 152] accepted the kinetic data of Bradbury but expanded the model to include additional kinetic data for the direct production of char from cellulose (i.e., without activation) and for the direct production of small quantities of gas (which he terms "prompt" gas) from active cellulose. Direct char production is reported to occur via an extremely slow, low-temperature pyrolysis process. After consultation with Diebold and considering the lack of

corroboration in the literature, the author concluded that these reactions, if they indeed existed as described, were inconsequential for modelling purposes. Consequently, they were not dealt with in the discussion on pyrolysis pathways (Sections 2.5 and 2.6) and are not dealt with further in this review of pyrolysis kinetics. However, it is important to note that this author acknowledges that "prompt" gas is indeed produced during primary fast pyrolysis, but that it is direct byproduct of the fragmentation and depolymerization; i.e., not a product of a competing primary pyrolytic reaction. This is dealt with in greater detail in Chapters 8 (Sections 8.4, 8.5 and 8.8) and 9.

Broido [33, and as reported in 11] had reported activation energies which were much higher than those associated with the k_v and k_c values of Bradbury, under similar experimental conditions. Until 1982, the literature reported kinetics data which were clearly divided, and apparently irreconcilable, in their support of the two sets of data. Antal, whose early work [6,11] had agreed with Broido, then confirmed the results of Bradbury and explained the discrepancy in terms of a failure to properly account for heat transfer effects [11,13,101]. Antal's subsequent experimental work and that of other researchers has substantiated the Bradbury model [11,13,14.188,189,190].

The Bradbury kinetic model can be applied in a very simple manner to confirm the mechanistic conclusions (Section 2.5) that volatilization reactions (depolymerization and fragmentation) begin to take over from dehydration (char-forming) reactions in

the temperature range of 280 to 300°C. Since the model is first-order and describes the disappearance of a single common reactant (ie. activated cellulose), the rates of both the volatilization and dehydration reactions are directly proportional to the value of their respective rate constants (k). Therefore, if we let $k_v = k_c$, we can then determine at what temperature the rates are the same. This temperature is about 285°C, and the Bradbury model is therefore consistent with empirical mechanistic studies. The model also indicates that at pyrolysis temperatures of 190°C (typical of conventional pyrolysis), the dehydration reaction rate is about 10 times that of the volatilization rate. At 450°C (typically a minimum temperature for fast pyrolysis), volatilization proceeds at about 10 times the rate of dehydration.

It is important to reiterate that the kinetic equations presented above were developed for the two-pathway model, before the third primary pathway was rediscovered and confirmed. It is very likely that empirical kinetic parameters (i.e., k_v in Equation 8) associated with "volatilization" pathway in Figure 8 represent the combined kinetic parameters of the primary depolymerization and fragmentation pathways of Figure 6. Indeed, many of carbonyl and related compounds, now known to be primary fragmentation products, were detected in the product distributions of the "volatilization" pathway which was being kinetically modelled by Bradbury, Shafizadeh , Antal and others. As was stated previously, these researchers typically assumed

that the carbonyls were secondary products arising from the anhydrosugars which had presumably been produced by the depolymerization of cellulose. Nevertheless, these kinetic equations have remained as valuable tools to accurately describe cellulose activation and to model the general volatilization of cellulose. The next generation of kinetic models, now being developed, will be required to distinguish between fragmentation and depolymerization products and will thus allow for selection and optimization of the desired fast pyrolysis product distribution.

2.7.2 Primary Fast Pyrolysis Kinetics

The present literature review has failed to locate any kinetics studies which deal *explicitly* with the primary fragmentation mechanism in the fast pyrolysis pathway. However, as stated in the previous discussion, the "k_v" reaction of Bradbury in Figure 8 (i.e., the volatilization route) likely lumps both fragmentation and depolymerization together in the production of "volatiles". This model has been found to accurately represent cellulose disappearance over a broad range of pyrolysis conditions [11,13,55,152]. Furthermore, Antal [13] states that accurate estimates of high temperature fast pyrolysis rates can be accurately obtained by extrapolating Bradbury's kinetic data. Therefore, since primary fast pyrolysis has been defined as activation followed by fragmentation (Sections 2.6.1 and 2.6.3), it is assumed for the remainder of this thesis that the kinetics of primary pyrolysis

can be modelled using Bradbury's "k_i" and "k_v" parameters (Section 2.7.1 and Figure 8). This data will suffice until specific fragmentation kinetic parameters are developed and are clearly distinguished from depolymerization parameters.

2.7.3 Secondary Fast Pyrolysis Kinetics

Secondary fast pyrolysis reactions have been characterized primarily in terms of vapour-phase cracking (Section 2.6.2). The water-gas shift can play a significant, though non-predominant, role at temperatures above 810°C, and is dealt with in detail in Chapter 8 (Section 8.7). The predominant cracking reactions therefore remain as the focus of this present discussion.

Comparatively little research has been conducted to determine the kinetics of the cracking of biomass-derived fast pyrolysis vapours, and this is the principal reason why this task was identified as one of the primary objectives of the thesis work. Antal [11-15,199], Diebold [55, and as referenced in 152], Peters and coworkers [86,90,130,,131,136, 137], Thurner and Mann [207] and Scott [173,175] are among the few researchers who have published literature in this area. All of these publications are relatively recent, and represent research which was conducted concurrently with the thesis work. The author and his coworkers at the University of Western Ontario have also published work on this topic during the course of this experimental study (Appendix 1).

The published work falls into one of two broad categories; those kinetic studies which deal with the complete cracking of

the solid biomass feedstock to permanent gases, and those which deal directly with the cracking of biomass-derived vapours. Since the secondary cracking reactions are rate-limiting (compared to primary activation and volatilization reactions) in the fast pyrolysis sequence [55,173], it can be reasonably concluded that studies within the first category can indeed give good kinetic data for vapour-phase cracking. In other words, volatiles are fully produced before significant cracking occurs within the typical reaction conditions of fast pyrolysis processes, and the kinetics will therefore represent rates for the cracking of the vapours to secondary permanent gases.

In general, the researchers have assumed simple first-order decomposition or formation mechanisms. The kinetic parameters are summarized in Table 1, with the exception of the kinetic data from the authors work, which is presented in Chapter 9.

It would appear that in 1980, Peters and coworkers [86,90, 131,136,137] were the first researchers to determine kinetic parameters for the decomposition of solid cellulose and wood feedstocks to secondary gases under fast pyrolysis conditions. Thurner and Mann [207] followed with data for wood in 1981, while Graham (Appendix 1) and Scott [173,175] have published kinetic parameters for the cracking of solid cellulose and hardwood feedstocks to vapours and gases both jointly and separately since 1984. It should be noted that the kinetic parameters published by Scott were determined from the combined fast pyrolysis results of Graham and Scott. These two sets of

data exhibited excellent agreement even though they were generated in two different reactor systems (Section 8.8). Furthermore, Scott's parameters were first determined by a coworker, Liden, and were then further refined by Scott himself to give a better fit. The distinction between the initial Liden parameters and the refined data is indicated in Table 1.

Antal [12,13], in 1983, was the first fast pyrolysis researcher to initiate kinetic studies dealing specifically with direct vapour-phase cracking of cellulose-derived volatiles. Diebold [55] followed with direct vapour-phase cracking of softwood-derived volatiles in 1985.

TABLE 1. KINETIC PARAMETERS FOR FIRST-ORDER VAPOUR-PHASE CRACKING REACTIONS UNDER CONDITIONS OF FAST PYROLYSIS.

RESEARCHER	FEEDSTOCK	KINETIC PARAMETERS	
		Ea (kJ/kmol)	A (s^{-1})
Peters, et.al. [86,90,131,137]	Cellulose	133.4	2.00×10^{8}
	Hardwood	69.0	3.39×10^{4}
Thurner/Mann [207]	Hardwood	106.5	2.47×10^{6}
Liden [173]	Hardwood	107.5	4.28×10^{6}
Scott [173,175]	Hardwood	107.5	2.00×10^{6}
	Cellulose	107.5	3.10×10^{6}
Antal [12,13]	Cellulose-Derived Vapours	204	3.57×10^{11}
Diebold [55]	Softwood-Derived Vapours	87.6	1.55×10^{5}

Antal [12,14], Peters and coworkers [86,90,131,137], and Graham and coworkers [Appendix 1] were the first researchers to publish kinetic parameters for the *formation* of individual gas components produced from vapour-phase cracking reactions during biomass fast pyrolysis. Their respective research was conducted and published concurrently. The parameters reported by Antal and Peters are given in Table 2. The parameters of Graham are the subject of this thesis and are reported in Chapter 9.

Diebold [55] models the production of permanent gases during fast pyrolysis by assuming the occurrence of three initial reactions followed by hydrocarbon cracking reactions. The initial reactions include:

1. The production of "prompt gas" (primarily CO_2 and CO) from activated biomass concurrently with vaporization.
2. The production H_2, CO, CO_2, CH_4 and C_2+ hydrocarbons from the cracking of primary vapour.
3. The production of CO_2 and water during the formation of secondary tar from primary vapours.

Diebold then proposes an empirically-determined stoichiometry for the production of permanent gases directly from the activated biomass and primary vapours. The kinetic parameters associated with the disappearance of the biomass and primary vapours (for the three initial reactions) are then used to give an initial permanent gas composition as a function of time. Consecutive hydrocarbon cracking reactions are then introduced to complete the model using kinetic rate constants gleaned from the literature. A complex set of reactions is numerically integrated to predict the overall gas composition as a function

of time and temperature. As such, the kinetic parameters for the appearance of each gas component are not determined *per se*.

TABLE 2. KINETIC PARAMETERS* FOR THE FORMATION OF PERMANENT GASES PRODUCED VIA VAPOUR-PHASE CRACKING DURING FAST PYROLYSIS.

RESEARCHER	FEEDSTOCK	GAS COMPONENT	KINETIC PARAMETERS	
			Ea (kJ/kmol)	A (s^{-1})
Antal [12,14]	Cellulose	H_2	146.5	-
		CO	251.2	-
		CO_2	87.9	-
		CH_4	280.5	-
		C_2H_4	230.3	-
		C_2H_6	159.1	-
		C_3H_6	230.3	-
	Hardwood	H_2	276.3	-
		CO	104.7	-
		CO_2	-	-
		CH_4	96.3	-
		C_2H_4	209.3	-
		C_2H_6	71.2	-
		C_3H_6	171.7	-
Peters,et al. [86,90,131,137]	Cellulose	Total Gas	133.1	2.00×10^{8}
		CO	220.8	5.62×10^{11}
		CO_2	98.1	2.45×10^{5}
		CH_4	251.4	1.00×10^{13}
		C_2H_4	208.6	6.61×10^{10}
		C_2H_6	174.0	1.15×10^{9}
		C_3H_6	254.0	8.51×10^{14}
	Hardwood	Total Gas	49.4	7.59×10^{2}
		CO	61.1	2.29×10^{3}
		CO_2	59.0	5.89×10^{3}
		CH_4	69.5	6.17×10^{3}
		C_2H_4	80.4	2.57×10^{4}
		C_2H_6	99.2	7.41×10^{5}
		C_3H_6	179.2	1.58×10^{11}

* The kinetic parameters are given for first order reactions describing the production of permanent gases directly from the biomass feedstock (Peters) and the biomass-derived vapours (Antal).

2.8 PYROLYSIS OF BIOMASS CONSTITUENTS

The thesis experimental work is concerned primarily with the fast pyrolysis of cellulose, and the literature review has therefore focused on this principal biomass component. A brief review of pyrolysis of the other principal biomass components is given in the following paragraphs.

It has often been assumed that the pyrolysis of a given biomass material was simply the sum of the pyrolytic behaviour of its individual lignocellulosic components (ie. cellulose, lignin and hemicellulose). Presently there is general agreement that the sum of primary pyrolysis products from individual constituents is very similar but not identical to whole biomass pyrolysis, and that synergistic effects are evident [1,2,5,14, 34,90,119,165,190,194,215]. If the secondary cracking reactions of fast pyrolysis are allowed to proceed to any appreciable extent, Antal [3] suggests that the behaviour of the whole wood material is similar to the sum of each of the components.

In any event, it is clear that a study of the pyrolysis of individual cellulose, hemicellulose and lignin compounds will be useful in predicting the behaviour of a given biomass material of known lignocellulosic composition. Of all principal lignocellulosic components (cellulose, hemicellulose and lignin), the thermal decomposition of cellulose has been best characterized and has been dealt with in great detail in previous sections.

2.8.1 Hemicellulose Pyrolysis

Hemicellulose, whose decomposition is initiated as low as 120°C and is completed by 325°C, is the most reactive of the three major biomass components [2,21,93,148,177,221]. A pyrolytic degradation pathway is proposed which is similar to that of cellulose in that dehydration reactions are important at temperatures less than 280°C and are replaced by rapid fragmentation and depolymerization as the temperature is increased [21,183]. Dehydration is characterized by random cleavage of the C-O bonds producing branched-chain anhydride fragments, water-soluble acids, char and light gases [2,21,34, 183].

In the case of high-temperature hemicellulose pyrolysis, a characteristic intermediate (i.e., the analogue of hydroxy-acetaldehyde or levoglucosan in cellulose pyrolysis) is assumed to exist from kinetic data, and is thought to be furan or furfural for hemicellulosic pentosans, but has not been clearly identified [2,5,34,44,146,221]. These furan derivatives are difficult to isolate due to their extremely rapid formation and decomposition. The secondary high-temperature products from hemicellulose rapid pyrolysis include those gases produced from cellulose [5,183], although in different proportions. Furthermore, the yields of char, organic acids (eg., acetic acid) and water from hemicellulose fast pyrolysis are typically higher than those from cellulose [44,146].

2.8.2 Lignin Pyrolysis

The mechanism and kinetics of the primary pyrolysis of lignin have not been as extensively investigated as those of cellulose pyrolysis, and a single major characteristic primary pyrolysis products have not been identified [2,5,13,21,34,138, 177,183]. This lack of a clear understanding can be directly attributed to the complex structure of lignin which varies significantly as a function of species and method of preparation. Indeed, it is very difficult to isolate and recover a representative "natural" lignin, and a standardized feed material is therefore difficult to define.

In general, lignin is more thermally stable than other biomass components and under similar pyrolysis conditions, whether fast or slow, produces more char and a higher fraction of aromatics in the liquid product than does cellulose or hemicellulose [13,21,34,77,78,93,102,130,132,148,183,190,221]. Antal [13] proposes a primary pathway consisting of three parallel reactions, similar to cellulose pyrolysis. The low temperature pathway gives high yields of char, water and aqueous condensibles, CO_2 and CO. Methanol and acetone are the most abundant organic components in the aqueous phase [13,44].

Lignin pyrolysis at medium temperatures results in a complex mixture of "monomers" which can further react to form refractory condensibles (secondary tar) or permanent gases. No single predominant monomer or intermediate has been identified which is analogous to levoglucosan or hydroxyacetaldehyde in

cellulose pyrolysis, but recent lignin pyrolysis experiments using direct mass spectrometry show a family of methoxy phenols as predominant primary pyrolysis products [119].

High temperature lignin pyrolysis produces high yields of CO, H_2 and reactive vapours. With extended reaction times, the reactive vapours will form secondary char and permanent gases. Above 1000°C, CH_4 and C_2H_2 are the predominant permanent gases.

It has been proposed that primary lignin fast pyrolysis occurs with the cleavage of the straight carbon chains which connect the aromatic units. Antal [5,13] speculates that rapid pyrolysis may initially result in the formation of monomeric phenylpropane units (which are joined by ether linkages), patterning to some extent the depolymerization of cellulose by the cleavage of the glycosidic bond. Further pyrolysis gives rise to phenols, cresols, catechols, xylenols, etc., and char from aromatic monomers, and produces carbon oxides, hydrocarbons, aqueous acids and char from the straight carbon chain [34].

Shafizadeh and Chin [183] summarize the primary volatilization (depolymerization and fragmentation) of the three major wood components as follows:

1. Hemicellulose is the most reactive component and volatilizes between 225 and 325°C.

2. Lignin is the most thermally stable component and decomposes gradually between 250 and 500°C.

3. Cellulose is intermediate in terms of its reactivity and decomposes between 325 and 375°C (decomposition is initiated at a higher temperature than lignin but occurs rapidly within a much narrower range).

2.9 HEAT AND HEAT TRANSFER EFFECTS

It would appear that fast pyrolysis has now been fully defined in terms of the required reaction conditions, the nature of desired products and specific pyrolytic reaction pathways. However, a final consideration involves heat transfer and the resultant biomass heating rate during pyrolysis. If heat transfer to and through the biomass is inadequate in the reactor system, a significant temperature gradient will exist and, depending on the size of the biomass feed material, a substantial fraction will remain unreacted or will pursue an alternate pyrolytic pathway.

If a biomass particle is infinitely thin and an adequate amount of heat is available at an appropriate reaction temperature, then no temperature gradient exists and fast pyrolysis certainly occurs without heat transfer limitations. However, one can imagine a very large piece of biomass fixed in a high-velocity hot gaseous stream. It is possible that the surface reactions would be typical of fast pyrolysis, and primary vaporized products would be swept from the reacting surface. Since biomass has a low thermal conductivity (ie. a good insulator), it is also possible that a large temperature gradient would exist for a significant period of time from surface to centre. Under these conditions, even if the reactor temperature was in the fast pyrolysis regime, slow pyrolysis reactions and secondary thermal reactions could occur in the solid and condensed phases at or below the surface.

Nevertheless, Diebold [48,56,152,178] demonstrated that "ablative" or "contact" heat transfer could result in the fast pyrolysis of even large biomass feedstocks. This type of heat transfer is characterized by direct intimate contact between a hot non-reacting surface moving over the reacting biomass surface. The biomass surface was found to react, vaporize and retreat at a rate which was much faster than the rate of heat conduction, and essentially no temperature gradient was realized. Diebold described ablation as "solid convective heat transfer" and demonstrated it elegantly by rapidly slicing through a wooden dowel with a hot nichrome wire.

Clearly, fast pyrolysis must be defined in terms of the heating rate of the particle such that temperature gradients in the particle do not *effectively* exist. That is, they exist for a period of time which is less than is required for slow pyrolysis reactions to occur. Heat transfer must be adequate to ensure that this minimal heating rate is achieved, and therefore physical and thermodynamic properties of the biomass, size of the particles and reaction rates must all be considered in the analysis.

Detailed analyses of heat transfer and heating rate in the context of fast pyrolysis have been conducted by the author and his co-workers [80], Diebold and co-workers [48,56,150,152,178], and by Scott and co-workers [173,174,175,]. Such detail is beyond the scope of this thesis, but the results of the studies are reviewed in the following paragraphs.

Graham and co-workers [80] applied first principles of heat transfer and empirical correlations using published thermodynamic and physical properties of wood [89,95,114,136,137] to define fast pyrolysis in terms of heating rates. The analysis simply considered conduction through the wood particle given an array of heat fluxes which were related to typical heating environments. The resistance to conduction arising from the endothermicity of pyrolysis and the diffusion of products was ignored, as was the accelerated conduction occurring in ablative processes.

Figure 9 shows the time taken for a particle of a given size to reach a mean temperature which is half that of the heat transfer environment. The isochrones of Figure 9 are for heat-up times of 0.1 to 100 s during which the particle mean temperature will be half that of the "bath" (environment) [80]. In pyrolysis experiments with a bath temperature of 1000°C, they cover the range from 10 to 10,000°C/s. The curves indicate that fast pyrolysis requires heating milieus such as fluidized beds, and small particles in the range of 100 to 1000 μm. According to this model, massive particles such as wood chips can only be heated at rates of 50°C/s in fluidized beds. Techniques which allow ablative pyrolysis to occur, circumvent the restrictions implicit in Figure 9 by having solid-solid heat transfer at far higher rates coupled with abrasion of the reacting layer from the surface of the particle. Radiation heating techniques such as solar flash pyrolysis or laser irradiation show very little

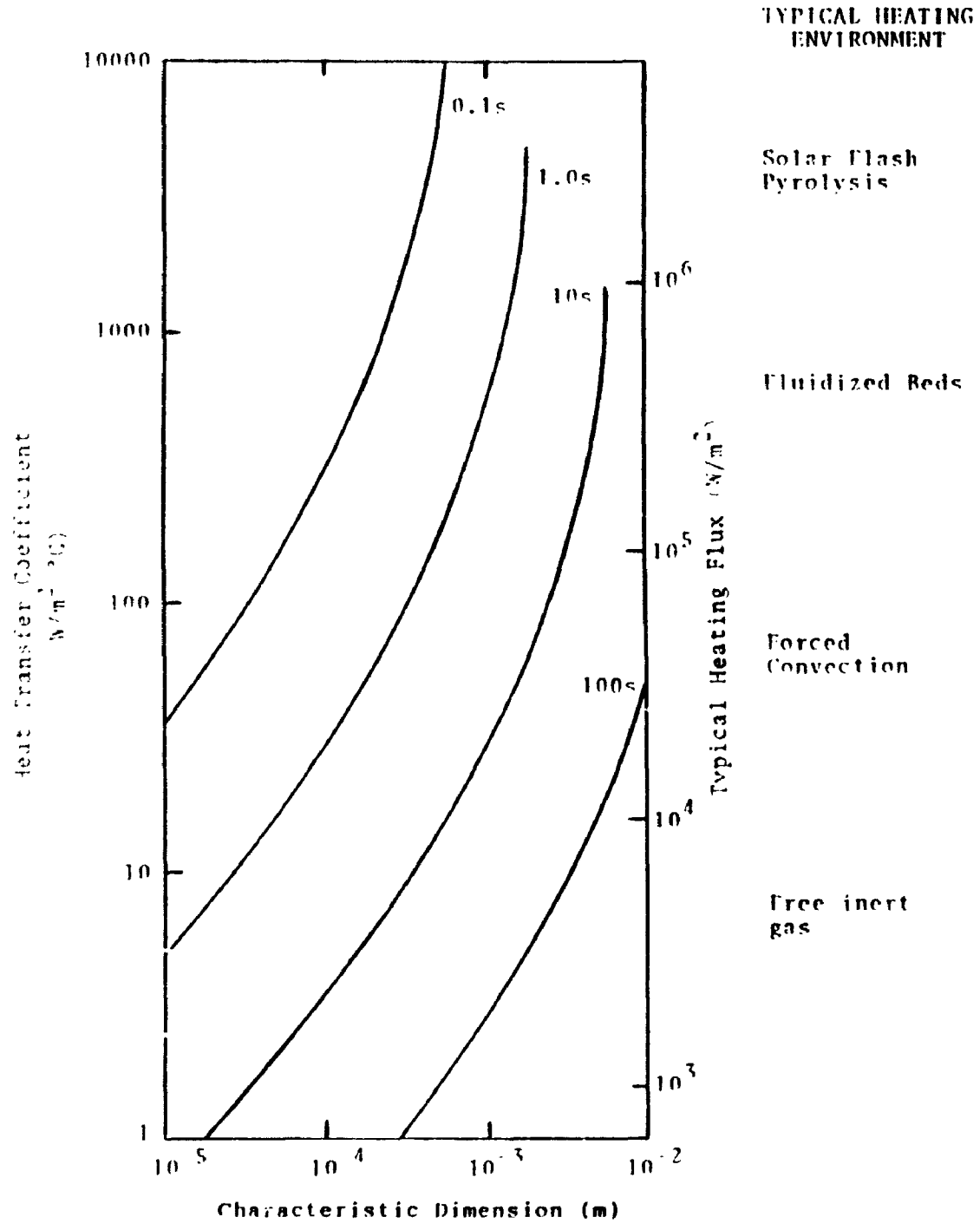

Figure 9. The Effect of Heat Transfer and Particle Size on Heating Rate [80]

penetration of the thermal front when applied to massive particles for brief periods.

For the purpose of discussion, Graham and co-workers [80] defined fast pyrolysis as referring to environments and particle sizes such that the mean rate of temperature rise was greater than or equal to 1000°C/s. Thus the sample would attain reasonable temperatures for reaction on a time scale corresponding to the "half life" of the reaction. Using averaged Arrhenius kinetic parameters for first-order biomass fast pyrolysis (i.e., a pre-exponential factor of approximately 10^9 s^{-1} and an activation energy of the order of 120 kJ/mole), then the half life of such a reaction is as follows:

Temperature (°C)	Half Life ($t_{1/2}$) (ms)
500	90
800	0.400
1000	0.058

In a dynamic experiment to avoid significant temperature gradients and reaction occurrence during heat-up, clearly the half times of sample heat-up, as derived from Figure 9, have to be less than these figures. For example, this simple model predicts that in a fluidized bed, the average particle size of the biomass particles would have to be less than 500 μm in order to achieve fast pyrolysis at 500°C. The model was useful as a first attempt to relate physical and chemical processes occurring in fast pyrolysis. However, subsequent expanded theoretical models and empirical studies with reactors which

utilize ablative heat transfer mechanisms (including transport reactors using hot particulate solids and cyclonic vortex systems) have clearly demonstrated that much larger particles can be reacted in a fast pyrolysis regime.

Scott and co-workers [173,174,175] outlined two methods for quantifying fast pyrolysis in terms of the biomass particle heating rate, by employing theoretical modelling and empirical data from two different fast pyrolysis reactor systems. One system was the Waterloo University fluidized bed and the other was the Ultrapyrolysis equipment used during the course of this thesis work. The first method simply defines fast pyrolysis as any pyrolysis process in which the biomass particle temperature reaches at least 95% of reaction temperature in a time period which is less than 20% of the particle residence time. The model assumes that biomass volatilization is complete at 500°C (ie. the biomass particle no longer exists as a solid), and therefore the time for the centre of particle to approach 500°C represents the heat-up time. In a fluidized bed, Scott estimated that the time for a 600 μm particle to reach 450°C (ie., 95% of the reaction temperature of 500°C on an absolute basis) was 618 ms. Since the particle residence time is between 2 and 6 seconds, the fast pyrolysis criterion is satisfied for this particle size. For a 100 μm size, the heat-up time is 62 ms and the particle residence time is at least 500 ms, and the fast pyrolysis criterion is therefore also satisfied. However, this method is perhaps inadequate since it does not deal

directly and quantitatively with the kinetics of fast pyrolysis reactions and their relationship to heating rates. The implicit assumption in the model is that if the particle temperature achieves fast pyrolysis temperatures within a certain fraction of its residence time, then slow pyrolysis reactions will be precluded and heat transfer will not be the rate-limiting step. One can imagine a slow pyrolysis process where the heating rate is such that fast pyrolysis temperatures are reached in a period of hours (meanwhile slow pyrolysis reactions have sufficient time to occur during heat-up) and the particle residence time is on the order of days. The criterion for fast pyrolysis is satisfied, but fast pyrolysis clearly does not occur.

The second method of Scott relates chemical rate equations to expressions for biomass particle heating rates, and arrives at a model which can be effectively applied on a broad basis. On the basis of empirical data, Scott proposes that fast pyrolysis occurs if the particle centre temperature reaches 450°C before more than 10% of the weight of the solid feedstock is lost. Heat rate expressions are derived from first principles using the physical and thermodynamic properties of wood and the kinetic parameters of Thurner and Mann [207] are used in a first-order Arrhenius rate equation. The model, which is moderately conservative given the kinetic parameters, predicts that for all particle sizes less than 2 mm, the criterion will be satisfied. This is confirmed in actual fluidized bed fast pyrolysis studies.

Diebold and co-workers [150,152] initially defined biomass fast pyrolysis in terms of heat transfer requirements, by relating the heat for pyrolysis and heat flux to char yields from cellulose. They proposed that fast pyrolysis of cellulose was indeed occurring when char yields were less than 1%, and then measured the heat flux required to achieve fast pyrolysis (according to the char yield criteria) in very thin "two-dimensional" cellulose particles. The heat for pyrolysis consisted of sensible heating, the heat of chemical reaction (heat of pyrolysis), melting and vaporization. The result of the study was that biomass fast pyrolysis requires about 2000 kJ/kg of heat to be supplied to a biomass surface at a temperature of at least 460°C with a flux somewhat above 500 kW/m^2. A review of pyrolysis kinetics confirmed that the resultant heating rate carried out to a final temperature of 500°C ensures that "the biomass spends an insignificant amount of time at the lower temperature" where slow pyrolysis reactions can occur. They reviewed the fundamental methods of heat transfer and related these to various practical heat transfer techniques. The conclusion was that reactor systems employing some form of solid convective heat transfer (ablation) would be necessary for a successful practical fast pyrolysis system. Subsequent modelling studies using a cyclonic ablative reactor system predicted that a 5mm particle could be fast pyrolysed and reduced to an escape particle size of about 50 μm in less than 700 ms.

The initial work of Diebold raises the question of determining the heat of pyrolysis for fast pyrolysis reactions. A considerable effort has been made to determine the heat of reaction for primary pyrolysis, and there is a considerable range of values reported in the literature. This range can likely be attributed to variations in the biomass feedstock, experimental equipment, reaction conditions, and the extent to which the reactions are permitted to occur in each case. There is, however, general agreement that primary fast pyrolysis pathways are moderately endothermic [2,8,27,41,42,54,56,103,105, 107,128,139,141,150,152,176,177,178,212,215]. A few authors speculate that fast pyrolysis is athermic (i.e., the heat of reaction equals zero) at approximately 700°C and increases in endothermicity with increasing temperature [42,107,212]. For engineering applications, the heat of reaction for primary pyolysis alone is often assumed to be negligible when compared to other heating effects such as melting, evaporation, sensible heating and secondary cracking [56,107,150,152,212]. Antal and co-workers [6,8,128] have experimentally determined the heat of reaction of primary pyrolysis (volatilization) to be between 100 and 400 kJ/kg in a differential scanning calorimeter apparatus at maximum temperatures of 500°C. They also observed that primary pyrolysis becomes athermic, and eventually exothermic, with increasing pressure as the vapour-phase polymerization and secondary char-forming reactions predominate. Values between 800 and 2000 kJ/kg over the temperature range of 500 to 1000°C

are reported for total heat requirements of fast pyrolysis processes designed for maximum liquid or olefin yields [42,54, 56,105,150,152,178]. The higher values reflect the additional heat required for secondary cracking. For rough engineering calculations, 10% of the heat of the higher heating value of the biomass feedstock gives an adequate estimate of the total required heat for fast pyrolysis [2,41,107,150,178].

The secondary gas-phase cracking reactions are the subject of the thesis experimental work, and a final heat transfer consideration involves these reactions. As indicated previously, the volatilization of biomass is complete when the temperature rises to a point between 450 and 500°C. However, if non-equilibrium gases (eg. olefins) are the desired products, then the temperature must be further elevated to produce these gases in appreciable yields and at acceptable rates. Heat transfer must continue in the vapour phase to raise the temperature and provide the endothermic heat for cracking. In other words, the quantity of heat and rate of transfer which was adequate for primary pyrolysis (vapourization) must also be adequate for the additional heat demand of secondary reactions.

This heat requirement must be considered when selecting hardware for experiments dealing with secondary fast pyrolysis. For example, plug flow reactors using gaseous heat carriers exhibit cooling along the reactor length as pyrolysis reactions proceed. Fluidized beds exhibit good heat transfer in the bed, but in the freeboard vapours may quickly cool because of the

endothermicity of cracking. This is often advantageous for the preservation of primary condensible products. However, unwanted secondary condensation and polymerization reactions may result if the reaction time is inordinately extended. If temperatures in the range of 700 to 1000°C are required (for the production of non-equilibrium gaseous products), efficient heat transfer must continue after vapourization is complete. A transported-bed of hot particulate solids is ideal for this requirement.

It is now clear that fast pyrolysis fundamentally differs from conventional pyrolysis in terms of reactor conditions, chemical mechanism, reaction rates, product yields and quality, and heat transfer requirements. Before proceeding to the thesis experimental work, it is worthwhile to briefly review reactor systems which are used for bench-scale research and which are under development for commercial applications.

2.10 FAST PYROLYSIS TECHNIQUES AND EQUIPMENT

Many techniques and types of equipment can theoretically achieve the process conditions required for fast pyrolysis. Depending on the heat transfer mechanism, some require extremely small particles while others can process sizes which are typical of wood "chips". Certain techniques are designed solely to conduct fundamental research in order to contribute to the science of fast pyrolysis. Others are intended for process development and applied engineering with eventual commercial scale-up being the ultimate objective.

Fundamental studies dealing with biomass fast pyrolysis were initiated by a handful of North American scientists more than thirty years ago. Since then, the interest and effort devoted to this topic have rapidly expanded, but have continued to be dominated by Canadian and American researchers. Only very recently has a concerted effort within the European Community been undertaken to systematically investigate rapid biomass pyrolysis. It is for this historical reason that the vast majority of fast pyrolysis processes which are now approaching commercialization are being developed in North America.

2.10.1 Fundamental Research

It is important to first review the types of reactor systems which have been used in fundamental research initiatives. Such initiatives are concerned primarily with characterization of the chemistry, product yields and quality, mechanisms and kinetics of the fast pyrolysis of biomass, and the equipment used is normally not suitable nor intended for eventual commercial scale-up. Early landmark kinetic studies were typically conducted in thermo-gravimetric (TGA) equipment [6,11,14,16,17,27,33,44,58,97,113,134,148,163,183,184 186,203] or small quartz, glass and stainless steel bench-scale reactors housed in electrical resistance ovens [8,9,12,14,28,199,207]. Experiments consisted of batch experiments using a maximum of several hundred mg of biomass in the reactor at the start of the run. Products were usually swept from the reacting biomass with a steam or hot inert gas carrier. The results of these

experiments have been dealt with in considerable detail in Sections 2.5, 2.6 and 2.7.

The discussions in Sections 2.5 and 2.9 have clearly illustrated the important contribution that the University of Waterloo researchers [73,139,140,141,146,169,170,171,172,173, 174,175,176] have made to the basic understanding of primary fast pyrolysis mechanisms and the optimization of yields of light primary liquids. Catalytic methanation, petrochemical optimization and pathway selection for maximum sugar yields from biomass are also areas in which significant advances were made. This work was carried out in a shallow fluidized bed at atmospheric pressure under steady-state conditions using a vast array of wood and wood-derived feedstocks, and agricultural residues. Hot sand in the bed was used to transfer heat to the biomass particles. Process development work, including two demonstration projects, have arisen from the fundamental work at Waterloo University. Other fluidized bed studies [19,57,66,212, 218] have been initiated to study the fast pyrolysis of biomass.

Recent research by Milne and co-workers [117,118,119,120, 121,122,123,154] in a molecular beam mass spectrometer apparatus, and by others using his technique [68], has confirmed the fast pyrolysis mechanisms outlined in previous discussions. Real time sampling, precise control of vapour residence times, and the development of an excellent adiabatic expansion technique to quickly (microseconds) freeze intermediate products have permitted the observation of the evolution of the primary

products as a function of time. With respect to secondary gas-phase reactions, preliminary results indicate that the "olefin window" (i.e., a time interval after primary pyrolysis during which maximum yields of olefins are apparent) occurs between 30 and 150 ms after the primary tars vapourize from the liquid surface of the pyrolysing biomass at 900°C.

These secondary gas-phase reactions are the principal focus of the thesis experimental work, and in the following paragraphs particular attention is therefore given to fundamental research dealing with this subject. A widely publicized system is based on the China Lake entrained-flow pyrolyzer [25,47,49,50,94,105] which subsequently gave rise to the SERI/NREL fast ablative "vortex" pyrolyzer [30,31,48,51,52,53,54,55,56,57,58,154]. The China Lake apparatus consisted of a screw feeder, a CO_2/steam injector, a coil tube heater housed in a propane-fired kiln, a char cyclone and a quenching/condensing train. Although the vast majority of the trials were carried out using a 250-μm free flowing municipal solid waste fuel, wood flour (less than 180 μm) and Avicel pH 102 cellulose (100 μm) were also pyrolyzed at 750°C for approximately 150 ms. Maximum yields of ethylene were 9.3 and 8.6% by mass for cellulose and wood, respectively. Less than 0.03% of the input wood remained as a char residue, and the cellulose char residue was negligible (less than 0.001%).

The SERI/NREL fast-ablative entrained flow vortex pyrolyzer is a cyclonic reactor, whose heated walls are designed to preferentially transfer heat to the entrained solids rather than

to the entraining gases. The biomass feedstock, whose particle size is typically less than 5 mm, enters the reactor tangentially and is centrifuged to the hot wall. Heat is transferred by ablative "solid convective) heat transfer to the biomass, and causes vapourization of the primary pyrolysis tars which are then carried quickly from the reactor in a high-velocity steam carrier or inert gas. After preliminary shakedown, an insulated recycle loop and cyclone were added to re-inject unpyrolyzed biomass and large char particles. A helical coil was also installed inside the reactor to extend the solid residence time by reducing the natural pitch of the spiral path of the particles.

The dilute vapours exiting from the reactor can be cooled and recovered as products, cracked in a thermal vapour cracker tube for 70 to 150 ms (where the temperature is raised to between 700 and 1000°C), or transferred to a close-coupled catalytic upgrader. Testing has been carried out in the SERI/NREL reactor system at wood feed rates between 3 and 23 kg/h, residence times between 400 and 1100 ms, temperatures of 500 to 750°C, and steam-to-biomass ratios of 1:5. Total liquid yields from wood of greater about 70% are reported for experiments where immediate cooling of the vapours is accomplished. When coupled to the vapour cracker, ethylene and total hydrocarbon non-condensible gas yields of 6.1 and 16.8% by mass of the feed, respectively, are reported. In general, particle size studies show very similar results over the range

0.18 to 5 mm with slight reductions in ethylene and total hydrocarbon yields with increasing size.

Work sponsored by Crown Zellerbach [74] has shown that ethylene is favoured at vapour phase temperatures of 700-900°C, while acetylene is favoured in the range of 1200-1500°C. Mixtures of various proportions occur between 900 and 1200°C. While the majority of experiments were conducted in an induction furnace at temperatures above 1000°C, some were carried out in plasma arc and electrical resistance ovens. Residence times varied between 0.1 ms and 2 s. Ethylene yields approaching 15% of the dry wood feedstock were achieved in the batch-mode bench-scale apparatus. Calculations predicted a 40% theoretical yield, and a 25% yield was assumed to be reasonable for a continuous commercial scale process.

Systematic studies of the effects of temperature (300 to 1100°C), solids residence time (0 to 30 s) and heating rate (less than 100 to 15,000°C/s) on the yields, composition and rates of formation of products from the rapid pyrolysis of small samples of wood, cellulose and lignin were performed at the Massachusetts Institute of Technology [30,86,90,130,131,137]. Biomass samples weighing approximately 100 mg were enclosed in a folded strip of 325 mesh stainless-steel screen wired into an electrical circuit. Temperature and residence time were found to be the most important reaction conditions in fast pyrolysis, while the heating rates were thought to be explicable in terms of their influence on these two parameters. The overall mass

loss (i.e., degree of volatilization) achieved from wood, cellulose and lignin was 93, 97 and 86%, respectively. Char yields decreased with increasing temperatures to a minimum of 3% by mass at 800°C and at shortest solid residence times. Maximum yields of ethylene occurred between 800 and 1000°C. Accurate estimates of vapour/gas residence times were not reported.

Fast pyrolysis of sawdust samples (100-300 mg; 25-400 μm) and wood chips (30 mm x 18 mm x 2.5 mm) was conducted at the University of Nancy (France) in a free falling system consisting of a vertical quartz tube in an electrical furnace with a temperature range of 500-1000°C [41,43,105,162]. The heating rate and the vapour residence time were not varied but were estimated to be 1000°C/s and less than 1 s, respectively. The char yield was consistently high and decreased with increasing temperature to a minimum of approximately 25% (by mass) at 800°C. It is assumed that secondary reactions and low-temperature carbonization was allowed to occur due to the insulating effect of the pyrolysing chip surface or outer particles (i.e., those farthest from the reactor axis). Ethylene yields were significant between 700 and 900°C with a maximum at 750°C.

A down-flow quartz tube reactor housed in an electrical resistance oven was also used for fast pyrolysis studies at the Swedish Royal Institute of Technology [65,155]. The heating rate for the particulate wood sample (400-500 μm) trials was fixed, and was estimated to be 1000°C/s. Solids residence time

was varied from 0.4 to 1.2 s. Char yields decreased with increasing temperatures levelling off to a minimum of approximately 10% at temperatures exceeding 650°C. Ethylene yields were significant between 700 and 950°C, with a maximum production at 800°C. Secondary thermal cracking of the primary fast pyrolysis volatiles significantly enhanced the yields of ethylene and methane, favouring ethylene at cracking temperatures exceeding 700°C.

Two studies at the Ames Research Centre, NASA [112] and the Colorado School of Mines [217] were designed primarily to study the effect of heating rate on fast pyrolysis. The Ames program employed an electrical resistance furnace, carbon arc, xenon flashtube and laser heat sources to achieve increasing heat rates for cellulose fast pyrolysis. Laser pyrolysis with an exposure time of 0.4 ms and surface temperature exceeding 600°C resulted in 100% conversion to gases (i.e., no tar, nor char produced). The Colorado researchers used a PYROPROBE unit to study the pyrolysis of wood particles (5 mg; less than 125 μm) at 1000°C and filament heating rates between 250 and 40,000°C/s. The highest heating rates gave the highest ethylene mass yields of approximately 15% of the wood feedstock.

Other fundamental fast pyrolysis studies of biomass have employed concentrated solar energy [3,4,5,7,8,9,45,105,106], microwaves [77,78,102] Curie-point techniques [167,168], vacuum pyrolysis equipment [6,11,28,34,35,66,155,164,165,179,183,185, 186,187,189,221] an assortment of entrained bed reactors [25,26,

31,49,50,57,66,98,99,174,176], ablative systems [152] and other apparati [29,30,31,57,66,107,112,199,207] to study the rates, mechanisms and chemistry of primary pyrolysis.

A significant amount of fast pyrolysis fundamental research has been carried out by investigators at Ensyn Technologies Inc. [83,84] This work includes optimization of liquid fuels (fuel oil substitutes), specialty chemicals, chemicals, petrochemicals and transportation fuels in recirculating transported-bed reactor systems. The work grew out of this thesis work which was initiated at the University of Western Ontario, and is detailed in subsequent Sections.

2.10.2 Process Development

The work reviewed in this section consists of those initiatives designed to engineer a process concept and hardware which may eventually be modified or directly scaled up to form the basis of a commercial fast pyrolysis process. It is not primarily concerned with the exploration of the fundamental chemistry and mechanisms of fast pyrolysis, but utilizes available empirical data and conventional or innovative engineering skills. The primary task for the development of each process is the rapid transfer of heat in a practical scalable reactor system. while at the same time preserving the requisite short residence times. Three basic techniques for heat transfer are evident in the emerging fast pyrolysis processes; ablative "solid convective " transfer from a hot inert surface to the biomass surface by intimate contact,

transfer from a hot gas to very fine (small particulate) feedstocks in a transport reactor, transfer from hot particulate solids to particulate biomass in a fluidized bed or transport reactors (which can involve ablative heat transfer). A fourth technique is vacuum pyrolysis, which does not strictly qualify as fast pyrolysis in terms of particle heating rate, but accomplishes a similar effect by drawing reaction products from the reactor system before they can react further to secondary products. Egemin NV, Ensyn Technologies Inc., Georgia Tech, Interchem Industries/NREL, Pyrovac/Laval and Waterloo U./ Encon/Union Electra Fenosa are the predominant groups which are currently involved in fast pyrolysis process development. Occidental is a company which was involved more than 10 years ago with "flash" pyrolysis demonstration, but was unsuccessful because the technology was ahead of the research and development.

Egemin NV [115]

Egemin NV is a private engineering company in Belgium which initiated fast pyrolysis process development in 1986 to deal with residue disposal problems in Belgian wood industries. The conceptual process (Figure 10) is an entrained downflow (transport) reactor system using hot combustion gases, generated from a fossil fuel source or pyrolysis products, to carry and transfer heat to fine particulate biomass (less than 1 mm). A 200 kg/h demonstration plant is currently being commissioned using fine wood sawdust from a local wood industry as the

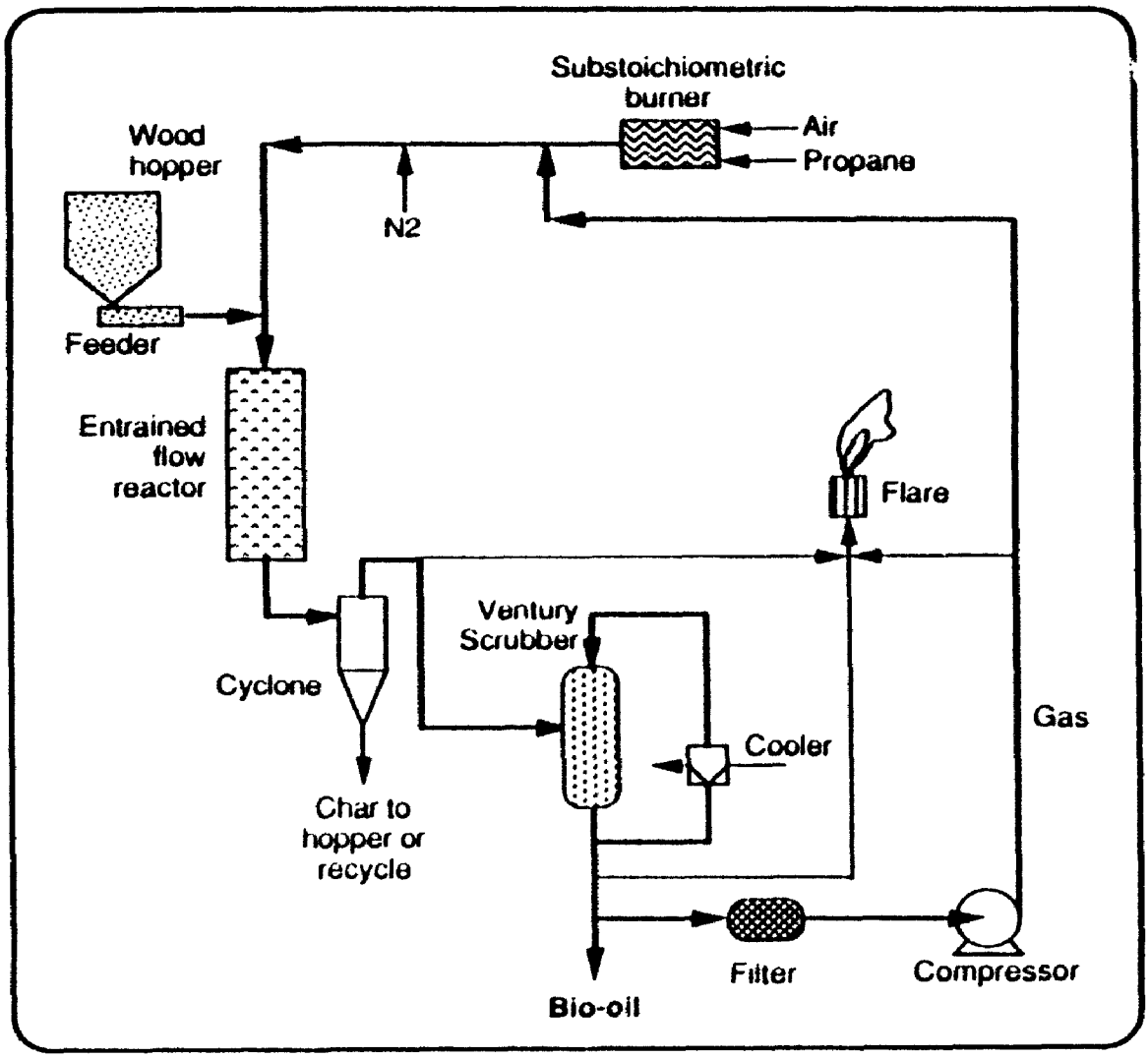

Figure 10. The Egemin Fast Pyrolysis Process [115]

feedstock. The desired product is bio-oil, for use in thermal applications. The process design is based on an oil yield of 60%. Egemin has no previous fast pyrolysis process development experience, but has formulated the design specifications based on a thorough review of the literature and the experience of prior fast pyrolysis systems.

Ensyn Technologies Inc. [29,30,31,83,84]

Ensyn Technologies Inc. is a private Canadian company with almost 10 years experience in fast pyrolysis process development. The technology, Rapid Thermal Processing (RTP) is derived from general principles upon which the University of Western Ontario Ultrapyrolysis process was based. Specifically, the use of hot particulate solids to transfer and carry heat to biomass in a transport reactor is the fundamental principle for RTP. Typically, biomass feedstocks must be less than 6 mm for successful conversion via RTP. The current reactor systems (Figure 11) are recirculating, transported beds which allow rapid heat transfer to be accomplished with precise control of the vapour residence time. Eight RTP systems have been built ranging from 5 kg/h to 25 tonne/day. These include research, development, demonstration and commercial installations. Product applications include specialty chemicals and bio-fuel oil on the short-term, and power fuels (turbines, engines), chemicals, petrochemicals and transportation fuels in the future. Liquid yields approaching 75% of the wood feedstock have been realized in commercial practice.

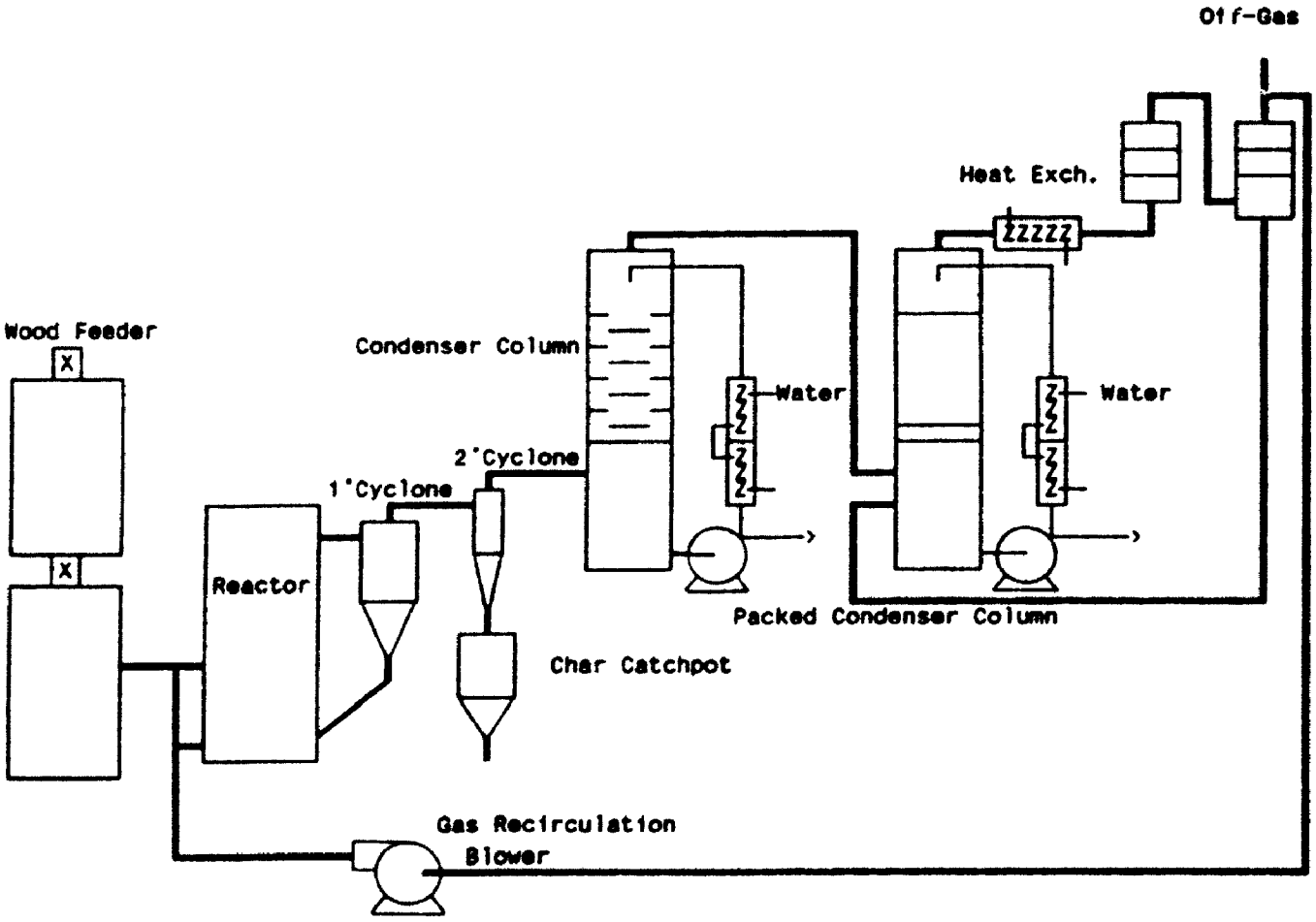

Figure 11. The Ensyn RTP Fast Pyrolysis Process [83]

Georgia Tech [29,30]

Development of the Georgia Tech process was initiated in 1980 with the support of the U.S. department of Energy. The principal objectives were to optimize oil yields from wood using an entrained flow pyrolyser [31], and to develop a scalable reactor system for eventual commercial applications. The reactor system has evolved through many stages to its present form which is an entrained upflow design (Figure 12). Wood is dried to less than 10% and milled to less than 1.5 mm, and then fed into the lower section of the reactor. Heat is carried to the reactor and transferred to the biomass by turbulent hot gases, produced from the combustion of propane. To date, the process has been demonstrated at a scale of about 60 kg/h. Total liquid yields are between 55 and 60% of the dried wood feedstock.

Interchem Industries/NREL [56,57,92]

Interchem Industries Inc. is a member of the Pyrolysis Materials Research Consortium which has a broad mandate to commercialize NREL's (formerly SERI's) pyrolysis technologies. Interchem's specific role is to scale-up the NREL ablative fast pyrolysis process (described in Section 10.1). Interchem is in the process of commissioning a 30 tonne/day demonstration unit in Southern Missouri (Figure 13) where the disposal of waste wood via Tee Pee burners is a serious environmental problem. Heat is supplied by combustion of pyrolysis byproducts in an envelope which surrounds the ablative reactor system. Heat is

then transferred through the reactor wall directly to biomass particles which are forced to the wall by cyclonic activity. Pyrolysis oil, whose yield is expected to be in the range of 55 to 60%, and cha--oal are the principal products for the short-term. Value-added phenolic resin technology, as developed by the consortium, will be transferred to Interchem for future commercialization.

Occidental Petroleum [55,57]

In the late 1970's, an unsuccessful attempt was made to scale up Occidental's municipal solid waste (MSW) flash pyrolysis process to a capacity of 100 tonne/day in El Cajon, California. Early studies in transport reactors using fine particles were successful in terms demonstrating that high yields of bio-oil could be generated from the biomass fraction of MSW. However, the fundamentals of fast pyrolysis (specifically, the significance of the interrelated effects of heat transfer and residence time) were inadequately understood resulting in a lack of performance at a larger scale. The process employed hot char particles entrained in hot combustion gases (from a fluidized bed thermal regenerator unit) to transfer and carry heat to the feed material in an entrained-bed upflow reactor. The *amount* of heat and apparent resi lence times were adequate for fast pyrolysis, but heat transfer was inadequate. The result was the production of secondary products which the downstream equipment and thermal regenerator could not handle.

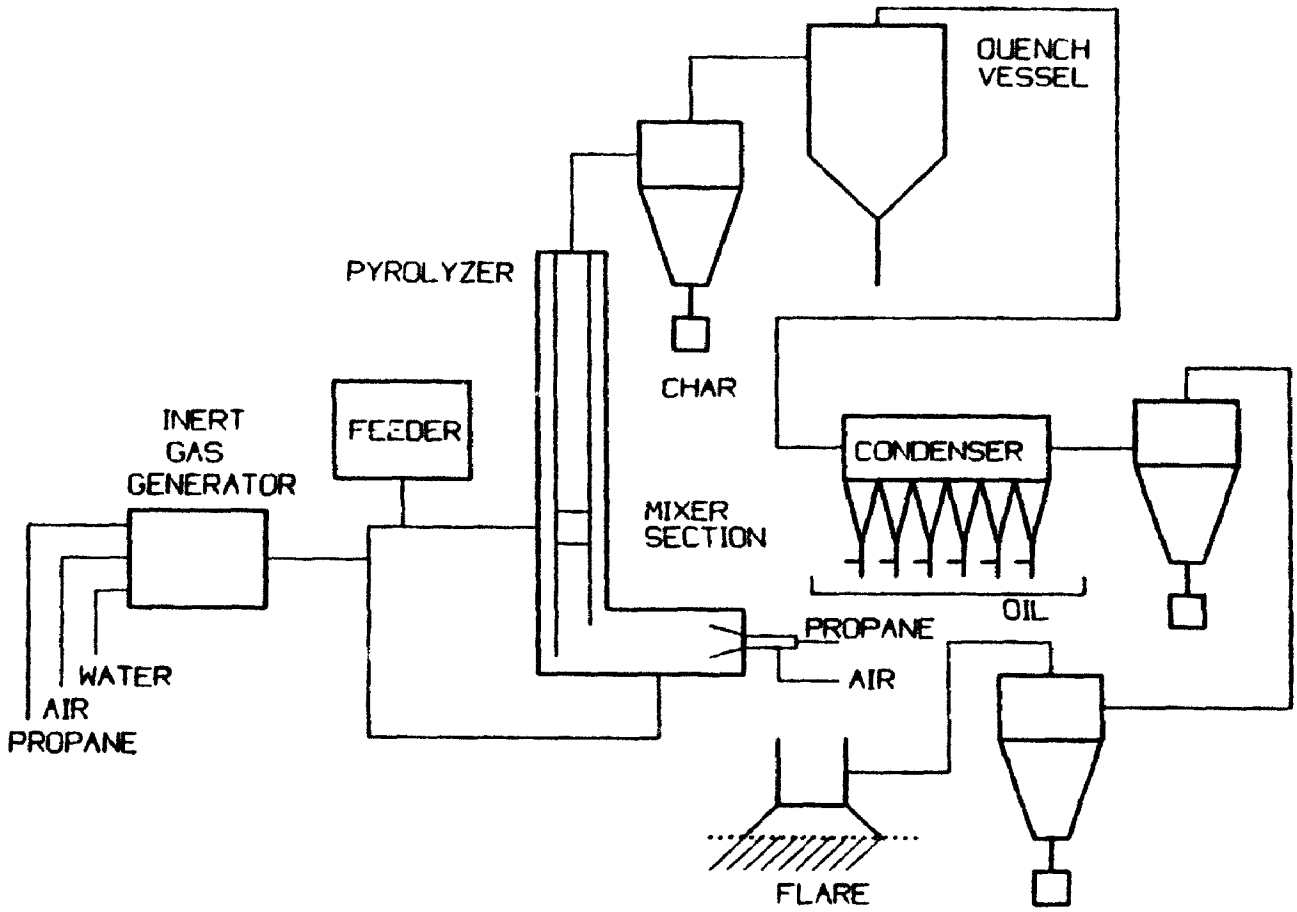

Figure 12. The Georgia Tech Fast Pyrolysis Process [57]

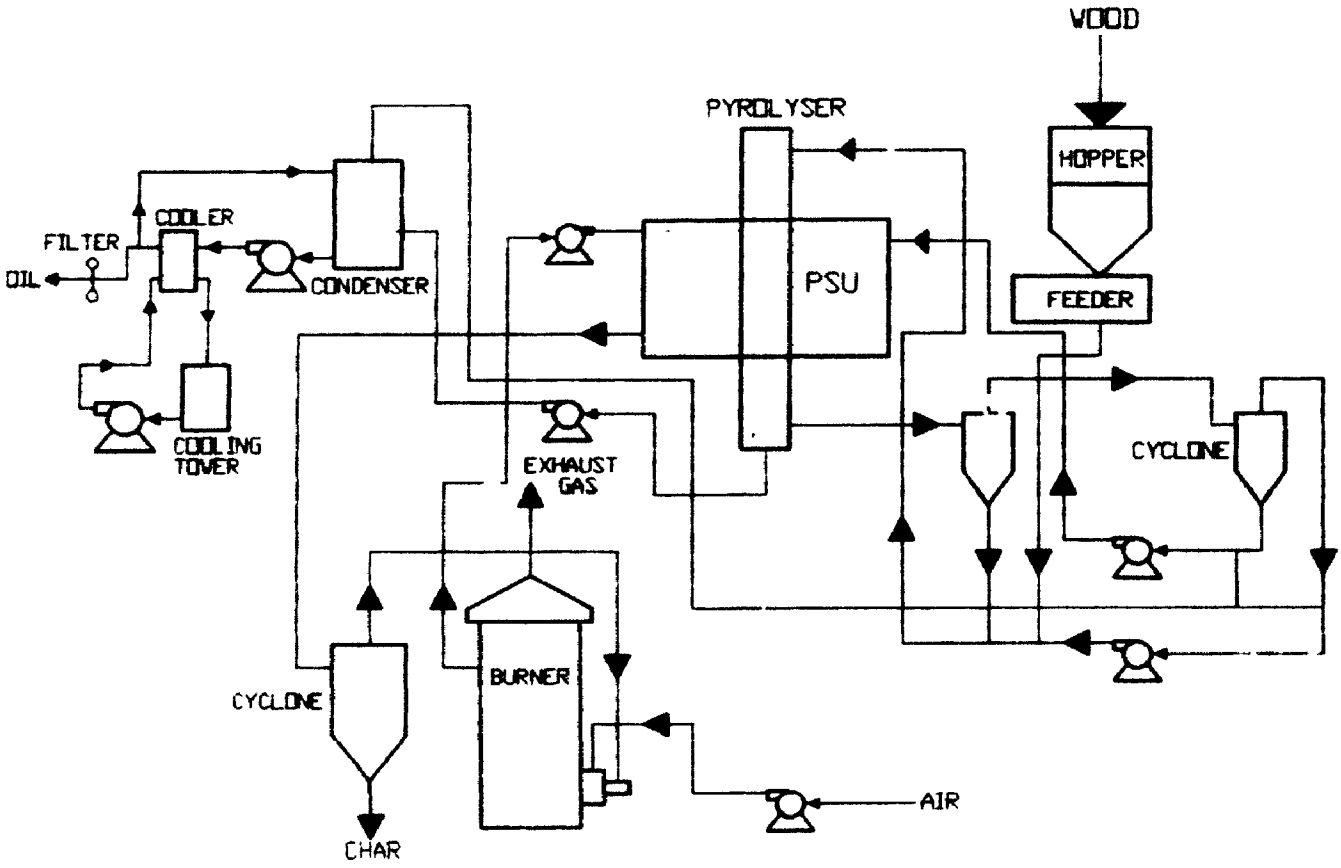

Figure 13. The Interchem/NREL Fast Pyrolysis Process [92]

Pyrovac/Laval University [29,30,31,164,165]

Vacuum pyrolysis is a particularly unique technology which has been under development at the Universities of Laval and Sherbrooke since the early 1980's. It is not strictly fast pyrolysis in terms of heat transfer requirements, but the relatively low heating rate of the solid biomass is not restrictive since primary products are drawn quickly from the reacting surface and out of the reactor as soon as they are formed. Secondary reactions are thereby precluded. Bench-scale batch units at Sherbrooke and Laval Universities resulted in a 40 kg/h process development unit being tested at Laval. Total liquid yields from wood were about 68%. A 200 kg/h continuous demonstration project was initiated but stopped in progress because of the licensee's financial difficulties. In general, vacuum processes tend to be expensive to operate on a commercial scale. For this reason, Pyrovac has chosen to move away from low value resources and products (biomass and fuel oil, respectively) to exploit environmental "niche" markets where high tipping fee wastes can be uniquely converted in a vacuum process to value-added chemicals.

Waterloo University/Encon/Union Electra Fenosa [29,30 70,173]

For more than 10 years, a shallow fluidized bed reactor system has been under development at Waterloo University for biomass fast pyrolysis. The initial bench-scale continuous unit was capable of processing 50 g/h, and was based on a coal flash pyrolysis technology developed at CSIRO in Australia. A larger

process development unit rated at 3 kg/h was subsequently built and tested. Under license, the process has been scaled up to 100 kg/h by Encon Enterprises for peat pyrolysis applications. Problems associated with liquid recovery and sand entrainment have restricted operation of this plant. A spanish electrical utility, Union Electra Fenosa, has initiated a demonstration project at a nominal scale of 200 kg/h, based on the Waterloo technology. This plant is currently being commissioned.

Misc. Systems

A cyclonic type fast pyrolysis reactor is being researched in Nancy, France, by the combined efforts of the University of Nancy and the Chemical Engineering Science Laboratory [106,107, 132,214,215]. Researchers are presently concentrating on the flow patterns, particle residence times, heat transfer between the heated walls and carrier gas/solid particles, and the nature of products obtained in an electrically-heated cyclone. The first continuous system will be designed to use solar energy as the heat source for pyrolysis. Preliminary work has been completed using solar energy for the fast pyrolysis of biomass feedstocks at a 1-MW solar furnace in Odeillo, France [4,9,5].

Other biomass fast pyrolysis process designs have incorporated single fluidized beds [57,212], twin fluidized beds [31,40,57,88, 91], entrained beds [30,31,57,91,98,99,115,201], single vessel circulating beds [104], molten baths [30,31,192] and atomized suspension techniques [142,143,144] for the rapid pyrolysis of various biomass materials.

2.11 FAST PYROLYSIS CHARACTERIZATION SUMMARY

The actual experimental work, which is the subject of this thesis, will be dealt with in the following chapters. Before proceeding, there are a number of general statements which can now be made to summarize what is currently known about biomass fast pyrolysis.

1. Fast pyrolysis is fundamentally different from conventional "slow" pyrolysis.

2. Fast pyrolysis processes require rapid heating rates exceeding 1000°C/s, temperatures greater than 450°C, and rapid product cooling.

3. When undergoing pyrolysis, three primary reactions pathways are available to the reacting biomass. Fragmentation is the term given to the pathway which characterizes fast pyrolysis.

4. Vapour-phase cracking reactions are representative of secondary fast pyrolysis reactions.

5. During primary pyrolysis, the rate of fragmentation appears to predominate over the other primary pathways, dehydration and depolymerization, as temperatures exceed 450°C.

6. Secondary fast pyrolysis reaction kinetics are rate-limiting.

7. Fast pyrolysis of whole wood appears to be approximately (not exactly) the sum of the pyrolysis of its major components.

8. Heat transfer must be adequate in fast pyrolysis to provide a heating rate such that the time that the biomass spends at lower temperatures is insufficient to allow the slow pyrolysis reactions to occur to any appreciable extent.

9. For very small biomass particles (ie., less than 500 μm), the method of heat transfer is of minor significance, and fast pyrolysis will occur as long as a sufficient quantity of heat is supplied at a temperature in the fast pyrolysis regime.

10. As the particle size is increased, the method of heat transfer becomes increasingly important. Some type of ablative mechanism is required to realize fast pyrolysis of particles approaching 5 or 6 mm.

11. A broad spectrum of techniques is available and adequate for bench-scale fast pyrolysis studies. In such studies, small particle sizes and intimate contact between the biomass and heat transfer medium ensure the heat transfer is not limiting.

12. For commercial-scale fast pyrolysis, adequate heat transfer becomes the central problem. Ablative systems, fluidized sand beds, and gas or particulate transport systems are emerging as the leading candidate reactors for industrial fast pyrolysis.

3.0 OVERVIEW OF THE EXPERIMENTAL STRATEGY

3.1 CONTEXT OF THE THESIS RESEARCH

The science of biomass fast pyrolysis has progressed considerably since its inception more than 30 years ago. Particular advances have been made with respect to an understanding of the requisite process conditions, the nature and yields of generic products, a general characterization of primary and secondary pathways, and heat transfer requirements. In addition to reviewing what is now known about biomass fast pyrolysis, the literature review in Chapter 2 has clearly highlighted those areas which require further attention. These areas, therefore, represent opportunities where unique contributions can be made to the science of fast pyrolysis, and the general tasks remaining are summarized as follows:

1. A continued characterization of primary pyrolysis products (analytical).

2. A further characterization of the mechanisms of primary fast pyrolysis (fragmentation), including the nature of the breakup of the polymeric and monomeric structures of the principal biomass components, and the origin of the primary products within these structures.

3. A clear distinction between the two higher-temperature primary fast pyrolysis pathways, fragmentation and depolymerization, particularly with respect to the chemical mechanisms and primary product distribution.

4. A clear determination of the rate equations (kinetics) for fragmentation and depolymerization. Currently, no distinction is made between the two in the kinetics literature.

5. A characterization of the mechanisms of secondary, vapour-phase, cracking reactions (Note: this is an extremely difficult task because of the number and complexity of primary products, and will not be accomplished until Tasks 1 to 3 are accomplished).

6. A determination of the composition of the non-equilibrium, non-condensible gas product and the component gas yields for the secondary cracking reactions of biomass fast pyrolysis.

7. A determination of empirical rate equations for the production of the total gas and principal gaseous components produced by the secondary vapour-phase cracking reactions.

Antal [2] summarizes the status of biomass fast pyrolysis research in a report to the Congress of the United States where he notes that the state of the art is "roughly comparable to that achieved one half century ago by the hydrocarbon processing industry in the steam cracking of alkanes to olefins".

3.2 GENERAL OBJECTIVES

This thesis work is concerned primarily with the latter two tasks identified in Section 3.1:

1. A determination of the gas composition and component yields for the secondary cracking reactions of biomass fast pyrolysis.

2. A determination of the kinetics of the production of gaseous components produced from the secondary cracking reactions of biomass fast pyrolysis.

Limited progress has historically been made in these areas because of the inability to precisely control both temperature and residence time in an experimental system which achieves the requisite heat transfer rates. Any progress in kinetic

modelling, including that achieved during the course of this thesis, will have to be restricted to that which is empirical, since the primary products from which the secondary gas-phase products are formed, are not yet fully identified. Furthermore, although the primary vapours from which the permanent secondary gases are derived are numerous, complex and not fully characterized, the theoretical number and identity of the individual secondary gases can be predicted in advance. Essentially, they are carbon oxides, hydrogen and hydrocarbons (alkanes, alkenes and alkynes) which are C_5's or less. The obvious place to initiate empirical kinetic modelling studies of secondary fast pyrolysis is therefore at the point which deals with the *formation* of permanent non-equilibrium gases (ie., not with the *disappearance* of primary vapours). It is on this point that the thesis experimental work is focused.

3.3 SPECIFIC OBJECTIVES

The specific objectives of the thesis work are summarized as follows:

1. Develop a fast pyrolysis research system which allows precise control of temperature and residence time while achieving rapid heat transfer rates to the biomass feedstock.

2. Conduct cracking studies of a model compound with known kinetics to confirm the integrity of the temperature and residence time measurements associated with the fast pyrolysis research system.

3. Compare the performance of an inert gaseous heat carrier with that of a an inert particulate (ie., sand) heat carrier to determine whether these can be used interchangeably in a small apparatus where biomass with an extremely small particle size is used.

4. Conduct studies of the fast pyrolysis of cellulose, the principal biomass component, which includes a characterization of the secondary cracking reaction product distribution (as a function of temperature and residence time) and the empirically-modelled reaction kinetics.

5. Should time permit, conduct optional studies of the fast pyrolysis of wood, the predominant bioenergy resource, which includes a characterization of the secondary cracking reaction product distribution (as a function of temperature and residence time) and the empirically-modelled reaction kinetics.

6. Conduct preliminary studies to empirically determine the maximum biomass particle size which can undergo fast pyrolysis without loss of performance, and then compare with theoretical studies.

7. Conduct a water-gas shift reaction study in the fast pyrolysis reactor system to determine its role in secondary pyrolysis, and compare with published data.

8. Conduct a cooperative study with an independent biomass fast pyrolysis research group to corroborate experimental results.

4.0 EQUIPMENT

The thesis experimental work was carried out in three reactor systems; the Ultrapyrolysis system at the University of Western Ontario, the Rapid Thermal Processing (RTP) system at Ensyn Technologies Inc., and the Shallow Fluidized Bed System at Waterloo University. The bulk of the research (essentially all of the cellulose work) was conducted in the Ultrapyrolysis reactor system. Some follow-on research, to supplement the wood pyrolysis data, was carried out in the scaled-up RTP equipment. A cooperative study on cellulose fast pyrolysis was conducted with researchers at Waterloo University, using a shallow fluidized bed reactor. The Ultrapyrolysis and RTP systems are described below, while the Waterloo apparatus is described within the context of the cooperative study, in Section 8.8.

4.1 ULTRAPYROLYSIS EQUIPMENT

The evolution of the design and development of the Ultrapyrolysis system is detailed in a previous publication (Appendix 1: Bergougnou,1983). Rapid, thorough and intimate mixing of the biomass feedstock (on the order of tens of milliseconds), and precise control over residence time were the two principal objectives associated with the design tasks. Published cold-model studies (Appendix 1: Meunier,1984; Berg, 1987) both in plexiglass models and in the final Ultrapyrolysis system indicated that these objectives were fully realized.

The major components of the Ultrapyrolysis (UP) system are illustrated in Figure 14. Rapid mixing and heat transfer are carried out in two conical vessels known as vortical contactors or "vortactors". The first, which is the heart of the Ultrapyrolysis system, has been termed a thermovortactor and allows heat to be transferred to the biomass from a heat carrying "thermofor" stream. The thermofor is gaseous nitrogen, suspended particulate solids, or a combination of the two. The second vortical unit is a cryovortactor and allows fast quenching of the products by the direct transfer of heat to a cold "cryofor" stream (i.e., cryogenic nitrogen). The thermovortactor, illustrated in Figure 15, has two opposing tangential inlets for the thermofor. One tangential stream effectively destroys the momentum of the other causing severe turbulence. Biomass feedstocks are then injected from the top of the thermovortactor through an air-cooled tube into the turbulent region where mixing occurs within 30 milliseconds. The hot gaseous product is rapidly cooled (i.e., in less than 30 ms) by the injection of a single tangential stream of a cryogenic nitrogen. The cryovortactor operates in a similar fashion.

Two mechanical table feeders are used to supply particulate solid biomass and thermofor solids to the reactor system. Solids pass from sealed hoppers, which have a sufficient inventory of solids for several experiments, through a double funnel system and are thereby metered onto a rotating table.

Two fixed armatures sit near the surface of the round table, and plough the solids off the outer circumference. From the table, the solids then fall into a conical chamber where they are picked up and carried into a transport line by nitrogen carrier gas. The overall range of the feed rate of the solids is controlled by setting the gap between the lower funnel and the table. Fine control is exercised by the rotation speed of the table.

Typically, the biomass feeder is set in the range of 0 to 20 grams per minute and the thermofor feeder is set to deliver 0 to 200 grams per minute. The biomass feeder is mounted on a 60 kg balance to facilitate mass balance procedures. When thermofor solids are required to supply the process heat (i.e., either in place of gaseous nitrogen thermofor or as a supplement), the thermofor feeder sends cold (ie., room temperature) particulate solids to a double preheater coil assembly, housed in electrical resistance ovens, where they are heated to the appropriate temperature. These solids are then sent on to the thermovortactor. Thermofor nitrogen can be sent directly to the preheater coil where it is heated, without any solids, to the set-point temperature.

The fast pyrolysis of biomass is initiated in the thermovortactor and continues in a plug-flow entrained bed downflow reactor. The reactor is simply a one-meter length of Inconel pipe in an electrical oven. The mixture of hot gases and biomass passes from the thermovortactor through the reactor

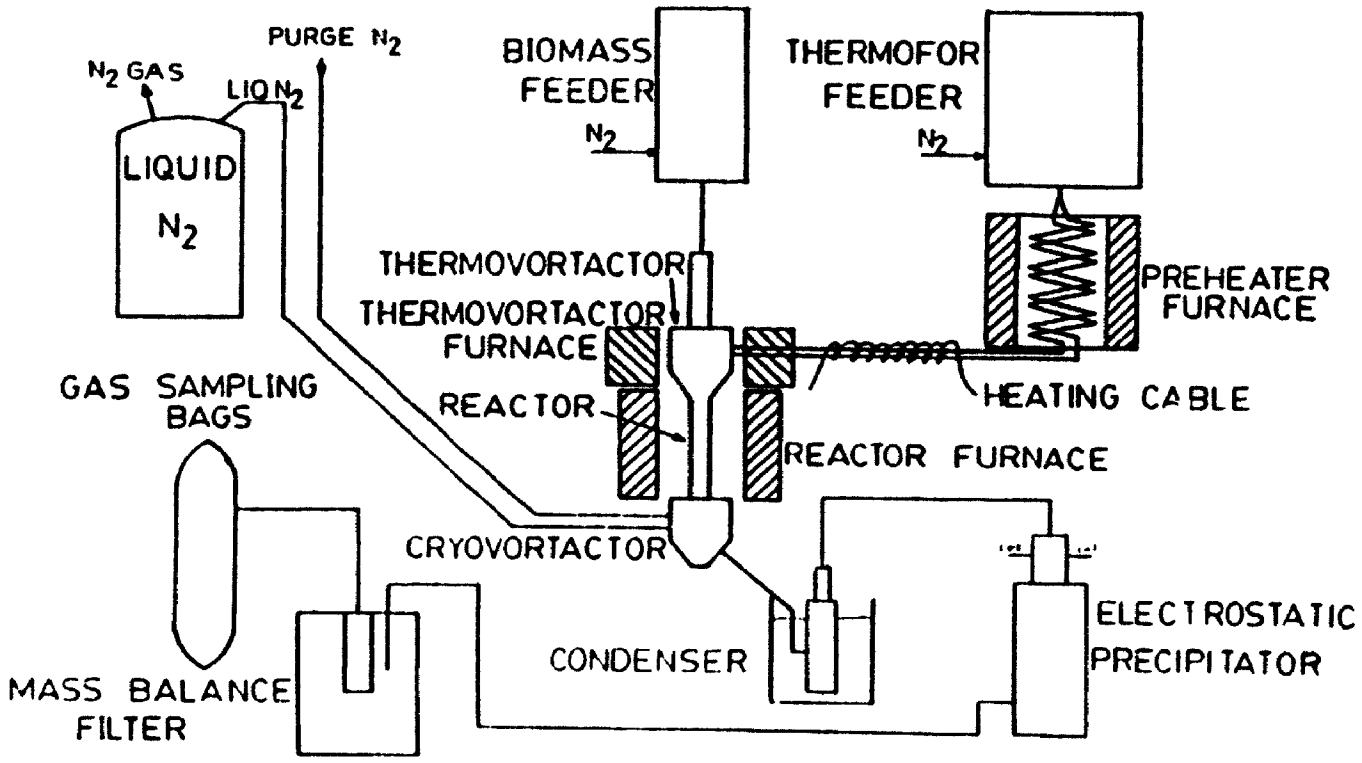

Figure 14. The Ultrapyrolysis Reactor System

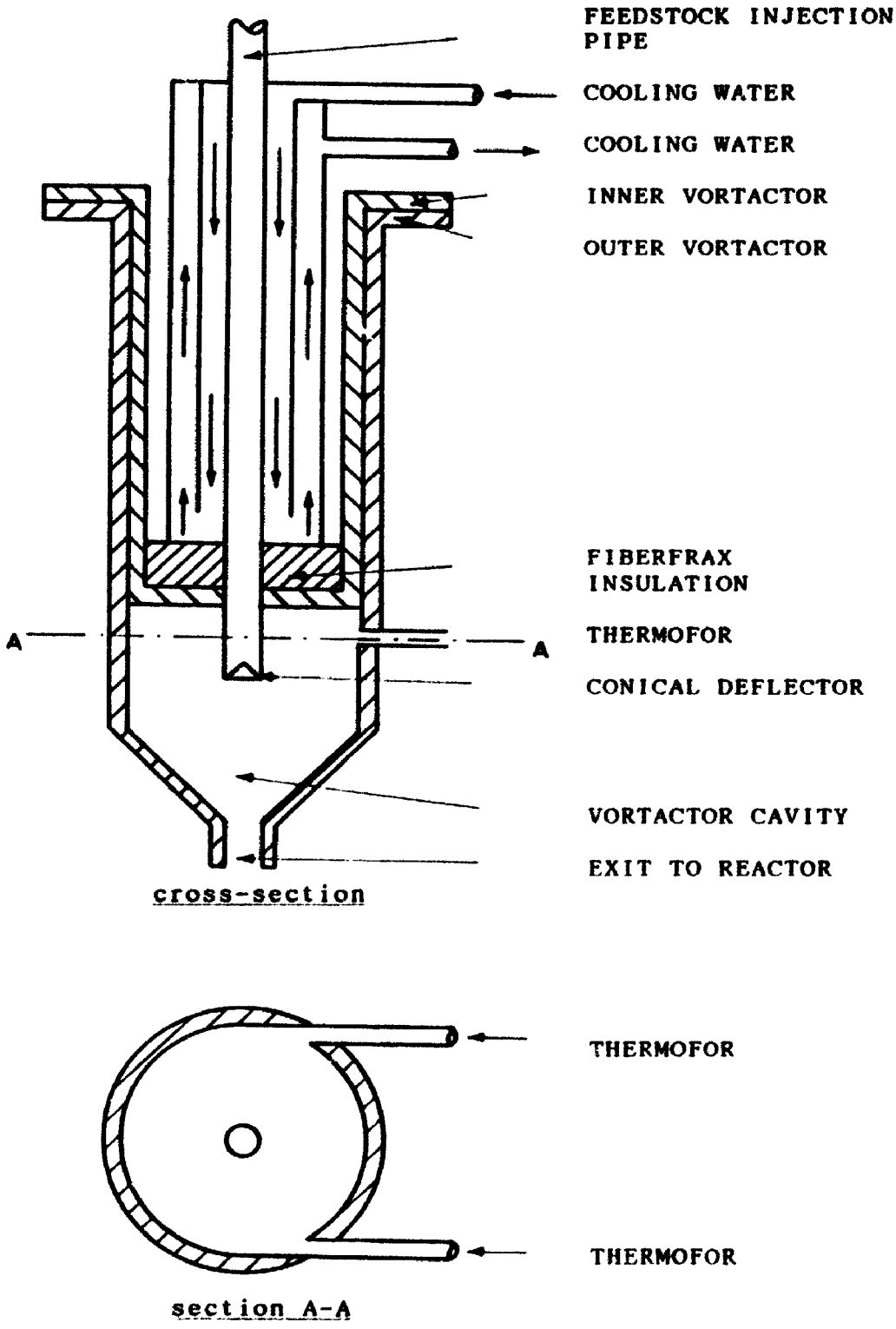

Figure 15. The Ultrapyrolysis "Thermovortactor" Reactor

to the cryovortactor. With the insertion of cylindrical inserts to reduce the reactor volume, and by manipulating thermofor and biomass flowrates, the residence time (i.e., the time from the heating of the biomass to the exit from the reactor) can be set between 30 and 900 ms. Reactor temperatures can be set in the range of 650 to 1000°C.

After exiting from the cryovortactor, the product stream passes through the product recovery train which consists of a water-cooled cyclonic condenser situated in an ice water bath, an optional electrostatic precipitator, a porous metal filter cartridge and a bank of four gas collection/sampling bags. The detailed designs of the cyclonic condenser, and electrostatic precipitator are given in previous publications (Appendix 1: Bergougnou,1986).

4.2 RAPID THERMAL PROCESSING (RTP) EQUIPMENT

The RTP-1 pilot plant, including its principal components, is illustrated in Figure 16. The plant is rated nominally at 5 to 10 kilograms per hour. Hot solids (i.e., sand or catalyst) flow from a number of "heat carrier" feeders to the reactor system where they are injected into the rapid thermal mixer. The carbonaceous feed material (solid, liquid, or gas) is delivered from one of several interchangeable feeders (i.e., the "biomass feeder" in the illustrated configuration) to the top of the reactor where it is injected into the cloud of turbulent hot solids. Extremely rapid heating of the feed material is

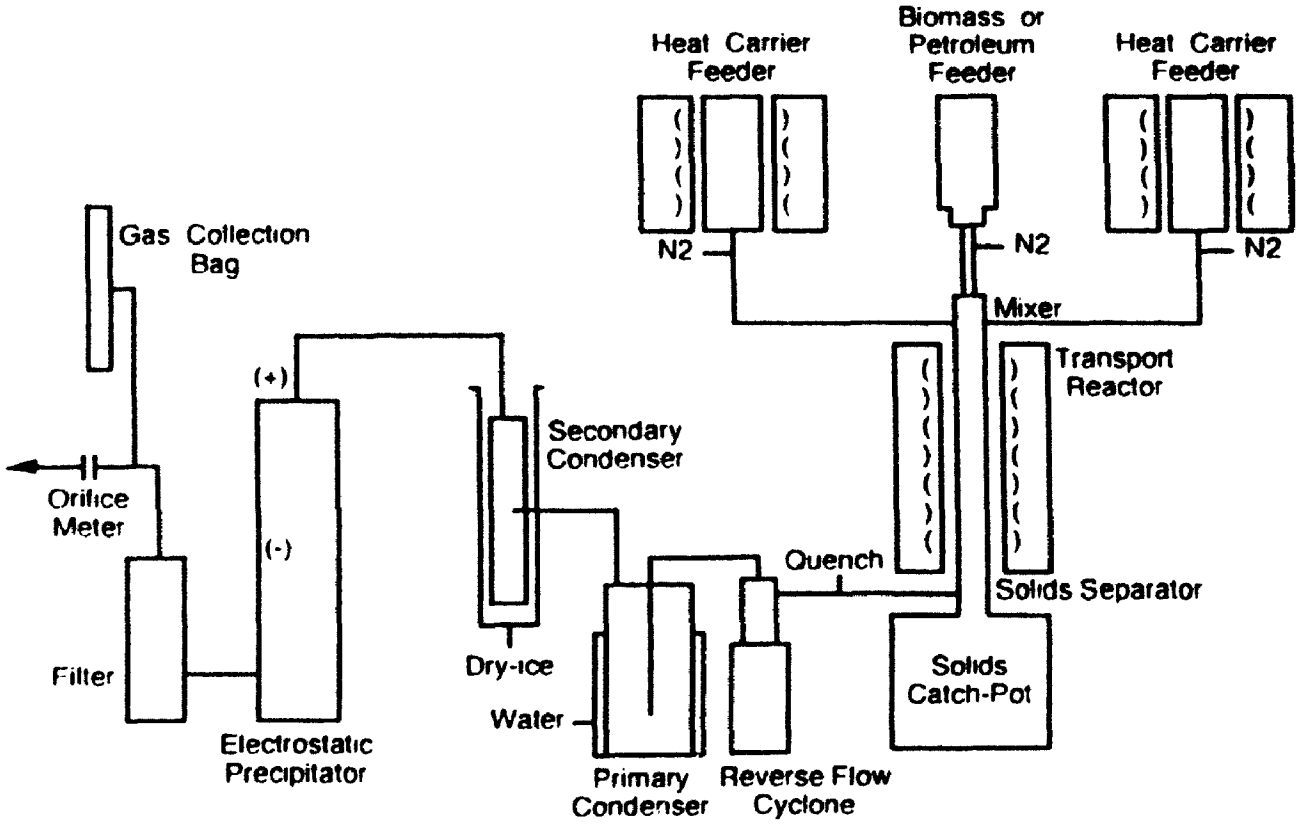

Figure 16. The RTP-1 Reactor System

achieved as the feed and hot sand particles are quickly and thoroughly mixed. After the fast, intimate mixing is complete, the feed and solid heat carrier pass through a tubular transport reactor, the length of which is adjusted to control the residence time.

The products are rapidly cooled with cryogenic nitrogen in a transfer line after the hot solids are removed in a solids "catch pot" or drop-out vessel. Additional cooling is carried out in the primary and secondary condensers, where condensation of vapours and recovery of liquids also occur. Parallel filters are used to collect persistent aerosols, and the clean gas is then directed through an orifice meter to quantify the flow for mass balance procedures. A fractional quantity of the product gas is continuously bled from the main stream to a gas sample bag for subsequent analyses. When the aerosol loading is particularly high, an electrostatic precipitator is installed between the condensers and the filters.

There are three identical heat carrier feeders which heat the sand heat carrier and deliver it to the transport lines. Each feeder is about 1.2 meters long and 150 mm outside diameter, and can hold 30 kg of silica sand. The maximum feed rate is approximately 60 kg per hour for each feeder, and the maximum temperature is 1100 °C. Feeder control is accomplished via a sparger tube and a non-mechanical, high temperature "J" valve.

A mechanical table feeder, with an inventory of about 4 kg, is used to supply the biomass to the reactor system. In a manner similar to that employed in the Ultrapyrolysis equipment, particulate biomass passes from a sealed hopper through a double funnel system and is thereby metered onto a rotating table. Two fixed armatures sit near the surface of the round table and plough the solids off the outer circumference. From the table, the solids then fall into a conical chamber where they are picked up and carried into a transport line by nitrogen carrier gas. The overall range of the feed rate of the solids is controlled by setting the gap between the lower funnel and the table. Fine control is exercised by the rotation speed of the table. Feed rates can be varied from 0 to about 10 kg per hour, and are independent of the transport gas flow rate and the solid heat carrier flowrate. The feeder is mounted on casters to allow for easy removal.

The reactor system consists of a rapid thermal mixer and two lengths of pipe which together constitute the transport reactor. The temperature of each pipe is controlled independently. Rapid mixing of the feedstocks with the sand heat carrier takes place in the rapid thermal mixer, and chemical reactions are then allowed to proceed in the transport reactor sections. The first reactor pipe is 1.2 m in length while the second is 0.6 m. The transport reactor system components, with inside diameters of 40 mm, are constructed of Inconel 601.

The solids catch pot is an inertial separator constructed of stainless steel and can hold about 100 kg of hot solids. Separation of the gases from the solids is based on the lower momentum of the gas/vapour product (compared to the hot sand) which can change direction more readily than the solids, and escape into the transfer line to be quenched directly with nitrogen gas.

The primary condenser is a water-jacketed carbon steel pipe (having both an inner and outer water-jacket) which is lined with a chemical resistant paint. The cooling water enters the condenser at approximately 19°C and cools the product to about 25°C. The secondary condenser is also a lined, carbon-steel pipe which is not jacketed but sits directly in an insulated acetone/dry ice bath. It has a tangential gas/vapour inlet which forces the products to the condenser wall, where efficient heat transfer can occur. The product gas stream typically exits from the secondary condenser at a temperature in the range of 4 to 8 °C.

To ensure the removal of any entrained condensed liquid or fine solid residue, a final filtration system is included in the product recovery stream. There are three parallel filters which are constructed of stainless steel, and have a pore size of 0.5 microns. They are housed in a single filter vessel.

5.0 EXPERIMENTAL PROCEDURE

5.1 ULTRAPYROLYSIS PROCEDURE

In preparation for an experiment, the Ultrapyrolysis system is purged with nitrogen. The furnaces are then turned on and allowed to reach their setpoint temperatures. When the desired temperatures are reached, cryogenic nitrogen is injected into the cryovortactor. Thermofor (i.e., nitrogen-transported silica sand or inert nitrogen gas) is then introduced into the system and the cryogenic nitrogen flowrate is adjusted to ensure that the cryovortactor temperature is less than 350°C. Gaseous nitrogen was used as the thermofor for all of the experiments reported in this thesis. During the startup period, the stream exiting from the reactor system is vented to atmosphere. The biomass feeder is activated and its feedrate is verified by directing the flow to a collection device mounted on an electronic balance. A cellulose feedrate of 2 to 6 grams per minute is typical for the thesis experiments.

Immediately prior to the actual steady-state experiment, the thermofor/cryofor stream, exiting from the cryovortactor, is directed to the mass balance filter and recovery train. The biomass is then directed to the thermovortactor and the actual fast pyrolysis experiment is thereby initiated. Products which are initially cooled to a temperature in the range of about 300 to 350°C in the cryovortactor, are further cooled to room temperature in a water-cooled cyclonic condenser/heat exchanger.

Solids and condensibles are deposited in the condenser and the filter, and the entire non-condensible product gas is collected in three gas collection bags which are connected in parallel. The multi-layered gas bags, from Calibrated Instruments Inc., have a capacity of 170 litres each. For extremely short residence time trials (when the yield of "condensibles" increases), an electrostatic precipitator unit can easily be integrated in the downstream gas line.

During the steady-state experiment, nineteen temperatures are monitored and recorded. These include ambient air and nitrogen temperatures, the six controller temperatures associated with the four system ovens (coil, thermovortactor, injector and reactor ovens) , and those associated with the coil transport lines, injector transport lines, thermovortactor, reactor cavity, two locations along the reactor wall and cryovortactor. The reactor system thermocouple locations are indicated in Appendix 8.0. Six system pressures are monitored at ports from the feeder systems to the cryovortactor exit, and are recorded on general experiment data sheets. Three rotameters are used to measure the flow to the reactor system, and one rotameter indicates the flow of quench nitrogen gas into the cryovortactor.

The steady-state experiment continues for 5 to 20 minutes. At the end of the experiment, the biomass flow is redirected from the reactor system to the bypass line and its feeder motor is turned off. The inert thermofor and cryofor streams,

however, are maintained for a short period of time in order to ensure that all products are carried to the recovery system. After purging, the recovery train (including filter, transport lines and condenser) is dismantled and washed with acetone to collect any condensibles. When sufficient quantities are produced, pure condensibles are poured from the condenser prior to solvent extraction. Recovery of the acetone-extracted pyrolysis liquids is accomplished using a rotary evaporator. The equipment is reassembled and feeders are charged with fresh sand or biomass in preparation for the next experiment.

At least three gas samples are taken from each of the collection bags and analyzed for hydrogen, carbon monoxide, carbon dioxide and C_1 to C_6 hydrocarbons using a Carle refinery gas chromatograph (Model 111-H/197A). The C_5/C_6 fraction is analyzed as a single constituent. When gas analysis of the bag contents is completed, the gas is drawn into an evacuated Superior 123 USWG Propane tank of known volume. The magnitude of the change in tank pressure and the gas analysis are used to determine the quantity of the product gas.

Data which is recorded during the experiment (i.e., temperatures, pressures, rotameter readings, etc.) is entered, along with the results of the gas analysis, into a personal computer (PC). The computer calculates the reactor residence time and the yields of total gas and gas components, and then prints out a summary of the operating conditions, experimental data and product yields (mass balance).

The residence times are calculated using the reactor system volume (as a function of temperature to account for thermal expansion) and the mean volumetric flow rate. Since the large bulk of the volume is due to inert nitrogen carrier gas (90%), it is reasonable to assume a constant volumetric flow rate. In the residence time model (used in the computer programs), however, linear decomposition kinetics of a characteristic primary tar (Molecular Mass = 100) at the reactor inlet to the final product gas composition (Molecular Mass = 24) at the reactor outlet, were assumed. This crude refinement gives a slightly better estimate of the average molecular weight of the gaseous stream within the reactor (which is used to calculate volumetric flowrate) than the assumption that the stream has an average molecular weight equal to that of its nitrogen carrier gas.

A complete mass balance, where char is recovered and liquid products are solvent-extracted and recovered by rotary evaporation, is not carried out for all of the cellulose and wood pyrolysis trials. This is a practical consideration since these procedures are relatively time-consuming. Complete mass balances are reported for about 30% of the cellulose experiments and about 70% of the wood experiments. A limited number of elemental balances (C,H and O) were carried out on cellulose fast pyrolysis trials after the liquids were analyzed by B.C. Research, Vancouver B.C.

5.2 RTP EXPERIMENTAL PROCEDURE

The furnaces which house the heat carrier (i.e., sand) feeders, mixer and the reactor lengths are activated about 8 hours prior to an experiment. The sand feeder ovens are set at a temperature which is about 150 °C greater than the desired reaction temperature. This temperature differential accounts for transport and reactor systems thermal losses and provides the heat required to raise the feedstock from ambient to reaction temperature.

During the heat-up period, a number of system checks, calibrations and peripheral system activations are carried out:

- the gas chromatograph is calibrated using a gas sample of known composition;
- the system is pressure-tested to detect and correct leaks;
- nitrogen is allowed to continually purge the system of air and residual product gas;
- water is fed to the primary condenser water-jacket;
- the secondary condenser bath is filled with liquid CO_2;
- the gas sampling bag is purged and evacuated;
- the chart recorder for reactor temperatures is activated;
- computer programs are run to assist in setting the carrier gas flows (these allow selection of the desired residence time as a function of temperature and reactor volume).

Just prior to the beginning of the experiment, the following steps are taken:

- the quench gas (which cools the product stream) is delivered to the gas exit line;
- system transport gas (nitrogen) flow is initiated in the "bypass" mode;

- transport gas is delivered to the heat carrier feeders and the feeder vibrators are activated;
- the feeder transport gas is diverted to the heat carrier feeder, and solids flow is verified using a thermocouple;
- fluidization gas in the heat carrier feeder is adjusted until the desired reactor inlet temperature is reached;
- the reactor temperatures are monitored on a chart recorder to ensure that the desired setpoint has been realized.

The actual experiment begins when the biomass feeder is activated and the wood is delivered to the reactor. At this point, the gas sampling bag valve is opened and a constant flow of product gas is bled from the main gas line to the gas bag. Orifice measurements for determining gas flow are taken every 30 seconds. System temperatures, gas flows (via rotameters and an orifice meter) and pressures are monitored continually.

Sand heat carrier flowrates are adjusted as required, to maintain the desired reactor temperatures and to ensure isothermal conditions. After the desired quantity of biomass has been fed, the steady-state experiment is terminated when the biomass feeder is turned off. The data recorders, system furnaces and carrier gas flows are then shut down (the quench gas is the last transport gas flow to be turned off).

At least three gas samples are taken from the sampling bag and analyzed for hydrogen, carbon monoxide, carbon dioxide and C_1 to C_6 in a Carle (Model 111-H/1997A) refinery gas analyzer. The C_5/C_6 fraction is analyzed as a single constituent. After gas analyses, the quantity of sampled gas is determined by evacuation into a vacuum tank of known, fixed volume.

Data which is recorded on standardized data sheets during the experiment (i.e., temperatures, pressures, rotameter readings, etc.) is collated and then entered, along with the results of the gas analysis, into a PC. The computer calculates the reactor residence time and the yields of total gas and gas components. It then prints out a systematic summary of the operating conditions, experimental data and product yields (mass balance).

The product recovery system (catch pot, cyclones, condensers, filters, transport lines, etc.) is disassembled and flushed with acetone to recover pyrolytic liquids. Solids which have been collected with the liquids (i.e. the small fraction which has not been collected in the solids catch pot) are filtered from the solvent, quantified by gravimetry and then ashed for char determination. The filtered mixture of pyrolytic liquid and solvent is rotary-evaporated to recover and quantify the raw liquid product. Selected samples are sent to B.C. Research for analyses.

After cooling in the inert atmosphere of the catch pot (to prevent spontaneous combustion when exposed to air), the bulk recovered solids are riffled, sampled and ashed to determine the solid residue (i.e., char) yield. Ashing is carried out (on the samples and a sand "control") in a muffle furnace according to ASTM procedures. The equipment is reassembled and feeders are charged with fresh sand or biomass in preparation for the next experiment.

6.0 CHARACTERIZATION OF BIOMASS FEEDSTOCKS AND HEAT CARRIER

6.1 CELLULOSE AND WOOD FEEDSTOCKS

Woody biomass materials consist primarily of the three major constituents, cellulose, lignin and hemicellulose. In the thesis work, the vast majority of experiments were conducted using cellulose as the feed material. At the end of the systematic cellulose study, there was sufficient time to perform additional preliminary experiments on wood. Wood was also used in the particle size study (Section 8.6), and cellulose was then used in the joint study with Waterloo University (Section 8.8).

Avicel PH-102 crystalline cellulose, supplied by the FMC corporation, was used as the representative cellulose feedstock in the thesis research program. This Avicel grade is a free-flowing white powder with an average particle size of 100 μm, an "as received" moisture content of 4.0 percent by mass (wet basis), and an empirical formula of $CH_{1.73}O_{0.87}$. It was dried to about 0.9% moisture prior to pyrolysis. Among the biomass feedstocks tested during the course of this project, cellulose had the highest hydrogen/carbon and oxygen/carbon mole ratios. The ultimate (elemental) analysis on a mass basis is given in Table 3. Avicel has been recommended as a standard for use in cellulose pyrolysis studies by the American biomass community at the National Science Foundation Workshop on "Research Goals of the Scientific Community concerned with the Thermochemical Conversion of Biologically-Based Raw Materials".

The raw wood feedstocks were "standard" IEA (International Energy Agency) poplar chips and red maple sawdust. Both were dried to an average moisture content of 0.9 %. The poplar was ground and sieved to an average particle size of 100 μm, and the maple was sieved to 1mm (average) for the particle size study (Section 8.6). Standard IEA poplar has an empirical formula of $CH_{1.47}O_{0.67}$, and is well characterized in terms of elemental composition (Table 3), higher heating value (19.5 MJ/kg), age (7 yrs) and clone (D38 populus deltoides). The lignocellulosic composition has been reported as 53.4% cellulose, 23.4% lignin, 19.8% hemicellulose, 3% extractives and 0.5% ash. The as-received moisture content was 5.2%. Only the elemental analysis (Table 3) and the as-received moisture (7.0%) were reported for the red maple. From the elemental analysis, the empirical formula $CH_{1.52}O_{0.68}N_{0.01}$ was calculated. Theander [206] reports a typical lignocellulosic composition of 42.0% cellulose, 25.4% lignin, 29.4% hemicellulose and 3.2% extractives for red maple.

TABLE 3. CELLULOSE AND WOOD FEEDSTOCK ANALYSIS

FEEDSTOCK	ELEMENTAL ANALYSIS (% dry basis)						"AS RECEIVED"+ MOISTURE	EMPIRICAL FORMULA			
	C	H	O	N	S	Ash	(% wet basis)	C	H	O	N
Cellulose (Avicel)	43.3	6.3	50.3	0.02	0.001	0.03	4.0	1.00	1.73	0.87	-
IEA Poplar	49.3	6.1	44.1	0.10	-	0.40	5.2	1.00	1.47	0.67	-
Red Maple	48.5	6.2	44.2	0.50	-	0.60	7.0	1.00	1.52	0.68	0.01

+ All feedstocks were sized to 100 um and dried to 0.9% moisture (wet basis) prior to pyrolysis.

6.2 HEAT CARRIER

Although the heat carrier (thermofor) was gaseous nitrogen for the large majority of tests which constitute the thesis experimental work, a series of trials using solid particulate thermofor was conducted as well. The solid thermofor was simply F-140 grade non-porous silica sand supplied by Indusmin, St. Canut, Quebec. The mean diameter particle size is 256 μm and the moisture content was less than 0.5% by mass. Particle size data is given in Table 4, along with other physical properties, and chemical composition is reported in Table 5.

TABLE 4. SOLID HEAT CARRIER (SILICA SAND) CHARACTERIZATION

SIEVE SIZE (microns)	MEAN PARTICLE SIZE Dp(I)	WEIGHT (g)	WEIGHT PERCENT W(I)	CUMULATIVE WEIGHT PERCENT	W(I)/Dp(I)
589	711	0.7	0.7	100.0	0.000984
417	503	10.9	10.9	99.3	0.021669
295	356	33.2	33.2	88.4	0.093258
208	251.5	35.1	35.1	55.2	0.139562
147	177.5	14.8	14.8	20.1	0.083380
104	125.5	3.9	3.9	5.3	0.031075
74	89	1.1	1.1	1.4	0.012359
pan	37	0.3	0.3	0.3	0.008108
		100.0	100.0		0.390399

Maximum Particle Size	=	833 μm
Sauter Mean Diameter	=	256.15 μm
Uncompacted Density	=	1390.0 kg/m^3
Loss on Ignition	=	0.07 %

TABLE 5. SOLID HEAT CARRIER CHEMICAL ANALYSIS

CONSTITUENT	MASS %
SiO_2	99.60
Fe_2O_3	0.06
Al_2O_3	0.24
CaO	0.04

7.0 SYSTEM CALIBRATIONS

All of the components involved in the measurement of the system operating conditions (pressure, temperature and flow) and mass balance (volume) were calibrated by at least one independent method. A general summary of the calibrations is given in the following paragraphs, and the detailed results are given in Appendix 2.

7.1 PRESSURE GAUGE CALIBRATIONS

All of the Ultrapyrolysis system Bourdon pressure gauges were calibrated with mercury manometers where:

$$P = \rho g h \qquad (8)$$

P = pressure (Pa)

ρ = mercury density at test conditions (kg/m^3)

g = gravitational constant ($9.81\ m/s^2$)

h = height of mercury column (m)

The readings from the pressure gauges were correlated to the actual pressure (P), as indicated by the mercury manometers, for a number of points over the scale range. A linear regression of the data gave an equation relating scale reading to actual pressure. For twelve pressure gauges, the correlation coefficients ranged from 0.989 to 1.000 (Appendix 2.1).

7.2 THERMOCOUPLE CALIBRATIONS

Although the type K thermocouples (Brampton Thermoelectric, Inc.) used in the Ultrapyrolysis system are certified to be at least ± 0.15% over the 0 to 1300°C temperature range, they were calibrated with reference temperatures of 0°C, room temperature and 100°C using a high-precision certified NSB thermometer. Furthermore, relative agreement of the thermocouples was checked by inserting them simultaneously in an aluminum block which was then placed in an electrical resistance oven set at 400°C. The thermocouple readings were given by a high accuracy DORIC TRENDICATOR 412A Indicator. The results clearly showed that the manufacturer certified accuracy was exceeded (Appendix 2.2).

7.3 ROTAMETER CALIBRATIONS

The rotameter sets used in the Ultrapyrolysis system were calibrated with a sharp-edged orifice meter (ie., corner taps) and checked with a wet test meter (corrected for vapour saturation). The rotameters were also calibrated in the factory by the manufacturer with dry air, and this calibration agreed very well with orifice meter and wet test meter (WTM) results using dry air. However, the "corrected" manufacturers' calibration using nitrogen did not agree well with the orifice meter and WTM results (even though the orifice and WTM gave similar results). A review of the literature indicated that the normal extrapolation of calibration curves from one gas to another (by molecular weight comparison) does <u>not</u> work well for "round float" orifice meters. In fact, the non-round float

calibrations performed in the first phase of the work on rotameters which were not used in the final Ultrapyrolysis system configuration, did exhibit good agreement between the manufacturers' calibrations (with air) and empirical calibrations, regardless of the type of calibration gas used. The results of the orifice and WTM calibrations using nitrogen were therefore combined and correlated to the range of rotameter settings by linear regression analysis. Correlation coefficients ranged from 0.9985 to 0.9996 (Appendix 2.3). The resulting equations were then used in the computer programs which calculated the residence time and mass balance. The pressure regression equations were also used in these programs.

7.4 MASS BALANCE CALIBRATIONS

The reliability of the mass balance procedures depends largely on the ability to accurately measure the mass of the non-condensible gas product. The mass of the condensible liquid and solid (ie., char and ash) products are determined quite accurately by gravimetric methods, as long as the recovery process is reliable. As outlined in Chapter 5, the mass of the non-condensible product gas is measured by evacuating the entire gas product into a tank (Superior Propane 123 USWG) of known volume. The pressure change is recorded, the average molecular mass is calculated from the gas analysis, and the results are used to calculate the total gas mass by applying the ideal gas law. The accuracy of this procedure was verified by determining

the volume of the tank by a reliable physical method, and by testing the procedure using a known mass of gas.

The tank volume was measured by the most practical and direct physical method available. The mass of water required to fill the vessel was measured and its density at test conditions was used to calculate the volume. Two tests, conducted by different researchers, gave results of 434.8 l and 435.2 litres. The average value, 435.0 litres, was used in the mass balance procedure. A second method of calibration using a wet test meter (with flow corrected to remove the saturation volume) coupled to the pressurized tank, gave a volume estimate of 437 litres.

The integrity of the mass balance procedure for gas mass determination was verified using two separate methods. The first method closely resembled an actual experimental run with the exception that the mass and composition of the "product" gas was known a priori. Using a small gas bottle of fixed volume (0.967 l) and known pressure, a known amount of tracer gas was injected into the Ultrapyrolysis system along with an appropriate flow of nitrogen carrier gas to simulate the dilution occurring during actual experimental conditions. The tracer gas was a GC standard calibration gas. Using normal operating analytical and experimental procedures, 2.56 g of gas was injected into the system and 2.57 g was accounted for in the analysis (Appendix 2.4).

The second method of mass balance procedure verification was less complex and time consuming, and was therefore repeated periodically during the project. Pure nitrogen was simply directed to the calibrated rotameters, through the Ultrapyrolysis system and eventually to the gas collection bags. The gas was then evacuated to the gas tank where its mass was determined by normal procedures (ideal gas law and pressure change at a given temperature). This value was then compared with the corresponding value calculated from the rotameter readings. No significant deviations were observed.

7.5 MISC. CALIBRATIONS

Perhaps the most profound "calibrations" are implicit in the Ethane Cracking Study (Section 8.2) and the Joint Study with Waterloo University (Section 8.8). If the system process conditions were being inaccurately determined, then the reported residence times and yields (mass balance) would also be incorrect and would not correspond to the true values. However, the data derived from the Ultrapyrolysis system, in the course of the two studies referred to above, exhibits excellent agreement with published empirical and theoretical literature (in the case of the Ethane Cracking Study) and with an independent fast pyrolysis system (in the case of the Joint Study with Waterloo University).

8.0 RESULTS AND DISCUSSION

8.1 OVERVIEW

In this Chapter, the results of the thesis experimental program are presented within seven general sections which represent natural divisions of the work. First, an ethane cracking study was carried out to test the "integrity" of the Ultrapyrolysis equipment and to give a practical confirmation of the general importance of secondary cracking reactions in fast pyrolysis. Ethane is an ideal model reactant since cracking studies of this hydrocarbon are well characterized and quantified in the literature.

A suitable number of fast pyrolysis experiments were conducted using both solid (particulate sand) and gaseous (nitrogen) thermofor to confirm that there is no significant difference in pyrolysis behaviour *for small biomass particles* (ie. 100 microns). *Small* particles are functionally defined as those in which there are negligible heat transfer limitations. Once confirmed, the results using nitrogen thermofor can then be used to predict results with sand thermofor. This is an extremely practical consideration since gaseous thermofor experiments are much easier to conduct, product recovery is less complicated and the turn-around time is much shorter.

The large majority of the thesis work, leading to the kinetic modelling of secondary vapour-phase cracking, involved the fast pyrolysis of Avicel cellulose using gaseous nitrogen as

the thermofor. A sufficient number of experiments were conducted to fully characterize the total and component gas yields over a broad range of temperatures and residence times, and to accomplish a full statistical analysis (Chapter 9) of the kinetics for the production of principal gases from cellulose.

A study of the fast pyrolysis of wood was an optional task contingent upon the availablility of time after completion of the cellulose experiments. After thorough cellulose experiments were completed, preliminary pyrolysis experiments were carried out using IEA standard poplar, and gave a good indication of the yields of gases, liquids and char produced during fast pyrolysis. The number of wood pyrolysis experiments *in the Ultrapyrolysis system*, however, was not adequate to accomplish a meaningful statistical analysis of the kinetic parameters. Nevertheless, the author was able to conduct additional experiments under similar fast pyrolysis conditions in the RTP system at Ensyn Technologies Inc. (Ottawa), and a *preliminary* kinetics analysis was completed (Chapter 9).

A brief study of biomass particle size was conducted to confirm the predictions of theoretical heating rate models (Section 2.9). For example, even the models which are based on the most conservative assumptions predict that it should be possible to effectively convert biomass particles up to 1 or 2 mm under conditions of fast pyrolysis, without significant heat transfer limitations.

A brief study of the water-gas shift was also conducted to determine whether it plays a significant role in fast pyrolysis. Because of operational problems in the Ultrapyrolysis system during the shift study, only general, non-quantitative conclusions were drawn, and insufficient time was available for further investigations in this area.

Finally, cellulose Ultrapyrolysis data were compared with the cellulose flash pyrolysis data from the Waterloo University fluidized bed process. The intention of this comparison was to check compatibility of the results, summarize the trends of the products yields over an extended temperature range, and to once more confirm the integrity of the Ultrapyrolysis data.

8.2 ETHANE CRACKING

The ethane cracking experiments were carried out by Mr. A. Vogiatzis, a summer student of Dr. J.R. Bolton (Chemistry Dept., U.W.O.) , under the supervision of the thesis author. The principal goal was to observe the pyrolysis of pure ethane in the Ultrapyrolysis system, and to compare the observed cracking kinetics with well-characterized published kinetics. In this manner, the integrity of the Ultrapyrolysis reactor system temperature and residence time measurements could be assessed.

The pyrolysis or "cracking" of pure hydrocarbons and hydrocarbons in inert atmospheres has been studied by a number of researchers [18,37,67,72,96,111,116,135,150,156,157,158,196, 197,198]. The pyrolysis of ethane is of particular interest

since it represents the primary reaction for the commercial production of ethylene. Accordingly, the kinetics are well understood and the free-radical mechanisms have been documented [8,67,72,111,116,135,150,157,158,197,198]. It is beyond the scope of this thesis to present an exhaustive review of the free-radical mechanisms. However, appropriate rate equations and kinetic constants from the literature are given because of their relevance to the observed Ultrapyrolysis kinetics.

Minor modifications were made to the Ultrapyrolysis system prior to the ethane experiments. Rotameters were installed, calibrated by direct methods and integrated into the existing reactor system. The ethane gas was procured from the Linde company as C.P. grade specialty gas (Group 2). It was 98.91% pure and had two principal impurities - carbon dioxide at 1.05% and methane at 0.04%.

Ethane was fed to the reactor system and mixed with the inert nitrogen heat carrier at a dilution (i.e., concentration) which approached that of the corresponding gases produced during cellulose pyrolysis alone. In other words, the quantity of ethane added during an experiment was similar to the amount of ethane which would be expected to be produced from the cellulose pyrolysis reactions. Experiments were conducted at 750 and 850 °C with residence times between 100 and 520 milliseconds. The ethane cracking literature suggested that ethane decomposition would occur at these conditions and would exhibit first-order or three-halves order kinetic behaviour.

TABLE 6. ETHANE CRACKING EXPERIMENTS: DATA SUMMARY

RUN NO.	TEMPERATURE (°C)	RESIDENCE TIME (ms)**	PRODUCT DISTRIBUTION (molar %)*							
			H_2	CO_2	C_2H_4	C_2H_6	C_2H_2	CH_4	C_3H_6	BENZ.
EK1	850	153	20.6	0.4	23.7	54.3	-	1.1	-	-
EK2		152	21.4	0.4	24.1	53.3	-	0.8	-	-
EK3		103	16.9	0.4	22.8	59.9	-	0.6	-	-
EK4		103	17.1	0.4	21.9	59.9	-	0.6	-	-
EK5		385	35.7	0.5	35.2	26.2	0.5	1.9	0.1	0.1
EK6		459	37.1	0.6	35.7	23.9	0.5	1.1	-	-
EK20		271	30.5	0.5	30.5	36.5	0.2	1.4	0.1	0.1
EK7	750	424	4.9	0.9	10.0	84.0	-	0.3	-	-
EK8		511	6.2	1.0	11.5	81 3	-	-	-	-
EK10		111	2.4	0.9	2.4	96.7	-	-	-	-
EK11		164	3.2	1.0	3.2	95.9	-	-	-	-
EK12		112	2.4	0.9	2.4	96.7	-	-	-	-
EK15		167	3.1	0.9	3.1	96.0	-	-	-	-
EK16		296	5.3	0.9	5.3	93.8	-	-	-	-
EK21		422	4.4	0.5	9.3	85.8	-	-	-	-
EK22		509	5.6	0.4	10.2	83.7	-	-	-	-
EK23		298	8.4	0.6	8.4	91.0	-	-	-	-

* The molar % is expressed on a nitrogen-free basis (i.e., the inert nitrogen carrier gas is not included).

** Residence time is measured from the mixer inlet to the quench gas inlet (incl. 8 ms heat-up time at 850°C).

The results of the ethane cracking experiments are given in Table 6. The principal pyrolysis products such as hydrogen and ethylene are observed at all temperatures and residence times investigated. The presence of carbon dioxide in the product is a consequence of the impurity of the ethane feedstock gas. At 850°C, methane is a minor product at all residence times while acetylene, benzene and propylene are apparent only at the longer residence times. These minor pyrolysis products are not detected at 750°C, with the exception of methane which was detected in one of the duplicate runs at approximately 420 milliseconds. Of the primary products of ethane pyrolysis, ethylene and hydrogen are reported in the literature to

predominate while minor amounts of methane are known to occur [72]. The principal secondary product is acetylene (with a proportional amount of hydrogen) with minor production of benzene, propylene, naphthalene and coke [135].

A plot of the disappearance of ethane and the appearance of primary pyrolysis products at 850°C as a function of residence time is given in Figure 17. As expected from the reaction stoichiometry, approximately equal concentrations of ethylene and hydrogen are produced. The product distribution as illustrated in Figure 17 is consistent with the widely accepted theoretical kinetic model for ethane pyrolysis known as the Rice-Herzfeld mechanism [157].

The Rice-Herzfeld model is a free-radical mechanism whose rate is first-order in ethane, and which has been experimentally verified. Therefore the empirical demonstration of first-order ethane pyrolysis kinetics in the Ultrapyrolysis system and comparable rate constants would confirm the validity of this reactor system for utility in kinetic studies. In a first-order model, a plot of the natural logarithm of the ratio of the initial reactant concentration (C_o) to the reactant concentration at time "t" (C_t) vs the residence time (t) should give a straight line. Table 7 presents a summary of the data required to generate such a plot for the pyrolysis of ethane at 750 and 850 °C. The corresponding curves are given for the two temperatures in Figures 18 and 19, respectively.

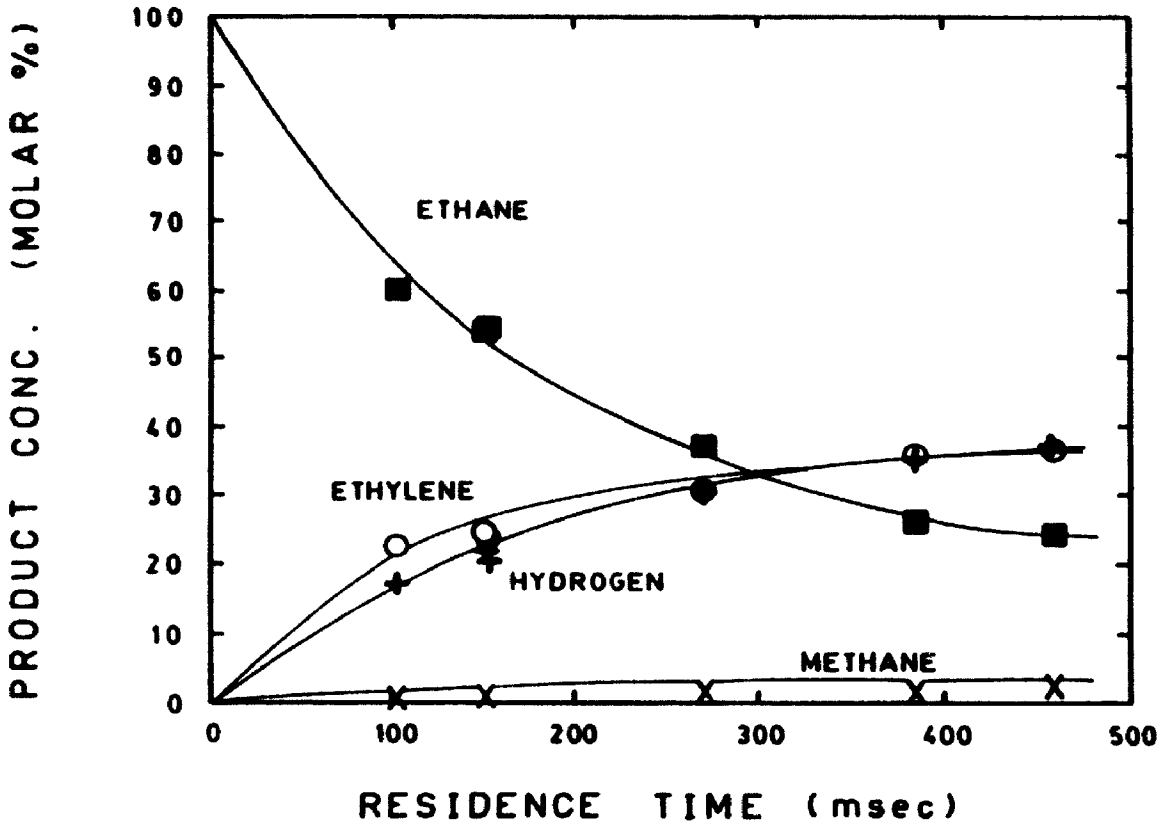

Figure 17. Ethane Cracking at 850°C: Ethane Disappearance and Primary Product Appearance vs Residence Time

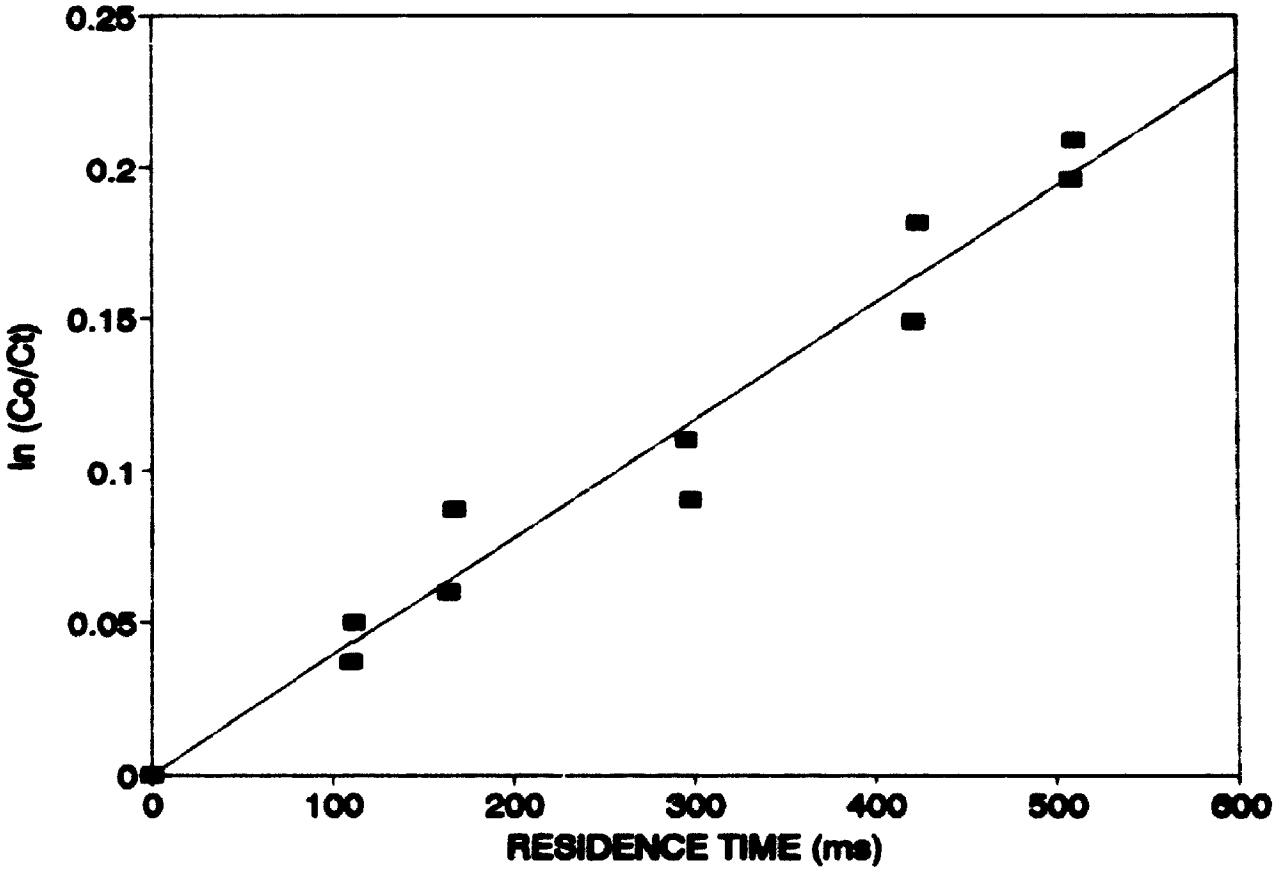

Figure 18. First-Order Plot for Ethane Cracking at 750°C (Run Numbers and Data in Table 7)

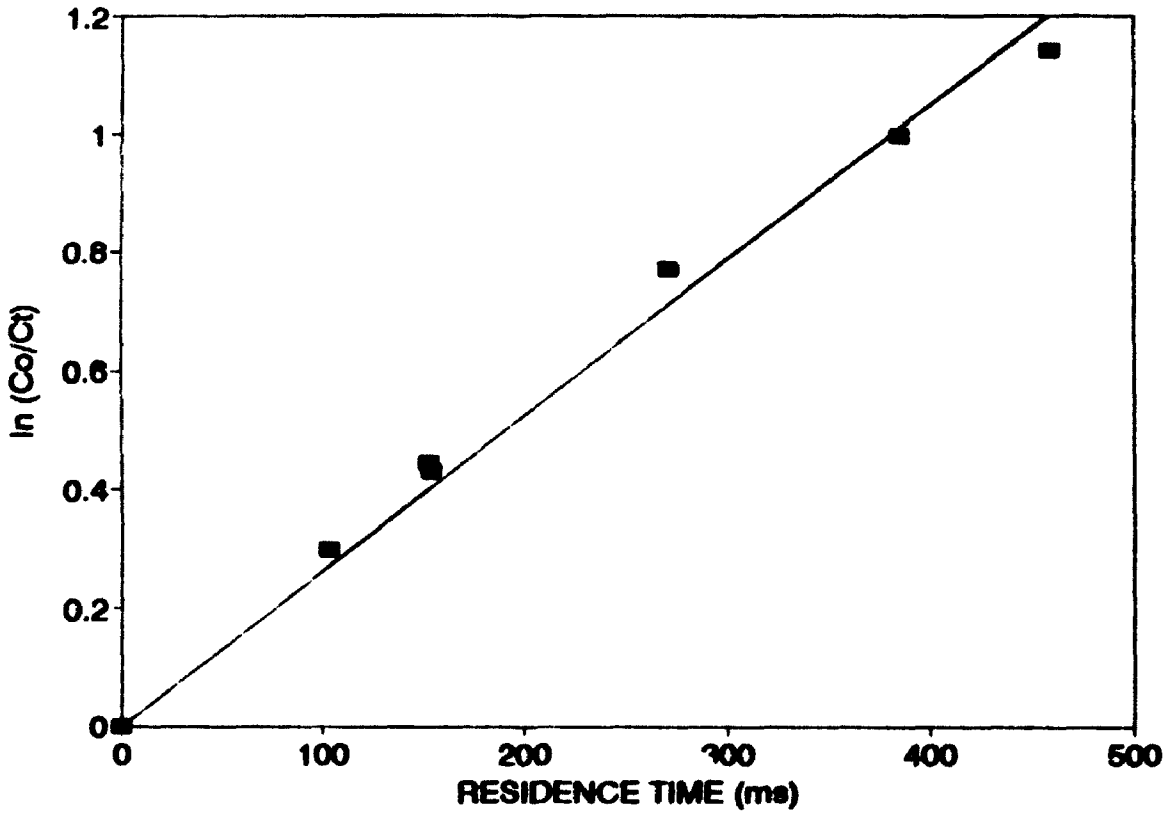

Figure 19. First-Order Plot for Ethane Cracking at 850°C (Run Numbers and Data in Table 7)

TABLE 7. FIRST-ORDER DATA FOR ETHANE CRACKING AT 750 AND 850 °C

RUN NO.	TEMPERATURE (C)	RESIDENCE TIME (ms)	ETHANE CONCENTRATION * $[C2H6]_0$	$[C2H6]_t$	$\ln(C_0/C_t)$
EK7	750	424	13.2	11.0	0.182
EK8		511	15.9	12.9	0.209
EK10		111	8.2	7.9	0.037
EK11		164	12.0	11.3	0.060
EK12		112	8.2	7.8	0.050
EK15		167	12.0	11.0	0.087
EK16		296	21.2	19.0	0.110
EK21		422	13.0	11.2	0.149
EK22		509	15.7	12.9	0.196
EK23		298	9.3	8.5	0.090
EK1	850	153	10.9	7.1	0.429
EK2		152	10.9	7.0	0.443
EK3		103	7.4	5.5	0.297
EK4		103	7.4	5.5	0.297
EK5		385	11.9	4.4	0.995
EK6		459	14.5	4.5	1.170
EK20		271	19.2	8.9	0.769

* Units of concentration are (moles/liter) x 10^4
Initial C2H6 concentration = $[C2H6]_0 = C_0$
Final C2H6 concentration (at time "t") = $[C2H6]_t = C_t$

The first-order plot for ethane pyrolysis at 750°C (Figure 18) is clearly linear, and the kinetics are first-order in ethane as expected. The slope, which represents the first-order rate constant, has a value of 0.39 s^{-1}. Working in a similar temperature range, Marek and McCluer [116] give the following equation for the first-order rate constant:

$$\log k = 15.12 - 15970/T \qquad (9)$$

where T is the reaction temperature in degrees Kelvin and k is

the rate constant in s^{-1}. At 750°C (1023°K), the rate constant is calculated to be 0.33 s^{-1}. The deviation of the Ultrapyrolysis value from this literature value is 18 percent. Lin and Back [111] also working at temperatures in the range of 750°C, give the following rate equation:

$$\log k = (16.22 \pm 0.11) - [(77600 \pm 600)/(2303\ RT)] \quad (10)$$

where T is the reaction temperature in degrees Kelvin, and k is the gas constant (1.987 cal k^{-1} mol^{-1}). At 750°C, the rate constant is calculated to be 0.44 s^{-1}, and the range (accounting for the limits) is 0.26 to 0.76 s^{-1}. The Ultrapyrolysis value is well within this range. Overall, the first-order rate constant for ethane pyrolysis at 750°C (as estimated from the Ultrapyrolysis data) seems to be in good agreement with the literature values. This is quite remarkable since the Ultrapyrolysis system is relatively large, and an error of ± 5°C in the measurement of the reactor temperature at 750°C would give a range of 0.27 to 0.39 s^{-1} for the rate constant from the Marek-McCluer equation and a range of 0.37 to 0.53 s^{-1} from the Lin-Back equation.

The first-order plot for ethane pyrolysis at 850°C (Figure 19) is also linear, thereby indicating that the kinetics are first-order in ethane as expected. The first-order rate constant (calculated from the slope of the plot) is 2.5 s^{-1}. Steacie and Shane [198] report a rate constant of 2.76 s^{-1} at 850°C. The Ultrapyrolysis value deviates from the literature value by about 9 percent. Based on the primary product

distribution and the empirical kinetics of ethane pyrolysis at 850°C, the Ultrapyrolysis results are consistent with the literature.

It can be generally concluded from the results of the pyrolysis of ethane at 750 and 850 °C, that the estimated time-temperature history of the Ultrapyrolysis system is not significantly different from the actual values. If the estimates of either the residence time or reactor temperature were in significant error, then the calculation of the kinetic constants would also deviate significantly from the literature values. The results confirm the "integrity" of the reactor system as a reliable tool for kinetic studies, and also provide a basis for incorporating kinetic models for other hydrocarbons (i.e., literature models) into the cellulose Ultrapyrolysis model without actually pyrolyzing those hydrocarbons independently in the system.

8.3 HEAT CARRIER STUDY

It was stated previously in this report that one of the principal potential advantages of a commercial-scale Ultra-pyrolysis or RTP fast pyrolysis system would be the extremely compact reactor size (i.e., low capital costs for a given plant capacity) because of the use of sand as the heat carrier. A gaseous thermofor would require a much larger volume (at similar reactor conditions) to carry an equivalent amount of heat. In addition, the heat transfer from solid particles to a solid

feedstock is much more efficient than the heat transfer from a gas (because of the "ablative" heat transfer), and therefore much larger biomass particles could be fast pyrolyzed in the system. In spite of these considerations, it is desirable in a *research* system to employ only a gaseous nitrogen heat carrier. The resultant operational advantages have been highlighted in Section 8.1. It was assumed by the Ultrapyrolysis researchers that *for small particles*, the fast pyrolysis product yields would be independent of the type of thermofor as long as the thermofor was chemically inert (i.e., non-reactive and/or non-catalytic). Implicit in this assumption are the following corollaries:

1. Sand thermofor is not catalytic at the temperatures, residence times and other reactor conditions under investigation during the Ultrapyrolysis program.
2. For small biomass particles such as were used in the Ultrapyrolysis experiments (i.e., 100 μm), the heat transfer is sufficient using either sand or nitrogen such that the time for the particle to heat up to reactor temperature is a fraction of the total vapour residence time.

Since nitrogen is much more convenient than sand for use in the Ultrapyrolysis apparatus and since the liquid and char products can be recovered much more easily when sand is excluded, it was decided to conduct the large proportion of the experiments using nitrogen as the heat carrier. A number of cellulose pyrolysis experiments using sand thermofor were conducted at a single temperature (i.e., 800°C) to compare with

nitrogen trials. A mass ratio of thermofor to cellulose of 10:1 was typically employed (reflecting the predicted ratio for a commercial design). The results of the thermofor comparison study are given in Table 8. It is important to note that all of the residence times investigated were in an asymptotic yield region at 800°C where the yields of total gas, gaseous components and total liquid remain constant over a particular range of reactor residence times.

TABLE 8. COMPARISON OF FAST PYROLYSIS EXPERIMENTS AT 800°C USING GASEOUS (NITROGEN) AND SOLID (SAND) THERMOFOR

TYPE OF THERMOFOR	RUN NO.	RESIDENCE TIME (ms)	TOTAL GAS AND COMPONENT GAS YIELDS (% by mass)									
			Gas	H2	CO	CO2	C2H4	C3H6	C2H2	CH4	C2H6	* B/T
NITROGEN	CK379	390	79.1	1.7	57.4	5.3	6.1	1.1	0.8	5.3	0.5	1.1
	CK400	370	78.6	1.4	57.0	4.9	6.0	1.0	0.9	6.1	0.6	0.8
	CK401	369	80.4	1.5	57.0	5.2	6.2	1.0	0.6	5.7	0.6	0.8
	CK402	370	81.1	1.5	57.0	5.2	6.2	1.0	0.7	5.7	0.6	0.9
	MEAN VALUES		79.80	1.53	57.10	5.15	6.13	1.03	0.75	5.70	0.58	0.90
	STD. DEV'N		1.00	0.11	0.17	0.15	0.08	0.04	0.11	0.28	0.04	0.12
SAND	TS1	387	80.5	1.3	58.0	6.1	6.1	1.1	0.8	5.5	0.7	1.0
	TS2	371	82.0	1.5	59.8	5.4	6.3	1.1	0.6	5.6	0.6	1.0
	TS3	367	78.9	1.4	57.8	5.0	6.0	1.1	0.7	5.3	0.6	0.9
	TS4	367	77.1	1.3	56.5	5.2	5.8	1.1	0.5	5.2	0.5	1.0
	MEAN VALUES		79.63	1.38	58.03	5.43	6.05	1.10	0.65	5.40	0.60	0.98
	STD. DEV'N		1.82	0.08	1.18	0.41	0.18	0	0.11	0.16	0.07	0.04

* B/T - benzene/toluene

A qualitative review of the data in Table 8 suggests that there is little or no difference associated with the type of thermofor used for the fast pyrolysis of small biomass particles. The mean yields of total gas at 800°C, for example, are 79.8 and 79.6 percent by mass using nitrogen and sand thermofor, respectively. The ethylene yield was 6.1 percent in both cases. Two statistical "T" tests (summarized in Table 9) also confirm that at the 95% confidence level, no difference in total gas or component yields is apparent, with the exception of propylene. One test assumes that the two "population" variances (i.e., one for the nitrogen thermofor pyrolysis and the other for sand thermofor pyrolysis) are equal, while the other assumes that the population variances are not equal. The outcomes were similar for both tests.

TABLE 9. GASEOUS AND SOLID THERMOFOR EXPERIMENTS AT 800°C: SUMMARY OF T-TEST STATISTICS

GAS PRODUCT	N2 THERMOFOR		SAND THERMOFOR		T - TEST RESULTS					
	MEAN YIELD	STD DEV.	MEAN YIELD	STD DEV.	SIMILAR VARIANCE V	T	Tc	DISSIMILAR VARIANCE V	T	Tc
Total Gas	79.80	1.00	79.63	1.82	6	0.163	2.45	5	0.163	2.57
Hydrogen	1.53	0.11	1.38	0.08	6	2.205	" "	5	2.205	2.57
Carb. Monox.	57.10	0.17	58.03	1.18	6	1.560	" "	3	1.560	3.18
Carb. Diox.	5.15	0.15	5.43	0.41	6	1.282	" "	4	1.282	2.78
Ethylene	6.13	0.08	6.05	0.18	6	0.812	" "	4	0.812	2.78
Propylene	1.03	0.04	1.10	0	6	3.499	" "	3	3.499	3.18
Acetylene	0.75	0.11	0.65	0.11	6	1.285	" "	6	1.285	2.44
Methane	5.70	0.28	5.40	0.16	6	1.860	" "	5	1.860	2.57
Ethane	0.58	0.04	0.60	0.0	6	0.496	" "	5	0.496	2.57
Benz./Tol.	0.90	0.12	0.98	0.0	6	1.264	" "	4	1.264	2.78

* Statistical Criteria: Taken at 95% confidence interval and for two cases.
First case - assumes the two "population" variances are equal.
Second case - assumes the two "population" variances are not equal.

Therefore, these tests confirm the assumption that no difference exists when comparing the use of the two types of thermofor during the pyrolysis of small particles of cellulose at 800°C. More comprehensive wood pyrolysis tests (Section 8.5) in the Ultrapyrolysis unit (using gaseous thermofor) and the Ensyn RTP plant (using sand thermofor) have shown excellent agreement between the two methods of heat transfer. The joint study (Section 8.8) which compared results from the U.W.O. Ultrapyrolysis unit and the Waterloo flash pyrolysis system (using sand to transfer heat in a fluidized bed) also confirmed good agreement regardless of thermofor type (for small biomass particles). Both studies were conducted over a broad range of temperatures and residence times.

8.4 CELLULOSE FAST PYROLYSIS

The cellulose fast pyrolysis study is the cornerstone of the thesis work. As stated previously, the principal objective was to investigate the production of the total gas and principal gaseous components *as a function of temperature and residence time*. From this investigation, the kinetics of the formation of the gases can in turn be determined (which was in fact accomplished, as reported in Chapter 9). Since the non-condensible gas is derived from the cracking of the primary products in the vapour-phase and since these kinetics are rate-limiting, the kinetics of non-condensible gas formation therefore represent the kinetics of vapour-phase cracking as discussed in Chapter 2.

An average of 17 experiments was conducted for each temperature, and 8 temperatures were selected in the range of 650 to 900 °C. Out of 136 experiments which were attempted to generate data for kinetics, about 75% or 101 were deemed to be "good" runs where there were no mechanical, procedural or analytical failures.

A sample data sheet, sample printouts from the residence time and mass balance computer programs, and a product recovery data sheet are given for a typical Avicel cellulose pyrolysis experiment in Appendix 3.0. The "mass balance" as reported in the appended computer printouts is not complete; it accounts only for the gas product (i.e., no liquids) and is therefore consistently and significantly under 100 percent. The true mass balance is calculated by combining the results of the computer mass balance (i.e., for gases) to the liquid yields determined by rotary evaporation of the solvent-extracted products.

The results of the production of total gas and the individual gaseous components produced during the fast pyrolysis of Avicel cellulose at temperatures between 650 and 900°C, are given in Tables 10 to 17. The yields of total gas and liquid are plotted as a function of residence time in Figures 20 to 27. Plots of the principal individual gas component yields are given in Chapter 9. The solid lines on the curves which correspond to the gas and liquid yield data, represent the fit of the data to a first-order kinetic model (Chapter 9).

TABLE 10. AVICEL CELLULOSE FAST PYROLYSIS EXPERIMENTS AT 650°C

RUN NO.	RESIDENCE TIME (ms)	PRODUCT MASS YIELD (%)									
		Gas	H_2	CO	CO_2	C_2H_4	C_3H_6	C_2H_2	CH_4	C_2H_6	B/T *
366	513	23.8	0.4	17.6	2.4	1.2	0.6	0.0	0.7	0.0	0.8
367	332	21.1	0.1	15.9	2.3	1.1	0.6	0.0	0.6	0.0	0.7
368	257	13.9	0.0	10.1	2.0	0.7	0.4	0.0	0.3	0.0	0.5
369	196	14.1	0.0	10.4	1.8	0.7	0.4	0.0	0.4	0.0	0.4
370	147	12.8	0.0	9.3	1.8	0.6	0.4	0.0	0.3	0.0	0.3
371	109	11.9	0.0	8.1	1.9	0.7	0.4	0.0	0.3	0.0	0.5
372	828	26.8	0.3	20.0	2.5	1.3	0.7	0.0	0.9	0.2	0.8
373	504	23.3	0.3	17.5	2.1	1.2	0.7	0.0	0.7	0.0	0.7
374	294	17.0	0.2	12.1	1.9	1.0	0.5	0.0	0.5	0.0	0.6
375	246	16.9	0.0	12.6	1.8	0.9	0.4	0.0	0.5	0.0	0.6
376	146	14.0	0.0	10.3	1.9	0.6	0.3	0.0	0.3	0.0	0.5
377	788	27.0	0.3	20.2	2.5	1.3	0.8	0.0	1.0	0.2	0.6

* B/T - benzene/toluene

TABLE 11. AVICEL CELLULOSE FAST PYROLYSIS EXPERIMENTS AT 700°C

RUN NO.	RESIDENCE TIME (ms)	PRODUCT MASS YIELD (%)									
		Gas	H_2	CO	CO_2	C_2H_4	C_3H_6	C_2H_2	CH_4	C_2H_6	B/T *
230	783	53.9	0.9	39.8	3.7	3.8	1.1	0.6	2.9	0.4	0.8
233	867	54.6	0.9	39.9	4.2	3.8	1.1	0.4	2.9	0.5	0.8
259	73	19.7	0.1	15.2	2.3	1.1	0.5	0.3	0.5	0.0	0.0
260	122	27.4	0.2	21.3	2.7	1.7	0.7	0.3	0.8	0.0	0.0
261	185	30.6	0.3	23.3	3.0	1.8	0.8	0.4	1.1	0.0	0.0
262	320	36.9	0.4	28.3	2.8	2.5	0.9	0.3	1.6	0.0	0.0
266	142	26.3	0.2	19.3	2.4	1.5	0.7	0.3	0.8	0.1	0.8
267	74	21.2	0.1	15.8	2.1	1.1	0.5	0.3	0.6	0.0	0.6
268	229	32.5	0.4	24.1	2.5	1.9	0.9	0.3	1.3	0.2	0.9
269	203	32.3	0.4	23.7	3.2	1.9	0.8	0.3	1.1	0.2	0.7
324	668	56.1	0.9	41.1	4.0	3.3	1.4	0.2	2.8	0.4	0.9
389	594	47.1	0.9	35.3	3.7	2.6	1.2	0.1	2.1	0.3	0.9
390	364	38.1	0.6	28.3	3.0	2.2	1.0	0.3	1.5	0.2	0.9
391	131	25.6	0.4	18.8	2.4	1.4	0.7	0.2	0.8	0.0	0.8
392	818	43.4	0.8	32.5	3.1	2.6	1.1	0.2	2.0	0.3	0.8
393	651	49.5	1.1	36.9	4.0	2.8	1.2	0.1	2.2	0.3	0.9
394	526	42.7	0.7	31.9	3.7	2.3	1.1	0.2	1.7	0.3	1.0

* B/T - benzene/toluene

TABLE 12. AVICEL CELLULOSE FAST PYROLYSIS EXPERIMENTS AT 750°C

RUN NO.	RESIDENCE TIME (ms)	PRODUCT MASS YIELD (%)									
		Gas	H_2	CO	CO_2	C_2H_4	C_3H_6	C_2H_2	CH_4	C_2H_6	B/T *
231	456	68.1	1.2	49.6	4.8	5.4	1.0	0.9	3.9	0.5	0.8
234	806	71.2	1.4	51.9	4.9	5.6	1.0	0.6	4.7	0.5	0.8
236	575	70.5	1.3	51.2	4.9	5.4	1.1	0.8	4.3	0.4	1.0
237	177	49.2	0.7	35.9	4.0	3.5	1.0	0.7	2.1	0.3	0.9
270	103	40.0	0.5	29.4	3.4	2.5	1.0	0.5	1.6	0.2	0.8
271	74	34.5	0.4	25.5	3.0	2.2	0.9	0.4	1.1	0.3	0.9
272	216	60.3	1.0	44.4	3.7	4.2	1.3	0.8	3.4	0.4	1.1
273	304	64.6	1.1	47.4	4.0	4.6	1.2	0.8	4.0	0.5	1.0
283	287	62.2	1.2	45.4	5.1	4.1	1.2	0.5	3.5	0.4	0.9
284	66	40.4	0.6	29.8	3.3	2.7	1.0	0.6	1.3	0.4	1.0
311	717	74.4	1.3	54.1	5.4	5.4	1.4	0.6	4.7	0.6	1.0
325	606	64.9	1.2	47.6	4.6	4.4	1.2	0.4	4.1	0.5	0.9
395	692	68.8	1.3	50.8	4.7	4.5	1.5	0.4	4.0	0.6	0.9

* B/T - benzene/toluene

TABLE 13. AVICEL CELLULOSE FAST PYROLYSIS EXPERIMENTS AT 800°C

RUN NO.	RESIDENCE TIME (ms)	PRODUCT MASS YIELD (%)									
		Gas	H_2	CO	CO_2	C_2H_4	C_3H_6	C_2H_2	CH_4	C_2H_6	B/T *
263	124	61.4	0.9	45.4	4.5	5.2	1.0	0.9	3.3	0.1	0.0
264	69	52.8	0.7	39.7	3.8	4.3	1.0	1.0	2.3	0.0	0.0
265	203	69.6	1.3	50.6	4.9	5.4	1.1	0.8	4.3	0.5	0.8
274	100	62.3	1.1	45.5	4.0	4.9	1.2	1.0	3.2	0.4	0.9
275	202	79.1	1.6	57.1	5.4	6.3	1.2	1.1	5.0	0.5	0.9
276	178	75.7	1.5	54.5	5.3	6.0	1.1	1.0	4.8	0.5	0.9
288	218	73.7	1.4	52.9	5.4	5.5	1.2	1.0	4.7	0.6	1.0
289	73	51.2	0.8	37.6	3.3	3.6	1.2	0.8	2.3	0.3	1.2
290	112	55.9	0.9	40.7	4.0	3.9	1.1	0.9	2.8	0.4	1.1
308	290	83.6	1.5	60.2	5.9	6.2	1.3	1.2	5.4	0.7	1.2
309	463	81.7	1.6	58.8	5.9	6.0	1.1	1.0	5.8	0.5	0.9
312	230	71.8	1.3	51.5	5.4	5.7	1.2	1.0	4.2	0.5	1.1
378	390	79.1	1.7	57.4	5.3	6.1	1.1	0.8	5.3	0.5	1.1

* B/T - benzene/toluene

TABLE 14. AVICEL CELLULOSE FAST PYROLYSIS EXPERIMENTS AT 825°C

RUN NO.	RESIDENCE TIME (ms)	PRODUCT MASS YIELD (%)									
		Gas	H_2	CO	CO_2	C_2H_4	C_3H_6	C_2H_2	CH_4	C_2H_6	B/T *
291	543	80.3	1.7	58.2	5.8	6.3	0.6	0.6	5.9	0.5	0.7
292	267	79.9	1.5	57.6	5.7	6.3	0.9	1.1	4.9	0.5	0.9
293	165	73.0	1.3	52.6	5.2	5.7	1.0	1.1	4.2	0.5	1.2
294	109	68.5	1.2	49.8	4.9	5.3	1.2	1.0	3.5	0.5	1.0
295	65	57.2	0.9	41.5	4.1	4.5	1.1	1.0	2.5	0.5	1.1
296	550	82.5	1.7	59.4	5.4	6.6	0.7	0.9	6.2	0.5	0.9
297	216	81.0	1.4	58.5	5.8	6.6	1.0	1.3	4.6	0.6	0.8
298	94	64.0	1.0	46.6	4.4	5.1	1.1	1.1	3.2	0.5	1.1
313	244	77.4	1.4	55.4	5.5	6.3	1.0	1.3	5.2	0.6	1.0
317	246	80.9	1.5	57.7	5.8	6.7	1.0	1.5	4.9	0.6	0.8
379	383	82.4	1.9	59.4	5.5	6.7	0.9	1.0	5.7	0.6	0.8

* B/T - benzene/toluene

TABLE 15. AVICEL CELLULOSE FAST PYROLYSIS EXPERIMENTS AT 850°C

RUN NO.	RESIDENCE TIME (ms)	PRODUCT MASS YIELD (%)									
		Gas	H_2	CO	CO_2	C_2H_4	C_3H_6	C_2H_2	CH_4	C_2H_6	B/T *
277	280	82.0	1.6	58.7	5.5	6.9	0.7	1.4	5.8	0.5	0.9
278	199	80.8	1.6	57.9	5.4	6.4	0.8	1.5	5.7	0.6	1.0
279	94	73.4	1.4	52.7	5.3	6.0	1.0	1.4	3.9	0.7	0.9
310	376	83.6	1.6	59.7	5.8	7.0	0.7	1.5	5.9	0.6	1.0
314	65	62.3	1.1	44.7	4.5	5.1	1.0	1.4	2.8	0.7	1.0
318	328	83.6	1.6	59.7	6.0	7.0	0.7	1.6	5.7	0.6	0.8
319	233	83.5	1.6	59.8	5.8	7.0	0.8	1.3	5.7	0.6	1.0
320	130	81.2	1.5	58.0	5.8	6.6	1.1	1.5	4.8	0.7	1.0
321	106	73.1	1.3	52.6	5.1	5.9	1.1	1.4	3.9	0.7	1.0
380	763	84.1	1.8	60.6	5.5	7.0	0.4	1.1	6.5	0.4	0.7

* B/T - benzene/toluene

TABLE 16. AVICEL CELLULOSE FAST PYROLYSIS EXPERIMENTS AT 875°C

RUN NO.	RESIDENCE TIME (ms)	PRODUCT MASS YIELD (%)									
		Gas	H_2	CO	CO_2	C_2H_4	C_3H_6	C_2H_2	CH_4	C_2H_6	B/T *
299	184	84.5	1.6	60.2	5.7	7.1	0.6	1.9	5.5	0.6	1.3
300	263	86.3	1.7	61.9	5.7	7.2	0.6	1.8	6.0	0.6	0.9
301	157	85.5	1.7	61.5	5.9	6.9	0.7	1.6	5.5	0.6	0.9
302	96	84.5	1.7	60.4	5.8	6.8	0.8	1.8	4.6	0.8	1.1
303	96	76.3	1.4	54.4	5.7	6.4	0.8	1.8	4.2	0.8	0.8
304	78	78.5	1.3	55.9	5.9	6.7	1.1	2.0	4.0	0.7	0.8
305	156	77.7	1.5	55.4	5.4	6.5	0.8	1.5	5.1	0.6	0.9
306	228	87.2	1.7	62.2	5.7	7.4	0.4	1.6	6.7	0.5	1.0
307	485	87.9	1.7	62.8	5.7	7.5	0.4	1.6	6.7	0.5	1.0
387	363	87.2	1.9	62.4	5.7	7.4	0.5	1.5	6.4	0.5	0.9
398	57	74.5	0.8	53.9	5.5	6.1	1.1	1.5	4.1	0.6	0.9
399	57	74.4	0.7	54.0	5.1	6.1	1.2	1.5	4.1	0.6	1.0

* B/T - benzene/toluene

TABLE 17. AVICEL CELLULOSE FAST PYROLYSIS EXPERIMENTS AT 900°C

RUN NO.	RESIDENCE TIME (ms)	PRODUCT MASS YIELD (%)									
		Gas	H_2	CO	CO_2	C_2H_4	C_3H_6	C_2H_2	CH_4	C_2H_6	B/T *
253	234	87.9	1.7	62.4	6.3	7.4	0.5	1.8	6.1	0.6	1.2
254	164	87.1	1.6	62.0	6.1	6.8	0.4	2.3	6.2	0.5	1.3
280	255	86.2	1.7	61.4	5.9	7.7	0.4	1.9	5.9	0.5	0.8
281	182	85.6	1.8	60.8	6.1	7.3	0.6	1.8	5.9	0.6	0.9
282	105	85.1	1.7	60.7	5.8	7.3	0.8	1.8	5.3	0.7	0.9
381	678	92.8	2.2	66.8	5.9	7.6	0.2	1.6	7.2	0.3	1.0
382	104	82.7	1.6	59.4	5.7	6.9	0.7	1.9	5.1	0.7	0.8
383	435	90.8	1.9	64.8	6.0	7.7	0.3	2.0	6.8	0.4	1.0
384	592	86.1	1.9	61.9	5.5	7.1	0.2	1.7	6.6	0.3	1.0
385	93	86.1	2.0	61.4	5.8	7.1	0.8	1.8	5.3	0.7	1.0
386	408	89.3	1.9	63.6	6.5	7.3	0.3	1.8	6.5	0.4	1.0
396	56	80.9	0.7	58.3	5.8	6.6	1.1	1.7	4.6	0.7	0.9
397	56	79.3	0.8	57.1	5.8	6.6	1.1	1.7	4.5	0.7	1.0

* B/T - benzene/toluene

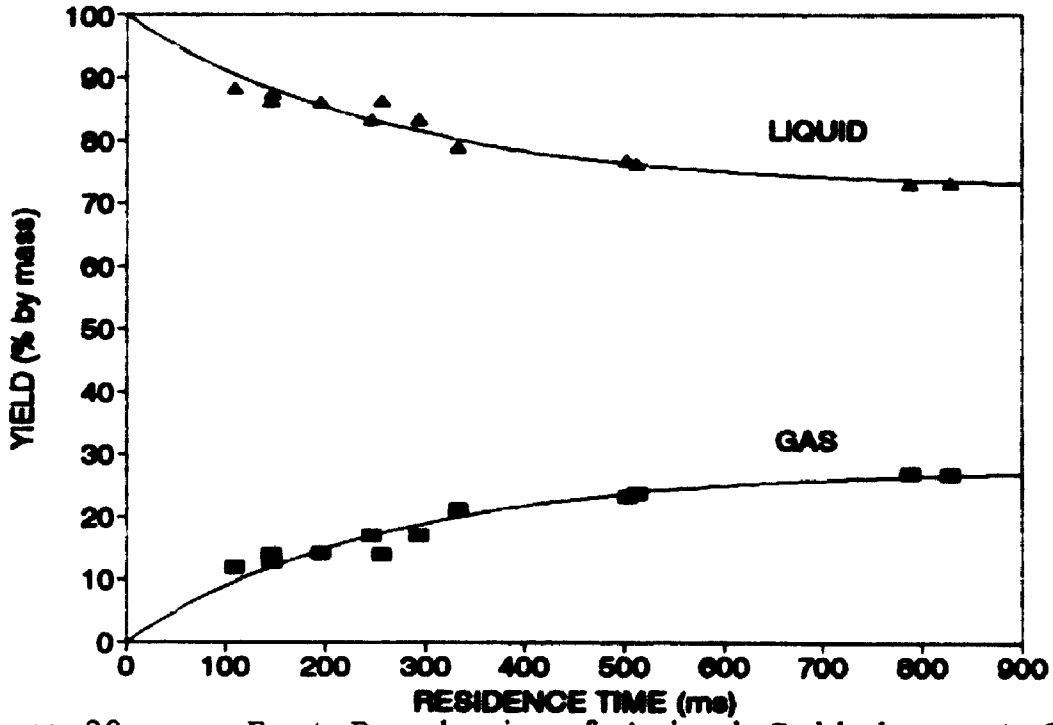

Figure 20. Fast Pyrolysis of Avicel Cellulose at 650°C: Total Gas and Liquid Yields vs. Residence Time (Run Numbers and Data in Table 10)

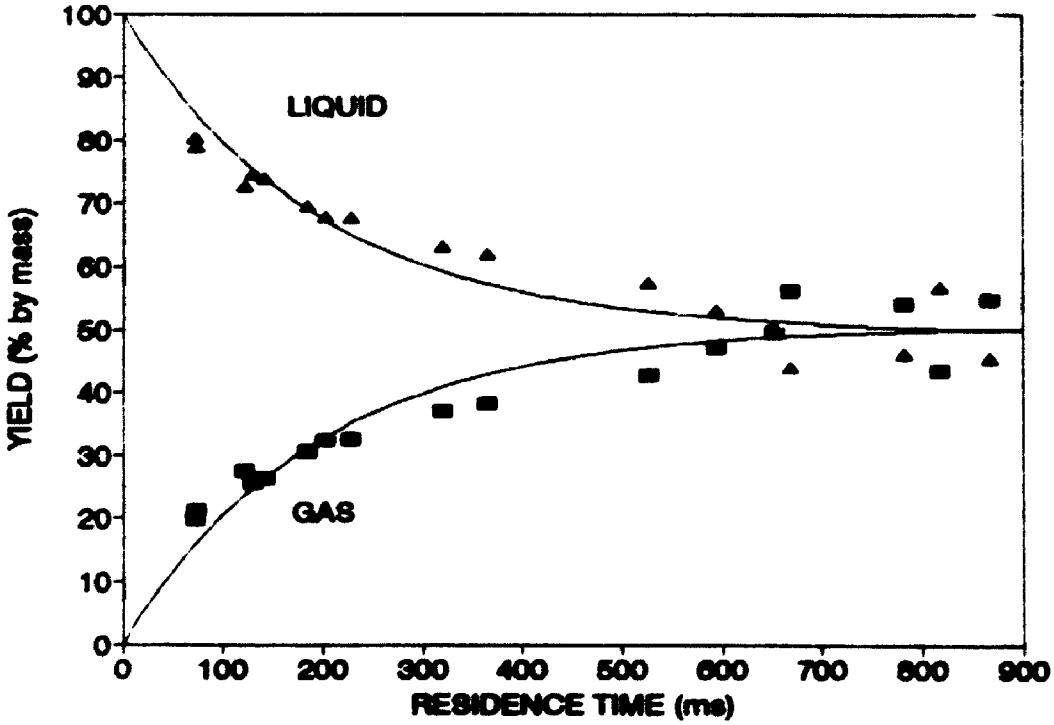

Figure 21. Fast Pyrolysis of Avicel Cellulose at 700°C: Total Gas and Liquid Yields vs. Residence Time (Run Numbers and Data in Table 11)

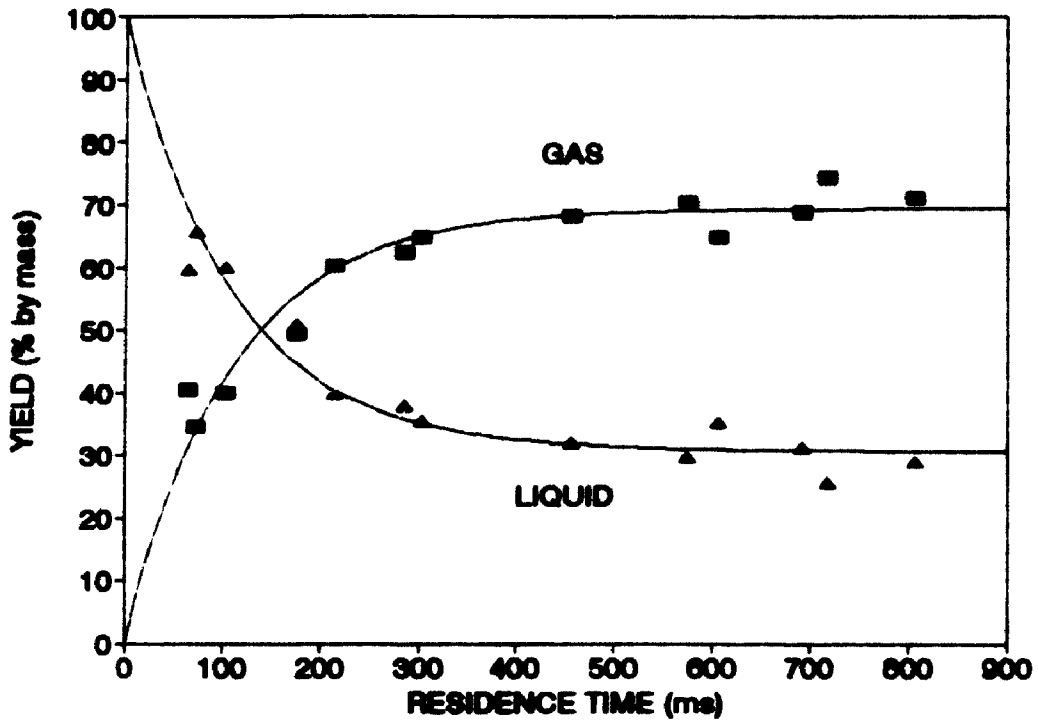

Figure 22. Fast Pyrolysis of Avicel Cellulose at 750°C: Total Gas and Liquid Yields vs. Residence Time (Run Numbers and Data in Table 12)

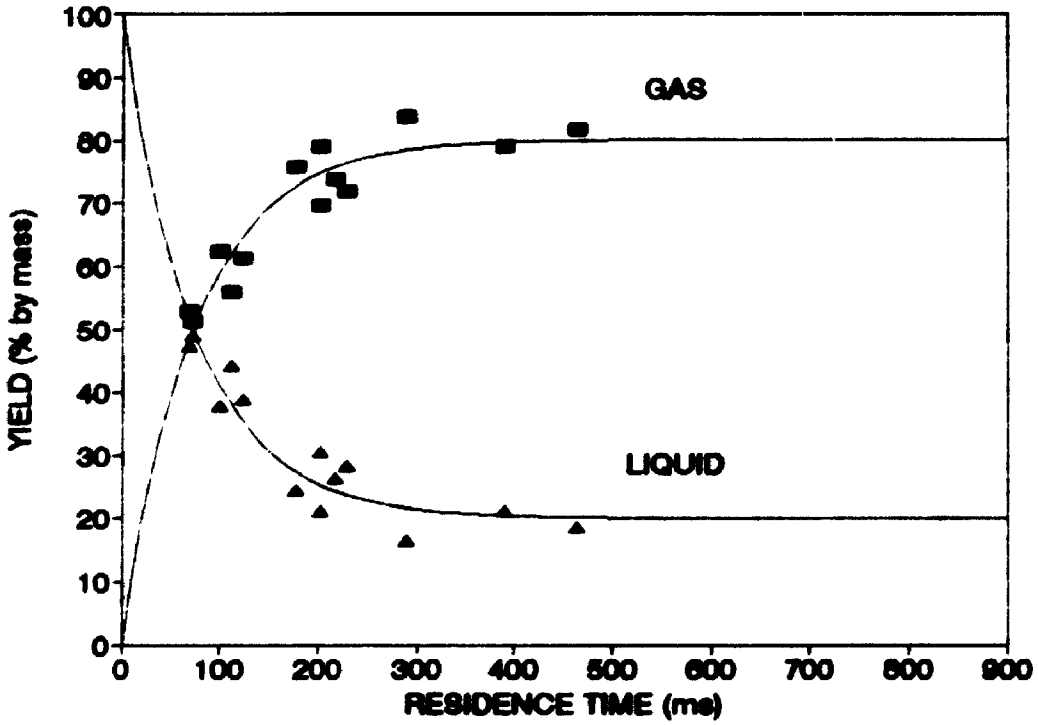

Figure 23. Fast Pyrolysis of Avicel Cellulose at 800°C: Total Gas and Liquid Yields vs. Residence Time (Run Numbers and Data in Table 13)

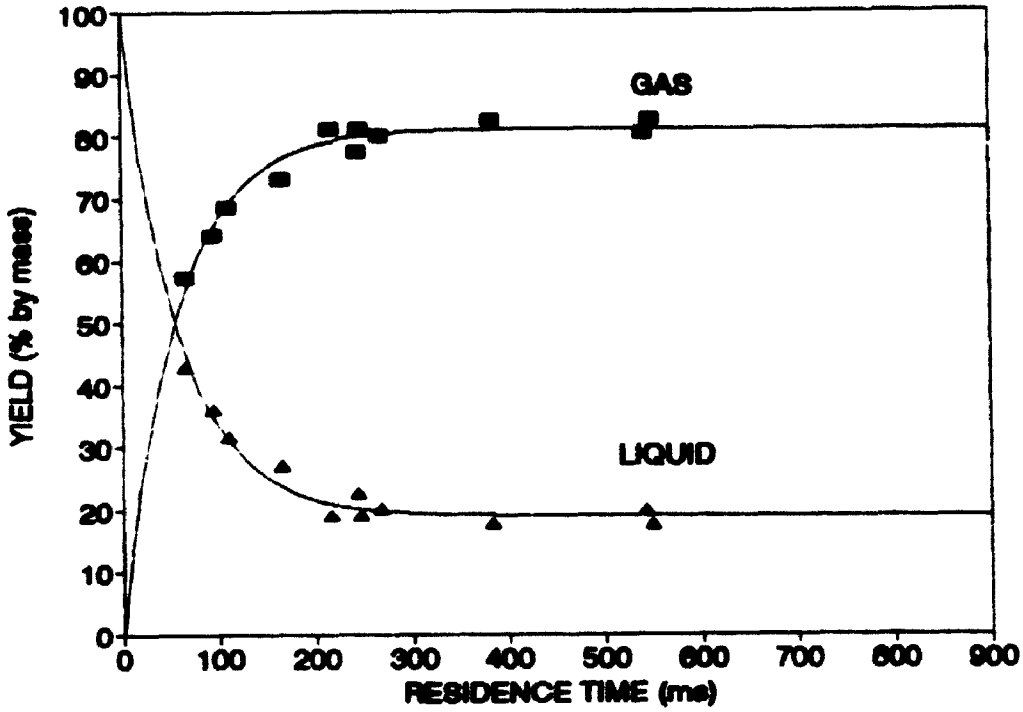

Figure 24. Fast Pyrolysis of Avicel Cellulose at 825°C: Total Gas and Liquid Yields vs. Residence Time (Run Numbers and Data in Table 14)

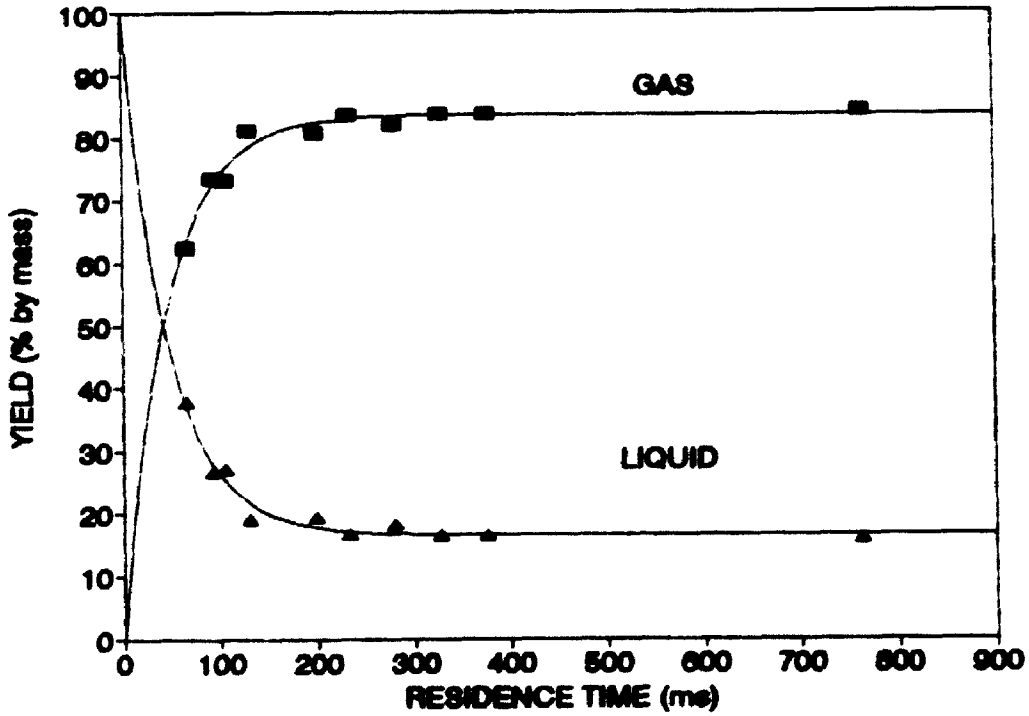

Figure 25. Fast Pyrolysis of Avicel Cellulose at 850°C: Total Gas and Liquid Yields vs. Residence Time (Run Numbers and Data in Table 15)

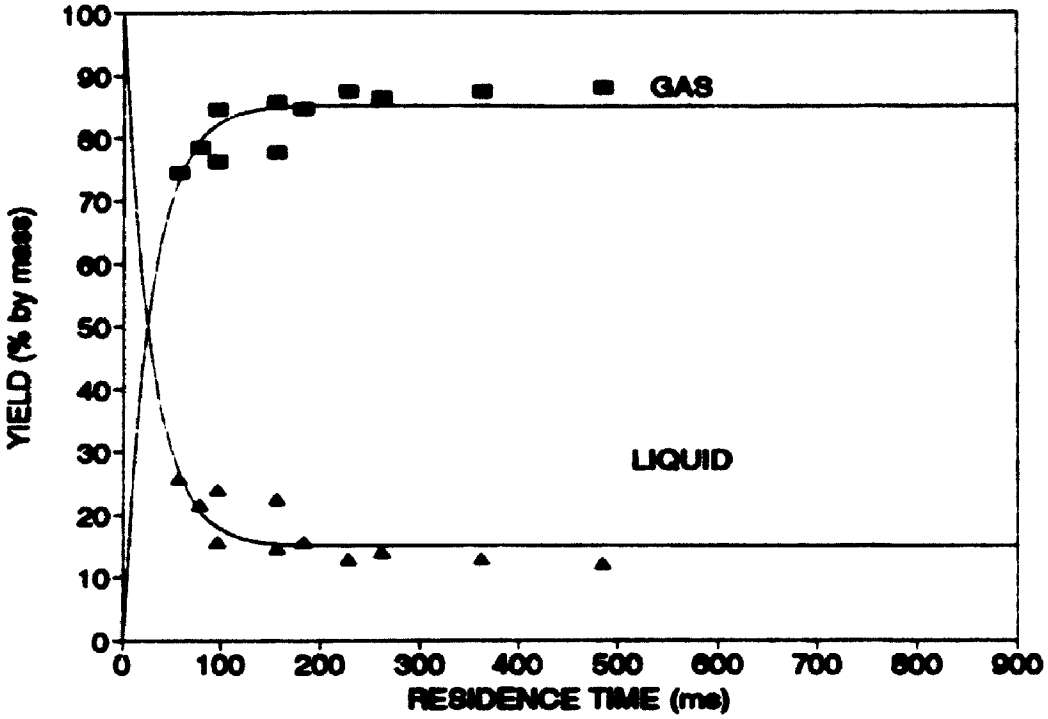

Figure 26. Fast Pyrolysis of Avicel Cellulose at 875°C: Total Gas and Liquid Yields vs. Residence Time (Run Numbers and Data in Table 16)

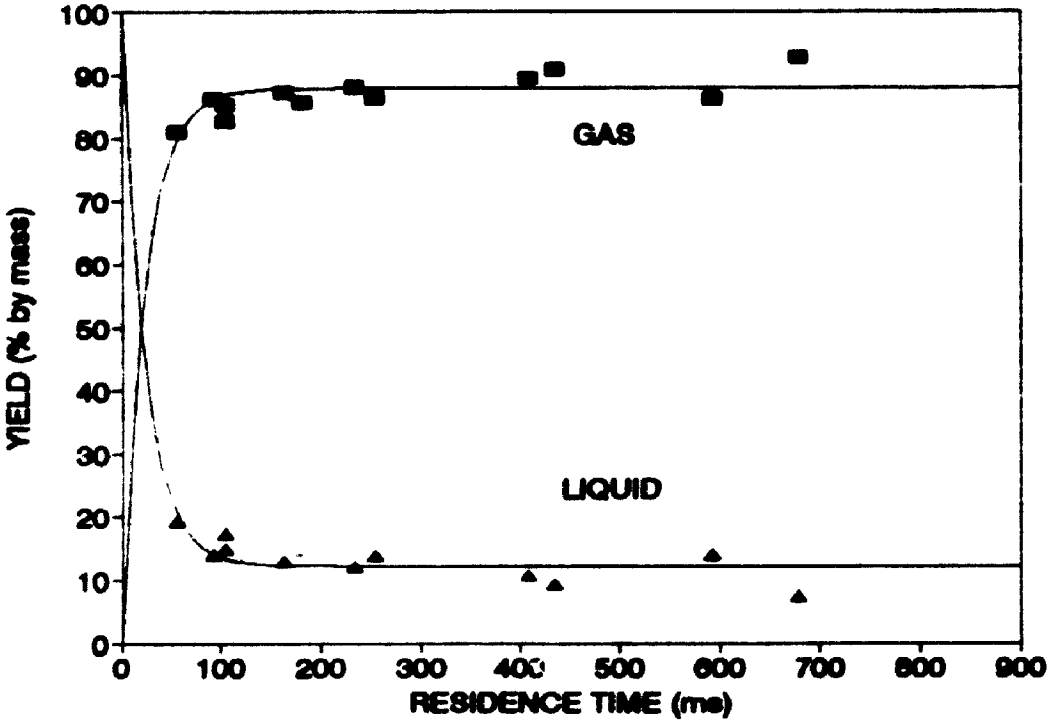

Figure 27. Fast Pyrolysis of Avicel Cellulose at 900°C: Total Gas and Liquid Yields vs. Residence Time (Run Numbers and Data in Table 17)

The general shape of the total gas yield curves (Figures 20 to 27) is consistent for each temperature, and indicates an initial rapid production rate followed by a tapering off to an asymptotic (constant maximum) yield. This characteristic shape has been observed by other researchers [8,12,14,175,213], and is representative of the shape of the curves for the yields of all *principal* gas components. From the experimental data, it is clear that the principal gaseous components are CO, CO_2, H_2, CH_4, C_2H_4, and C_2H_2. Other biomass fast pyrolysis researchers have also found that these are the predominant products of the secondary vapour-phase cracking reactions [8,11,12,13,14,26,49, 55,73,86,90,131,137,218]. Of the major components, CO is by far the most abundant component and is clearly a principal product of the secondary cracking reactions. The minor gaseous components include ethane and propylene. Their yield curves do not exhibit the asymptotic behaviour which is characteristic of the major products, since at elevated temperatures these gases are cracking as they appear [8].

The initial production rates of the principal gases, as represented by the slopes of the lines, vary both with temperature and gas component. Consistent with kinetic theory, the rates increase with increasing temperature. It is also evident that the asymptotic total gas yield increases from 28 to 88 percent (by mass) as the temperature is increased from 650°C to 900 °C. Over this same temperature range, the maximum

asymptotic mass yields of carbon monoxide, carbon dioxide and hydrogen increase from 21 to 63, and 2.3 to 6.0, and 0.3 to 1.9 percent, respectively. Corresponding values for ethylene (a significant petrochemical feedstock), total unsaturated hydrocarbons (olefins and alkynes) and total hydrocarbons are 1.3 to 7.3, 2.1 to 10.3, and 3.3 to 17.5 percent, respectively. These asymptotic values are taken from the results of the regression analysis, as reported in the kinetic modelling study (Chapter 9), and not directly from the data tables.

Although not fully apparent from an initial analysis of the cellulose pyrolysis data, there is evidence to confirm that a significant amount of CO and CO_2 (and consequently, total gas) is already present as prompt gas before subsequent production via the secondary cracking reactions. As discussed previously (Chapter 2), prompt gas is the relatively small quantity of non-condensible gases which are produced during primary pyrolysis. The composition of prompt gas from cellulose pyrolysis and its effect on kinetic modelling is dealt with in much greater detail in Section 8.8 and Chapter 9, respectively. Furthermore, its significance has already been noted and described by other researchers [8,11,55,73,80,131,152,173,174,175].

The production of ethane, acetylene and propylene clearly does not fully follow the pattern which is characteristic of the production of principal gaseous products, as described in the preceding paragraphs. Typically, ethane is not in the product distribution at 650°C and is therefore not a primary prompt gas

product. It appears consistently at 700°C and follows the asymptotic trend at this temperature where it reaches a maximum yield of about 0.4%. At 750°C, it also behaves asymptotically where it reaches a maximum yield of about 0.5%. Residence times exceeding 800 ms are not sufficient to allow cracking of the ethane product at temperatures up to 750°C (Tables 10 to 12). At temperatures greater than 750°C (Tables 13 to 17), the ethane yield reaches a maximum at some intermediate residence time, and then begin to decrease as cracking reactions are initiated. For example, at 800°C the maximum ethane yield averages about 0.6% at approximately 300 ms. The corresponding value at 850 and 900°C is 0.7% for both temperatures, at about 110 ms and 80 ms, respectively. As the temperature is increased, the decrease in residence time at which the maximum occurs is indicative of the increasing rate of ethane cracking.

Acetylene is not produced until reaction temperatures approach 700°C. Its constant maximum yield at each temperature, increases systematically from about 0.4% to about 1.8% as the temperature is increased from 700 to 800 °C. At 850°C, the acetylene yield is about 1.5% as the residence time approaches 130 ms and remains constant up to about 400 ms. From 400 ms to about 760 ms the yield drops to 1.1% as acetylene cracking begins to occur at this temperature. At 900 °C, a maximum acetylene yield of 2.3% is realized by about 260 ms, and then drops to about 1.6% at approximately 680 ms.

Since there are no published biomass fast pyrolysis results based on a systematic study of the effects of both temperature *and* residence time (typically only the temperature is methodically investigated), it is difficult to systematically compare the above results with those of other researchers. Nevertheless, where temperatures and residence times overlap and where researchers have paid attention to the importance of heat transfer, there is remarkable agreement [8,12,14,49,55,173,174, 175]. An example of the good agreement between independent fast pyrolysis data and the data presented in this Section is given in considerable detail in Section 8.8. Where researchers have considered residence time and temperature without fully regarding the importance of heat transfer, there is clearly poor agreement [74,86,90,102,112,137].

The *total* liquid yields (ie., product water plus organics) as a function of temperature are also represented by solid lines in Figures 20 to 27. Since the char yields from cellulose are negligible over the entire temperature range studied, the liquid yield curves are simply the inverse of the gas yield curves (i.e., 100 percent minus the gas yields). The validity of this technique is confirmed by the mass balance results which exhibit consistently good closure (Table 18). Liquid yields decrease to an asymptotic minimum value as a function of residence time for each temperature. The asymptotic values decrease from 72 to 12 percent by mass as temperature is increased from 650 to 900°C. It is apparent from the curves that total liquid yields can be

increased at each temperature by reducing the residence time. The maximum liquid yield observed during the thesis work was 88.1 percent (by mass) at 650°C and 109 ms.

The fact that the liquid yield curve appears to approach 100 % as the residence time approaches zero is simply an artifact of the modelling procedure (Chapter 9). In reality, it is clear that the liquid yield is zero at t_o (i.e., the solid feedstock has not yet reacted). Nevertheless, the model represents a reasonable approximation, since according to the published kinetics, the biomass is converted to an "active" state (a viscous liquid plus prompt gas) within a few milliseconds. This is relatively "instantaneous" on the vapour cracking time scale.

A summary of the mass balance results for selected cellulose pyrolysis experiments is given in Table 18. The average value of the product recovery is 96.1 percent of the mass of cellulose pyrolysed. This consistent deficit in the mass balance can be easily accounted for as the uncondensed water vapour in the saturated nitrogen carrier gas which exits from the condenser at 8 to 10°C. In addition, the small amount of light organic volatiles which is condensed during the experiment but then lost with the solvent during rotary evaporation, cannot be accounted for in the mass balance. Nevertheless, any light volatiles which remain in the saturated nitrogen carrier gas are analyzed as a single peak ("C_5/C_6") on the Carle gas chromatograph. The product recovery ranged from

TABLE 18. AVICEL CELLULOSE FAST PYROLYSIS MASS BALANCE SUMMARY

RUN NUMBER	CELLULOSE FED (g)	PRODUCT RECOVERY (g) * GAS	LIQUID	CHAR	TOTAL	TOTAL RECOVERY (% by mass)
CK300	35.6	30.45	3.86	0.06	34.4	96.6
CK303	26.5	20.04	5.75	0.09	25.9	97.7
CK304	21.2	16.49	3.64	0.12	20.3	95.8
CK305	49.7	38.28	9.46	0.04	47.8	96.2
CK306	39.5	34.13	2.60	0.08	36.8	93.2
CK307	41.8	36.42	2.70	0.06	39.2	93.8
CK309	51.8	41.92	7.40	0.04	49.4	95.4
CK310	50.7	42.17	6.30	0.05	48.5	95.7
CK311	43.3	31.93	9.45	0.21	41.6	96.1
CK313	34.2	26.22	5.94	0.10	32.3	94.4
CK314	23.3	14.40	7.98	0.34	22.7	97.4
CK318	37.7	31.25	4.65	0.06	36.0	95.5
CK319	39.0	32.28	5.12	0.09	37.5	96.2
CK320	37.5	30.17	6.18	0.06	36.4	97.1
CK321	30.8	22.32	7.56	0.05	29.9	97.1
CK324	32.0	17.80	13.52	0.25	31.6	98.8
CK325	35.2	22.63	11.84	0.10	34.6	98.3
CK366	16.4	3.87	11.73	0.40	16.0	97.6
CK367	11.6	2.43	9.54	0.10	12.1	104.3
CK369	21.6	3.01	17.41	0.44	20.9	96.8
CK370	21.6	2.74	17.69	0.35	20.8	96.3
CK374	26.3	4.42	20.92	0.25	25.6	97.3
CK375	23.6	3.95	18.98	0.46	23.4	99.1
CK379	21.8	17.80	2.05	0.02	19.9	91.3
CK381	20.8	19.12	1.00	0.03	20.2	97.1
CK382	22.2	18.19	2.31	0.05	20.6	92.8
CK383	25.4	22.86	2.02	0.02	24.9	98.0
CK384	29.7	25.36	3.10	0.00	28.5	96.0
CK385	24.4	20.81	2.94	0.01	23.8	97.5
CK393	21.0	10.29	10.21	0.04	20.5	97.6
CK394	24.6	10.42	13.65	0.07	24.1	98.0

* "Liquid" includes liquids recovered by solvent extraction and light volatiles in product gas stream.

91.3 to 104.3 percent by mass. This latter value was the only one over 100 percent.

A summary of the elemental balance results for several selected cellulose pyrolysis experiments is given in Table 19. The elemental analysis of the liquids was carried out by B.C. Research (Vancouver) while that of the gases was provided by appropriate calculations using the gas chromatograph results. The elemental composition of the char component was taken from typical values in the literature. Any errors associated with this assumption for char will be negligible since the mass yield of char from cellulose pyrolysis is practically negligible. The carbon balance ranged form 94 to 101 percent (output/input) with a mean of 98%. Hydrogen and oxygen balances ranged from 100 to 127 and 97 to 103 percent, respectively, with mean values of 108 and 99 percent, respectively.

TABLE 19. AVICEL CELLULOSE FAST PYROLYSIS ELEMENTAL BALANCE SUMMARY

RUN NUMBER	ELEMENTAL MASS (g)						ELEMENTAL BALANCE (% Output/Input)		
	OUTPUT			INPUT					
	C	H	O	C	H	O	C	H	O
CK366	7.1	1.1	8.0	7.0	1.0	8.2	101	106	98
CK369	8.8	1.4	10.8	9.3	1.4	10.5	95	100	103
CK370	8.7	1.5	10.6	9.3	1.4	10.9	94	107	97
CK374	11.1	1.9	13.0	11.3	1.5	13.3	98	127	98
CK375	10.1	1.6	12.1	10.1	1.5	12.0	100	107	101
								*	
MEAN VALUES (ELEMENTAL BALANCE)							98	105	99

* As discussed in the text, this "adjusted" mean does not include the value of 127%. The non-adjusted mean is 109%.

Although the results of the elemental balance are quite remarkable considering that five samples were randomly selected and products were analyzed at two independent laboratories (i.e., the gases at U.W.O. and the liquid products at B.C. Research), the relatively high value of the hydrogen balance is largely due to a single sample (127%). If the results of this sample are discarded (assuming the analysis may be in error), then the "adjusted" mean for the hydrogen balance is 105 percent. Overall, the results of the elemental and mass balances support the accuracy of the individual product analyses and also give credence to the reported mass yields of the individual components. In turn, this supports the utility of the data for kinetic modelling.

8.5 WOOD FAST PYROLYSIS

Upon completion of the cellulose Ultrapyrolysis study at the University of Western Ontario, there was sufficient time and resources to conduct a *preliminary* investigation of the fast pyrolysis of wood. About 65 IEA poplar Ultrapyrolysis experiments were carried out in the temperature range of 650 to 850°C. This number was inadequate for kinetic modelling but was suitable to give an indication of general product yields and also the product distribution for gaseous components. However, the author was able to continue pyrolysis studies of IEA poplar at the Ensyn RTP facility in Ottawa. Approximately 55 additional experiments were conducted to provide data at 900°C,

and to supplement the Ultrapyrolysis data in the temperature range of 650 to 850 °C. Preliminary modelling studies were conducted using this data, as presented in Chapter 9, but lacked the depth of treatment that was given to the cellulose data (for example, no wood fast pyrolysis experiments were conducted at 875°C). The general wood pyrolysis results are therefore presented here in their entirety to make them available to the bioenergy research community. Other researchers are encouraged to further analyze the wood pyrolysis data for mechanistic and kinetic modelling.

The results of the production of total gas and the component gases produced during the fast pyrolysis of the IEA poplar wood at temperatures between 650 and 900 °C, are given in Tables 20 to 26. The "UP" series of runs designates those experiments conducted at the U.W.O. Ultrapyrolysis mini-pilot plant, while the runs labelled "POP" are those experiments carried out in the Ensyn RTP equipment.

TABLE 20. IEA POPLAR FAST PYROLYSIS EXPERIMENTS AT 650°C

RUN NO.	RESIDENCE TIME (ms)	PRODUCT MASS YIELD (%)									
		Gas	H_2	CO	CO_2	C_2H_4	C_3H_6	C_2H_2	CH_4	C_2H_6	B/T *
POP-09	800	32.9	0.1	16.5	9.9	1.6	0.0	0.2	3.3	0.4	0.5
POP-31	324	31.0	0.1	19.2	6.3	1.3	0.1	0.0	2.2	0.3	0.6
POP-32	524	33.1	0.1	21.1	6.2	1.4	0.1	0.0	2.4	0.4	0.4
POP-38	640	33.6	0.1	21.1	6.9	1.5	0.0	0.0	2.1	0.4	0.7
POP-44	390	30.4	0.1	19.1	5.6	1.6	0.1	0.0	2.2	0.3	0.7
POP-52	287	25.8	0.0	12.5	7.1	2.1	0.0	0.1	1.3	0.3	1.5
POP-53	325	30.9	0.1	17.7	6.3	2.2	0.0	0.1	1.8	0.3	1.7
POP-56	210	24.9	0.1	13.5	6.9	1.4	0.0	0.0	1.1	0.3	0.8

* B/T - benzene/toluene

TABLE 21. IEA POPLAR FAST PYROLYSIS EXPERIMENTS AT 700°C

RUN NO.	RESIDENCE TIME (ms)	PRODUCT MASS YIELD (%) Gas	H_2	CO	CO_2	C_2H_4	C_3H_6	C_2H_2	CH_4	C_2H_6	B/T *
POP-30	450	37.7	0.2	21.3	8.3	1.2	0.3	0.0	5.4	0.2	0.7
POP-36	624	37.7	0.1	24.3	6.5	1.8	0.5	0.2	3.0	0.4	0.9
POP-39	771	40.7	0.2	25.9	6.4	2.3	0.7	0.2	3.3	0.5	0.9
POP-40	950	37.8	0.2	23.3	7.0	1.8	0.7	0.1	3.0	0.4	0.9
POP-41	206	37.8	0.2	23.8	6.8	1.9	0.5	0.2	2.8	0.4	0.9
POP-42	340	37.1	0.2	23.4	6.2	2.1	0.7	0.3	2.5	0.4	1.3
POP-46	570	39.9	0.3	25.4	6.2	2.5	0.4	0.3	3.4	0.4	0.8
POP-54	305	38.6	0.1	25.3	6.5	2.2	0.5	0.3	2.5	0.4	0.7
POP-55	197	36.5	0.2	22.2	7.5	2.2	0.3	0.2	2.1	0.5	0.6
UP-10	462	39.9	0.2	24.2	8.1	2.0	0.5	0.2	2.4	0.5	1.6
UP-11	298	36.9	0.2	21.9	7.8	1.8	0.7	0.2	2.3	0.4	1.6
UP-12	204	33.0	0.1	19.0	7.9	1.4	0.6	0.2	1.8	0.5	1.5
UP-13	123	28.7	0.1	16.0	7.7	1.1	0.5	0.0	1.5	0.4	1.3
UP-14	90	25.4	0.0	14.0	7.1	1.0	0.5	0.0	1.3	0.5	1.1
UP-16	345	32.2	0.2	18.7	7.4	1.4	0.6	0.1	2.1	0.4	1.3
UP-17	177	32.7	0.1	19.2	7.7	1.3	0.6	0.2	1.8	0.4	1.4
UP-18	123	25.0	0.1	14.6	6.2	0.9	0.5	0.1	1.3	0.3	1.0
UP-19	671	36.8	0.2	22.9	6.6	1.8	0.8	0.2	2.5	0.3	1.5
UP-20	323	38.2	0.2	23.6	7.1	1.9	0.7	0.3	2.4	0.4	1.7
UP-21	719	40.3	0.3	25.1	7.1	2.0	0.8	0.2	2.7	0.4	1.8
UP-37	510	40.2	0.3	25.7	7.0	1.9	0.8	0.2	2.5	0.4	1.3

* B/T - benzene/toluene

TABLE 22. IEA POPLAR FAST PYROLYSIS EXPERIMENTS AT 750°C

RUN NO.	RESIDENCE TIME (ms)	PRODUCT MASS YIELD (%) Gas	H_2	CO	CO_2	C_2H_4	C_3H_6	C_2H_2	CH_4	C_2H_6	B/T *
POP-34	630	60.4	0.3	37.7	9.9	3.7	0.6	0.4	5.5	0.6	1.7
POP-35	520	58.8	0.4	37.8	8.7	3.8	0.5	0.4	5.3	0.6	1.3
POP-37	731	55.6	0.4	36.1	8.5	3.4	0.7	0.3	5.0	0.6	0.4
POP-43	380	52.5	0.3	31.8	9.6	3.3	0.8	0.5	3.8	0.5	1.6
POP-45	600	61.2	0.4	39.0	8.8	4.3	0.4	0.5	5 9	0.4	1.2
POP-48	500	52.0	0.2	33.1	7.8	3.3	0.7	0.5	4.7	0.5	1.3
POP-49	300	52.0	0.2	33.2	7.7	3.7	0.3	0.3	4.4	0.5	1.5
POP-57	205	48.4	0.4	31.3	7.8	3.1	0.3	0.4	3.9	0.5	0.7
UP-39	496	59.6	0.6	37.1	9.3	3.4	1.1	0.5	4.6	0.6	2.4
UP-41	339	54.7	0.6	34.2	8.7	3.0	1.0	0.4	3.9	0.6	2.3
UP-42	166	43.8	0.4	27.5	7.4	2.2	0.8	0.3	2.8	0.4	1.8
UP-43	114	41.8	0.4	26.4	6.9	2.1	0.8	0.3	2.7	0.4	1.8
UP-44	595	58.7	0.7	36.3	9.4	3.3	1.1	0.4	4.5	0.5	2.5
UP-45	205	45.9	0.4	27.3	9.0	2.4	0.8	0.3	3.0	0.5	2.1
UP-46	356	59.3	0.6	34.2	11.9	3.2	1.1	0.4	4.6	0.6	2.8
UP-47	251	54.5	0.5	31.5	11.0	2.9	1.0	0.4	4.1	0.8	2.4
UP-48	151	44.7	0.4	26.2	9.5	2.2	0.8	0.3	2.9	0.5	2.0
UP-49	199	46.5	0.4	27.1	9.5	2.3	0.9	0.2	3.1	0.7	2.2
UP-50	133	47.2	0.4	27.3	9.8	2.3	0.9	0.3	3.0	0.9	2.4
UP-74	65	37.0	0.1	22.7	7.8	1.7	0.7	0.3	1.9	0.5	1.5

* B/T - benzene/toluene

TABLE 23. IEA POPLAR FAST PYROLYSIS EXPERIMENTS AT 800°C

RUN NO.	RESIDENCE TIME (ms)	PRODUCT MASS YIELD (%)									
		Gas	H_2	CO	CO_2	C_2H_4	C_3H_6	C_2H_2	CH_4	C_2H_6	B/T *
POP-50	570	63.6	0.5	43.3	6.8	4.0	0.3	0.5	6.7	0.4	1.0
POP-58	190	56.7	0.5	38.0	8.4	3.3	0.3	0.4	4.3	0.5	0.6
POP-74	374	65.3	0.4	41.3	8.9	4.8	0.2	1.0	5.4	0.6	1.9
POP-94	553	65.9	0.7	41.2	9.2	4.5	0.3	1.5	6.3	0.3	2.0
UP-22	527	69.1	0.9	41.9	10.8	4.3	1.0	0.6	5.6	0.6	3.3
UP-24	236	60.3	0.6	37.1	9.4	3.5	0.9	0.6	4.5	0.7	3.1
UP-25	141	52.3	0.6	31.9	9.2	2.7	0.9	0.4	3.2	0.6	2.6
UP-26	92	48.5	0.5	29.4	8.6	3.1	0.8	0.5	2.8	0.7	2.2
UP-29	71	42.8	0.4	26.0	7.9	2.2	0.7	0.4	2.5	0.7	1.9
UP-30	474	65.3	0.9	40.2	9.6	4.3	0.9	0.7	5.5	0.6	2.8
UP-31	273	66.5	0.8	41.0	9.9	4.3	1.0	0.7	5.0	0.7	3.0
UP-32	345	65.3	0.8	39.9	10.1	4.2	0.9	0.7	5.4	0.6	2.7
UP-33	623	69.6	1.1	42.0	10.6	4.7	0.9	0.8	5.9	0.6	2.9
UP-34	195	65.1	0.8	40.0	10.0	3.9	1.0	0.7	5.0	0.6	3.0
UP-35	128	55.9	0.6	34.8	8.6	3.3	1.0	0.5	3.9	0.7	2.5
UP-36	107	51.8	0.6	32.5	7.9	3.0	0.9	0.5	3.7	0.5	2.2
UP-38	76	53.3	0.6	33.8	7.8	3.2	0.9	0.6	3.2	0.8	2.6
UP-75	61	52.2	0.2	30.6	7.1	3.1	1.0	0.5	3.4	0.9	2.4
UP-83	62	45.1	0.2	29.7	5.1	2.6	0.8	0.4	3.1	0.9	2.3

* B/T - benzene/toluene

TABLE 24. IEA POPLAR FAST PYROLYSIS EXPERIMENTS AT 825°C

RUN NO.	RESIDENCE TIME (ms)	PRODUCT MASS YIELD (%)									
		Gas	H_2	CO	CO_2	C_2H_4	C_3H_6	C_2H_2	CH_4	C_2H_6	B/T *
POP-80	200	66.8	0.3	41.1	10.4	4.7	0.6	0.6	4.7	0.7	2.9
UP-62	334	70.5	0.9	41.5	11.5	4.6	0.9	0.8	6.0	0.7	3.6
UP-63	282	74.7	0.9	44.2	12.7	4.8	1.1	0.8	6.4	0.8	3.1
UP-64	233	70.9	0.9	41.5	12.4	4.5	1.1	0.7	5.9	0.8	3.2
UP-65	139	63.6	0.8	37.5	11.1	3.9	1.0	0.6	4.9	0.7	3.0
UP-66	580	72.8	1.0	42.5	12.1	4.8	1.0	0.7	6.5	0.6	3.7
UP-67	117	69.8	0.8	40.4	12.8	4.0	1.2	0.7	5.3	0.9	3.6
UP-68	442	74.6	1.0	44.0	12.2	4.9	1.0	0.8	6.5	0.7	3.5
UP-69	530	74.9	0.9	44.3	12.5	4.9	1.0	0.7	6.6	0.6	3.4
UP-70	177	71.2	0.7	40.9	13.1	4.2	1.2	0.7	5.6	0.8	4.0
UP-71	154	64.4	0.7	37.5	11.7	4.0	1.0	0.6	5.2	0.7	3.0
UP-72	185	71.6	0.8	42.4	12.8	4.2	1.2	0.7	5.7	0.8	3.1
UP-80	61	49.3	0.2	29.6	9.1	2.8	0.8	0.4	3.2	1.1	2.1
UP-82	61	51.4	0.3	31.2	9.0	2.8	0.9	0.5	3.6	0.8	2.4

* B/T - benzene/toluene

TABLE 25. IEA POPLAR FAST PYROLYSIS EXPERIMENTS AT 850°C

RUN NO.	RESIDENCE TIME (ms)	PRODUCT MASS YIELD (%)									
		Gas	H_2	CO	CO_2	C_2H_4	C_3H_6	C_2H_2	CH_4	C_2H_6	B/T *
POP-75	200	73.7	0.6	46.0	10.4	4.9	0.6	1.6	6.1	0.5	1.9
POP-76	350	73.5	0.5	45.7	11.1	4.8	0.4	1.5	6.0	0.5	2.8
POP-83	330	68.9	0.3	42.6	9.9	4.8	0.4	1.8	5.4	0.5	3.1
POP-86	180	73.6	0.6	45.6	10.2	5.7	0.5	1.5	6.1	0.6	3.0
POP-88	262	73.0	0.5	45.3	10.1	5.5	0.5	1.6	6.3	0.4	2.7
POP-90	310	75.2	0.7	46.3	10.7	5.0	0.7	1.4	6.4	0.5	3.2
UP-51	321	72.0	1.0	42.5	12.1	4.8	0.9	0.9	6.1	1.0	2.7
UP-52	398	74.4	1.2	43.8	12.2	5.1	0.7	1.0	6.7	0.6	3.1
UP-55	588	76.7	1.2	46.2	12.0	5.3	0.7	1.0	6.9	0.6	3.0
UP-56	121	75.9	0.9	43.0	11.9	4.6	1.0	0.8	5.9	1.0	3.8
UP-57	108	67.4	0.8	39.8	11.2	4.3	1.0	0.8	5.2	0.9	3.4
UP-58	582	71.4	1.3	42.8	11.2	4.9	0.7	0.9	6.5	0.6	2.7
UP-59	85	70.0	0.8	41.8	11.8	4.2	0.9	0.9	4.8	0.9	4.1
UP-60	368	74.2	1.1	44.5	11.8	5.1	0.9	0.9	6.5	0.6	2.8
UP-61	97	69.0	0.8	40.4	12.1	4.2	1.1	0.7	5.5	0.9	3.4
UP-73	87	64.7	0.7	38.4	11.1	4.0	1.0	0.8	4.8	0.9	3.2
UP-77	248	72.0	0.5	44.1	11.3	4.9	0.9	0.9	6.3	0.8	2.4
UP-78	270	74.5	0.8	44.5	11.5	4.9	0.9	0.9	6.3	0.7	4.0
UP-79	62	65.1	0.4	38.6	11.3	4.0	1.1	0.8	4.3	1.2	3.5
UP-81	325	71.2	0.8	42.8	11.5	4.7	0.9	0.7	6.3	0.6	2.9

* B/T - benzene/toluene

TABLE 26. IEA POPLAR FAST PYROLYSIS EXPERIMENTS AT 900°C

RUN NO.	RESIDENCE TIME (ms)	PRODUCT MASS YIELD (%)									
		Gas	H_2	CO	CO_2	C_2H_4	C_3H_6	C_2H_2	CH_4	C_2H_6	B/T *
POP-77	350	77.8	0.8	48.4	10.9	5.0	0.4	2.0	6.6	0.4	3.3
POP-78	300	78.5	0.3	48.0	11.0	5.0	0.3	2.4	6.1	0.5	4.9
POP-79	200	74.3	0.6	46.2	10.2	5.4	0.2	1.9	6.0	0.5	3.2
POP-84	260	79.8	0.6	49.8	11.8	6.1	0.5	0.8	7.0	0.3	2.8
POP-89	300	75.4	0.8	46.0	11.3	5.0	0.4	1.9	6.5	0.4	2.9
POP-91	341	78.6	1.1	49.0	11.1	5.3	0.4	1.2	7.4	0.3	2.4
POP-92	400	78.5	1.0	48.4	11.3	4.9	0.3	1.4	7.4	0.3	3.2
POP-93	182	75.1	0.4	46.8	10.6	5.8	0.5	1.5	6.3	0.5	2.7
POP-95	80	73.0	0.3	45.5	10.3	5.4	0.5	1.3	5.8	0.6	3.3

* B/T - benzene/toluene

The yields of total gas, liquid (including product water and organics), and char are plotted as a function of residence time in Figures 28 to 34. Corresponding curves for some of the component gases are given in Chapter 9. The solid lines which correspond to the gas yield data represent kinetic modelling results (Chapter 9). The curves for liquid yields from poplar are generated by taking the difference between the total poplar feedstock mass and the mass of total gas plus char. The constant char yields were determined from the mass balance procedures in which complete product collection took place, and were confirmed with Waterloo pyrolysis data [175]. It is implicitly assumed that any minor deficiency in the mass balance (ie. an average of 3 to 4 %) is because of evaporative losses of the lightest fraction of the liquids during recovery.

As was the case with cellulose fast pyrolysis results, the general shape of the total gas yield curves (Figures 28 to 34) is consistent for each temperature, and is characterized by an initial rapid production rate followed by levelling to an asymptotic maximum yield. This is representative of the shape of the curves for the yields of all *principal* gas components. From the experimental data, it is clear that the principal gaseous components are CO, CO_2, H_2, CH_4, C_2H_4, and C_2H_2. The minor gaseous components are ethane and propylene. Their yield curves do not exhibit the characteristic asymptotic behaviour since at elevated temperatures, these gases are cracking as they appear [8].

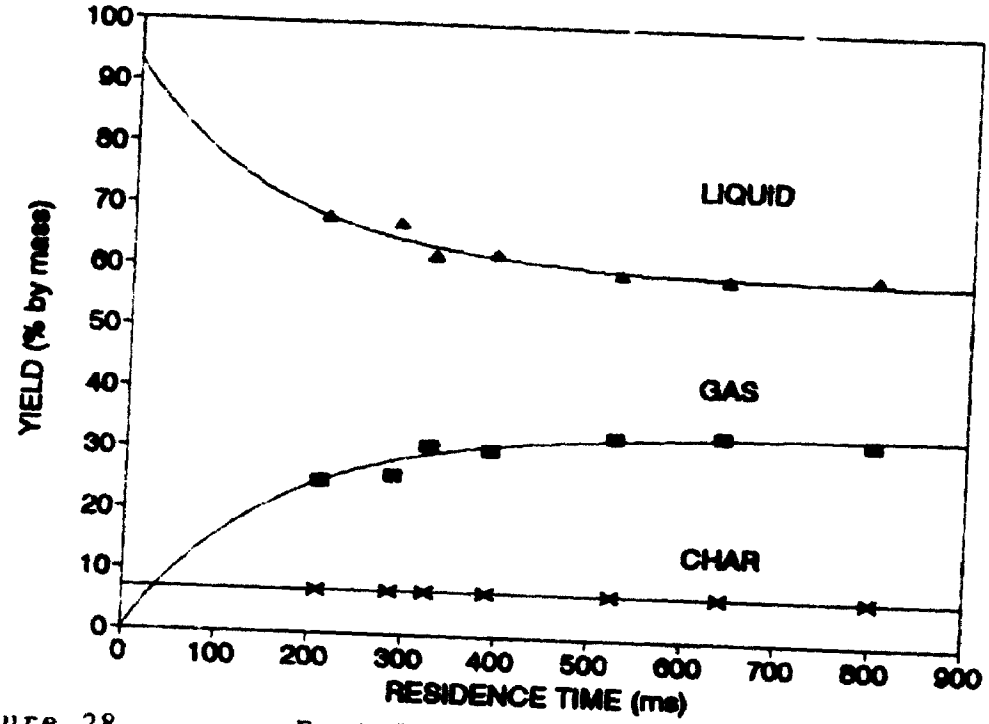

Figure 28. Fast Pyrolysis of IEA Poplar at 650°C: Total Gas, Liquid and Char Yields vs. Residence Time (Run Numbers and Data in Table 20)

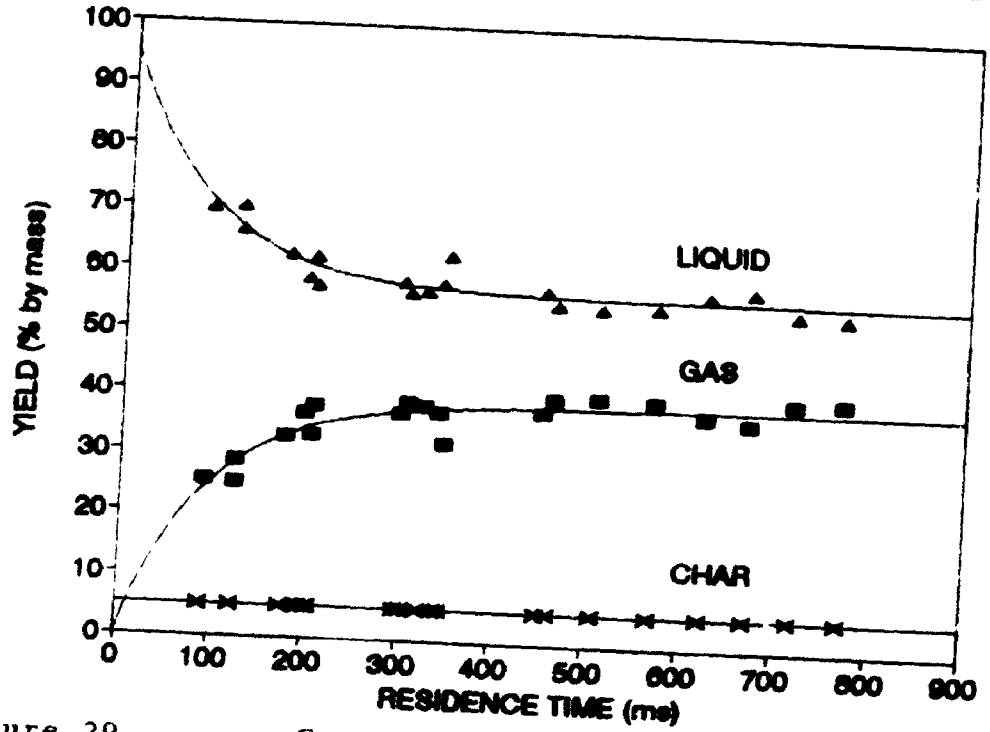

Figure 29. Fast Pyrolysis of IEA Poplar at 700°C: Total Gas, Liquid and Char Yields vs. Residence Time (Run Numbers and Data in Table 21)

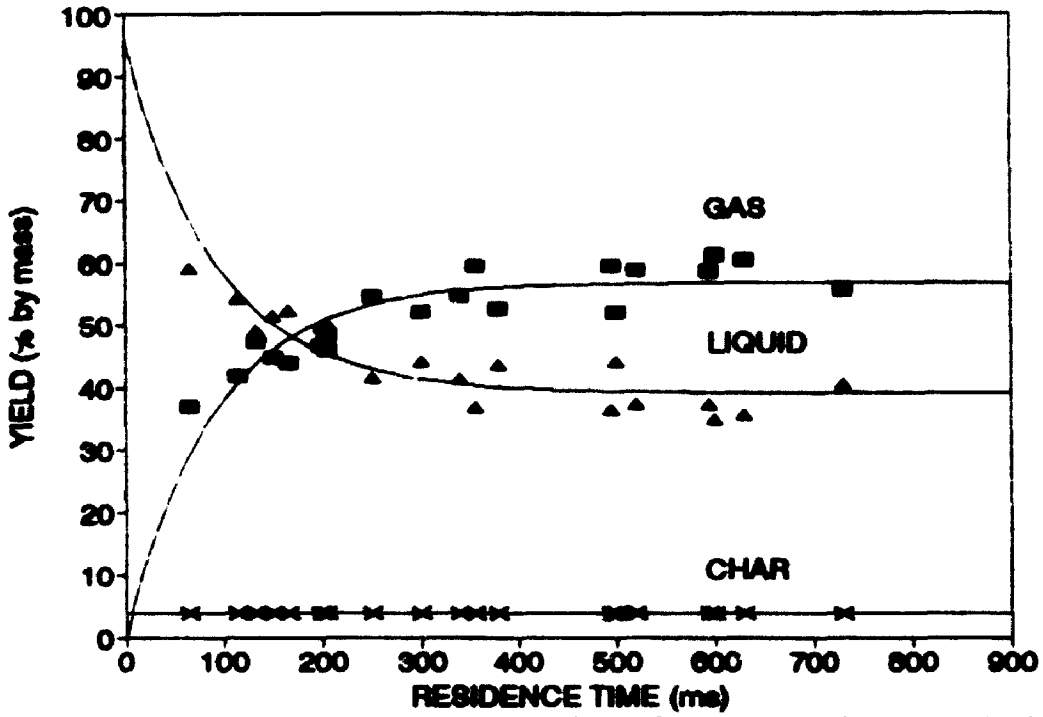

Figure 30. Fast Pyrolysis of IEA Poplar at 750°C: Total Gas, Liquid and Char Yields vs. Residence Time (Run Numbers and Data in Table 22)

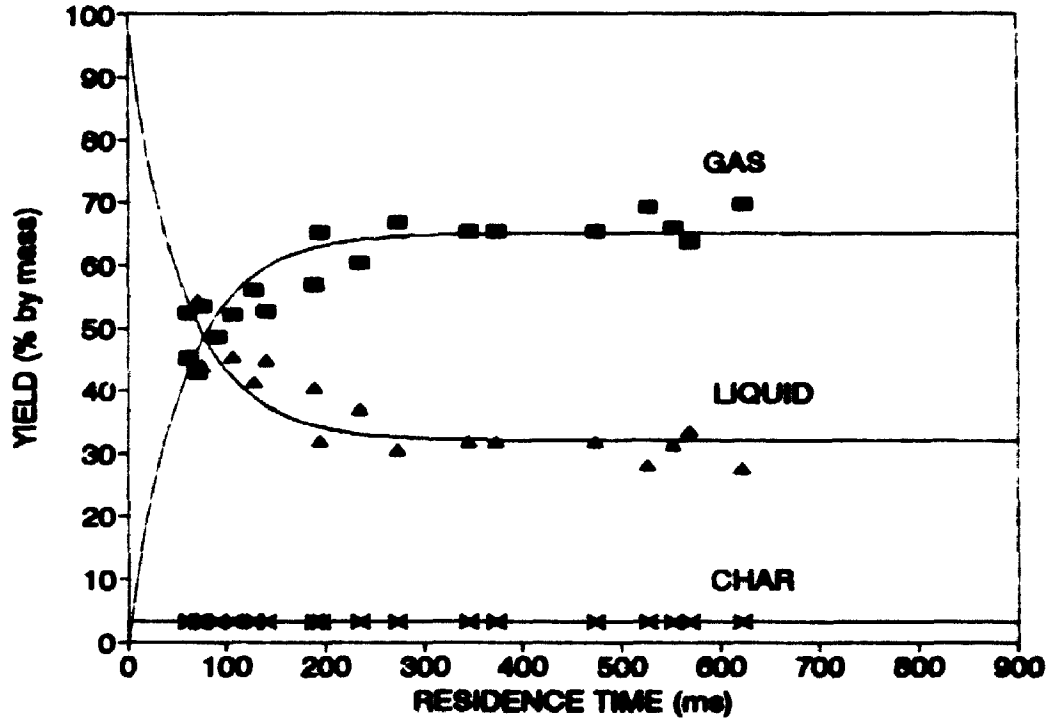

Figure 31. Fast Pyrolysis of IEA Poplar at 800°C: Total Gas, Liquid and Char Yields vs. Residence Time (Run Numbers and Data in Table 23)

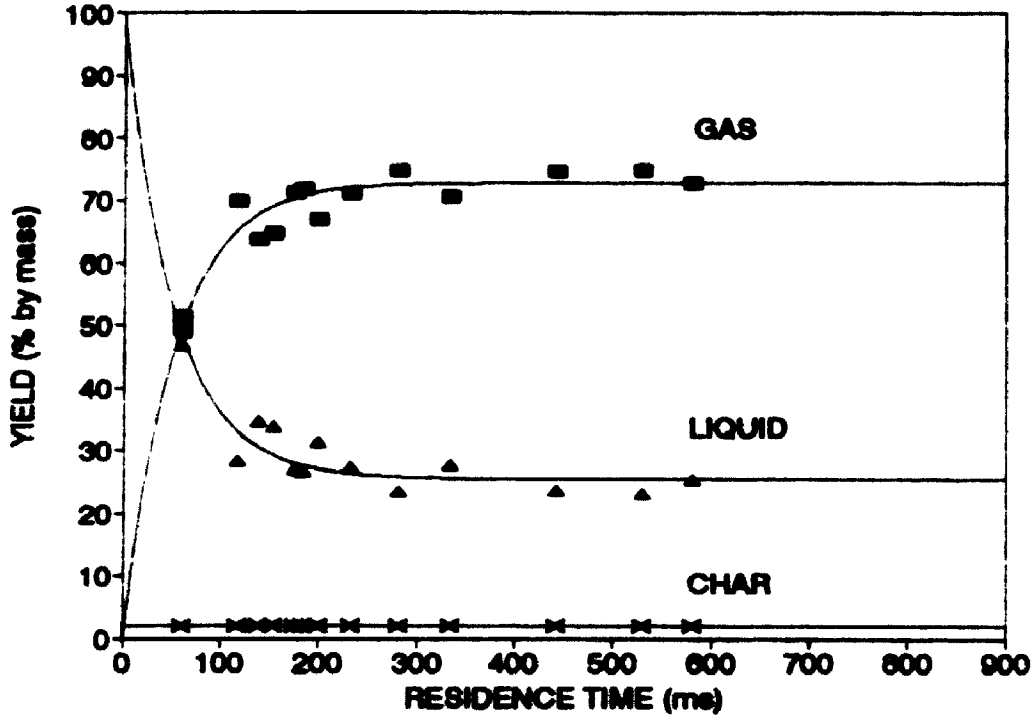

Figure 32. Fast Pyrolysis of IEA Poplar at 82[illegible]°C: Total Gas, Liquid and Char Yields vs. Residence Time (Run Numbers and Data in Table 24)

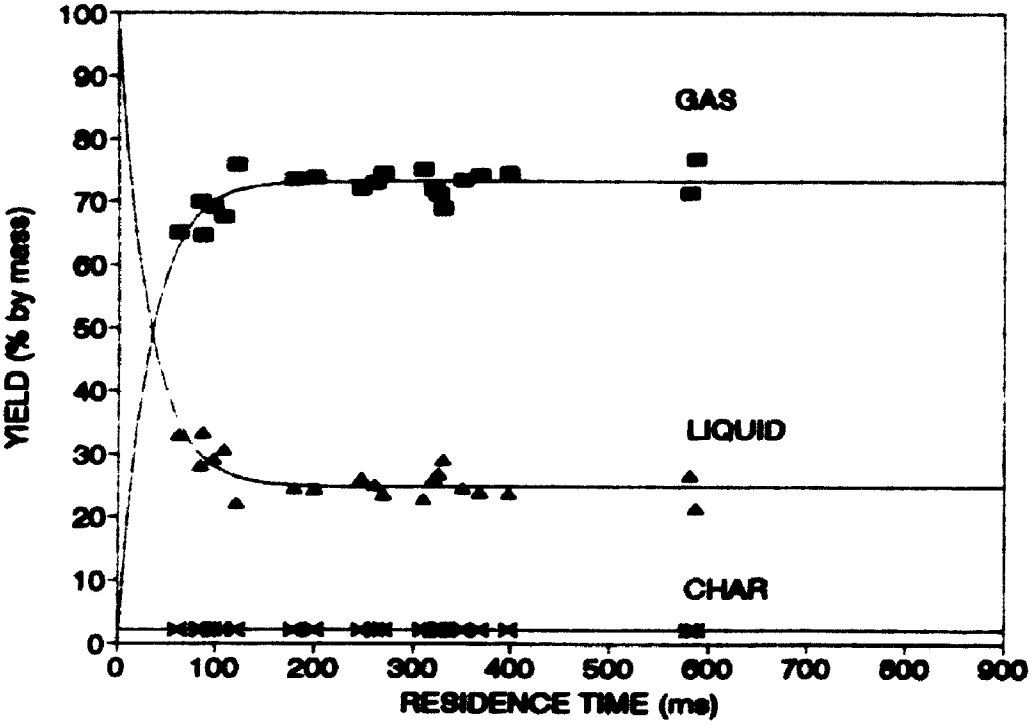

Figure 33. Fast Pyrolysis of IEA Poplar at 850°C: Total Gas, Liquid and Char Yields vs. Residence Time (Run Numbers and Data in Table 25)

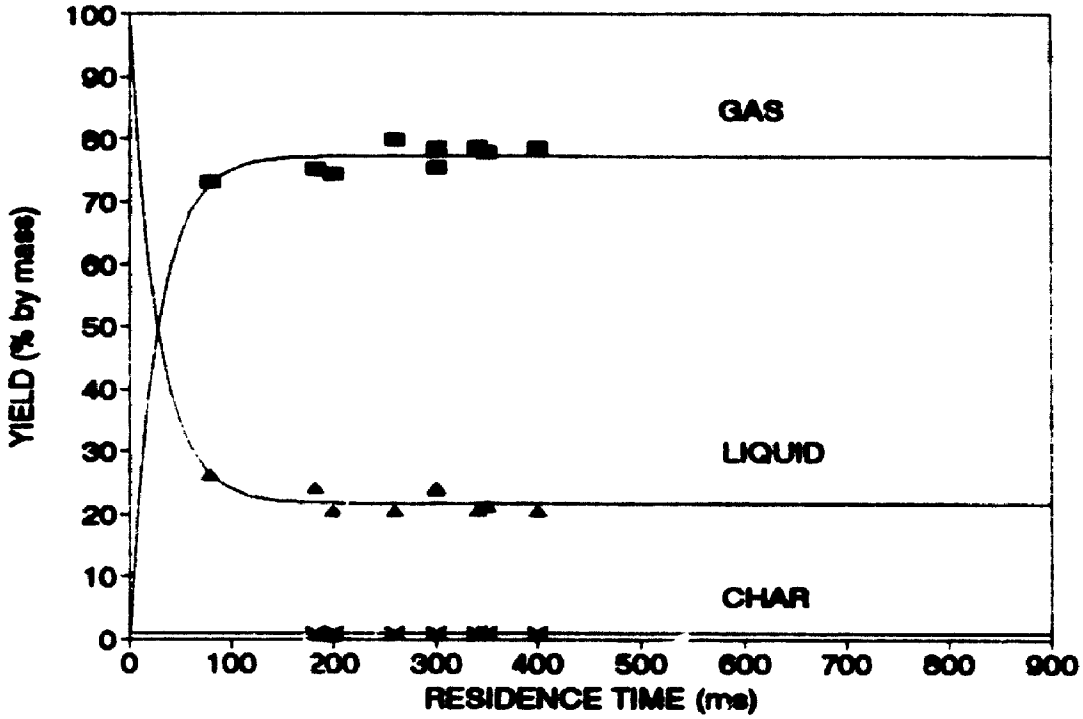

Figure 34. Fast Pyrolysis of IEA Poplar at 900°C: Total Gas, Liquid and Char Yields vs. Residence Time (Run Numbers and Data in Table 26)

The initial production rates of the principal gases, as represented by the slopes of the lines, vary both with temperature and gas component. Consistent with kinetic theory, the rates increase with increasing temperature. It is also evident that the asymptotic total gas yield increases from 33.9 percent (by mass) to 77.3 percent as the temperature is increased from 500°C to 900°C. Over this same temperature range, the maximum asymptotic mass yields of hydrogen, carbon monoxide and carbon dioxide increase from 0.0 to 1.0, 20.1 to 47.9, and 7.2 to 11.4 percent, respectively. Corresponding values for ethylene, total unsaturates (i.e., olefins and alkynes) and total hydrocarbons are 1.7 to 5.4, 1.8 to 7.5, and 5.5 to 15.0 percent, respectively. These asymptotic values are taken from the results of the regression analysis, as reported in the kinetic modelling study (Chapter 9), and not directly from the data tables.

Once again, there is evidence both from the data and modelling (Chapter 9) which suggests that CO and CO_2 (and consequently, total gas) are already present as prompt gas before subsequent production via the secondary cracking reactions. The composition of this gas is described in subsequent paragraphs.

The production of ethane, acetylene and propylene clearly does not fully follow the pattern which is characteristic of the production of principal gaseous products, as described in the

preceding paragraphs. In contrast to cellulose pyrolysis, ethane appears in the product distribution at 650°C with a yield of about 0.4% which is independent of residence time. This may suggest that a small amount of ethane is a prompt gas product. Additional evidence for this is the fact that ethane yield remains constant at about 0.4%, even when the pyrolysis temperature is 700°C. At 750°C, ethane increases from 0.4 to 0.8 % with increasing residence time, and then drops to about 0.5% as it begins to crack at the longest residence times. This behaviour, exhibited at 750°C, is repeated at temperatures up to 900°C, and the residence time at which cracking begins predictably decreases with increasing temperature.

Acetylene is not produced until reaction temperatures approach 750°C. Its constant maximum yield at each temperature, increases systematically from about 0.5% to about 1.0% as the temperature is increased from 750 to 800 °C. At 850°C, the acetylene yield increases to about 1.5% as the residence time approaches 180 ms and remains constant up to about 300 ms. From 300 ms to about 600 ms the yield drops to 0.9% as acetylene cracking begins to occur. At 900°C, a maximum acetylene yield of 2.4% is realized by about 300 ms, and then drops to about 1.3% at approximately 400 ms.

Aside from the fact that propylene is not present at 650°C, its behaviour closely resembles that of ethane at temperatures from 700 to 900 °C At 700°C, its yield gradually increases from about 0.4% to 0.8% with an increase in residence time. At

elevated temperatures, there is evidence of propylene cracking since a maximum yield is evident at some intermediate residence time followed by a decrease with a further increase in residence time. Propylene and acetylene are not present at the lowest pyrolysis temperatures and are therefore not prompt products of primary wood fast pyrolysis.

The wood-derived prompt gas yield and composition can be determined implicitly from the data presented in this Section and explicitly from the modelling results presented in Chapter 9. Consequently, the prompt gas yield is estimated to be approximately 7% of the mass of the poplar feedstock. About 70% of this is CO_2 (equivalent to about 5% of the poplar mass) and 20% is CO (equivalent to about 1.5% of the poplar mass). Methane and other hydrocarbons each constitute approximately 5% of the prompt gas (together, equivalent to 0.5% of the feed).

Diebold [55] states that the prompt gas from fast pyrolysis amounts to about 4% of the mass of the wood feedstock. He deems the composition to be approximately 55% CO_2, 40% CO, 3% CH_4 and 1% C_2H_4. The balance is made up of trace amounts of hydrogen and C_3+ hydrocarbons. The data presented in this thesis is in general agreement with the composition of Diebold's prompt gas. However, in quantitative terms there are significant differences. For example, the thesis data suggests that the amount of CO_2 in the wood-derived prompt gas exceeds that of CO by a factor of about 3. Diebold's corresponding factor is less than 2. The difference could be explained in terms of feedstock

material since Diebold used a mixed softwood sawdust while IEA poplar (hardwood) was for the wood pyrolysis experiments reported here. In any event, the quantity of prompt gas is relatively small compared to the overall gas yield, particularly at elevated temperatures and long residence times.

The asymptotic values of the liquid yields (representing the minimum liquid yields at each temperature) decrease from 62 to 20% by mass as the temperature is increased from 650 to 900 °C. The total liquid yields could be drastically increased at each temperature simply by reducing the reactor residence time from the asymptotic region. The maximum liquid yields from IEA poplar observed during the thesis experimental work was approximately 70% at 650 °C and 210 ms. It is important to note, however, that the asymptotic liquid yields are still increasing as the temperature is reduced to 650°C. Higher liquid yields are therefore expected at lower temperatures, and this has been confirmed in subsequent studies (Appendix 1) and by other researchers [139,140,171-178].

Char yields were measured for 90 percent of the Ultrapyrolysis poplar experiments. It was apparent from the results that these yields were dependent upon reactor temperature but relatively independent of the residence time. As illustrated in Figures 28 to 34, the char yields decrease from 7 to 1 percent of the poplar feedstock mass as the temperature is increased from 650 to 900°C.

Mass balances were carried out on more than half of the Ultrapyrolysis poplar experiments, and a summary of the results is given in Table 27. The average value of the product recovery is 96.5 percent of the mass of poplar pyrolysed. As was the case for cellulose experiments, the minor consistent deficit in the mass balance can easily be accounted for as uncondensed water vapour in the saturated carrier gas and evaporative losses. The product recovery ranged from 92.9 to 105.6 percent by mass. Only two values (out of 36 mass balance experiments) were over 100 percent.

There are clearly some significant differences between the fast pyrolysis of cellulose and that of the representative wood. The maximum yield of total gas is 90% for cellulose and 80% for wood. Corresponding values for total liquids are 88% for cellulose and 75% for wood. Cellulose did not produce any char over the temperature or residence time ranges studied while wood produced 7 to 1 % char as the pyrolysis temperature increased from 650 to 900 °C. Wood produced almost 50% more prompt gas than did cellulose, and the dominant wood-derived prompt gas product was CO_2. The dominant cellulose-derived prompt gas product was CO. The mass ratio of CO_2 to CO was greater than 2:1 for wood prompt gas and was 1:2 for cellulose prompt gas. Wood pyrolysis gave more CO2 (a maximum yield of 12% vs 6% for cellulose). Cellulose produced more CO (a maximum yield of 67% vs 50% for wood), H_2 (a maximum yield of 2% vs 1% for wood) and hydrocarbons (a maximum of 18% vs 15% for wood) than did wood.

TABLE 27. IEA POPLAR FAST PYROLYSIS MASS BALANCE SUMMARY

RUN NUMBER	POPLAR FED (g)	PRODUCT RECOVERY (g) *				TOTAL RECOVERY (% by mass)
		GAS	LIQUID	CHAR	TOTAL	
PWK12	24.9	8.1	15.6	0.7	24.4	98.0
PWK14	25.8	6.5	17.8	1.1	25.4	98.5
PWK15	28.8	9.2	19.6	1.6	30.4	105.6
PWK17	23.9	7.8	14.2	1.2	23.2	97.1
PWK18	24.9	6.2	16.9	1.2	24.3	97.6
PWK19	19.0	6.6	11.4	0.8	18.8	98.9
PWK20	16.9	6.4	9.2	0.8	16.4	97.0
PWK24	23.0	13.7	9.1	0.7	23.5	102.2
PWK25	20.9	10.8	8.6	0.7	20.1	96.2
PWK26	17.7	8.5	7.8	0.5	16.9	95.5
PWK27	24.0	12.2	10.6	0.7	23.5	97.9
PWK28	21.0	11.0	8.9	0.9	20.8	99.0
PWK29	17.7	7.5	8.8	0.6	16.9	95.5
PWK30	23.8	15.4	7.3	0.2	22.9	96.2
PWK31	13.8	9.1	3.7	0.3	13.1	94.9
PWK32	29.0	18.8	8.4	0.4	27.6	95.2
PWK33	29.0	20.0	6.9	0.8	27.7	95.5
PWK34	20.8	13.4	5.9	0.5	19.8	95.2
PWK35	23.8	13.2	9.0	0.5	22.7	95.4
PWK36	13.7	7.0	5.6	0.4	13.0	94.9
PWK37	31.9	12.7	16.4	1.4	30.5	95.6
PWK38	17.2	9.1	6.8	0.6	16.5	95.9
PWK39	25.9	15.3	8.8	0.7	24.8	95.8
PWK41	24.0	13.0	8.9	1.0	22.9	95.4
PWK42	29.9	13.0	14.8	0.7	28.5	95.3
PWK43	29.8	12.4	16.1	0.5	29.0	97.3
PWK44	26.0	15.1	8.8	0.8	24.7	95.0
PWK45	14.4	6.6	6.7	0.4	13.7	95.1
PWK46	15.0	8.9	4.9	0.7	14.5	96.7
PWK47	22.9	12.4	9.0	0.6	22.0	96.1
PWK48	21.8	9.7	10.5	0.7	20.9	95.9
PWK49	23.9	11.0	10.9	0.8	22.7	95.0
PWK50	19.8	9.3	9.1	0.4	18.8	95.0
PWK51	21.8	15.2	5.2	0.3	20.7	95.0
PWK52	19.8	14.2	4.0	0.2	18.4	92.9
PWK55	22.0	17.9	2.8	0.4	21.1	95.9

8.6 BIOMASS PARTICLE SIZE STUDY

From the point of view of fast pyrolysis commercialization, the limitation of maximum feedstock particle size is extremely important. Rensfelt (155) has shown that the reduction of a biomass particle from "chip" sizes (10 to 30 mm) to about 1 mm requires *relatively* small quantities of energy for comminution. However, there is a rapid exponential growth in the energy requirement for the comminution of biomass from 1 mm to "powder" (ie. under 500 um), since in this circumstance, the biomass fibre itself must be severely disrupted and disintegrated.

As reviewed in Section 2.9, *theoretical* investigations have predicted that fast pyrolysis could be successfully achieved with biomass particles up to 1 or 2 mm. "Successful" may be defined as pyrolysis with no significant change in product distribution using larger particles. A preliminary experimental study was initiated to *empirically* examine the effect of particle size on product yields during fast pyrolysis. In terms of heat transfer, the worst-case scenario for such a study is for the fast pyrolysis system to be operated at moderate temperatures, between 400 and 600 °C, rather than at higher temperatures. This is clearly evident in a study by Reed [150] where the surface ablation rate is shown to be directly proportional to the difference between the pyrolysis "bath" temperature and the initial particle temperature. Temperatures in the lower range were therefore selected for the study. Wood feedstocks were used rather than cellulose because the reference

cellulose feedstock (Avicel) was not available at the desired larger particle size of 1.0 mm.

The results of the investigation are summarized in Table 28, and indicate that the pyrolysis of wood with an average particle size of 1.0 mm (1.5 mm maximum) compares quite favourably with the pyrolysis of 100 um wood under similar conditions of temperature and residence time. The first four runs listed in Table 28 were conducted at residence times which place the overall product distributions in the asymptotic region of the yield curves (Sections 8.4 and 8.5). At 500°C, the asymptotic total gas yield is 10.9% for 1.0 mm particles and 10.0 for 0.1 mm particles. Corresponding liquid yields are 72.6% and 73.0%. At 525°C, the asymptotic yields for large and small particles are 15.4% and 15.3%, respectively for gas, and 70.9% and 70.7%, respectively for liquid.

The last four experiments listed in Table 28 were conducted at residence times which place the product distributions in the transition region of the yield curves (ie. where yields are strongly dependent on residence time). At 525°C and approximately 350 ms, the total gas yields from large and small wood particles are 9.2% and 10.1%, repectively, and the liquid yields from large and small wood particles are 73.7% and 75.9% respectively. At 525°C and approximately 300 ms, the total gas yields for large and small wood particles are 12.7% and 12.0%, repectively, and the liquid yields from large and small wood particles are 70.8 and 74.0%, respectively.

The necessary action of the particulate (sand) heat carrier during fast pyrolysis, and its role in bringing about rapid heat transfer, was clearly illustrated during the course of the peripheral particle size experiments. Out of the nine "formal" runs which were undertaken using 1 mm wood feedstocks, five of the experiments resulted in a significant quantity of unpyrolyzed material in the product stream. During these five experiments only one of the three system heat carrier jets was used. The two remaining jets were inoperable because of maintenance work on the injectors and their corresponding thermofor ovens. Nevertheless, it was decided to proceed using the single jet. As a result, the turbulence and mixing between the hot sand and feedstock was greatly reduced and a significant amount of wood passed through the system unpyrolyzed or simply charred. The solid residues (including char and unpyrolyzed material) were 19 to 28% of the feedstock mass instead of 12 to 17% (char yield) which is normally expected in the temperature range of study (500 to 550 °C). The results which are given in Table 28 are exclusively those runs where the multiple jet heat carriers configuration was used.

It is clear that although this study is preliminary and does not involve full statistical analysis, there does not appear to be any significant loss of yield as the particle size is increased from 0.1 mm to greater than 1mm. This has been borne out in subsequent pilot plant studies [83,84] with wood particle sizes up to 4 mm.

TABLE 28. BIOMASS PARTICLE SIZE STUDY EXPERIMENTAL RESULTS

REACTION TEMPERATURE (°C)	PARTICLE SIZE (mm)	RUN NUMBER	RESIDENCE TIME (ms)	PRODUCT YIELD (% by mass)		
				Gas	Liquid	Solid
500	1.5	PS-11	1030	10.9	72.6	16.6
	0.1	PS-60	886	10.0	73.0	17.0
525	1.5	PS-10	950	15.4	70.9	13.7
	0.1	PS-06	900	15.3	70.7	14.0
525	1.5	PS-02	350	9.2	73.7	17.1
	0.1	PS-23	363	10.1	75.9	14.0
525	1.5	PS-03	280	12.7	70.8	16.5
	0.1	PS-25	329	12.0	74.0	14.0

8.7 WATER-GAS SHIFT REACTION STUDY

The literature review presented earlier in this report suggested that the water-gas shift reaction might play some role in determining the final product distribution of the fast pyrolysis gases. This reaction is represented as follows:

$$CO_2 + H_2 = CO + H_2O \quad (11)$$

It was decided to conduct a limited number of experiments in the Ultrapyrolysis system, and to monitor the extent of the homogeneous reaction on a time scale comparable to that for the fast pyrolysis of biomass. Carbon dioxide and hydrogen were selected as the feedstock gases due to their convenience with respect to procurement, feeding and metering (i.e., the reverse would require steam generation and flow metering). A mixture

consisting of 82.45 molar % hydrogen and 17.55 molar % carbon dioxide was procured from Matheson in Whitby, Ontario. The experimental procedure was similar to that reported for biomass experiments with the exception that feedstock gas flow was controlled and measured with rotameters. Feedstock gases were injected through the biomass injection tube where they were rapidiy heated to the reaction temperature by the inert nitrogen thermofor. The resulting mixture was diluted such that the nitrogen accounted for about 80% (by volume) of the total reacting gas. Experiments were conducted at 850 and 900°C.

The results of the water-gas shift reaction, investigated in the Ultrapyrolysis system, are given in Table 29. The initial H_2 and CO_2 concentrations (i.e., the concentrations at t = 0) are tabulated along with the concentration of CO_2 and CO at the indicated residence times. Equilibrium concentrations of CO_2 and CO, accounting for the reactor conditions of pressure, temperature and initial concentrations, are also tabulated.

The predicted concentration of CO_2 ($[CO_2]_p$) for each experiment is based on a homogeneous kinetic model for the forward direction of the reaction (i.e., $CO_2 + H_2 \rightarrow CO + H_2O$) as reported by Kochubei and Moin [100]. The reaction has been treated as an irreversible process since a literature review failed to provide the homogeneous kinetics of the reverse reaction (published heterogeneous reaction kinetic studies were numerous). However, the treatment of this reaction as irreversible proved to be adequate since an analysis of the

homogeneous model revealed that the rate is too slow to be a factor in the context of fast pyrolysis. In other words, if the reaction were properly treated as reversible, the net forward rate would be even slower than the estimated irreversible forward rate, and would thus remain insignificant under the stated experimental conditions. The results of this kinetic analysis are summarized as the predicted CO_2 concentrations ($[CO_2]_p$) in Table 29, and a sample of the results of the computer analysis is given for two shift experiments in Appendix 4.0.

TABLE 29. WATER-GAS SHIFT REACTION EXPERIMENTS AT 850 AND 900 °C: DATA SUMMARY

RUN NO.	TEMPERATURE (C)	RESIDENCE TIME (ms)	COMPONENT CONCENTRATION (molar x 10^4) $[H_2]_o$	$[CO_2]_o$	$[CO_2]_t$	$[CO_2]_e$	$[CO_2]_p$	$[CO]_t$	$[CO]_e$	APPROACH TO EQUILIBRIUM $[CO]_t/[CO]_e$
WG-2	850	178	19.2	3.93	3.61	0.65	3.93	0.43	3.40	0.13
WG-3		342	25.9	5.31	4.52	0.87	5.31	0.94	4.59	0.20
WG-4		91	29.4	6.02	5.75	0.99	6.02	0.42	5.18	0.08
WG-12		434	31.4	6.44	4.45	1.06	6.44	1.58	5.55	0.28
WG-5	900	98	26.0	5.34	4.79	0.78	5.34	0.68	4.69	0.14
WG-6		191	20.6	4.21	3.67	0.62	4.21	0.64	3.72	0.17
WG-7		350	26.7	5.47	4.19	0.80	5.47	1.44	4.81	0.30

* Initial concentrations of CO and H_2O are zero. The concentrations of H_2O at time "t" and at equilibrium are equal to the concentration of CO at time "t" and at equilibirum, respectively. The concentrations of H_2 at time "t" is equal to the initial concentration of H_2 minus the quantity $[CO2]_o - [CO2]_t$.

SUBSCRIPTS:

o	initial conditions
t	conditions at residence time "t" ms
e	equilibrium conditions
p	conditions predicted by theoretical kinetic model at time "t" (assumes homogeneous irreversible kinetics)

It is obvious that the actual experimental data ($[CO_2]_t$) does not agree with the results predicted by the kinetic model ($[CO_2]_p$). In fact, for all of the residence times and temperatures investigated, the theoretical homogeneous model predicts that the reaction will not proceed to any appreciable extent (ie. $[CO_2]_o = [CO_2]_p$). The actual extent of the reaction was indicated by measuring the approach to equilibrium. The approach to equilibrium (Table 29) was measured by taking the ratio of the actual CO concentration ($[CO]_t$) to that expected at equilibrium ($[CO]_e$). The results which are plotted as a function of residence time in Figure 35, indicate that while equilibrium has not been reached, the reaction has proceeded to a significant extent over the fast pyrolysis time scale. The kinetic model predicts that the reaction will not occur to any significant extent. A 5% reduction in initial CO_2 concentration is predicted at about 25 seconds for experiments conducted at 900°C, and at approximately 100 seconds for 850°C experiments (Appendix 4.0).

The disagreement in the data can perhaps be resolved in terms of an unfortunate oversight in the operating procedure. The water-gas shift experiments were conducted after the cellulose pyrolysis series was completed and before the systematic wood pyrolysis experiments were initiated. However, several preliminary trials with wood were carried out prior to the water-gas shift study in order to gain experience and to

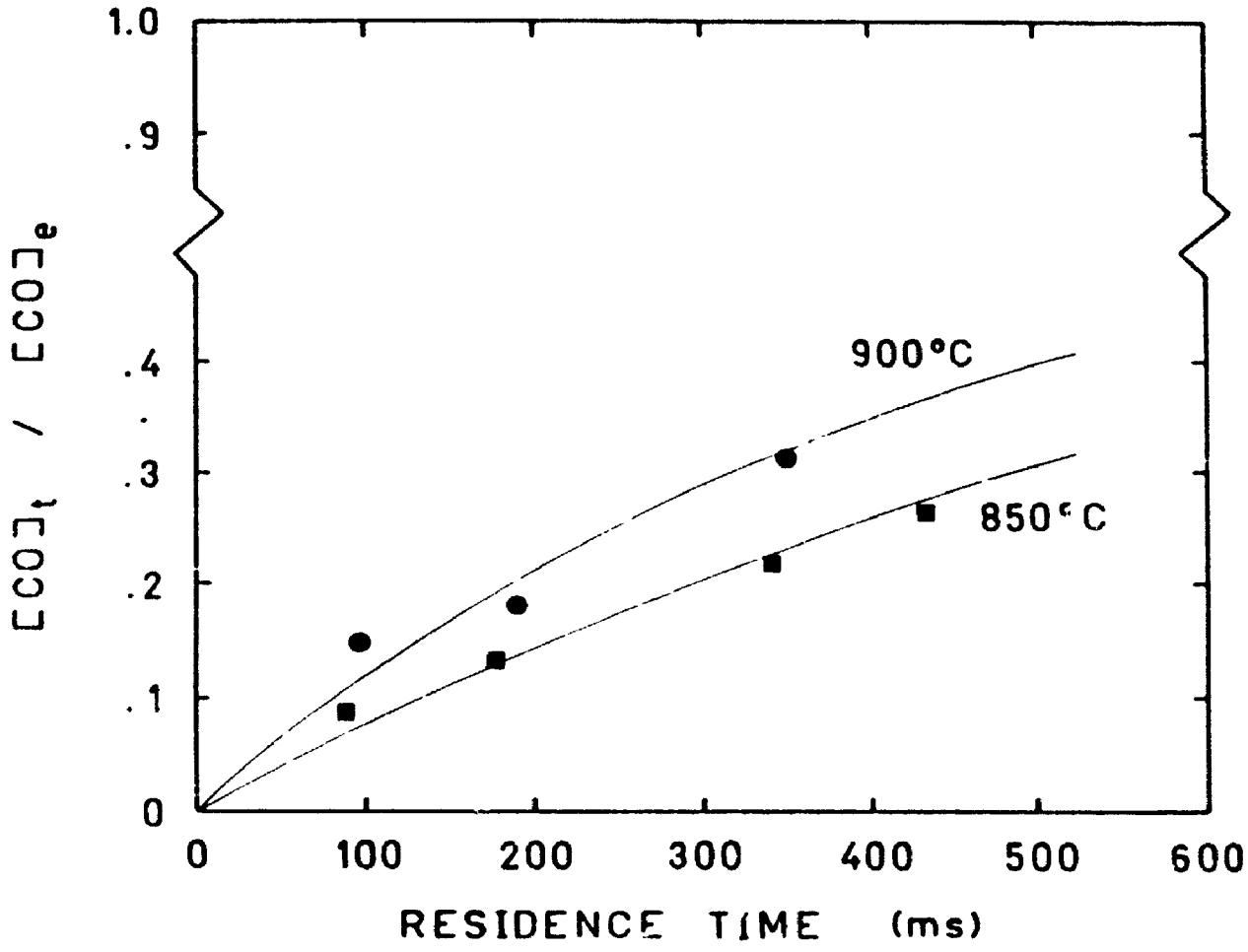

Figure 35. Water-Gas Shift Reaction Approach to Equilibrium: $[CO]_t/[CO]_e$ vs Residence Time

note qualitative differences between wood and cellulose trials (i.e., differences in liquid and char yields which must be handled by the downstream recovery units). Since these wood experiments were of a preliminary nature and since no char accumulation occured during cellulose experiments, the reactor system was not routinely inspected for solids accumulation.

Upon completion of the water-gas study, the reactor system was inspected and a 3 cm plug of char/ash, deposited during the preliminary wood pyrolysis trial, was found in the tubular reactor. Smaller plugs were also found, and it was very likely that surface catalysis was occurring in the "porous bed" reactor. Therefore, the reactions occuring during the actual water-gas shift experiments could not be described by a homogeneous kinetic model.

The results of the cellulose and wood fast pyrolysis experiments (Sections 8.4 and 8.5, and Chapter 9) confirm that the water-gas shift reaction does not play a significant role in the secondary vapour-phase reactions. The yields of CO, CO_2, and H_2 remain constant in non-equilibrium concentrations in the asymptotic region of the total gas yield curves, even at the highest reaction temperature and longest residence time. If the heterogeneous water-gas shift reaction were occuring because of catalytic effects associated with the reactor wall or solid heat carrier, the yields of the participant reactants would change with residence time. Other fast researchers observe that the water-gas shift is not a significant factor under typical fast

pyrolysis conditions [26,65,173,175]. It therefore appears that the water-gas shift reaction is in fact more closely represented by homogeneous reaction kinetics than by heterogenous kinetics.

The water-gas shift study did not accomplish its intended objective which was to monitor the homogeneous reaction. The published homogenous kinetic model and actual results from the fast pyrolysis of cellulose and wood, suggest that homogeneous water-gas shift reaction kinetics are much too slow to allow this reaction to play a significant role during fast pyrolysis. It was hoped that an independent study in the Ultrapyrolysis system would confirm this. The study did indicate that the heterogeneous (catalyzed) reaction is significant on a fast pyrolysis time scale.

8.8 JOINT STUDY WITH WATERLOO UNIVERSITY

During the course of the Ultrapyrolysis project, a cooperative project was initiated between rapid pyrolysis researchers at Waterloo University and those at the University of Western Ontario. Using different pieces of equipment, both groups were able to achieve the rapid heating rates which are characteristic of fast pyrolysis. The Waterloo group has conducted fast pyrolysis experiments for several years in a fluidized bed reactor system using silica sand as the fluidizing medium. Since the operating temperature and residence time ranges of the Waterloo fluidized bed are 400 to 750°C and 300 to 1500 milliseconds, respectively, while the corresponding ranges

for the U.W.O. Ultrapyrolysis reactor are 500 to 900°C and 50 to 900 milliseconds, respectively, it was apparent that there was sufficient overlap in operating conditions to attempt to get a congruent picture of cellulose rapid pyrolysis from 400 to 900°C. It was therefore decided to compare the pyrolysis of an identical Avicel cellulose feedstock in the two reactor systems with the idea of matching the Ultrapyrolysis reactor residence time (at each temperature) to that of the fluidized bed.

The Ultrapyrolysis system and experimental procedure have already been presented. Two fluidized bed reactor systems were used at the University of Waterloo facilities. One was a bench-scale unit with a capacity of about 50 grams per hour while the second was a small pilot plant with a capacity of 3 kg per hour. In the pilot plant system (Figure 36), dry particulate biomass is fed from a hopper by a variable speed twin-screw feeder to a discharge zone where it is picked up by a preheated transport gas and carried into the fluidized bed reactor. The reactor is wrapped with heating coils such that heat can be added selectively to the bed and freeboard space as desired. Pyrolysis products are swept from the reactor to a cyclone where the particulate char and ash are separated from the product gases and vapours. The gas product and vapours are then piped to two condensers in series, the first of which is a "warm" condenser while the second uses ice water as the condensing medium. The gas passes from the condensers through a series of filters to remove residual aerosols.

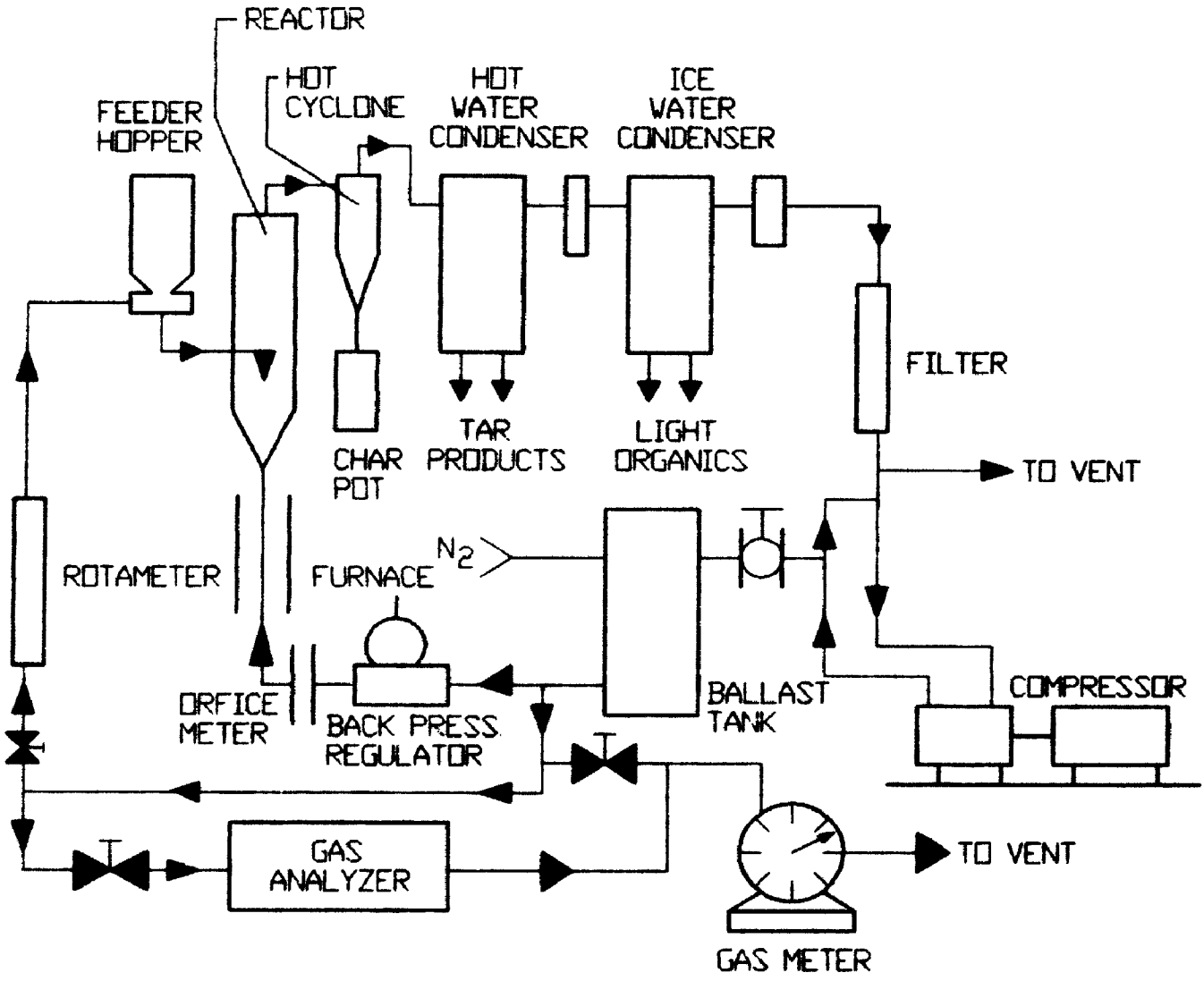

Figure 36. University of Waterloo Fluidized Bed Pilot Plant [174]

After a fluidized bed run, the condensers are washed with acetone, the solution is filtered, and the solvent is evaporated under vacuum to yield the liquid fraction. Additional liquids are collected in the filters which are weighed before and after the experiment. All liquid products are soluble in acetone. The char, which is very reactive and can easily combust with air when hot, is carefully collected from the char pot and weighed. The residue from the acetone extraction which is not soluble, is included in the char fraction. Gases are analyzed for CO and CO_2 by on-line infra-red analysis, and complete off-line gas analysis of selected samples is accomplished using gas chromatography. A more complete description of the fluidized bed units and procedures is given elsewhere [73,170-176].

The pyrolysis experiments in the fluidized beds were carried out at gas residence times of 450 to 550 milliseconds. For temperatures above 650°C, this corresponds to the asymptotic product yields in the Ultrapyrolysis transport reactor. As stated previously in this thesis, the asymptotic region corresponds to a range of residence times where gas yields in the transport reactor rise to a maximum, liquid yields drop to a minimum, and the yields of both remain independent of reactor residence time. Appropriately, Ultrapyrolysis data from this region was compared to the data from the fluidized bed reactor. The results of the joint study, as presented in the following paragraphs, have been published in their entirety in refereed journals [174,175] and other publications [173].

The results of pyrolysis experiments using Avicel cellulose are shown in Figures 37 to 41. All yields are expressed as a mass percent of the dried feedstock. Figure 37 illustrates that the yields of gas, liquids and char from two different types of reactor systems operated by two independent research groups, are in very close agreement over the range of 450 to 900°C. This good agreement is also evident for the yields of CO (Figure 38), CO_2 (Figure 39), CH_4 (Figure 40), and C_2 unsaturates such as ethylene and acetylene (Figure 41). The general congruence of the data also confirms that the temperature measurements in the systems, and to a lesser degree the residence time measurements, must either be accurate or else any errors are coincidentally similar in three distinct fast pyrolysis reactors.

The yields of total gas, CO, CO_2, and CH_4 approach a minimum at the lowest pyrolysis temperatures investigated (ie. <500°C). These minimum values reflect the prompt gas which is produced during primary pyrolysis, as identified by Diebold [55] and discussed in Chapter 2 and Sections 8.4. The yield and composition of cellulose pyrolysis prompt gas can be determined from the curves. Thus, the total prompt gas yield is about 4 or 5 % of the Avicel cellulose feed material [Figure 37]. Carbon oxides make up 90%, by mass, of the prompt gas (60% CO and 30% CO_2), and the remaining 10% consists mostly of methane with some ethylene. This prompt gas yield and composition is consistent with the results of the cellulose study in this thesis (Section 8.4 and Chapter 9), and with the estimates of Diebold [55].

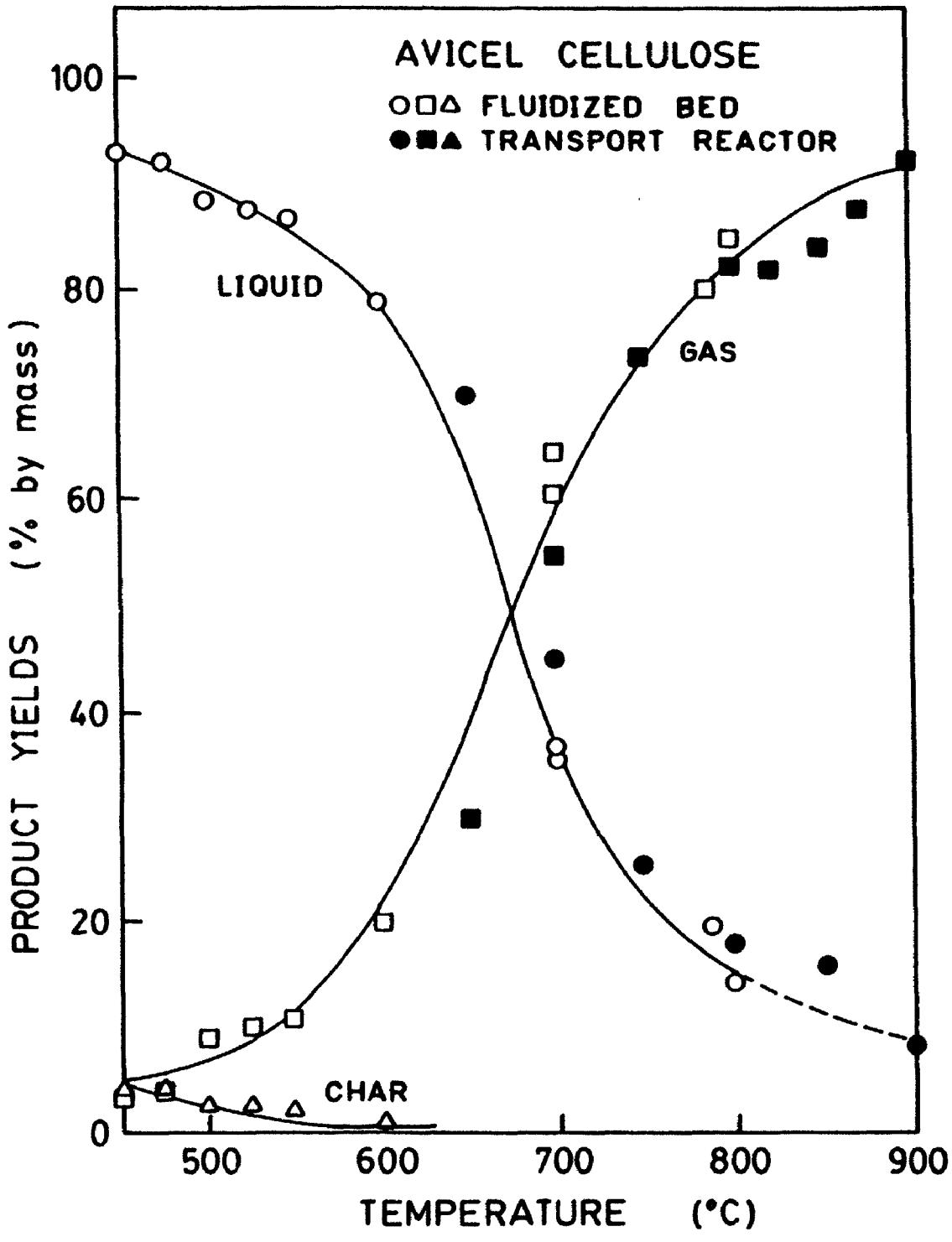

Figure 37. Fast Pyrolysis of Avicel Cellulose: Product Yields from the Waterloo Fluidized Beds and Ultrapyrolysis Reactor Systems

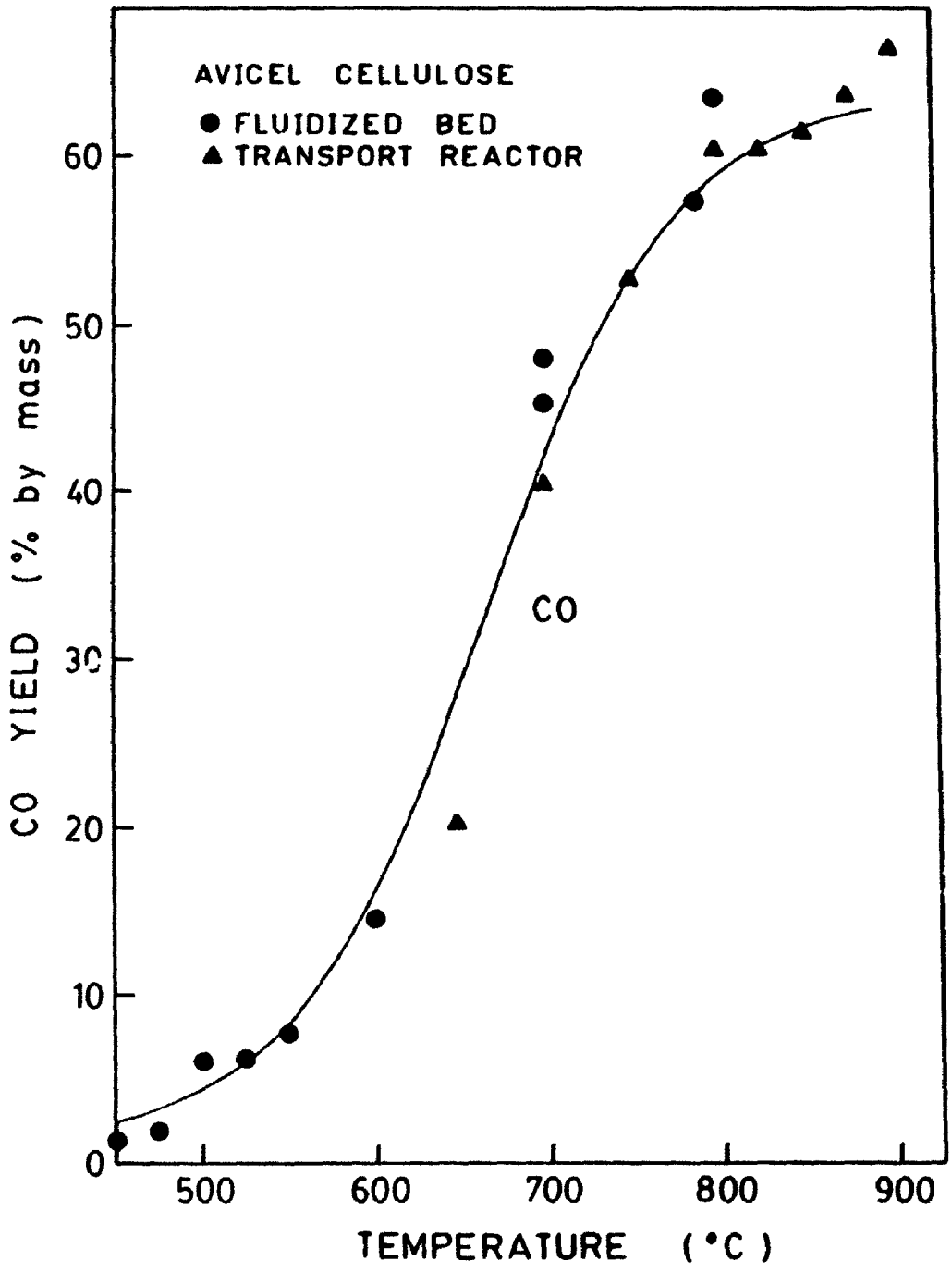

Figure 38. Fast Pyrolysis of Avicel Cellulose: CO Yields from the Waterloo Fluidized Beds and Ultrapyrolysis Reactor Systems

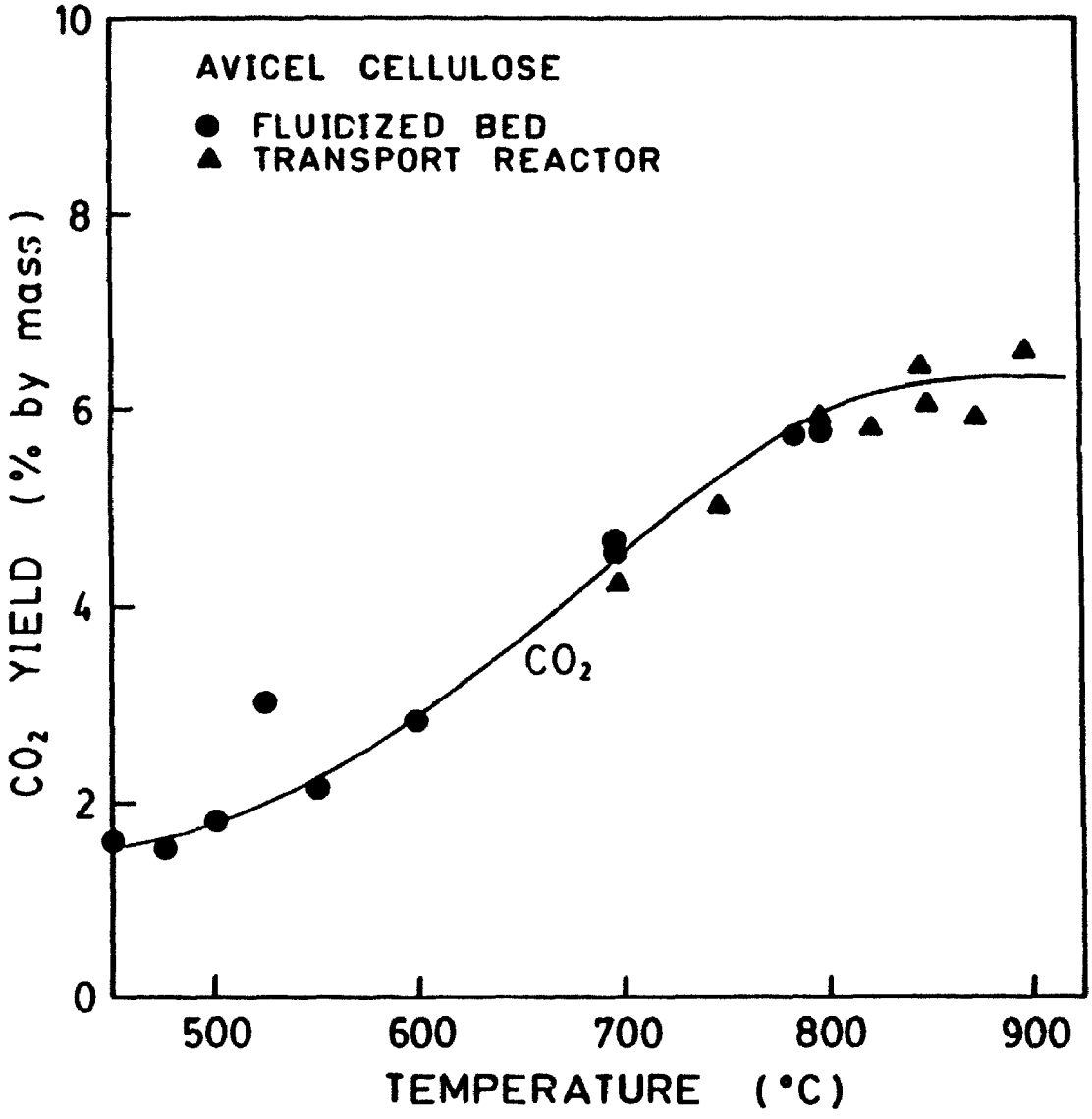

Figure 39. Fast Pyrolysis of Avicel Cellulose: CO_2 Yields from the Waterloo Fluidized Beds and Ultrapyrolysis Reactor Systems

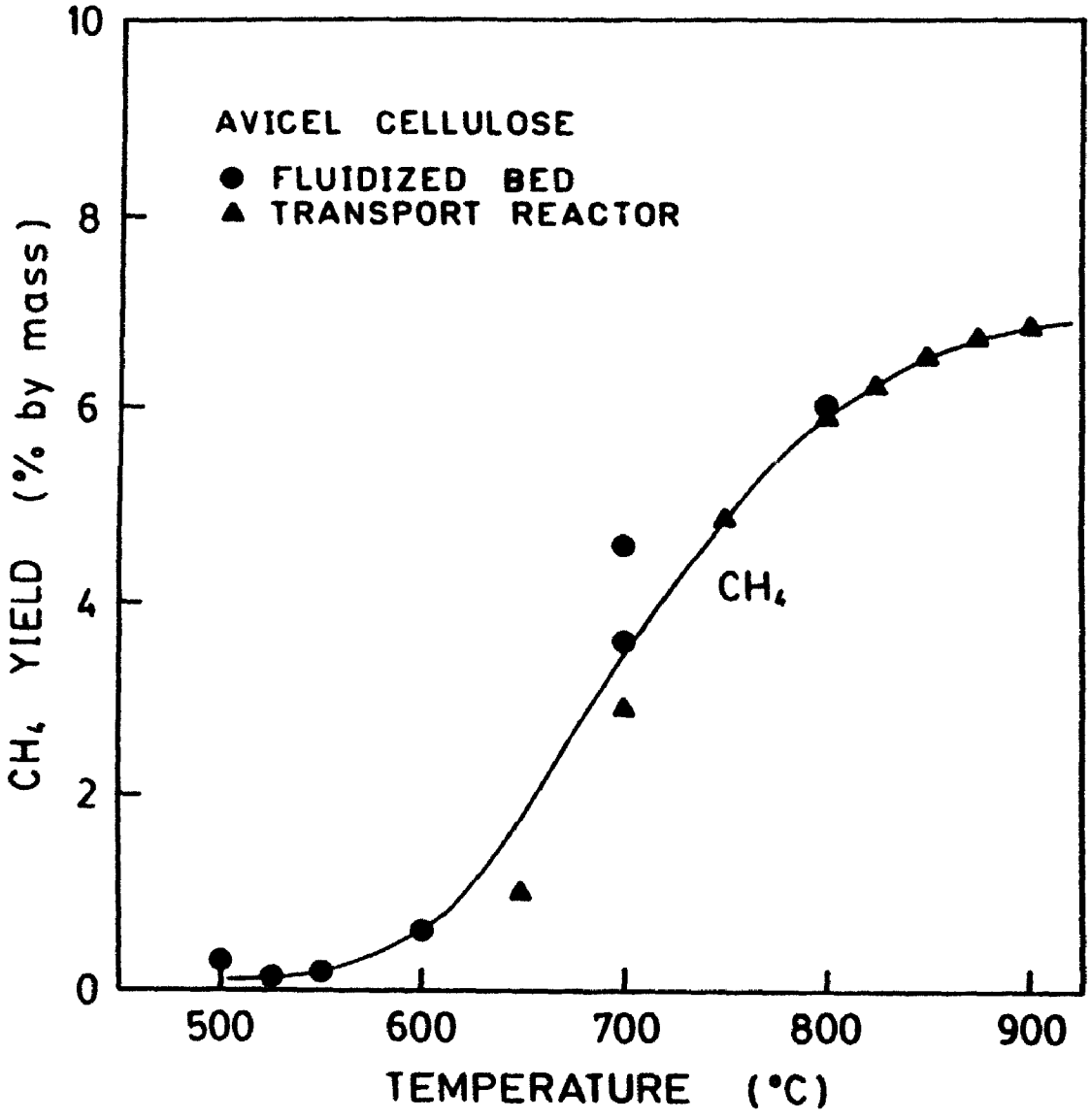

Figure 40. Fast Pyrolysis of Avicel Cellulose: CH_4 Yields from the Waterloo Fluidized Beds and Ultrapyrolysis Reactor Systems

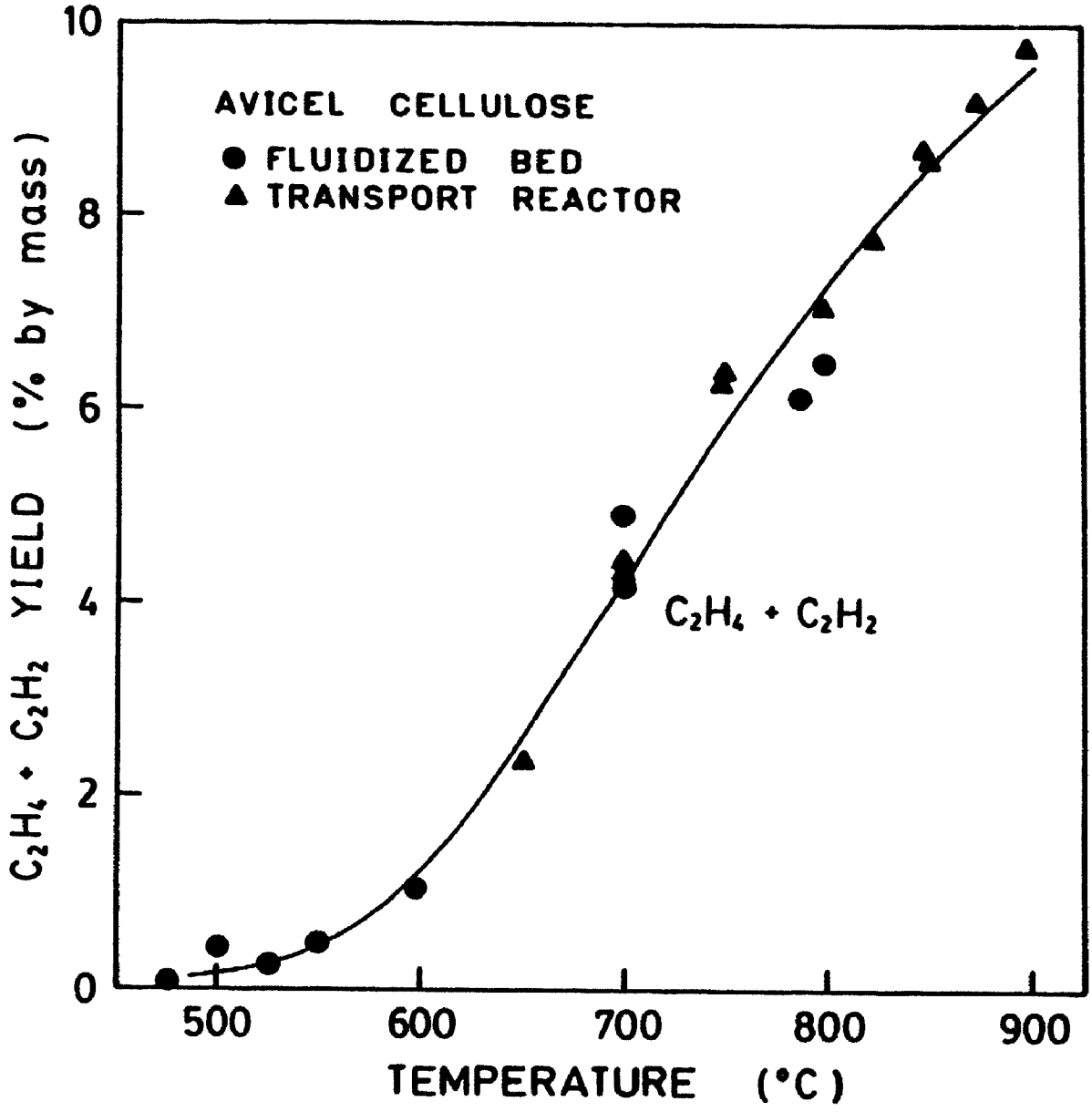

Figure 41. Fast Pyrolysis of Avicel Cellulose: C_2H_4 Plus C_2H_2 Yields from the Waterloo Fluidized Beds and Ultrapyrolysis Reactor Systems

Researchers at the Universities of Waterloo and Western Ontario [173-175], and other researchers [86,90,137], point out that the apparent rapid escalation in total gas, CO, and CO_2 yields at approximately 500°C, which is most dramatically illustrated in the CO_2 curve (Figure 39), is real. It is not simply the random error associated with that particular experiment. Scott proposes that this is evidence of the transition between the predominance of primary reactions which produce prompt gas along with the primary vapours, and the predominance of secondary reactions. This phenomenon is quite obvious on the CO_2 curve since the prompt CO_2 represents approximately 25% of the total maximum yield of CO_2. On the other hand, the prompt total gas and prompt CO represent only about 4% of their eventual maximum yields. Clearly, the prompt CO_2 *must* be dealt with when modelling the production of CO_2 from secondary reactions. Prompt total gas and CO *should* be dealt with in order to provide a model which will satisfy the purist. However, it is likely that the small relative "prompt" amounts will have little effect on the modelling results for these components. This is dealt with in Chapter 9.

The total gas yield from cellulose rises quickly from a prompt yield of about 5% to greater than 90%, at the expense of the yield of condensible vapours, once again confirming that secondary reactions consist of the cracking of primary vapours to low molecular-mass, non-condensible gases (Figure 37). Carbon monoxide is by far the most abundant secondary product

reaching a maximum yield of about 65%, from its prompt yield of about 3%, at 900°C (Figure 38). Carbon dioxide is also a significant secondary product, and rises from its primary prompt yield of about 1.5% to a final yield exceeding 6% at 900°C (Figure 39).

There is very little evidence of prompt hydrocarbon gases being produced by primary reactions (Figures 40 and 41), although Diebold [55] and the data presented elsewhere in this thesis (Sections 8.4 and 8.5, and Chapter 9) suggest that minor amounts of methane and ethylene (together amounting to less than 0.5% of the cellulose feedstock mass) are indeed primary products. Nevertheless, methane (Figure 40) and C_2 unsaturates (Figure 41) are significant products of secondary cracking reactions, and their yields increase from negligible amounts at 500°C to 7% and 10%, respectively, at 900°C. Figure 41 indicates that the yield of C_2 unsaturates is still increasing (ie. has not yet reached a maximum) at 900°C. This appears to be evidence that the secondary cracking of hydrocarbons, likely ethane, propylene, C_4's and C_5's, is continuing after the initial cracking of the oxygenated vapours has ceased. This is confirmed by the data presented in Section 8.4 and the asymptotic character of the total gas and liquid yield curves (Figure 37).

The data for liquid yields shown in Figure 37 refer to *total* condensibles, including organic compounds and product water formed during pyrolysis. Product water is variable and

tends to increase weakly with temperature, so that the organic liquid yield decreases more rapidly than indicated by the decreasing total liquid yield curve in Figures 37. An optimum maximum liquid yield is not observed from cellulose over the temperature range studied. In fact, the liquid yields continue to increase to about 92 percent as the temperature decreases to the lowest value of 450°C. Total gas yield for the cellulose is essentially the inverse of the liquid yield, with negligible char yields except at the lowest temperatures (i.e., 4 percent at 450°C).

The results shown in Figures 37 to 41 represent experiments done in a transport reactor and two fluidized bed reactors (bench scale and pilot plant), and which were conducted by various workers over a period of time. The agreement of all the results has implications for all fast pyrolysis processes where heat transfer is not a rate limiting factor [174,175].

9.0 EMPIRICAL MODELLING

Two general objectives of the thesis research were identified in Section 3.2:

1. To determine the gas composition and gas component yields for the secondary vapour-phase cracking reactions of biomass fast pyrolysis.

2. To determine the kinetics of the secondary vapour-phase cracking reactions (ie. those which produce non-condensible gases), and the kinetics of the formation of the individual gas products.

Chapter 8 dealt principally with the first objective, and the focus is now turned towards kinetic modelling. More specifically, in this chapter an attempt is made to provide kinetic equations and parameters for the final step in the defined sequence of fast pyrolysis reactions. As stated previously, this final step is the cracking of primary fragmentation reaction products in the vapour-phase (Figure 6). In the model proposed by Diebold (Figure 7), this final step includes both the production of "transient oxygenated fragments" and "CO, CH_4, H_2, CO_2 and olefins".

A pivotal question which arises is how can one model vapour-phase cracking reactions from the experimental work which is reported in Chapter 8, when in fact that experimental work includes both primary fragmentation and secondary cracking reactions. As discussed in section 2.7.2, the secondary cracking reactions are indeed fast, but are still rate-limiting when compared with the primary cellulose volatilization

reactions (ie., either fragmentation or depolymerization). Therefore, a determination of the kinetics of the production of secondary products directly from biomass. will reflect the kinetics of the rate-limiting secondary cracking reactions. This is a fundamental assumption in the strategy of the current kinetic modelling exercise, and can be substantiated by available kinetic data.

For example, the volatilization kinetic constants as reported by Bradbury [28] and reviewed in Section 2.7.1, and those of other researchers [12,13,55,86,90,131,137,173,175,207] for the vapour-phase cracking reactions (summarized in Table 1, Section 2.7.2) can be used to calculate rate constants for primary and secondary reactions, respectively, over the temperature range investigated during this thesis work. The ratio of rate constants then provides an indication of the dominance of one set of reactions over the other. Using Antal's parameters [12,13] over the range of 650 to 900 °C, the first-order reaction rate of the primary reaction exceeds that of the first-order secondary reaction by a relatively constant factor of about 2000. With the kinetic constants derived by Peters [86,90], the primary reaction rate exceeds the secondary reaction rate by a factor of 330 to 2000, as the reaction temperature is increased from 650 to 900 °C, respectively. Corresponding rate factors increase from 770 to 10,000 over the same temperature range, using the kinetic data reported by Scott [173,175].

This rather simple kinetic analysis confirms the pivotal assumption of the kinetic modelling approach presented in this chapter. Details of the analysis are provided in Appendix 5.0, and a similar exercise is carried out using this author's data after kinetic parameters are derived (Section 9.2).

9.1 KINETIC MODEL CHARACTERIZATION

The purpose of the kinetic study was to generate an empirical kinetic model as opposed to a theoretical mechanistic model. As reflected in the kinetic literature, it is extremely difficult to evaluate the detailed mechanisms of fast pyrolysis without sophisticated analytical equipment because of the complexity and number of the primary products. Alternatively, an empirical kinetic model is much more flexible in that it is useful in engineering applications as a predictive tool to optimize yields of desirable products, and also to assist in reactor design. This latter method was therefore adopted to provide an adequate model for the rate of *appearance* of the principal gaseous products from biomass. This is equivalent to the rate of *disappearance* of primary fragmentation products by vapour-phase cracking.

A convenient approach to kinetic modelling assumes that the solid biomass decomposes directly to each individual gas component by a single independent pathway and that the kinetics of the decomposition can be represented by a unimolecular first-order reaction. As discussed previously, this model in fact

provides rate equations for the secondary cracking reactions, since the primary volatilization reactions are rate-limiting under true fast pyrolysis conditions. The appearance of total non-condensible gas in effect mirrors the disappearance, by cracking, of the primary vapour products. This approach has been widely used to represent the kinetics of the thermal decomposition of many solid feedstocks [5,6,19,71,86,90,131,137, 213]. The following rate equation is thereby derived from first principles (details of the derivation from first principles are presented in Appendix 6.0):

$$V = V^{\circ} (1 - e^{-kt}) \qquad (12)$$

where V represents the yield (% by mass of the dry feedstock) of the product at residence time "t" and temperature "T"; V° is the maximum attainable (i.e., asymptotic) yield (% by mass) of the product at temperature "T"; and k is the Arrhenius rate constant.

The Arrhenius expression is given by:

$$k = A\, e^{-Ea/RT} \qquad (7b)$$

where A is the frequency factor or pre-exponential constant; E_a is the apparent activation energy of the reaction; R is the universal gas constant; and T is the absolute reaction temperature.

In the Ultrapyrolysis and RTP equipment, the heat transfer rate and temperature control (in a "sea" of pre-heated sand) are such that the heat-up period is instantaneous compared with the reaction time, and the temperature is effectively constant until quenching. Furthermore, in these systems, pre-selection of the desired residence time is possible and precise control of this

important variable is realized. In the author's opinion, this combination is unique with respect to published biomass fast pyrolysis kinetic studies. The development of kinetic data is therefore simplified since equations can be integrated over constant reaction temperature, and errors associated with data acquisition and analyses are thereby minimized.

A variation of the model expressed in equation (12) is used to account for prompt gas which is produced during primary volatilization reactions, and therefore is not a direct product of the cracking reactions. If the contribution of the prompt gas to the final gas product is not dealt with, there will be errors associated with the derivation of parameters V^*, A and Ea. The model which accounts for prompt gas production is given by:

$$V = P_i + V^* (1 - e^{-kt}) \qquad (13)$$

where P_i represents the yield (expressed as a % by mass of the dry feedstock) of the total prompt gas or the individual prompt gas components.

In the kinetic models represented by equations (12) and (13), V^* and k may be determined from the experimental data using nonlinear regression analysis. "P_i" can be set as a constant based on values reported in the literature, or it can be derived using the experimental data and regression analysis. For the remainder of this thesis, the first model (equation 12) will be termed the "zero-intercept" model since it assumes that the curve will pass through the origin. The second (equation 13) will be referred to as the "prompt gas" model since it accounts

for prompt gas production and as a result, does not pass through the origin. The Arrhenius constants A and Ea are derived from the intercept and slope, respectively, of Arrhenius plots ($\ln k$ vs 1/T) using the k parameters derived from the zero-intercept and prompt gas models.

9.2 REGRESSION ANALYSIS: CELLULOSE FAST PYROLYSIS

In order to estimate the parameters of the first-order models described by equations (12) and (13), the cellulose pyrolysis data for total gas and the principal individual gas components (Section 8.4) were used in a nonlinear regression routine available from S.A.S. (Statistical Analysis Systems). The S.A.S. routine, based on an algorithm deve.oped by Maquardt and Levenberg (Appendix 7.0), determines the best values for V^*, k, and P_i (where applicable) along with the standard errors associated with each parameter estimate. From the standard error, which is the square root of the variance and includes both the experimental error and any model inadequacies, the significance of each parameter is determined. A good fit to the model (based on a 95% confidence interval) is assumed if the parameter estimate is "significant". A standard linear regression is then used along with the Arrhenius expression to determine the activation energy (Ea) and the pre-exponential constant (A).

9.2.1 Zero-Intercept Model

The first set of regression analyses were based on the model expressed by equation (12) which includes both the primary prompt gas and secondary cracking product gas in the total gas yields (ie., prompt gas is not accounted for and is therefore not excluded from the total). The analyses were conducted on total gas, carbon monoxide (CO), carbon dioxide (CO_2), ethylene (C_2H_4), methane (CH_4), hydrogen (H_2) and acetylene (C_2H_2). Representative results using the regression analysis and the basic kinetic model are given for the total gas yield data, over the temperature range of 650 to 900 °C, in Figures 42 to 49. Corresponding figures are given for the individual gas components in Appendix 7.1. Each figure consists of three plots. The main plot is a curve representing the actual and predicted yields of total gas or gas component vs residence time. Individual dots on this curve represent the actual experimental values. The solid lines represent the best fit of the kinetic parameters V^* and k to the zero-intercept model, as expressed in equation (12). Also illustrated, to provide a visual representation of the suitability of the model, is a plot of predicted value vs. the actual experimental value. Finally, in each figure, there is a plot of residual vs. residence time. The residual is the numerical difference between the observed and predicted values, and also gives an indication of the acceptability of the model.

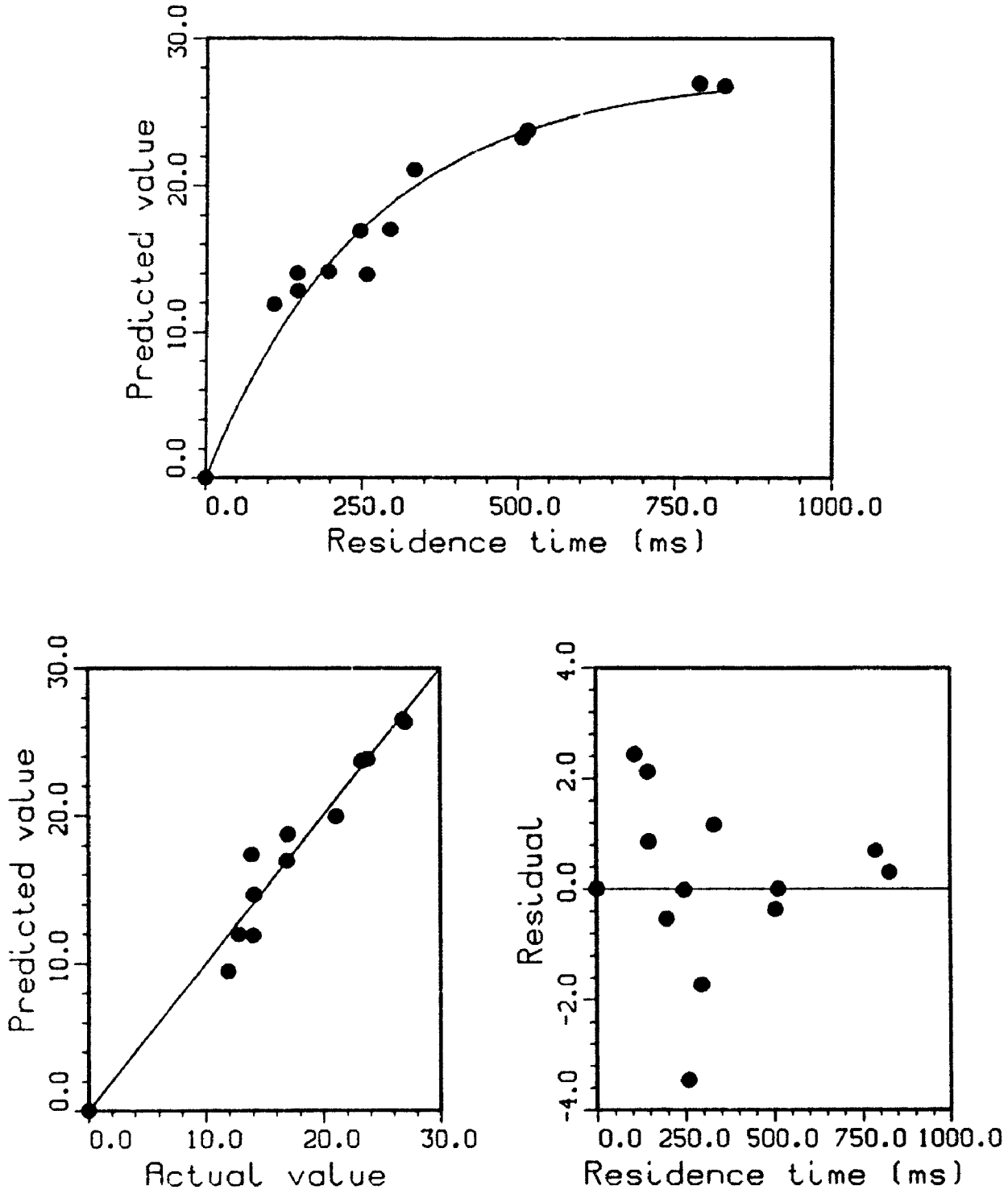

Figure 42. Zero-Intercept Kinetic Model (Equation 12) For Total Gas from Cellulose: Fast Pyrolysis at 650 °C (Run Numbers and Data in Table 10)

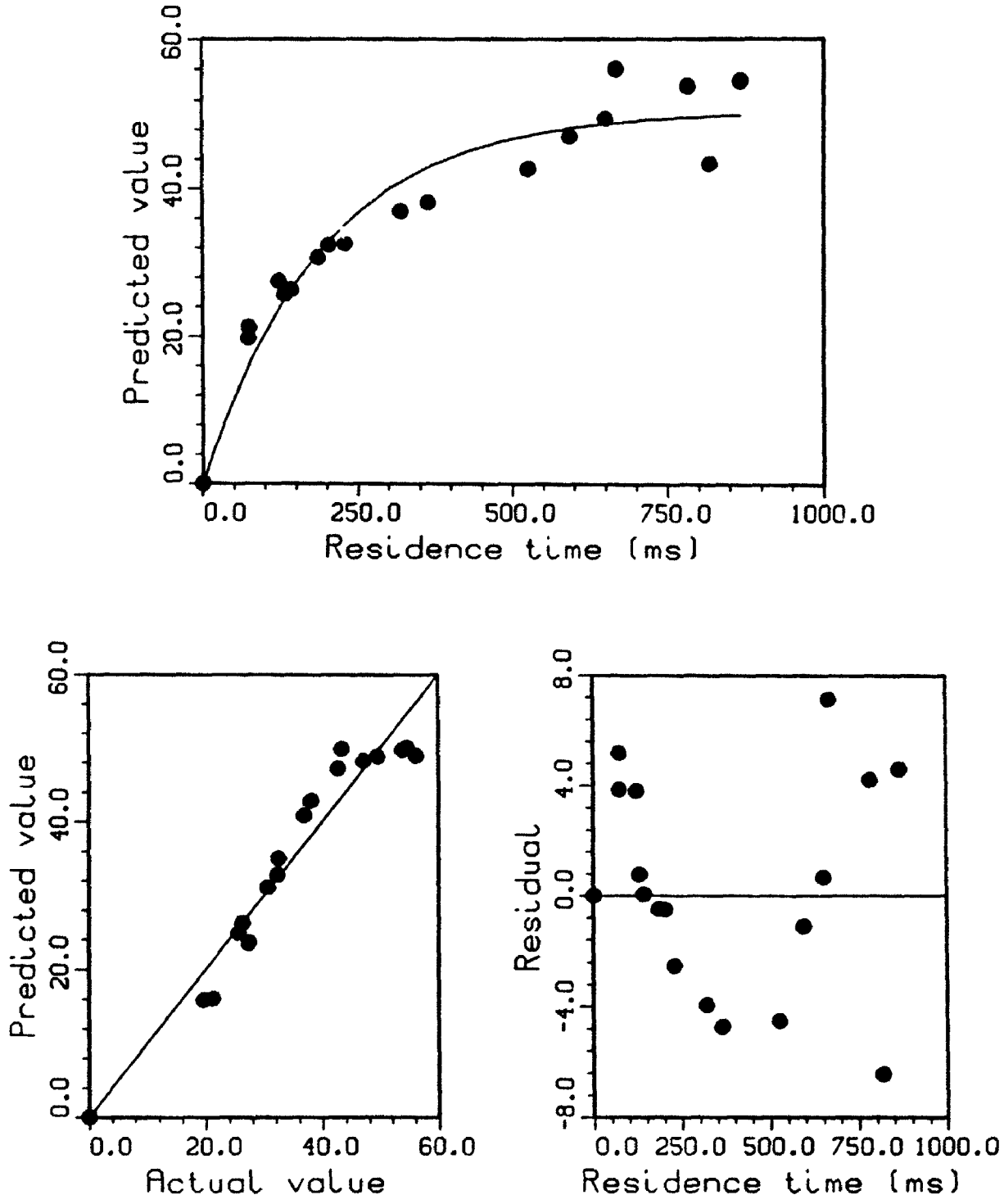

Figure 43. Zero-Intercept Kinetic Model (Equation 12) For Total Gas from Cellulose: Fast Pyrolysis at 700 °C (Run Numbers and Data in Table 11)

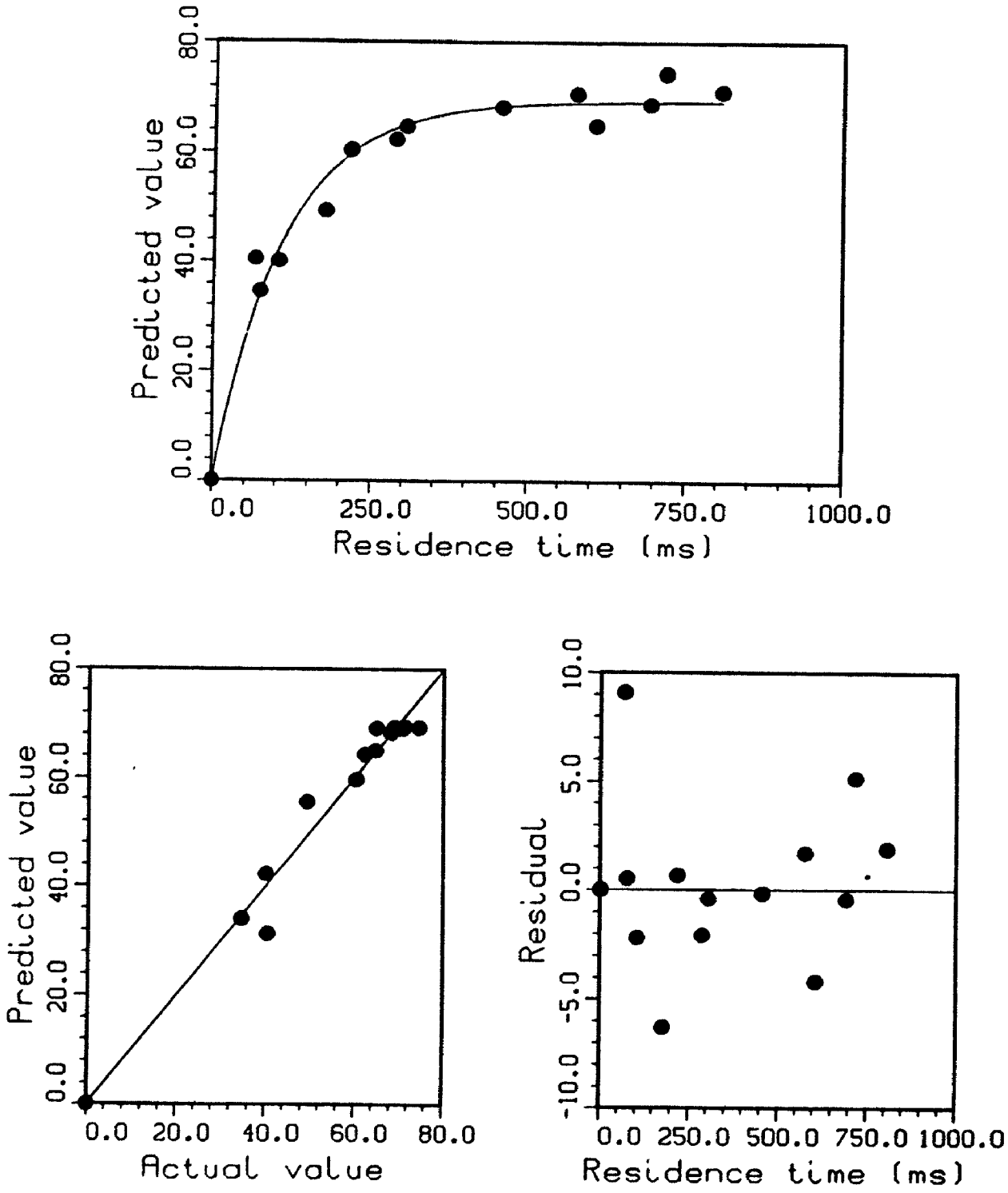

Figure 44. Zero-Intercept Kinetic Model (Equation 12) For Total Gas from Cellulose: Fast Pyrolysis at 750 °C (Run Numbers and Data in Table 12)

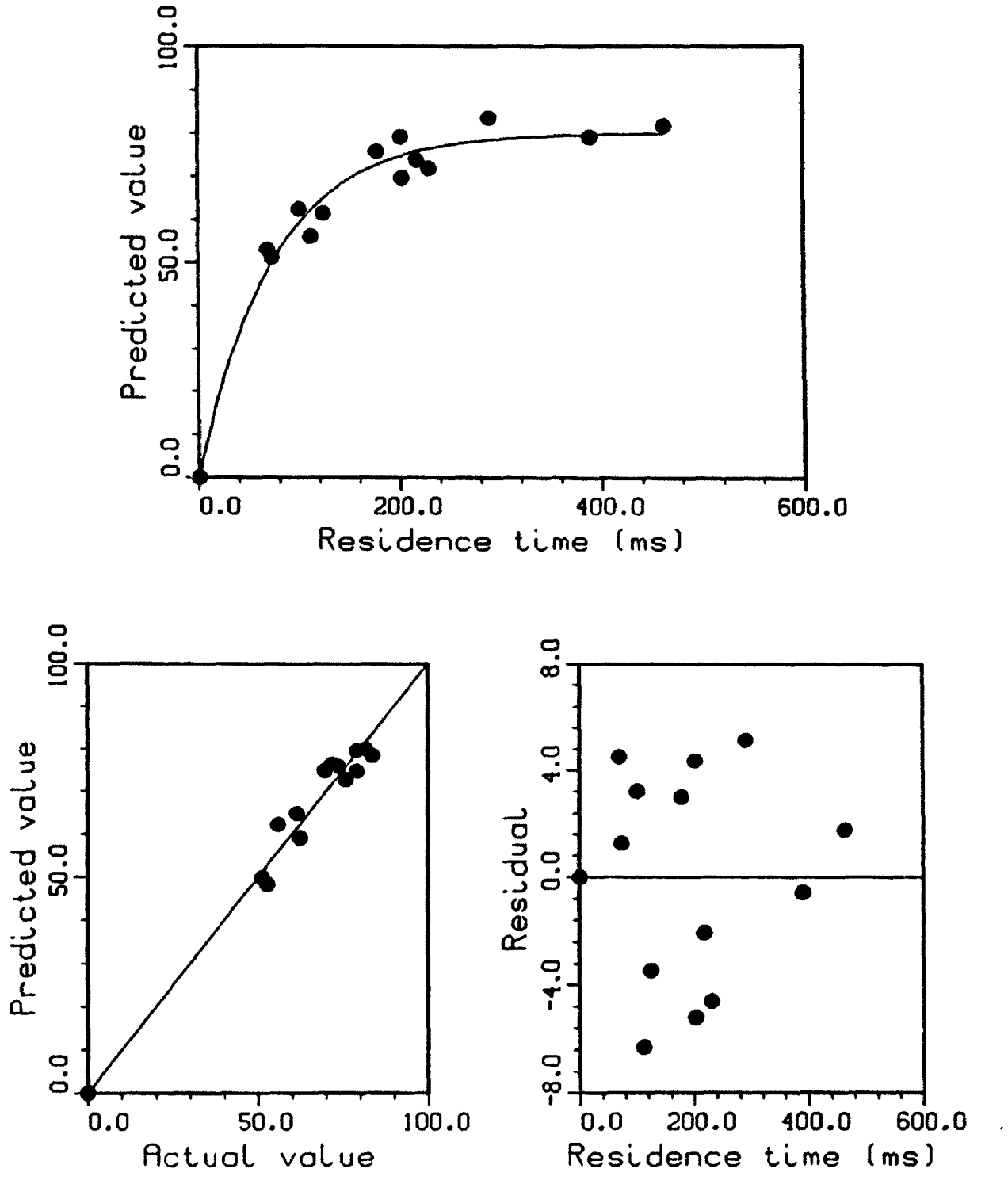

Figure 45. Zero-Intercept Kinetic Model (Equation 12) For Total Gas from Cellulose: Fast Pyrolysis at 800 °C (Run Numbers and Data in Table 13)

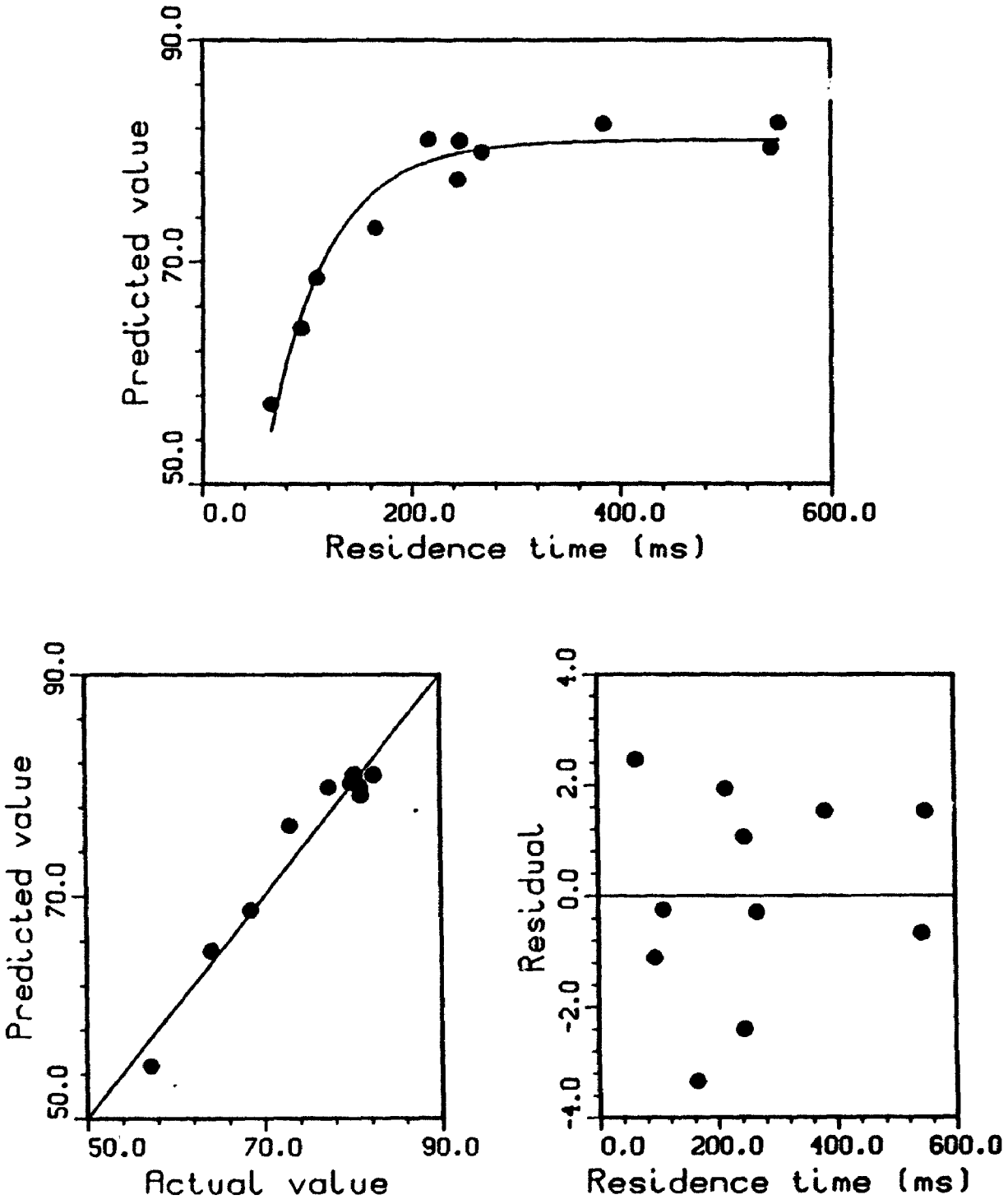

Figure 46. Zero-Intercept Kinetic Model (Equation 12) For Total Gas from Cellulose: Fast Pyrolysis at 825 °C (Run Numbers and Data in Table 14)

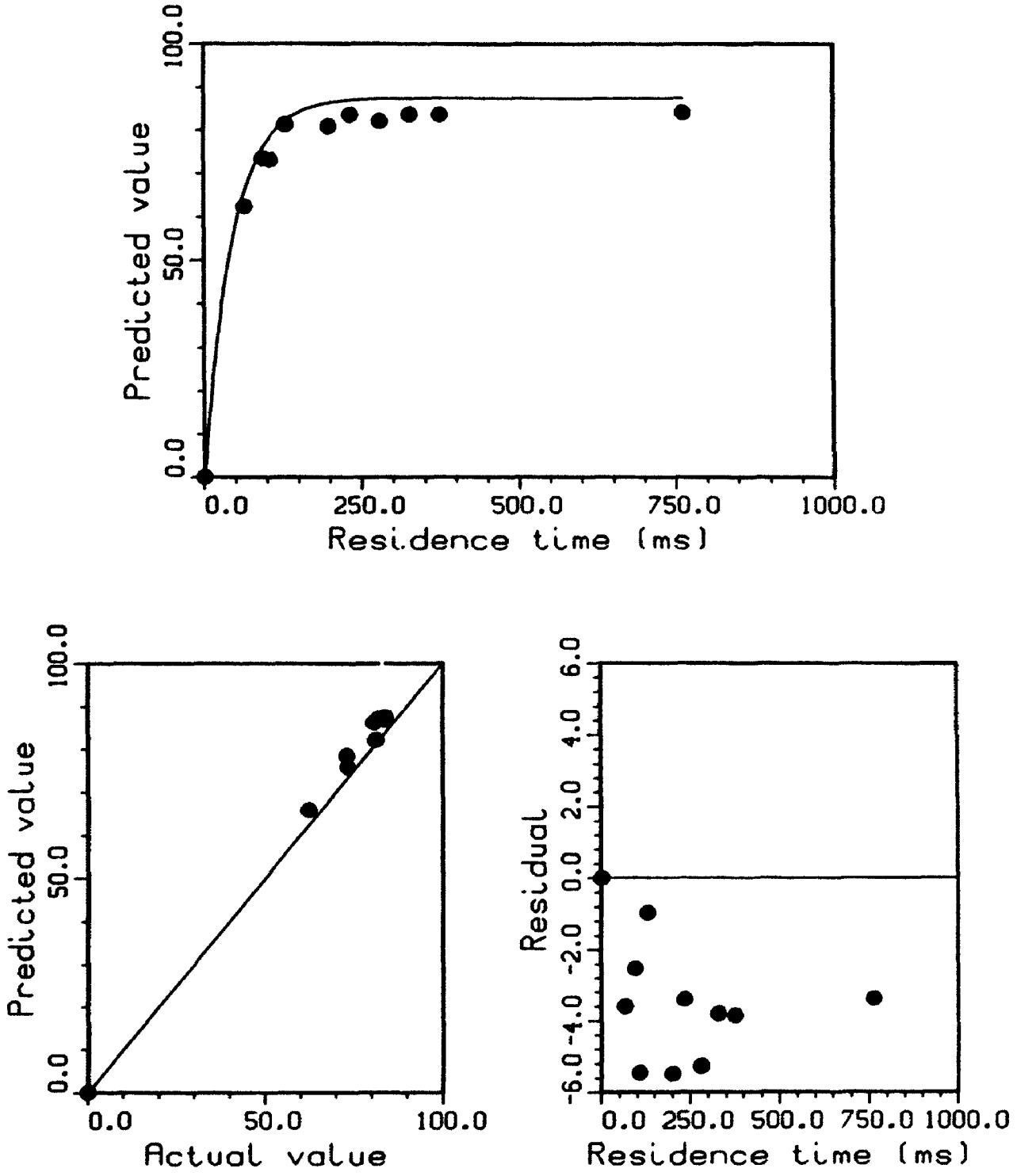

Figure 47. Zero-Intercept Kinetic Model (Equation 12) For Total Gas from Cellulose: Fast Pyrolysis at 850 °C (Run Numbers and Data in Table 15)

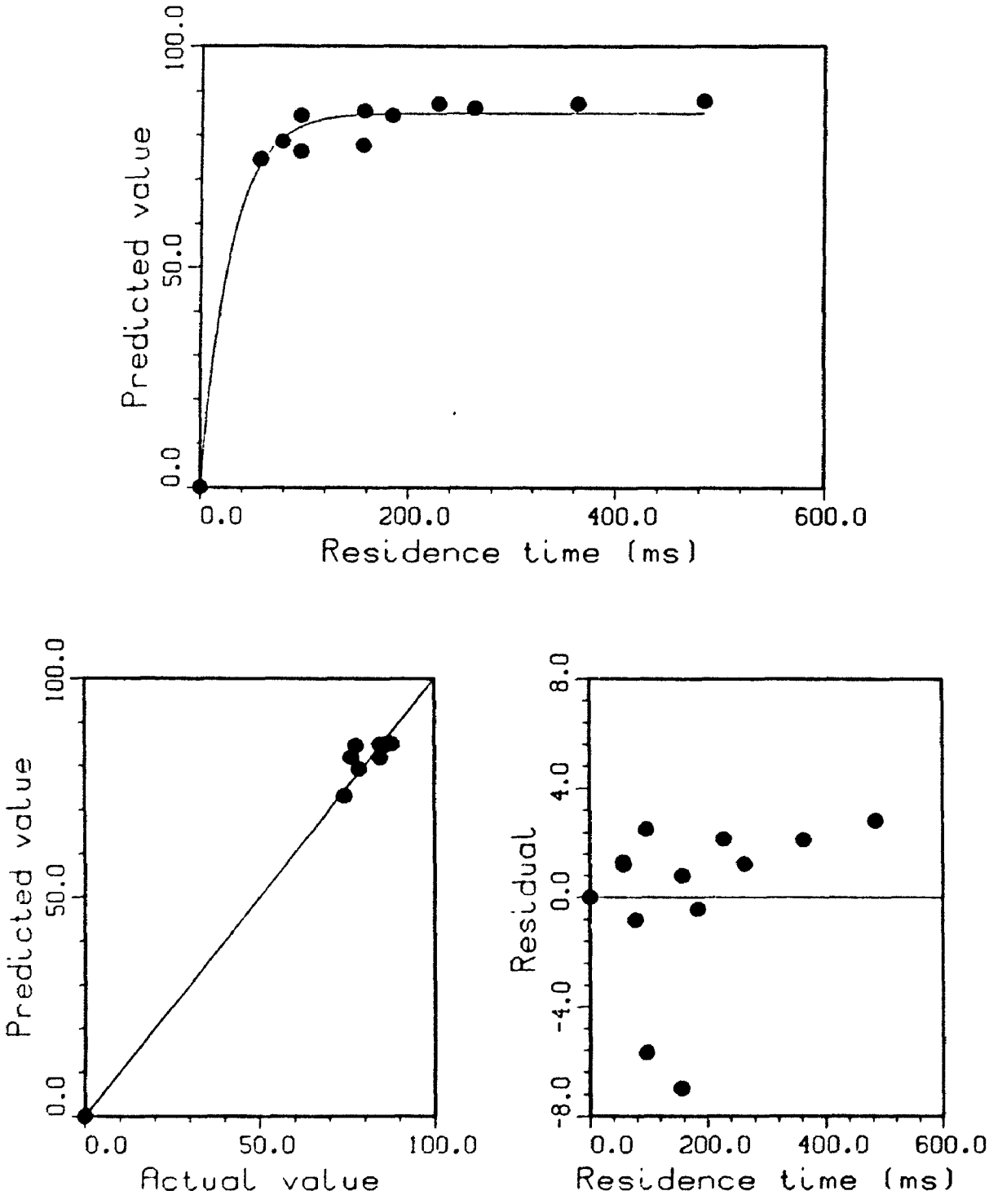

Figure 48. Zero-Intercept Kinetic Model (Equation 12) For Total Gas from Cellulose: Fast Pyrolysis at 875 °C (Run Numbers and Data in Table 16)

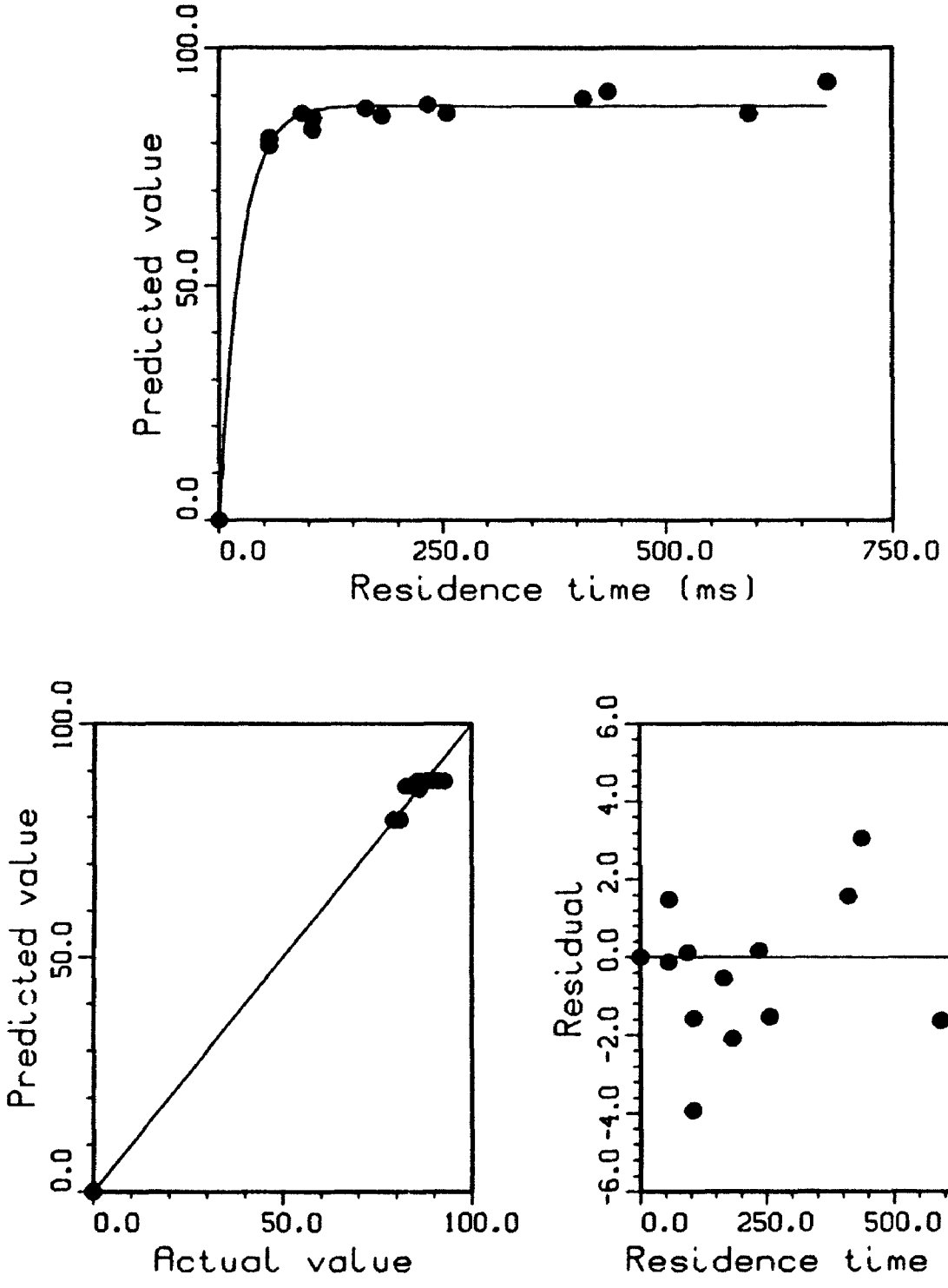

Figure 49. Zero-Intercept Kinetic Model (Equation 12) For Total Gas from Cellulose: Fast Pyrolysis at 900 °C (Run Numbers and Data in Table 17)

The kinetic parameter estimates of V^* and k for the total gas and the principal gas components are summarized, along with corresponding statistical analyses, in Tables 30 to 36. It is clear that for all principal gas products, with the exception of acetylene, there is a good fit to the first-order, zero-intercept model. The k parameters can therefore be used to determine the kinetic constants A and Ea using the Arrhenius equation. A representative Arrhenius plot for total gas production is given in Figure 50. Plots of predicted value vs. actual value, and residuals vs 1/T are also included in this figure. Corresponding figures for each of the principal gas components are given in Appendix 7.2.

TABLE 30. ZERO-INTERCEPT KINETIC MODEL PARAMETER ESTIMATES FOR TOTAL GAS FROM CELLULOSE

TEMPERATURE (°C)	PARAMETER	PARAMETER ESTIMATE	STANDARD ERROR	LOWER 95%	UPPER 95%	SIGNIFICANT
650	V^*	27.64	1.41	24.53	30.74	yes
	k	3.85	0.44	2.87	4.83	yes
700	V^*	50.57	1.91	46.54	54.64	yes
	k	5.15	0.57	3.94	6.37	yes
750	V^*	69.37	1.58	65.94	72.81	yes
	k	9.11	0.83	7.30	10.91	yes
800	V^*	80.10	2.07	75.59	84.61	yes
	k	13.38	1.24	10.68	16.07	yes
825	V^*	80.98	0.81	79.16	82.81	yes
	k	17.34	0.89	15.33	19.36	yes
850	V^*	83.49	0.59	82.16	84.82	yes
	k	21.53	0.86	19.58	23.47	yes
875	V^*	85.08	1.19	82.46	86.71	yes
	k	34.54	3.49	26.85	42.23	yes
900	V^*	87.73	0.77	86.04	89.42	yes
	k	42.09	3.94	33.50	50.69	yes

Units: V*, mass % k, s^{-1}

TABLE 31. ZERO-INTERCEPT KINETIC MODEL PARAMETER ESTIMATES FOR CARBON MONOXIDE (CO) FROM CELLULOSE

TEMPERATURE (°C)	PARAMETER	PARAMETER ESTIMATE	STANDARD ERROR	LOWER 95%	UPPER 95%	SIGNIFICANT
650	V^*	20.94	3.63	18.29	23.58	yes
	k	3.63	0.45	2.62	4.64	yes
700	V^*	37.35	1.38	34.40	40.29	yes
	k	5.32	0.59	4.06	6.57	yes
750	V^*	50.62	1.20	47.98	53.25	yes
	k	9.25	0.88	7.31	11.19	yes
800	V^*	57.40	1.54	54.01	60.79	yes
	k	14.13	1.42	11.01	17.25	yes
825	V^*	58.24	0.59	56.89	59.59	yes
	k	17.75	0.95	15.60	19.91	yes
850	V^*	59.79	0.43	58.80	60.77	yes
	k	21.66	0.89	19.62	23.71	yes
875	V^*	60.74	0.94	58.65	62.83	yes
	k	35.81	4.20	26.45	45.17	yes
900	V^*	62.59	0.61	61.26	63.92	yes
	k	43.90	4.83	33.27	54.52	yes

TABLE 32. ZERO-INTERCEPT KINETIC MODEL PARAMETER ESTIMATES FOR CARBON DIOXIDE (CO_2) FROM CELLULOSE

TEMPERATURE (°C)	PARAMETER	PARAMETER ESTIMATE	STANDARD ERROR	LOWER 95%	UPPER 95%	SIGNIFICANT
650	V^*	2.27	0.10	2.05	2.50	yes
	k	10.64	2.09	5.97	15.30	yes
700	V^*	3.61	0.15	3.29	3.93	yes
	k	9.22	1.44	6.16	12.28	yes
750	V^*	4.75	0.16	4.40	5.10	yes
	k	12.99	2.06	8.45	17.52	yes
800	V^*	5.72	0.15	5.39	6.05	yes
	k	12.58	1.12	10.12	15.05	yes
825	V^*	5.65	0.08	5.47	5.83	yes
	k	18.23	1.39	15.09	21.37	yes
850	V^*	5.71	0.09	5.49	5.93	yes
	k	24.95	2.77	18.56	31.33	yes
875	V^*	5.72	0.06	5.58	5.87	yes
	k	49.65	7.43	33.09	66.21	yes
900	V^*	5.97	0.08	5.79	6.16	yes
	k	59.84	17.67	20.95	98.73	yes

Units: V^*, mass % k, s^{-1}

TABLE 33. ZERO-INTERCEPT KINETIC MODEL PARAMETER ESTIMATES FOR ETHYLENE (C_2H_4) FROM CELLULOSE

TEMPERATURE (°C)	PARAMETER	PARAMETER ESTIMATE	STANDARD ERROR	LOWER 95%	UPPER 95%	SIGNIFICANT
650	V^*	1.34	0.08	1.17	1.51	yes
	k	4.28	0.58	2.99	5.57	yes
700	V^*	3.22	0.21	2.76	3.67	yes
	k	4.32	0.78	2.65	5.99	yes
750	V^*	5.12	0.20	4.68	5.56	yes
	k	7.49	1.07	5.12	9.86	yes
800	V^*	6.10	0.22	5.62	6.59	yes
	k	13.98	1.86	9.89	18.07	yes
825	V^*	6.52	0.10	6.30	6.75	yes
	k	16.38	1.22	13.60	19.16	yes
850	V^*	6.94	0.08	6.75	7.13	yes
	k	20.11	1.25	17.20	23.01	yes
875	V^*	7.14	0.11	6.89	7.39	yes
	k	32.16	3.34	24.71	39.60	yes
900	V^*	7.34	0.09	7.14	7.53	yes
	k	39.67	4.63	29.48	49.86	yes

TABLE 34. ZERO-INTERCEPT KINETIC MODEL PARAMETER ESTIMATES FOR METHANE (CH_4) FROM CELLULOSE

TEMPERATURE (°C)	PARAMETER	PARAMETER ESTIMATE	STANDARD ERROR	LOWER 95%	UPPER 95%	SIGNIFICANT
650	V^*	1.19	0.16	0.84	1.55	yes
	k	1.88	0.41	0.95	2.80	yes
700	V^*	3.11	0.39	2.28	3.94	yes
	k	2.13	0.51	1.04	3.22	yes
750	V^*	4.60	0.20	4.15	5.05	yes
	k	4.73	0.62	3.36	6.09	yes
800	V^*	5.94	0.32	5.24	6.64	yes
	k	7.02	0.87	5.11	8.93	yes
825	V^*	6.02	0.14	5.71	6.33	yes
	k	7.47	0.48	6.38	8.57	yes
850	V^*	6.24	0.14	5.91	6.57	yes
	k	10.08	0.73	8.39	11.56	yes
875	V^*	6.36	0.24	5.82	6.91	yes
	k	13.86	1.69	10.09	17.64	yes
900	V^*	6.47	0.15	6.13	6.81	yes
	k	18.58	1.93	14.34	22.83	yes

Units: V*, mass % k, s^{-1}

TABLE 35. ZERO-INTERCEPT KINETIC MODEL PARAMETER ESTIMATES FOR HYDROGEN (H_2) FROM CELLULOSE

TEMPERATURE (°C)	PARAMETER	PARAMETER ESTIMATE	STANDARD ERROR	LOWER 95%	UPPER 95%	SIGNIFICANT
700	V^*	1.23	0.21	0.78	1.68	yes
	k	1.77	0.54	0.63	2.92	yes
750	V^*	1.34	0.05	1.22	1.45	yes
	k	5.64	0.69	4.11	7.16	yes
800	V^*	1.69	0.10	1.46	1.92	yes
	k	8.29	1.30	5.43	11.14	yes
825	V^*	1.71	0.07	1.56	1.86	yes
	k	9.46	1.20	6.75	12.17	yes
850	V^*	1.65	0.03	1.58	1.73	yes
	k	17.05	1.56	13.44	20.66	yes
875	V^*	1.80	0.10	1.58	2.02	yes
	k	14.00	2.40	8.64	19.36	yes
900	V^*	1.93	0.11	1.69	2.18	yes
	k	14.67	3.09	7.57	21.16	yes

TABLE 36. ZERO-INTERCEPT KINETIC MODEL PARAMETER ESTIMATES FOR ACETYLENE (C_2H_2) FROM CELLULOSE

TEMPERATURE (°C)	PARAMETER	PARAMETER ESTIMATE	STANDARD ERROR	LOWER 95%	UPPER 95%	SIGNIFICANT
750	V^*	0.65	0.06	0.52	0.77	yes
	k	21.03	11.52	-4.33	46.38	no
800	V^*	0.98	0.04	0.89	1.07	yes
	k	35.03	16.05	-0.30	70.37	no
825	V^*	1.09	0.08	0.90	1.29	yes
	k	37.35	38.30	-49.29	123.99	no
850	V^*	1.41	0.05	1.30	1.53	yes
	k	72.67	190.30	-366.17	511.50	no
875	V^*	1.69	0.06	1.56	1.83	yes
	k	51.12	26.60	-8.15	110.38	no
900	V^*	1.86	0.06	1.74	1.98	yes
	k	44.01	15.09	10.78	77.23	yes

Units: V*, mass % k, s^{-1}

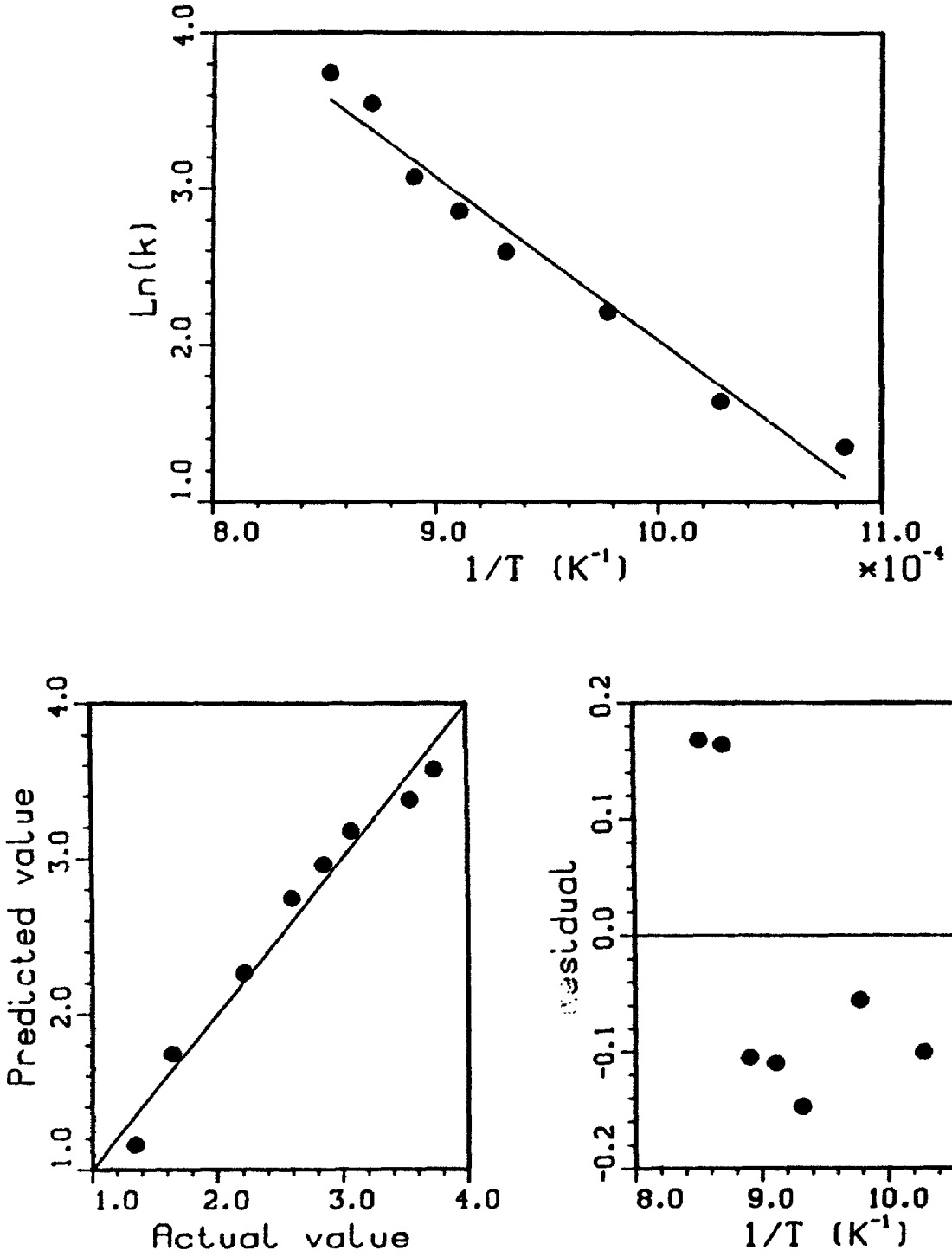

Figure 50. Zero-Intercept Kinetic Model (Equation 12) For Total Gas from Cellulose: Arrhenius Plot (Data from Table 30)

From the zero-intercept model Arrhenius plots (Figure 50 and Appendix 7.2), the activation energies (Ea) and pre-exponential constants (A) for total gas and the principal gas components are determined. A summary of these is given in Table 37. The slope of the Arrhenius curve (ln*k* vs 1/T) is Ea/R, and using a value of 0.008314 kJ/mole-K for the gas constant (R), the Activation Energy is expressed in units of kJ/mole.

TABLE 37. ESTIMATES OF ACTIVATION ENERGIES AND PRE-EXPONENTIAL CONSTANTS: CELLULOSE PYROLYSIS ZERO-INTERCEPT MODEL

KINETIC CONSTANT	GAS PRODUCT						
	Total Gas	CO	CO2	C_2H_4	CH_4	H_2	C_2H_2
Activation Energy (kJ-mole)							
Ea	86.9	89.3	51.2	85.3	83.8	99.9	59.6
Standard Error	6.2	5.7	16.3	8.5	6.4	14.8	24.0
Pre-exponential Const. (s^{-1})							
ln [A]	12.5	12.8	9.4	12.2	11.6	12.4	10.2
Standard Error	0.7	0.6	1.6	0.9	0.9	1.4	2.6
A (10^5 s^{-1})	2.68	3.62	0.12	1.99	1.09	2.43	0.27

A good fit of the data to the Arrhenius equation, based on the zero-intercept first-order model, is apparent for total gas and all gaseous components, with the exception of carbon dioxide and acetylene. This would suggest the gas-phase reactions generally follow first-order behaviour as described by the model. Nevertheless, in the zero-intercept curves (Figures 42

to 49 and Appendix 7.1), it appears that the actual yields of total gas, carbon monoxide, carbon dioxide and perhaps methane, do not pass through the origin as the residence time approaches zero. That is, the yields of those products are positive when extrapolated back to zero residence time "t_o". This phenomenon is particularly evident in the case of carbon dioxide, and for total gas and carbon dioxide at lower temperatures. The zero-intercept model requires that the curve pass through the origin, and the result is a moderate deviation of actual data from first-order behaviour at the lower pyrolysis temperatures.

Several explanations can be presented for those gas yield curves which do not appear to pass through the origin as the residence time approaches zero:

1. There are physical transport limitations (such as heat or mass transfer) to the pyrolysis process in the RTP equipment.
2. There is some rate-limiting latent period of activation associated with biomass fast pyrolysis.
3. The estimates of reactor residence times are in error.

If there were physical limitations or latency, *none* of the product yields would be expected to pass through the origin at t_o, and the yields would remain at zero until some positive residence time "t". In fact, *all* product yields do appear to pass through the origin with the exception of total gas and CO (particularly at lower temperatures), and CO_2. In addition, those gases whose yields do not pass through the origin have *positive* values at t_o.

As documented by the calibration tests (Chapter 7.0) and peripheral experimental studies (Chapter 8, Sections 8.2 and 8.8), it is very unlikely that there are errors associated with estimates of the residence time. Furthermore, the injector Reynold's numbers coupled with the basic tubular reactor design confirms the supposition that a narrow residence time distribution is achieved.

A more suitable explanation of the moderate deviation from zero-intercept, first-order behaviour clearly involves the production of prompt gas during primary volatilization of the solid biomass feedstock. Since the primary reactions are significantly more rapid than secondary reactions under fast pyrolysis conditions, the CO, CO_2 and small quantities of methane which have been identified as principal prompt gas constituents (Chapter 8), appear as "instantaneous" products relative to the appearance of the secondary reaction products. The instantaneous total gas yield is simply the sum of the yields of the individual prompt gas constituents.

The standard errors associated with the CO_2 kinetic parameters (Table 37) are relatively large, even though the estimates are statistically accep able, reflecting the fact that the maximum total CO_2 yield is never very high. Therefore, the ratio of prompt CO_2 to secondary CO_2 is comparably high for all reaction temperatures, and the effect of prompt gas yields in the model is always significant. However, the secondary yields

of total gas and CO are relatively high compared to those for the primary prompt gases, and the effect of prompt gas is therefore somewhat dampened, particularly at elevated temperatures.

An analysis of the Arrhenius plots (Figure 50 and Appendix 7.2) for total gas, CO and CO_2 gives an indication of the effect of prompt gas on the model. For example, there is an apparent "curve" away from the expected straight line at lower temperatures (ie., higher values of 1/T). This phenomenon is particularly evident in the CO_2 plot where the prompt quantity represents a large fraction of the total, but is also evident in the total gas and CO plots. If the prompt gas were removed, the estimate of the rate constants would be drastically reduced at the lower temperatures, while only moderately reduced at elevated temperatures. Accordingly, the Arrhenius curve would "bend" back giving a statistically better straight-line fit.

An estimation of prompt gas yields from in-house and independent experimental data permits the zero-intercept model to be modified, thus allowing for a better fit of kinetic parameters for those gases which are produced both by primary and secondary reactions. This model was described in Equation (13), and is the focus of the next section.

9.2.2 Prompt Gas Model

Equation (13) contains the term "P_i" to account for prompt gas. This constant can either be calculated using a non-linear regression routine (while calculating the kinetic parameters V^*

and k), or it can be estimated from an assessment of both in-house and independent experimental fast pyrolysis data. An attempt was made, without success, to calculate the P_i values by regression analyses. The lack of convergence for total gas, CO, CO_2 or CH_4 was likely because of the relative deficiency of data points in the shortest "transition" residence time region. It is the quantity and reliability of data in this region (close to the yield curve intercept) which provide for a significant parameter estimate for P_i.

The P_i values for total gas, CO, CO_2 or CH_4 were then fixed at 5.0, 3.0, 1.5 and 0.5 percent, respectively, based on the estimates presented in Chapter 8 (Section 8.8). The regression analyses were then carried out over the temperature range of 650 to 900 °C using the prompt gas model described by equation (13). Regression plots for total gas, CO, CO_2, and CH_4 (analogous to Figures 42 to 49 for the total gas, zero-intercept model) are given in Appendix 7.3.

The kinetic parameter estimates of V^* and k, derived from the prompt gas model regression analyses for the total gas, CO, CO_2 and CH_4, are summarized with statistical analyses in Tables 38 to 41. As was the case with the zero-intercept model, it is clear that the prompt gas model gave a good fit. A qualitative comparison of the parameter standard errors suggests that the prompt gas model results in a better fit, with the exception of CH_4 data. However, a quantitative comparison is possible once the A and Ea parameters are calculated, via Arrhenius plots.

TABLE 38. PROMPT GAS KINETIC MODEL PARAMETER ESTIMATES FOR TOTAL GAS FROM CELLULOSE

TEMPERATURE (°C)	PARAMETER	PARAMETER ESTIMATE	STANDARD ERROR	LOWER 95%	UPPER 95%	SIGNIFICANT
650	V_1^*	25.65	2.06	21.06	30.23	yes
	k_1	2.43	0.36	1.63	3.22	yes
700	V_2^*	47.01	2.09	42.55	51.48	yes
	k_2	4.21	0.51	3.13	5.37	yes
750	V_3^*	64.83	1.58	61.35	68.30	yes
	k_3	8.23	0.77	6.54	9.93	yes
800	V_4^*	75.58	2.21	70.72	80.45	yes
	k_4	12.51	1.24	9.77	15.24	yes
825	V_5^*	76.14	0.78	74.37	77.91	yes
	k_5	16.49	0.84	14.60	18.38	yes
850	V_6^*	78.55	0.64	77.07	80.04	yes
	k_6	20.74	0.93	18.60	22.88	yes
875	V_7^*	80.14	1.25	77.35	82.93	yes
	k_7	33.42	3.60	25.39	41.45	yes
900	V_8^*	82.75	0.81	80.97	84.54	yes
	k	40.95	4.07	32.00	49.91	yes

TABLE 39. PROMPT GAS KINETIC MODEL PARAMETER ESTIMATES FOR CARBON MONOXIDE (CO) FROM CELLULOSE

TEMPERATURE (°C)	PARAMETER	PARAMETER ESTIMATE	STANDARD ERROR	LOWER 95%	UPPER 95%	SIGNIFICANT
650	V_1^*	19.77	1.61	16.18	23.36	yes
	k_1	2.52	0.38	1.67	3.38	yes
700	V_2^*	35.10	1.42	32.08	38.12	yes
	k_2	4.55	0.52	3.46	5.66	yes
750	V_3^*	47.88	1.15	45.34	50.42	yes
	k_3	8.53	0.80	6.77	10.29	yes
800	V_4^*	54.67	1.56	51.23	58.10	yes
	k_4	13.38	1.37	10.37	16.40	yes
825	V_5^*	55.33	0.58	54.02	56.64	yes
	k_5	17.04	0.91	14.98	19.09	yes
850	V_6^*	56.82	0.44	55.81	57.84	yes
	k_6	21.00	0.90	18.92	23.08	yes
875	V_7^*	57.77	0.94	55.68	59.86	yes
	k_7	34.85	4.14	25.63	44.07	yes
900	V_8^*	59.60	0.61	58.27	60.94	yes
	k	42.94	4.78	32.42	53.46	yes

Units: V^*, mass % k, s^{-1}

TABLE 40. PROMPT GAS KINETIC MODEL PARAMETER ESTIMATES FOR CARBON DIOXIDE (CO_2) FROM CELLULOSE

TEMPERATURE (°C)	PARAMETER	PARAMETER ESTIMATE	STANDARD ERROR	LOWER 95%	UPPER 95%	SIGNIFICANT
650	V^*	1.28	0.32	0.56	2.00	yes
	k	1.83	0.76	0.15	3.51	yes
700	V^*	2.38	0.20	1.95	2.81	yes
	k	3.95	0.88	2.06	5.83	yes
750	V^*	3.38	0.16	3.02	3.73	yes
	k	7.75	1.38	4.70	10.80	yes
800	V^*	4.41	0.20	3.97	4.84	yes
	k	8.93	1.07	6.57	11.29	yes
825	V^*	4.19	0.09	3.99	4.39	yes
	k	14.48	1.35	11.43	17.54	yes
850	V^*	4.22	0.10	3.98	4.45	yes
	k	21.11	2.84	14.56	27.65	yes
875	V^*	4.22	0.07	4.08	4.37	yes
	k	45.06	7.80	27.66	62.45	yes
900	V^*	4.48	0.08	4.29	4.66	yes
	k	53.56	16.54	17.15	89.97	yes

TABLE 41. PROMPT GAS KINETIC MODEL PARAMETER ESTIMATES FOR METHANE (CH_4) FROM CELLULOSE

TEMPERATURE (°C)	PARAMETER	PARAMETER ESTIMATE	STANDARD ERROR	LOWER 95%	UPPER 95%	SIGNIFICANT
700	V^*	8.04	10.24	-13.79	29.87	no
	k	0.38	0.55	-0.80	1.56	no
750	V^*	4.26	0.29	3.61	4.91	yes
	k	3.80	0.69	2.28	5.31	yes
800	V^*	5.63	0.40	4.75	6.52	yes
	k	5.98	0.89	4.01	7.94	yes
825	V^*	5.65	0.13	5.36	5.93	yes
	k	6.52	0.38	5.66	7.38	yes
850	V^*	5.80	0.16	5.42	6.19	yes
	k	9.11	0.77	7.34	10.89	yes
875	V^*	5.94	0.24	5.39	6.48	yes
	k	12.45	1.53	9.05	15.86	yes
900	V^*	6.00	0.15	5.67	6.33	yes
	k	17.14	1.78	13.23	21.05	yes

Units: V*, mass % k, s^{-1}

The prompt gas model Arrhenius plots for total gas, CO, CO_2 and CH_4 are given in Appendix 7.4, and the kinetic constants Ea and A which are derived from these plots are listed in Table 42. As predicted, there is generally an increase in the activation energy and a decrease in the standard error. The exception is methane where the poor fit is not likely a rejection of the prompt gas model, but is a reflection of the experimental variability. This variability results in background "noise" which is particularly noticeable at such low methane yields.

TABLE 42. ESTIMATES OF ACTIVATION ENERGIES AND PRE-EXPONENTIAL CONSTANTS: CELLULOSE PYROLYSIS PROMPT GAS MODEL

KINETIC CONSTANT	GAS PRODUCT			
	Total	CO	CO_2	CH_4
Activation Energy (kJ/mole)				
Ea	100.8	100.3	116.6	160.9
Standard Error	4.3	5.7	10.9	25.1
Pre-exponential Const. (s^{-1})				
ln [A]	13.9	13.9	15.7	19.4
Standard Error	0.5	0.5	1.2	2.8
A (10^6 s^{-1})	1.09	1.09	6.58	266

The modelling results, as presented in Section 9.2.1 and 9.2.2, provide substantial evidence for the appearance of a *primary* prompt gas product. The proposed composition and yield of prompt gas as reported in the literature and the thesis data (Chapter 8, Sections 8.4 and 8.8) are in good agreement, and result in a good fit when applied to the prompt gas model.

9.3 MECHANISTIC INTERPRETATION

The fundamental purpose of the thesis work was to provide an *empirical* model for cellulose fast pyrolysis, particularly the vapour-phase, cracking reactions. As such, only a limited amount of mechanistic interpretation is possible. Some general inferences are highlighted in the following paragraphs.

The first-order prompt gas model adequately describes the *appearance* of secondary gases produced from cellulose by the cracking reactions. The Arrhenius expression for the kinetics of these secondary, vapour-phase reactions is given as follows:

$$k_{cr} = 1.09 \times 10^{6} \ (e^{-100.8/RT}) \qquad (14)$$

This expression exhibits relatively good agreement with the kinetic expression of Scott [173,175], as reported in Chapter 2 (Section 2.7.2). Scott's expression, which follows, was derived using Avicel cellulose pyrolysis data from the Waterloo U. research program, combined with data from this thesis work:

$$k_{cr} = 3.10 \times 10^{6} \ (e^{-107.5/RT}) \qquad (15)$$

The value of 100.8 kJ/mole for the activation energy in equation (14) clearly indicates that the reactions are operating in a regime which is kinetically determined, and not limited by diffusion (mass transfer) or heat transfer. If mass or heat transfer were limiting, the apparent activation would typically be less than 50 kJ/mole.

A comparison of the thesis rate constant expression for secondary vapour-phase cracking reactions (equation 14) to the corresponding expression for the primary fragmentation

reactions, similar to the comparisons made previously with literature data, can now be made. Such a comparison (Appendix 5.0) indicates that the secondary reaction rate as described by equation (14) exceeds the estimated primary rate by factors of 900 to 14,000 over the temperature range investigated during the course of this thesis experimental program.

It has been reported that carbon monoxide (with prompt CO removed) and hydrogen are quintessential biomass pyrolysis cracking products [8,12]. It is therefore expected that the kinetic parameters derived from CO and H_2 yield data should closely correspond to the kinetic parameters for total gas (which represent overall fast pyrolysis cracking kinetics). This is in fact the case. The activation energies for the appearance of CO and H_2 are 100.3 (Table 42) and 99.9 (Table 37) kJ/mole, respectively. The corresponding value for total gas is 100.8 kJ/mole. The H_2 parameters are particularly significant since they are based on raw experimental data with no subsequent adjustment for prompt gas removal. Mechanistic pyrolysis research confirms that CO and H_2 are indeed formed together via a catastrophic fragmentation of the cellulose ring [11,180,188]. CO arises from the decarbonylation of ring fragments, particularly the aldehyde intermediates [180, 188].

The kinetic constants reported in Table 37 suggest that CH_4 and C_2H_4 are formed from a common pathway, since the activation energies for methane- and ethylene-forming reactions are about 84 and 85 kJ/mole, respectively. Antal [8,12,14] has previously

noted that these two hydrocarbons track each other during pyrolysis, and concludes that they are formed together.

The reaction mechanism for carbon dioxide production is complex and therefore difficult to model. There is certainly general agreement that primary reactions yield a significant amount of CO_2 [8,13,55,73,131,139]. Antal [8,13], Diebold [55] and Piskorz [139] conclude that CO_2 is *exclusively* a primary product. Piskorz suggests that it is derived from the C_1 and C_2 cellulose ring positions, and is formed by decarboxylation reactions as described by Shafizadeh [188]. However, Shafizadeh [188] speculates that in addition to formation from primary reactions, carbon dioxide may be formed from the high temperature cracking of ring fragments via decarboxylation.

The data presented in this thesis clearly confirms that CO_2 arises both from primary and secondary reactions. For example, the data presented in Chapter 8 (Section 8.4) indicates that the asymptotic maximum yield of CO_2 continues to rise over the entire temperature range. Furthermore, the relatively low value for E_a (51 kJ/mole), reported in Table 37, is a typical for a multi-reaction pathway which has been modelled as a single reaction.

9.4 PRELIMINARY MODELLING: FAST PYROLYSIS OF WOOD

The wood fast pyrolysis data, as summarized in Chapter 8 (Section 8.5), was analyzed by regression analyses using the same procedures as were used for the analyses of cellulose data (Section 9.2). As has been indicated throughout this thesis,

the extent of the initial wood pyrolysis experiments was limited by time constraints, and the kinetic modelling must therefore be considered as preliminary. Furthermore, two pyrolysis systems (i.e., Ultrapyrolysis and RTP) were used, and the larger RTP system may have added to data variability. Nevertheless, the preliminary analyses are reported here as a foundation upon which future wood pyrolysis studies can be constructed.

Wood pyrolysis regression curves for the total gas, using the zero intercept model, are given in Appendix 7.5. As with cellulose pyrolysis, the curves for the principal gas components (CO, CO_2, C_2H_4, CH_4, H_2, and C_2H_2) are similar to the total gas curves in general form. Corresponding figures for total gas, using the prompt gas model, are given in Appendix 7.6.

Zero-intercept model estimates for the activation energies (Ea) and the pre-exponential constants (A) are given for the total gas and principal gas component products in Table 43. Prompt gas model estimates are given in Table 44. The values of "Pi" used in the prompt gas model for total gas, CO_2, CO, and CH_4 were 7.0, 5.0, 1.0, and 0.5, respectively (refer to Section 8.5). As with cellulose pyrolysis, the prompt gas model gives a better fit for CO. However, there seems to be no improvement when fitting the total gas data to the prompt gas model (the standard errors are essentially the same). Perhaps any real improvement using the prompt gas model, if existent, is eclipsed by the experimental variability introduced by data generated in a second fast pyrolysis system (i.e., RTP). The zero-intercept

model seems to provide kinetic parameter estimates which are closer to those of Diebold [55] while the prompt gas model estimates approximate those of Thurner and Mann [207], Liden [173] and Scott [175], as summarized in Table 1 (p.52).

Assuming that the prompt gas model for total gas product best represents the kinetics of the vapour-phase reactions for wood fast pyrolysis (while noting that further experimentation and analyses are required to verify or refute this assumption), the activation energy and pre-exponential constants of these first-order, secondary reactions are 99.7 kJ/mole and 3.3×10^4 s^{-1}, respectively. The first-order Arrhenius expression is:

$$k_{cr} = 3.3 \times 10^4 \ (e^{-99.7/RT}) \qquad (15)$$

9.5 MODELLING COMMENTS

Although the zero-intercept and prompt gas models provided reasonable estimates for kinetic parameters (and estimates which agree with other published data), it is important to note some of the general shortcomings of the modelling procedure itself. With additional time and effort these shortcomings could be addressed. For example, the random error in the data (which is determined in replication runs as reported in Appendix 9.0.) should be compared with the "lack-of-fit" error in the models.

Furthermore, the "goodness-of-fit" is not only measured by the kinetic parameter statistics but also by an analysis of the residuals. A plot of residuals should exhibit a random distribution, which typically appears to be the case. However,

some of the residual plots (i.e., Figure 43) seem to indicate a quadratic trend which is not accounted for in the modelling procedure. This requires further analysis. Finally, the regression procedure is based on an assumption that the V^* and k parameters are uncorrelated. Theoretically, one expects that the maximum yield (V^*) at a given temperature is independent of the rate (k) at which that yield is approached. However, a thorough analysis should include some form of correlation test.

TABLE 43 ESTIMATES OF ACTIVATION ENERGIES AND PRE-EXPONENTIAL CONSTANTS: WOOD PYROLYSIS ZERO-INTERCEPT MODEL

KINETIC CONSTANT	GAS PRODUCT						
	Total Gas	CO	CO_2	C_2H_4	CH_4	H_2	C_2H_2
Activation Energy (kJ/mole):							
Ea	89.6	96.6	66.0	97.1	127.8	103.4	112.3
Standard Error	10.5	9.3	3.6	14.0	19.2	24.4	38.4
Pre-exponential Const. (s^{-1}):							
ln [A]	9.9	10.4	8.4	10.1	12.2	10.3	11.8
Standard Error	0.8	0.7	0.3	1.0	1.2	1.2	2.9
A (10^4 s^{-1})	2.0	3.3	0.44	2.4	19.9	3.0	13.3

TABLE 44. ESTIMATES OF ACTIVATION ENERGIES AND PRE-EXPONENTIAL CONSTANTS: WOOD PYROLYSIS PROMPT GAS MODEL

KINETIC CONSTANT	GAS PRODUCT			
	Total	CO	CO_2	CH_4
Activation Energy (kJ/mole):				
Ea	97.7	98.5	83.3	153.6
Standard Error	11.1	8.8	20.7	19.6
Pre-exponential Const. (s^{-1}):				
ln [A]	10.4	10.5	9.8	14.3
Standard Error	0.9	0.7	1.4	1.6
A (10^4 s^{-1})	3.3	3.6	1.8	162

10.0 CONCLUSIONS AND RECOMMENDATIONS

Significant gains have been made in the advancement of the science of biomass fast pyrolysis during the course of this thesis work. Fast pyrolysis has been defined in terms of chemistry, characteristic product distributions, kinetics, heat transfer requirements and requisite process requirements.

Fast pyrolysis consists of biomass activation followed by fragmentation and cracking. The thesis experimental work focused primarily on secondary cracking reaction products and their corresponding rate equations. However, initial studies on ethane cracking were conducted to prove the "integrity" of the equipment and procedure. There was close agreement between published data and the Ultrapyrolysis ethane cracking data. Initial studies also demonstrated that an inert gas (ie., nitrogen) could be used in place of sand as a suitable heat carrier for small biomass particles (ie., less than 200 um). This greatly simplified the mass balance procedure.

Avicel cellulose was the principal feedstock investigated, but wood was also investigated in a preliminary manner. The gas product distribution for the secondary cracking reactions was determined as a function of residence time at constant temperatures. It appears that this is the first biomass fast pyrolysis study where residence time is precisely controlled, and its effect on product distribution is studied over a

relatively broad range of temperatures (650 to 900 °C). Carbon monoxide is clearly the predominant product from secondary reactions, followed by ethylene and carbon dioxide. Methane and hydrogen are also significant secondary products. The yield of these principal gases via cracking follows a characteristic pattern over time, rising from a negligible or low "prompt gas" quantity to a maximum value at some time after pyrolysis has commenced. This behaviour is clearly reflected by the yield of total gas. The existence of prompt gas (ie., initial gases produced during primary reactions) was confirmed, and the composition was determined for cellulose and wood pyrolysis.

The primary accomplishment was the determination of rate equations for the secondary cracking reactions of cellulose and wood fast pyrolysis. The kinetic equations were not mechanistic, *per se*, but were empirical expressions suitable for reactor design and optimization of products over a defined range of experimental fast pyrolysis conditions.

A joint fast pyrolysis study was conducted with the cooperation of researchers at the University of Waterloo. This study was carried out at two independent laboratories using three reactor systems. The pyrolysis results exhibited excellent agreement over a very broad temperature range of 450 to 900°C, while overlapping in the range of 650 to 800 °C.

Although significant progress has been made in the science of fast pyrolysis, much remains to be done. The principal remaining tasks involve the identification of detailed

mechanisms of the primary fragmentation and secondary cracking reactions. Inextricably linked to this is the analysis and identification of the principal primary products (intermediates) from which the secondary cracking products are derived.

The ultrapyrolysis and RTP systems are potentially very well-suited to this task because of their characteristic precise control of residence time. However, additional analytical capabilities would be required to identify and quantify the liquid (vapour) intermediates. Their *disappearance* could then be monitored as a function of time, analogous to the present method of tracking the *appearance* of secondary gas products. An accurate determination of the secondary reaction mechanism would be possible since the intermediate reactants and secondary products would both be well characterized in time. The mechanism of the primary reactions could be inferred, with less confidence, from the product distribution of the intermediates.

Another remaining task is to determine the kinetics of the primary fragmentation and depolymerization pyrolysis reactions. Presently there is no quantitative *kinetic* evidence differentiating these two distinct primary pathways. The ultrapyrolysis and RTP reactor systems are not presently suitable for this task since the reaction times are too short, and precise control of the residence is simply not possible under 50 or 60 ms. Therefore, the analysis of products could not be related to residence time with confidence.

A final significant task is a reliable characterization of the mechanism of primary fast pyrolysis (ie., fragmentation). This should include the nature of the breakup of the polymeric and monomeric structures of the principal biomass components, and the origin of the primary products (intermediates) within these structures. For reasons outlined in the previous paragraph, the Ultrapyrolysis and RTP pilot plant systems in their present configurations are not well suited for this assignment. Some of the bench-scale fast pyrolysis apparati reviewed in Chapter 2 (Section 2.10.1) are more suitable for fundamental mechanistic investigations involving *primary* fast pyrolysis pathways.

Biomass fast pyrolysis has reached commercial viability, albeit in limited markets, over a relatively short period of development time. This has occurred as a direct result of meticulous and focussed fundamental research conducted by many researchers in various laboratories. The successful completion of the remaining tasks will provide a more complete understanding of the potential for fast pyrolysis, conceivably giving rise to a multi-product biomass "refinery" industry based on a renewable resource.

11.0 REFERENCES

1. Aho, M. and J. Huotari. "The Effects of Atmosphere on Pyrolysis of Solid Fuel Produced in Finland". In Fundamentals of Thermochemical Biomass Conversion. R.P. Overend et al., Editors. Elsevier Applied Science Publishers Ltd., New York, NY (1985), pp. 429-435.

2. Antal, M.J. "Thermochemical Conversion of Biomass. The Scientific Aspects". A Report to the Office of Technology Assessment of the Congress of the United States U.S. Congress, Washington, D.C. (1980).

3. Antal, M.J. "Pyrolysis as a Source of Chemicals and Feedstocks". Bio-Energy '80 World Congress and Exposition, Atlanta, GA. April 21-24. Bio-Energy Council, Washington, D.C. (1980), pp. 174-176.

4. Antal, M.J., C. Royere and A. Vialaron. "Biomass Gasification at the Focus of the Odeillo (France) 1-MW(Thermal) Solar Furnace". In Thermal Conversion of Solid Wastes and Biomass. J.L. Jones and S.B. Radding, Editors. ACS Symposium Series 130. American Chemical Society, Washington, D.C. (1980), pp. 237-255.

5. Antal, M.J. "Solar Flash Pyrolysis: A New Source of Fuels and Chemicals from Biomass". Annual Meeting of the AIChE. Philadelphia, PA. June. American Institute of Chemical Engineers, New York, NY (1980).

6. Antal, M.J., H.L. Friedman and F.E. Rogers. "Kinetics of Cellulose Pyrolysis in Nitrogen and Steam". Combustion Science and Technology 21 (1980): 141-152.

7. Antal, M.J., L. Hofmann and J.R. Moriera. "Bench Scale Radiant Flash Pyrolysis of Biomass". In Specialists' Workshop on Fast Pyrolysis of Biomass. James Diebold, Editor. SERI/CP-622-1096. Solar Energy Research Institute, Golden, CO (1980). pp. 175-182.

8. Antal, M.J. "The Effects of Residence Time, Temperature and Pressure on the Steam Gasification of Biomass". In Biomass as a Non-Fossil Fuel Source. D.L. Klass, Editor. ACS Symposium Series 144. American Chemical Society, Washington, D.C. (1981), pp. 313-334.

9. Antal, M.J., L. Hofman, C.T. Brown and R. Steenblick. "Design and Operation of a Solar Fired Biomass Flash Pyrolysis Reactor". In Energy from Biomass and Wastes V. Donald L. Klass, Editor. Institute of Gas Technology, Chicago, IL (1981), pp. 881-913.

10. Antal, M.J. "Biomass Conversion to Methane". In Methane: Fuel for the Future. P. McGeer and E. Durbin, Editors. Plenum Publishing Corporation, New York, NY (1982), pp.59-69.

11. Antal, M.J. "Biomass Pyrolysis: A Review of the Literature Part 1 - Carbohydrate Pyrolysis". In Advances in Solar Energy. K.W. Boer and V.A. Duffie, Editors. American Solar Energy Society, New York, NY (1983), pp. 61-111.

12. Antal, Michael Jerry. "Effects of Reactor Severity on the Gas-Phase Pyrolysis of Cellulose- and Kraft Lignin-Derived Volatile Matter". Industrial and Engineering Chemistry Product Research and Development 22 (1983): 366-375.

13. Antal, Michael Jerry. "Biomass Pyrolysis: A Review of the Literature Part 1 - Lignocellulose Pyrolysis". In Advances in Solar Energy. K.W. Boer and V.A. Duffie, Editors. American Solar Energy Society, New York, NY (1985), pp. 175-255.

14. Antal, M.J. "A Review of the Vapor Phase Pyrolysis of Biomass Derived Volatile Matter". In Fundamentals of Thermochemical Biomass Conversion. R.P. Overend et al., Editors. Elsevier Applied Science Publishers Ltd., New York, NY (1985), pp. 511-537.

15. Antal, M.J., W.S.L. Mok, J.C. Roy and A.T-Raissi. "Pyrolytic Sources of Hydrocarbons from Biomass". Journal of Analytical and Applied Pyrolysis 8 (1985): 291-303.

16. Arsenau, Donald F. and J.J. Stanwick. "A Study of Reaction Mechanisms by DSC and TG". Thermal Analysis 3 (1971): 319-326.

17 Arsenau, Donald F. "Competitive Reactions in the Thermal Decomposition of Cellulose" Canadian Journal of Chemistry 49 (1971): 632-638

18. Back, M.H. and R.A. Back. "Thermal Decomposition and Reactions of Methane". In Pyrolysis Theory and Industrial Practice. L.F. Albright et al., Editors. Academic Press, New York, NY (1983), pp. 1-24.

19. Barooah, J.N. and V.D. Long. "Rates of Thermal Decomposition of Some Carbonaceous Materials in a Fluidized Bed". Fuel 55 (1976): 116-120.

20. Basu, S.N. and P.C. Stangeby. "A Study on the Rapid Devolatilization Hydrogenation of Biomass Material Phase II". Enfor Report C-98. Canadian Forestry Service, Environment Canada, Ottawa, Canada (1981).

21. Beall, F.C. and H.W. Eickner. "Thermal Degradation of Wood Components: A Review of the Literature". Research Paper FPL 130. Forest Products Laboratory, U.S. Department of Agriculture, Madison, WI (1970).

22. Bergougnou, M.A., H.I. de Lasa, L.K. Mok, R.G. Graham and J. Hazlett. "High Intensity Flash Pyrolysis of Wood Using Solid Heat Carriers (Ultrapyrolysis)". In Third Bioenergy R&D Seminar. B. Summers, Editor. National Research Council of Canada, Ottawa, Canada (1981), pp. 277-282.

23. Bergougnou, M.A., H.I. de Lasa, J. Hazlett, L.K. Mok and R.G. Graham. "Ultraflash Pyrolysis (ULTRAPYROLYSIS) Process for Coal, Wood and Other Carbonaceous Materials". 64th Canadian Chemical Conference and Exhibition, Halifax, N.S. May 31 - June 3. Chemical Institute of Canada, Ottawa, Canada (1981).

24. Bergougnou, M.A., H.I. de Lasa, L.K. Mok, R.G. Graham, B.A. Freel and J.D. Hazlett. "Ultrapyrolysis of Cellulose and Wood Components". Enfor C-147 Final Report. Environment Canada. Ottawa, Canada (1983).

25. Bohn, M. and C. Benham. "An Experimental Investigation Into Fast Pyrolysis of Biomass Using an Entrained Flow Reactor". In Specialists' Workshop on Fast Pyrolysis of Biomass. James Diebold, Editor. Solar Energy Research Institute, Golden, CO (1980). pp. 287-301.

26. Bohn, M. and C. Benham. "Biomass Pyrolysis with an Entrained Flow Reactor". Industrial and Engineering Chemistry Process Design and Development 23 (2) (1984): 355-363

27. Boyd, M., C. Anderson, De Vera and M.C. Hawley. "Pyrolysis and Gasification of Hybrid Poplar SPP". Symposium 78 - Pyrolysis for Production of Chemicals and Food. American Institute of Chemical Engineers, New York, NY (1979).

28. Bradbury, Allan .G., Yoshio Sakai and Fred Shafizadeh. "A Kinetic Model for Pyrolysis of Cellulose". Journal of Applied Polymer Science 23 (1979): 3271-3280.

29. Bridgwater, A.V. and J.M. Double. "Pyrolysis Liquids: Problems and Opportunities for Utilization". In Pyrolysis as a Basic Technology for Large Agro-Energy Projects E. Mattucci, Editor. Commission of the European Communities. Brussels, Belgium (1989). pp. 167-171.

30. Bridgwater, A.V. "Biomass Pyrolysis Technologies". In Biomass for Energy and Industry. G. Grassi, Editor. Elsevier Applied Science. London (1990), pp. 2.489-2.496

31. Bridgwater, A.V. and S.A. Bridge. "A Review o. Biomass Pyrolysis and Pyrolysis Technologie:". In Biomass Pyrolysis Liquids Upgrading and Utilization. A.V. Bridgwater and G. Grassi, Editors. Elsevier Applied Science. London (1991), pp. 11-92.

32. Brink, D.L. and M.S. Massoudi. "A Flow Reactor Technique for the Study of Wood Pyrolysis. A. Experimental". Journal of Fire and Flammability 9 (1978): 176-188.

33. Broido, A. "Kinetics of Solid Phase Cellulose Pyrolysis". In Thermal Uses and Properties of Carbohydrates and Lignins. F. Shafizadeh, Editor. Academic Press, New York, NY (1976), pp. 19-36.

34. Browne, F.L. "Theories of the Combustion of Wood and Its Control". FPL Report No. 2136. Forest Products Laboratory, US Department of Agriculture, Madison, WI (1963).

35. Byrne, G.A., D. Gardner and F.H. Holmes. "The Pyrolysis of Cellulose and the Action of Flame Retardants II. Further Analysis and Identification of Products". Journal of Applied Chemistry 16 (1966): 81-88.

36. Chang, P.W., K. Duri-Swamy and E.W. Knell. "Kinetics of Coal Pyrolysis Reactions in a Flash Pyrolysis Process". Coal Processing Technology 6 (1980): 20-27.

37. Chen, C.J., M.H. Back and R.A. Back. "Mechanism of the Thermal Decomposition of Methane". In Industrial and Laboratory Pyrolysis. American Chemical Society Symposium Series 32 (1976), pp. 1-16.

38. Contractor, R.M. "Commercial Hydrocarbon Cracking Processes". In Specialists' Workshop on Fast Pyrolysis of Biomass. James ~ ebold, Editor. Solar Energy Research Institute, Golden, CO (1980), pp. 45-55.

39. Dave, R., J.L. Hauzelot and J. Villermaux. "A Novel and Simple Jet-Stirred Reactor for Homogeneous and Heterogeneous Reactions with Short Residence Times". Chemical Engineering Science 34(6) (1979): 867-876.

40. Deglise, X., P. Marliere and Ph. Schlicklin. "Mass and Energy Balances for a Two-Fluidized Bed Pilot Plant which Operates on Wood Fast Pyrolysis". In Energy from Biomass 1st E.C. Conference. A. Strub et al., Editors. Applied Science Publishers, London, England (1981), pp. 569-573.

41. Deglise, X., C. Richard, A. Rolin and H. François. "Fast Pyrolysis/Gasification of Lignocellulosic Materials at Short Residence Time". In Energy from Biomass 1st E.C. Conference. A. Strub et al., Editors. Applied Science Publishers, London, England (1981), pp. 548-562.

42. Deglise, X. and J. Lede. "The Upgrading of the Energy of Biomass by Thermal Methods". International Chemical Engineering 22 (1982): 631-646.

43. Deglise, X. and G. Martin. "Pyrolyse Rapide de Plaquettes de Hetre et de Douglas". Laboratoire de Photochimie Appliquée. Université de Nancy 1, B.P. 239, 54506 Vandoeuvre-les-Nancy, Cedex, France (1982).

44. Degroot, William F., Wei-Ping Pan, M. Dalilur Rahman and Geoffry N. Richards. "Early Products of Pyrolysis of Wood". American Chemical Society. Division of Fuel Chemistry 32 (2) (1987): 36-39

45. DeJenga, Chine I., Michael Jerry Antal and Maitland Jones. "Yields and Composition of Sirups Resulting from the Flash Pyrolysis of Cellulosic Materials Using Radiant Energy". Journal of Applied Polymer Science 27 (1982): 4313-4322.

46. Desrosiers, R. "Gasification Engineering". 12th Biomass Thermochemical Conversion Contractor's Meeting, Washington, D.C. March 18-19. Pacific Northwest Laboratory, Batelle Memorial Institute, Richland, WA (1981).

47. Diebold, J.P. "Gasoline from Solid Wastes by a Noncatalytic Thermal Process". In Thermal Conversion of Solid Wastes and Biomass. J.L. Jones and S.B. Radding, Editors. ACS Symposium Series 130. American Chemical Society, Washington, D.C. (1979), pp. 209-226.

48. Diebold, J.P. "Ablative Pyrolysis of Macroparticles of Biomass". In Specialists' Workshop on Fast Pyrolysis of Biomass. James Diebold, Editor. Solar Energy Research Institute, Golden, CO (1980), pp. 237-251.

49. Diebold, J.P. and C.B. Benham. "Pyrolysis Experiments at China Lake Using a Tubular Entrained Flow Reactor". In Specialists' Workshop on Fast Pyrolysis of Biomass. James Diebold, Editor. Solar Energy Research Institute, Golden, CO (1980), pp. 271-280.

50. Diebold, James and Garyl Smith. "Commercialization Potential of the China Lake Trash-to-Gasoline Process". In Design & Management for Resource Recovery. Volume 1. Energy from Waste. T.C. Frankiewicz, Editor. Ann Arbor Science Publishers Inc., Ann Arbor, MI (1980).

51. Diebold, J. and J. Scahill. "Progress in the Entrained Flow, Fast Ablative Pyrolysis of Biomass". 12th Biomass Thermochemical Conversion Contractor's Meeting, Washington, D.C. March 18-19. Pacific Northwest Laboratory, Batelle Memorial Institute, Richland, WA (1981).

52. Diebold, J. and J. Scahill. "October 1981 Update on the Progress in the Entrained Flow, Fast Ablative Pyrolysis of Biomass". 13th Biomass Thermochemical Conversion Contractor's Meeting, Arlington, VA. October 27-29. Pacific Northwest Laboratory, Batelle Memorial Institute, Richland, WA (1981).

53. Diebold, J. and J. Scahill. "Ablative Entrained Flow Fast Pyrolysis Status". 15th Biomass Thermochemical Conversion Contractor's Meeting, Atlanta, GA. March 16-17. Pacific Northwest Laboratory, Batelle Memorial Institute, Richland, WA (1983).

54. Diebold, J. and J. Scahill. "Ablative Pyrolysis of Biomass in the Entrained-Flow Cyclonic Reactor of SERI". Annual Report. October 1, 1981 - November 30, 1982., SERI/PR-234-1883. Solar Energy Research Institute, Golden, CO (1983).

55. Diebold, J.P. "The Cracking Kinetics of Depolymerized Biomass Vapors in a Continuous, Tubular Reactor". Master of Science in Chemical and Petroleum-Refining Engineering Thesis. Colorado School of Mines, Denver, CO (1985).

56. Diebold, James and Arthur Power. "Engineering Aspects of the Vortex Pyrolysis Reactor to Produce Primary Pyrolysis Oil Vapors for use in Resins and Adhesives". In Research in Thermochemical Biomass Conversion. A.V. Bridgwater and J.L. Kuester, Editors. Elsevier Applied Science. London (1988). pp. 629-638.

57. Diebold, James. "Development of Pyrolysis Reactor Concepts in the USA". In Biomass Pyrolysis Liquids Upgrading and Utilization. A.V. Bridgwater and G. Grassi, Editors. Elsevier Applied Science. London (1991), pp. 341-350.

58. Diebold, J., J. Scahill, R. Bain, H. Chum, S. Black, T. Milne, R. Evans and B. Rajal. "Biomass Liquefaction at SERI". Proceedings of R&D Contractors Meeting on Biomass Liquefaction. Alternate Energy Branch. Canmet. Energy, Mines and Resources, Ottawa (1991). pp. 101-108.

59. Eddinger, R.T. "The Pyrolysis Route to Gasification". Proceedings of the 14th Intersociety Energy Conversion Engineering Conference. American Chemical Society, Washington, D.C. (1979).

60. Edrich, R., T. Bradley and M.S. Graboski. "The Gasification of Ponderosa Pine Charcoal". In Fundamentals of Thermochemical Biomass Conversion. R.P. Overend et al., Editors. Elsevier Applied Science Publishers Ltd., New York, NY (1985), pp. 557-566.

61. Edwards, J.H., I.W. Smith, R.J. Tyler and P.C. Wailes. "Conversion of Coal to Liquid Products by Flash Pyrolysis". Institute of Chemical Engineers Symposium Series 62 (1980): Q1-Q16.

62. Edwards, J.H. and I.W. Smith. "Flash Pyrolysis of Coals: Behaviour of Three Coals in a 20 Kg/h Fluidized Bed Pyrolyzer". CSIRO Division of Process Technology. P.O. Box 136, North Ryde, N.S.W., Australia 2113 (1982).

63. Edwards, J.H., I.W. Smith and R.J. Tyler. "Flash Pyrolysis of Coals: Comparison of Results from 1 g/h and 20 kg/h Reactors". CSIRO Division of Process Technology, P.O. Box 136, North Ryde, N.S.W., Australia 2113 (1982).

64. Eisenhut, I. "Pyrolysis of Solid Carbonaceous Materials". Proceedings of the Future Sources of Organic Raw Materials World Conference, L.E. St. Pierre et al., Editors. Pergamon Press (1980), pp. 257-267.

65. Ekstrom, C. and E. Rensfelt. "Flash Pyrolysis of Biomass in Sweden". In Specialists' Workshop on Fast Pyrolysis of Biomass. James Diebold, Editor. Solar Energy Research Institute, Golden, CO (1980), pp. 303-325.

66. Elliott, D.C., D. Beckman, A.V. Bridgwater, J.P. Diebold, S.B. Gevert and Y. Solantausta. "Developments in Direct Thermal Liquefaction of Biomass 1983-1990. Energy and Fuels 5 (1991): 399-410.

67. Eltenton, G.C. "The Detection of Free Radicals by Means of a Mass Spectrometer". Journal of the Chemical Physics 10 (1942): 403.

68. Evans, R.J., F.A. Agblevor, H.L. Chum, J.B. Woolten, D.B. Chadwick and S.D. Baldwin. "New Approaches to the Study of Cellulose Pyrolysis" American Chemical Society. Division of Fuel Chemistry 36 (2) (1991): 1-11

69. Fallon, P.T., B. Bhatt and M. Steinberg. "The Flash Hydropyrolysis of Lignite and Sub-Bituminous Coals to Both Liquid and Gaseous Hydrocarbon Products". Fuel Processing Technology 3 (1980): 155-168.

70. Fransham, P.B. "Fast Pyrolysis Demonstration Plant". R&D Contractors Meeting on Biomass Liquefaction. Alternate Energy Branch. Canmet. Energy, Mines and Resources, Ottawa (1991). pp. 74-85.

71. Freel, B.A., R.G. Graham, M.A. Bergougnou, R.P. Overend and L.K. Mok. "The Kinetics of the Fast Pyrolysis (Ultrapyrolysis) of Cellulose in a Fast Fluidized Bed Reactor". In New Developments in Fluidization and Fluid Particle Systems Wen-Ching Wang, Editor. AIChE Symposium Series 255. Volume 83 (1987): 105-111.

72. Frey, F.E. and D.F. Smith. "Thermal Decomposition of Ethane, Ethylene, Propane and Propylene". Industrial and Engineering Chemistry 20 (1928): 948-951.

73. Funazukuri, Toshitaka, Robert R. Hudgins and Peter 1. Silveston. "Correlation of Products from Fast Cellulose Pyrolysis" Industrial and Engineering Chemistry Process Design and Development 25 (1986): 172-181.

74. Goheen, D.W. "High Temperature Electric Arc RF Energy and Combustion Gas Heated Pyrolysis of Powdered Biomass". In Specialists' Workshop on Fast Pyrolysis of Biomass. James Diebold, Editor. Solar Energy Research Institute, Golden, CO (1980), pp. 137-151.

75. Graboski, M.S. "Fast Pyrolysis of Biomass for Energy or Chemicals". Bioenergy '80 World Congress. Atlanta, GA (1980), pp. 211-219.

76. Graboski, M.S. "Purification and Uses of Fast Pyrolysis Gases Made from Biomass". In Specialists' Workshop on Fast Pyrolysis of Biomass. James Diebold, Editor. Solar Energy Research Institute, Golden, CO (1980), pp. 393-414.

77. Graef, M., A.G. Graham and B.H. Krieger. "Rapid Pyrolysis of Biomass/Lignin for Production of Acetylene". Symposium on Biomass as a Non-Fossil Fuel Source. Honolulu, HI, April 1-6. American Chemical Society. Division of Fuel Chemistry (1979), pp. 432-444.

78. Graef, M., A.G. Graham and B.H. Krieger. "Product Distribution in the Rapid Pyrolysis of Biomass/Lignin for Production of Acetylene". American Chemical Society Symposium Series 144 (1981), pp. 293-312.

79. Graham, R.G., L.K. Mok, M.A. Bergougnou and H.I. de Lasa. "Fast Pyrolysis of Biomass for the Production of Chemicals and Fuels from Wood". In Fourth Bioenergy R&D Seminar. B. Summers, Editor. National Research Council of Canada, Ottawa, Canada (1982), pp. 397-410.

80. Graham, R.G., M.A. Bergougnou and R.P. Overend. "Fast Pyrolysis of Biomass". Journal of Analytical and Applied Pyrolysis 6 (1984):363-374.

81. Graham, R.G., M.A. Bergougnou, L.K. Mok and H.I. de Lasa. "Fast Pyrolysis (ULTRAPYROLYSIS) of Biomass Using Solid Heat Carriers". In Fundamentals of Thermochemical Biomass Conversion, R.P. Overend et al., Editors. Elsevier Applied Science Publishers Ltd. New York, NY (1985), pp. 397-410.

82. Graham, R.G., M.A. Bergougnou and B.A. Freel. "The Production of Pyrolytic Liquids from Cellulose by Fast Pyrolysis (Ultrapyrolysis)". Symposium on Production, Analysis and Upgrading of Pyrolysis Oils from Wood. 193rd ACS National Meeting. Denver, CO. April 5-10. The Cellulose, Paper and Textile Division and The Fuel Division. American Chemical Society. Washington, DC. (1987).

83. Graham, Robert G., Barry A. Freel and M.A. Bergougnou. "Rapid Thermal Processing (RTP): Biomass Fast Pyrolysis Overview". R&D Contractors Meeting on Biomass Liquefaction. Alternate Energy Branch. Canmet. Energy, Mines and Resources, Ottawa (1990), pp. 52-63.

84. Graham, Robert G., Barry A. Freel, Donald R. Huffman and M.A. Bergougnou. "Developments in Rapid Thermal Processing (RTP): Biomass Fast Pyrolysis". In Sixth European Conference on Biomass for Energy, Industry and Environment. G. Grassi, Editor. Elsevier Applied Science, London (1991). In Press.

85. Gumz, W. Gas Producers and Blast Furnaces. Wiley, New York, NY (1980), p. 18.

86. Hajaligol, M.R., W.A. Peters, J.B. Howard and J.P. Longwell. "Product Compositions and Kinetics for Rapid Pyrolysis of Cellulose". Industrial and Engineering Chemistry Process Design and Development 21 (1982): 457-465.

87. Hallen, R.T., L.J. Sealock and R. Cuello. "Influence of Alkali Carbonate on Biomass Volatilization". In Fundamentals of Thermochemical Biomass Conversion. R.P. Overend et al., Editors. Elsevier Applied Science Publishers Ltd., New York, NY (1985), pp. 157-166.

88. Harkness, J.B.L., R.D. Doctor and W.H. Seward "Environmental Control Technology for Biomass Flash Pyrolysis". In Energy from Biomass and Wastes IV. Donald L. Klass, Editor. Institute of Gas Technology, Chicago, IL (1980), pp. 617-643.

89. Holman, J.R. Heat Transfer, 4th Edition. McGraw-Hill Book Company, New York, NY (1976).

90. Howard, J.B., M.R. Hajaligol, J.P. Longwell, T.R. Nunn and W.A. Peters. "Pyrolysis of Biomass". Proceedings of the AIChE/CIESC Joint Meeting of Chemical Engineers, Beijing, China. September 19-22. American Institute of Chemical Engineers, New York, NY (1982).

91. Huffman, W.J., J.E. Halligan, R.L. Peterson and E. de La Garza. "Ammonia Synthesis Gas and Petrochemicals from Cattle Feedlot Manure". Proceedings of the Symposium on Clean Fuels from Biomass, Lake Buena Vista, FL. January 24-28. Institute of Gas Technology, Chicago, IL (1977).

92. Johnson, D.A., W.A. Ayres and G. Tomberlin. "Scale-up of the Ablative Fast Pyrolysis Process". R&D Contractors Meeting on Biomass Liquefaction. Alternate Energy Branch. Canmet. Energy, Mines and Resources, Ottawa (1990), pp. 236-239.

93. Jönsson, O. "Thermal Cracking of Tars and Hydrocarbons by Addition of Steam and Oxygen in the Cracking Zone". In Fundamentals of Thermochemical Biomass Conversion. R.P. Overend et al., Editors. Elsevier Applied Science Publishers Ltd., New York, NY (1985), pp. 733-746.

94. Kam, A. "Hydrocarbon Liquids and Heavy Oil from Biomass: Technology and Economics". In Energy from Biomass and Wastes IV. Donald L. Klass, Editor. Institute of Gas Technology, Chicago, IL (1980), pp. 589-615.

95. Kanury, A.M. "Thermal Decomposition Kinetics of Wood Pyrolysis". Combustion and Flame 18 (1972): 75-83.

96. Khan, M.S. and B.L. Crynes. "Survey of Recent Methane Pyrolysis Literature". Industrial and Engineering Chemistry 62 (1970): 54-59.

97. Kilzer, F.J. and A. Broido. "Speculations on the Nature of Cellulose Pyrolysis". Pyrodynamics 2 (1965): 151-163.

98. Knight, J.A., C.W. Gorton and T.H. Murphy. "Thermochemical Conversion of Biomass to Syngas Via the Georgia Tech Entrained Pyrolysis/Gasification Process". 11th Thermochemical Conversion Contractor's Meeting, Richland, WA. September 23-24. Pacific Northwest Laboratory, Batelle Memorial Institute, Richland, WA (1980).

99. Knight, J.A., C.W. Gorton, R.J. Kovac and L.W. Elston. "Entrained Flow Pyrolysis of Biomass". 14th Biomass Thermochemical Conversion Contractor's Meeting, Arlington, VA. June 23-24. Pacific Northwest Laboratory, Batelle Memorial Institute, Richland, WA (1982).

100. Kochubei, V.F. and F.B. Moin. "Kinetics of the Reaction of CO_2 with Hydrogen". Kinetics and Catalysis 10 (1969): 992-997.

101. Kothari, Virendra and Michael Jerry Antal. "Numerical Studies of the Flash Pyrolysis of Cellulose". Fuel 64 (1985): 1487-1494.

102. Krieger, B. "Microwave Pyrolysis of Biomass". In Specialists' Workshop on Fast Pyrolysis of Biomass. James Diebold, Editor. Solar Energy Research Institute, Golden, CO (1980), pp. 191-214.

103. Kung, H-C. and A.S. Kaielkar. "On the Heat of Reaction in Wood Pyrolysis". Combustion and Flame 20 (1973): 91-103.

104. Kuramoto, M., F. Takehiko and D. Kunii. "New Circulation of Fluidized Solids Applied to Biomass Gasification". Department of Chemical Engineering, University of Tokyo, Japan (1982).

105. Lede, J., P. Berthelot, J. Villermaux, A. Rolin, A. François and X. Deglise. "Pyrolyse-flash de déchets lignocellulosiques en vue de leur valorisation par l'énergie solaire concentrée". Revue de Physique Appliquée 15 (1980):545-552.

106. Lede, J., F. Verzaro and J. Villermaux. "Le cyclone: un nouveau réacteur chimique solaire gas-solide. Application à la mise en oeuvre en continu de la pyrolyse flash de sciure de bois". Revue de Physique Appliquées 15 (1980): 535-543.

107. Lede, J., F. Verzaro, B. Antoine and J. Villermaux. "Cyclone Reactor for Flash Pyrolysis of Solid Particles". In Specialists' Workshop on Fast Pyrolysis of Biomass. James Diebold, Editor. Solar Energy Research Institute, Golden, CO (1980), pp. 327-345.

108. Lewellen, P.C., W.A. Peters and J.B. Howard. "Cellulose Pyrolysis Kinetics and Char Formation Mechanism". The 16th International Symposium on Combustion. The Combustion Institute, Pittsburgh, PA (1977), pp. 1471-1480.

109. Liberick, W. "Thermochemical Conversion of Wastes/Biomass to Gasoline". In Energy from Biomass and Wastes IV. Donald L. Klass, Editor. Institute of Gas Technology, Chicago, IL (1980), pp. 747-763.

110. Liinanki, L., N. Lindman, S.O. Sjoberg and E. Strom. "Methane Yield from Biomass Gasification at High Temperature and Pressure". In Fundamentals of Thermochemical Biomass Conversion. R.P. Overend et al., Editors. Elsevier Applied Science Publishers Ltd., New York, NY (1985), pp. 923-936.

111. Lin, M.C. and M.H. Back. "The Thermal Decomposition of Ethane". Canadian Journal of Chemistry 44 (1966): 505-514.

112. Lincoln, K.A. "High Radiative Heat Flux Pyrolysis of Thin Biomass". In Specialists' Workshop on Fast Pyrolysis of Biomass. James Diebold, Editor. Solar Energy Research Institute, Golden, CO (1980), pp. 153-164.

113. Lipska-Quinn, A.E., S.H. Zeronian and K.M. McGee. "Thermal Degradation of Rice Straw and Its Components". In Fundamentals of Thermochemical Biomass Conversion. R.P. Overend et al., Editors. Elsevier Applied Science Publishers Ltd., New York, NY (1985), pp. 453-471.

114. MacLean, J.D. Transactions of the American Society of Heating and Ventilating Engineers 47 (1971): 323-354.

115. Maniatis, K., J. Baeyens, H. Peeters and G. Roggeman. "Flash Pyrolysis in an Entrained Bed Pilot Plant Reactor". R&D Contractors Meeting on Biomass Liquefaction. Alternate Energy Branch. Canmet. Energy, Mines and Resources, Ottawa (1991). pp. 39-43.

116. Marek, L.F. and W.B. McCluer. "Velocity Constants for the Thermal Dissociation of Ethane and Propane". Industrial and Engineering Chemistry 23 (1931): 878-881.

117. Milne, T.A. "Pyrolysis - Thermal Behaviour of Biomass Below 600°C". In A Survey of Biomass Gasification, Volume II. Principles of Gasification. Solar Energy Research Institute, Golden, CO (1979), p. 79.

118. Milne, T.A. and M. Soltys. "Kinetics and Mechanisms of Fast Pyrolysis". 12th Thermochemical Conversion Contractor's Review Meeting, Washington, D.C. March 18-19. Pacific Northwest Laboratory, Batelle Memorial Institute, Richland, WA (1981).

119. Milne, T.A. and M. Soltys. "Fundamental Pyrolysis Studies". Quarterly Report. October-December 1981. SERI/PR-234-1537. Solar Energy Research Institute, Golden, CO (1982).

120. Milne, T.A. and M. Soltys. "Fundamental Pyrolysis Studies". Quarterly Report. January-March 1982. SERI/PR-234-1617. Solar Energy Research Institute, Golden, CO (1982).

121. Milne, T.A. and M.N. Soltys. "Fundamental Pyrolysis Studies". 14th Biomass Thermochemical Conversion Contractor's Meeting, Arlington, VA. June 23-24. Pacific Northwest Laboratory, Batelle Memorial Institute, Richland, WA (1982).

122. Milne, T.A., R.J. Evans and N. Michael. "Fundamental Pyrolysis Studies". Annual Report. October 1, 1981 - November 30, 1982. SERI/PR-234-1884. Solar Energy Research Institute, Golden, CO (1983).

123. Milne, T.A. and M.N. Soltys. "The Direct Mass-Spectrometric Study of the Primary and Secondary Pyrolysis Behaviour of Biomass and its Constituents". In Fundamentals of Thermochemical Biomass Conversion. R.P. Overend et al., Editors. Elsevier Applied Science Publishers Ltd., New York, NY (1985), pp. 361-383.

124. Mok, L.K., R.G. Graham, M.A. Bergougnou and H.I. de Lasa. "Continuous Ultra-Flash Pyrolysis of Wood Using Solid Heat Carriers and Vortical Contactors (Ultrapyrolysis)". Industrial Wood Energy Forum '82 Conference, Washington, D.C. March 8-10. Forest Products Research Society, Madison, WI (1982), pp. 292-298.

125. Mok, L.K., H.I. de Lasa, M.A. Bergougnou and R.G. Graham. "Continuous Ultra-Flash Pyrolysis of Wood Using Solid Heat Carriers and Double Jet Vortical Contactors (Ultrapyrolysis)". In Fourth Bioenergy R&D Seminar. B. Summers, Editor. National Research Council of Canada, Ottawa, Canada (1982), pp. 337-341.

126. Mok, L.K., R.G. Graham, H.I. de Lasa and M.A. Bergougnou. "Laboratory Apparatus for the Ultra-Fast Pyrolysis (Ultrapyrolysis) of Biomass and Other Carbonaceous Materials Using Ultra Fast Fluidized Reactors". Proceedings of the International Powder and Bulk Solids Conference, Rosemont, IL. May 11-13. Cahners Exposition Group, Des Plaines, IL (1982).

127. Mok, L.K., R.G. Graham, H.I. de Lasa, B.A. Freel and M.A. Bergougnou. "Application of Ultra-Fast Fluidization to the Fast Pyrolysis of Cellulose (Ultrapyrolysis)". American Institute of Chemical Engineers Symposium Series 234. Volume 80 (1984): 70-79.

128. Mok, William. S. and Michael J. Ant[illegible]. "Effects of Pressure on Biomass Pyrolysis". 14tn Thermochemical Conversion Contractor's Meeting, Washington, D.C. June 23-24. Pacific Northwest Laboratory, Batelle Memorial Institute, Richland, WA (1982).

129. Nandi, S.P. and M. Onischak. "Gasification of Chars from Maple and Jack Pine Woods". In Fundamentals of Thermochemical Biomass Conversion. R.P. Overend et al., Editors. Elsevier Applied Science Publishers Ltd., New York, NY (1985), pp. 567-587.

130. Nunn, T.R., J.B. Howard and J.P. Longwell. "Product Compositions and Kinetics in the Rapid Pyrolysis of Milled Wood Lignin". Energy Laboratory and Department of Chemical Engineering, Massachusetts Institute of Technology, Cambridge, MA (1982).

131. Nunn, T.B., J.B. Howard, J.P. Longwell and W.A. Peters. "Studies of the Rapid Pyrolysis of Sweet Gum Hardwood". In Fundamentals of Thermochemical Biomass Conversion. R.P. Overend et al., Editors. Elsevier Applied Science Publishers Ltd. New York, NY (1985), pp. 293-314.

132. Nuttal, H.E. "Heating Carbonaceous Particulate Material". United States Patent Number 4108732 (August 22, 1978).

133. Overend, Ralph P. Biosyn Biomass Gasification: Executive Summary Alternate Energy Division. Canmet. Energy Mines and Resources, Canada. Ottawa (1988).

134. Pavlath, A.E. and K.S. Gregorski. "Thermoanalytical Studies of Carbohydrate Pyrolysis". In Fundamentals of Thermochemical Biomass Conversion. R.P. Overend et al., Editors. Elsevier Applied Science Publishers Ltd., New York, NY (1985), pp. 437-452.

135. Pease, R.N. "The Thermal Dissociation of Ethane, Propane, Butane and Isobutane Preliminary Study". Journal of the American Chemical Society 50 (1928): 1779-1785.

136. Peters, W.A. Massachusetts Institute of Technology. Personal Communication (1983).

137. Peters, W.A. "Studies of the Pyrolysis Behaviour of Condensed Phase Fuels with Applications to Fuel Conversion Technology". In Fifth International Symposium on Analytical Pyrolysis. K.J. Voorbees et al., Editors. Butterworth, New York, NY (1983).

138. Petrocelli, F.P. and M.T. Klein. "Simulation of Kraft Lignin Pyrolysis". In Fundamentals of Thermochemical Biomass Conversion. R.P. Overend et al., Editors. Elsevier Applied Science Publishers Ltd., New York, NY (1985), pp. 257-273.

139. Piskorz, Jan, Desmond Radlein and Donald S. Scott. "On the Mechanism of the Rapid Pyrolysis of Biomass". Journal of Analytical and Applied Pyrolysis 9 (1986): 121-137.

140. Piskorz, J. and D.S. Scott. "The Composition of Oils Obtained by the Fast Pyrolysis of Different Woods" American Chemical Society. Division of Fuel Chemistry 32 (2) (1987): 215-223.

141. Piskorz, Jan. Desmond ST.A.G. Radlein, Donald S.Scott and Stefan Czernik. "Liquid Products from the Fast Pyrolysis of Wood and Cellulose" In Research in Thermochemical Biomass Conversion. A.V. Bridgwater and J.L. Kuester, Editors. Elsevier Applied Science. London (1988).

142. Prahacs, S. "Pyrolytic Gasification of Na-, Ca- and Mg-Base Spent Pulping Liquors in an AST Reactor". Advances in Chemistry Series 69. The 152nd Meeting of the American Chemical Society, Division of Fuel Chemistry (1966), pp. 230-242.

143. Prahacs, S., H.G. Barclay and S. Bhatia. "A Study of the Possibilities of Production Synthetic Tonnage Chemicals from Lignocellulosic Residues". Pulp and Paper Magazine of Canada 72 (1971): 69-83.

144. Prahacs, S., H.G. Barclay and S. Bhatia. "Possibilities of Large-Scale Utilization of Lignocellulosic Residues by Partial or Complete Gasification". American Institute of Chemical Engineers Symposium Series 133. Volume 69 (1973): 11-19.

145. Preston, G.T. "Resource Recovery and Flash Pyrolysis of Municipal Refuse". Clean Fuels from Biomass, Sewage, Urban Refuse and Agricultural Wastes Symposium, Lake Buena Vista, FL. January 27. Sponsored by the Institute of Gas Technology, Chicago, IL (1976).

146. Radlein, D.St.A.G., J. Piskorz, A. Grinshpun and D.S. Scott. "Fast Pyrolysis of Pretreated Wood and Cellulose". American Chemical Society. Division of Fuel Chemistry 32 (2) (1987): 29-34.

147. Raman, Pattabi, Walter P. Walawender, L.T. Fan and C.C. Chang. "Mathematical Model for the Fluid Bed Gasification of Biomass Materials. Application to Feedlot Manure". Industrial and Engineering Chemistry Process Design and Development 20 (1981): 686-692.

148. Ramiah, M.V. "Thermogravimetric and Differential Thermal Analysis of Cellulose, Hemicellulose and Lignin". Journal of Applied Polymer Science 14 (1970): 1323-1337.

149. Reed, T.B. "Biomass Gasification: Yesterday, Today and Tomorrow". Energy Generation and Cogeneration from Wood Conference, Atlanta, GA. February 18-20. Forest Products Research Society, Madison, WI (1980), p. 50.

150. Reed, T.B., J.P. Diebold and R. Desrosiers. "Perspectives in Heat Transfer Requirements and Mechanisms for Fast Pyrolysis". In Specialists' Workshop on Fast Pyrolysis of Biomass. James Diebold, Editor. Solar Energy Research Institute, Golden, CO (1980), pp. 7-19.

151. Reed, T.B., J.P. Diebold and R. Desrosiers. "Biomass Gasification for Production of Gaseous and Liquid Fuels". 3rd Symposium on Biotechnology in Energy Production and Conservation, Gatlinburg, TN. May 12-15. United States Department of Energy, Washington, D.C. (1981).

152. Reed, Thomas B. and Craig D. Cowdery. "Heat Flux Requirements for Fast Pyrolysis and a New Method for Generating Biomass Vapor". American Chemical Society. Division of Fuel Chemistry 32 (2) (1987): 68-81

153. Reed, Th.B. and C.C. Cowdery. "A Pyrolysis Mill for Fast Pyrolysis of Biomass". In Pyrolysis as a Basic Technology for Large Agro-Energy Projects E. Mattucci, Editor. Commision of the European Communities. Brussels, Belgium (1989).

154. Rejai, B. R.J. Evans, T.A. Milne, J.P. Diebold and J.W. Scahill. "The Conversion of Biobased Feedstocks to Liquid Fuels Through Pyrolysis". Chemical Conversion Research Branch. Solar Energy Research Institute. Golden, CO. (1990).

155. Rensfelt, E., G. Blomkvist, C. Ekstrom, S. Engstrom, B.G. Espenas and L. Liinanki. "Basic Gasification Studies for Development of Biomass Medium - BTU Gasification Processes". Energy from Biomass and Wastes Conference, Washington, D.C. August 14-18. Institute of Gas Technology, Chicago, IL (1978), pp. 465-494.

156. Rice, F.O. and M.D. Dooley. "Thermal Decomposition of Organic Compounds from the Standpoint of Free Radicals. IV. The Dehydrogenation of Paraffin Hydrocarbons and the Strength of the C-C Bond". Journal of the American Chemical Society 55 (1933): 4245-4247.

157. Rice, F.C. and K.F. Herzfeld. "Thermal Decomposition of Organic Compounds from the Standpoint of Free Radicals. IV. The Dehydrogenation of Parrafin Hydrocarbons and the Strength of the C-C Bond". Journal of the American Chemical Society 56 (1934): 4245-4247.

158. Rice, F.O. and K.F. Herzfeld. "The Mechanism of Some Chain Reactions". Journal of Chemical Physics 7 (1939): 671-674.

159. Richards, Geoffry N. "Glycoaldehyde from Pyrolysis of Cellulose" Journal of Analytical and Applied Pyrolysis 10 (1987): 251-255.

160. Roberts, A.F. "A Review of Kinetics Data for the Pyrolysis of Wood and Related Substances". Combustion and Flame 14 (1970): 261-272.

161. Roberts, A.F. "The Kinetic Behavior of Intermediate Compounds During the Pyrolysis of Cellulose". Journal of Applied Polymer Science 14 (1970): 244-247

162. Rolin, A. "Pyrolyse Rapide de Composés Lignocellulosiques". (Thèse). Laboratoire de Photochimie Appliquée, Université de Nancy, Nancy, France (1981).

163. Ross, R.A. and P. Fong. "Catalytic Conversion of Wood Barks to Fuel Gases". Industrial and Engineering Chemistry Process Design and Development 20(1) (1981): 197-203.

164. Roy, C., B. de Caumia, P. Plante and H. Menard. "Production of Liquids from Biomass by Vacuum Pyrolysis. Development of Data Base for Continuous Process". In Energy from Biomass and Wastes VII. Donald L. Klass, Editor. Institute of Gas Technology, Chicago IL (1983), p. 1147.

165. Roy, C., B. de Caumia, D. Brouillard and H. Ménard. "The Pyrolysis Under Vacuum of Aspen Poplar". In Fundamentals of Thermochemical Biomass Conversion. R.P. Overend et al., Editors. Elsevier Applied Science Publishers Ltd., New York, NY (1985), pp. 237-256.

166. Schaffer, E.L. "An Approach to the Mathematical Prediction of Temperature Use Within a Semi-Infinite Wood Slab Subjected to High Temperature Conditions". Pyrodynamics 2 (1965): 117-132.

167. Schulten ,H.-R., U. Bahr and W. Gortz. "Curie-Point Pyrolysis Field Ionization Mass Spectrometry of Carbohydrates. Part B: Polysaccharides" Journal of Analytical and Applied Pyrolysis 3 (1981): 137-150.

168. Schulten ,H.-R., U. Bahr and W. Gortz. "Pyrolysis Field Ionization Mass Spectrometry of Carbohydrates. Part A: Methodology" Journal of Analytical and Applied Pyrolysis 3 (1981): 137-150.

169. Scott, D.S. and J. Piskorz. "Flash Pyrolysis of Biomass". In Fuels from Biomass and Wastes. D.L. Klass and G.H. Emert. Editors. Ann Arbor Science Publishers Inc., Ann Arbor, MI (1981).

170. Scott, D.S. and J. Piskorz. "The Flash Pyrolysis of Aspen-Poplar Wood". The Canadian Journal of Chemical Engineering 60 (1982): 666-674.

171. Scott, D.S. and J. Piskorz. "Continuous Flash Pyrolysis of Wood for Production of Liquid Fuels". In Energy from Biomass and Wastes III. Donald L. Klass, Editor. Institute of Gas Technology, Chicago, IL (1983), pp. 1123-1146.

172. Scott, Donald S., Jan Piskorz and Desmond Radlein. "Liquid Products from the Continuous Flash Pyrolysis of Biomass". Industrial and Engineering Chemistry Process Design and Development 24 (1985): 581-588

173. Scott, Donald S. Technical Evaluation of the Waterloo Fast Pyrolysis Process. Alternate Energy Division. Canmet. Energy Mines and Resources Canada. Ottawa (1986)

174. Scott, Donald S., J. Piskorz, A. Grinshpun and R.G. Graham. "The Effect of Temperature on Liquid Product Composition from the Fast Pyrolysis of Cellulose". American Chemical Society. Division of Fuel Chemistry 32 (2) (1987): 1-11.

175. Scott, Donald S., Jan Piskorz, Maurice A. Bergougnou, Robert Graham and Ralph P. Overend. "The Role of Temperature in the Fast Pyrolysis of Cellulose and Wood". Industrial and Engineering Chemistry Research 27 (1988): 8-15.

176. Scott, D.S., D. Radlein, J. Piskorz and P. Majerski. "Potential of Fast Pyrolysis for the Production of Chemicals" R&D Contractors Meeting on Biomass Liquefaction. Alternate Energy Branch. Canmet. Energy, Mines and Resources, Ottawa (1991). pp. 171-178.

177. SERI. A Survey of Biomass Gasification. Volume II - Principles of Gasification. SERI/TR-33-239. Solar Energy Research Institute. Golden, CO (1979).

178. SERI. Specialists' Workshop on Fast Pyrolysis of Biomass. James Diebold, Editor. SERI/CP-622-1096. Solar Energy Research Institute, Golden, CO (1980).

179. Shafizadeh, F. "Pyrolysis and Combustion of Cellulosic Materials". Advances in Carbohydrate Chemistry 23 (1968): 419-465.

180. Shafizadeh, F. and Y.Z. Lai. "Thermal Degradation of 1,6-Anhydro-B-D-glucopyranose". Journal of Organic Chemistry 37 (2) (1972): 278-283.

181. Shafizadeh, F. and Y.L. Fu. "Pyrolysis of Cellulose". Carbohydrate Research 29 (1973): 113-122.

182. Shafizadeh, F. "Industrial Pyrolysis of Cellulosic Materials". Applied Polymer Symposium 28. John Wiley & Sons, New York, NY (1975), pp. 153-174.

183. Shafizadeh, F., and P.P.S. Chin. "Thermal Deterioration of Wood". 172nd National American Chemical Society Meeting, San Francisco, CA. August 30 - September 6. American Chemical Society, Washington, D.C. (1976), p. 57.

184. Shafizadeh, F. and W.F. DeGroot. "Thermal Analysis of Forest Fuels". In Fuels and Energy from Renewable Resources. Academic Press Inc., New York, NY (1977).

185. Shafizadeh, F. "Utilization of Biomass by Pyrolytic Methods". TAPPI Forest Biology Wood Chemistry Conference, Madison, WI (1977), p. 191.

186. Shafizadeh, F., R.H. Furneaux, T.G. Cochran, J.P. Scholl and Y. Sakai. "Production of Levoglucosan and Glucose from Pyrolysis of Cellulose Materials". Journal of Applied Polymer Science 23 (1979): 3525-3539.

187. Shafizadeh, F. "Introduction to Biomass Pyrolysis". In Specialists' Workshop on Fast Pyrolysis of Biomass. James Diebold, Editor. Solar Energy Research Institute, Golden, CO (1980), pp. 79-103.

188. Shafizadeh, F. "Introduction to Pyrolysis of Biomass" Journal of Analytical and Applied Pyrolysis 3 (1982): 283-305.

189. Shafizadeh, F. "Saccharification of Lignocellulosic Materials". Department of Chemistry, University of Montana, Missoula, Montana. Submitted to the Journal of Pure and Applied Chemistry (1982).

190. Shafizadeh, F. "Pyrolytic Reactions and Products of Biomass". In Fundamentals of Thermochemical Biomass Conversion. R.P. Overend et al., Editors. Elsevier Applied Science Publishers Ltd. New York, NY (1985), pp. 183-217.

191. Sitnai, O. "Kinetic Modelling of a Reactor for the Flash Pyrolysis of Coal". National Conference Publication. Institute of Engineers 76 (1979):22-30 (Australia).

192. Skaates, J.M. "Fast Pyrolysis on a Molten Lead Bath". In Specialists' Workshop on Fast Pyrolysis of Biomass. James Diebold, Editor. Solar Energy Research Institute, Golden, CO (1980), pp. 347-364.

193. Soltes, E.J. and T.J. Elder. "Thermal Degradation Routes to Chemicals from Wood". 8th World Forestry Congress Proceedings, Jakarta, Indonesia. October 2-6, (1978).

194. Soltes, E.J., T. Allen and S.C.K. Lin. "Biomass Pyrolysis Towards an Understanding of its Versatility and Potentials". 3rd Symposium on Biotechnology in Energy Production and Conservation, Gatlinburg, TN. May 12-15. U.S. Department of Energy, Washington, D.C. (1981).

195. Soltes, E.J. and T.J. Elder. "Pyrolysis". In Organic Chemicals from Biomass. I.S. Goldstein, Editor. CRC Press, Boca Raton, FL (1981).

196. Starch, H.H. "Acetylene Formation in Thermal Decomposition of Hydrocarbons". Industrial and Engineering Chemistry 26 (1934): 56-60.

197. Steacie, E.W.R. "The Kinetics of Elementary Reactions of the Simple Hydrocarbons". Chemical Reviews 22 (1935): 311-402.

198. Steacie, E.W.R. and G. Shane. "The Kinetics of the Decomposition Reactions of the Lower Paraffins. VII. The Nitric-Oxide Inhibited Decomposition of Ethane". Canadian Journal of Research 18B (1940): 351-357.

199. Stein, Yolanda S. and Michael Jerry Antal. "A Study of the Gas-Phase Pyrolysis of Glycerol" Journal of Analytical and Applied Pyrolysis 4 (1983): 283-296

200. Steinberg, M. and B. Bhatt. "Flash Pyrolysis and Hydropyrolysis of Coal". In Specialists' Workshop on Fast Pyrolysis of Biomass. James Diebold, Editor. Solar Energy Research Institute, Golden, CO (1980), pp. 57-78.

201. Steinberg, M. and P. Fallon. "Flash Pyrolysis of Biomass with Reactive and Non-Reactive Gases". 14th Biomass Thermochemical Conversion Contractor's Meeting, Arlington, VA. June 23-24. Pacific Northwest Laboratory, Batelle Memorial Institute, Richland, WA (1982).

202. Steinberg, M. and P.T. Fallon. "Make Ethylene and Benzene by Flash Methanolysis of Coal". Hydrocarbon Processing 61 (1982): 92-96.

203. Stern, E.W., A.S. Logiudice and H. Heinemann. "Approach to Direct Gasification of Cellulosics". Industrial and Engineering Chemistry Process Design and Development 4 (1965): 171-173.

204. Sundaram, K.M., P.S. Van Damme and G.F. Froment. Journal of the American Institute of Chemical Engineers 27 (1981): 946-951.

205. Sundaram, M.S., M. Steinberg and P.T. Fallon. "Flash Hydropyrolysis of Coal for Conversion to Liquid and Gaseous Fuels". U.S. Department of Energy Summary Report OOE/METC/82- 48. Prepared for Morgantown Energy Technology Center, Morgantown, WV (1982).

206. Theander, O. "Cellulose, Hemicellulose and Extractives". In Fundamentals of Thermochemical Biomass Conversion. R.P. Overend et al., Editors. Elsevier Applied Science Publishers Ltd., New York, NY (1985), pp. 35-60.

207. Thurner, Franz and Uzi Mann. "Kinetic Investigation of Wood Pyrolysis". Industrial and Engineering Chemistry Process Design and Development 20 (1981): 482-488.

208. Tran, D.G. and C. Rai. "A Kinetic Model for Pyrolysis of Douglas Fir Bark". Fuel 57 (1978): 293-298.

209. Tran, D.G. and C. Rai. "Pyrolytic Gasification of Bark". American Institute of Chemical Engineers Symposium Series 75, No. 184 (1979), pp. 41-49.

210. Tyler, R. "Flash Pyrolysis of Coals: Devolatilization of a Victorian Brown Coal in a Small Fluidized-Bed Reactor". CSIRO Division of Process Technology, P.O. Box 136, North Ryde, N.S.W. Australia 2113 (1983).

211. Tyler, R. "Flash Pyrolysis of Coals: Devolatilization of Bituminous Coals in a Small Fluidized-Bed Reactor". CSIRO Division of Process Technology, P.O. Box 136, North Ryde, N.S.W. Australia 2113 (1983).

212. Van den Aarsen, F.G., A.A.C.M. Beenackers and W.P.M. Van Swaaij. "Wood Pyrolysis and Carbon Dioxide Char Gasification Kinetics in a Fluidized Bed". In Fundamentals of Thermochemical Biomass Conversion. R.P. Overend et al., Editors. Elsevier Applied Science Publishers Ltd., New York, NY (1985), pp. 691-715.

213. Vargas, Jose M. and Daniel D. Perlmutter. "Interpretation of Coal Pyrolysis Kinetics" Industrial and Engineering Chemistry Process Design and Development 25 (1986): 49-54.

214. Villermaux, J. and B. Antoine. "Pyrolyse-éclair de solides devisés dans un réacteur continu 1...". Revue Générale de Thermique 19(227) (1980): 851-860.

215. Villermaux, J., F. Verzaro and J. Lede. "Pyrolyse-éclair de solides divisés dans un réacteur continu 2...". Revue Générale de Thermique 19 (1980): 861-869.

216. Villermaux, J., B. Antoine, J. Lede. and F. Soulignac. "A New Model for Thermal Volatilization of Solid Particles Undergoing Fast Pyrolysis" Chemical Engineering Science 41 (1) (1986): 151-157

217. Vorhees, K.J. and L.J. Hendricks. "A Comparison of Heating Techniques on the Pyrolysis of Douglas Fir". In Specialists' Workshop on Fast Pyrolysis of Biomass. James Diebold, Editor. Solar Energy Research Institute, Golden, CO (1980), pp. 183-190.

218. Walawender, W.P., D.A. Hoveland and L.T. Fan. "Steam Gasification of Alpha Cellulose in a Fluid Bed Reactor". In Fundamentals of Thermochemical Biomass Conversion. R.P. Overend et al., Editors. Elsevier Applied Science Publishers Ltd., New York, NY (1985), pp. 897-910.

219. Wan, E.I. and J.A. Simons. "Biofuel Synthesis". Bio-Energy '80 World Congress and Exposition, Atlanta, GA. April 21-24. Bio-Energy Council, Washington, D.C. (1980), pp. 204-208.

220. Wan, E.I. "Economics of Methanol Production from Indigenous Resources". In Energy from Biomass and Wastes VIII. Donald L. Klass, Editor. Institute of Gas Technology. Chicago, IL. (1984). pp. 1249-1274.

221. Wenzyl, H.F.J. "Further Destructive Processing of Wood". In The Chemical Technology of Wood. F.J. Herman, Editor. Academic Press, New York, NY (1970).

222. Wright, R.H. and A.M. Hayward. "Kinetics of the Thermal Decomposition of Wood". Canadian Journal of Technology 29 (1951): 503-510.

12.0 APPENDICES

APPENDIX 1.0 THESIS-RELATED FAST PYROLYSIS PUBLICATIONS

The following is a list of forty-two (42) fast pyrolysis papers which have been published as a result of thesis work. These papers were authored or co-authored by Robert G. Graham, and have been classified as fully refereed, refereed extended abstract, and non-refereed.

APPENDIX 1.1 FULLY REFEREED

Graham. Robert G., Barry A.Freel, D.R. Huffman and M.A. Bergougnou. "Applications of Rapid Thermal Processing of Biomass". In Advances in Thermochemical Conversion. A.V. Bridgwater, Editor. Elsevier Applied Science, London (1992). In Press.

Graham, Robert G., Barry A. Freel, Donald R. Huffman and M.A. Bergougnou. "The Production of Liquid Fuels and Chemicals from Biomass by Rapid Thermal Processing (RTP)". In 1st European Forum on Electricity Production from Biomass and Solid Wastes by Advanced Technologies. G. Grassi, Editor. Elsevier Applied Science, London (1992). In Press.

Huffman, D.R., A.J. Vogiatzis, R.G. Graham and B.A. Freel. "The Characterization and Combustion of Fast Pyrolysis Bio-Oils". In 1st European Forum on Electricity Production from Biomass and Solid Wastes by Advanced Technologies. G. Grassi, Editor. Elsevier Applied Science, London (1992). In Press.

Graham, Robert G., Barry A. Freel, Donald R. Huffman and M.A. Bergougnou. "Developments in Rapid Thermal Processing (RTP): Biomass Fast Pyrolysis". In Sixth European Conference on Biomass for Energy, Industry and Environment. G. Grassi, Editor. Elsevier Applied Science, London (1992). pp. 629-635.

Beckman, David, and Robert Graham. "Economic Assessment of a Wood Fast Pyrolysis Plant". In Advances in Thermochemical Conversion. A.V. Bridgwater, Editor. Elsevier Applied Science, London (1992). In Press.

Freel, Barry A., Robert G. Graham, Donald R. Huffman and Apostolos Vogiatzis. "Rapid Thermal Processing of Biomass (RTP) Development, Demonstration and Commercialization". In Energy from Biomass and Wastes XVI. Donald L. Klass, Editor. Institute of Gas Technology. Chicago, IL. (1992).

Graham, R.G. and Barry A. Freel. "Scale-Up and Commercialization of Rapid Biomass Pyrolysis for Fuel and Chemical Production. In Energy from Biomass and Wastes XIV. Donald L. Klass, Editor. Institute of Gas Technology. Chicago, IL. (1990).

Graham, R.G., B.A. Freel and M.A. Bergougnou. "The Production of Pyrolytic Liquids, Gas and Char from Wood and Cellulose by Fast Pyrolysis". In Research in Thermochemical Biomass Conversion. A.V. Bridgwater and J.L. Kuester, Editors. Elsevier Applied Science, London (1988). pp. 629-641.

Scott, Donald S., Jan Piskorz, Maurice A. Bergougnou, Robert Graham and Ralph P. Overend. "The Role of Temperature in the Fast Pyrolysis of Cellulose and Wood". Industrial and Engineering Chemistry Research 27 (1988): 8-15.

Freel, B.A., R.G. Graham, M.A. Bergougnou, R.P. Overend and L.K. Mok. "The Kinetics of the Fast Pyrolysis (Ultrapyrolysis) of Cellulose in a Fast Fluidized Bed Reactor". In New Developments in Fluidization and Fluid Particle Systems Wen-Ching Wang, Editor. AIChE Symposium Series 255. Volume 83 (1987): 105-111.

Scott, Donald S., J. Piskorz, A. Grinshpun and R.G. Graham. "The Effect of Temperature on Liquid Product Composition from the Fast Pyrolysis of Cellulose". American Chemical Society. Division of Fuel Chemistry 32 (2) (1987): 1-11.

Graham, R.G., et.al. "The Kinetics of Fast Pyrolysis of Cellulose at 900 C". In Energy from Biomass and Wastes X. Donald L. Klass, Editor. Institute of Gas Technology. Chicago, IL. (1986).

Graham, R.G., M.A. Bergougnou, L.K. Mok and H.I. de Lasa. "Fast Pyrolysis (Ultrapyrolysis) of Biomass Using Solid Heat Carriers". In Fundamentals of Thermochemical Biomass Conversion, R.P. Overend et al., Editors. Elsevier Applied Science Publishers Ltd. New York, NY (1985), pp. 397-410.

Graham, R.G., B.A. Freel, M.A. Bergougnou, R.P. Overend and L.K. Mok. "Fast Pyrolysis of Cellulose". In Energy from Biomass. W. Palz, J. Coombs and D.O. Hall, Editors. Elsevier Applied Science Publishers. London (1985). pp. 860-864.

Mok, L.K., R.G. Graham, B.A. Freel, M.A, Bergougnou and R.P. Overend. "Fast Pyrolysis (Ultrapyrolysis) of Cellulose and Wood Components" Journal of Analytical and Applied Pyrolysis 8 (1985): 391-400

Mok, L.K., R.G. Graham, R.P. Overend, B.A. Freel and M.A. Bergougnou. "Ultrapyrolysis: The Continuous fast Pyrolysis of Biomass" In Bioenergy 84. Volume III, Biomass Conversion. H. Egneus and A. Ellegard, Editors. Elsevier Applied Science Publishers. London (1985). pp. 23-30.

Graham, R.G., M.A. Bergougnou and R.P. Overend. "Fast Pyrolysis of Biomass". Journal of Analytical and Applied Pyrolysis 6 (1984): 363-374.

Mok, L.K., R.G. Graham, H.I. de Lasa, B.A. Freel and M.A. Bergougnou. "Application of Ultra-Fast Fluidization to the Fast Pyrolysis of Cellulose (Ultrapyrolysis)". American Institute of Chemical Engineers Symposium Series 234. Volume 80 (1984): 70-79.

Graham, R.G., M.A. Bergougnou, L.K. Mok, B.A. Freel and H.I. de Lasa. "Continuous Fast Pyrolysis of Biomass Using Solid Heat Carriers". In Energy from Biomass and Wastes VIII. Donald L. Klass, Editor. Institute of Gas Technology. Chicago, IL. (1984). pp. 1417-1433.

Bergougnou, M.A., H. de Lasa, J. Hazlett, L.K. Mok and R. Graham. "Ultraflash Pyrolysis (Ultrapyrolysis) Process for Coal, Wood and Other Carbonaceous Materials". In Coal: Phoenix of the '80's. A.M. Al Taweel, Editor. Canadian Society for Chemical Engineering. Ottawa (1982). pp. 523-529.

APPENDIX 1.2 REFEREED EXTENDED ABSTRACT

Graham, Robert G., Barry A. Freel and M.A. Bergougnou. "Rapid Thermal Processing (RTP): Biomass Fast Pyrolysis Overview". In Biomass Thermal Processing. E. Hogan et.al., Editors. CPL Press. London, UK (1992). pp. 52-63.

Graham, R.G., B.A. Freel and R.P. Overend. 1989. "Thermal and Catalytic Fast Pyrolysis of Lignin by Rapid Thermal Processing (RTP)". In Bioenergy. E.N. Hogan, Editor. National Research Council of Canada. Ottawa (1989). pp. 669-673.

Graham, R.G. "A Review of Fast Pyrolysis Process Development" In Sixth Canadian Bioenergy R&D Seminar. Cecile Granger, Editor. Elsevier Applied Science Publishers. New York, NY. (1987). pp. 448-452.

Berg, D.A., R.J. Sumner, R.G. Graham, et.al. "Ultra-rapid Pyrolysis of Biomass and Carbonaceous Feedstocks". In Sixth Canadian Bioenergy R&D Seminar. Cecile Granger, Editor. Elsevier Applied Science Publishers. New York, NY. (1987). pp. 443-447.

Graham, R.G., et.al. "The Ultra-Rapid Fluidized (URF) Reactor: Application to Determine the Kinetics of thr Fast Pyrolysis (Ultrapyrolysis) of Cellulose". Proceedings of the Fifth Engineering Foundation Conference of Fluidization. Helsingor, Denmark. May 18-23. Engineering Foundation (1986). pp. 473-480.

Graham, R.G., R.P. Overend, B.A. Freel, L.K. Mok and M.A. Bergougnou. "Development of the Ultra-Rapid Fluidized (URF) Reactor: Application to the Fast Pyrolysis of Cellulose". Proceedings of the 10th Annual Powder and Bulk Solids Conference. Rosemont, IL. May 7-9. Cahners Exposition Group, Des Plaines, IL. (1985). pp. 126-139.

Graham, R.G., M.A. Bergougnou, L.K. Mok, H.I. de Lasa and B.A. Freel. "Ultrapyrolysis of Cellulose and Wood Components" In Fifth Canadian R&D Seminar. S. Hasnain, Editor. Elsevier Applied Science Publishers. New York (1984). pp. 386-390.

Graham, R.G., L.K. Mok, M.A. Bergougnou and H.I. de Lasa. "Fast Pyrolysis of Biomass for the Production of Chemicals and Fuels from Wood". In Fourth Bioenergy R&D Seminar. B. Summers, Editor. National Research Council of Canada, Ottawa, Canada (1982), pp. 397-410.

Mok, L.K., R.G. Graham, M.A. Bergougnou and H.I. de Lasa. "Continuous Ultra-Flash Pyrolysis of Wood Using Solid Heat Carriers and Vortical Contactors (Ultrapyrolysis)". Proceedings of the Industrial Wood Energy Forum '82 Conference, Washington, D.C. March 8-10. Forest Products Research Society, Madison, WI (1982), pp. 292-298.

Mok, L.K., H.I. de Lasa, M.A. Bergougnou and R.G. Graham. "Continuous Ultra-Flash Pyrolysis of Wood Using Solid Heat Carriers and Double Jet Vortical Contactors (Ultrapyrolysis)". In Fourth Bioenergy R&D Seminar. B. Summers, Editor. National Research Council of Canada, Ottawa, Canada (1982). pp. 337-341.

Mok, L.K., R.G. Graham, H.I. de Lasa and M.A. Bergougnou. "Laboratory Apparatus for the Ultra-Fast Pyrolysis (Ultrapyrolysis) of Biomass and Other Carbonaceous Materials Using Ultra Fast Fluidized Reactors". Proceedings of the International Powder and Bulk Solids Conference, Rosemont, IL. May 11-13. Cahners Exposition Group, Des Plaines, IL. (1982). pp. 250-257.

Bergougnou, M.A., H.I. de Lasa, L.K. Mok, R.G. Graham and J. Hazlett. "High Intensity Flash Pyrolysis of Wood Using Solid Heat Carriers (Ultrapyrolysis)". In Third Bioenergy R&D Seminar. B. Summers, Editor. National Research Council of Canada, Ottawa, Canada (1981), pp. 277-282.

APPENDIX 1.3 NON-REFEREED

Graham, Robert G., Barry A. Freel and M.A. Bergougnou. "Overview of Rapid Thermal Processing (RTP): Biomass Fast Pyrolysis". Proceedings of the Symposium on Emerging Materials and Chemicals from Biomass and Wastes. Washington, August 26-31. American Chemical Society. Division of Cellulose, Paper and Textile. Washington, DC. (1990).

Huffman, D.R., B.A. Freel, R.G. Graham and L. Vogiatzis. "Thermal and Catalytic Fast Pyrolysis of Lignin by Rapid Thermal Processing (RTP)" Proceedings of the C.I.C. Congress. Halifax, N.S. July 15-20. Chemical Institute of Canada. Ottawa. (1990).

Freel, B.A. and R.G. Graham. Rapid Pyrolysis of Wood and Wood-Derived Liquids to Produce Olefins and High Quality Fuels. Alternate Energy Branch. Canmet. Energy Mines and Resources Canada. Ottawa. (1988).

Graham, R.G., M.A. Bergougnou and B.A. Freel. "The Production of Pyrolytic Liquids from Cellulose by Fast Pyrolysis (Ultrapyrolysis)". Proceedings of the Symposium on Production, Analysis and Upgrading of Pyrolysis OIls from Wood. 193rd ACS National Meeting. Denver, CO. April 5-10. The Cellulose, Paper and Textile Division and The Fuel Division. American Chemical Society. Washington, DC. (1987).

Graham, R.G., et.al. "Fast Pyrolysis (Ultrapyrolysis) of Poplar. Proceedings of the 36th CSChE Conference. Sarnia, Ont. October 5-8. Canadian Society for Chemical Engineering. Ottawa (1986).

Bergougnou, M.A., R.G. Graham, B.A. Freel and L. Vogiatzis. An Investigation of the Fast Pyrolysis of Cellulose and Wood. Energy Project Office. National Research Council of Canada. Ottawa. (1986).

Garnier, Gil,... R.G. Graham, et.al. "An Investigation of the Role of the Water-Gas Shift Reaction in Fast Pyrolysis". Proceedings of the 35th CSChE Conference. Calgary, Alta. October 7-9. Canadian Society for Chemical Engineering. Ottawa (1985).

Graham, R.G., B.A. Freel. L.K. Mok and M.A. Bergougnou. "Ultrapyrolysis of Cellulose, Wood and Lignin". Proceedings of the 34th CSChE Conference. Quebec, Que. September 30 - October 3. Canadian Society for Chemical Engineering. Ottawa (1984).

Meunier, M. ... R.G. Graham, et.al. "Ultra-Rapid Fluidization (URF). A New Advanced Reactor Concept: Application to Pyrolysis of Wood Components and to Other Industrial Processes". Proceedings of the 7th All-Union Heat and Mass Transfer Conference. Minsk, USSR. May 21-23. Institute of Heat and Mass Transfer. Minsk (1984).

Bergougnou, M.A., H.I. de Lasa, L.K. Mok, R.G. Graham, B.A. Freel and J.D. Hazlett. "Ultrapyrolysis of Cellulose and Wood Components". Enfor C-147 Final Report. Environment Canada. Ottawa, Canada (1983).

APPENDIX 2.0 SYSTEM CALIBRATIONS

APPENDIX 2.1 PRESSURE GAUGE CALIBRATIONS

Twelve (12) Bourdon pressure gauges (maximum pressure of 25 psig) were used in the Ultrapyrolysis system to measure rotameter pressures and process pressures from the feeder systems to the condenser exit. A vacuum pressure gauge (maximum vacuum of 25 inches of mercury) was used on the mass-balance evacuated gas tank. These gauges were all calibrated with mercury manometers according to the formula in Section 7.1. The gauges were calibrated over the range of 10 to 80 % of scale. The actual pressure (P_A), as determined by the manometers, was correlated to the gauge pressure reading (P_G) by linear regression analysis. An average of 11 pressure measurements were made per calibration (ie., per gauge). The results of the linear regression analysis are given, as follows.

$P_A = [\ M \times P_G\ ] + B$ Where, P_A = Actual Pressure
M = Slope
P_G = Gauge Pressure
B = Intercept

PRESSURE GAUGE NO.	SLOPE	INTERCEPT	CORRELATION COEFFICIENT
1	0.98902	0.16037	0.9995
2	1.00057	0.01718	0.9997
3	1.00733	0.25595	0.9982
4	1.00875	0.26773	0.9956
5	1.00230	-0.27183	0.9999
6	1.00100	0.02281	1.0000
7	1.02243	0.18792	0.9994
8	1.00789	0.10869	0.9999
9	1.02812	-0.30354	0.9997
10	0.99830	0.22337	1.0000
11	0.99849	0.33628	1.0000
12	0.95387	0.82135	1.0000
13 (Vacuum)	0.97632	-0.66696	0.9894

The equations derived by linear regression were used in the Ultrapyrolysis computer programs to determine actual pressures from gauge scale readings.

APPENDIX 2.2 THERMOCOUPLE CALIBRATIONS

Nine (9) of the Ultrapyrolysis system Type K Thermocouples (Brampton Thermoelectric) were calibrated with an NSB high precision thermometer in ice water, water, air and an electrical resistance oven. The results are given, as follows.

THERMOCOUPLE ENVIRONMENT	NSB THERMOM. TEMPERATURE (°C)	THERMOCOUPLE TEMPERATURES (°C)								
		T_1	T_2	T_3	T_4	T_5	T_6	T_7	T_8	T_9
Ice Water	0.50	0.50	0.50	0.60	0.50	0.50	0.40	0.50	-	-
" "	0.25	0.25	0.25	0.35	0.20	0.30	-0.30	0.25	0.20	0.25
" "	0.20	-	-	-	-	-	-	-	0.20	0.20
Tap Water	21.20	21.2	21.2	21.2	21.2	21.3	21.2	21.4	-	-
" "	21.80	21.8	21.8	21.8	21.8	21.8	21.8	21.8	-	-
" "	20.00	-	-	-	-	-	-	-	20.0	20.0
Boiling Water	100.20	101.0	101.1	100.2	100.2	100.2	102.6	100.7	-	-
" "	100.20	101.5	101.3	100.2	100.2	100.2	102.8	100.8	-	-
" "	100.20	101.5	101.2	100.2	100.4	100.4	102.2	100.8	-	-
" "	100.35	101.1	101.2	100.4	100.4	100.4	103.0	100.6	-	-
" "	99.60	-	-	-	-	-	-	-	100.1	101.0
" "	99.00	-	-	-	-	-	-	-	100.1	100.7
" "	99.40	-	-	-	-	-	-	-	101.0	101.0
" "	99.50	-	-	-	-	-	-	-	100.9	100.9
Ambient Air	25.50	25.7	25.5	25.5	25.5	25.7	24.8	25.7	-	-
" "	19.25	-	-	-	-	-	-	-	-	19.0
" "	19.45	-	-	-	-	-	-	-	19.5	-
" "	19.80	-	-	-	-	-	-	-	19.7	19.6
Furnace	N/A*	302.3	302.3	302.8	302.7	301.8	302.1	302.5	305.8	307.2
" "	N/A*	303.8	303.5	303.9	304.0	303.1	303.4	303.9	306.4	307.5
" "	N/A*	310.6	310.6	310.3	310.7	309.6	310.2	310.1	312.2	313.0

* Calibration was relative to each of the thermocouples, and not calibrated with the NSB thermometer.

APPENDIX 2.3 ROTAMETER CALIBRATIONS

The seven (7) Ultrapyrolysis system Brooks round-float rotameters were calibrated using *nitrogen* flow through a Wet Test Meter (WTM), corrected for saturation volume, and a straight-edged orifice meter. It was noted that the manufacture calibration curve for *air*, which was then transformed to a calibration curve for nitrogen by the rotameter equation (a molecular weight conversion), did not agree with those curves corresponding to the WTM and orifice calibrations. A literature review (in journals and from rotameter manufacturers) indicated that the rotameter equation does not apply when round floats are used.

Typically, four series of calibrations (using nitrogen) were carried out for each rotameter; one series with the Wet Test Meter and three with a sharp-edged orifice meter. The rotameters were tested over the range of 10 to 90% of scale, and 10 to 12 flow measurements were made per test series. A linear regression analysis on all calibration data was conducted to generate an "STP" calibration curve for use in the computer programs for residence time and mass balance. Actual system pressures were used in the computer programs to calculate actual volumetric flowrates from the STP calibration curves. The results of the linear regression are give, as follows.

$$F_S = [\ M \times RR\ ] + B$$

Where, F_S = Nitrogen Mass Flowrate at STP (kg/s)
M = Slope
RR = Rotameter Reading (mm)
B = Intercept

BROOKS ROTAMETER No.	Model	SLOPE (M)	INTERCEPT (B)	CORRELATION COEFFICIENT (R)
1.	R-6-15A	9.7420×10^{-6}	-1.0052×10^{-4}	0.9994
2.	R-6-15A	3.5458×10^{-6}	-2.0372×10^{-5}	0.9998
3.	R- -15B	3.4476×10^{-6}	-4.5755×10^{-5}	0.9970
4.	R-6-15B	3.5711×10^{-6}	-7.6856×10^{-6}	0.9998
5.	1307-08B-0000	6.9321×10^{-5}	4.1219×10^{-5}	0.9996
6.	1307-08F-LA1A	1.7669×10^{-5}	-5.9338×10^{-5}	1.0000
7.	1307-08B-0000	1.8395×10^{-6}	-5.4632×10^{-5}	0.9998

APPENDIX 2.4 MASS BALANCE CALIBRATIONS

The amount of gas produced during an Ultrapyrolysis test was determined by collecting the entire product in the gas sample bags (up to four 170 litre bags were used), determining the average gas composition (and therefore the average molecular mass) by gas chromatograhic (GC) analysis, and then evacuating the entire contents of the bags into a Superior Propane 123 USWG tank of known fixed volume. The ideal gas law was then applied to determine the mass of the product gas using the average molecular mass of the gas, the tank volume and temperature, and magnitude of the pressure change of the tank:

$$PV = nRT = (m/\bar{M})RT$$

Therefore, $$m = \frac{PV\bar{M}}{RT}$$

Where,
- P = change in tank pressure
- V = tank volume
- n = change in number of moles of gas in tank
- R = universal gas constant
- m = change in mass of gas in tank (ie. product gas plus N_2 carrier)
- $\bar{M}$ = average molecular mass of gas in tank

From the GC analysis, the fraction of product gas in the total gas stream (product plus N_2 carrier) was known, and the mass of the product gas was calculated:

$$m_p = y_g m$$

Where,
- m_p = mass of product gas
- y_g = fraction of product gas in total gas

An experimental procedure was prepared to calibrate and confirm this procedure. Using a small gas bottle of fixed volume (.967 l) and known pressure, a known amount of tracer gas was injected into the UP system along with an appropriate flow of nitrogen carrier gas to simulate the dilution occurring during actual experimental conditions. The tracer gas was a GC calibration gas mixture.

From the volume of the gas bottle, the known gas composition, and the pressure drop of the bottle (before and after tracer injection), it was calculated from the ideal gas law that 2.56 g of gas was injected into the system. In the mass balance test, and 2.57 g was accounted for in the analysis.

The detailed procedure is given as follows:

- Calculations were made to prepare a gas sample diluted in nitrogen which is a similar dilution to actual UP product gas samples.

- A one litre (nominal) gas bottle was utilized to accurately inject known volumes of gas into the gas bag. Its volume was determined by filling with water and weighing. The collection bag was half filled with approximately 80 litres of nitrogen which was metered by a calibrated rotameter. It was determined that approximately 8 volumes of the one litre bottle would be required to give the appropriate dilution. The sample gas injected was a GC calibration gas (Matheson), which was itself diluted by nitrogen (i.e. 64% by volume).

- The gas bottle was pressurized to approximately 1 atmosphere (gage) and its contents were then injected into the sample bag. The pressure drop, known volume of the bottle, and known composition of the gas were then used to calculate the total mass of *non-nitrogen* gas injected into the sample bag.

- Gas samples were withdrawn from the sample bag and analyzed. The entire sample bag contents were withdrawn into the Superior Propane 123 USWG tank, and the pressure increase recorded. The results of the sample analysis and tank volume, pressure increase and temperature were measurements were then used in the mass balance program (PC) to calculate the mass of the sample using the established mass balance procedure. This was compared with the known mass of the injected sample.

The following calculations were performed to confirm the integrity of the mass balance procedure:

1. Mass of Tracer Gas Injected

Total number of moles of gas (including N_2) injected:

$$N_T = \frac{PV}{RT}$$

$$= \frac{(7.463)(0.967)}{(0.08205)(295.1)}$$

$$= 0.298 \text{ moles}$$

Where, N_T = total moles of gas
P = bottle pressure drop (over 8 injections)
R = universal gas const.
T = absolute gas temp.

Number of moles of nitrogen-free gas injected:

$N_G = y_g N_T$ Where, N_G = number of moles of nitrogen-free gas

$= (0.3604)(0.298)$ y_g = fraction of standard calibration gas which is non-nitrogen

$= 0.107$ moles

Mass of nitrogen-free (tracer) gas injected:

$m_g = N_G \bar{M}_G$ Where, m_g = mass of nitrogen-free calibration (tracer) gas injected

$= (0.107)(23.95)$ $\bar{M}_G$ = avge. molecular mass of non-nitrogen calibration (tracer) gas

$= 2.56$ g
======

2. Mass of Tracer Gas Detected (mass balance procedure)

The mass balance procedure was followed as described above, and the calculated value for the amount of tracer gas is given, as follows:

$m_g = 2.57$ g
======

Copies of the actual data sheets from the experimental mass balance run are given in the following pages.

RUN MASSBAL TEST: GAS PRODUCT SUMMARY

TABLE 1. G.C. CALIBRATION SUMMARY

GAS COMPONENT	AVG CAL. AREA	AVG RF	AVG PEAK AREAS FOR ULTRAPYROLYSIS GAS SAMPLES				
			TRACER	BAG 1	BAG 2	BAG 3	BAG 4
Hydrogen	88326	11237.4	125072.4	9296.3	0	0	0
Carb Diox	117733	51637.1	580581.8	45724.8	0	0	0
Ethylene	59282	54387.4	120830.8	9497	0	0	0
Ethane	32071	57269.2	32811.6	2353.3	0	0	0
Acetylene	25062	45566.6	22758	1603.3	0	0	0
Oxygen	18405	33463.9	16422	3166.8	0	0	0
Nitrogen	3051457	40839.8	2612307.2	3934410	0	0	0
Methane	82071	35838.9	187180.8	13675.8	0	0	0
Carb Monox	352651	41635.3	170202.2	12582.5	0	0	0
Benz/Tol	3585	84952.6	0	0	0	0	0
Propane	37606	69640.1	32581.3	2543	0	0	0
Propylene	36508	68882.4	0	0	0	0	0
Butene-1	41936	80646.8	41017.3	2789	0	0	0

TABLE 2. G.C. COMPOSITION SUMMARY (Molar %)

GAS COMPONENT	ACTUAL G.C. MOLAR COMPOSITION					AIR FREE MOLAR COMPOSITION				
	TRACER	BAG 1	BAG 2	BAG 3	BAG 4	TRACER	BAG 1	BAG 2	BAG 3	BAG 4
Hydrogen	11.13	.827	0	0	0	11.349	.838	0	0	0
Carb Diox	11.243	.895	0	0	0	11.464	.897	0	0	0
Ethylene	2.222	.175	0	0	0	2.265	.177	0	0	0
Ethane	.573	.041	0	0	0	.584	.042	0	0	0
Acetylene	.499	.035	0	0	0	.509	.036	0	0	0
Oxygen	.491	.095	0	0	0	0	0	0	0	0
Nitrogen	63.965	96.338	0	0	0	63.339	97.246	0	0	0
Methane	5.223	.382	0	0	0	5.325	.387	0	0	0
Carb Monox	4.088	.302	0	0	0	4.168	.306	0	0	0
Benz/Tol	0	0	0	0	0	0	0	0	0	0
Propane	.468	.037	0	0	0	.477	.037	0	0	0
Propylene	0	0	0	0	0	0	0	0	0	0
Butene-1	.509	.035	0	0	0	.519	.035	0	0	0
TOTAL	100.41	99.151	0	0	0	100	100	0	0	0
MOL. WT	26.65	27.68	0	0	0	26.49	27.92	0	0	0

RUN MASSBAL TEST (cont'd)

TABLE 3. SUMMARY OF PRODUCT GAS COMPOSITION

GAS COMPONENT	MOL. WT.	NITROGEN/OXYGEN FREE MOLAR COMPOSITION					PRODUCT GAS AVG (1 BAG)		
		TRACER	BAG 1	BAG 2	BAG 3	BAG 4	MOLAR % AIR-FREE	MOLAR % N/O FREE	MASS FRACTION
Hydrogen	2.02	30.956	30.43	0	0	0	.838	30.43	.025
Carb Diox	44.01	31.27	32.573	0	0	0	.897	32.573	.592
Ethylene	28.05	6.179	6.423	0	0	0	.177	6.423	.074
Ethane	30.07	1.593	1.512	0	0	0	.042	1.512	.019
Acetylene	26.04	1.389	1.294	0	0	0	.036	1.294	.014
Oxygen	32	0	0	0	0	0	0	0	0
Nitrogen	28.02	0	0	0	0	0	97.246	0	0
Methane	16.04	14.526	14.037	0	0	0	.387	14.037	.093
Carb Monox	28.01	11.37	11.116	0	0	0	.306	11.116	.129
Benz/Tol	85.13	0	0	0	0	0	0	0	0
Propane	44.09	1.301	1.343	0	0	0	.037	1.343	.024
Propylene	42.08	0	0	0	0	0	0	0	0
Butene-1	56.1	1.415	1.272	0	0	0	.035	1.272	.029
TOTAL		100	100	0	0	0	100	100	1
MOL WT.		23.84	24.21	0	0	0	27.92	24.21	

TABLE 4. YIELD OF GAS IN EACH SAMPLE BAG

	BAG 1	BAG 2	BAG 3	BAG 4	TOTAL
TANK DP (Atm)	.219	0	0	0	.219
NO. MOLES (AF)	3.853	0	0	0	3.853
MASS (gm AF)	107.6	0	0	0	107.6
NO. MOLES (N/O FREE)	.106	0	0	0	.106
PRODUCT GAS (gm)	2.57	0	0	0	2.57

APPENDIX 3.0 SAMPLE DATA SHEETS AND COMPUTER PRINTOUTS FOR A TYPICAL CELLULOSE FAST PYROLYSIS EXPERIMENT

UP DATA SHEET: Run # CK-314 Date: 13/8/85 No. Inserts: 12

TEMPERATURES:

Ambient temp.	22 C	Coil Oven (top)	1100 C
Nitrogen	215 C	Coil Oven (bot)	1100 C
Reactor Oven (top)	862 C	Injector (M.I.)	83 V
Reactor Oven (bot)	860 C	Thermovort. Oven	830 C
Thermofor Line (1)	880 C	Reactor Wall (7)	850 C
Thermofor Line (2)	870 C	Cryovortactor (8)	320 C
Injector Oven (3)	960 C	Heat Exchang. (9)	— C
Thermovortactor (4)	850 C		
Reactor Cavity (5)	850 C	Preheater-T (11)	1020 C
Reactor Wall (6)	852 C	Preheater-B (12)	— C

PRESSURES: Ambient Pressure 764 mmHg

Time (m/s)	0	5	10		
Biom. Feeder (psig)					
Therm. Feeder (psig)	16	2	2.1		
Cryo. Exit (psig)	14	1.7	19		

(2 / 18)

ROTAMETER DATA: Time (m/s) 2 5 8

	psig	scale	psig	scale	psig	scale	psig	scale
Cryo.Ext.N2	14	110	18	110	19	110	20	110
Thermofor	—	—	—	—	—	—	—	—
Biomass	16	45	2		2.1			
B/T Ext.N2	64	80	7	80	7	80		

(16, 110 / 2, 45 / 7, 80)

BIOMASS FLOW:

Motor Setting	18 %	Calib. Flowrate	~2 g/min
Biomass Fed	240 g	Initial Time	6 s
Biom. Bypassed	07 g	Final Time	10'6 s
Biom. Pyrolyzed	233 g	Time of Pyrolysis	10'
Biomass Flowrate	2.33 g/min		

THERMOFOR FLOW:

Motor Setting	— %	Calib. Flowrate	— g/min
Time Interval	— s		

BAG PRESSURES:

	Bag 1	Bag 2	Bag 3	Bag 4
Initial P (mmHg)	730	411	693	—
Final P (mmHg)	414	95	365	
Delta P (mmHg)	316	316	328	
Tank Temp. (C)	24	25	26.5	

COMMENTS:

DAL
Initials

```
      ULTRAPYROLYSIS REACTOR RESIDENCE TIME PROGRAM
      ##############################################


EXPERIMENTAL RUN: CK-314       DATE: AUG.13/85

EXPERIMENTAL CONDITIONS:
      AMBIENT ROOM TEMPERATURE= 22 C
      AMBIENT ATMOSPHERIC PRESSURE= 1.005 Atm
      MEAN REACTOR TEMPERATURE= 850 C
      MEAN REACTOR PRESSURE= 1.128 Atm
      NUMBER OF REACTOR INSERTS= 12
      NITROGEN TRANSPORT GAS TEMPERATURE= 21.5 C
      BIOMASS FLOWRATE= 4.05000001E-05 kg/s (2.43 g/min)
      THERMOFOR (solids) FLOWRATE= 0 kg/s (0 g/min)

SOLIDS LOADING:
      BIOMASS LOADING (solids/gas) = .357
      THERMOFOR LOADING (solids/gas)= 0

MASS FLOWRATES OF NITROGEN TRANSPORT GAS:
      BIOMASS N2 TRANSPORT GAS= 1.1342181E-04 kg/s (6.805 g/min)
      THERMOFOR N2 TRANSPORT GAS= 0 kg/s (0 g/min)
      BIOMASS/THERMOFOR EXTRA N2= 8.01554905E-04 kg/s (48.093 g/min)
      CRYOFOR EXTRA N2= 3.79579221E-04 kg/s (22.775 g/min)
      TOTAL N2 FLOW TO RECOVERY TRAIN= 1.29455594E-03 kg/s (77.673 g/min)
      TOTAL N2 FLOW THROUGH REACTOR= 9.14976715E-04 kg/s (54.899 g/min)

RESIDENCE TIME:
      REACTOR RESIDENCE TIME (incl. thermovort.)= 64.902 ms
      PORTION OF RESIDENCE TIME DUE TO BIOMASS N2= 12.15 %
      PORTION OF RESIDENCE TIME DUE TO THERMOFOR N2= 0 %
      PORTION OF RESIDENCE TIME DUE TO BIOMASS/THERMOFOR EXTRA N2= 85.865 %
      PORTION OF RESIDENCE TIME DUE TO PRODUCT GAS= 1.985 %

REYNOLDS NUMBERS:
      REACTOR REYNOLDS NUMBER= 1278.1     VELOCITY= 7.9 m/s
      REACTOR INSERT/TV EXIT REYNOLDS NUMBER= 2605.7    VELOCITY= 32.7 m/s
      BIOMASS INLET = 1137.3  VELOCITY= 4.2 m/s
      THERMOFOR INLET = 4941.8  VELOCITY= 110.9 m/s

COMMENTS:
      NO THERMOFOR SOLIDS WERE INJECTED.
      REACTOR VOLUME = ? (TEMP.)
```

RUN CI-314: GAS PRODUCT SUMMARY

REACTOR TEMP. = 850 C
RESIDENCE TIME =65 ms

TABLE 1. G.C. CALIBRATION SUMMARY

GAS COMPONENT	AVG CAL. AREA	AVG RF	AVG PEAK AREAS FOR ULTRAPYROLYSIS GAS SAMPLES				
			DYNAMIC	BAG 1	BAG 2	BAG 3	BAG 4
HYDROGEN	78813	10195.8	0	5403	5346	6201	0
CARB DIOX	116531	51335.2	0	4927.5	5311.5	5237	0
ETHYLENE	62095	54469.3	0	9260.5	10147	9894	0
ETHANE	31323	58005.6	0	1528	1264.5	1453	0
ACETYLENE	23635	46343.6	0	2415	2679	2583	0
OXYGEN	16622	31964.6	0	9127	7850.5	12132	0
NITROGEN	3165470	42060.7	0	3938279	3985712	3973839	0
METHANE	74823	34964.1	0	5810.5	6209	5961	0
CARB MONOX	362092	43625.5	0	65907	72057.5	69104	0
BENZ/TOL	3985	98386.8	0	1123	1320	1126	0
PROPANE	40757	78378.2	0	0	0	0	0
PROPYLENE	38953	74910.3	0	1627	1828	1852	0
BUTENE-1	45258	88741.2	0	0	0	0	0

TABLE 2. G.C. COMPOSITION SUMMARY (Molar %)

GAS COMPONENT	ACTUAL G.C. MOLAR COMPOSITION					AIR FREE MOLAR COMPOSITION				
	DYNAMIC	BAG 1	BAG 2	BAG 3	BAG 4	DYNAMIC	BAG 1	BAG 2	BAG 3	BAG 4
HYDROGEN	0	.53	.524	.608	0	0	.549	.543	.635	0
CARB DIOX	0	.096	.103	.102	0	0	.099	.107	.106	0
ETHYLENE	0	.17	.186	.192	0	0	.176	.193	.19	0
ETHANE	0	.026	.022	.025	0	0	.027	.023	.026	0
ACETYLENE	0	.052	.058	.056	0	0	.054	.06	.058	0
OXYGEN	0	.286	.246	.38	0	0	0	0	0	0
NITROGEN	0	95.06	94.761	94.479	0	0	97.324	97.142	97.116	0
METHANE	0	.166	.178	.17	0	0	.172	.184	.178	0
CARB MONOX	0	1.511	1.652	1.584	0	0	1.564	1.71	1.653	0
BENZ/TOL	0	.011	.013	.011	0	0	.012	.014	.012	0
PROPANE	0	0	0	0	0	0	0	0	0	0
PROPYLENE	0	.022	.024	.025	0	0	.022	.025	.026	0
BUTENE-1	0	0	0	0	0	0	0	0	0	0
TOTAL	0	97.93	97.767	97.621	0	0	100	100	100	0
MOL. WT	0	27.32	27.27	27.22	0	0	27.88	27.88	27.86	0

RUN CK-314 (cont'd)

TABLE 3. SUMMARY OF PRODUCT GAS COMPOSITION

GAS COMPONENT	MOL. WT.	NITROGEN/OXYGEN FREE MOLAR COMPOSITION					PRODUCT GAS AVG (3 BAGS)			SPECIFIC GAS YIELD *
		DYNAMIC	BAG 1	BAG 2	BAG 3	BAG 4	MOLAR % AIR-FREE	MOLAR % N/O FREE	MASS FRACTION	
HYDROGEN	2.02	0	20.504	18.392	22.01	0	.576	20.523	.018	.011
CARB DIOX	44.01	0	3.714	3.748	3.692	0	.104	3.718	.072	.045
ETHYLENE	28.05	0	6.578	6.748	6.573	0	.186	6.633	.081	.051
ETHANE	30.07	0	1.019	.79	.906	0	.025	.903	.012	7E-03
ACETYLENE	26.04	0	2.016	2.094	2.017	0	.057	2.042	.023	.014
OXYGEN	32	0	0	0	0	0	0	0	0	0
NITROGEN	28.02	0	0	0	0	0	97.194	0	0	0
METHANE	16.04	0	6.43	6.432	6.17	0	.178	6.34	.044	.028
CARB MONOX	28.01	0	59.455	59.827	57.323	0	1.642	58.52	.717	.447
BENZ/TOL	85.13	0	.442	.486	.414	0	.013	.447	.017	.01
PROPANE	44.09	0	0	0	0	0	0	0	0	0
PROPYLENE	42.08	0	.84	.824	.895	0	.025	.874	.016	.01
BUTENE-1	56.1	0	0	0	0	0	0	0	0	0
TOTAL		0	100	100	100	0	100	100	1	.623
MOL WT.		0	22.86	23.28	22.47	0	27.98	22.87		

* mass yield of the gaseous component per unit mass of dry biomass

TABLE 4. YIELD OF GAS IN EACH SAMPLE BAG

	BAG 1	BAG 2	BAG 3	BAG 4	TOTAL
TANK DP (Atm)	.418	.414	.43	0	1.262
NO. MOLES (AF)	7.459	7.364	7.605	0	22.428
MASS (gm AF)	208	205.3	211.9	0	625.2
NO. MOLES (N/O FREE)	.2	.21	.219	0	.629
PRODUCT GAS (gm)	4.56	4.9	4.93	0	14.4

RUN CR-314 (cont d)

TABLE 5. MASS BALANCE (NO SOLVENT/WATER SOLVENTS)

COMPONENT	MASS (gm)
BIOMASS (as is)	23.3
DRY BIOMASS	23.09
GAS	14.4
WATER (by K-F) *	N/A
VOLATILES	0
TAR	0
CHAR	0
TOTAL INPUT	23.3
TOTAL OUTPUT	14.4

MASS BALANCE (products/biomass) = 61.8 %
FRACTIONAL CONVERSION ('as is' biomass to gas) = .618
FRACTIONAL CONVERSION (dry biomass to gas) = .623

* Water Predicted By Shift Equilibrium (gm) = 3E-03

TABLE 6. ELEMENTAL BALANCE

ELEMENT	DRY BIOMASS INPUT	DRY GAS OUTPUT
CARBON	10.26	7.05
HYDROGEN	1.44	.7
OXYGEN	11.39	6.64

CARBON BALANCE (carbon in gas/feedstock carbon) = 68.7 %

Mass Balance Summary Sheet

Run: CK-314 Temperature: 850 C Residence Time: 50 ms

1. Pure Liquid Sample:

	Mass before (g)	Mass after (g)	Difference (g)
Condenser	3742.5	3741.4	1.1

Weight of pure condenser sample (if any) for analysis = NONE g

2. Solid Residue:

	Mass before (g)	Mass after (g)	Difference (g)
Filter Paper	1.25	1.59	0.34

3. Roto-vaporation:

	Mass of Flask (g)	Flask + Organics (g)	Difference (g)
All system (MeOH)	357.1	364.8	7.7

TOTAL _____

4. Summary:

G.C. VOLATILES ("liquids")	0.28		
Total Solids Collected --->	0.34	g	1.46 %
Total Organic Liquids ---->	7.7	g	33.05 %
Total Collected ---------->	8.32	g	
Gas Produced --- --------->	14.4	g	61.80 %
Total Products ---------->	22.72	g	
Mass of Biomass Fed ------>	23.3	g	
Mass Percentage Recovered	97.4	%	

Date: _____

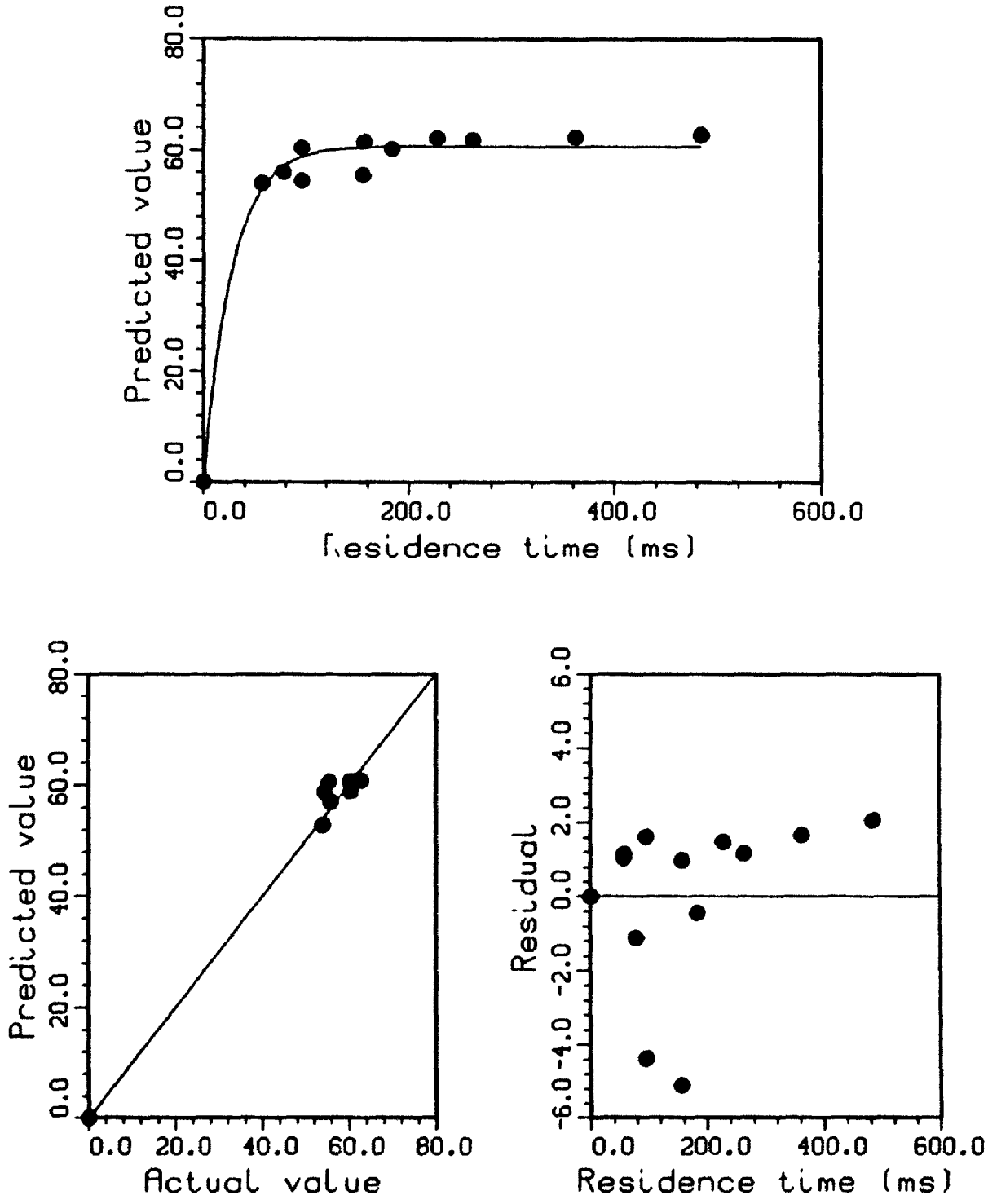

Figure A7.1.7. Zero-Intercept Kinetic Model (Equation 12) For CO from Cellulose: Fast Pyrolysis at 875 °C (Run Numbers and Data in Table 16)

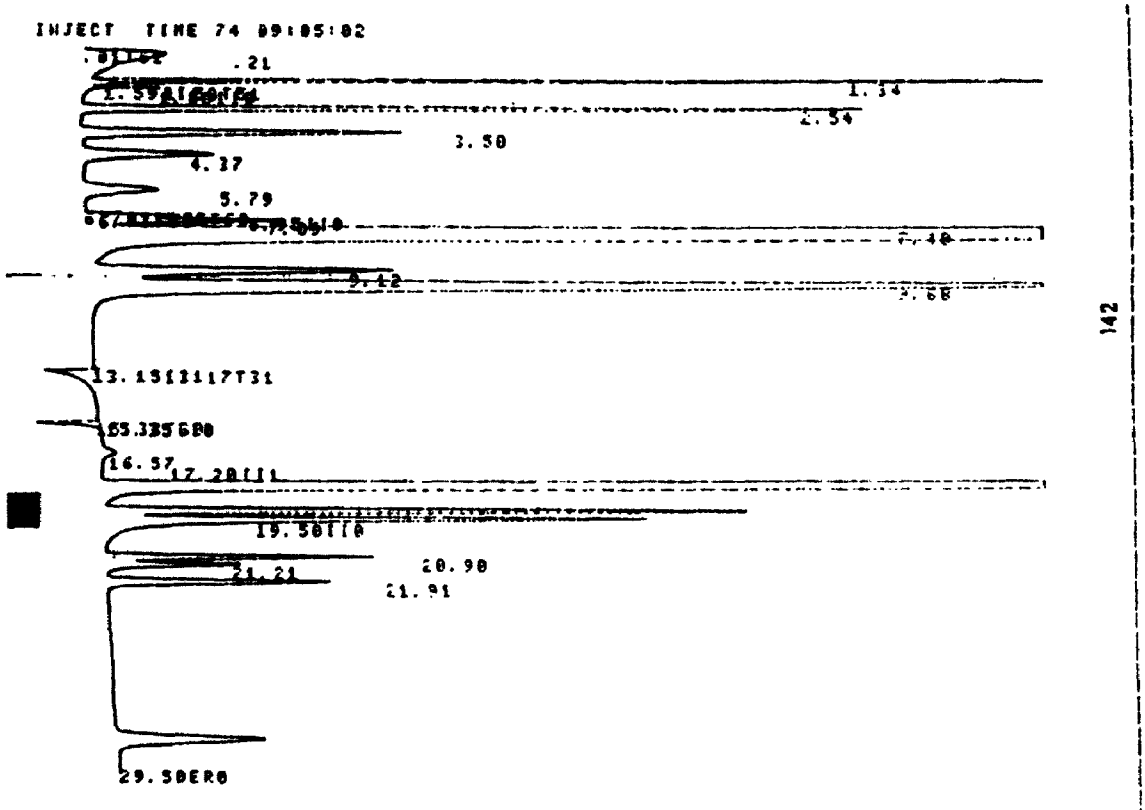

DUAL
FILE 2 METHOD 5. RUN *** INDEX 749

ANALYST: 7

NAME	CONC	RT	AREA	BC	RF
HYDROGEN	0.	1.24	79916	22	
CARB DIOX	0.	2.54	116659	01	
ETHYLENE	0.	3.5	61914	01	
ETHANE	0.	4.37	31654	01	
ACETYLENE	0.	5.79	22747	01	
OXYGEN	0.	7.09	16580	01	
NITROGEN	0.	7.48	3173239	01	
METHANE	0.	9.12	74948	02	
CARB MONOX	0.	9.68	363490	03	
BENZ/TOL	0.	16.57	1950	01	
PROPANE	0.	20.9	40707	02	
ACETYLENE	0.	21.21	23801	02	
PROPYLENE	0.	21.91	38629	01	
TOTALS	0.		4046426		

Sample Chromatogram: CK-314 Calibration Gas.

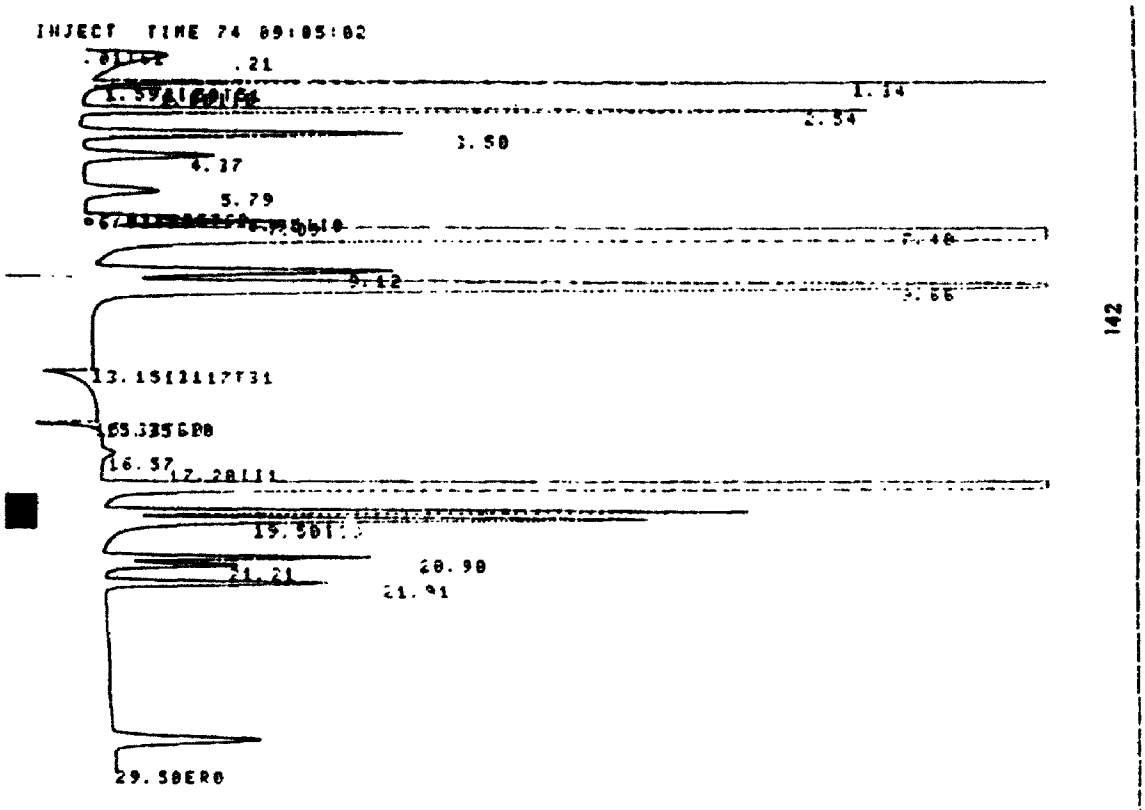

DUAL
FILE 2 METHOD 5. RUN *** INDEX 749

ANALYST: 7

NAME	CONC	RT	APER	EC	RF
HYDROGEN	0.	1.34	79916	00	
CARB DIOX	0.	2.54	116659	01	
ETHYLENE	0.	3.5	61914	01	
ETHANE	0.	4.37	31654	01	
ACETYLENE	0.	5.79	22747	01	
OXYGEN	0.	7.09	1650	01	
NITROGEN	0.	7.48	3172439	01	
METHANE	0.	9.12	74040	02	
CARB MONOX	0.	9.68	363490	07	
BENZ/TOL	0.	16.57	3950	01	
PROPANE	0.	20.9	40707	02	
ACETYLENE	0.	21.21	23801	02	
PROPYLENE	0.	21.91	38629	01	
TOTALS	0.		4046426		

Sample Chromatogram: CK-314 Calibration Gas.

APPENDIX 4.0 WATER-GAS SHIFT REACTION STUDY: SAMPLE DATA FROM COMPUTER MODELLING

CO_2 CONCENTRATION VS TIME AT 850°C

EXPERIMENT I.D.: WG-12
[CO2]o = 6.44E-04 molar
[H2]o = 3.14E-03 molar

[CO2] (molar)	TIME (s)
6.44E-04	0
6.118E-04	104.05
5.796E-04	214.29
5.474E-04	331.45
5.152E-04	456.37
4.83E-04	590.07
4.508E-04	733.77
4.186E-04	888.98
3.864E-04	1057.54
3.542E-04	1241.80
3.22E-04	1444.78
2.898E-04	1670.46
2.576E-04	1924.20
2.254E-04	2213.56
1.932E-04	2549.59
1.61E-04	2949.42
1.288E-04	3441.76
9.66E-05	4080.43
6.44E-05	4986.23
3.33E-05	6544.73

CO_2 CONCENTRATION VS TIME AT 850°C

EXPERIMENT I.D.: WG-7
[CO2]o = 5.47E-04 molar
[H2]o = 2.67E-03 molar

[CO2] (molar)	TIME (s)
5.47E-04	0
5.197E-04	26.25
4.923E-04	54.06
4.65E-04	83.62
4.376E-04	115.13
4.103E-04	148.86
3.829E-04	185.11
3.556E-04	224.26
3.282E-04	266.79
3.009E-04	313.27
2.735E-04	364.47
2.462E-04	421.40
2.188E-04	485.41
1.915E-04	558.40
1.641E-04	643.17
1.368E-04	744.03
1.094E-04	868.22
8.205E-05	1029.32
5.47E-05	1257.81
2.735E-05	1650.93

APPENDIX 5.0 COMPARISON OF CELLULOSE PRIMARY VOLATILIZATION AND SECONDARY CRACKING REACTION RATES

COMPARISON OF CELLULOSE VOLATILIZATION AND CRACKING REACTION RATES:

FIRST ORDER KINETICS GAS CONST: 0.008314 KJ/mol K

VOLATILIZATION KINETIC PARAMETERS: BRADBURY (Ea= 198 KJ/mol)

1. BRADBURY/ANTAL PARAMETERS:

CRACKING KINETIC PARAMETERS: ANTAL (Ea= 204 KJ/mol)

TEMPERATURE		PRE-EXPONENTIAL CONST.		ACTIVATION ENERGY		RATE CONSTANT		RATE RATIO
(C)	(K)	A (v)	A (cr)	Ea/RT (v)	Ea/RT (cr)	kv	kcr	kv / kcr
650	923.15	3.17E+14	3.57E+11	25.79657	26.57828	1984.953	1.022975	1940.373
700	973.15	3.17E+14	3.57E+11	24.47115	25.21270	7470.869	4.008011	1863.984
750	1023.15	3.17E+14	3.57E+11	23.27528	23.98059	24702.01	13.74131	1797.645
800	1073.15	3.17E+14	3.57E+11	22.19084	22.86329	73063.01	42.00154	1739.531
825	1098.15	3.17E+14	3.57E+11	21.68565	22.34279	121087.0	70.68279	1713.104
850	1123.15	3.17E+14	3.57E+11	21.20296	21.84547	196214.1	116.2248	1688.228
875	1148.15	3.17E+14	3.57E+11	20.74128	21.36980	311339.2	187.0158	1664.774
900	1173.15	3.17E+14	3.57E+11	20.29928	20.91441	484386.4	294.8855	1642.625

2. BRADBURY/PETERS PARAMETERS:

CRACKING KINETIC PARAMETERS: PETERS (Ea= 133 KJ/mol)

TEMPERATURE		PRE-EXPONENTIAL CONST.		ACTIVATION ENERGY		RATE CONSTANT		RATE RATIO
(C)	(K)	A (v)	A (cr)	Ea/RT (v)	Ea/RT (cr)	kv	kcr	kv / kcr
650	923.15	3.17E+14	2.00E+08	25.79657	17.32800	1984.953	5.964512	332.7938
700	973.15	3.17E+14	2.00E+08	24.47115	16.43769	7470.869	14.52878	514.2114
750	1023.15	3.17E+14	2.00E+08	23.27528	15.63440	24702.01	32.44092	761.4460
800	1073.15	3.17E+14	2.00E+08	22.19084	14.90597	73063.01	67.21228	1087.048
825	1098.15	3.17E+14	2.00E+08	21.68565	14.56662	121087.0	94.36770	1283.140
850	1123.15	3.17E+14	2.00E+08	21.20296	14.24239	196214.1	130.5080	1503.463
875	1148.15	3.17E+14	2.00E+08	20.74128	13.93227	311339.2	177.9586	1749.503
900	1173.15	3.17E+14	2.00E+08	20.29928	13.63537	484386.4	239.4752	2022.699

3. BRADBURY/SCOTT PARAMETERS:

CRACKING KINETIC PARAMETERS: SCOTT (Ea= 107.5 KJ/mol)

TEMPERATURE		PRE-EXPONENTIAL CONST.		ACTIVATION ENERGY		RATE CONSTANT		RATE RATIO
(C)	(K)	A (v)	A (cr)	Ea/RT (v)	Ea/RT (cr)	kv	kcr	kv / kcr
650	923.15	3.17E+14	3.10E+06	25.79657	14.00571	1984.953	2.563049	774.4497
700	973.15	3.17E+14	3.10E+06	24.47115	13.28610	7470.869	5.263547	1419.360
750	1023.15	3.17E+14	3.10E+06	23.27528	12.63683	24702.01	10.07522	2451.757
800	1073.15	3.17E+14	3.10E+06	22.19084	12.04805	73063.01	18.15330	4024.777
825	1098.15	3.17E+14	3.10E+06	21.68565	11.77377	121087.0	23.88220	5070.177
850	1123.15	3.17E+14	3.10E+06	21.20296	11.51170	196214.1	31.03774	6321.791
875	1148.15	3.17E+14	3.10E+06	20.74128	11.26105	311339.2	39.87947	7807.005
900	1173.15	3.17E+14	3.10E+06	20.29928	11.02107	484386.4	50.69546	9554.828

4. BRADBURY/GRAHAM PARAMETERS: (prompt gas removed)

CRACKING KINETIC PARAMETERS: GRAHAM (Ea= 100.8 KJ/mol)

TEMPERATURE		PRE-EXPONENTIAL CONST.		ACTIVATION ENERGY		RATE CONSTANT		RATE RATIO
(C)	(K)	A (v)	A (cr)	Ea/RT (v)	Ea/RT (cr)	kv	kcr	kv / kcr
650	923.15	3.17E+14	1.09E+06	25.79657	13.13280	1984.953	2.157365	920.0820
700	973.15	3.17E+14	1.09E+06	24.47115	12.45804	7470.869	4.236108	1763.616
750	1023.15	3.17E+14	1.09E+06	23.27528	11.84923	24702.01	7.786981	3172.219
800	1073.15	3.17E+14	1.09E+06	22.19084	11.29715	73063.01	13.52487	5402.121
825	1098.15	3.17E+14	1.09E+06	21.68565	11.03997	121087.0	17.49152	6922.607
850	1123.15	3.17E+14	1.09E+06	21.20296	10.79423	196214.1	22.36402	8773.651
875	1148.15	3.17E+14	1.09E+06	20.74128	10.55919	311339.2	28.28944	11005.49
900	1173.15	3.17E+14	1.09E+06	20.29928	10.33418	484386.4	35.42816	13672.35

APPENDIX 6.0 DERIVATION OF FIRST-ORDER KINETIC EQUATION FROM FIRST PRINCIPLES

1. General rate equations are given as follows:

$$r = \frac{dV}{dt}$$

where,
- r is the rate
- V is the mass or concentration of of reactant
- t is the residence (reaction) time

2. Another general expression for the rate is given:

$$r = k\,(V^{*} - V)^{n}$$

where,
- k is the Arrhenius rate constant
- V^{*} is the maximun yield at some extended residence time
- V is the yield at any residence time
- n is the order of the reaction

3. These two equations are equivalent:

$$\frac{dV}{dt} = k\,(V^{*} - V)^{n}$$

4. The rate constant k is defined by the Arrhenius expression:

$$k = A\,e^{-Ea/RT}$$

where,
- A is the pre-exponential constant (freq. factor)
- Ea is the activation energy
- R is the gas constant
- T is the reaction temp.

5. Substituting the Arrhenius equation (4) into (3):

$$\frac{dV}{dt} = A\, e^{-Ea/RT}\, (V^* - V)^n$$

6. If the reaction is first-order (as many complex pyrolysis reactions are assumed to be), then n=1. This can be substituted in equation 5. With rearrangement:

$$\frac{dV}{(V^*-V)} = A\, e^{-Ea/RT}\, dt = k\, dt$$

7. Integrating both sides of (6):

$$\ln [(V^*-V)/V^*] = -kt$$

or,

$$\frac{(V^*-V)}{V^*} = e^{-kt}$$

and,

$$V = V^* [1 - e^{-kt}]$$

APPENDIX 7.0 REGRESSION ANALYSES

The Statistical Analysis Systems (S.A.S.) routine for the non-linear regression analyses was based on the the Levenberg-Marquardt algorithm. References are given as follows:

Marquardt, D.W. and K. Levenberg. J. Soc. Instit. Appl. Math. 11(2):431 (1963).

APPENDIX 7.1 CELLULOSE PYROLYSIS REGRESSION CURVES: ZERO-INTERCEPT MODEL (EQUATION 12)

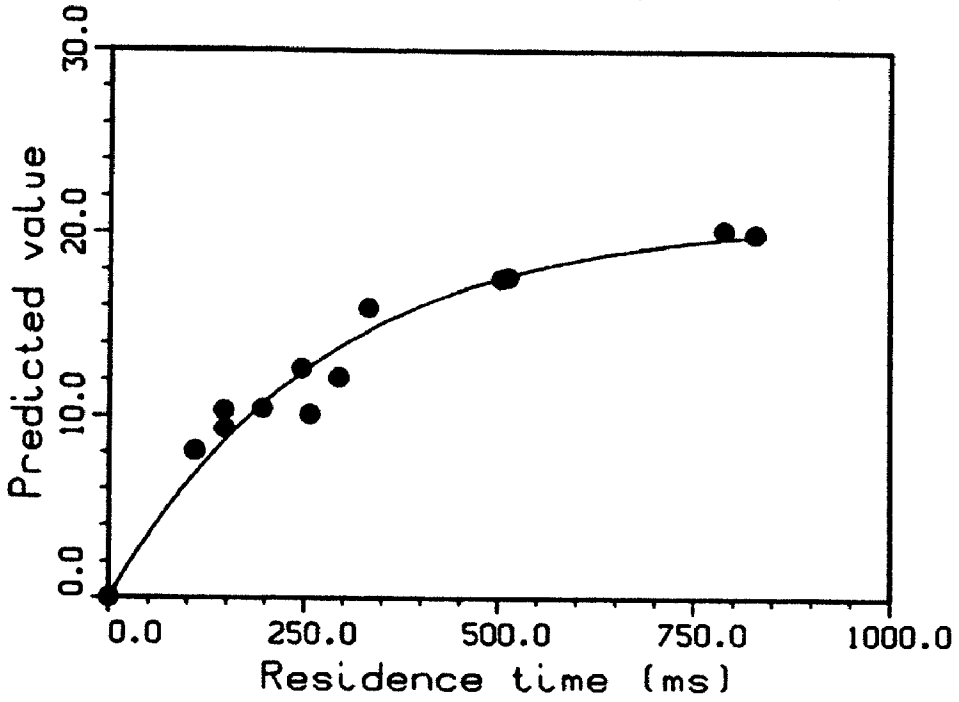

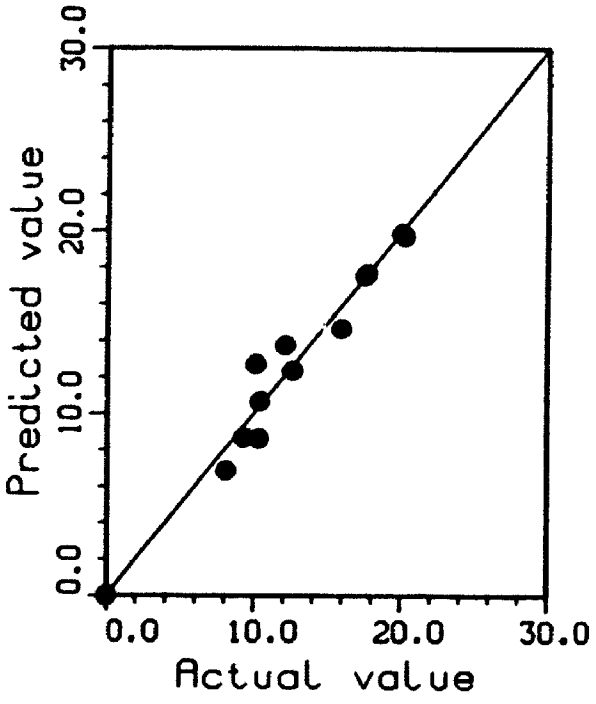

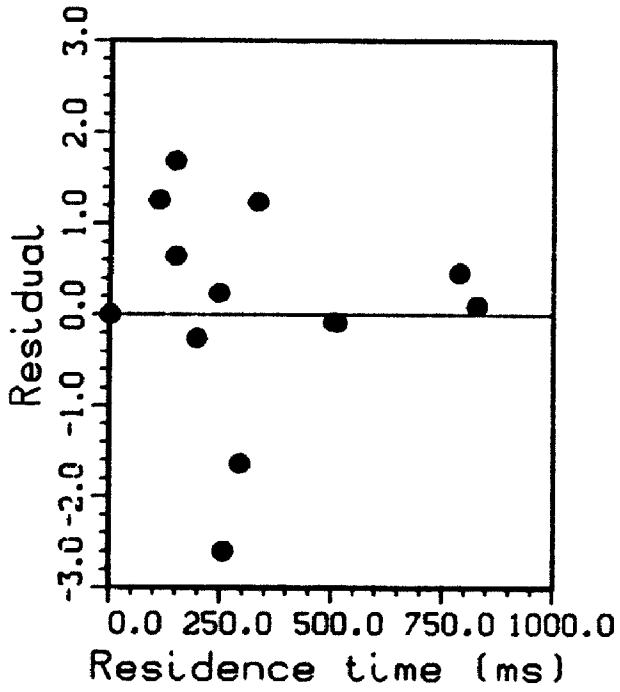

Figure A7.1.1. Zero-Intercept Kinetic Model (Equation 12) For CO from Cellulose: Fast Pyrolysis at 650 °C (Run Numbers and Data in Table 10)

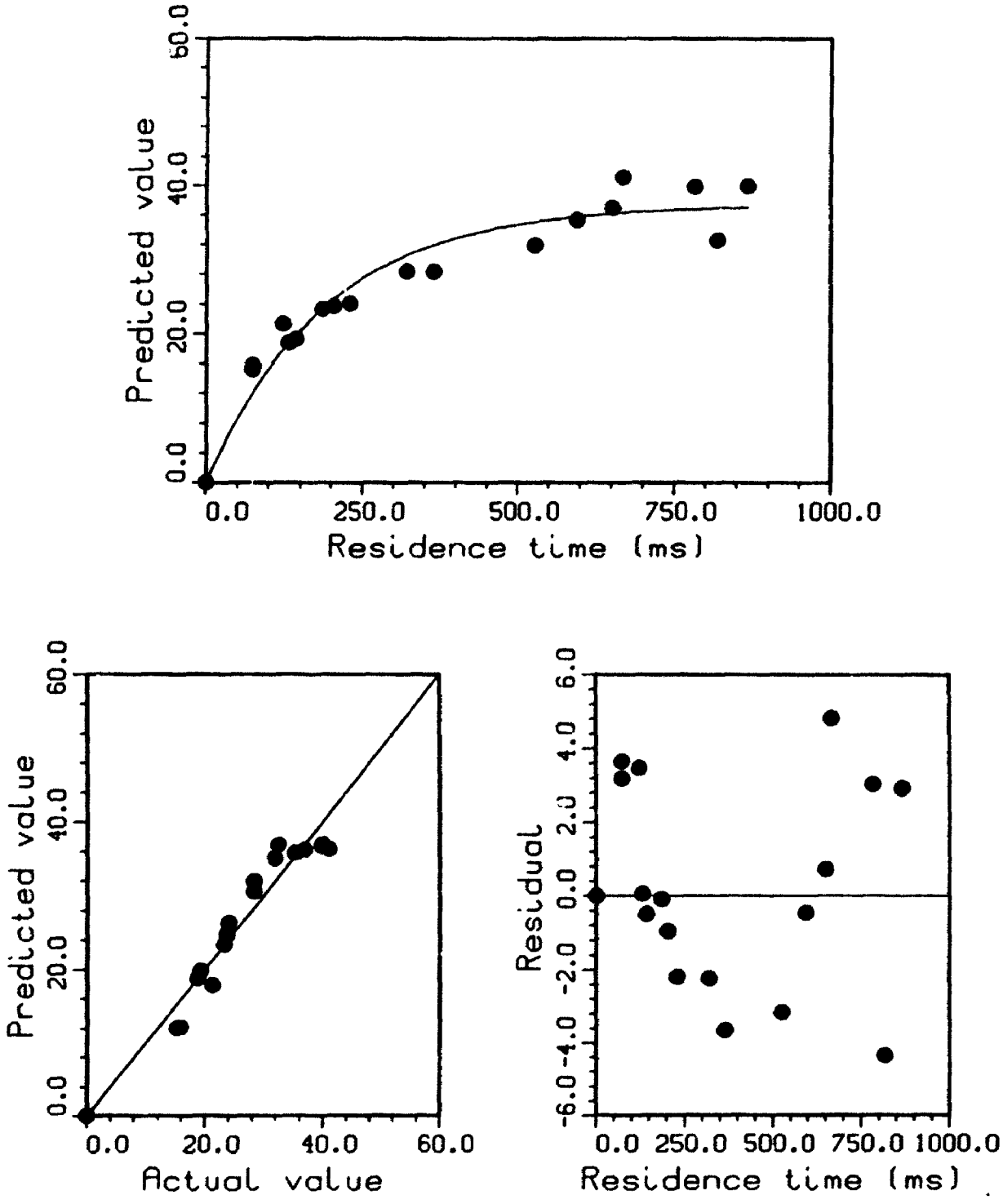

Figure A7.1.2. Zero-Intercept Kinetic Model (Equation 12) For CO from Cellulose: Fast Pyrolysis at 700 °C (Run Numbers and Data in Table 11)

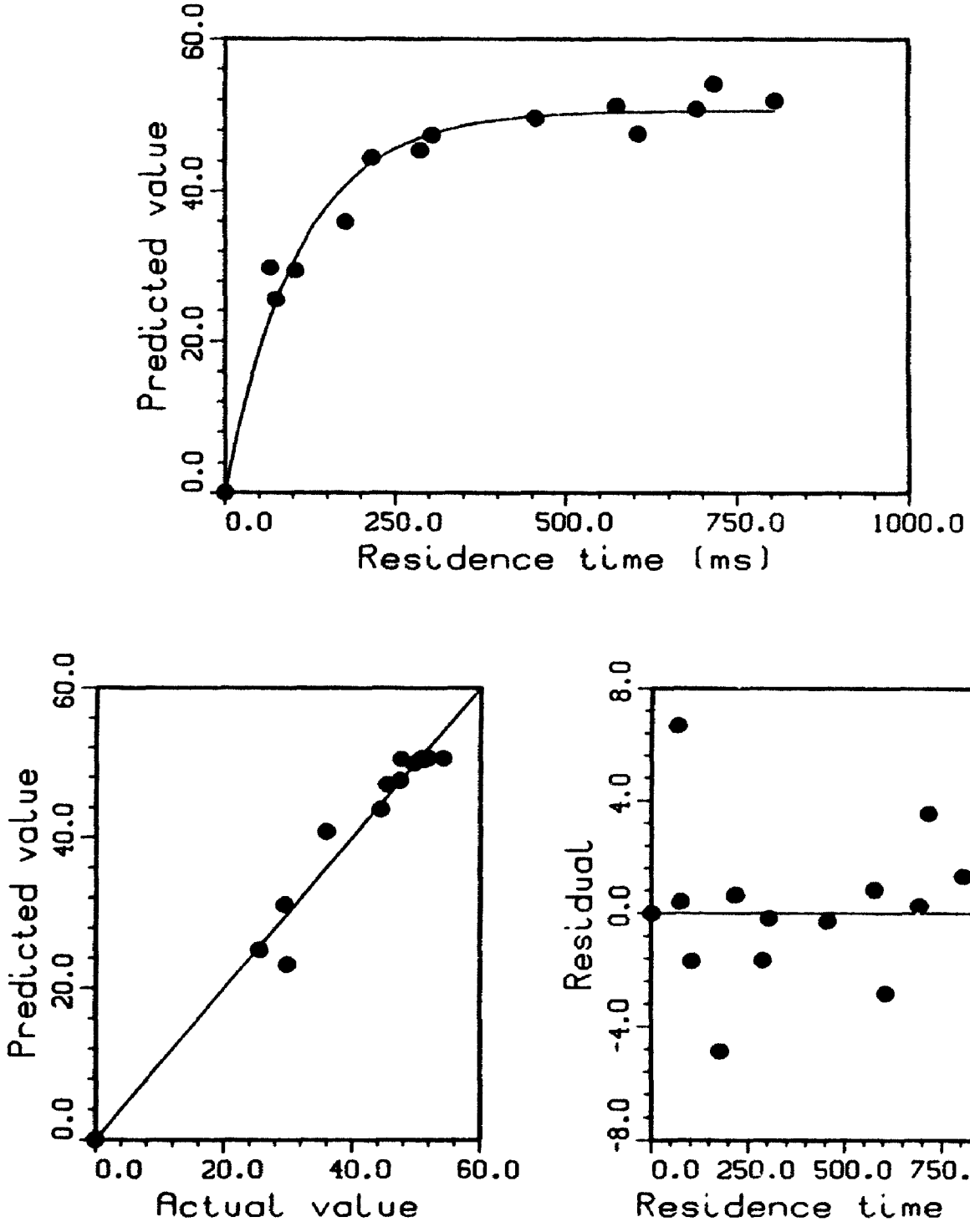

Figure A7.1.3. Zero-Intercept Kinetic Model (Equation 12) For CO from Cellulose: Fast Pyrolysis at 750 °C (Run Numbers and Data in Table 12)

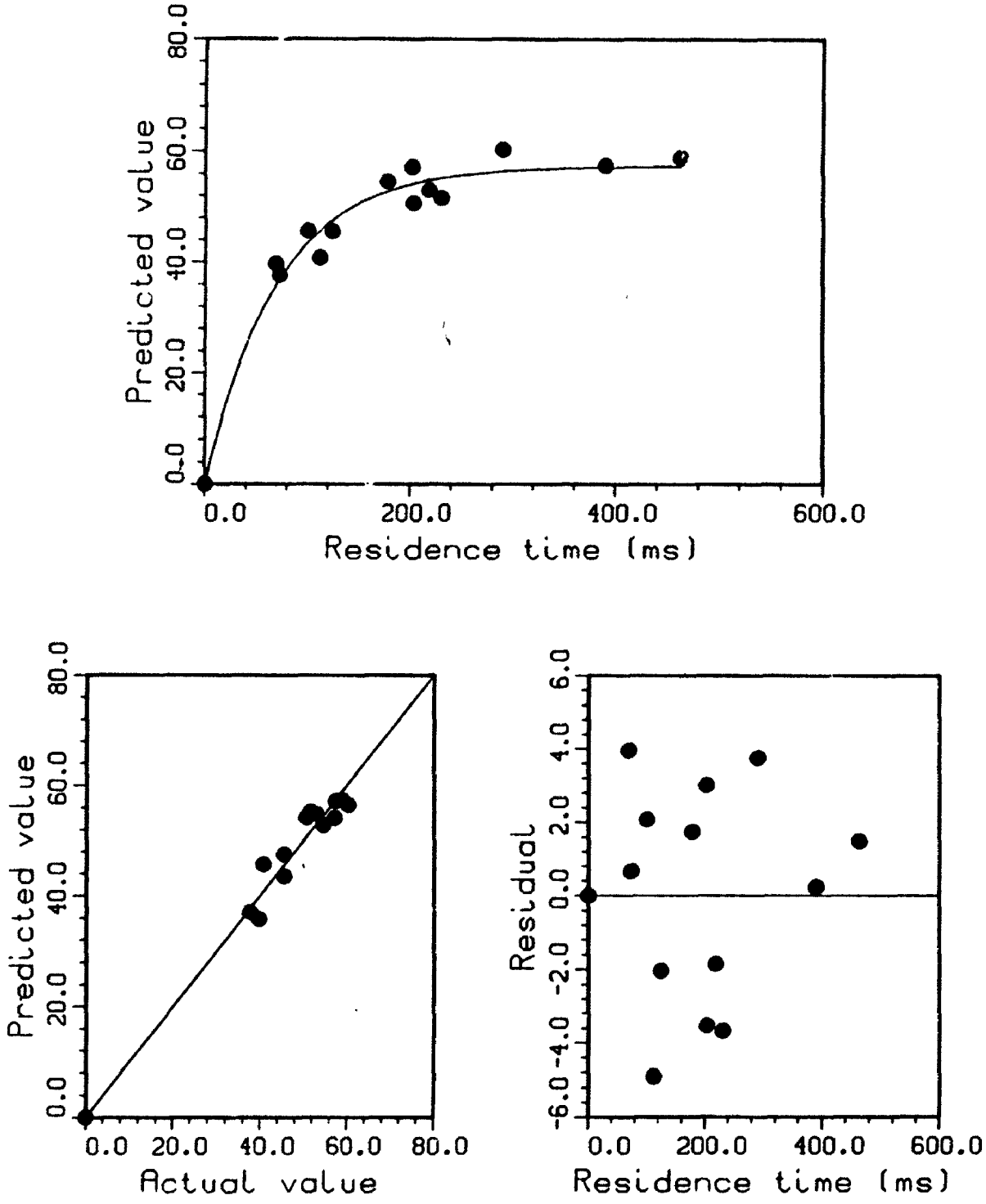

Figure A7.1.4. Zero-Intercept Kinetic Model (Equation 12) For CO from Cellulose: Fast Pyrolysis at 800 °C (Run Numbers and Data in Table 13)

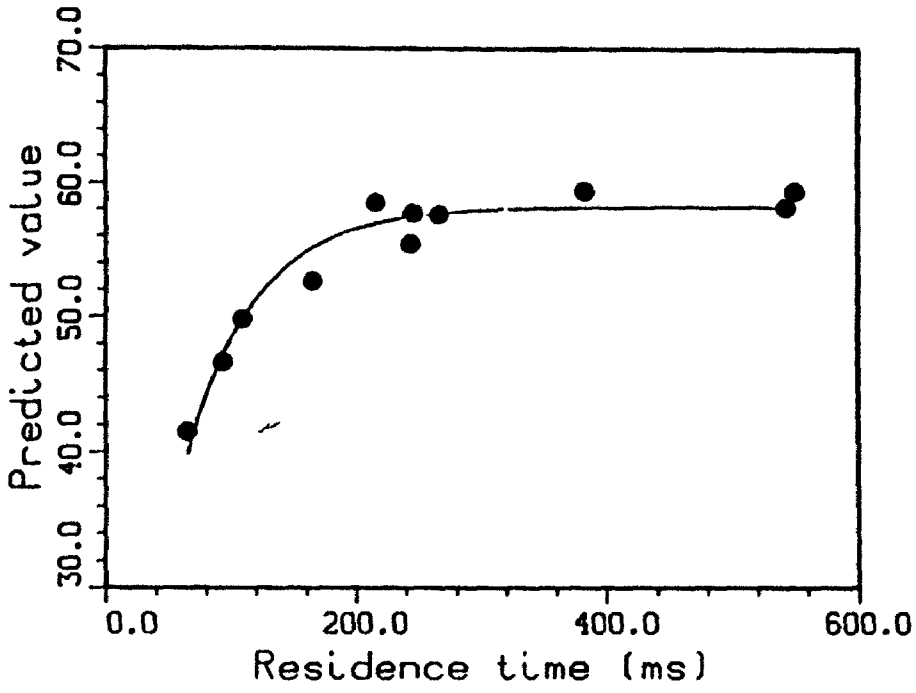

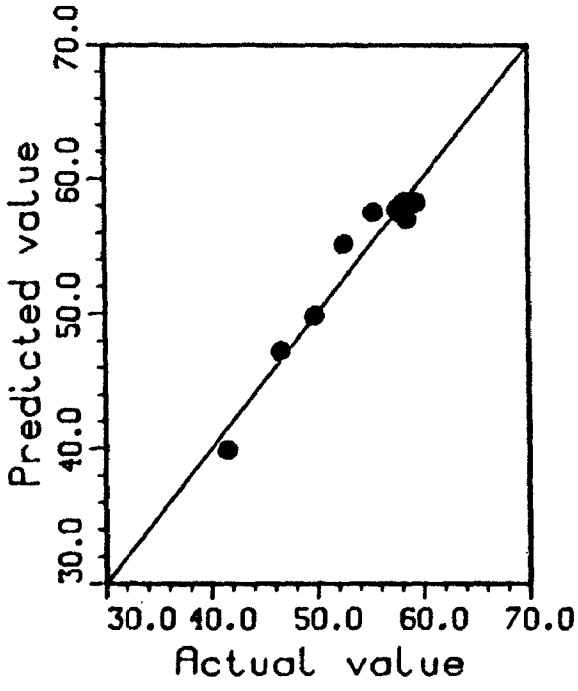

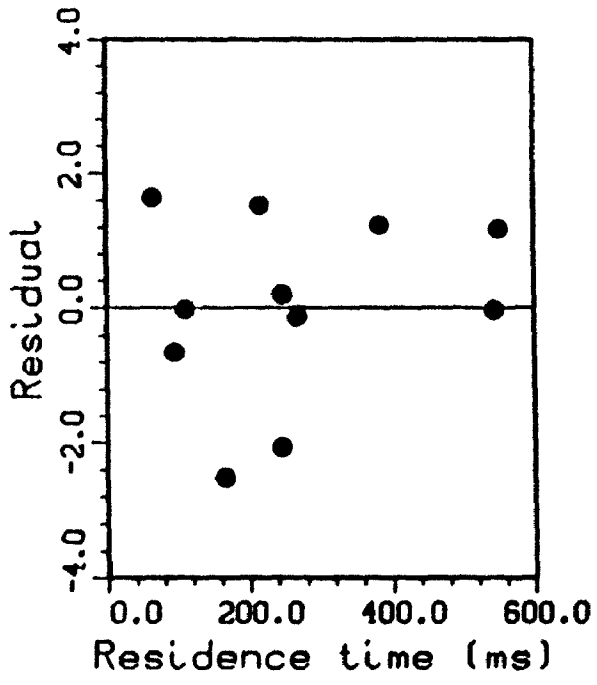

Figure A7.1.5. Zero-Intercept Kinetic Model (Equation 12) For CO from Cellulose: Fast Pyrolysis at 825 °C (Run Numbers and Data in Table 14)

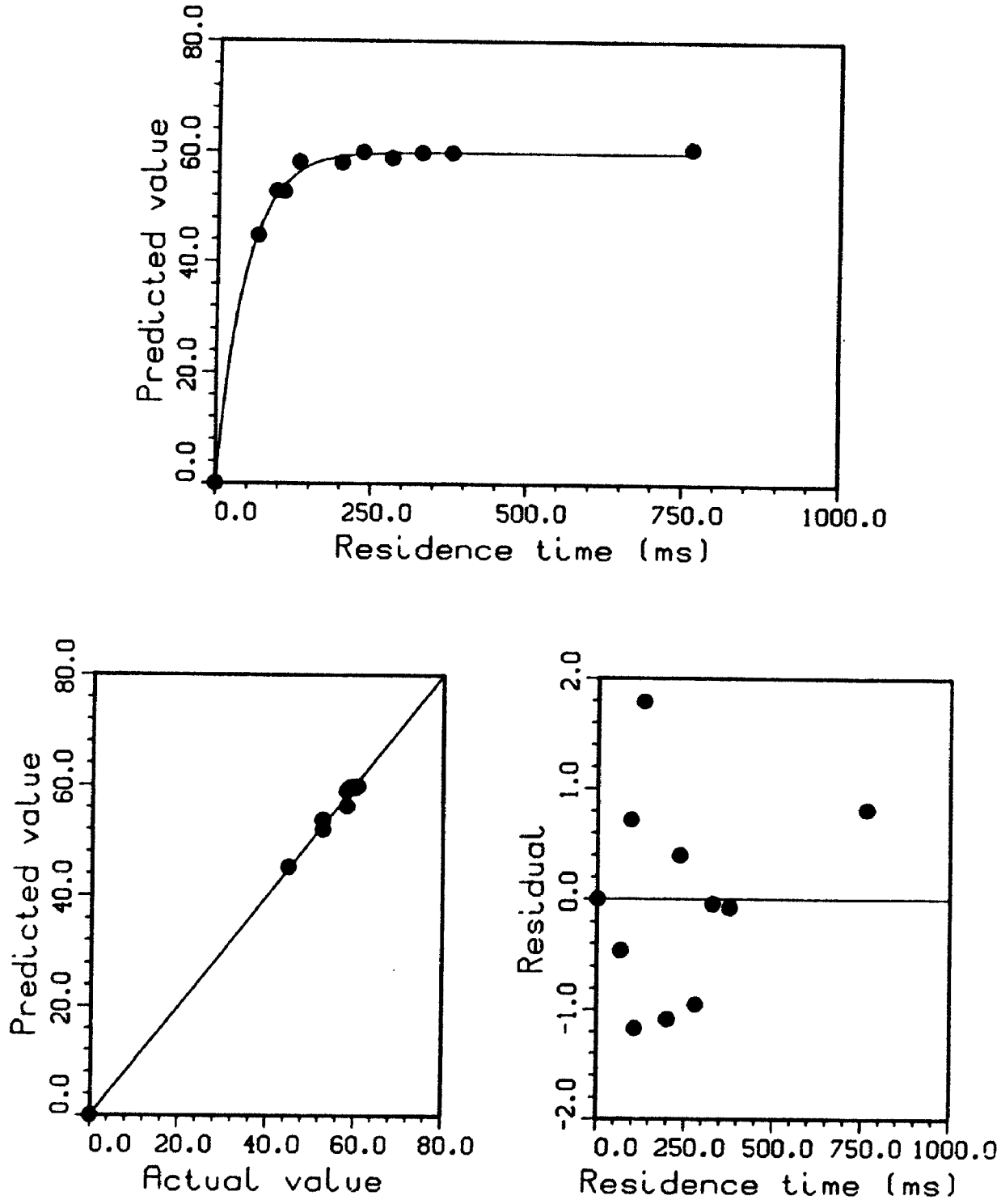

Figure A7.1.6. Zero-Intercept Kinetic Model (Equation 12) For CO from Cellulose: Fast Pyrolysis at 850 °C (Run Numbers and Data in Table 15)

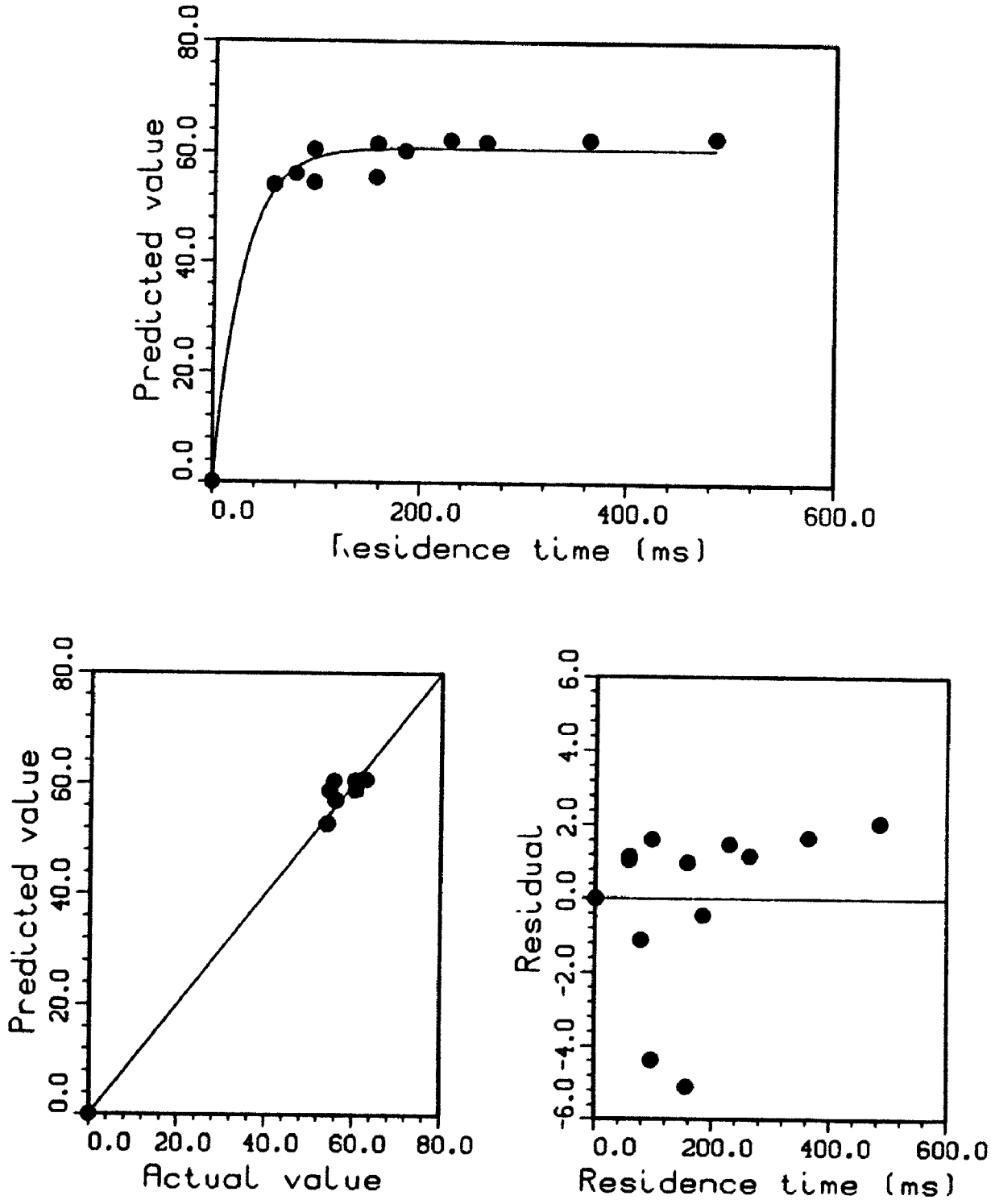

Figure A7.1.7. Zero-Intercept Kinetic Model (Equation 12) For CO from Cellulose: Fast Pyrolysis at 875 °C (Run Numbers and Data in Table 16)

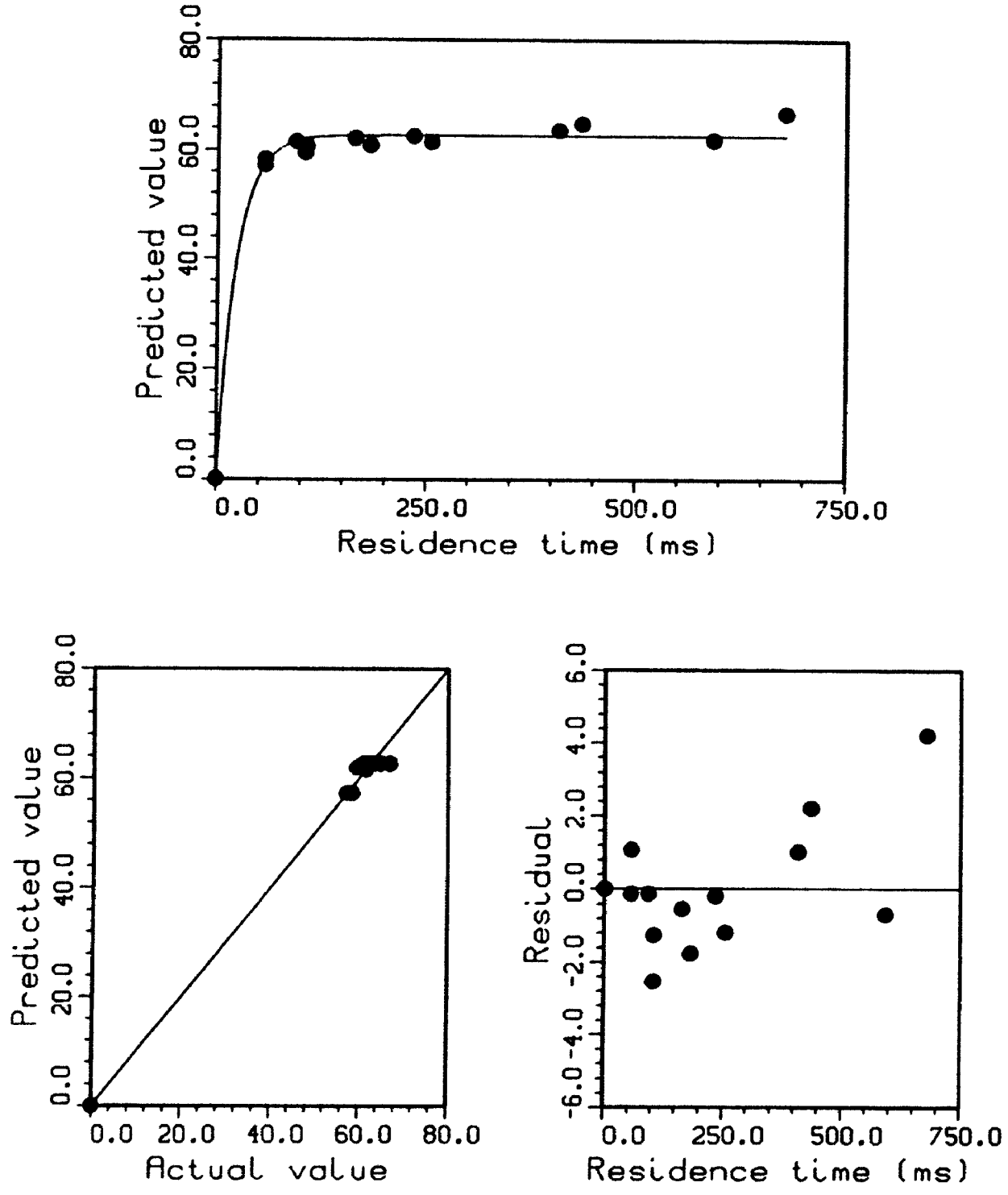

Figure A7.1.8. Zero-Intercept Kinetic Model (Equation 12) For CO from Cellulose: Fast Pyrolysis at 900 °C (Run Numbers and Data in Table 17)

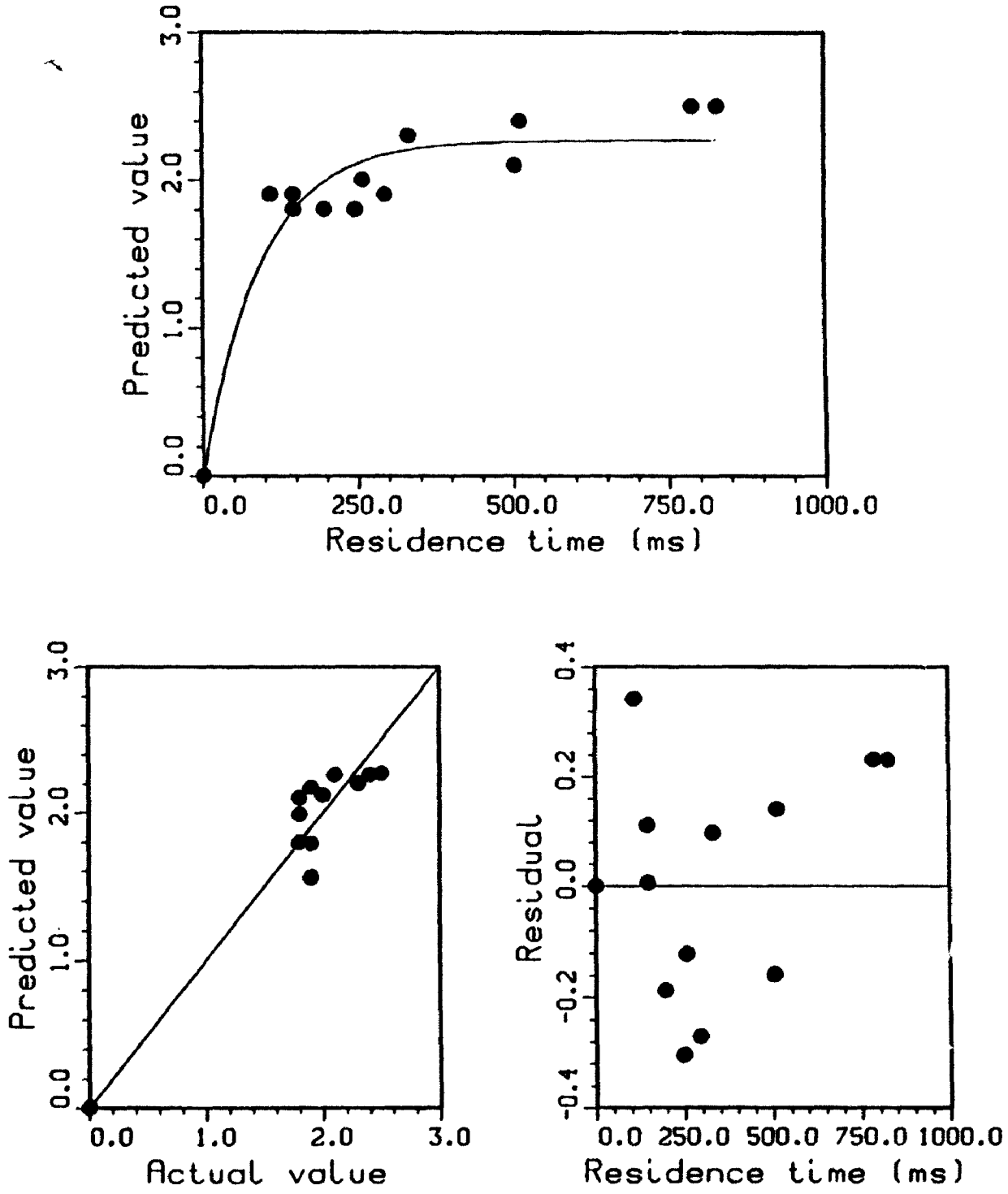

Figure A7.1.9. Zero-Intercept Kinetic Model For CO_2 from Cellulose: Fast Pyrolysis at 650 °C (Run Numbers and Data in Table 10)

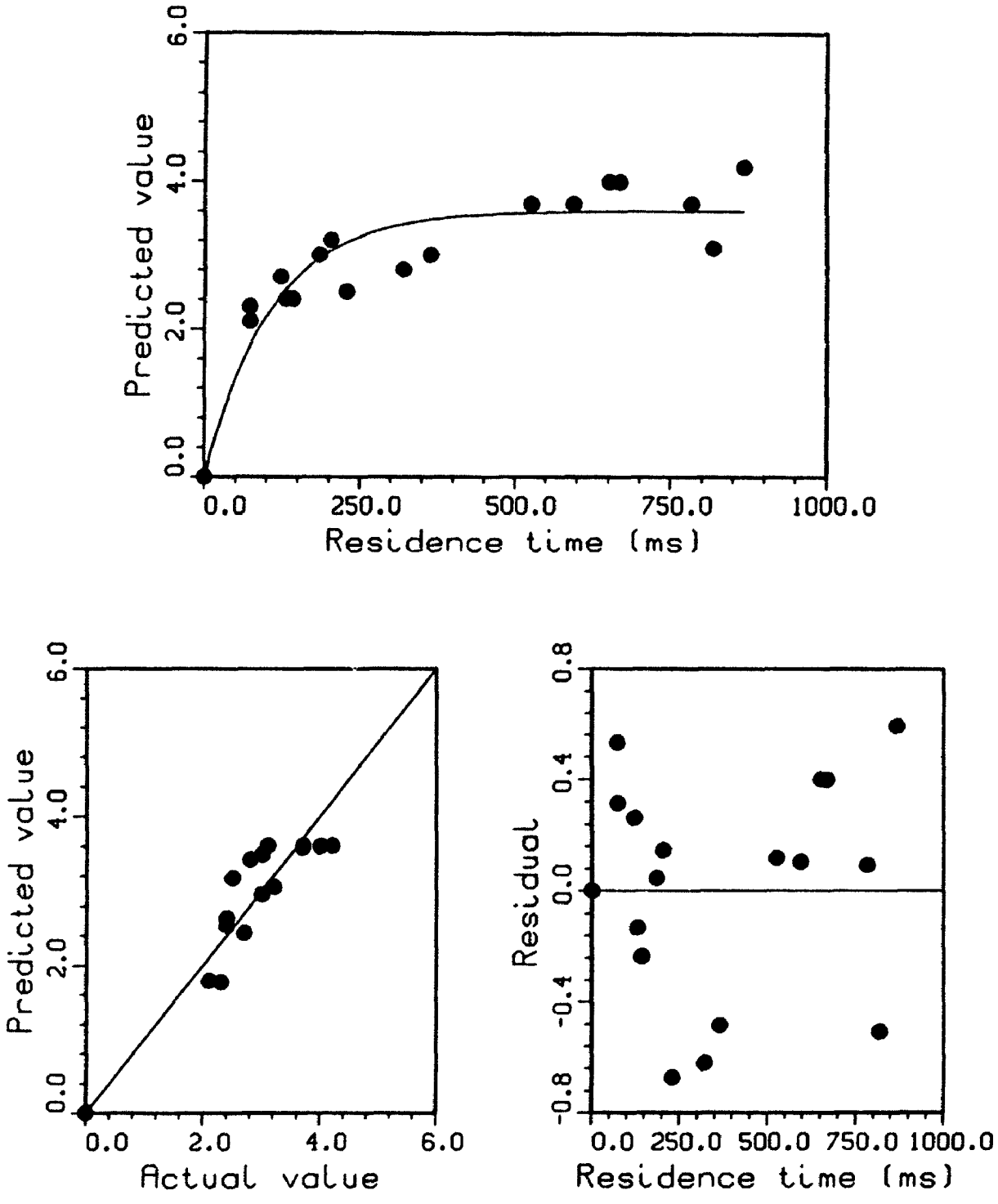

Figure A7.1.10. Zero-Intercept Kinetic Model For CO_2 from Cellulose: Fast Pyrolysis at 700 °C (Run Numbers and Data in Table 11)

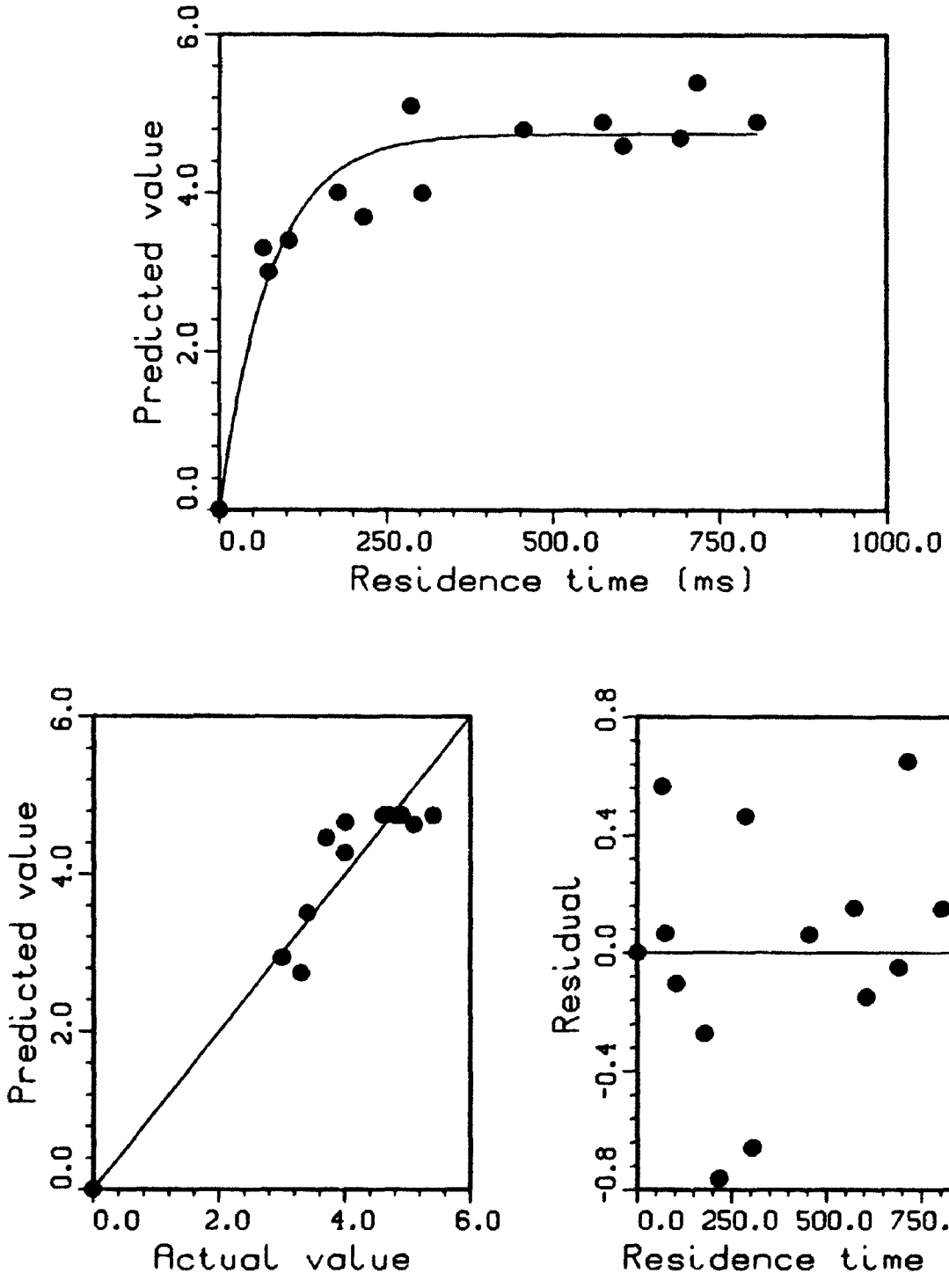

Figure A7.1.11. Zero-Intercept Kinetic Model For CO_2 from Cellulose: Fast Pyrolysis at 750 °C (Run Numbers and Data in Table 12)

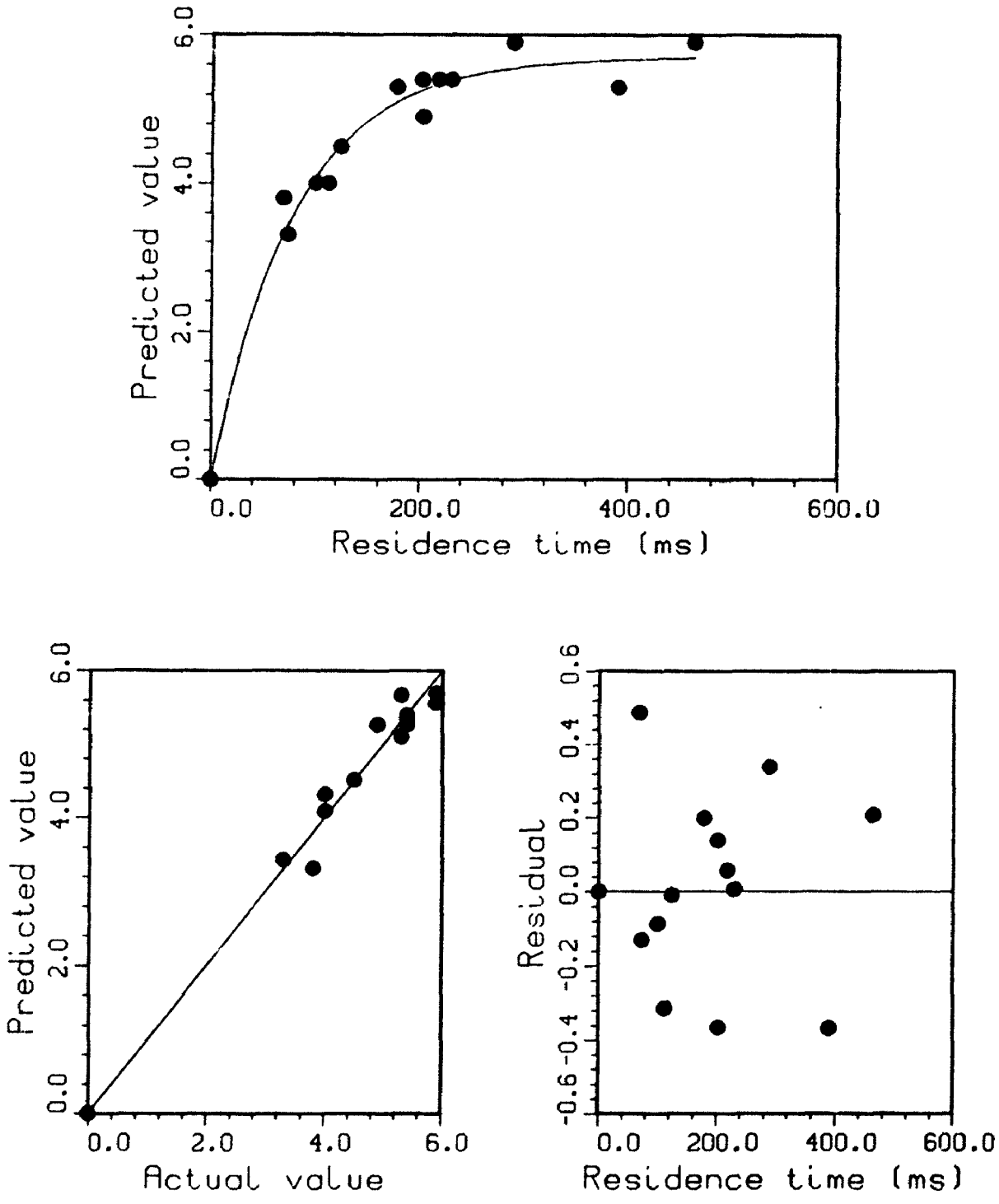

Figure A7.1.12. Zero-Intercept Kinetic Model For CO_2 from Cellulose: Fast Pyrolysis at 800 °C (Run Numbers and Data in Table 13)

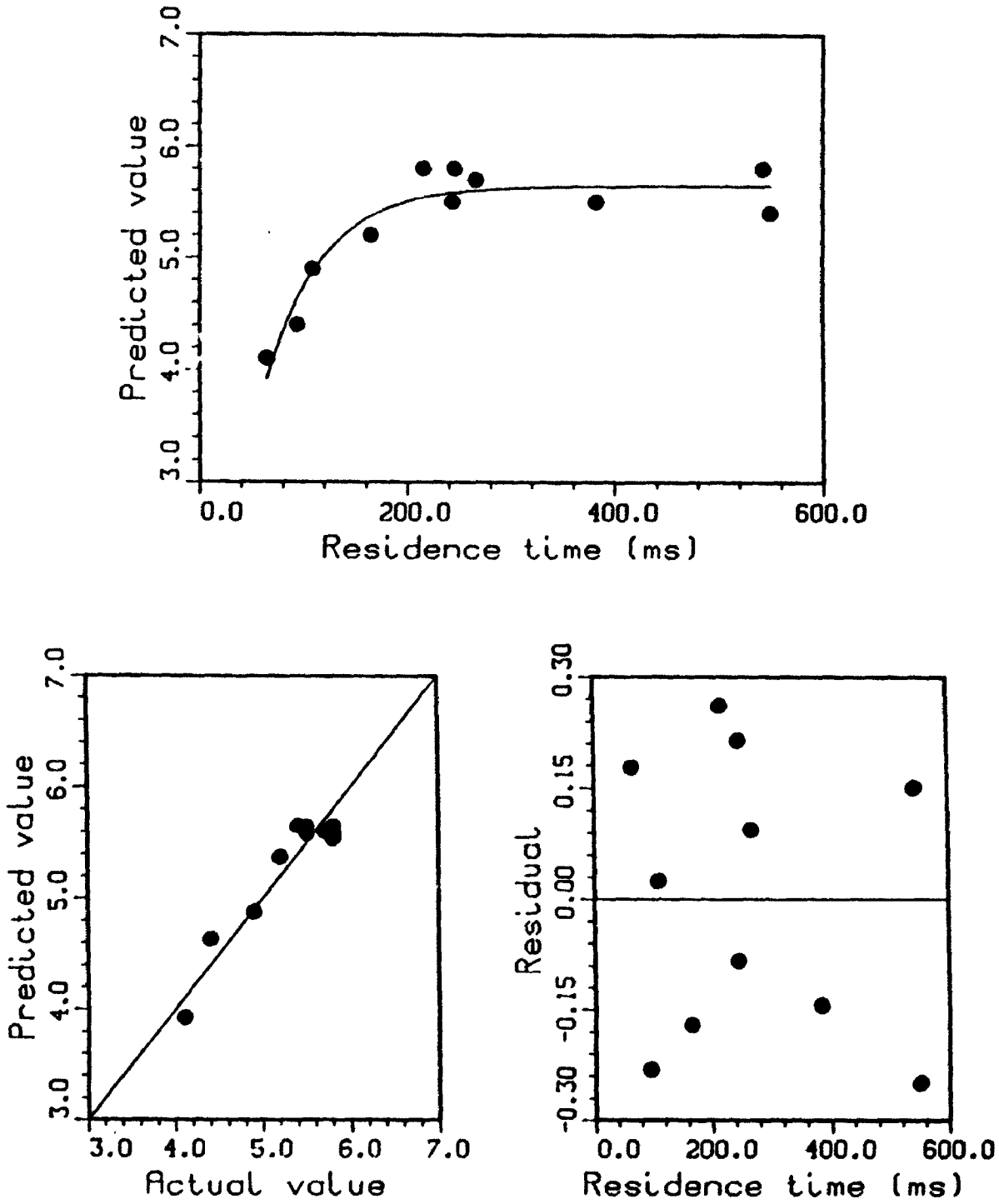

Figure A7.1.13. Zero-Intercept Kinetic Model For CO_2 from Cellulose: Fast Pyrolysis at 825 °C (Run Numbers and Data in Table 14)

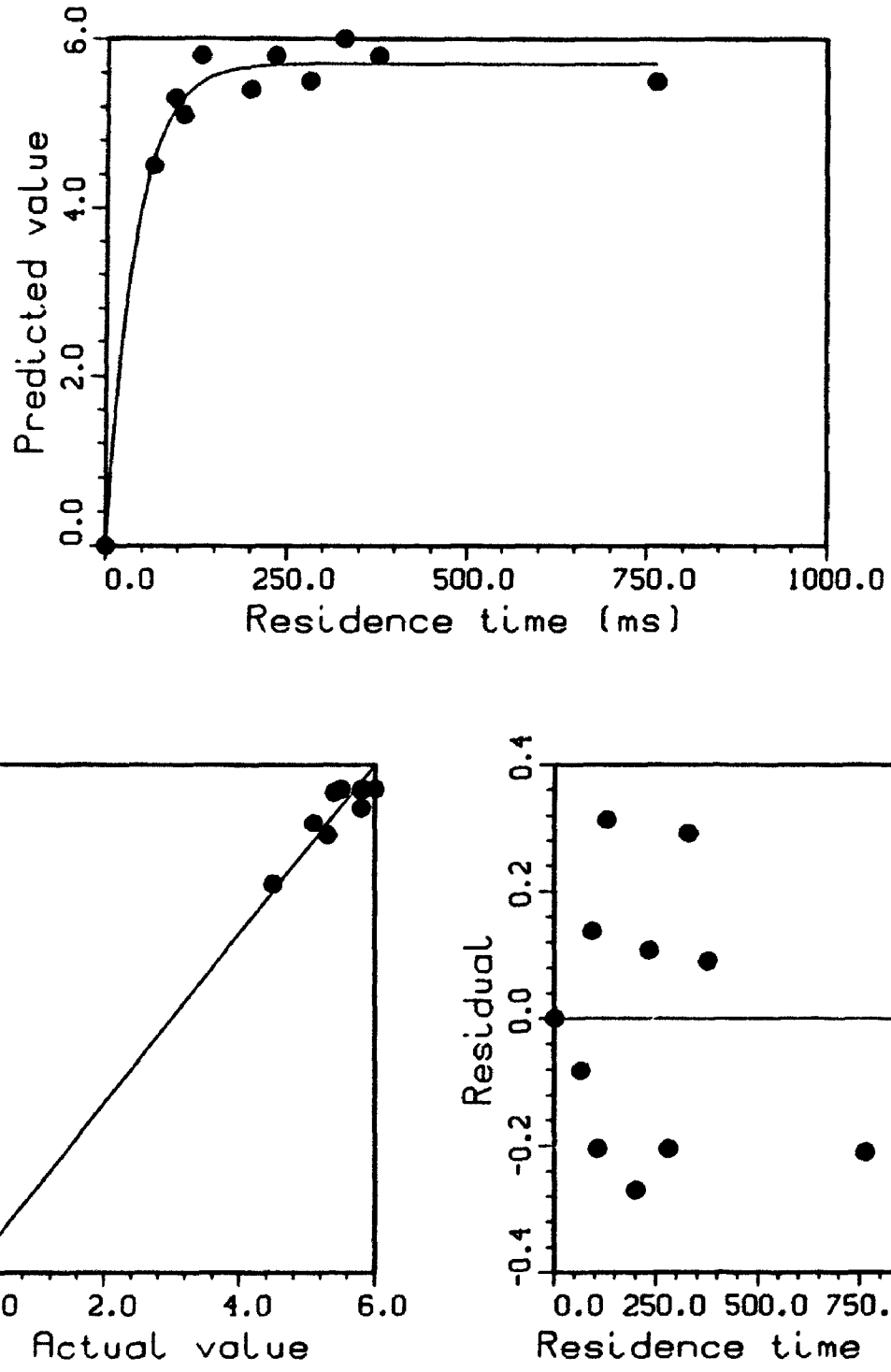

Figure A7.1.14. Zero-Intercept Kinetic Model For CO_2 from Cellulose: Fast Pyrolysis at 850 °C (Run Numbers and Data in Table 15)

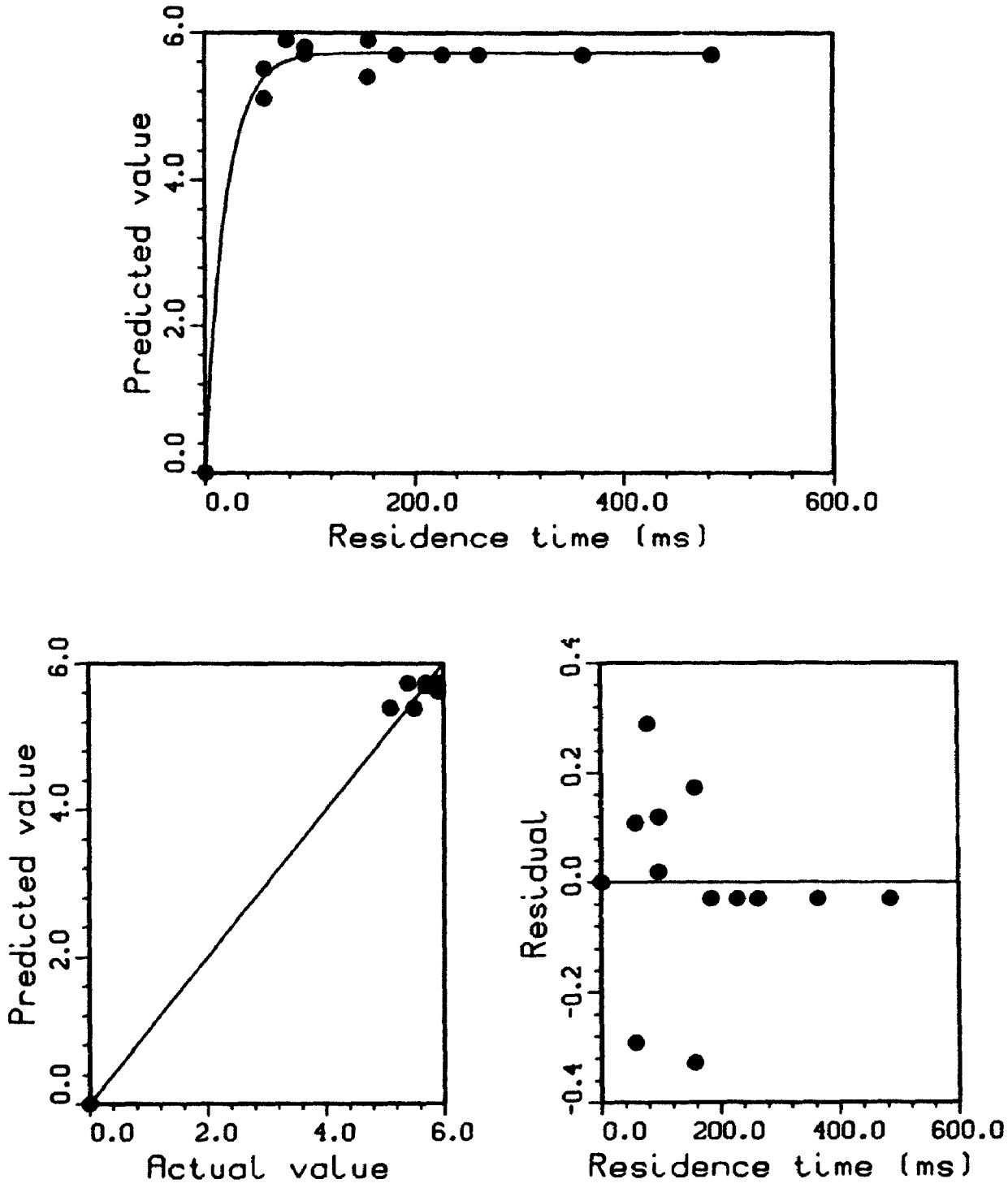

Figure A7.1.15. Zero-Intercept Kinetic Model For CO_2 from Cellulose: Fast Pyrolysis at 875 °C (Run Numbers and Data in Table 16)

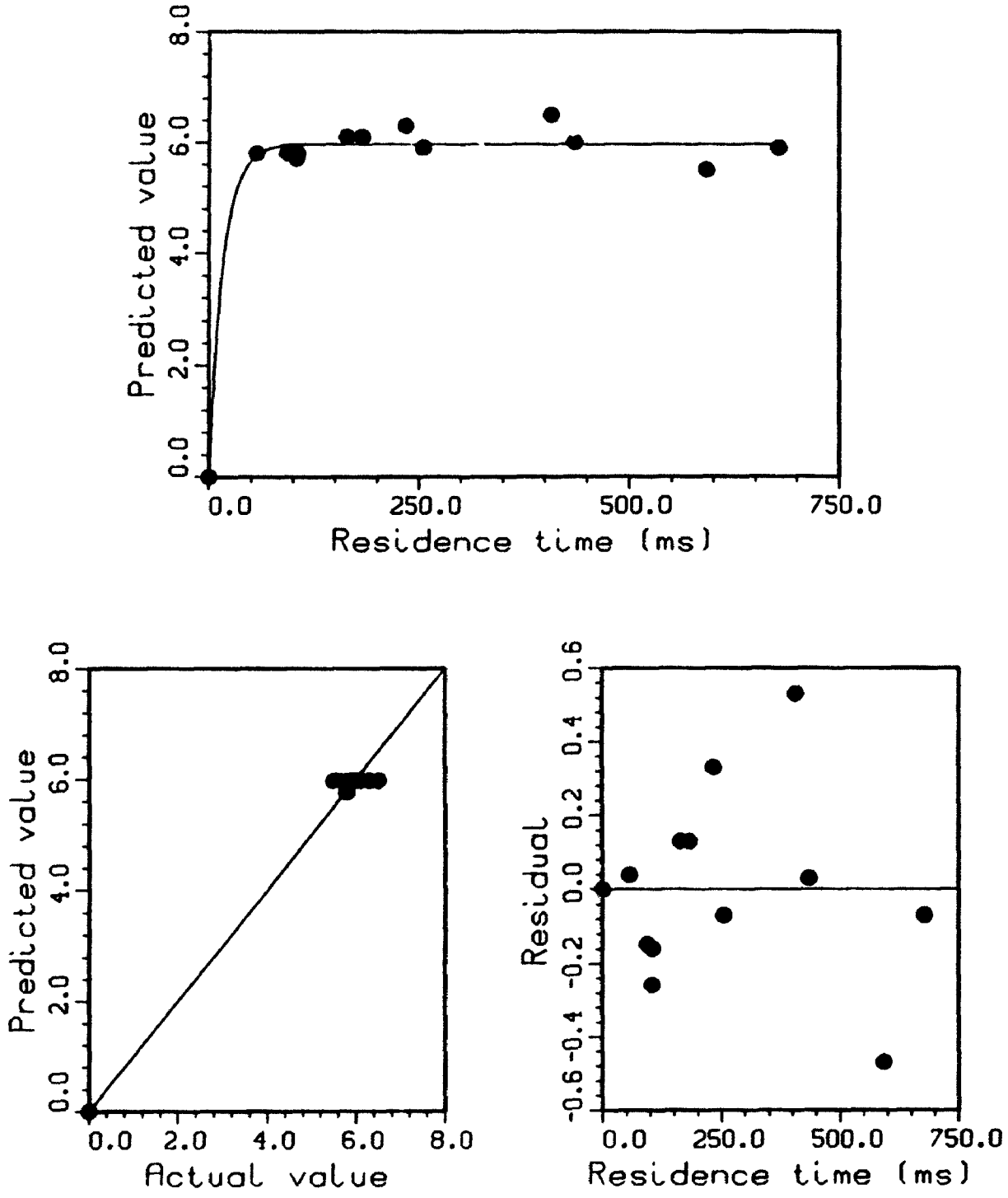

Figure A7.1.16. Zero-Intercept Kinetic Model For CO_2 from Cellulose: Fast Pyrolysis at 900 °C (Run Numbers and Data in Table 17)

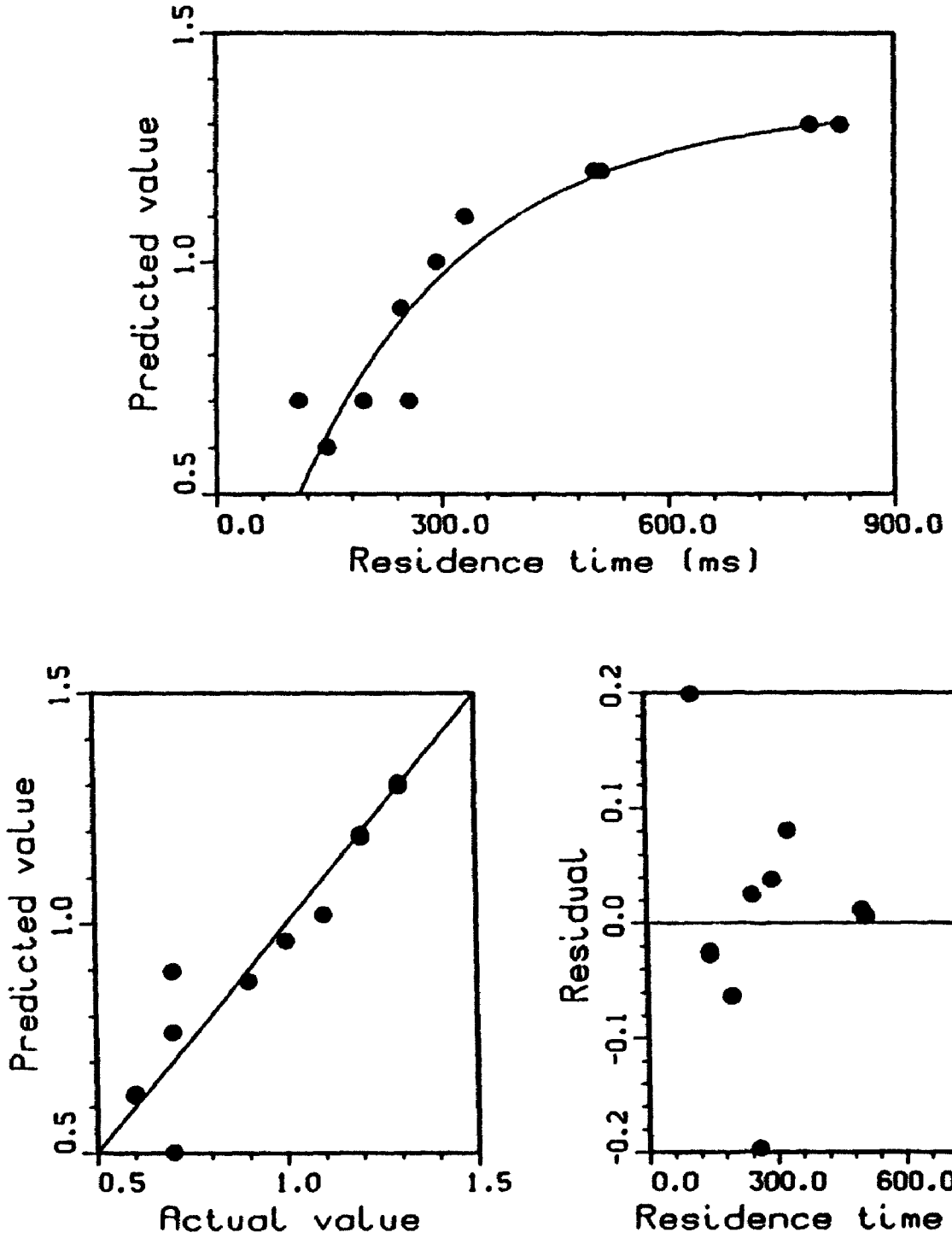

Figure A7.1.17. Zero-Intercept Kinetic Model For C_2H_4 from Cellulose: Fast Pyrolysis at 650 °C (Run Numbers and Data in Table 10)

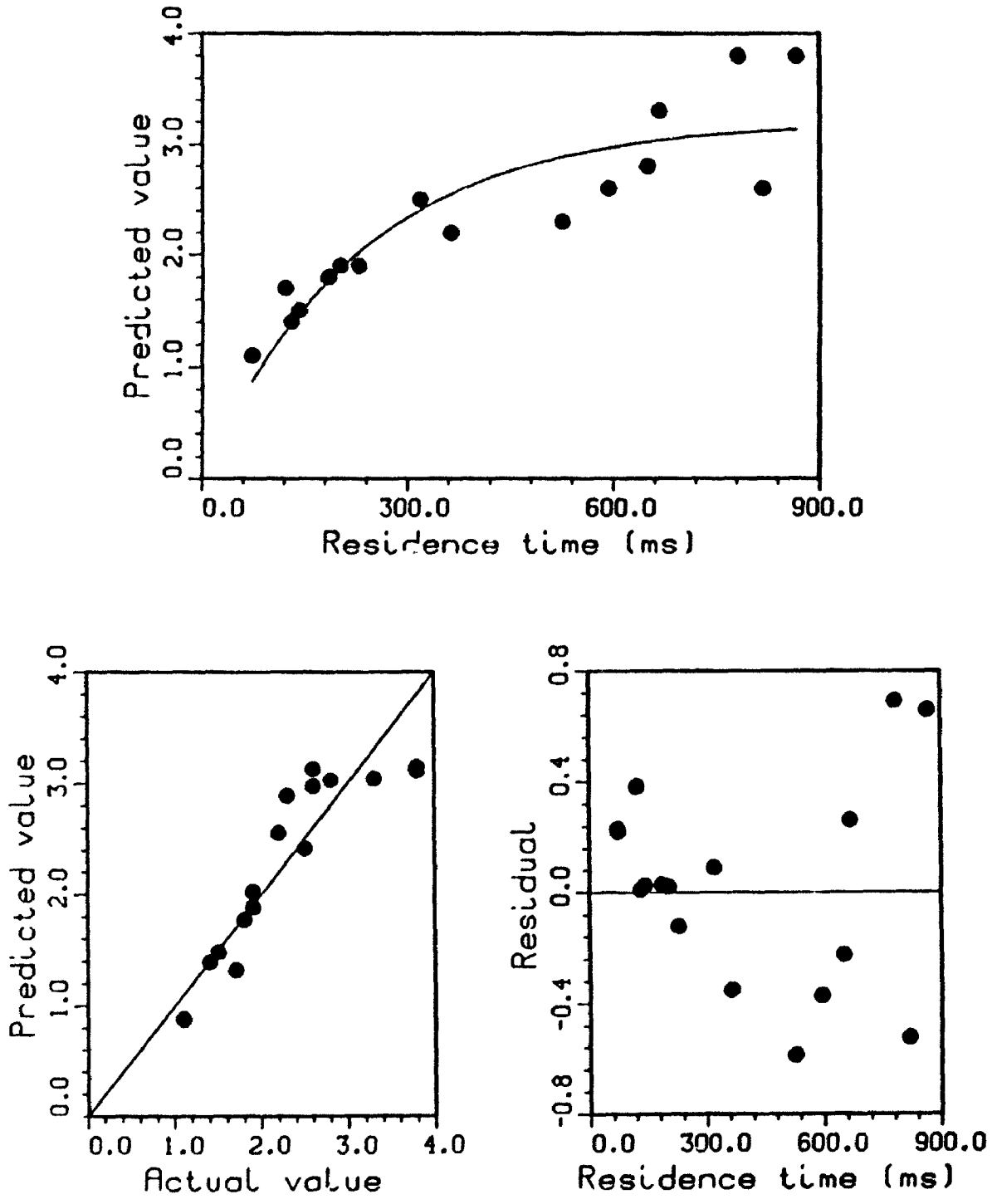

Figure A7.1.18. Zero-Intercept Kinetic Model For C_2H_4 from Cellulose: Fast Pyrolysis at 700 °C (Run Numbers and Data in Table 11)

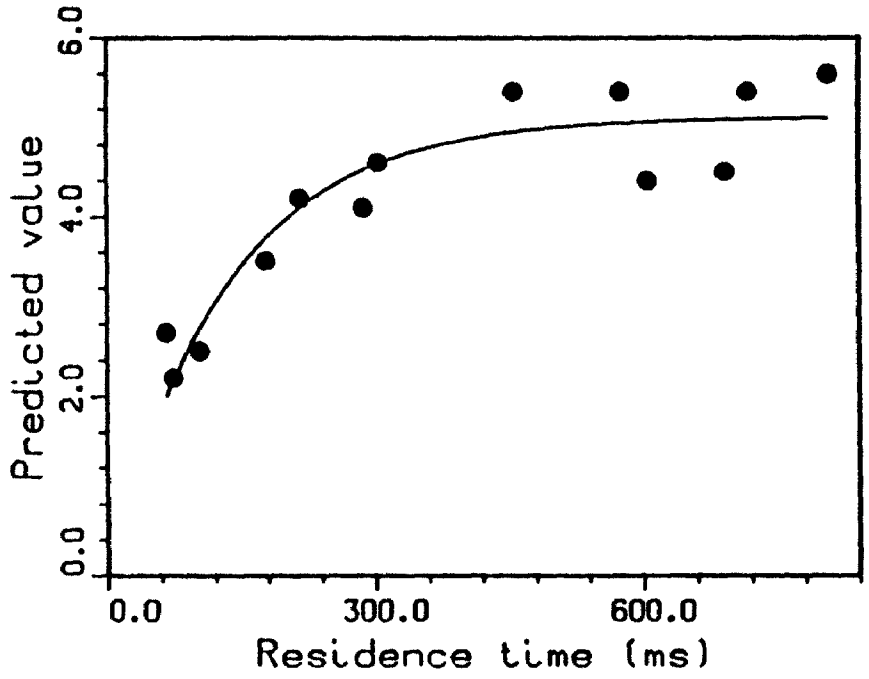

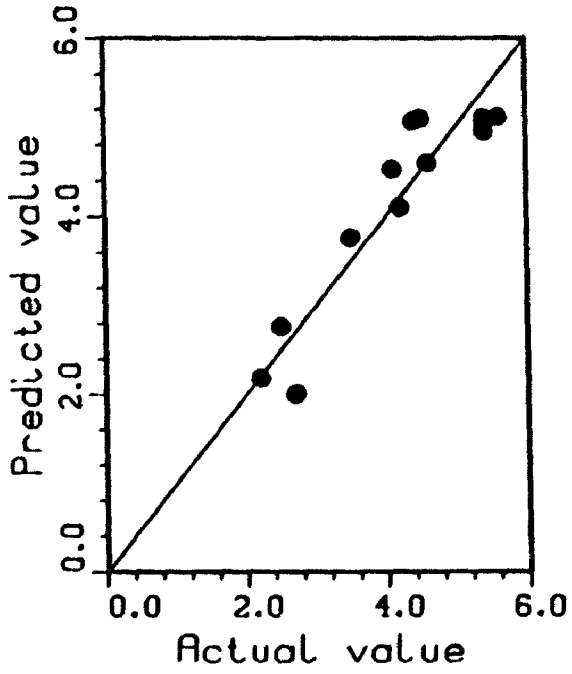

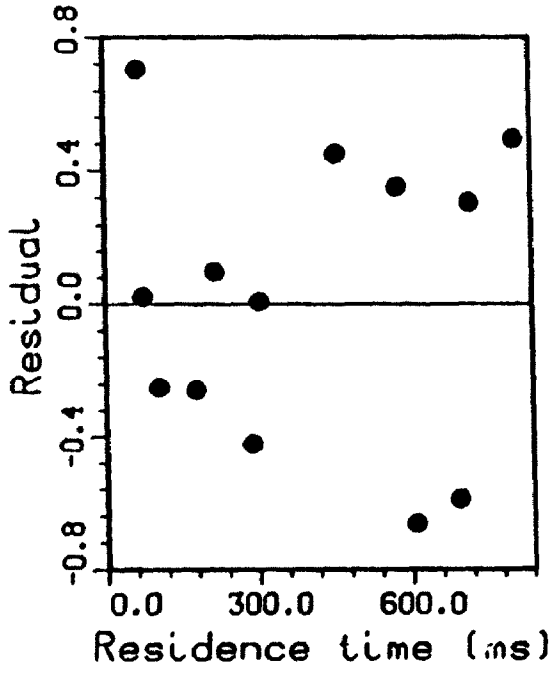

Figure A7.1.19. Zero-Intercept Kinetic Model For C_2H_4 from Cellulose: Fast Pyrolysis at 750 °C (Run Numbers and Data in Table 12)

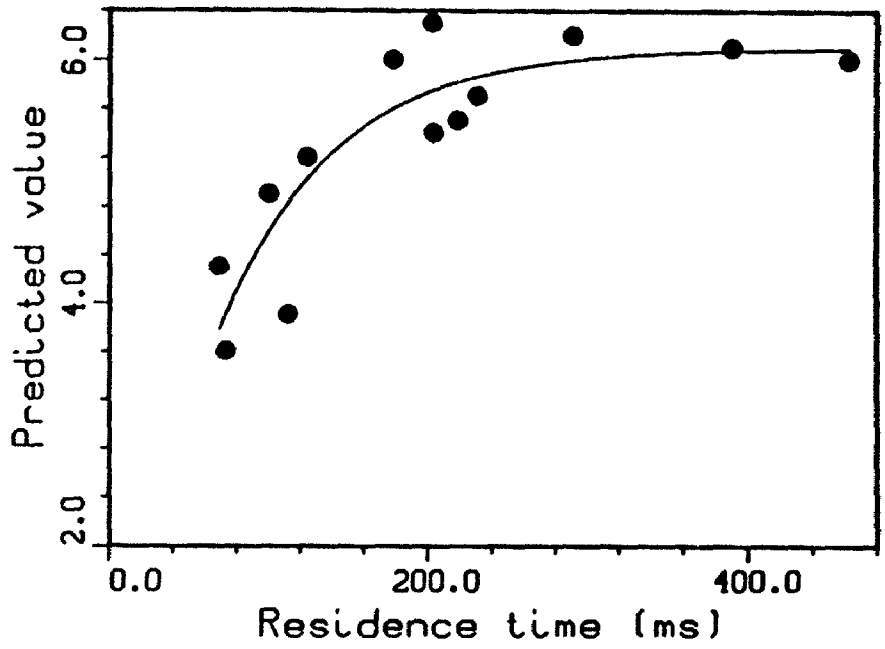

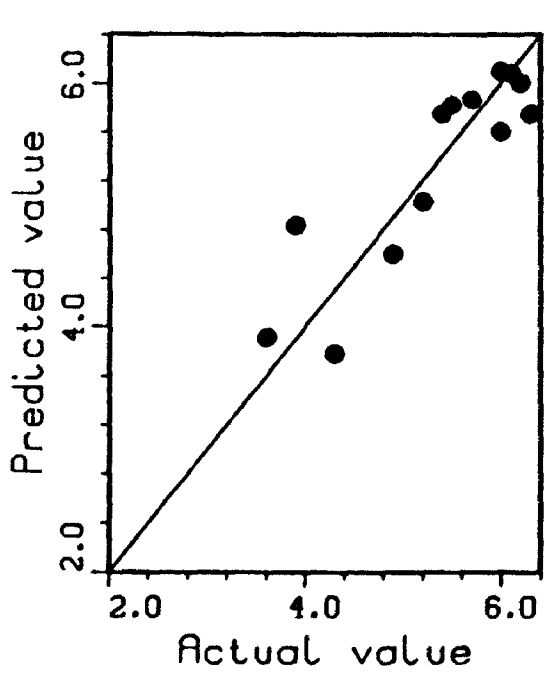

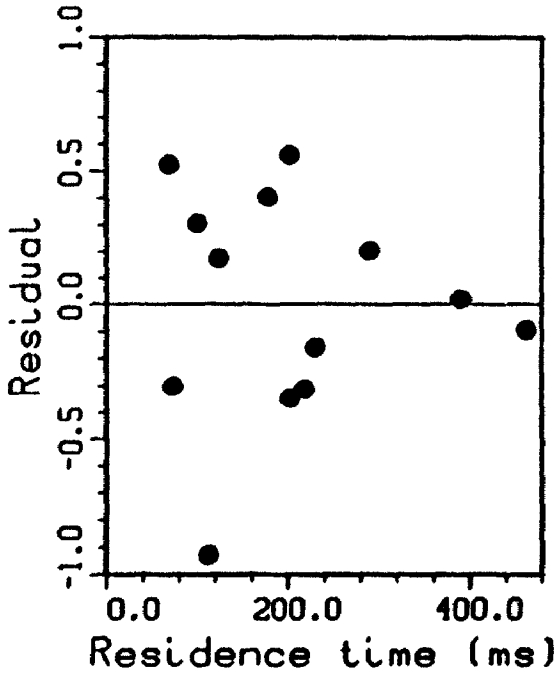

Figure A7.1.20. Zero-Intercept Kinetic Model For C_2H_4 from Cellulose: Fast Pyrolysis at 800 °C (Run Numbers and Data in Table 13)

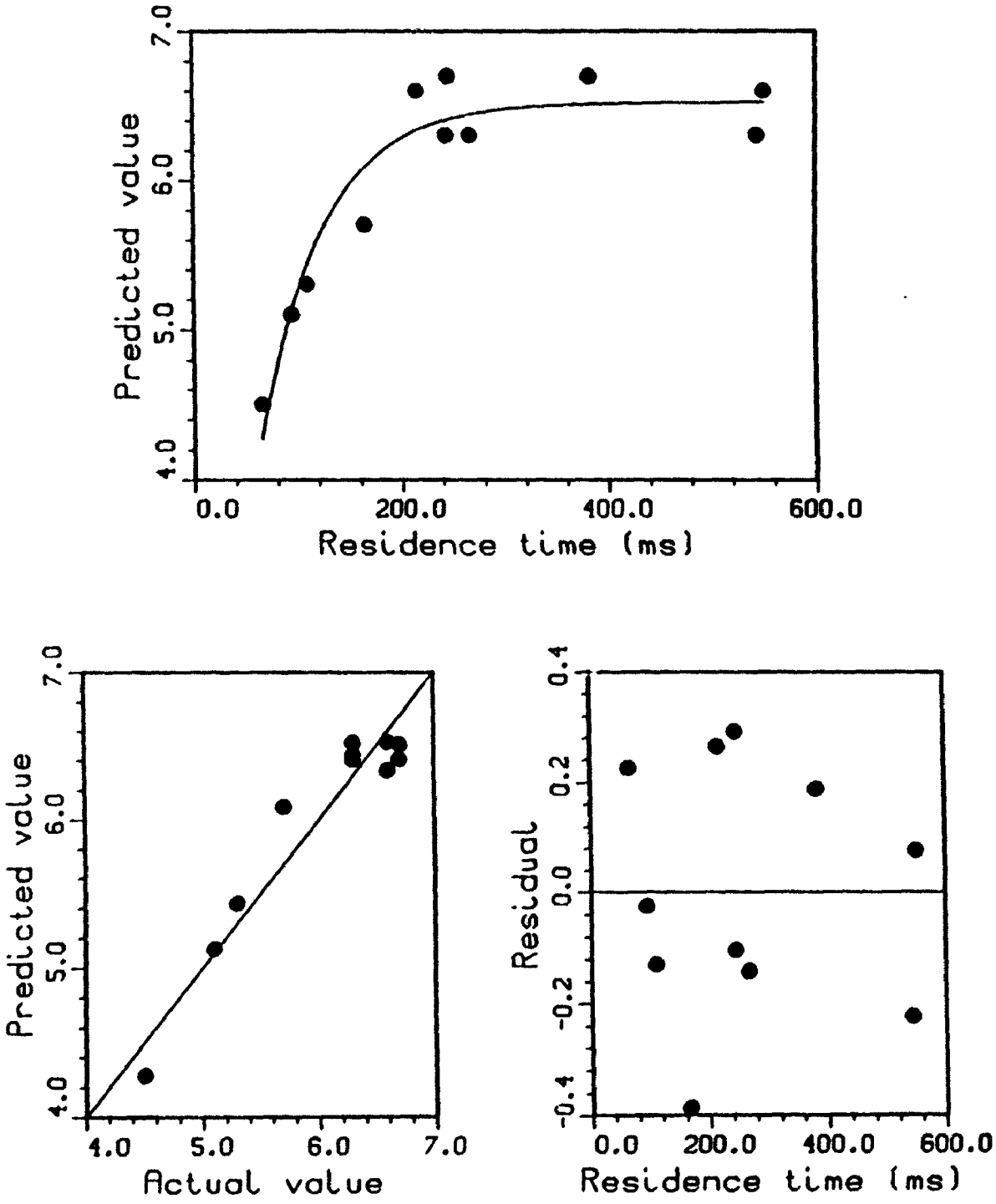

Figure A7.1.21. Zero-Intercept Kinetic Model For C_2H_4 from Cellulose: Fast Pyrolysis at 825 °C (Run Numbers and Data in Table 14)

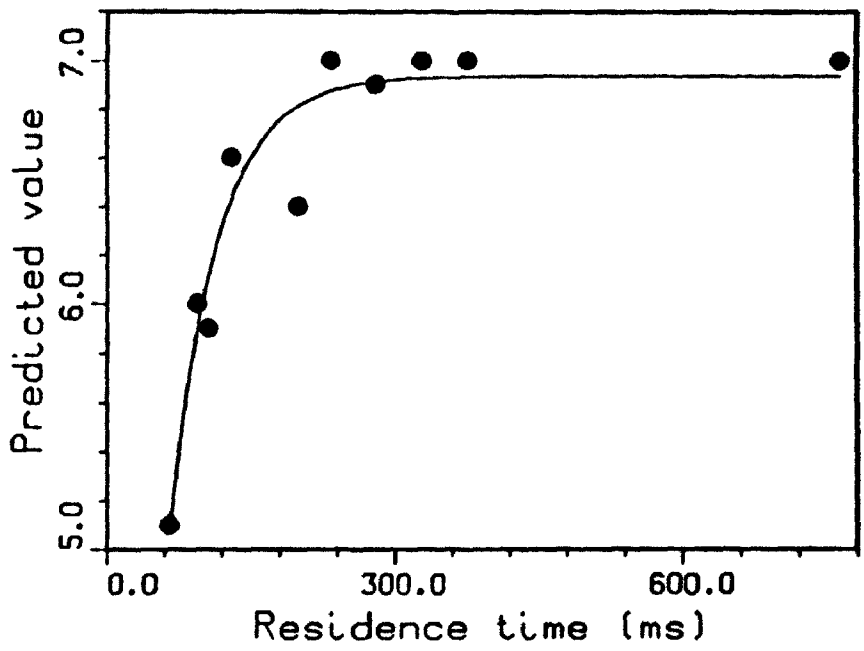

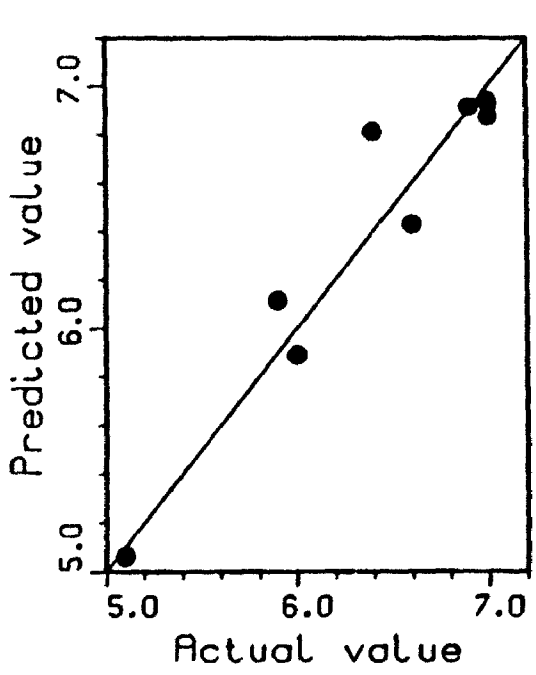

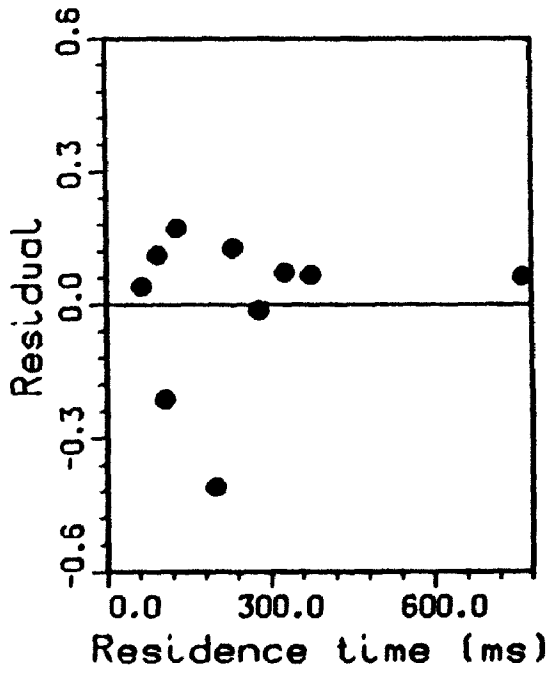

Figure A7.1.22. Zero-Intercept Kinetic Model For C_2H_4 from Cellulose: Fast Pyrolysis at 850 °C (Run Numbers and Data in Table 15)

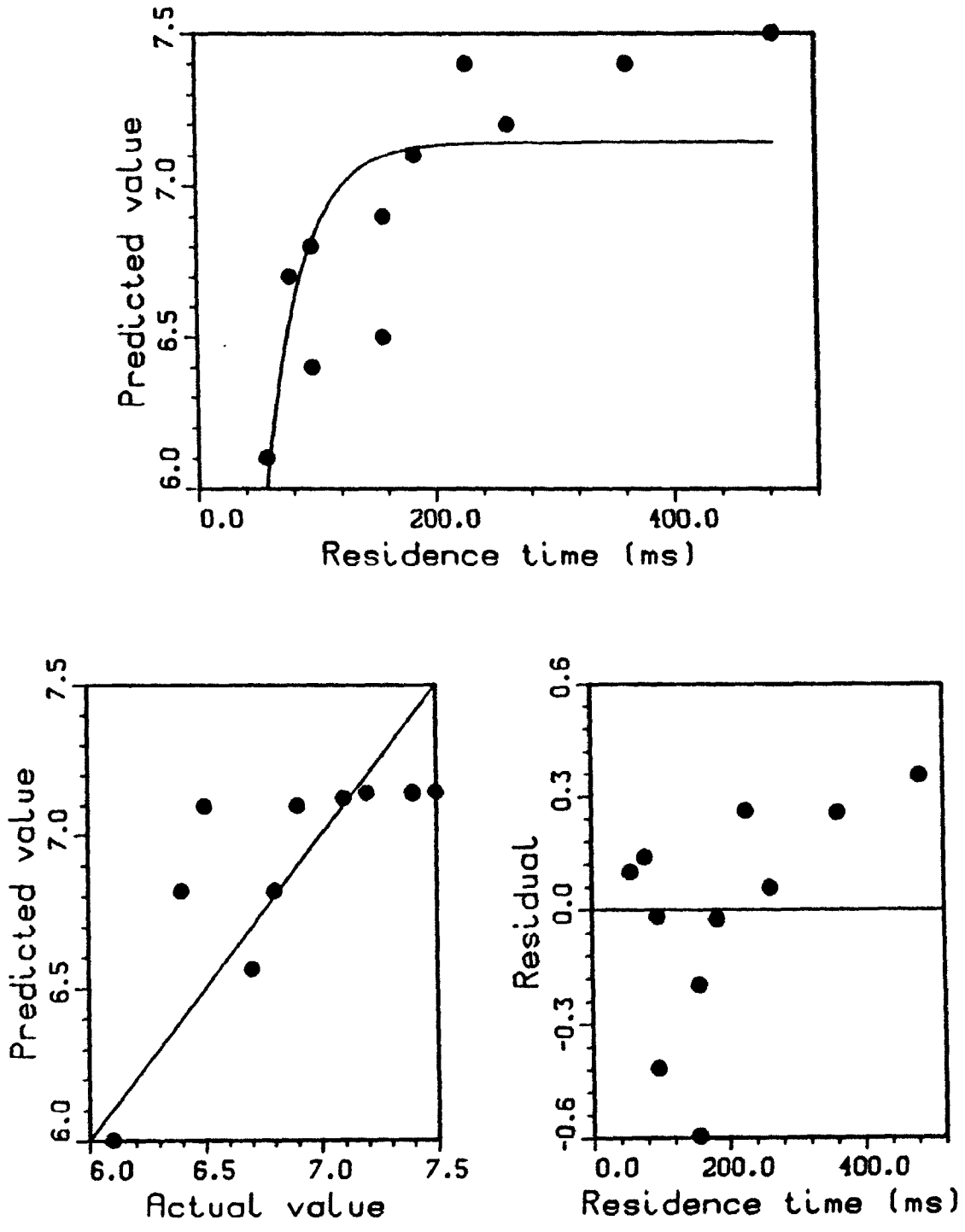

Figure A7.1.23. Zero-Intercept Kinetic Model For C_2H_4 from Cellulose: Fast Pyrolysis at 875 °C (Run Numbers and Data in Table 16)

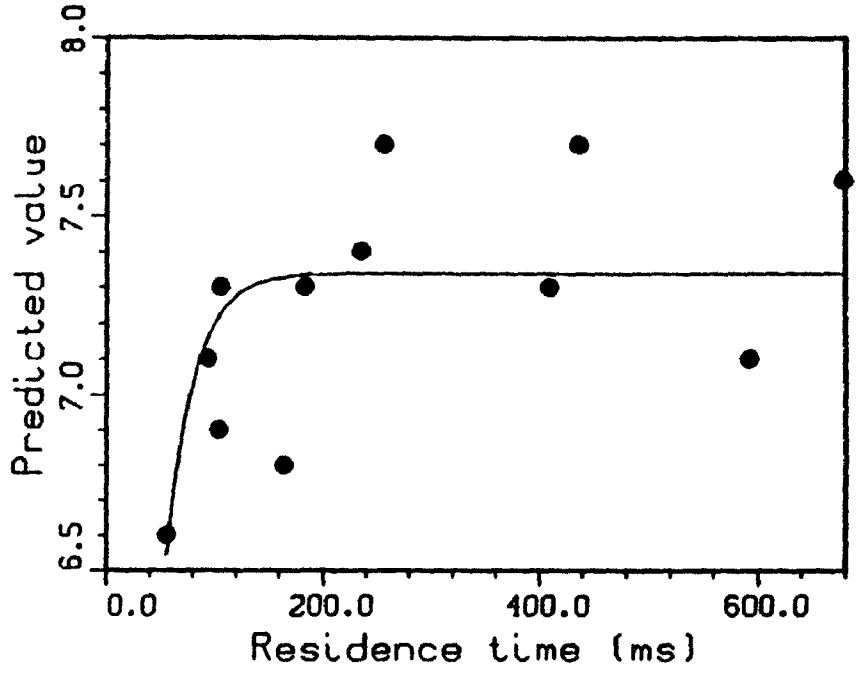

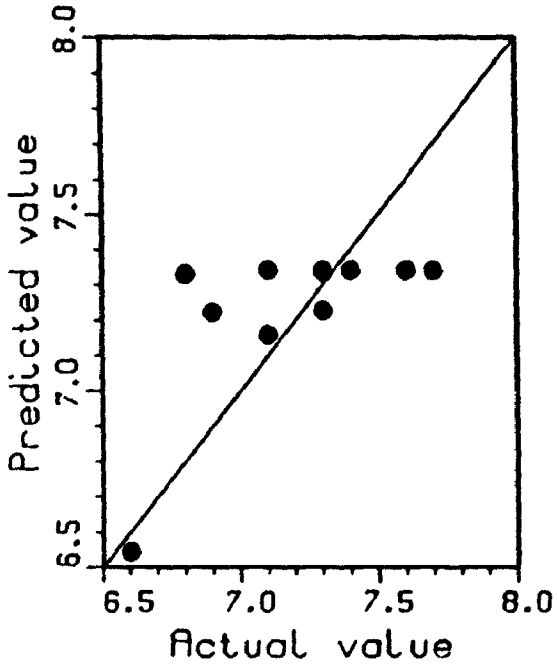

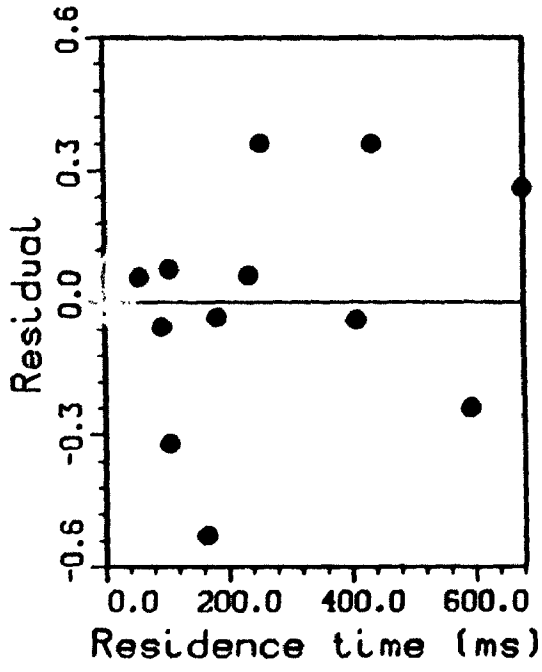

Figure A7.1.24. Zero-Intercept Kinetic Model For C_2H_4 from Cellulose: Fast Pyrolysis at 900 °C (Run Numbers and Data in Table 17)

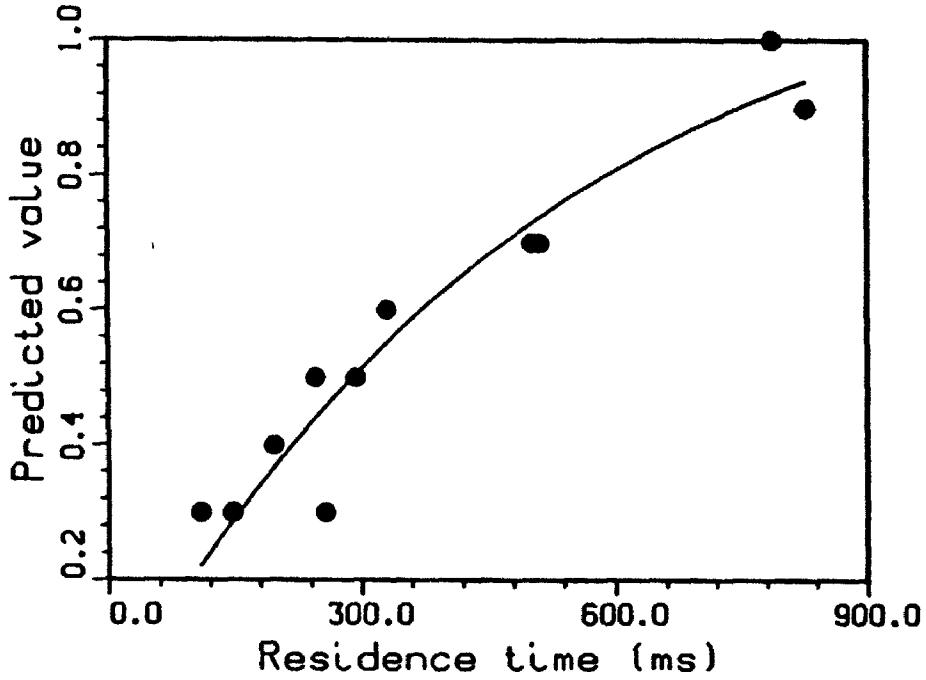

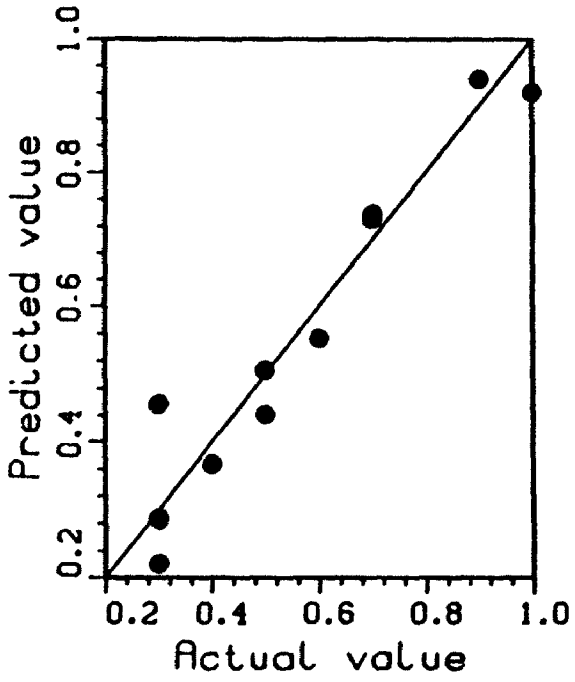

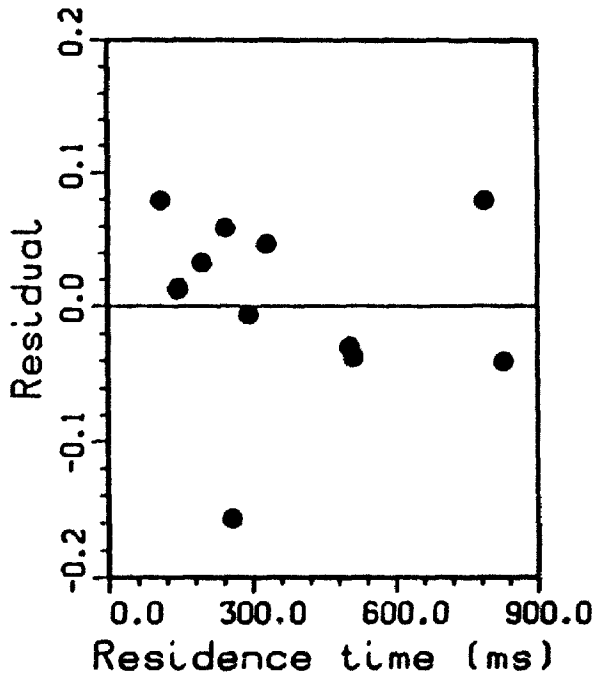

Figure A7.1.25. Zero-Intercept Kinetic Model For CH_4 from Cellulose: Fast Pyrolysis at 650 °C (Run Numbers and Data in Table 10)

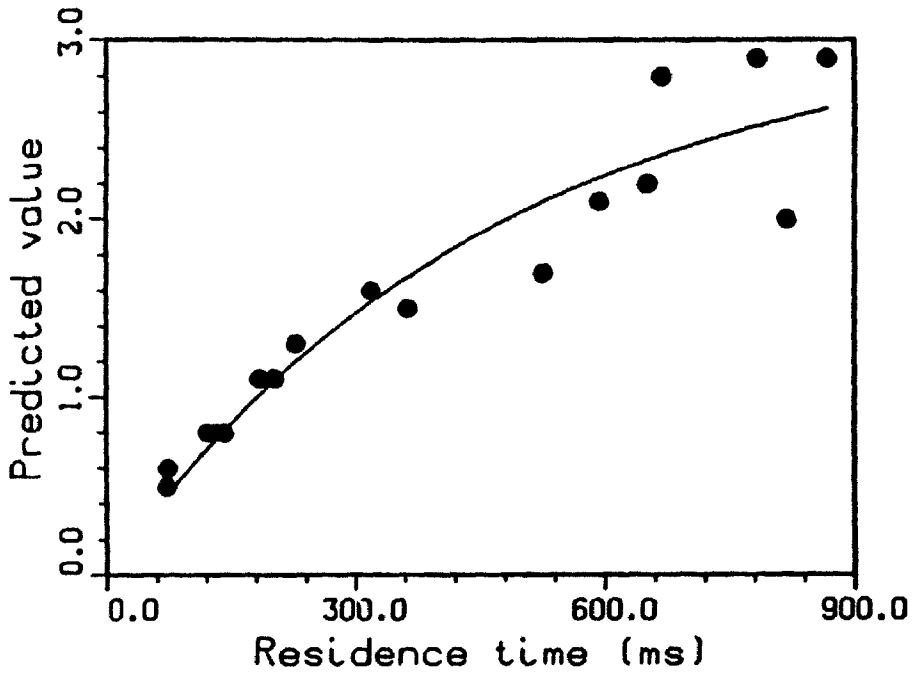

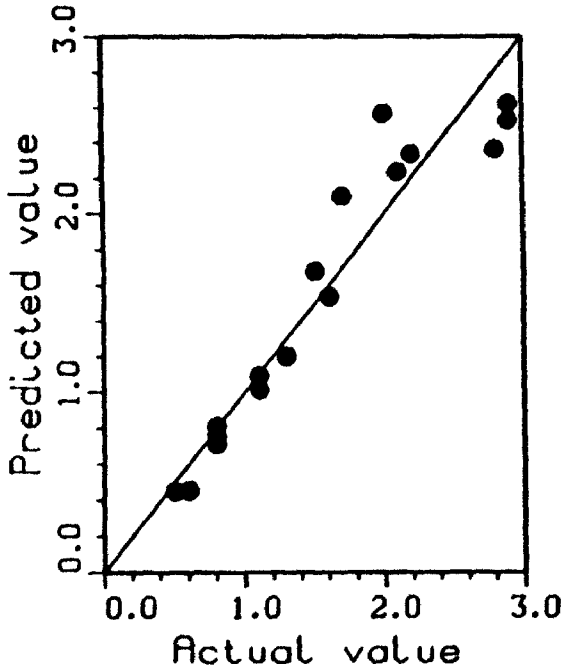

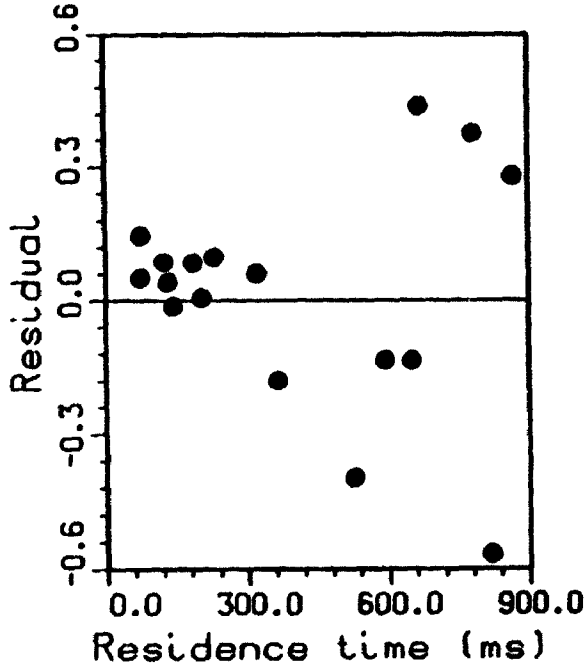

Figure A7.1.26. Zero-Intercept Kinetic Model For CH_4 from Cellulose: Fast Pyrolysis at 700 °C (Run Numbers and Data in Table 11)

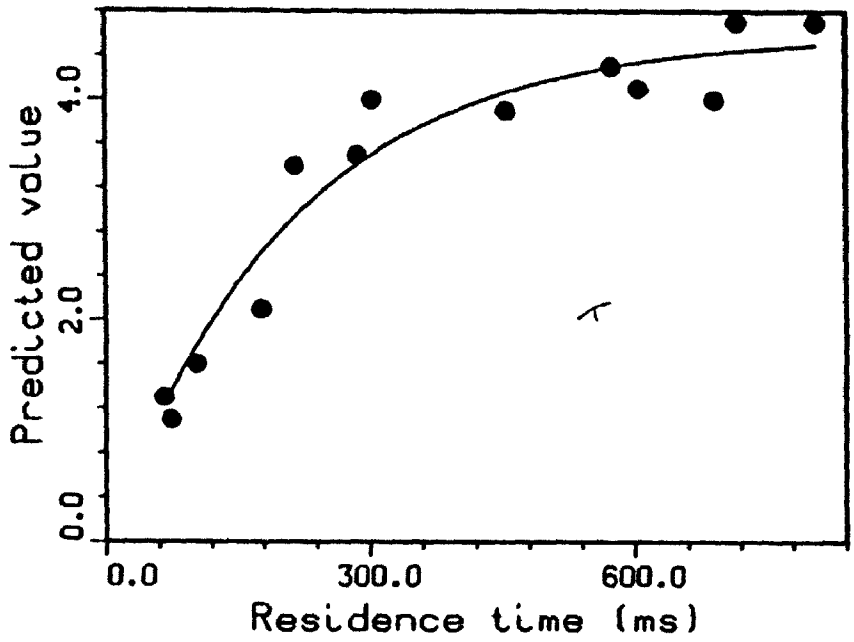

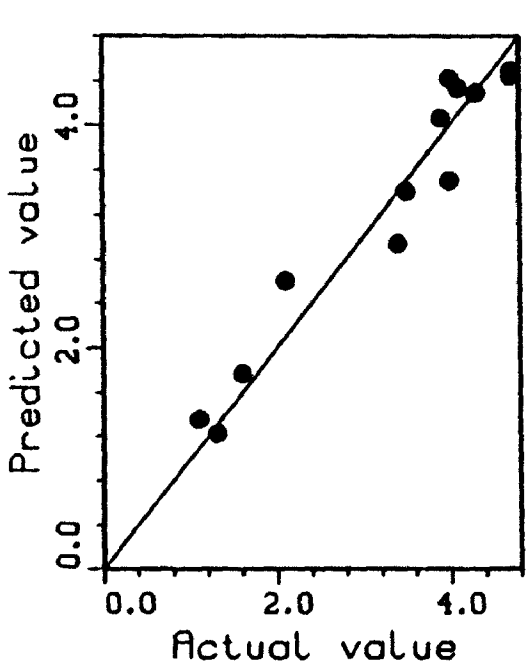

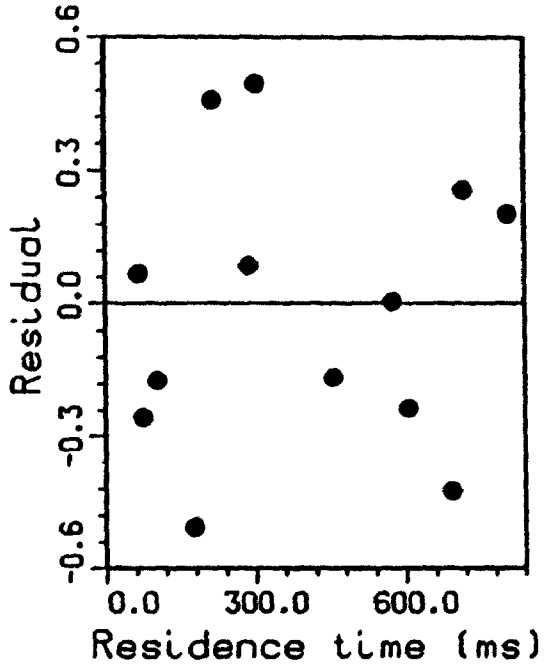

Figure A7.1.27. Zero-Intercept Kinetic Model For CH_4 from Cellulose: Fast Pyrolysis at 750 °C (Run Numbers and Data in Table 12)

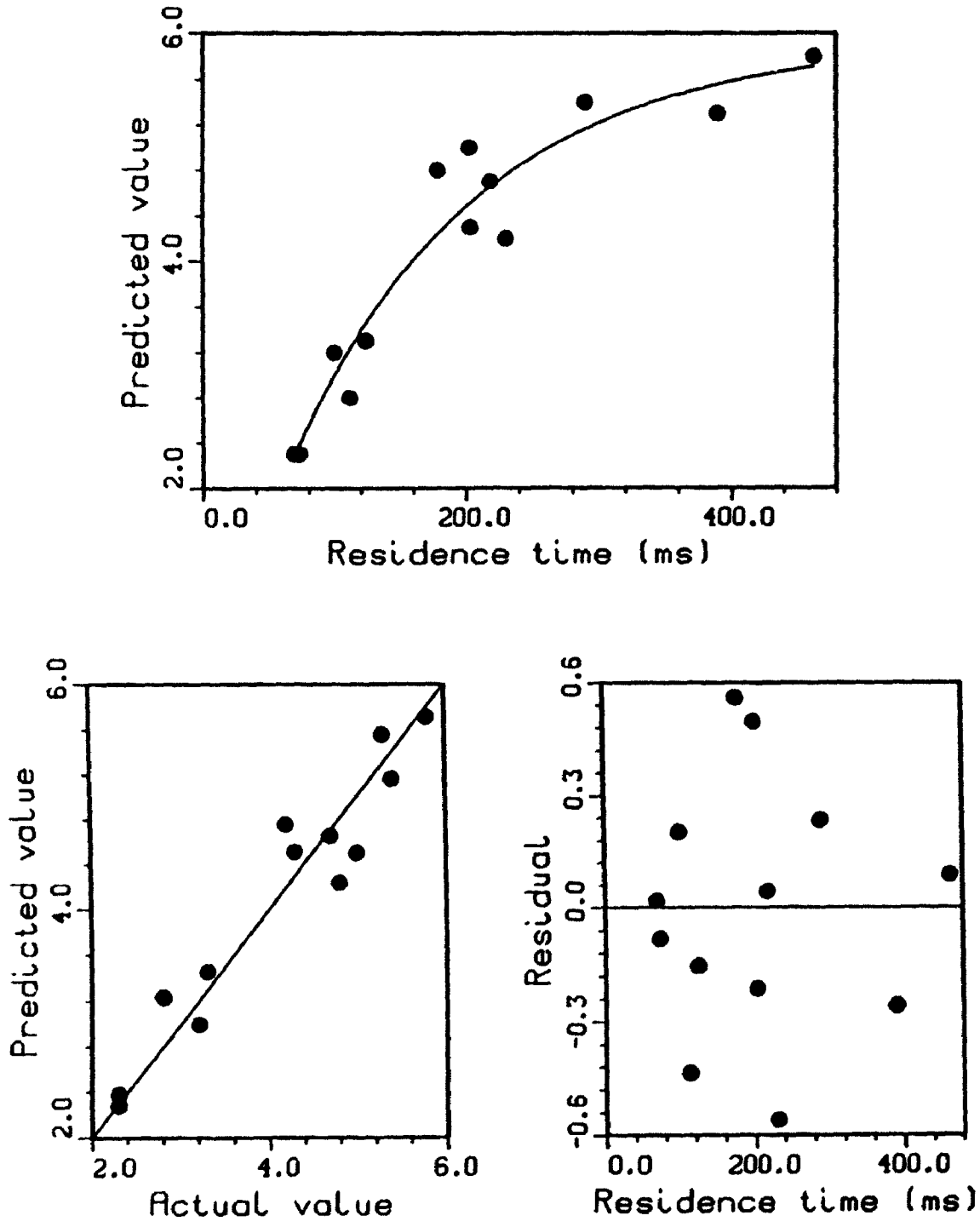

Figure A7.1.28. Zero-Intercept Kinetic Model For CH_4 from Cellulose: Fast Pyrolysis at 800 °C (Run Numbers and Data in Table 13)

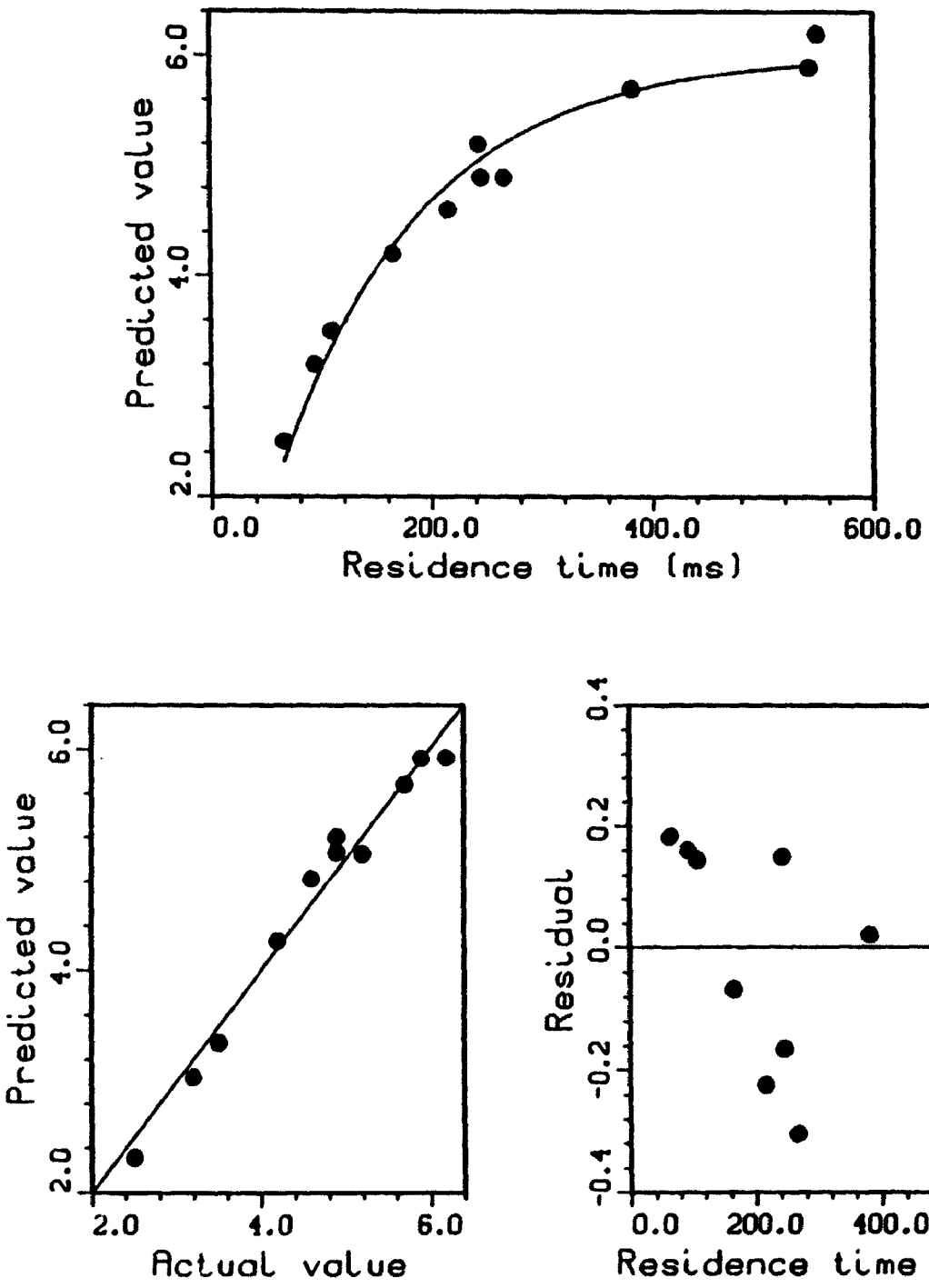

Figure A7.1.29. Zero-Intercept Kinetic Model For CH_4 from Cellulose: Fast Pyrolysis at 825 °C (Run Numbers and Data in Table 14)

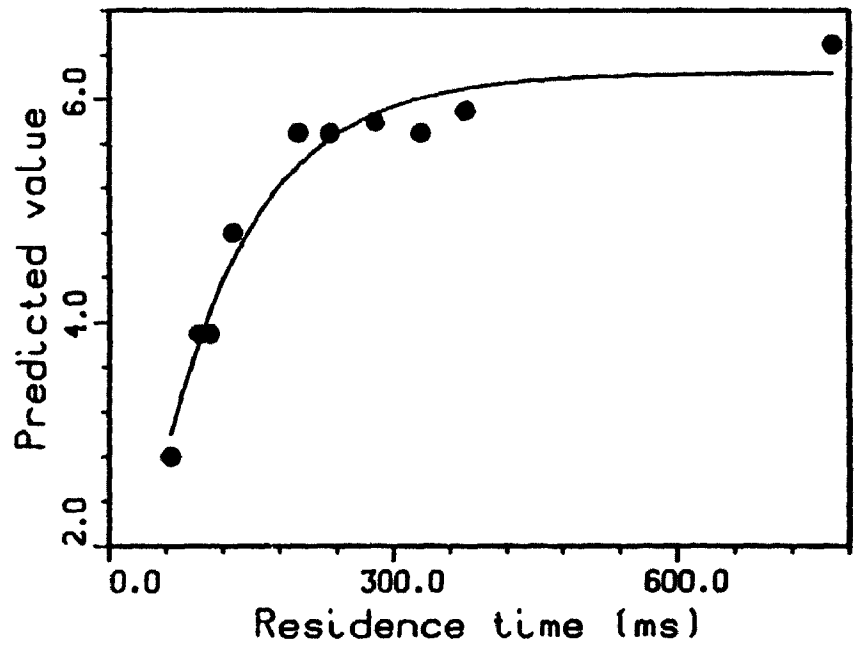

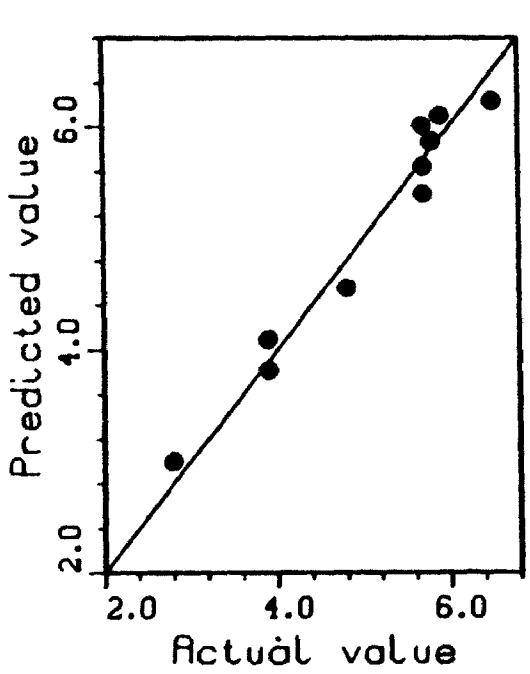

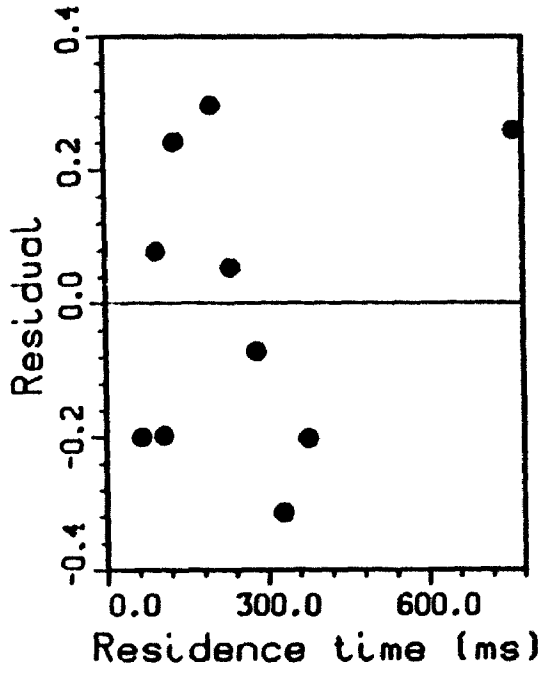

Figure A7.1.30. Zero-Intercept Kinetic Model For CH_4 from Cellulose: Fast Pyrolysis at 850 °C (Run Numbers and Data in Table 15)

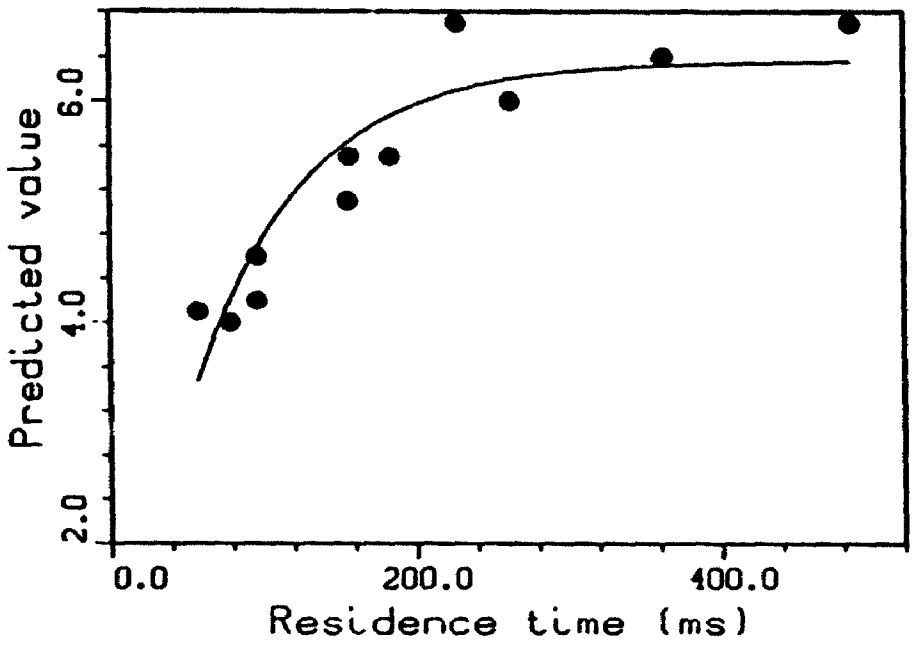

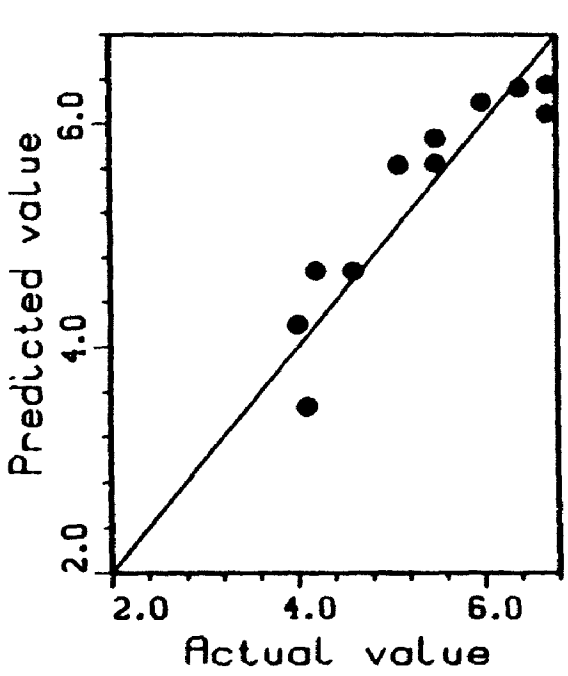

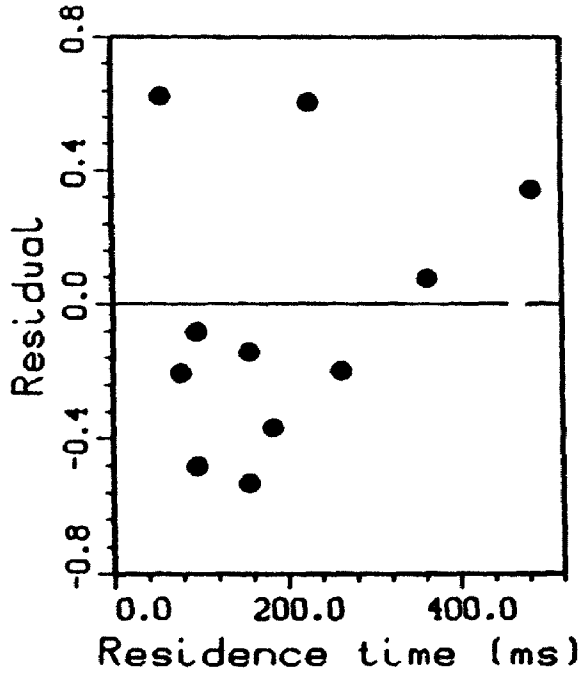

Figure A7.1.31. Zero-Intercept Kinetic Model For CH_4 from Cellulose: Fast Pyrolysis at 875 °C (Run Numbers and Data in Table 16)

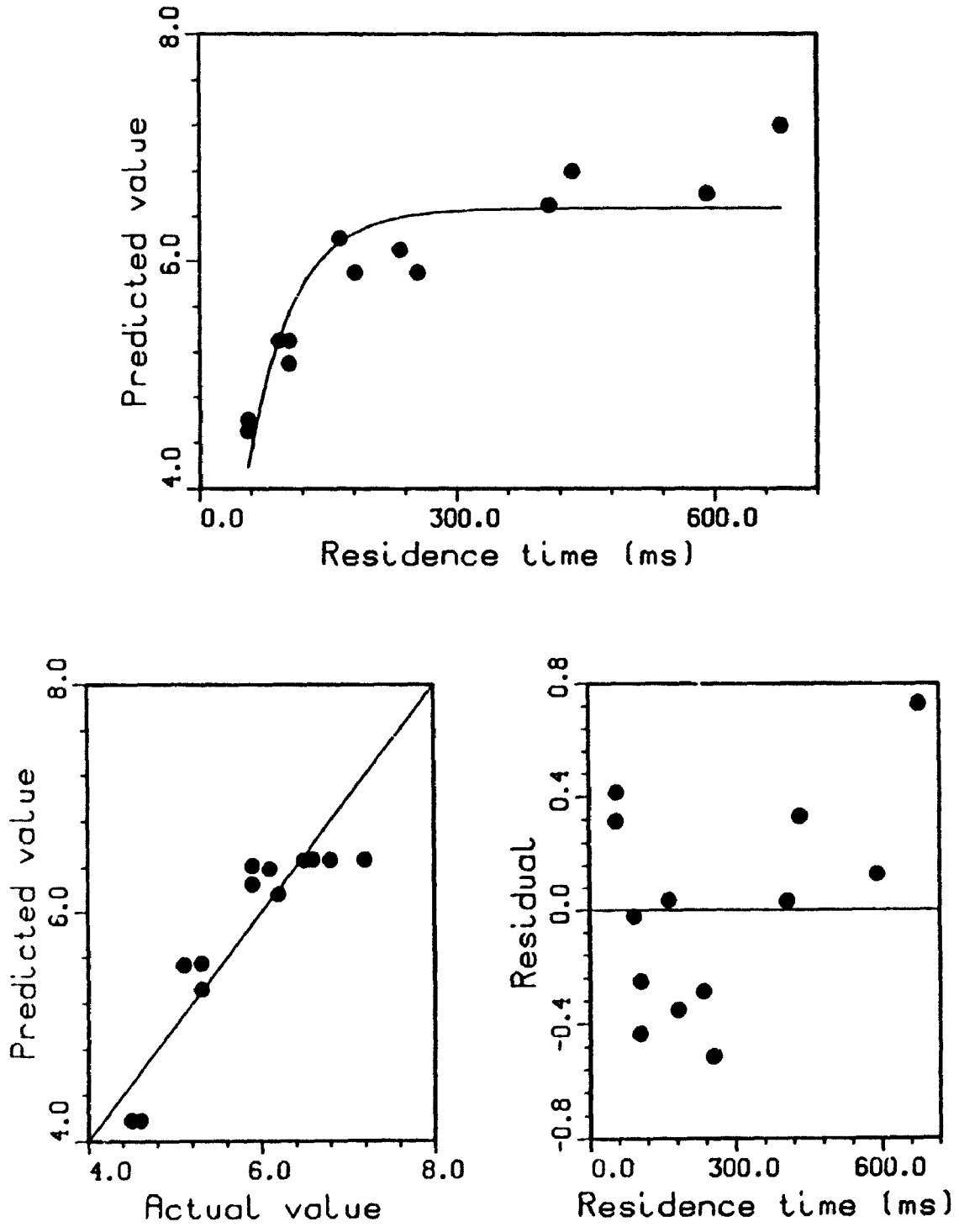

Figure A7.1.32. Zero-Intercept Kinetic Model For CH_4 from Cellulose: Fast Pyrolysis at 900 °C (Run Numbers and Data in Table 17)

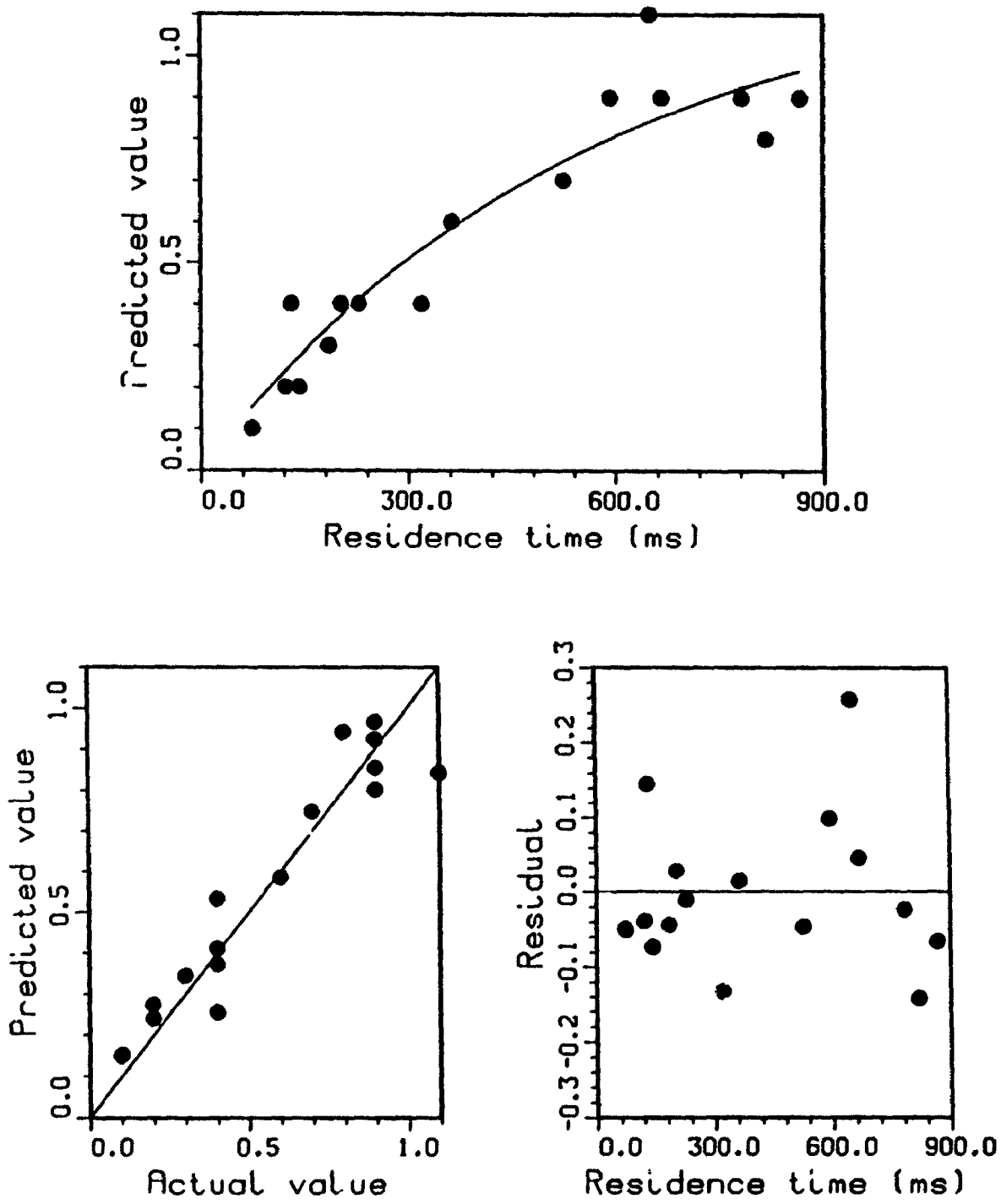

Figure A7.1.33. Zero-Intercept Kinetic Model For H_2 from Cellulose: Fast Pyrolysis at 700 °C (Run Numbers and Data in Table 11)

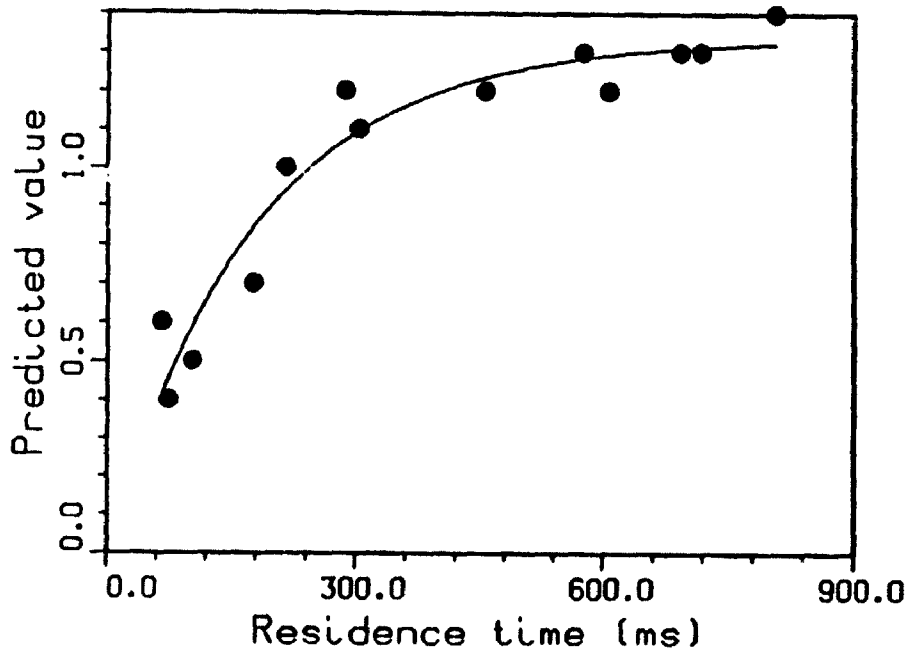

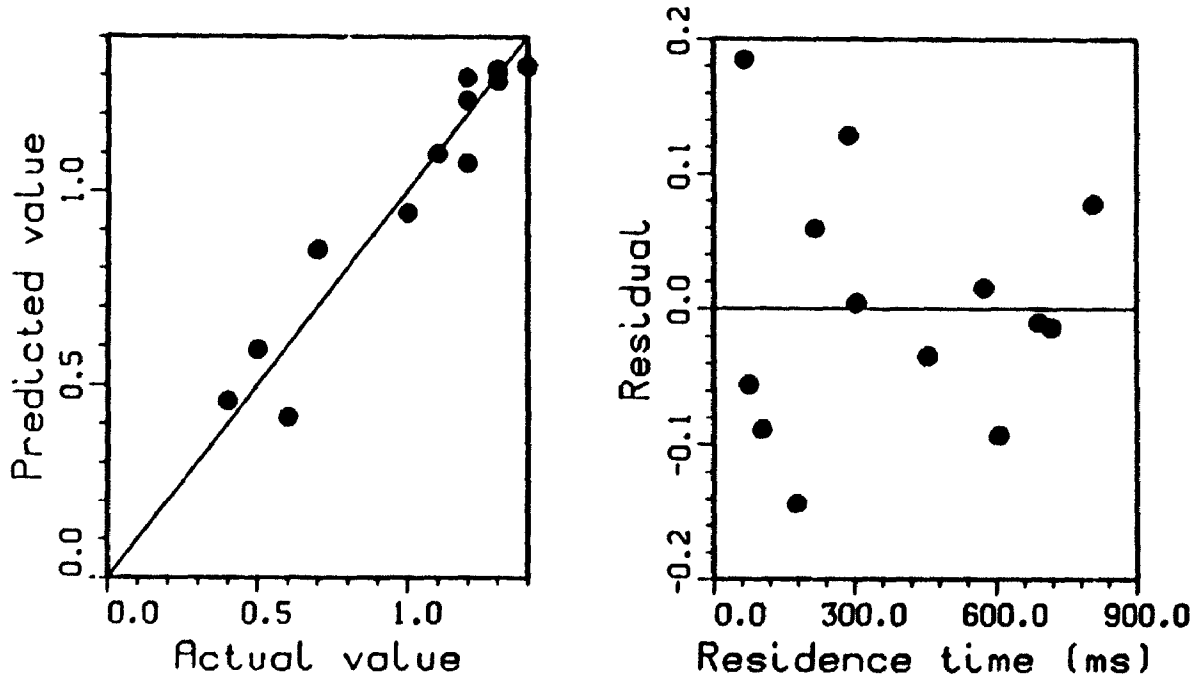

Figure A7.1.34. Zero-Intercept Kinetic Model For H_2 from Cellulose: Fast Pyrolysis at 750 °C (Run Numbers and Data in Table 12)

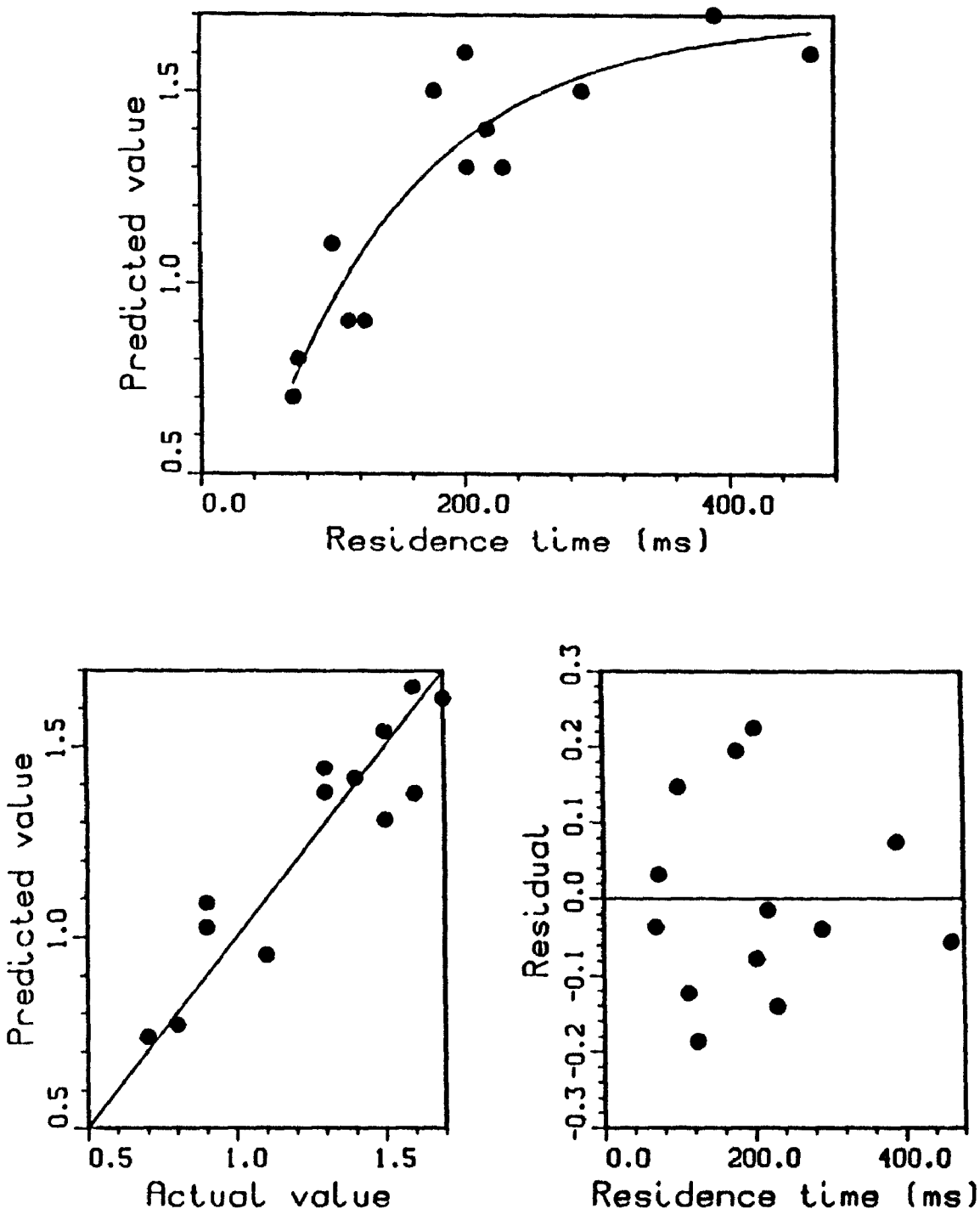

Figure A7.1.35. Zero-Intercept Kinetic Model For H_2 from Cellulose: Fast Pyrolysis at 800 °C (Run Numbers and Data in Table 13)

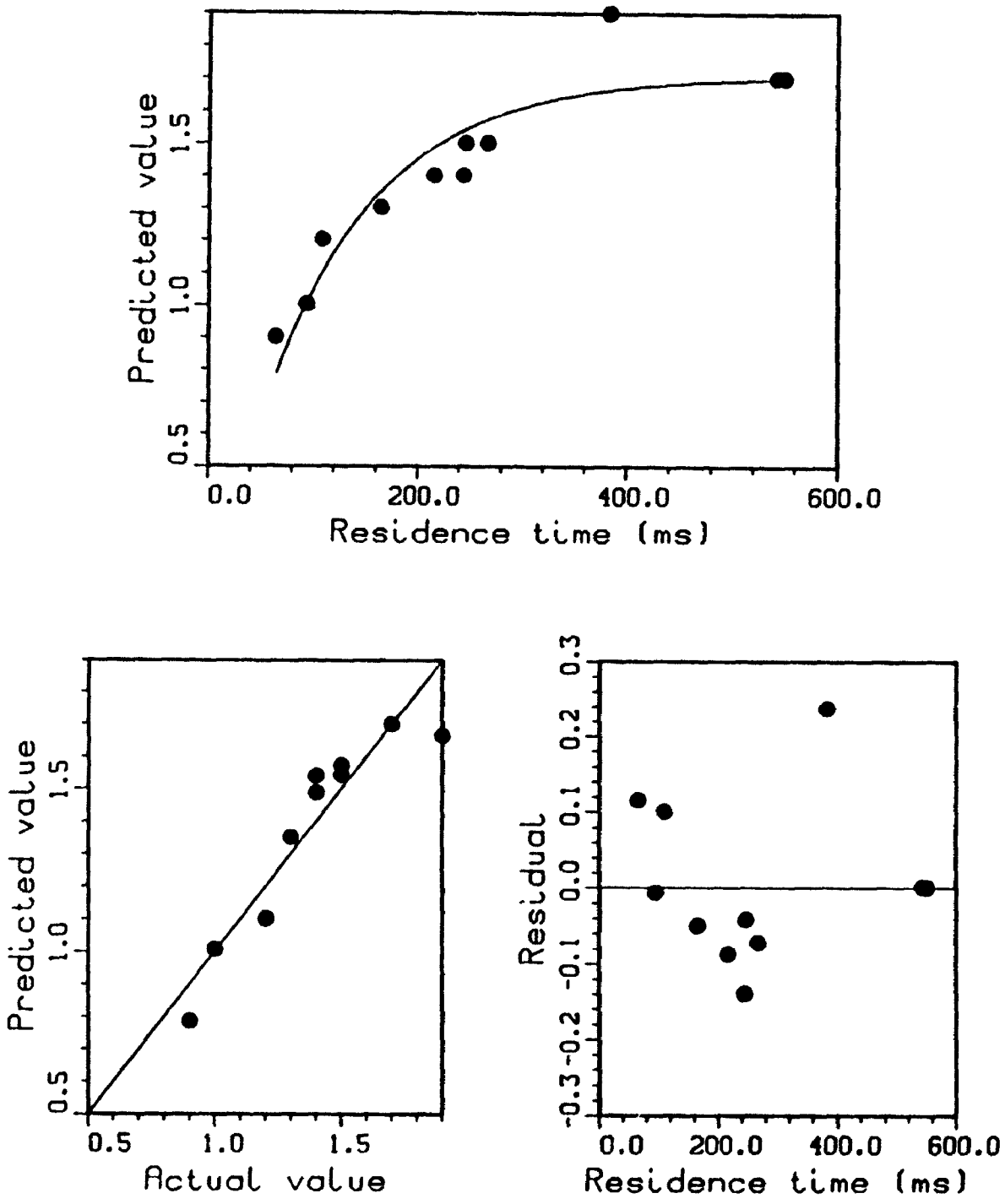

Figure A7.1.36. Zero-Intercept Kinetic Model For H_2 from Cellulose: Fast Pyrolysis at 825 °C (Run Numbers and Data in Table 14)

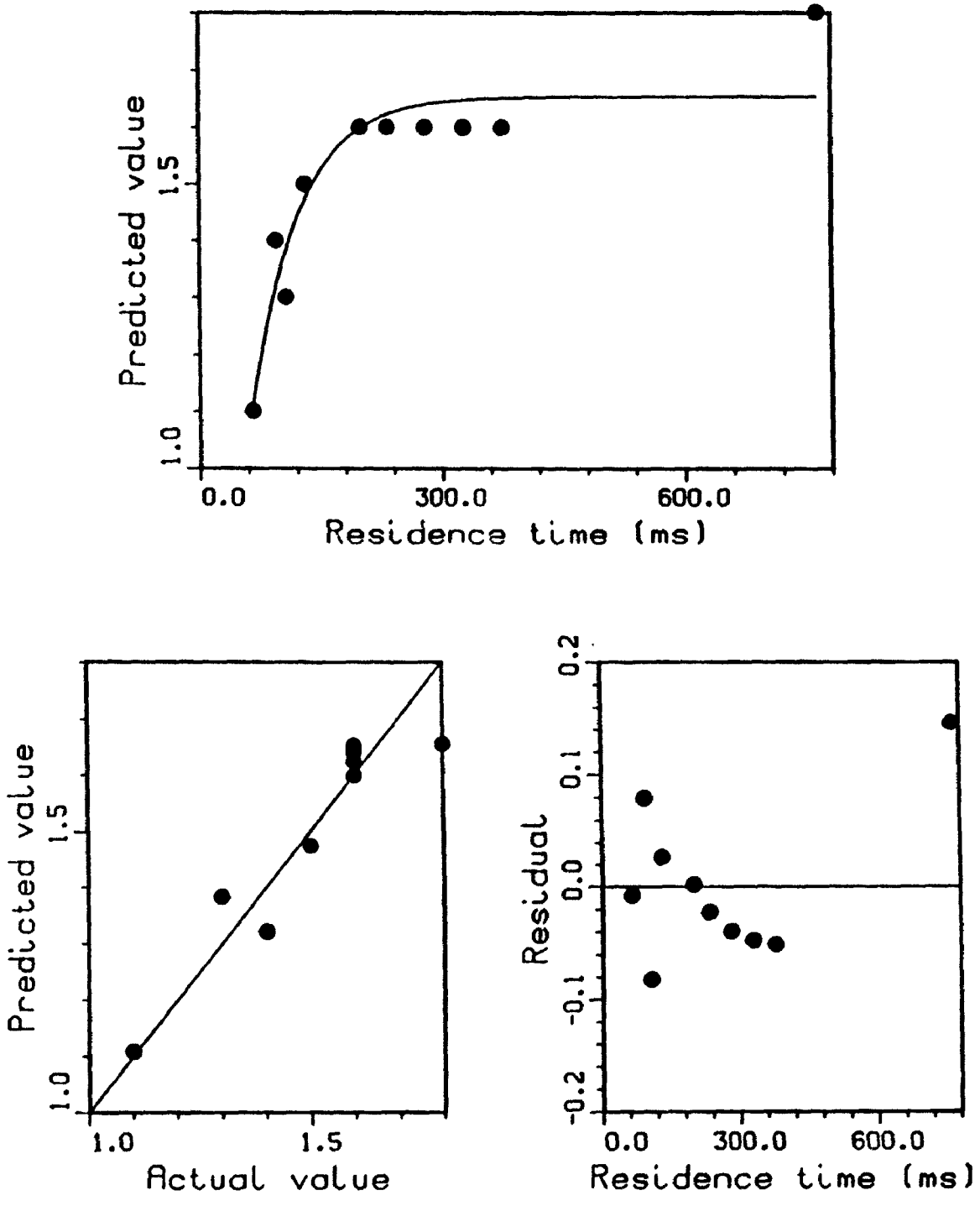

Figure A7.1.37. Zero-Intercept Kinetic Model For H_2 from Cellulose: Fast Pyrolysis at 850 °C (Run Numbers and Data in Table 15)

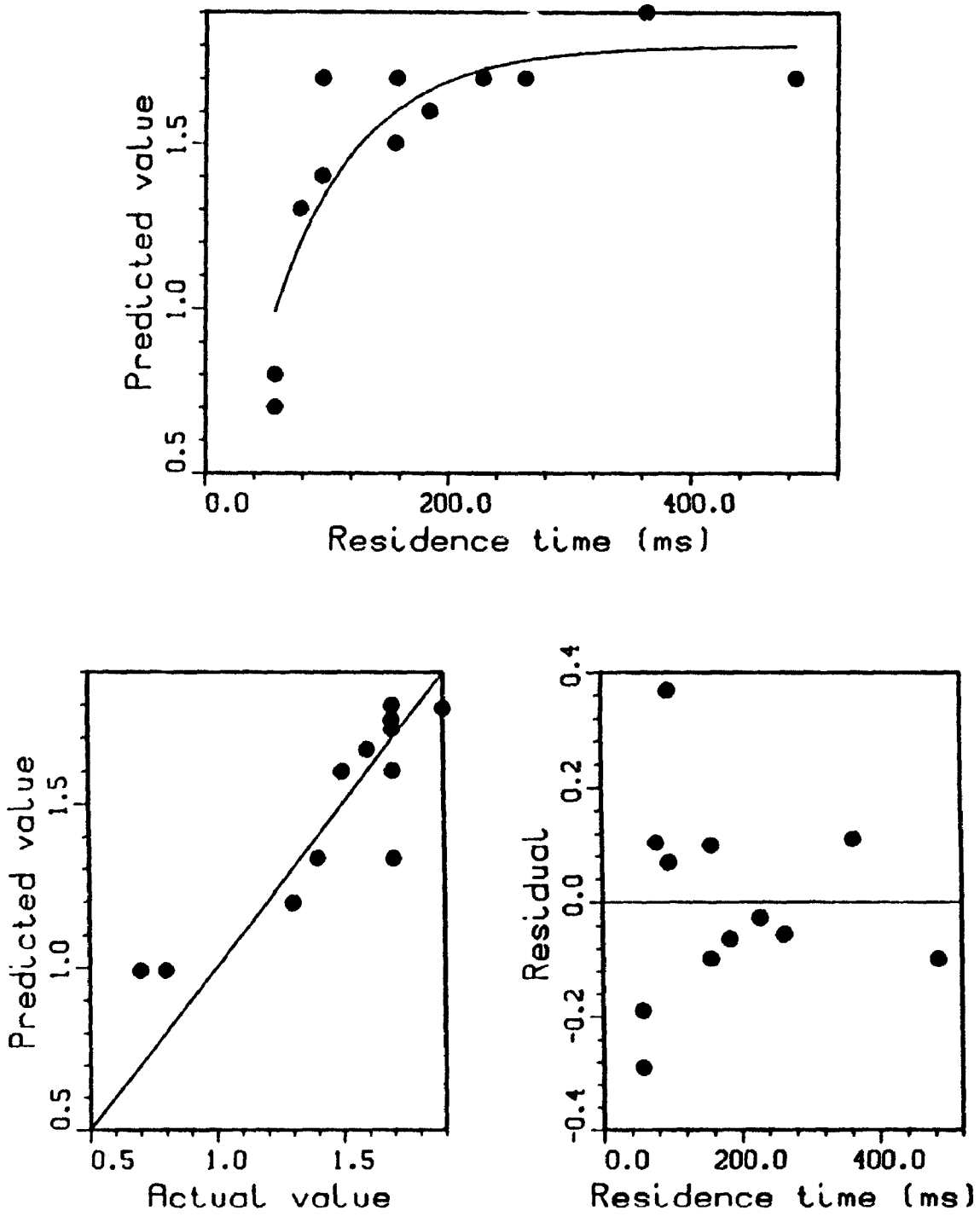

Figure A7.1.38. Zero-Intercept Kinetic Model For H_2 from Cellulose: Fast Pyrolysis at 875 °C (Run Numbers and Data in Table 16)

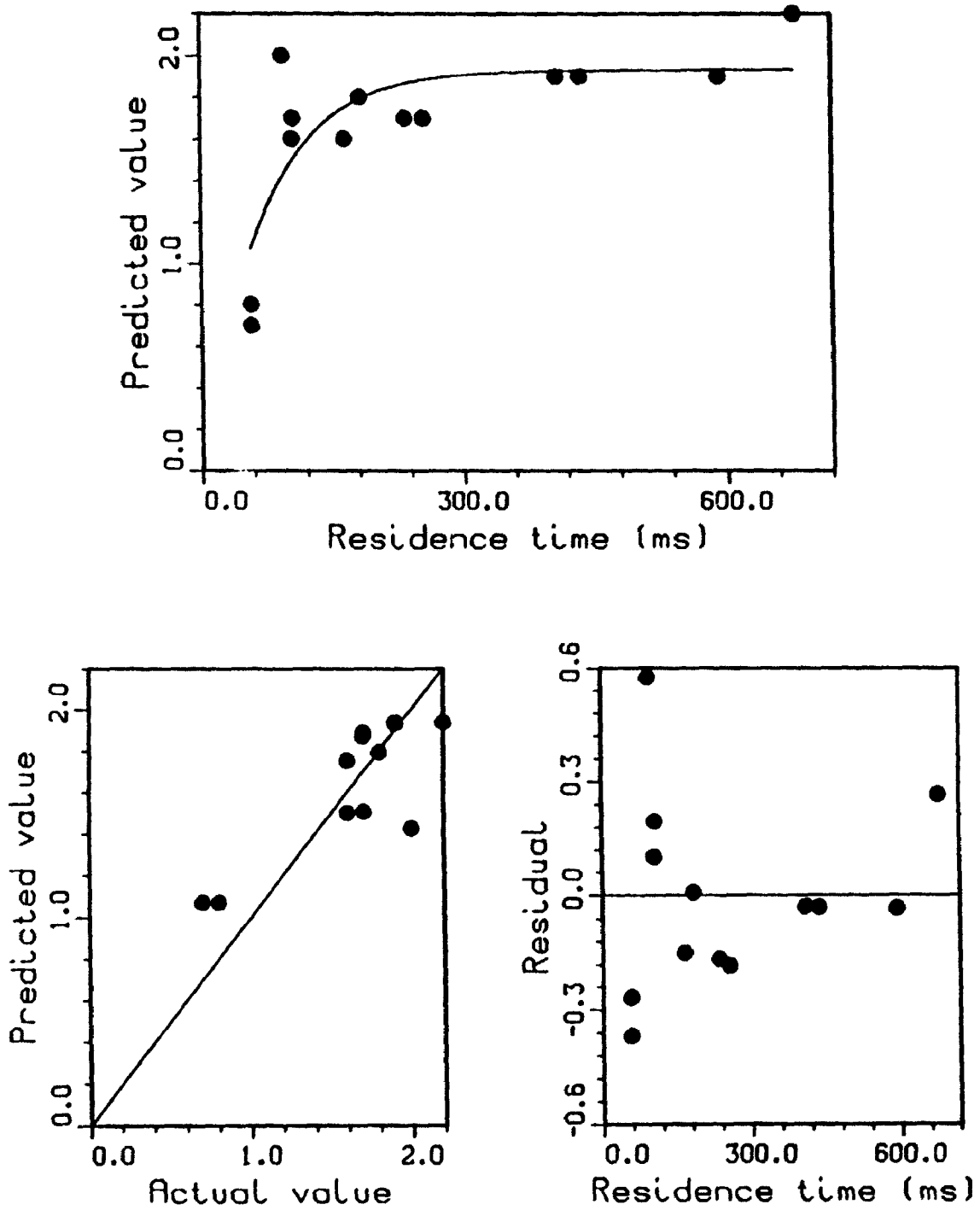

Figure A7.1.39. Zero-Intercept Kinetic Model For H_2 from Cellulose: Fast Pyrolysis at 900 °C (Run Numbers and Data in Table 17)

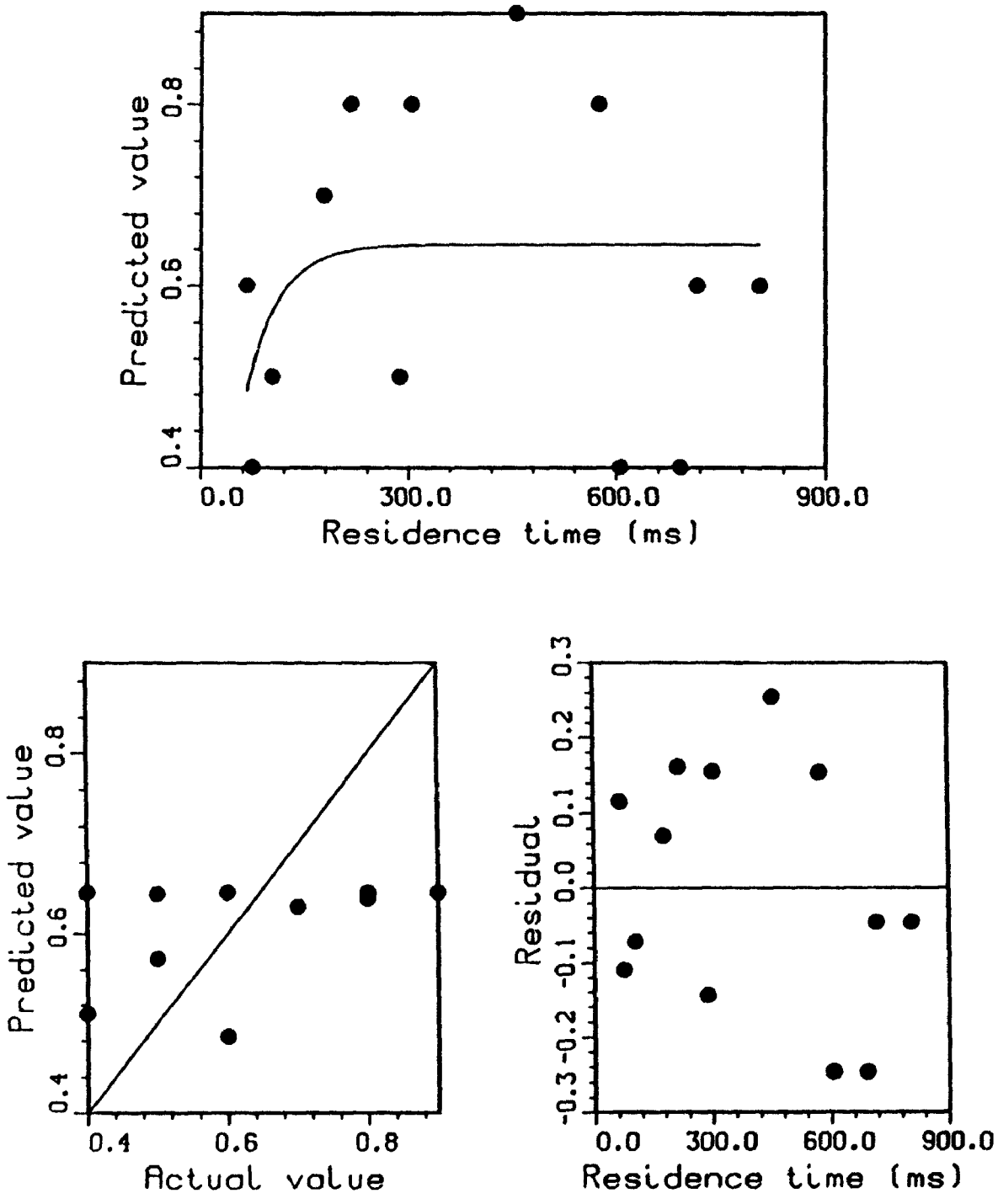

Figure A7.1.40. Zero-Intercept Kinetic Model For C_2H_2 from Cellulose: Fast Pyrolysis at 750 °C (Run Numbers and Data in Table 12)

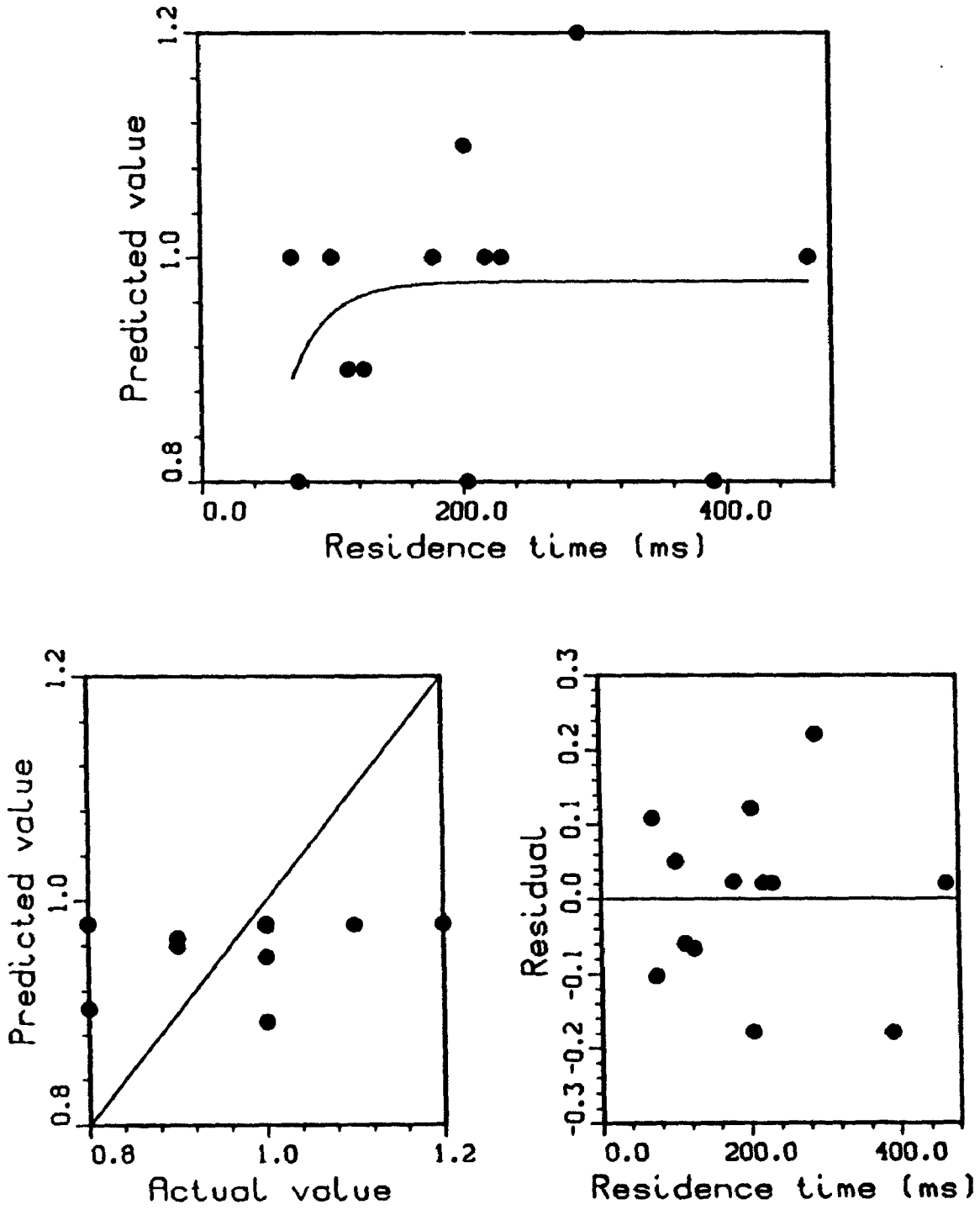

Figure A7.1.41. Zero-Intercept Kinetic Model For C_2H_2 from Cellulose: Fast Pyrolysis at 800 °C (Run Numbers and Data in Table 13)

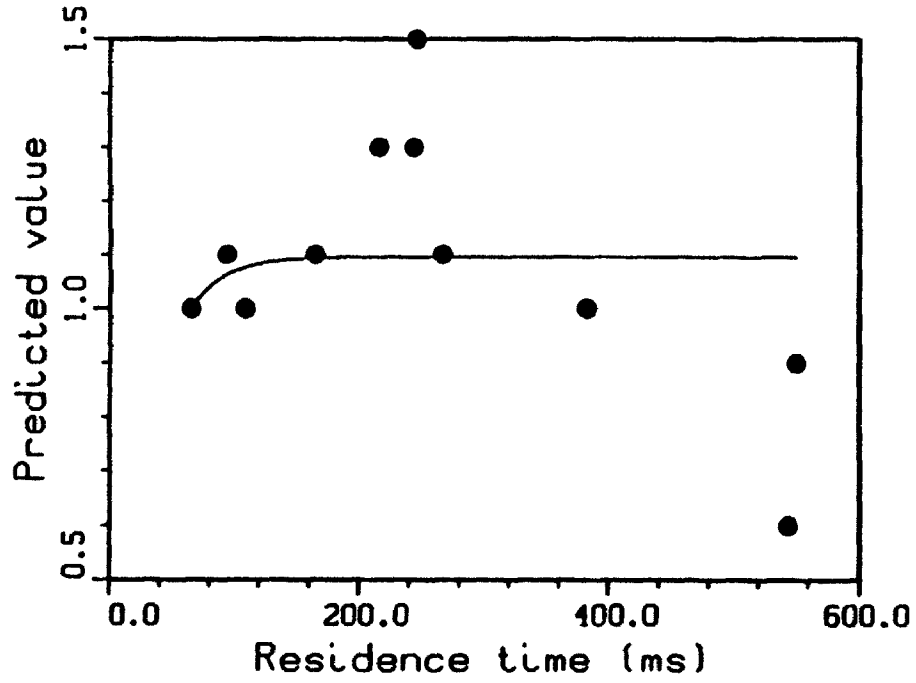

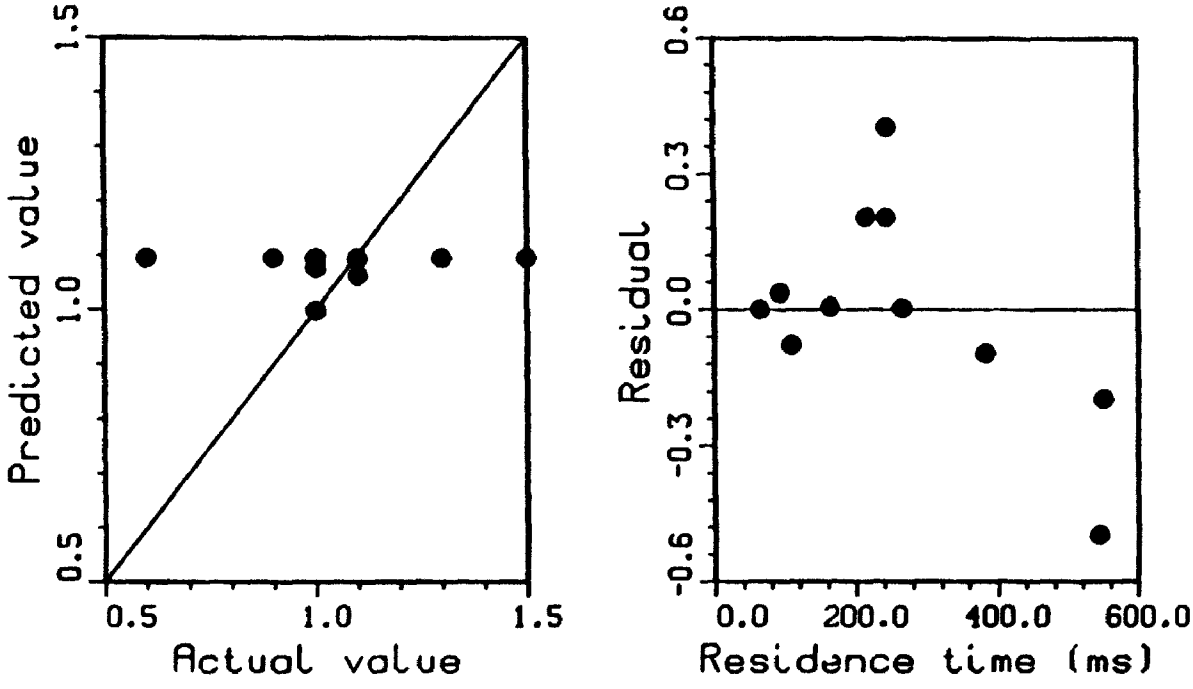

Figure A7.1.42. Zero-Intercept Kinetic Model For C_2H_2 from Cellulose: Fast Pyrolysis at 825 °C (Run Numbers and Data in Table 14)

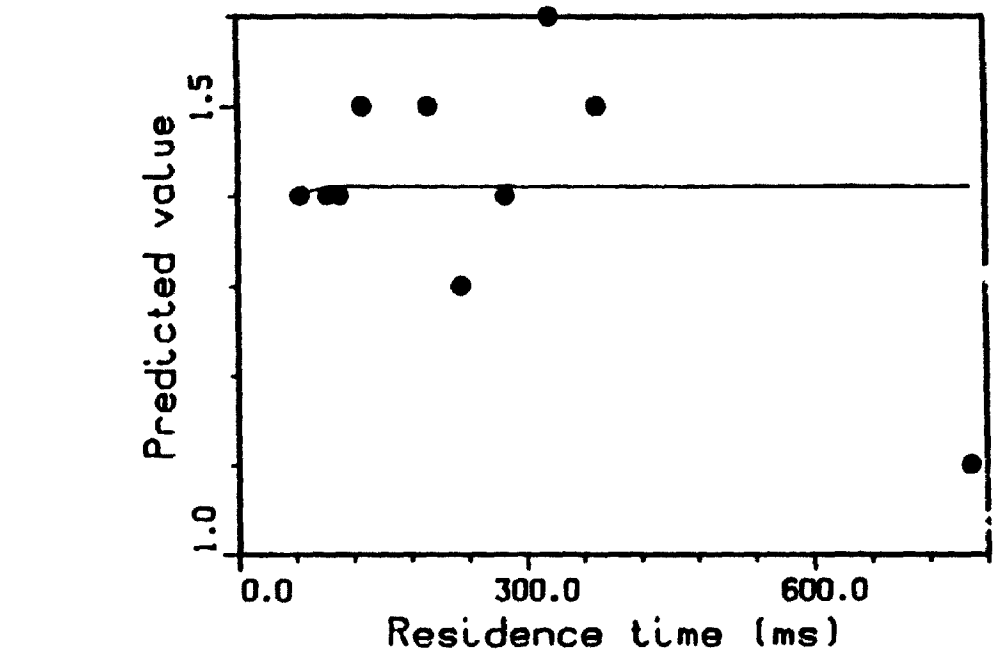

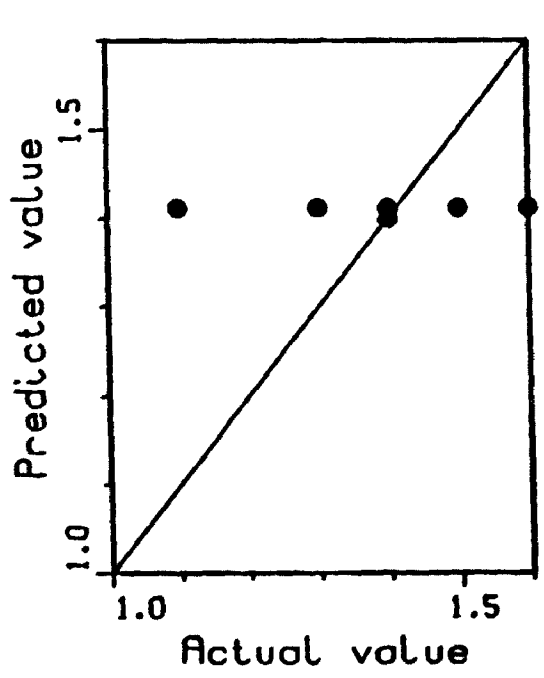

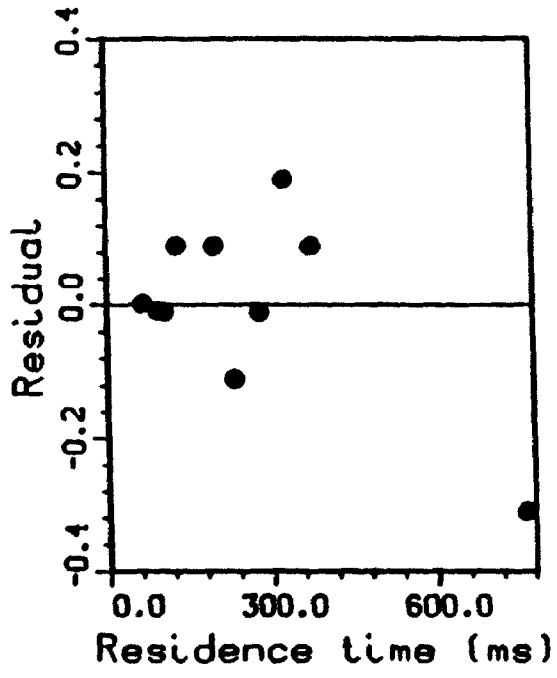

Figure A7.1.43. Zero-Intercept Kinetic Model For C_2H_2 from Cellulose: Fast Pyrolysis at 850 °C (Run Numbers and Data in Table 15)

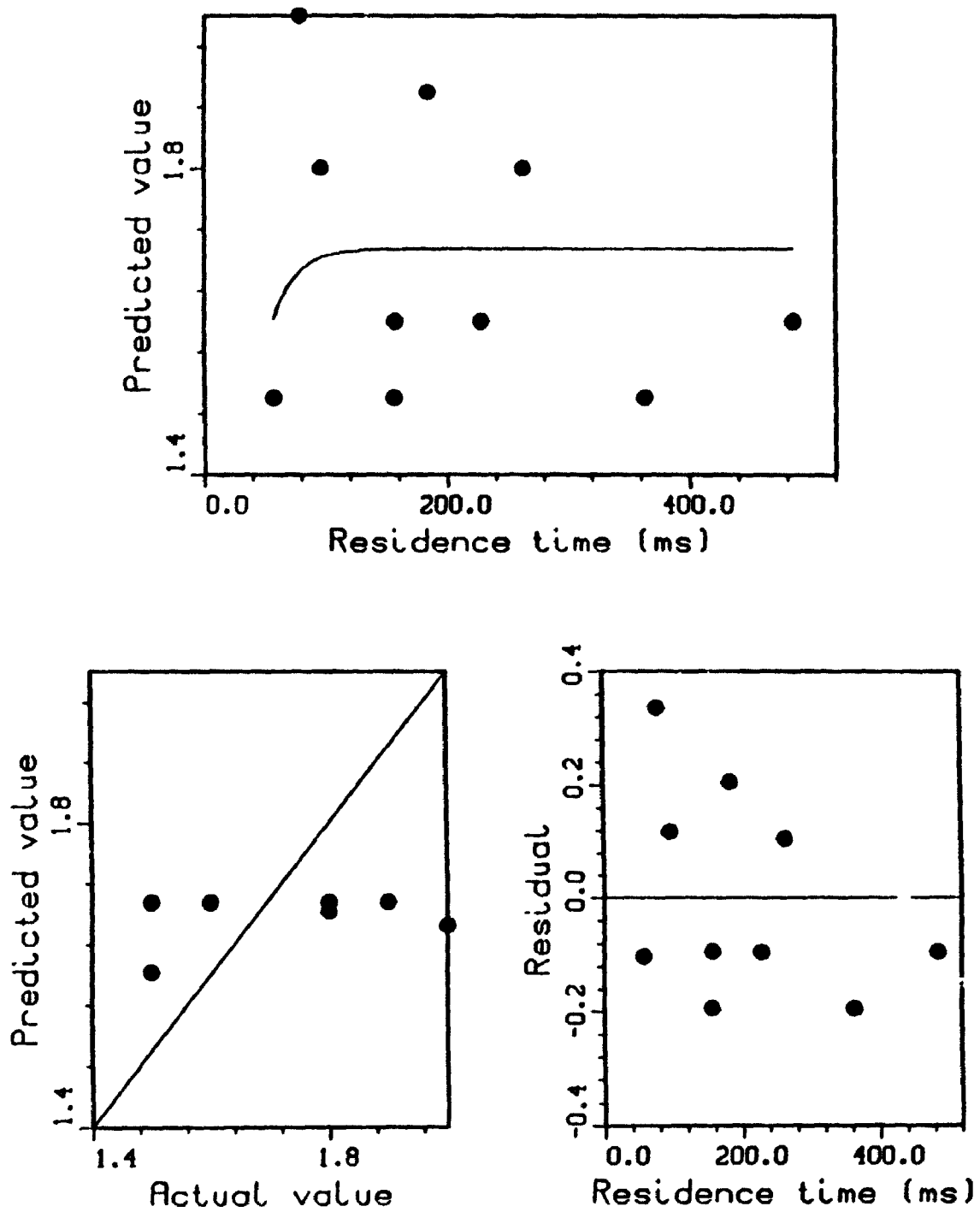

Figure A7.1.44. Zero-Intercept Kinetic Model For C_2H_2 from Cellulose: Fast Pyrolysis at 875 °C (Run Numbers and Data in Table 16)

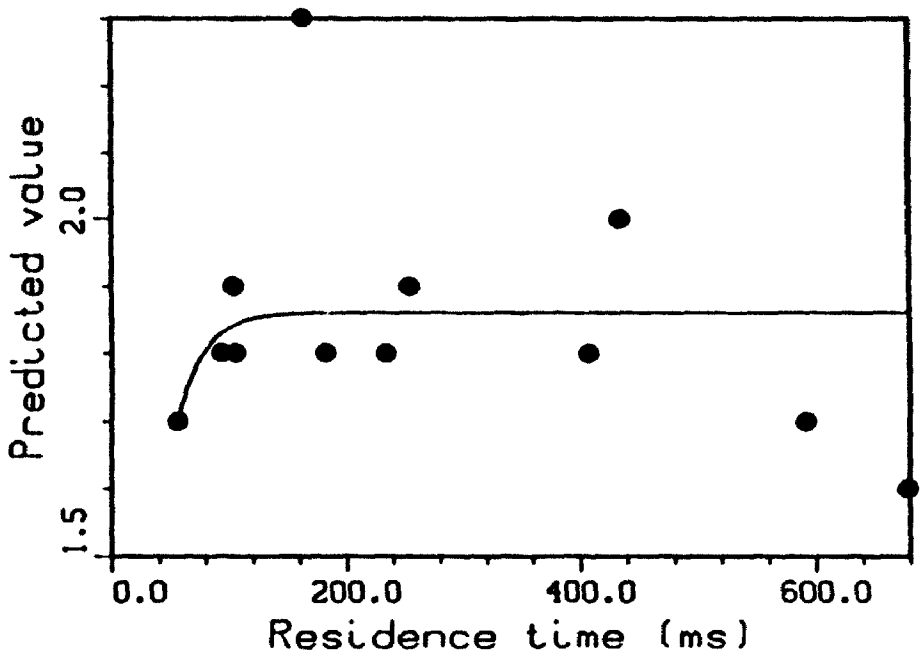

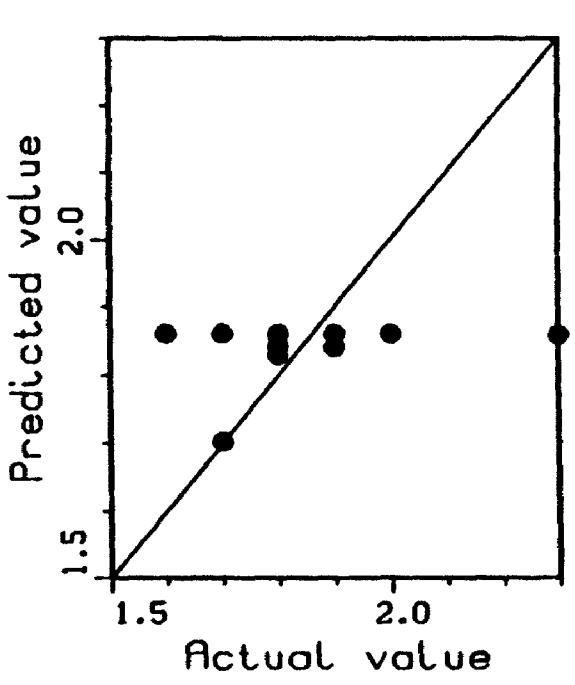

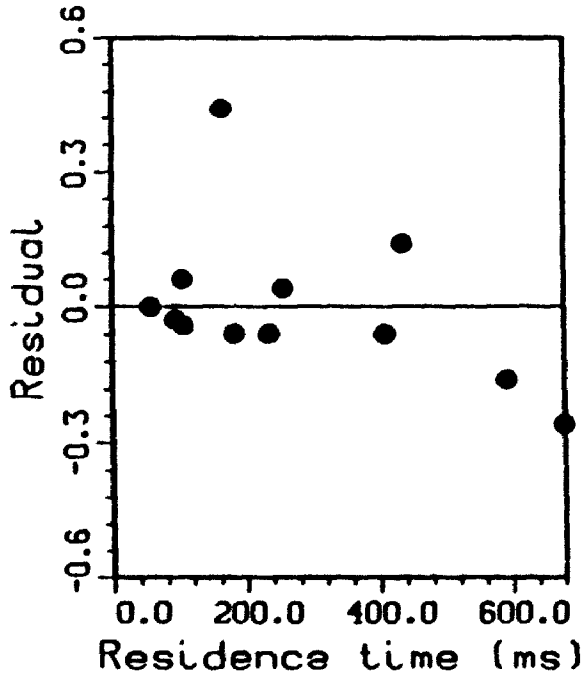

Figure A7.i.45. Zero-Intercept Kinetic Model For C_2H_2 from Cellulose: Fast Pyrolysis at 900 °C (Run Numbers and Data in Table 17)

APPENDIX 7.2 CELLULOSE PYROLYSIS ARRHENIUS PLOTS: ZERO-INTERCEPT MODEL

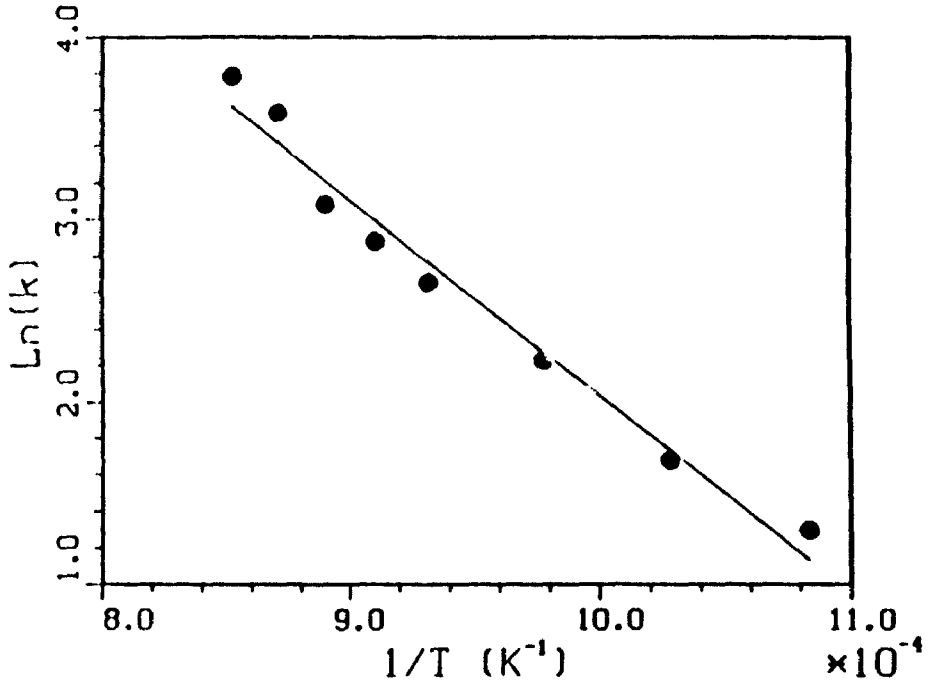

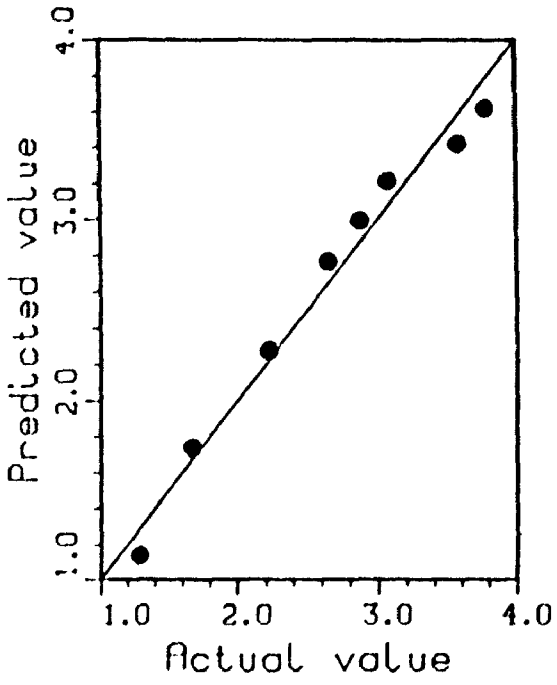

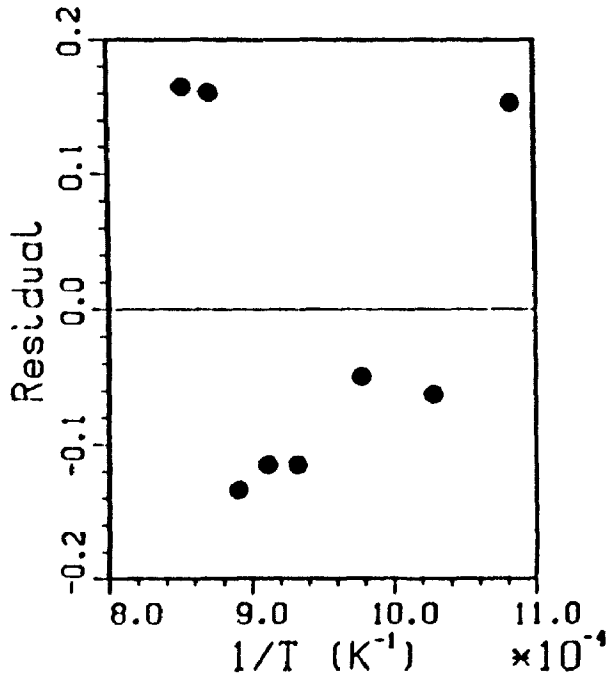

Figure A7.2.1. Zero-Intercept Model for CO from Cellulose: Arrhenius Plot (Data from Table 31)

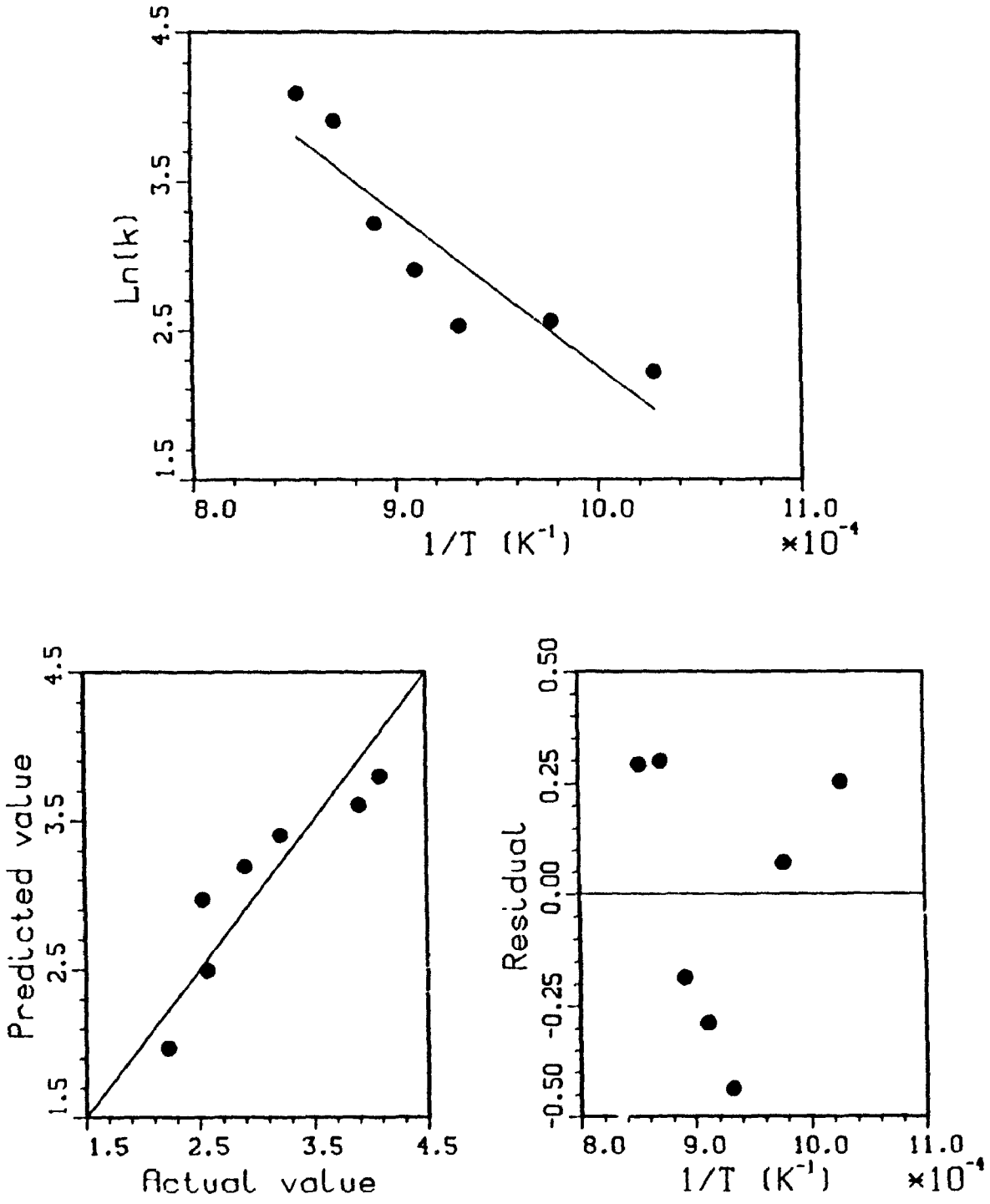

Figure A7.2.2. Zero-Intercept Model for CO_2 from Cellulose: Arrhenius Plot (Data from Table 32)

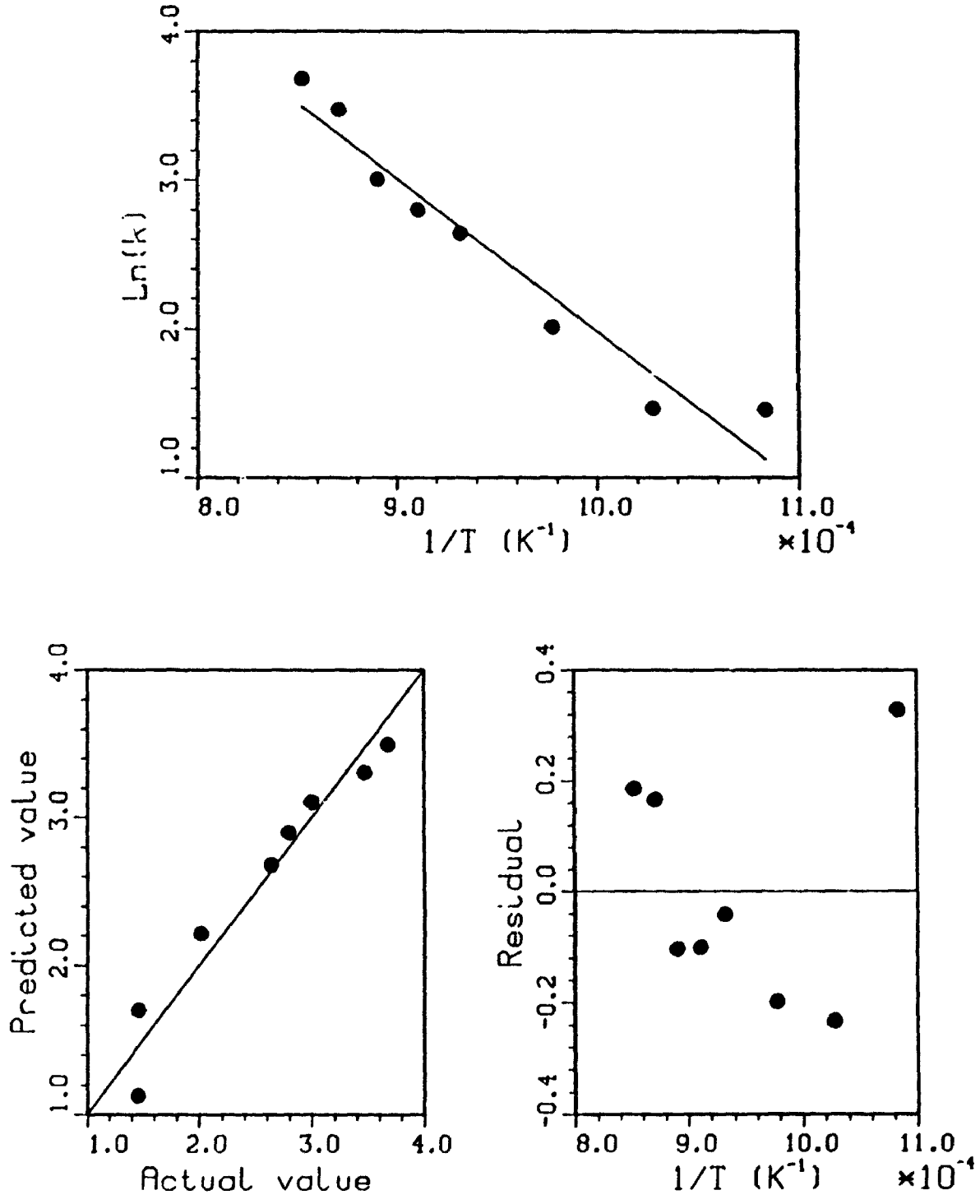

Figure A7.2.3. Zero-Intercept Model for C_2H_4 from Cellulose: Arrhenius Plot (Data from Table 33)

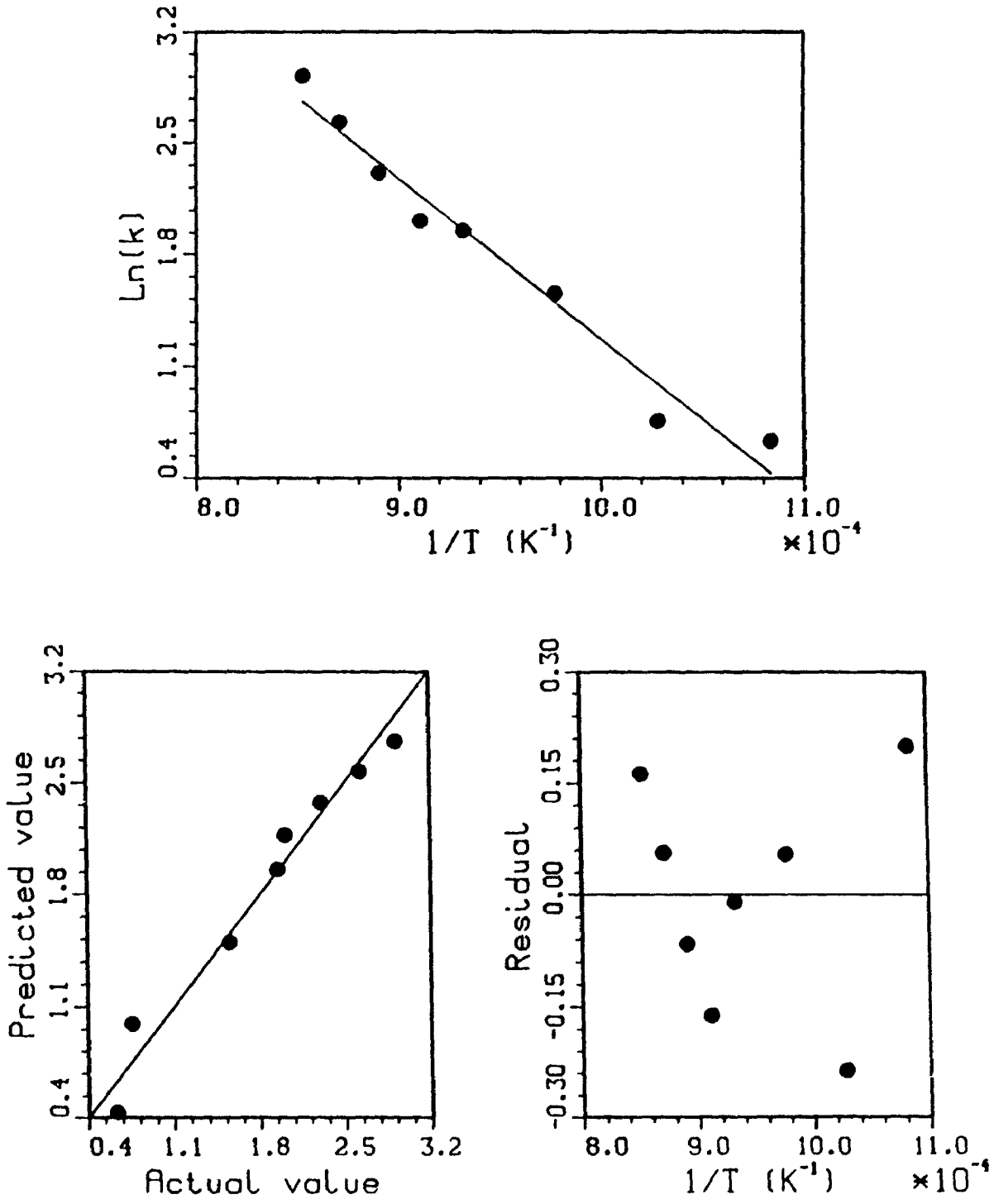

Figure A7.2.4. Zero-Intercept Model for CH_4 from Cellulose: Arrhenius Plot (Data from Table 34)

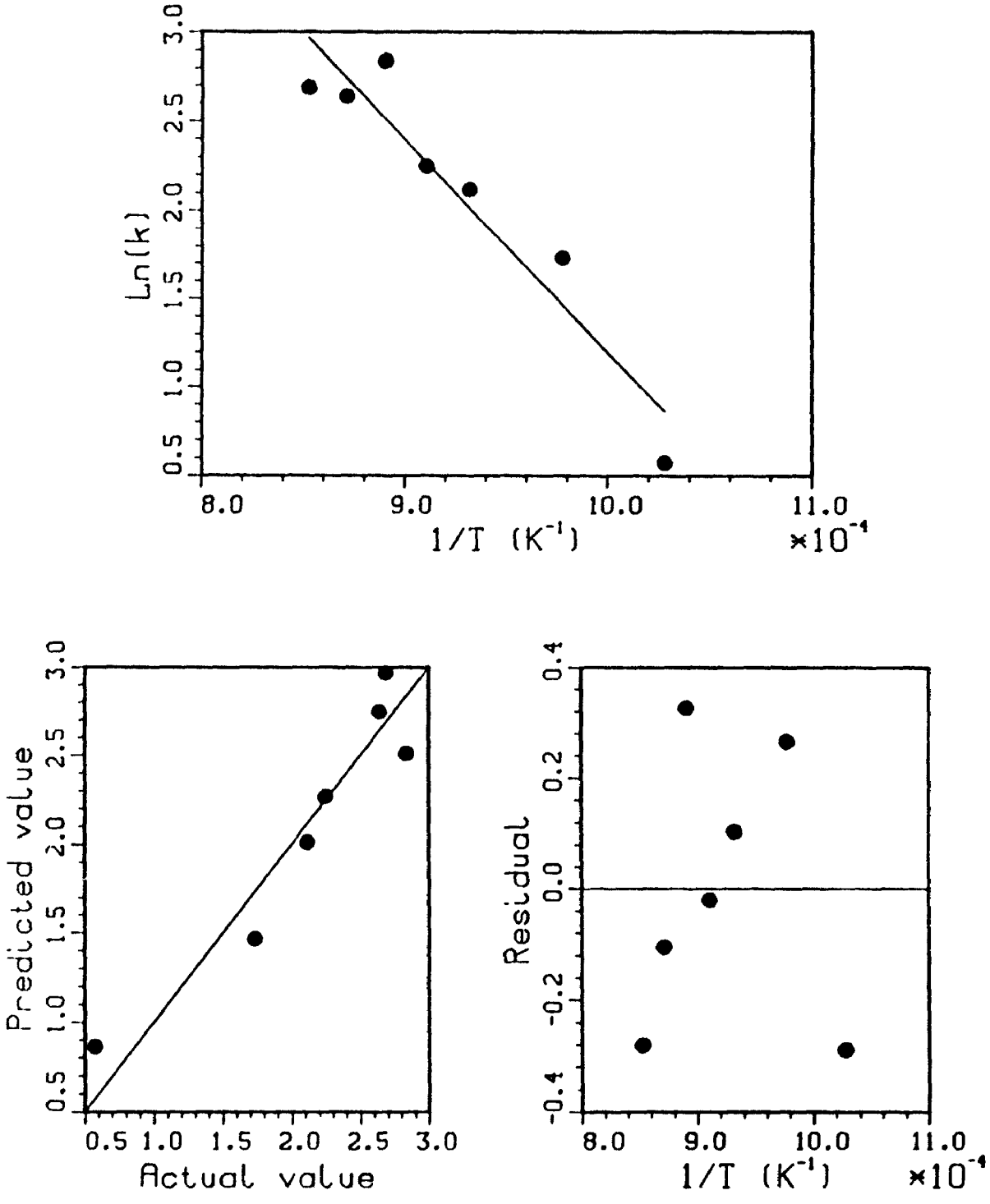

Figure A7.2.5. Zero-Intercept Model for H_2 from Cellulose: Arrhenius Plot (Data from Table 35)

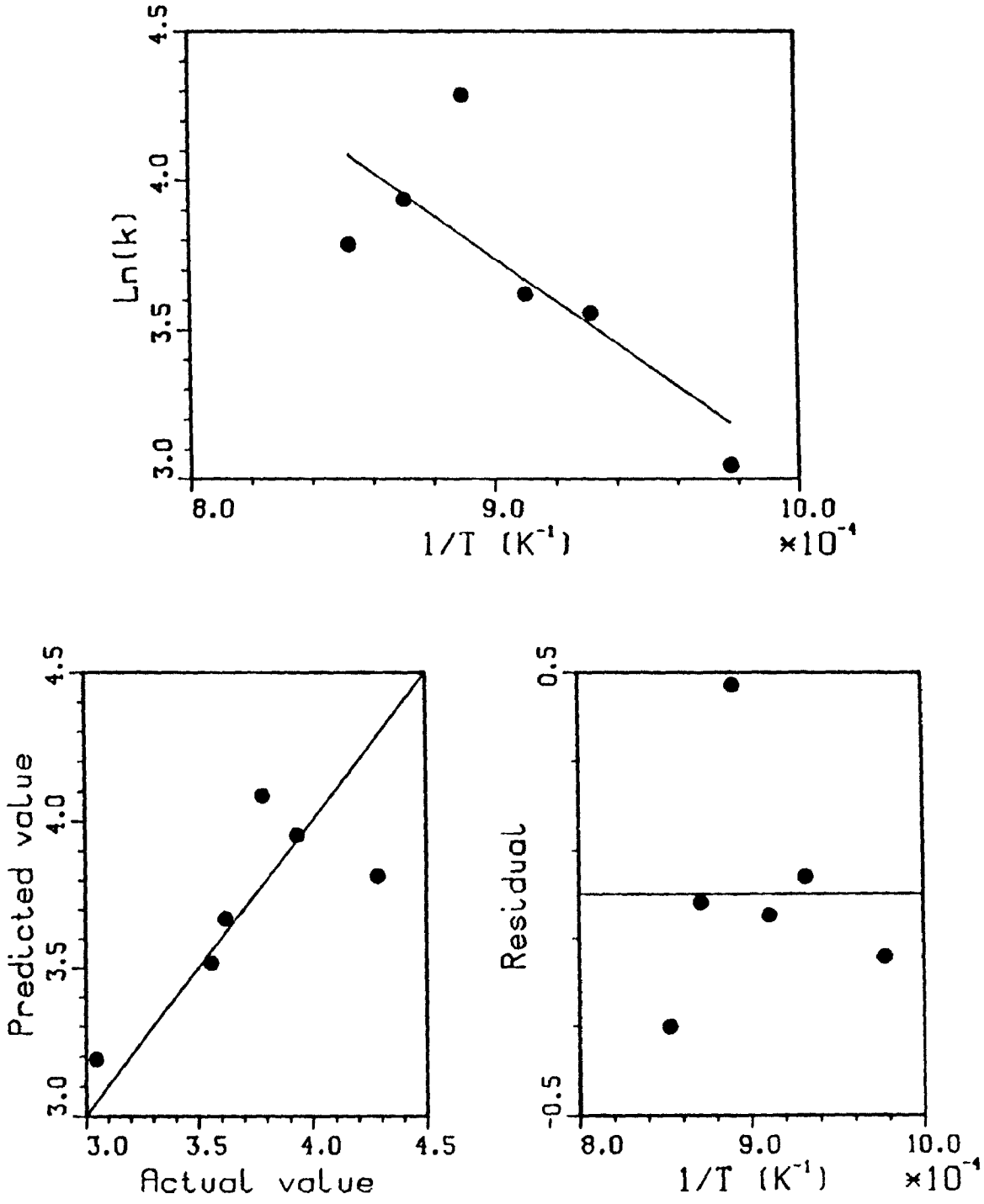

Figure A7.2.6. Zero-Intercept Model for C_2H_2 from Cellulose: Arrhenius Plot (Data from Table 36)

APPENDIX 7.3 CELLULOSE PYROLYSIS REGRESSION CURVES: PROMPT GAS MODEL

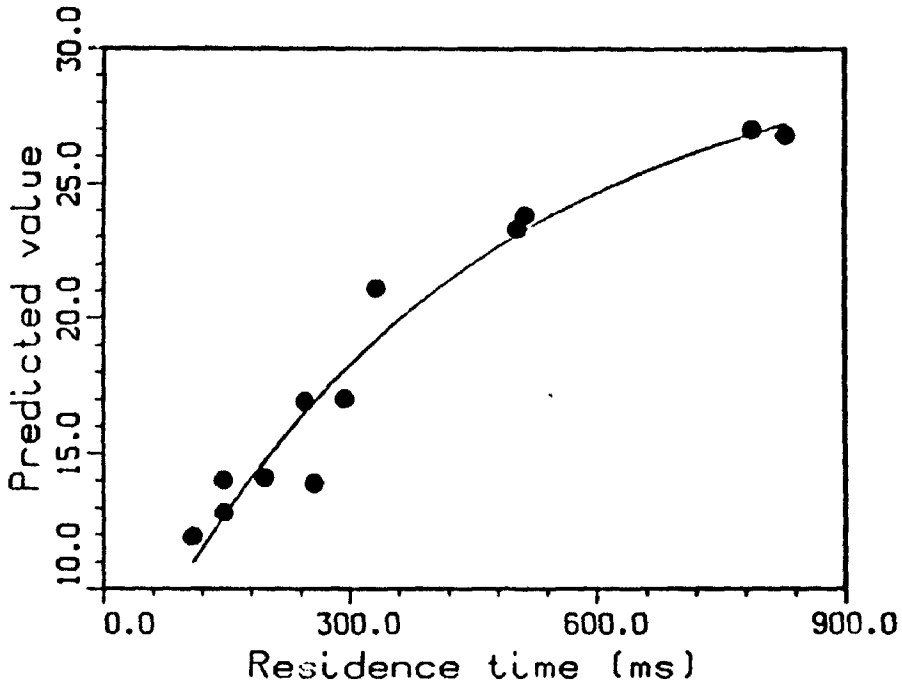

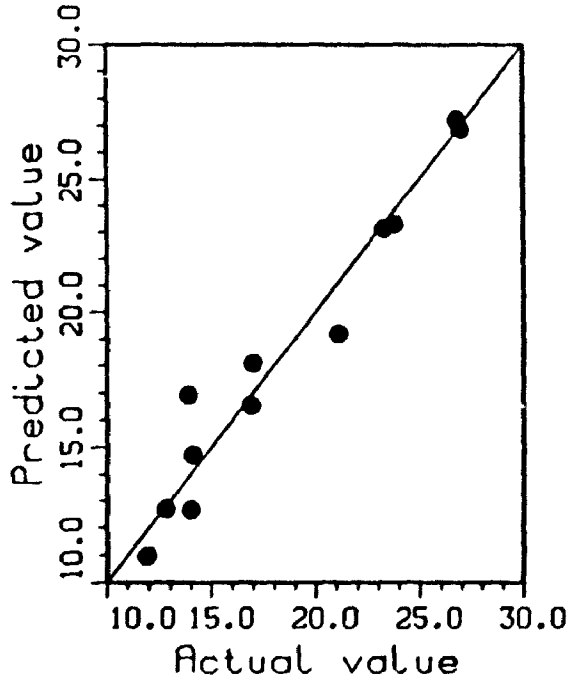

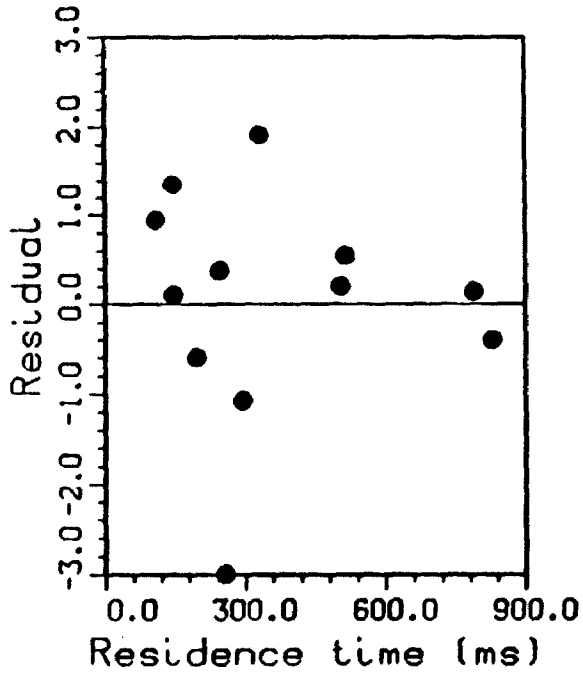

Figure A7.3.1. Prompt Gas Kinetic Model For Total Gas from Cellulose: Fast Pyrolysis at 650 °C

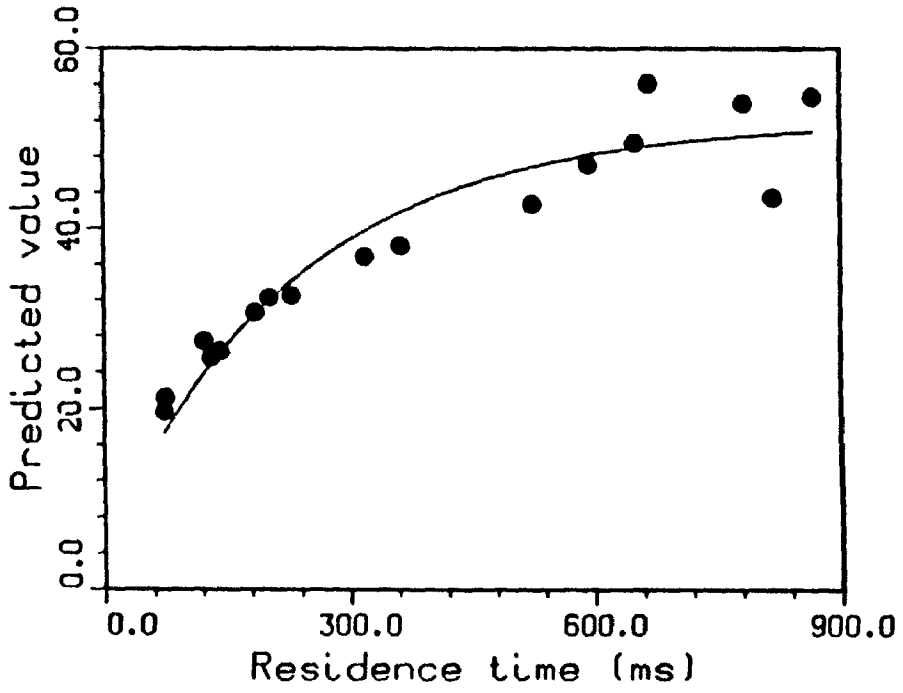

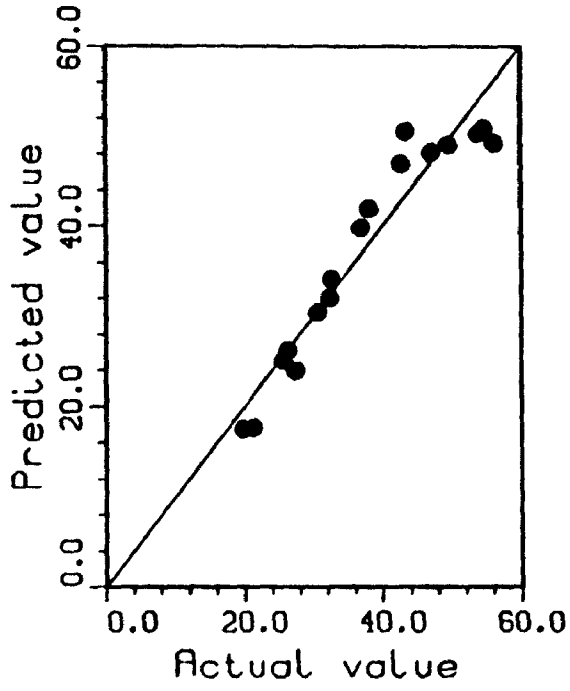

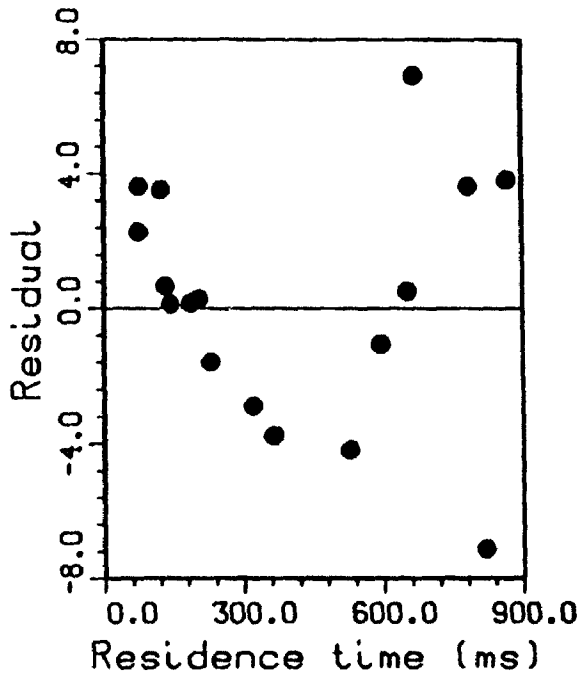

Figure A7.3.2. Prompt Gas Kinetic Model For Total Gas from Cellulose: Fast Pyrolysis at 700 °C

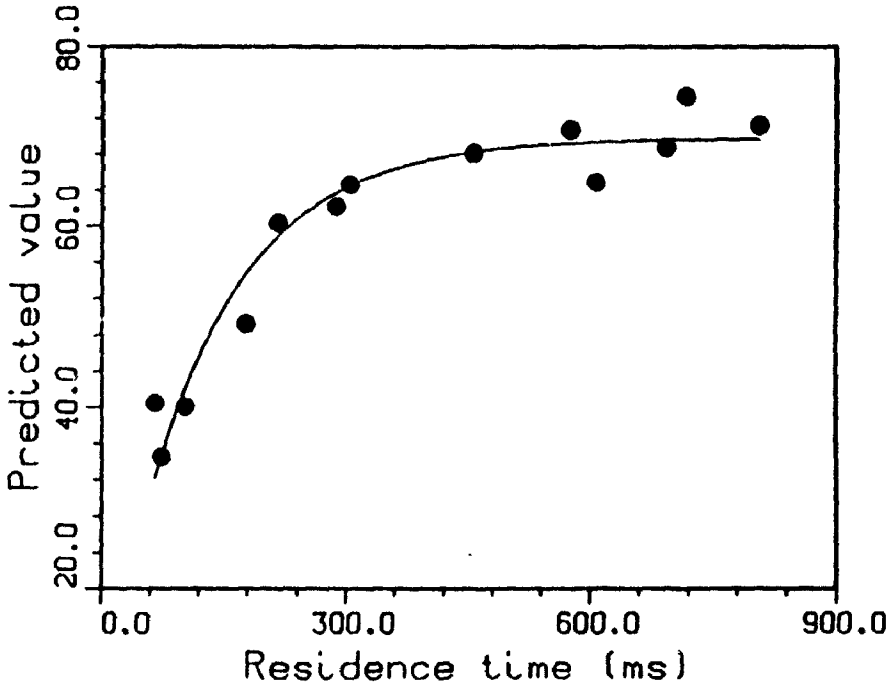

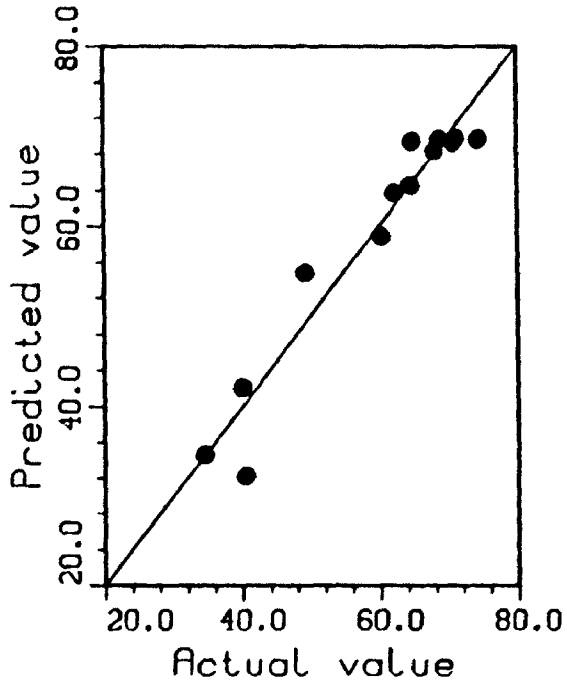

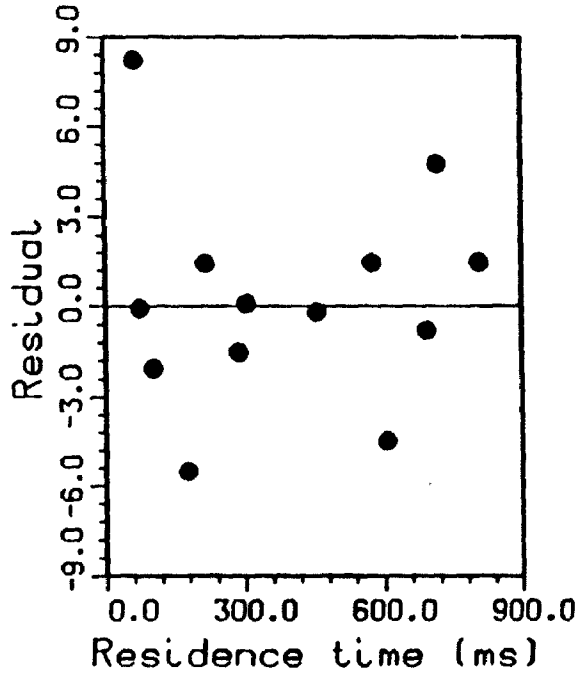

Figure A7.3.3. Prompt Gas Kinetic Model For Total Gas from Cellulose: Fast Pyrolysis at 750 °C

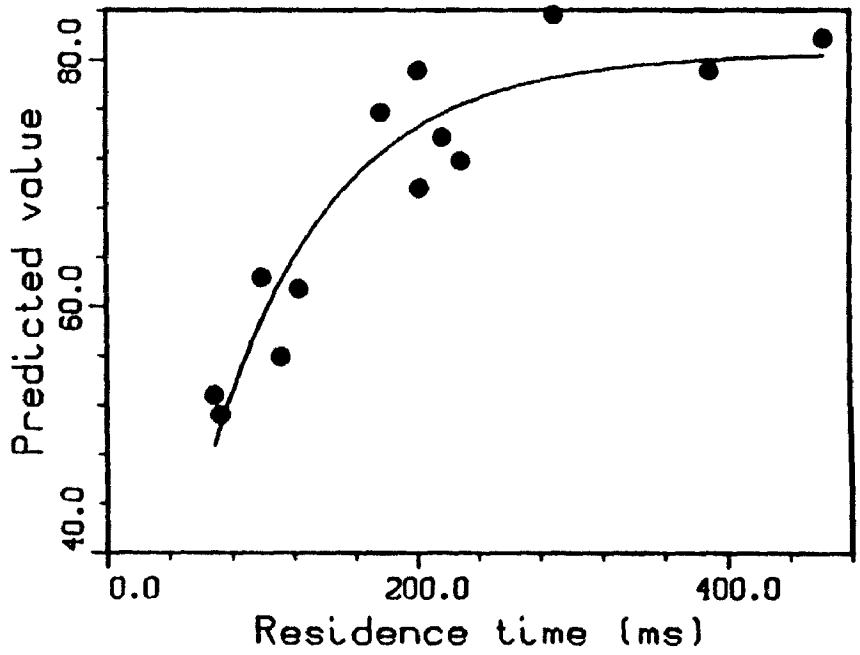

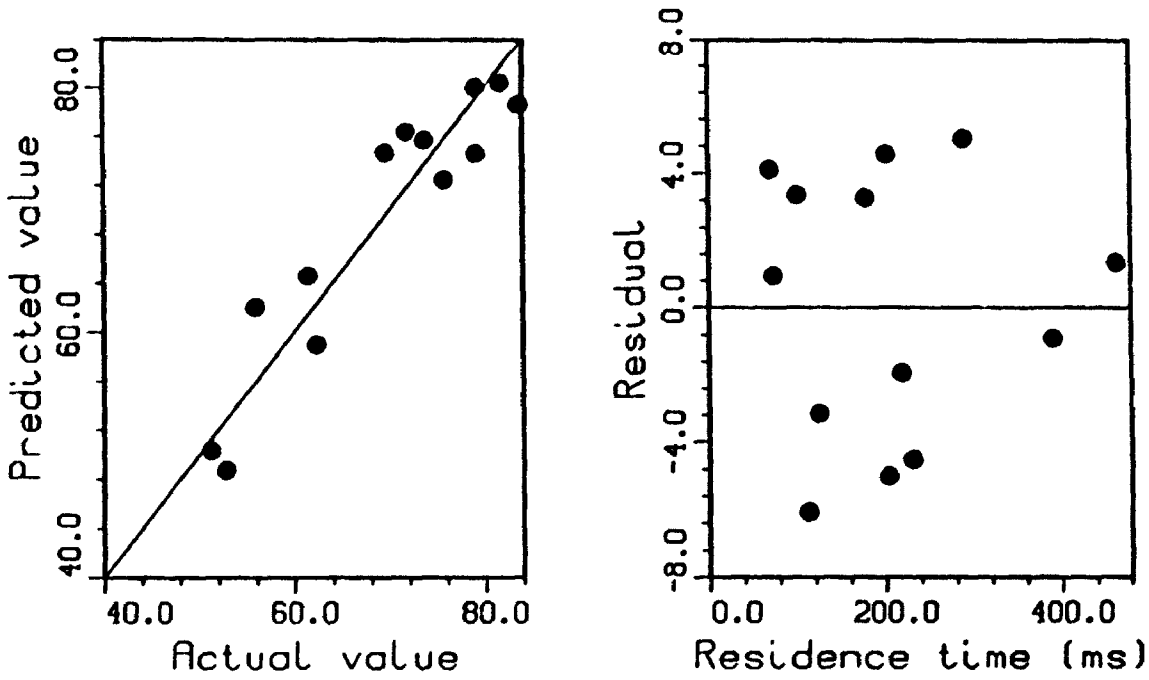

Figure A7.3.4. Prompt Gas Kinetic Model For Total Gas from Cellulose: Fast Pyrolysis at 800 °C

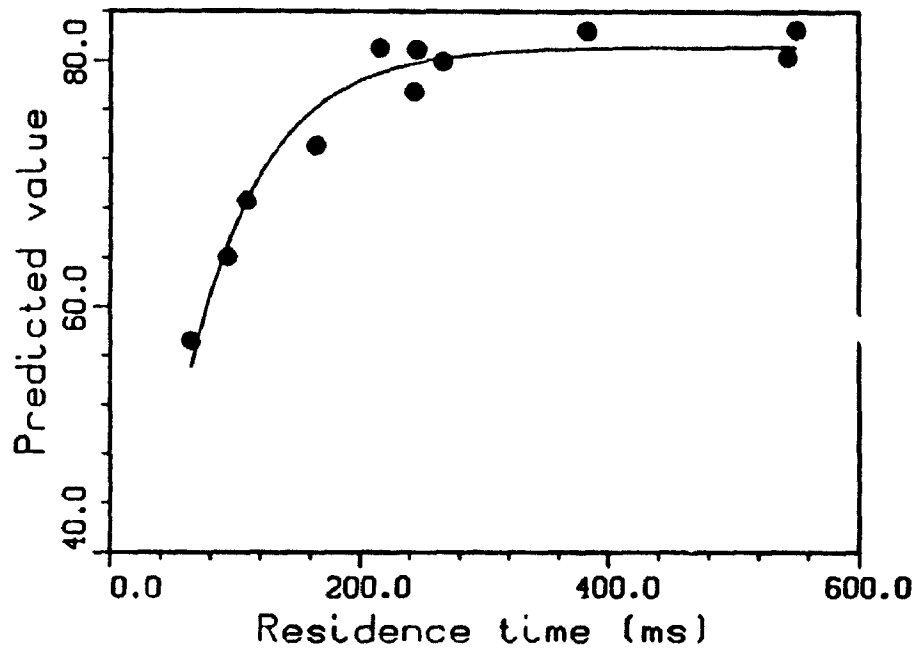

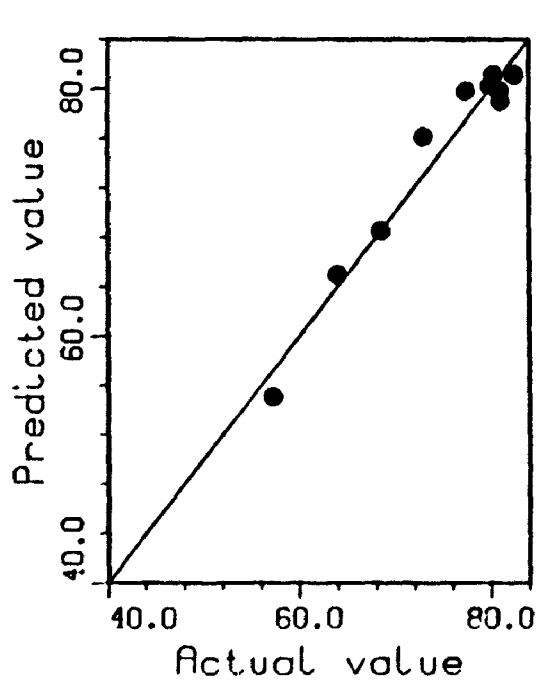

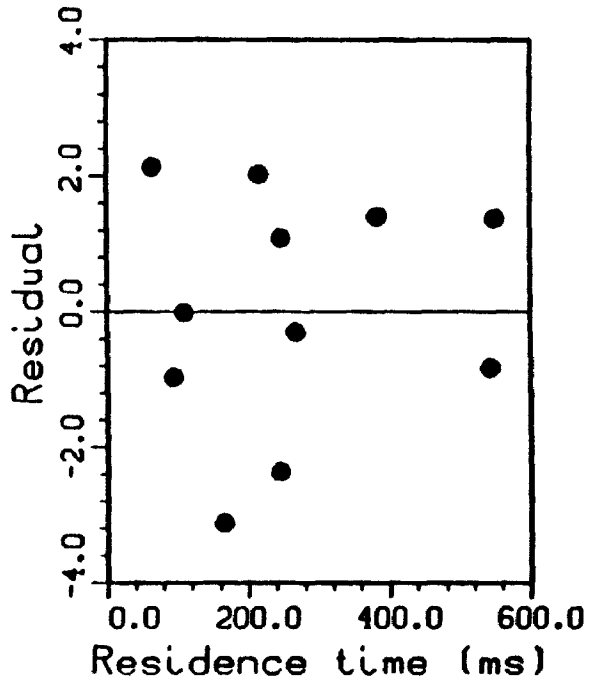

Figure A7.3.5. Prompt Gas Kinetic Model For Total Gas from Cellulose: Fast Pyrolysis at 825 °C

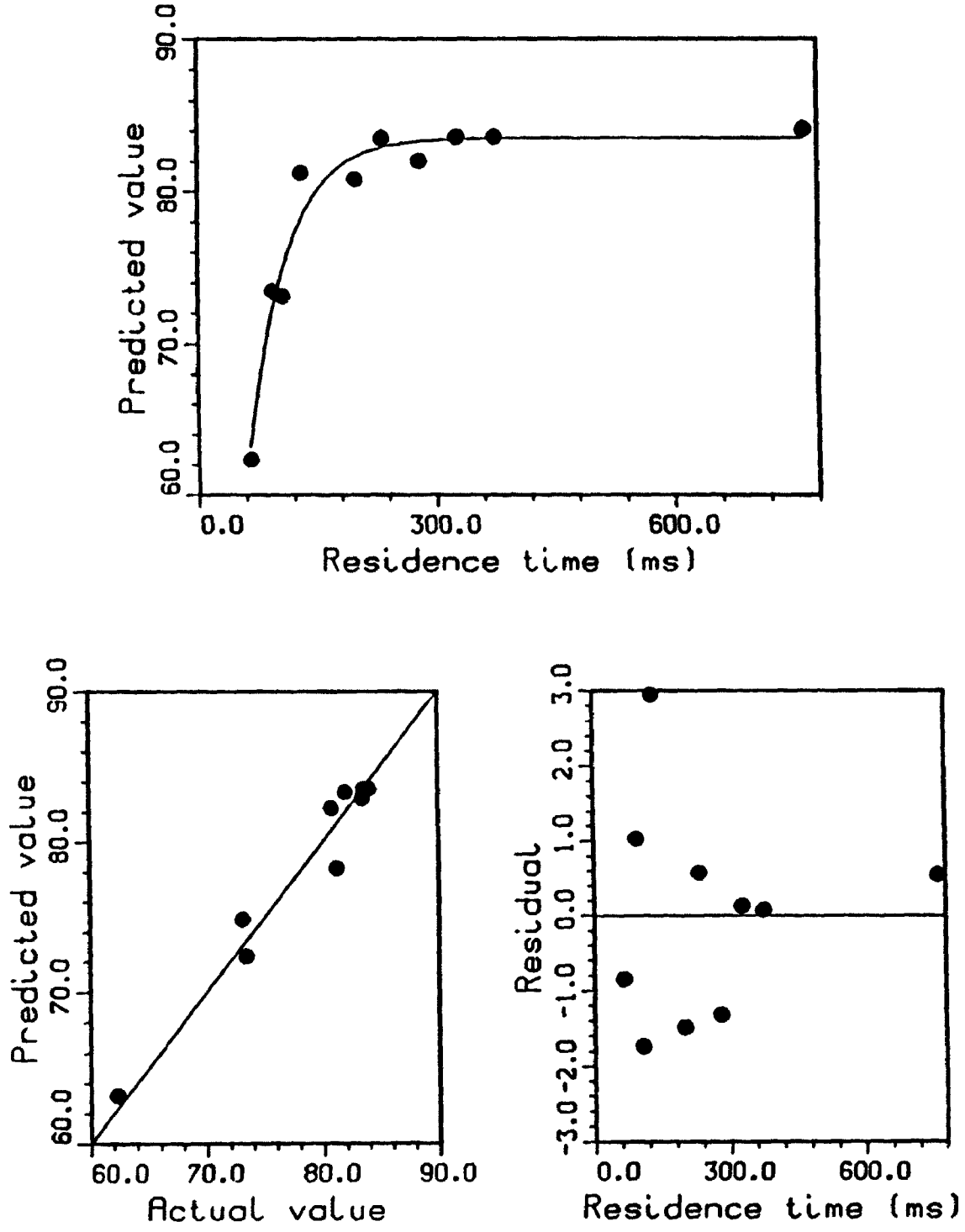

Figure A7.3.6. Prompt Gas Kinetic Model For Total Gas from Cellulose: Fast Pyrolysis at 850 °C

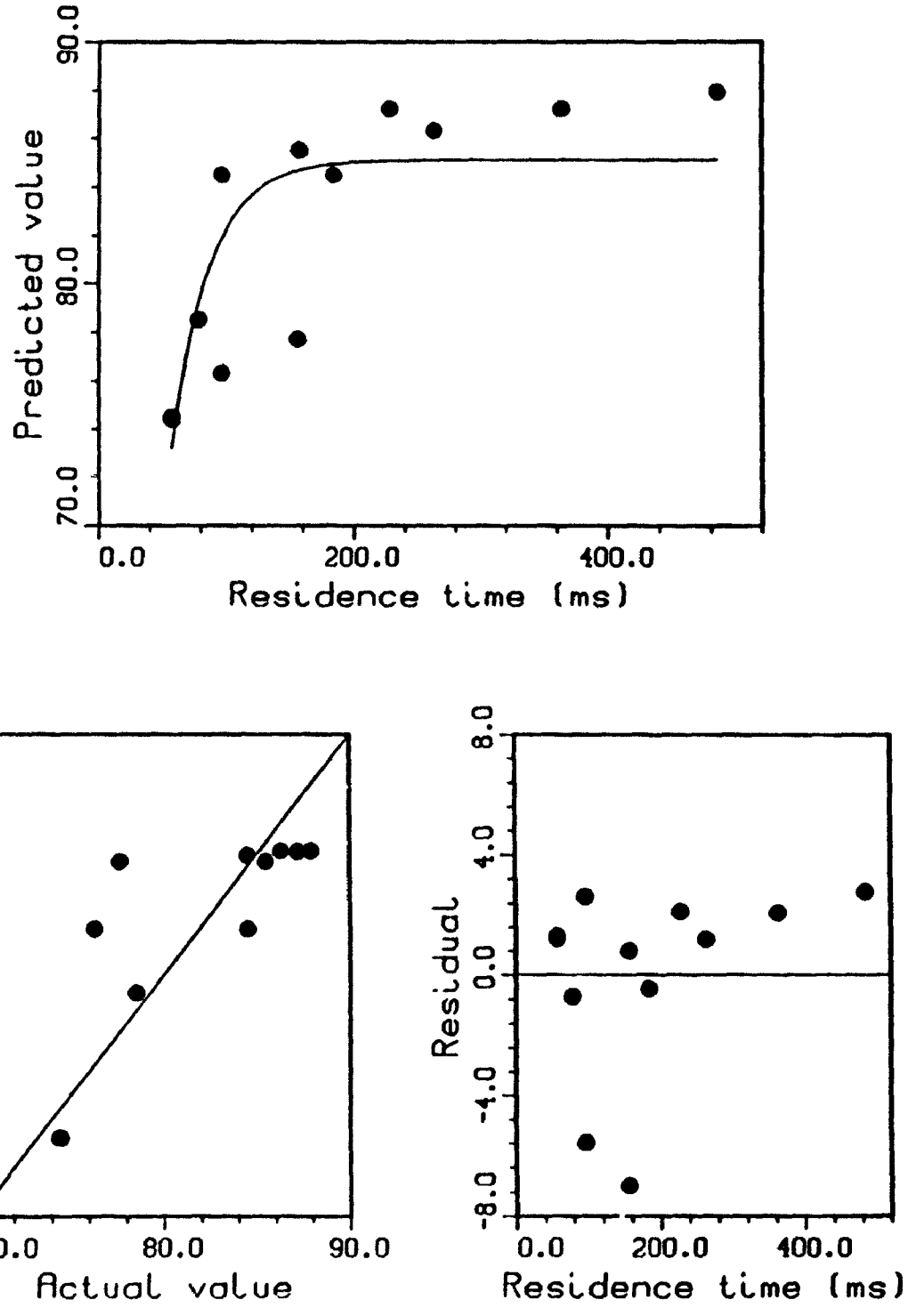

Figure A7.3.7. Prompt Gas Kinetic Model For Total Gas from Cellulose: Fast Pyrolysis at 875 °C

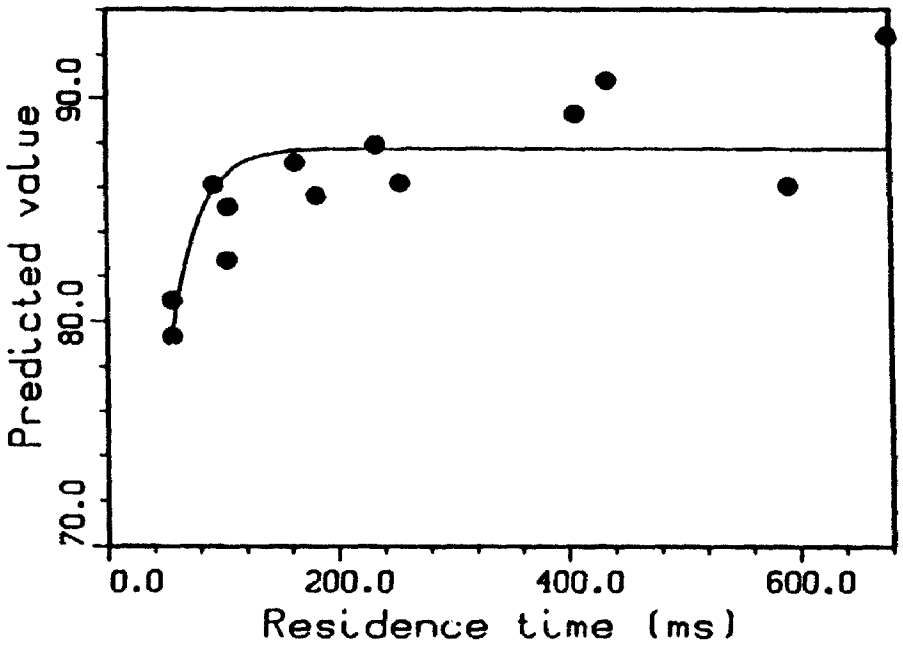

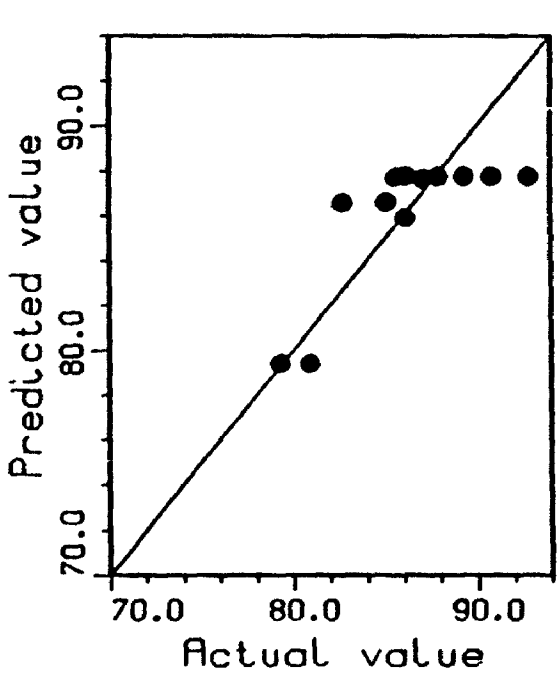

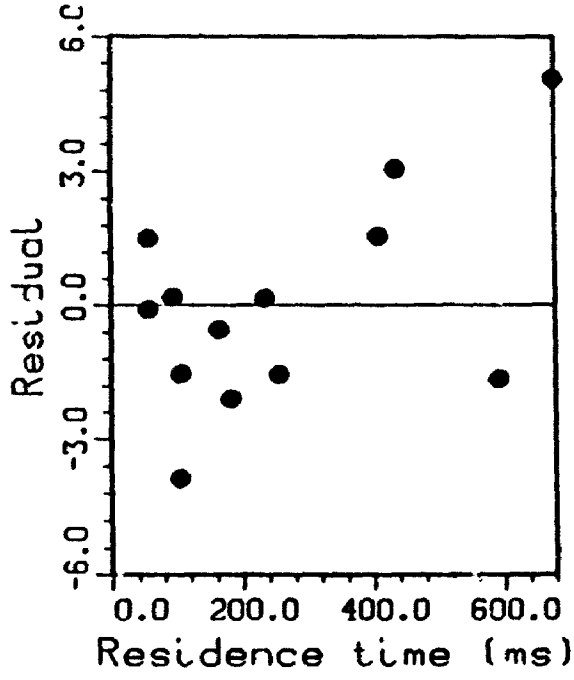

Figure A7.3.8. Prompt Gas Kinetic Model For CO from Cellulose: Fast Pyrolysis at 900 °C

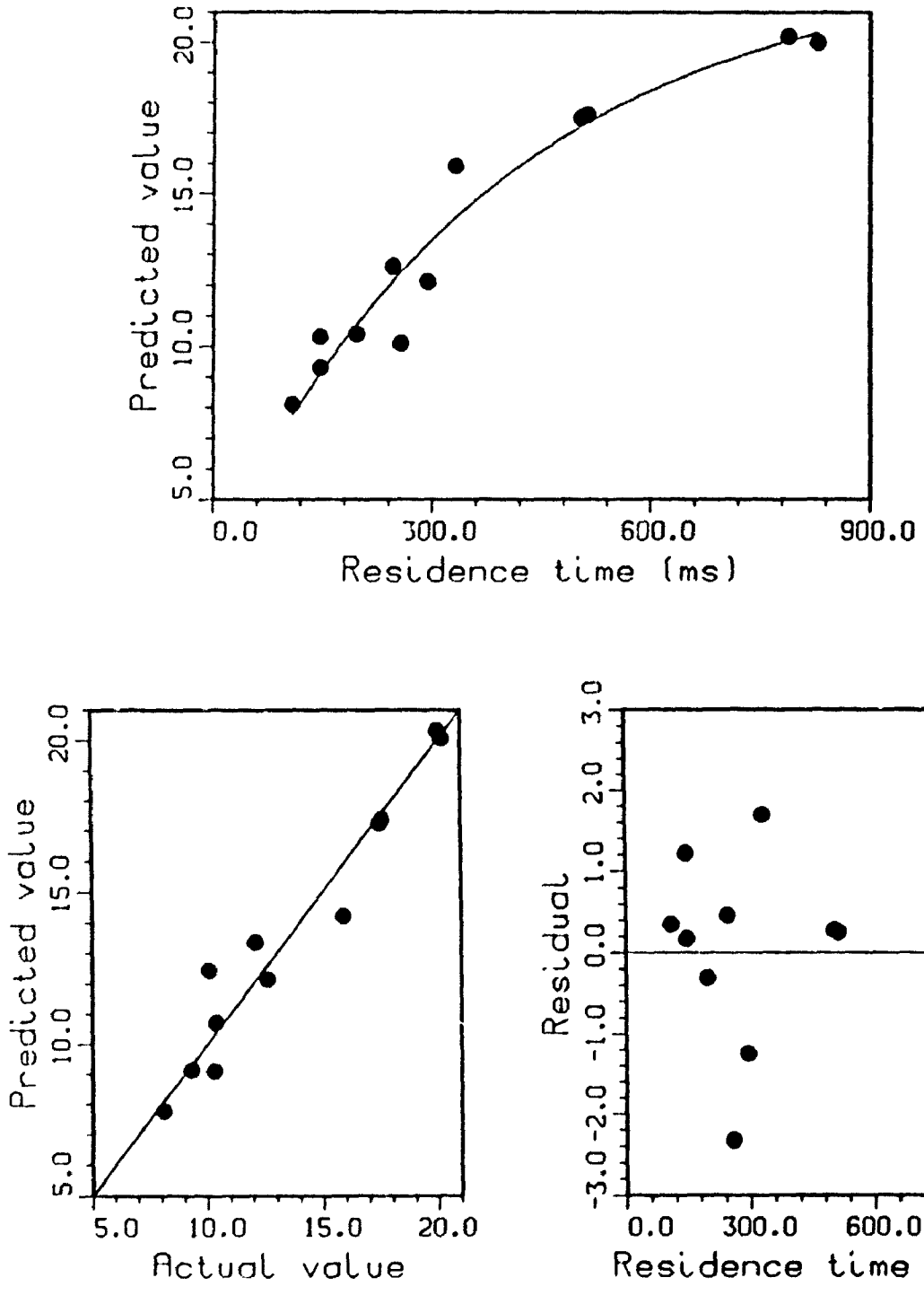

Figure A .3.9. Prompt Gas Kinetic Model For CO from Cellulose: Fast Pyrolysis at 650 °C

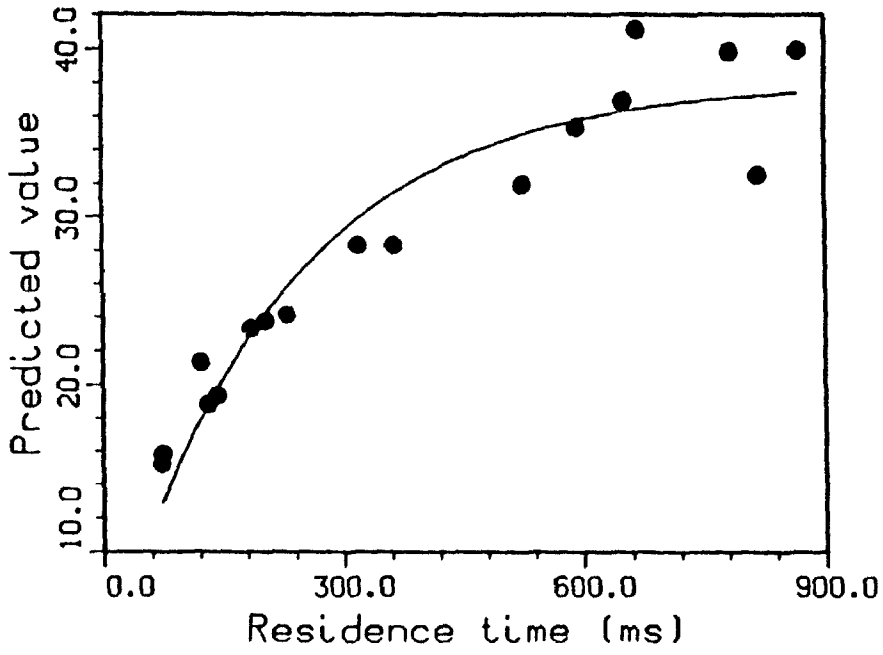

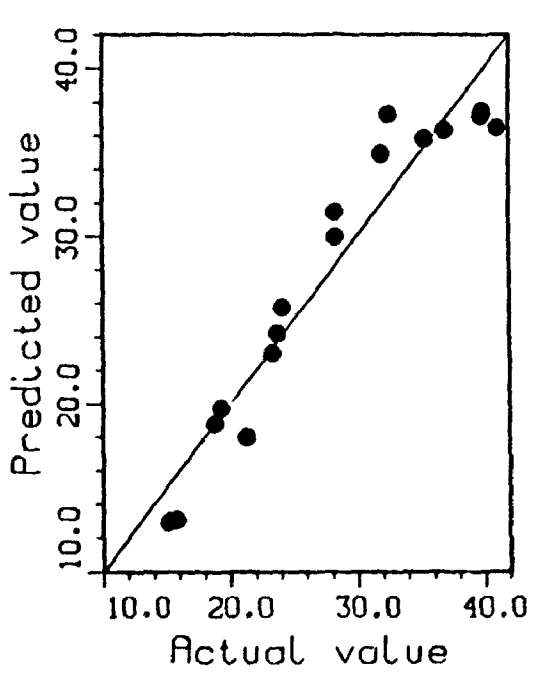

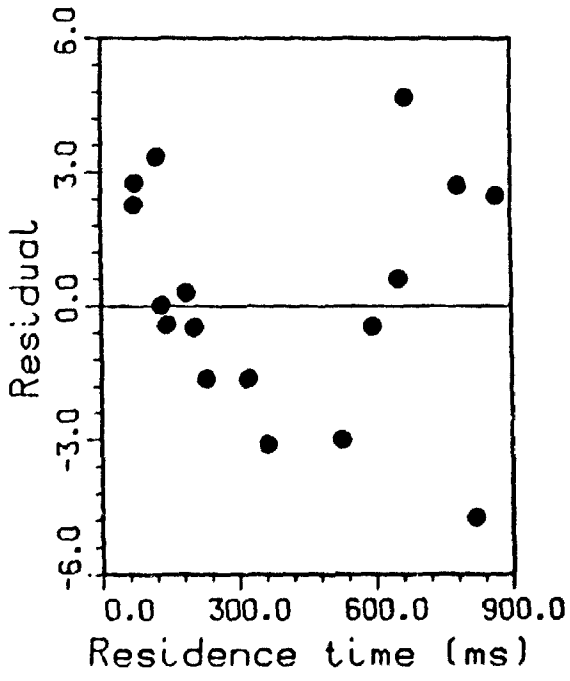

Figure A7.3.10. Prompt Gas Kinetic Model For CO from Cellulose: Fast Pyrolysis at 700 °C

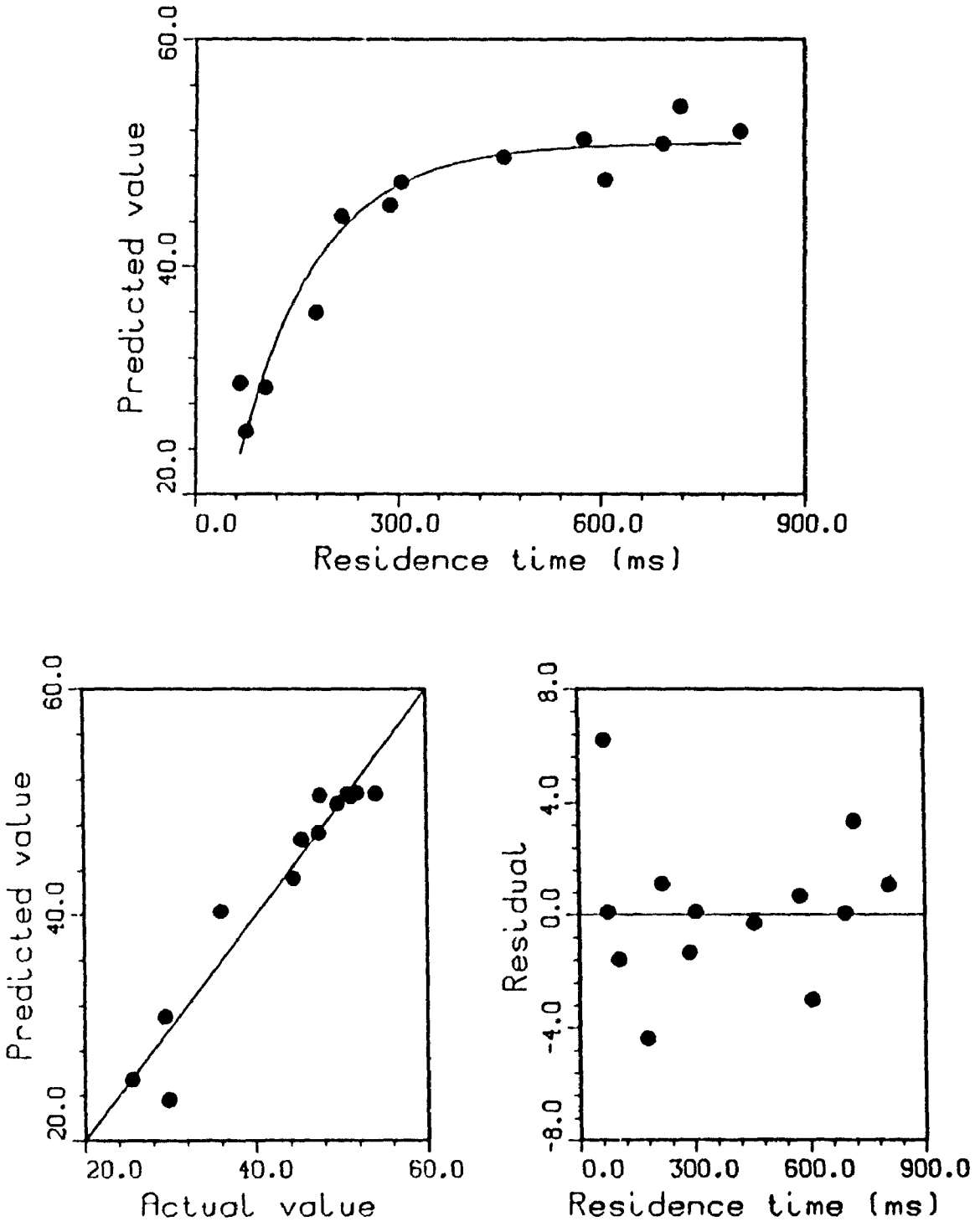

Figure A7.3.11. Prompt Gas Kinetic Model For CO from Cellulose: Fast Pyrolysis at 750 °C

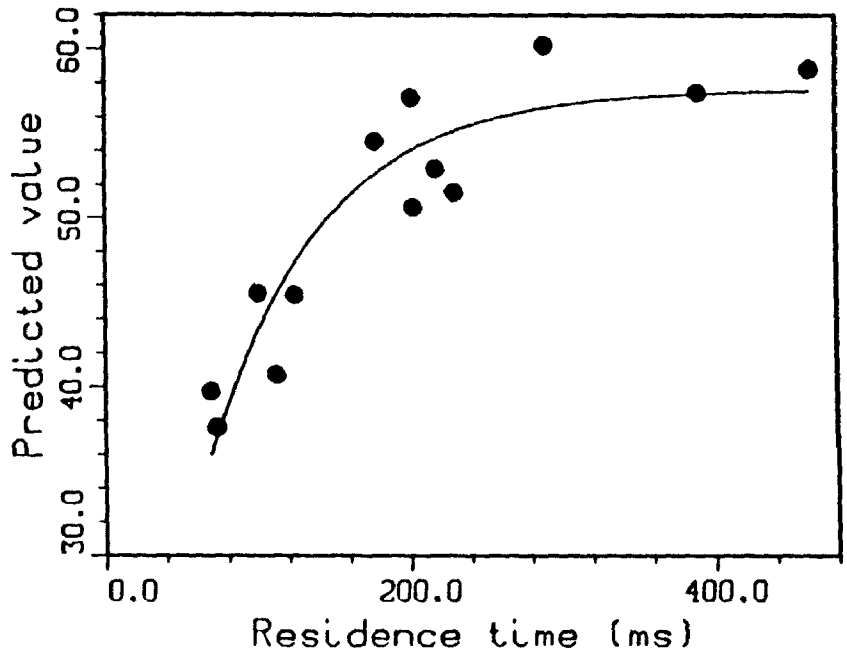

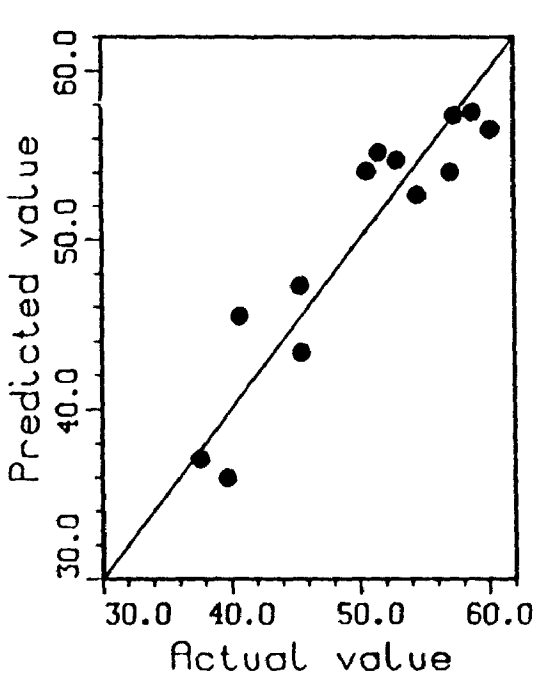

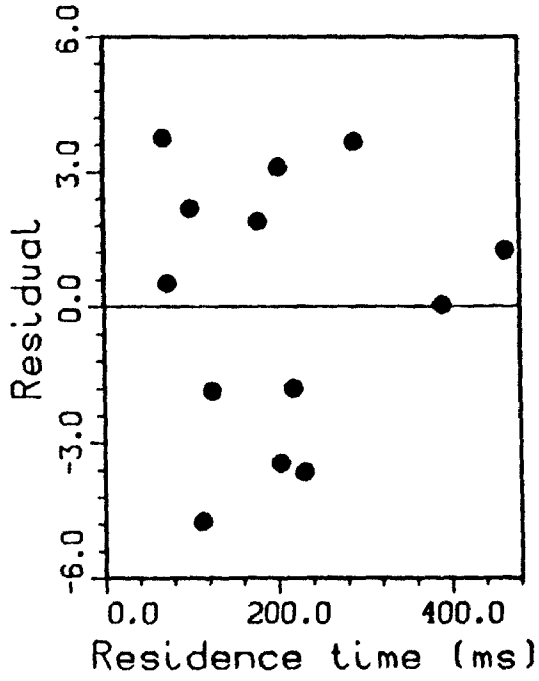

Figure A7.3.12. Prompt Gas Kinetic Model For CO from Cellulose: Fast Pyrolysis at 800 °C

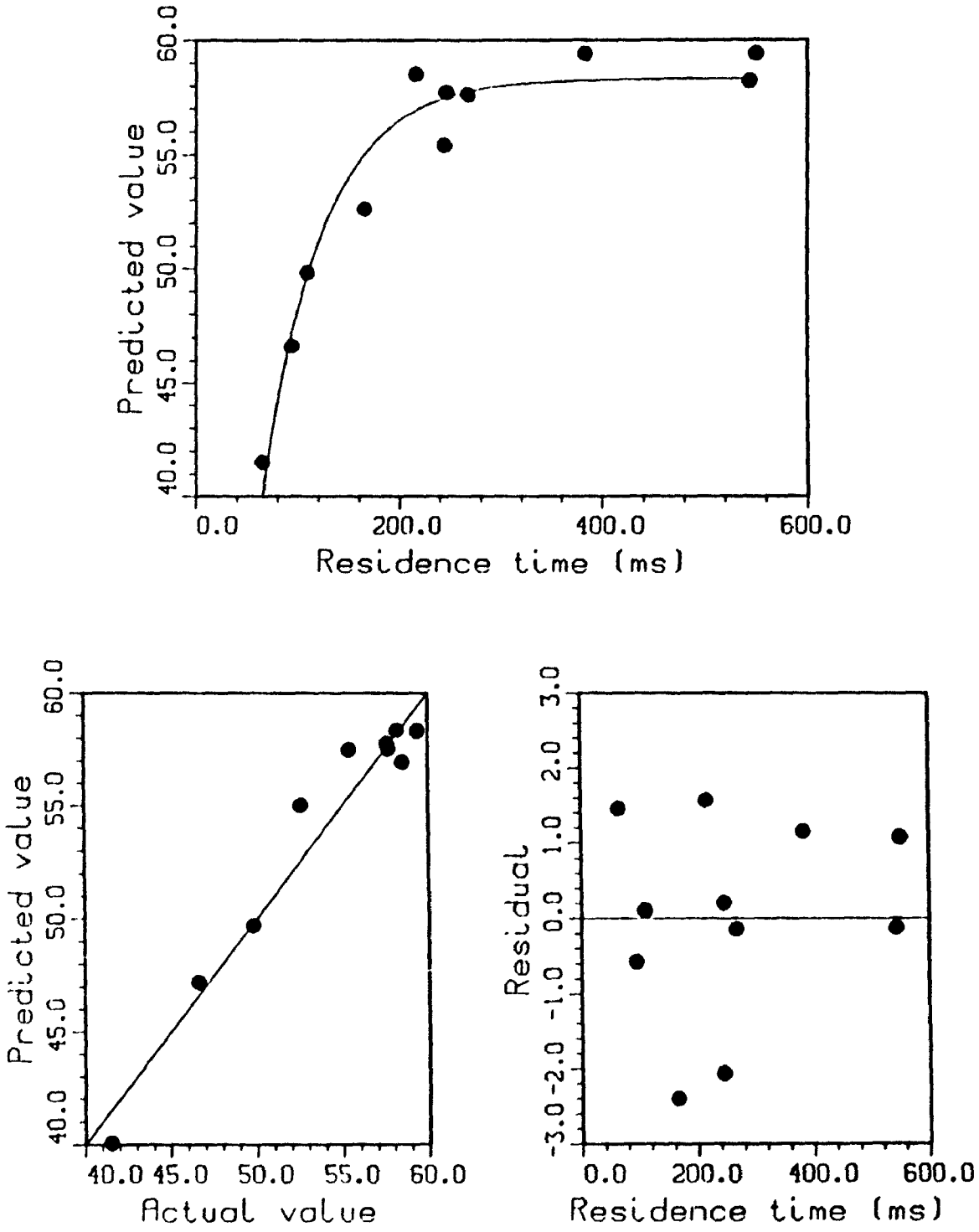

Figure A7.3.13. Prompt Gas Kinetic Model For CO from Cellulose: Fast Pyrolysis at 825 °C

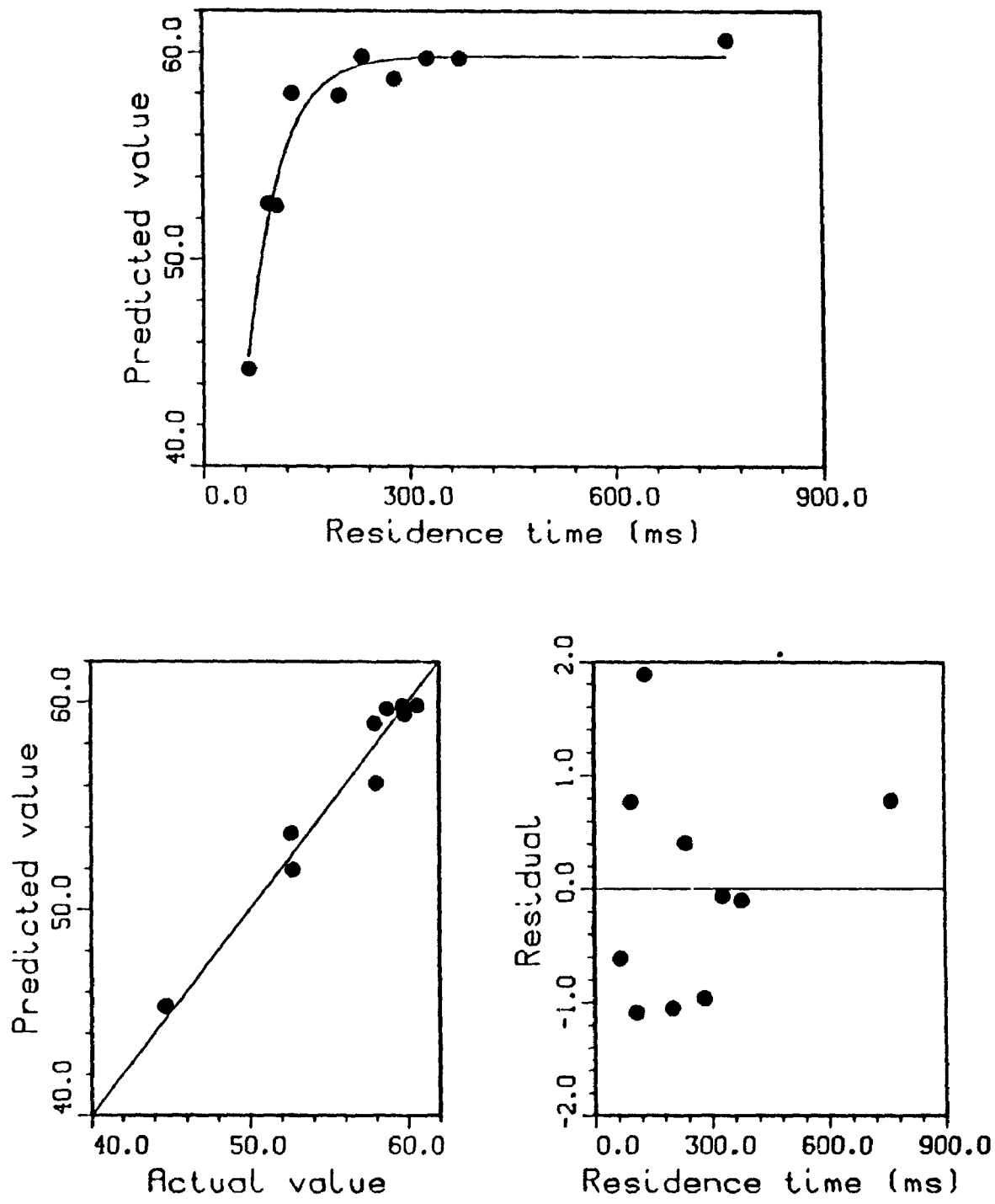

Figure A7.3.14. Prompt Gas Kinetic Model For CO from Cellulose: Fast Pyrolysis at 850 °C

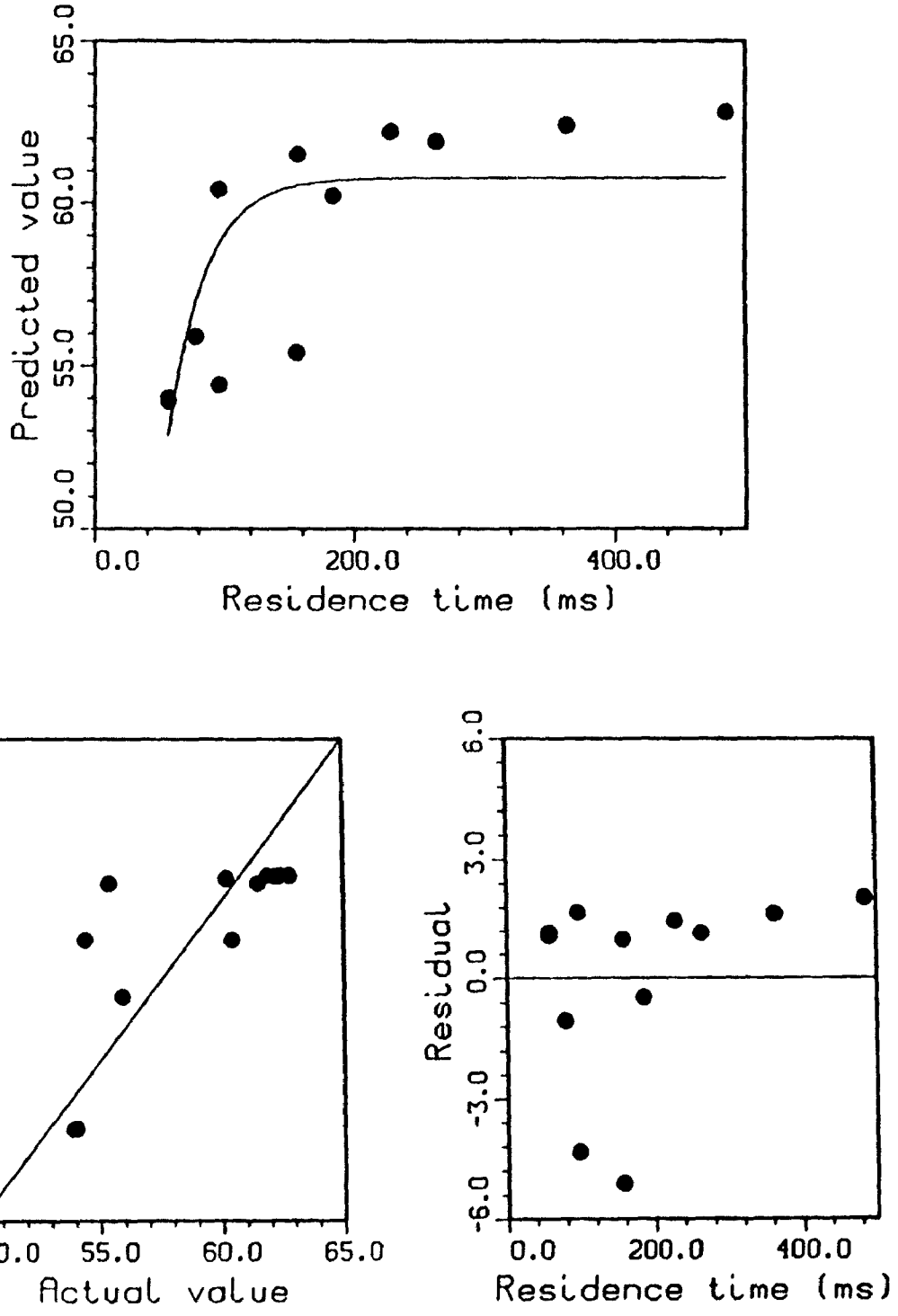

Figure A7.3.15. Prompt Gas Kinetic Model For CO from Cellulose: Fast Pyrolysis at 875 °C

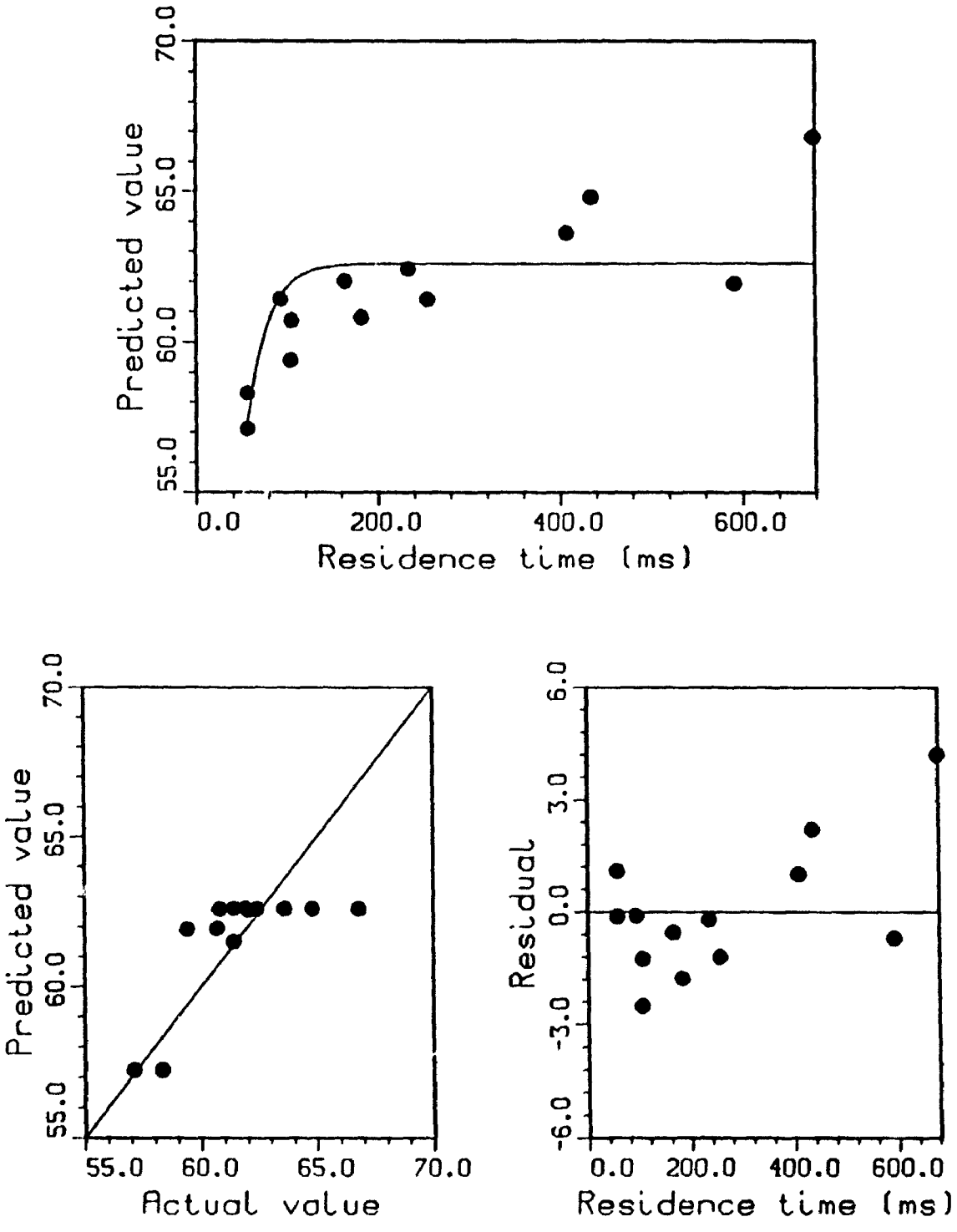

Figure A7.3.16. Prompt Gas Kinetic Model For CO from Cellulose: Fast Pyrolysis at 900 °C

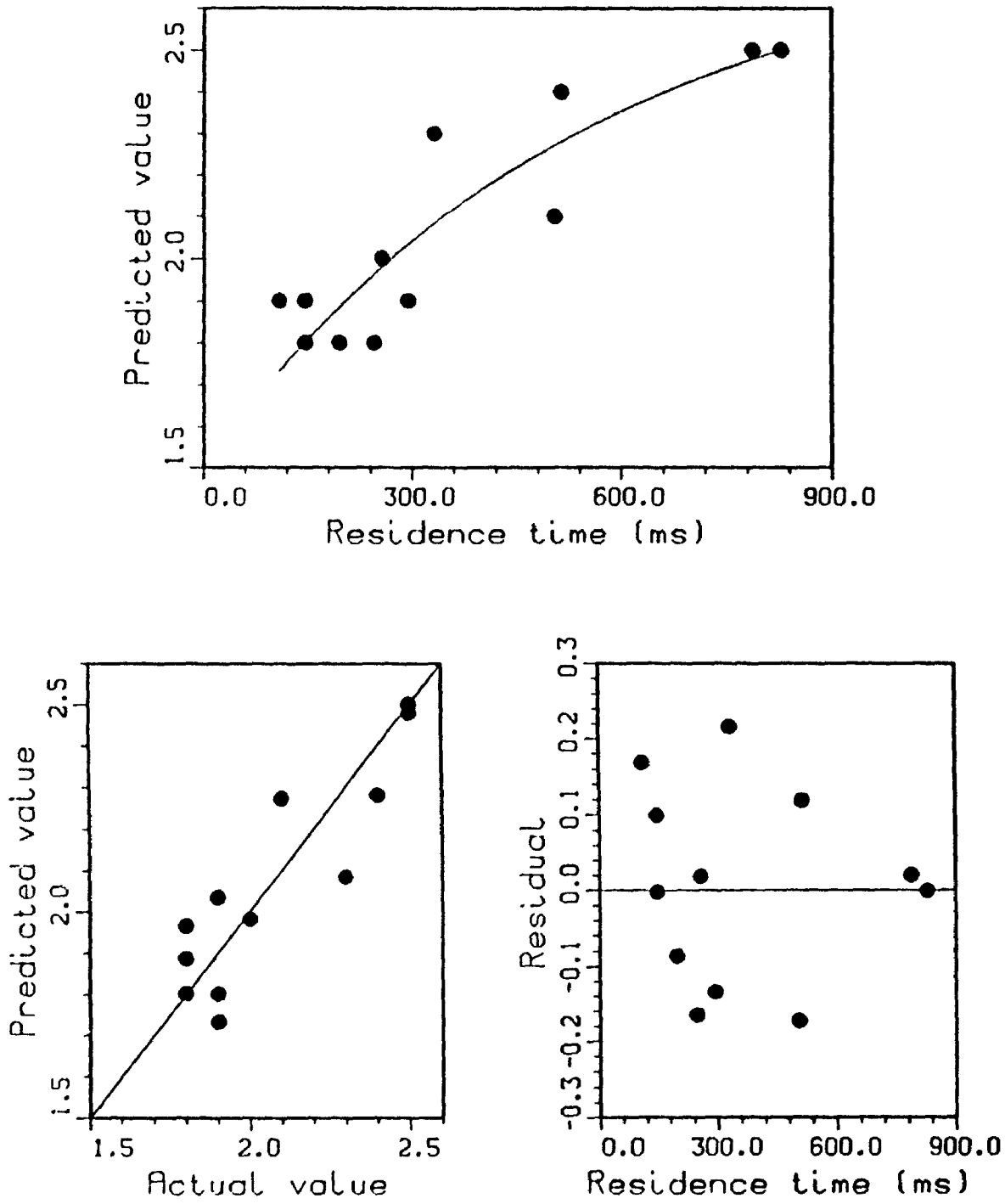

Figure A7.3.17. Prompt Gas Kinetic Model For CO_2 from Cellulose: Fast Pyrolysis at 650 °C

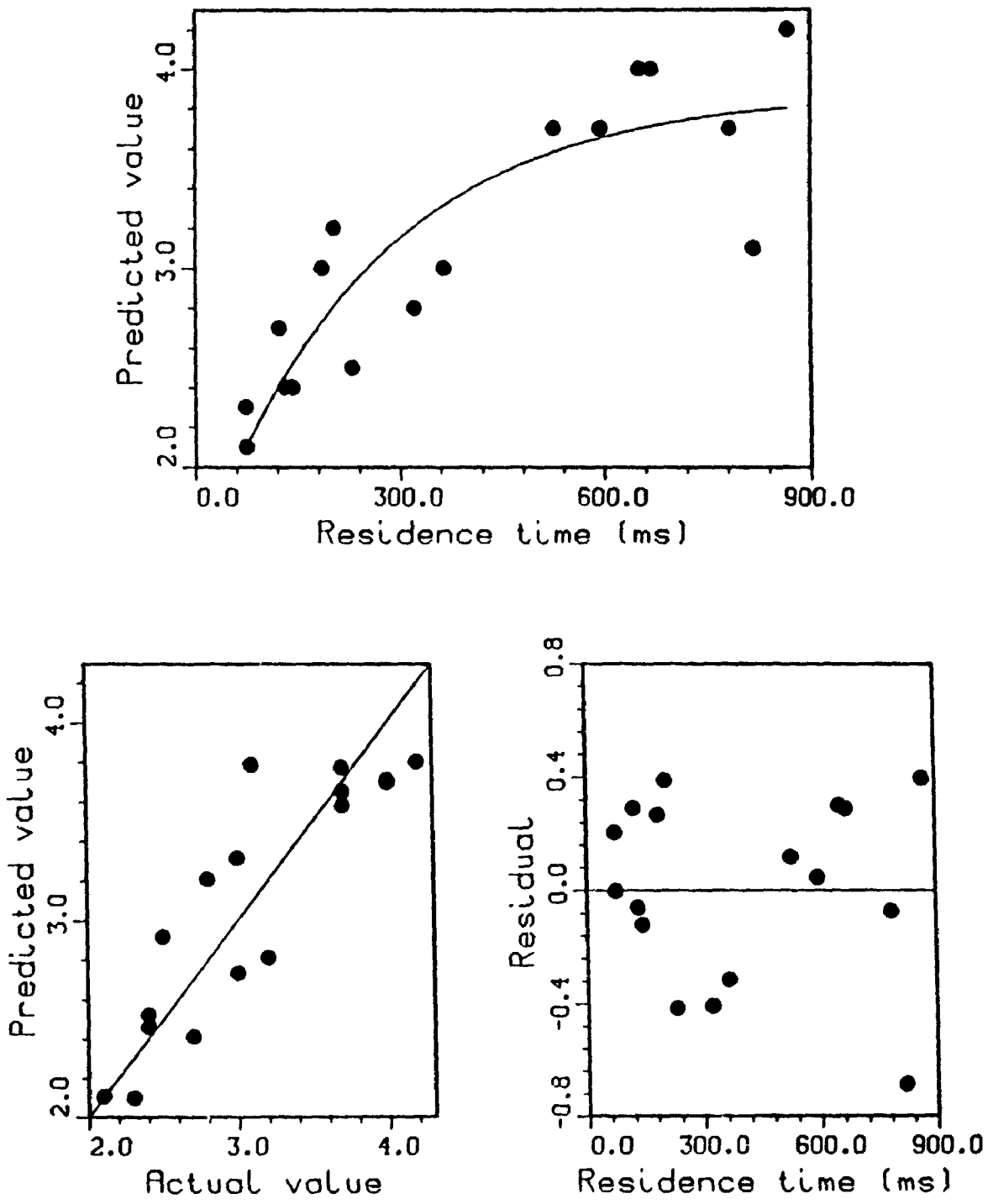

Figure A7.3.18. Prompt Gas Kinetic Model For CO_2 from Cellulose: Fast Pyrolysis at 700 °C

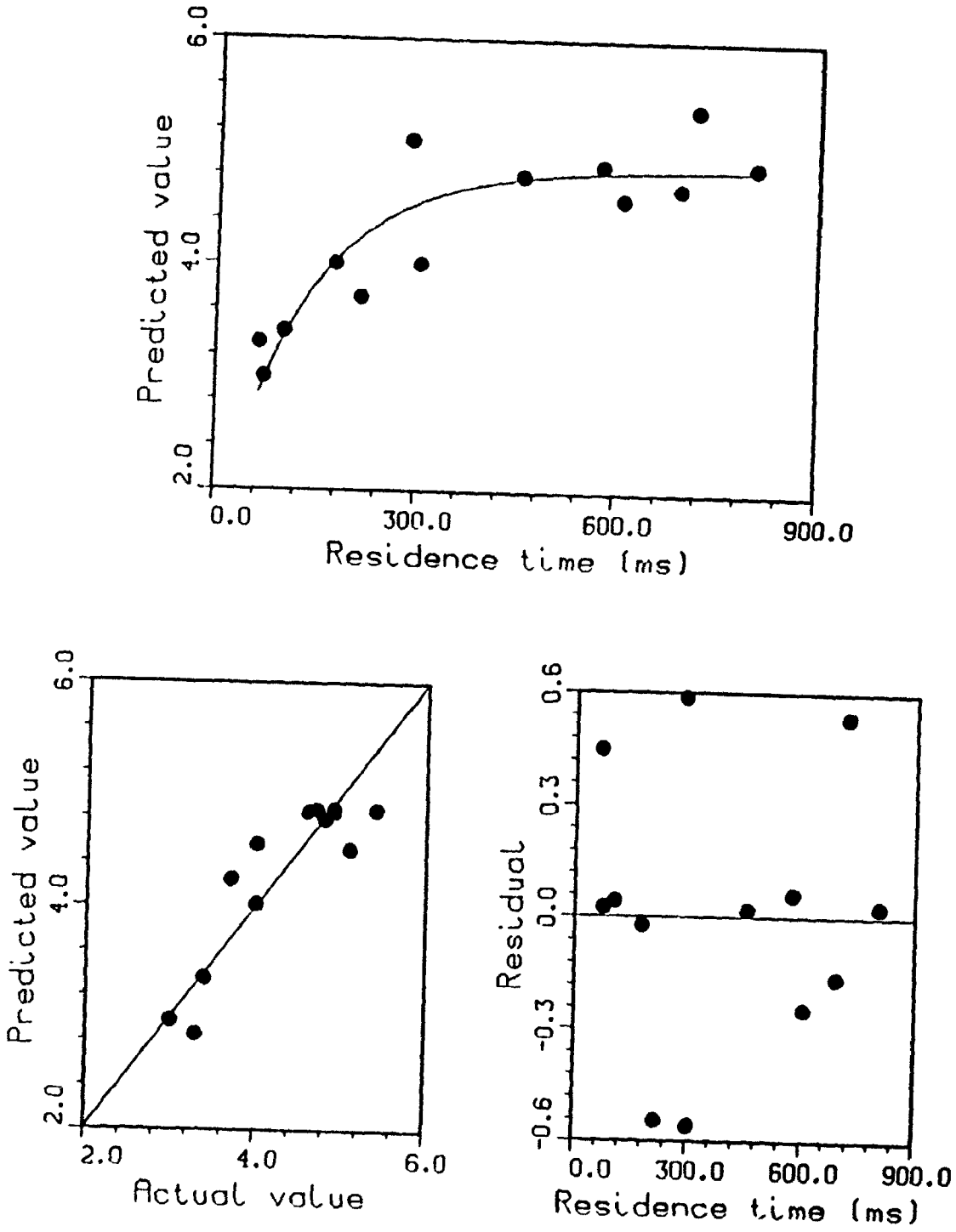

Figure A7.3.19. Prompt Gas Kinetic Model For CO_2 from Cellulose: Fast Pyrolysis at 750 °C

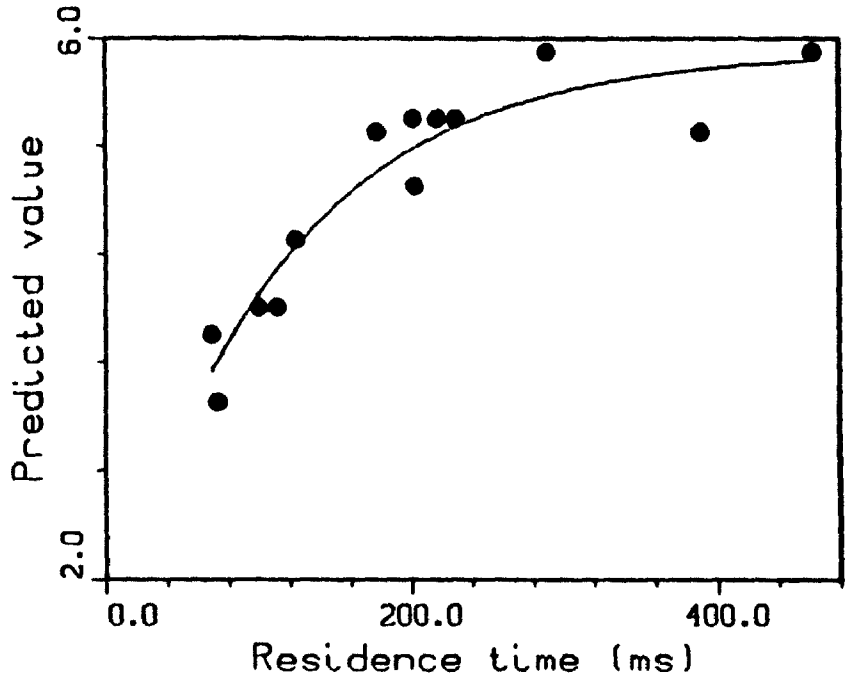

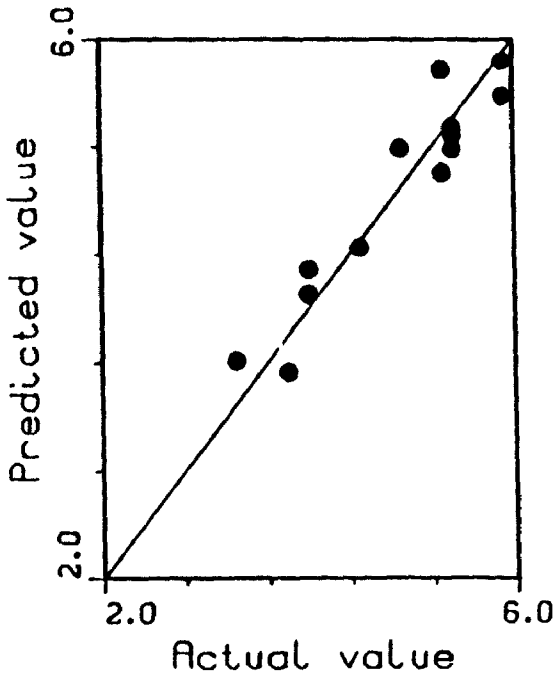

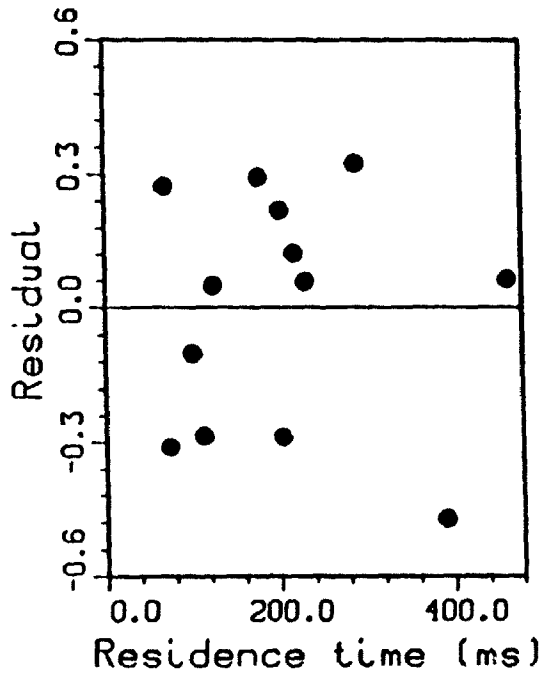

Figure A7.3.20. Prompt Gas Kinetic Model For CO_2 from Cellulose: Fast Pyrolysis at 800 °C

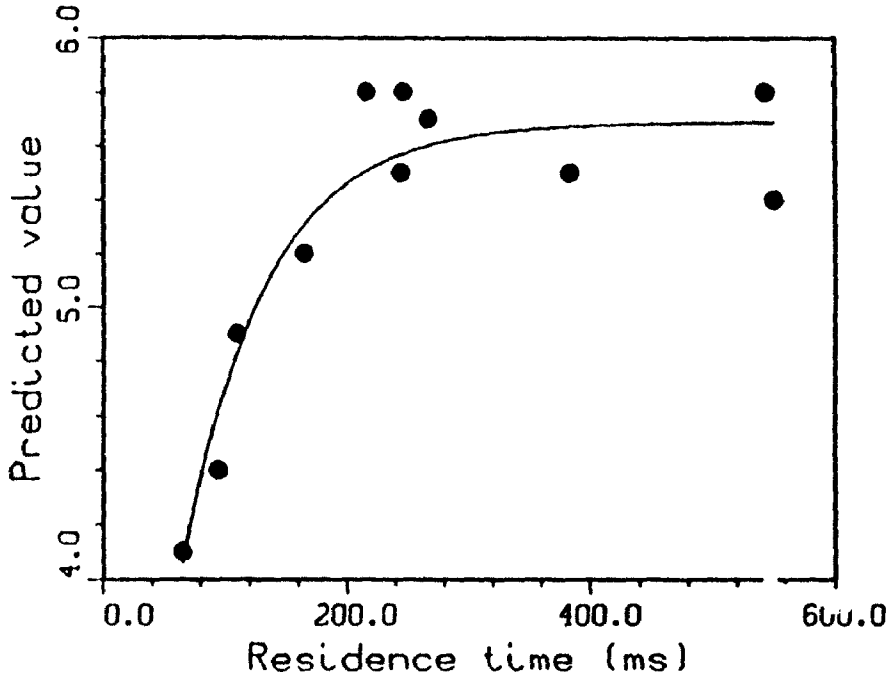

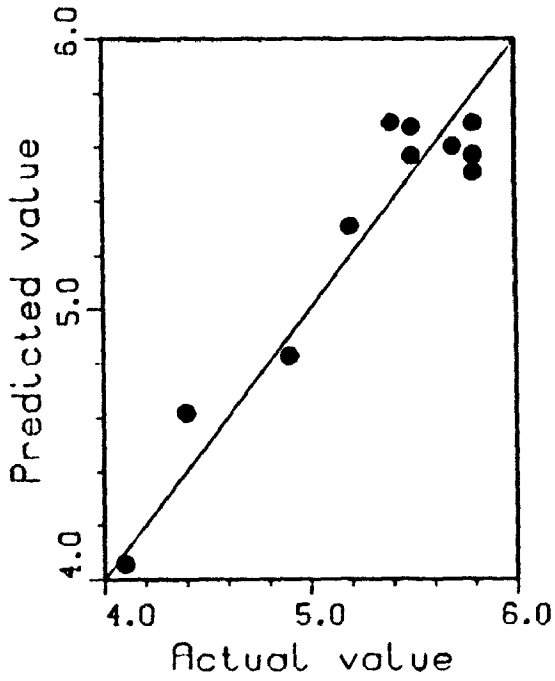

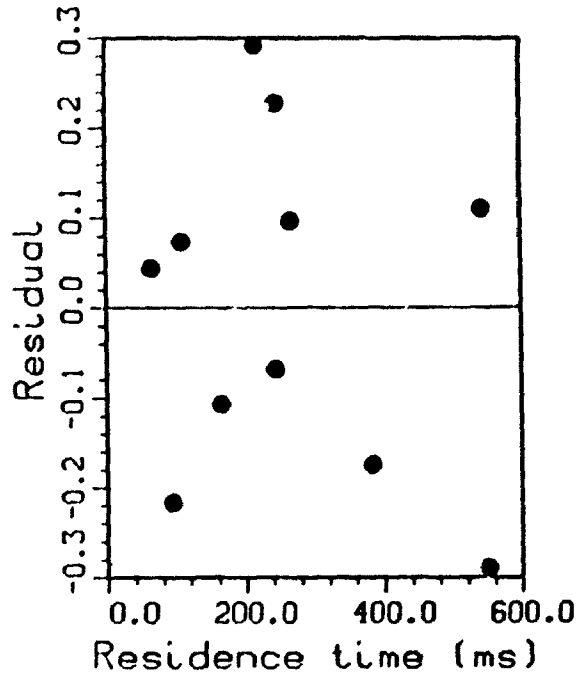

Figure A7.3.21. Prompt Gas Kinetic Model For CO_2 from Cellulose: Fast Pyrolysis at 825 °C

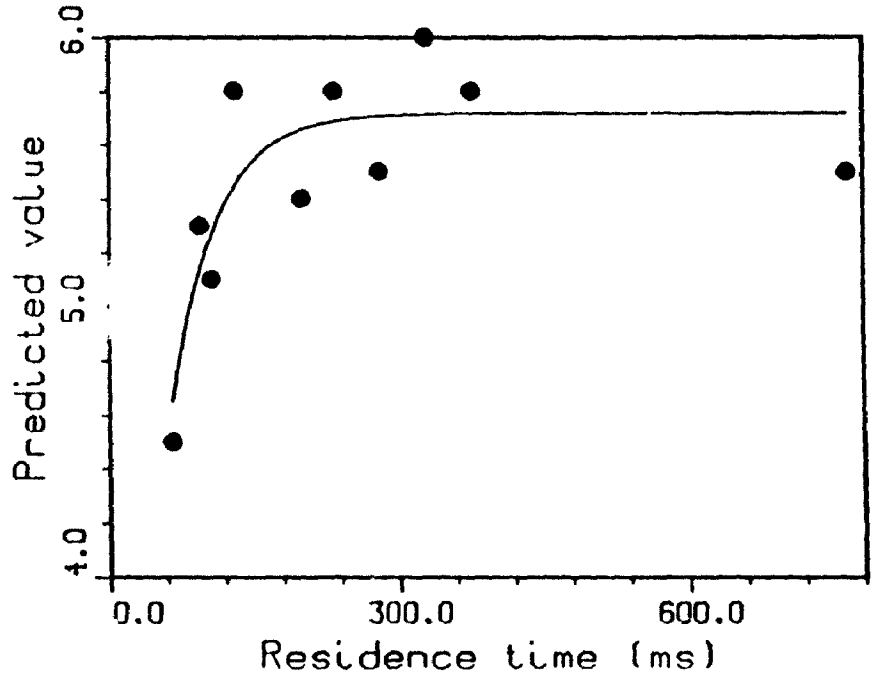

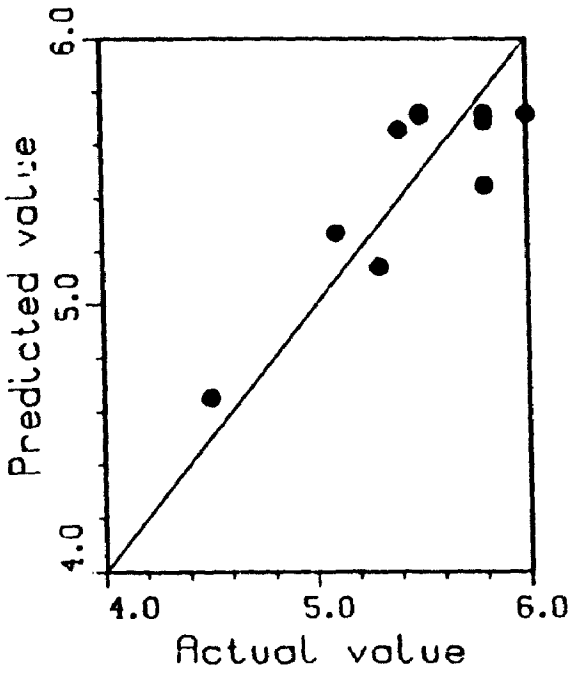

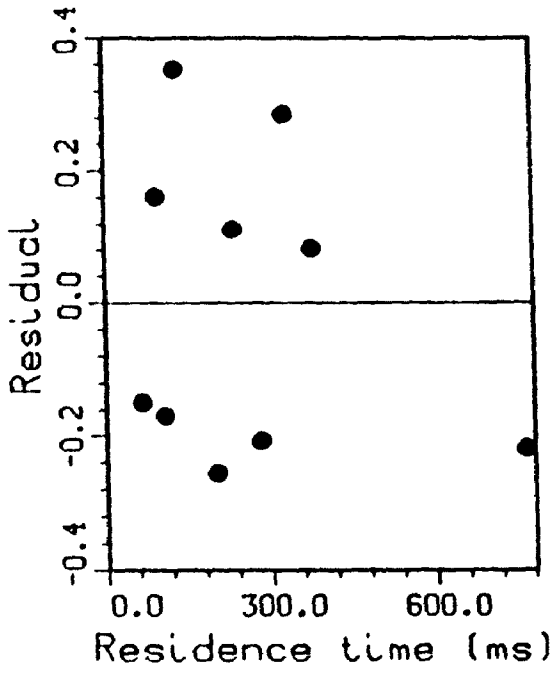

Figure A7.3.22. Prompt Gas Kinetic Model For CO_2 from Cellulose: Fast Pyrolysis at 850 °C

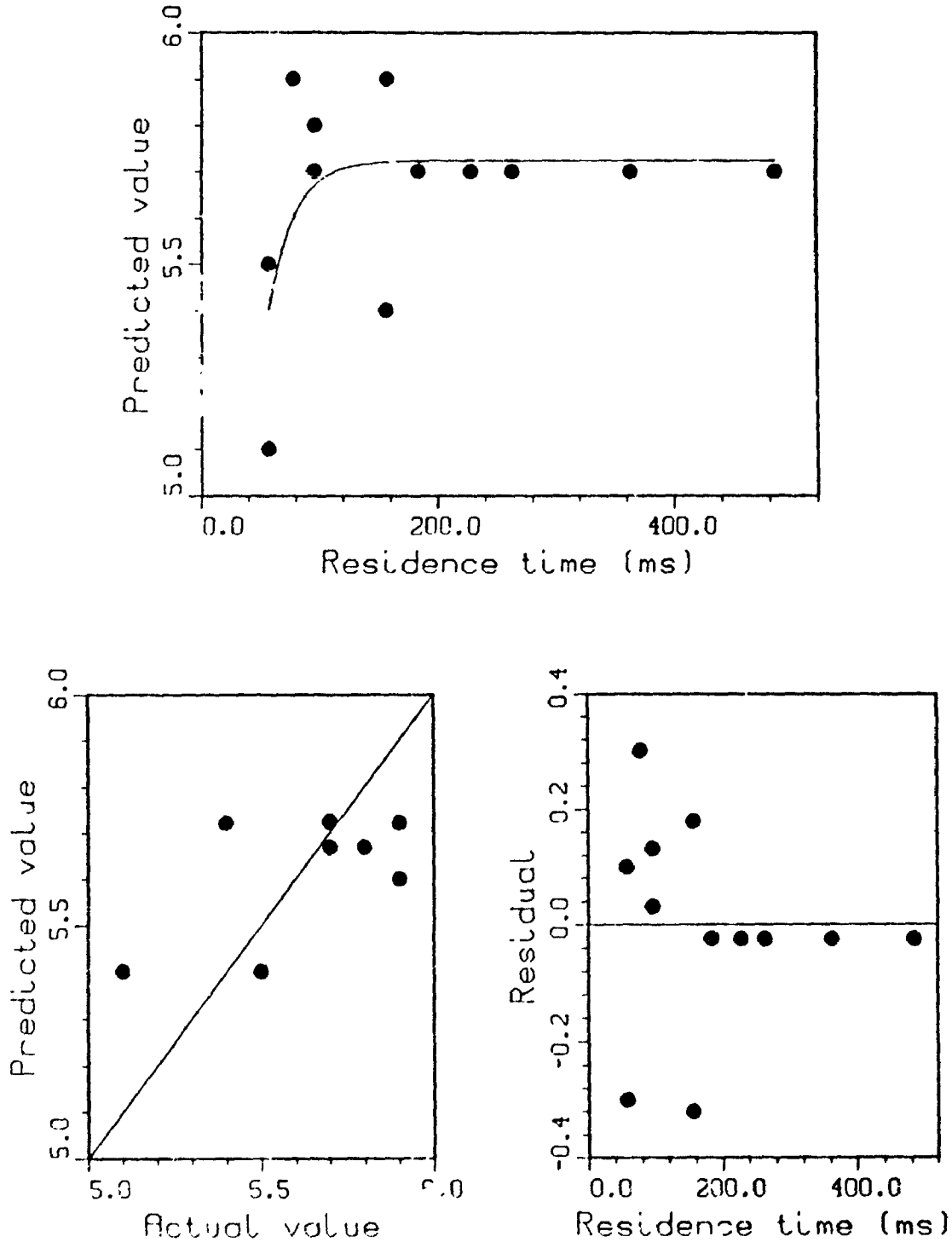

Figure A7.3.23. Prompt Gas Kinetic Model For CO_2 from Cellulose: Fast Pyrolysis at 875 °C

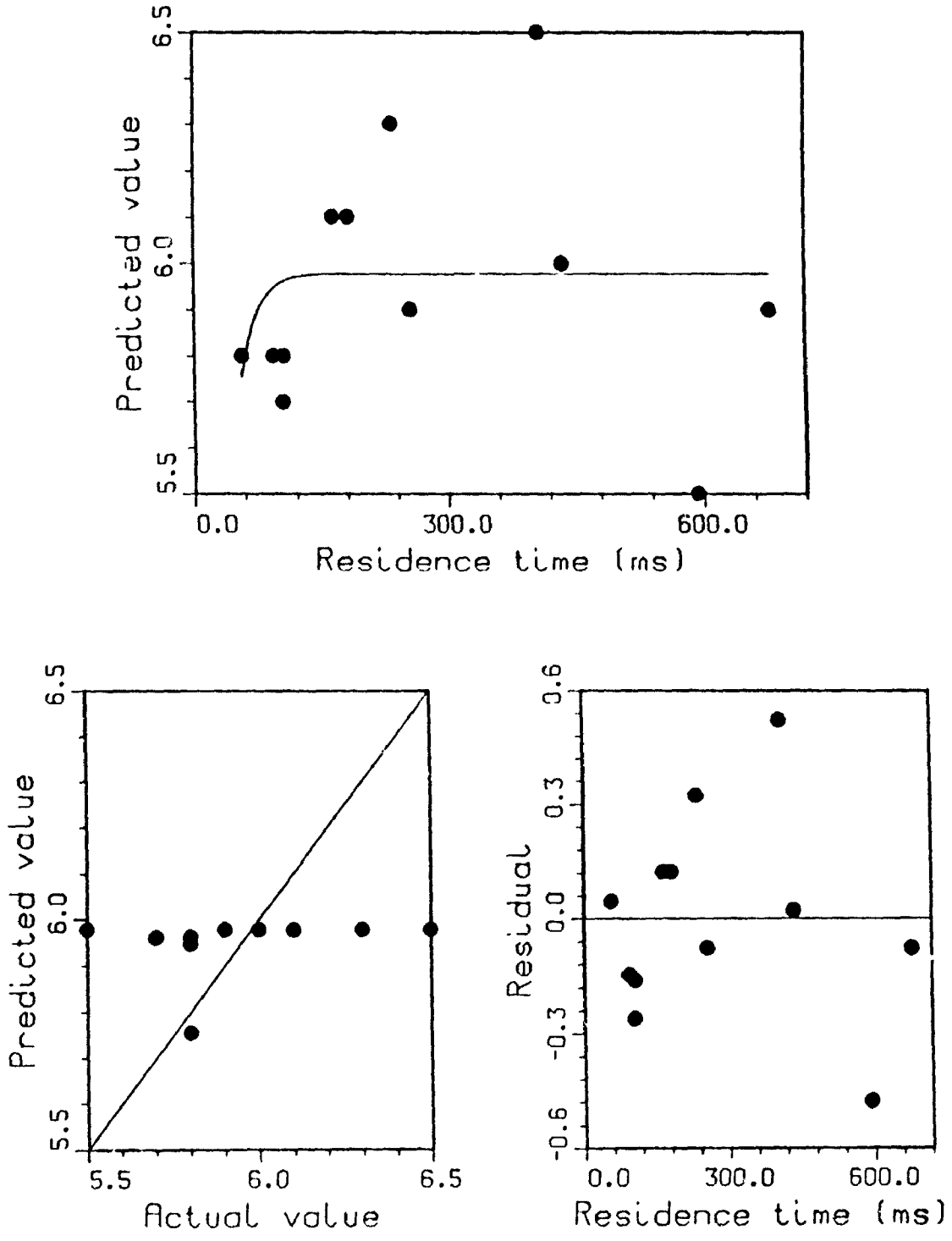

Figure A7.3.24. Prompt Gas Kinetic Model For CO_2 from Cellulose: Fast Pyrolysis at 900 °C

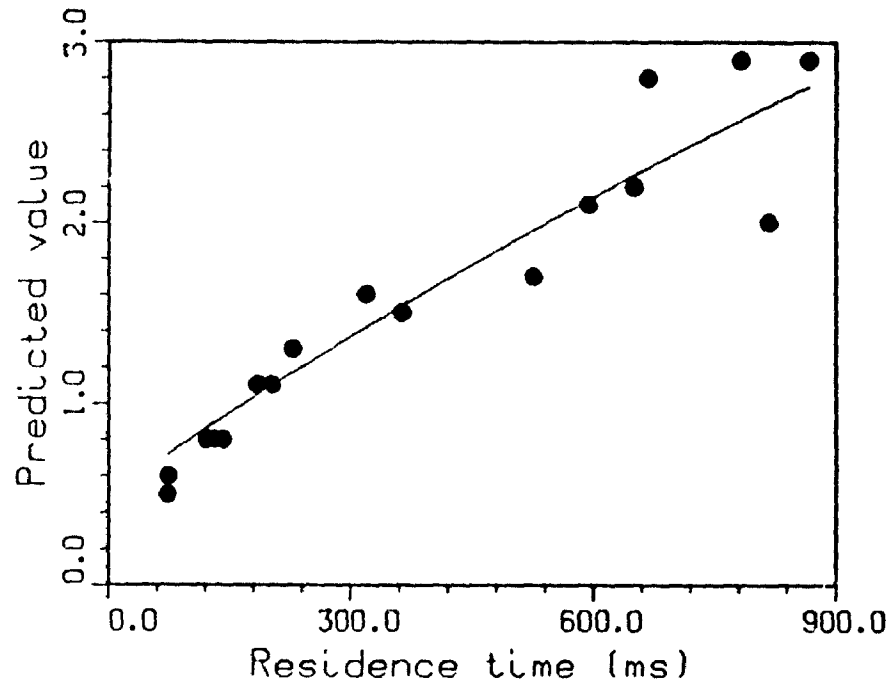

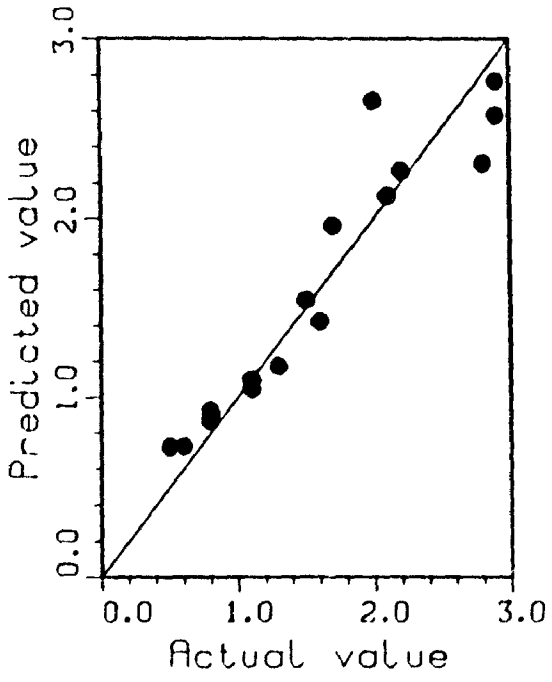

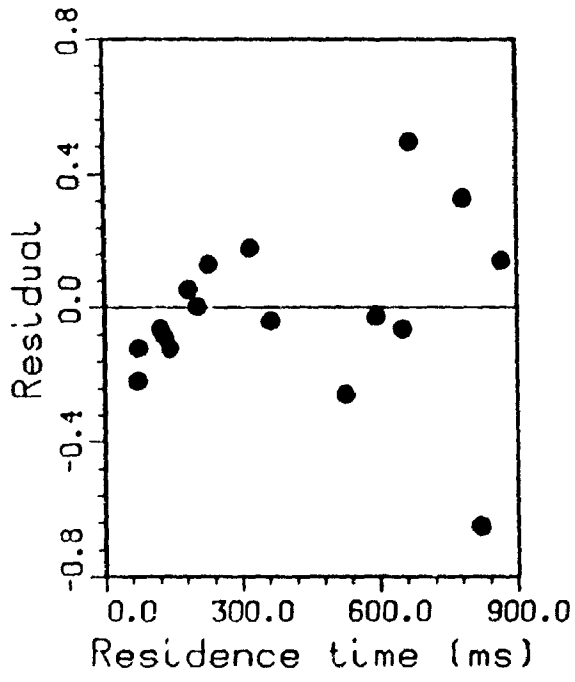

Figure A7.3.25. Prompt Gas Kinetic Model For CH_4 from Cellulose: Fast Pyrolysis at 700 °C

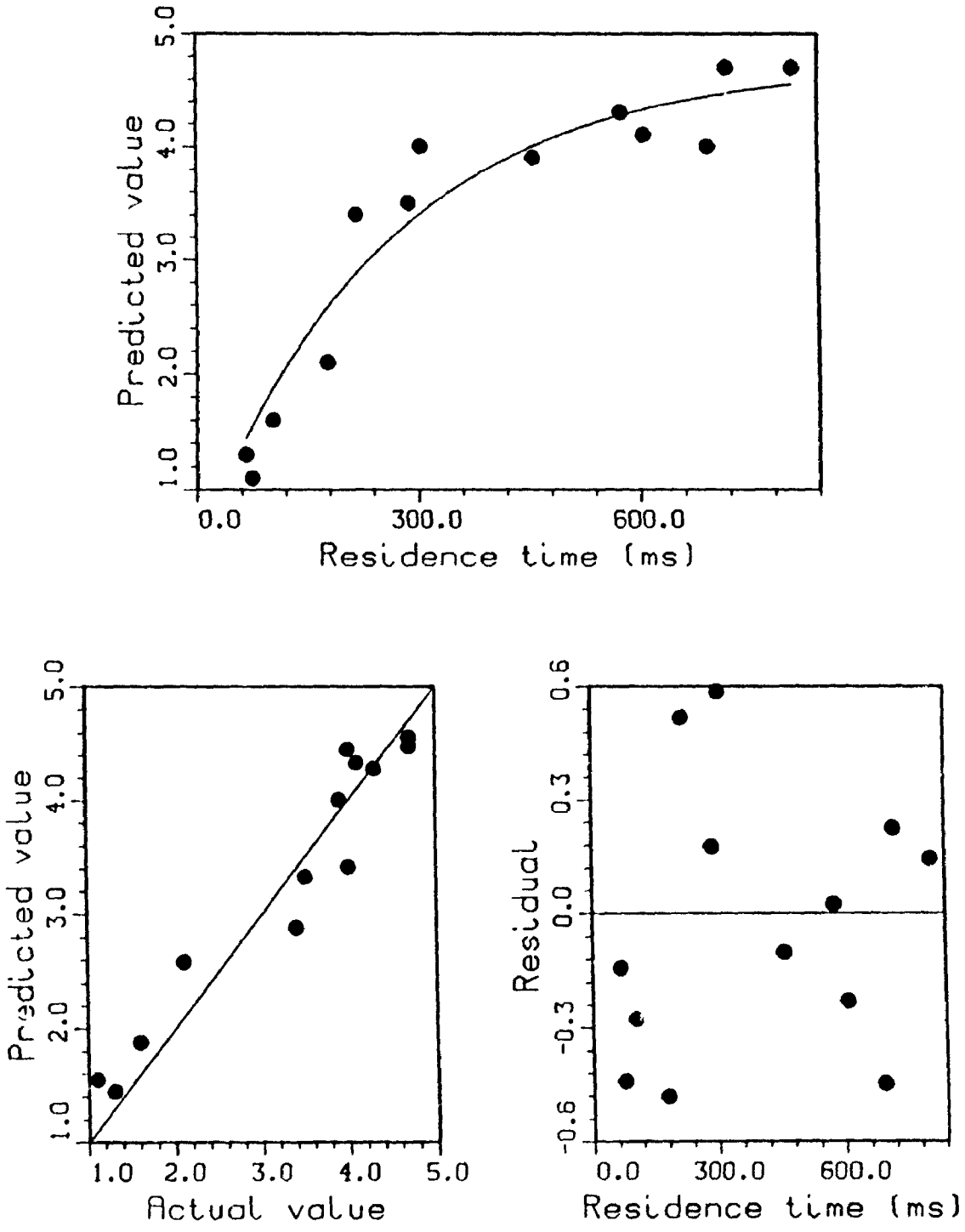

Figure A7.3.26. Prompt Gas Kinetic Model For CH_4 from Cellulose: Fast Pyrolysis at 750 °C

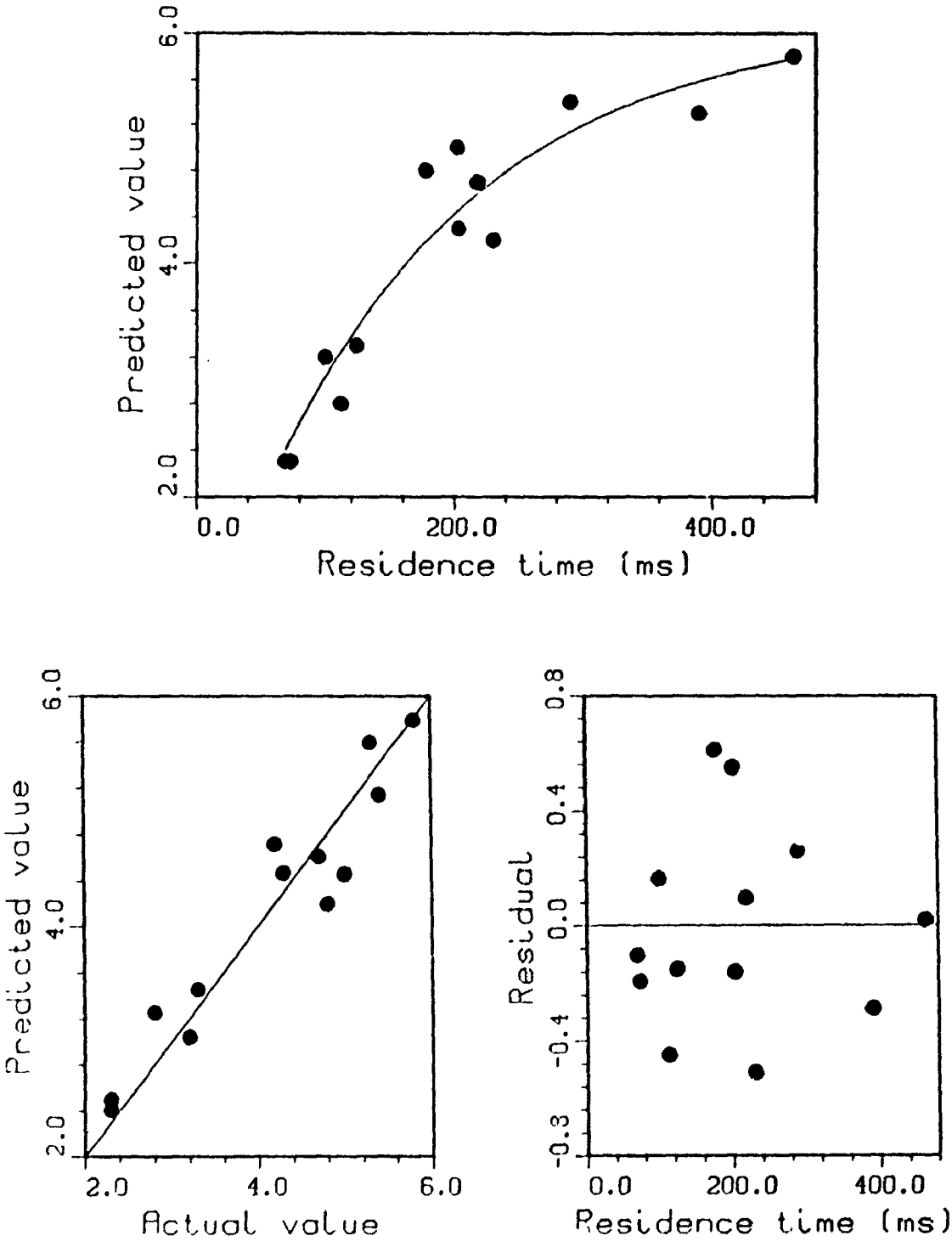

Figure A7.3.27. Prompt Gas Kinetic Model For CH_4 from Cellulose: Fast Pyrolysis at 800 °C

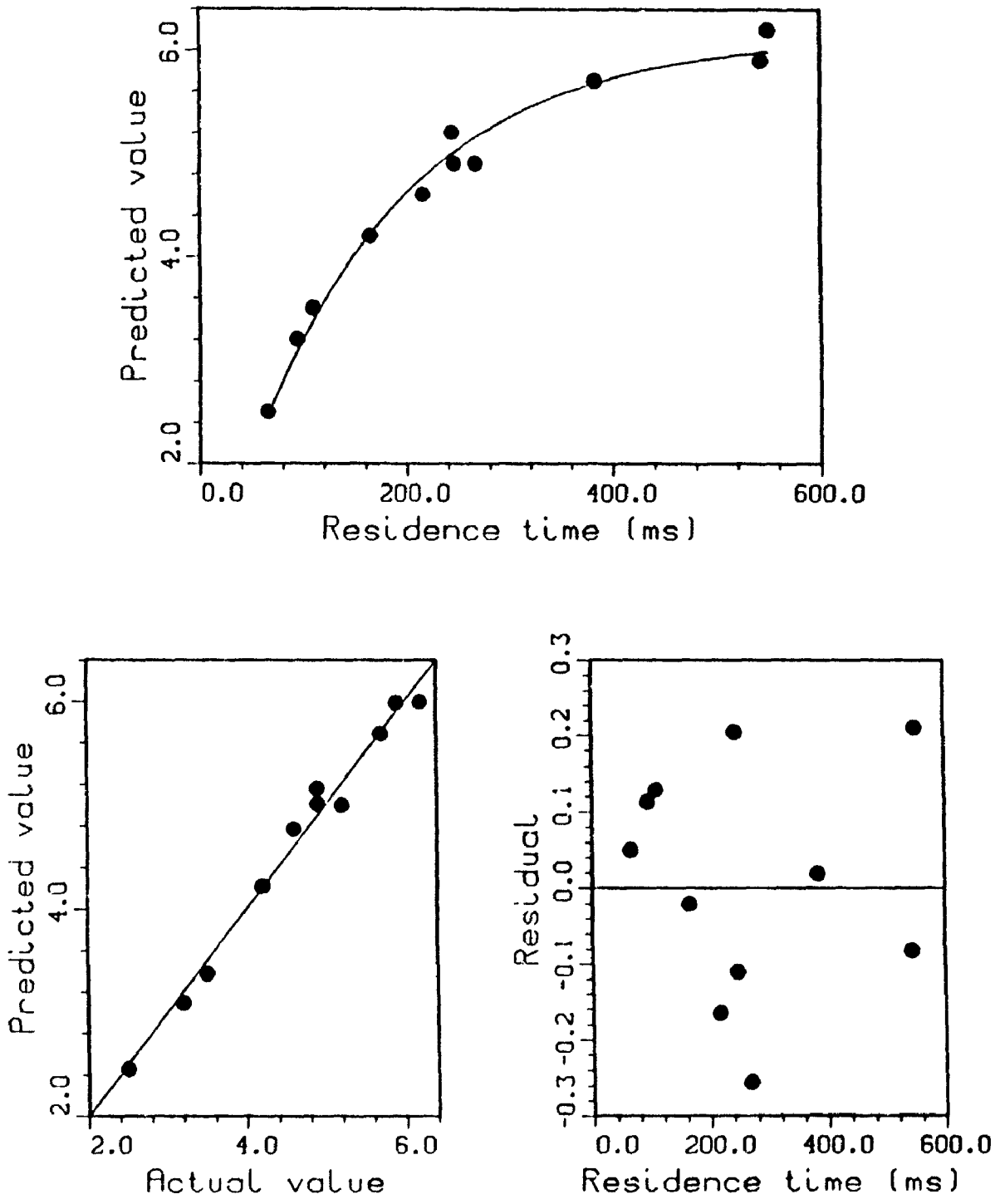

Figure A7.3.28. Prompt Gas Kinetic Model For CH_4 from Cellulose: Fast Pyrolysis at 825 °C

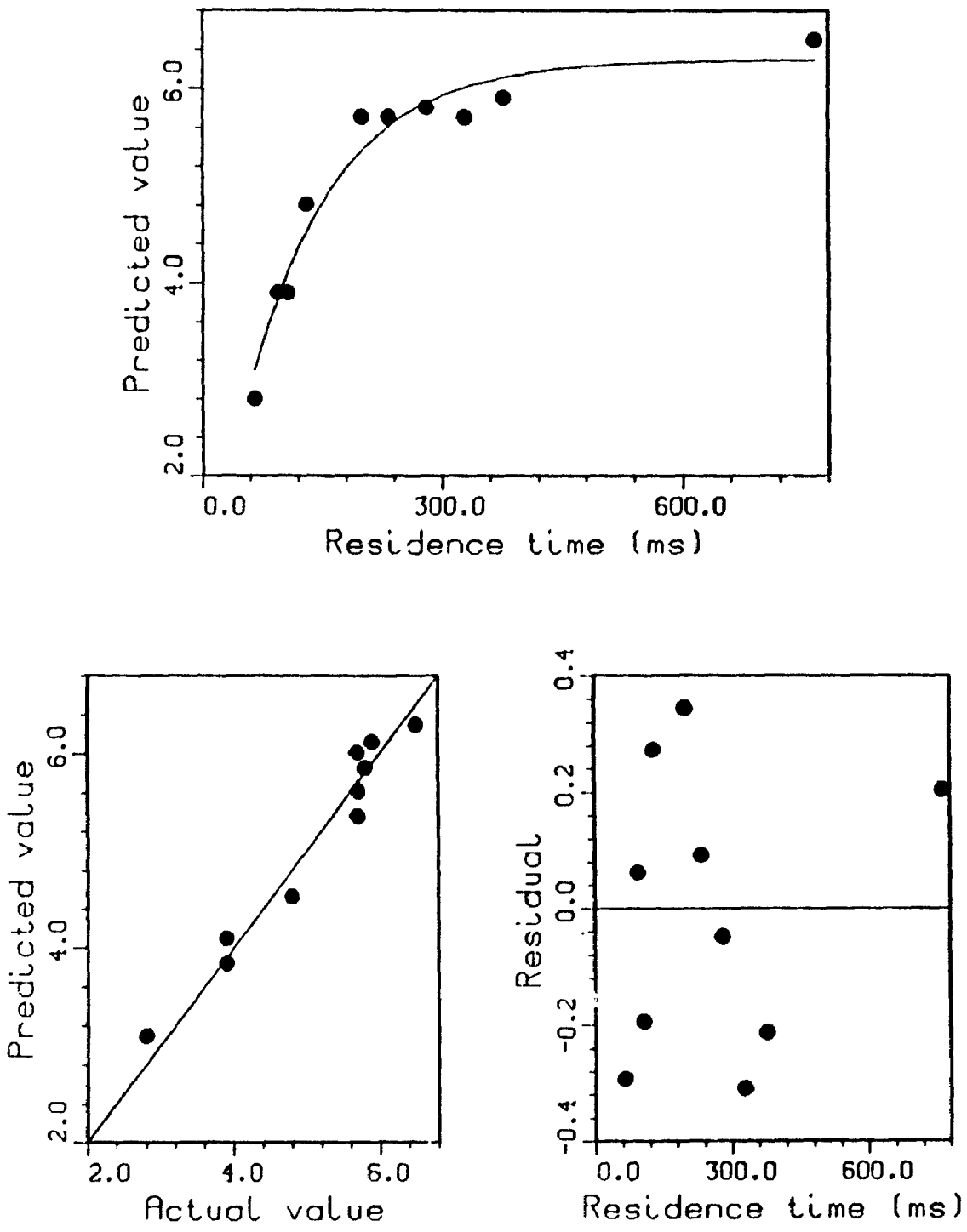

Figure A7.3.29. Prompt Gas Kinetic Model For CH_4 from Cellulose: Fast Pyrolysis at 850 °C

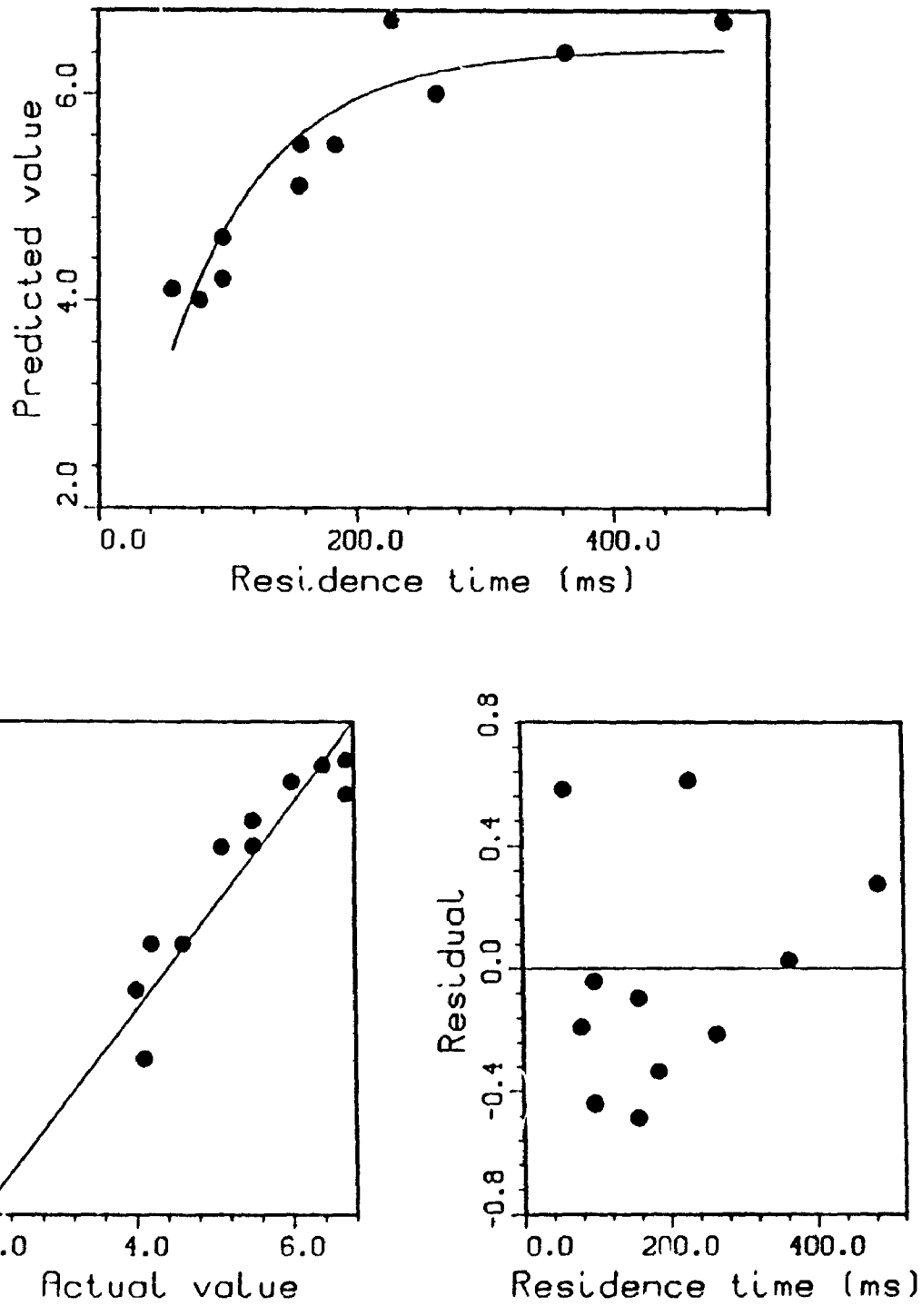

Figure A7.3.30. Prompt Gas Kinetic Model For CH_4 from Cellulose: Fast Pyrolysis at 875 °C

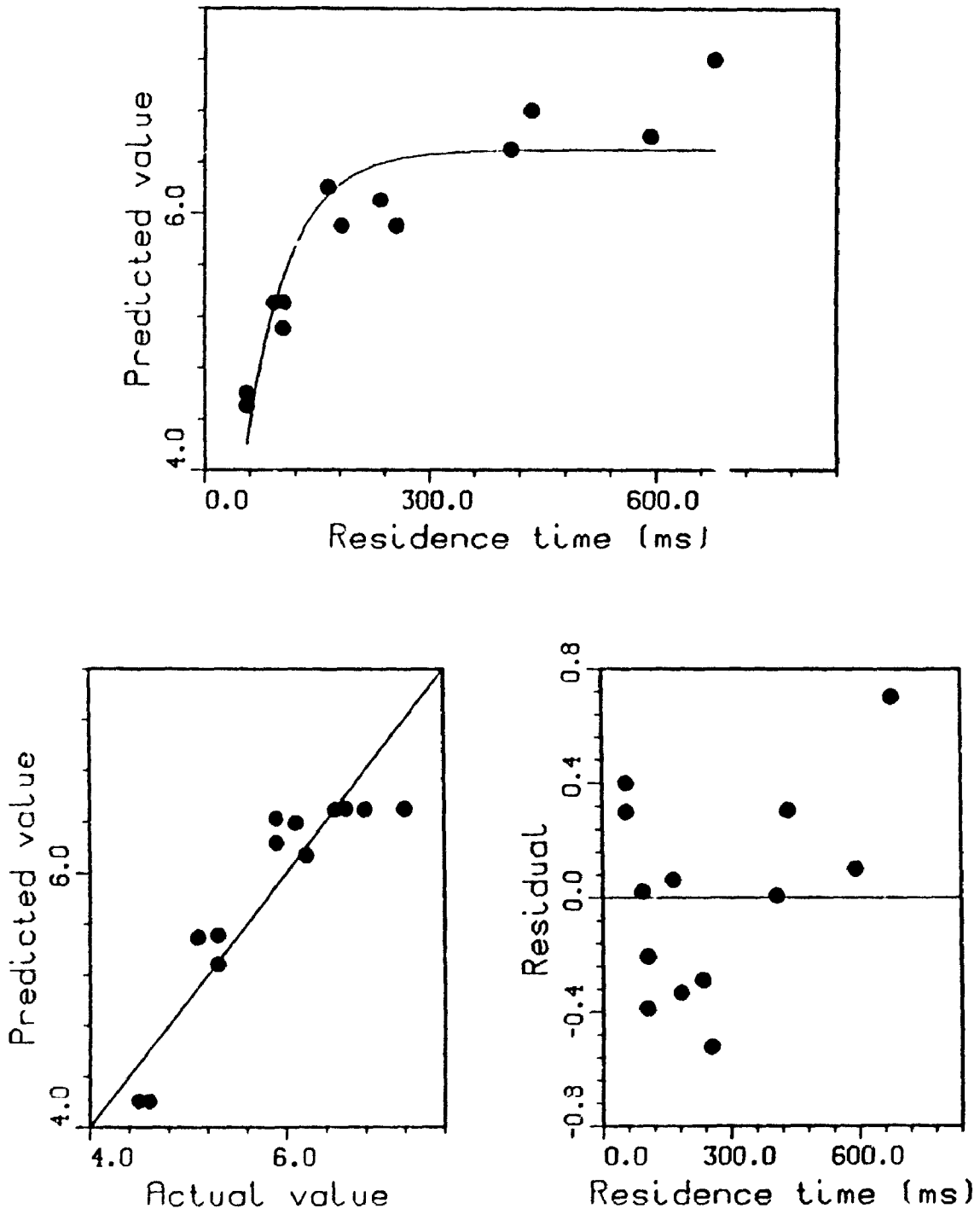

Figure A7.3.31. Prompt Gas Kinetic Model For CH_4 from Cellulose: Fast Pyrolysis at 900 °C

APPENDIX 7.4 CELLULOSE PYROLYSIS ARRHENIUS PLOTS: PROMPT GAS MODEL

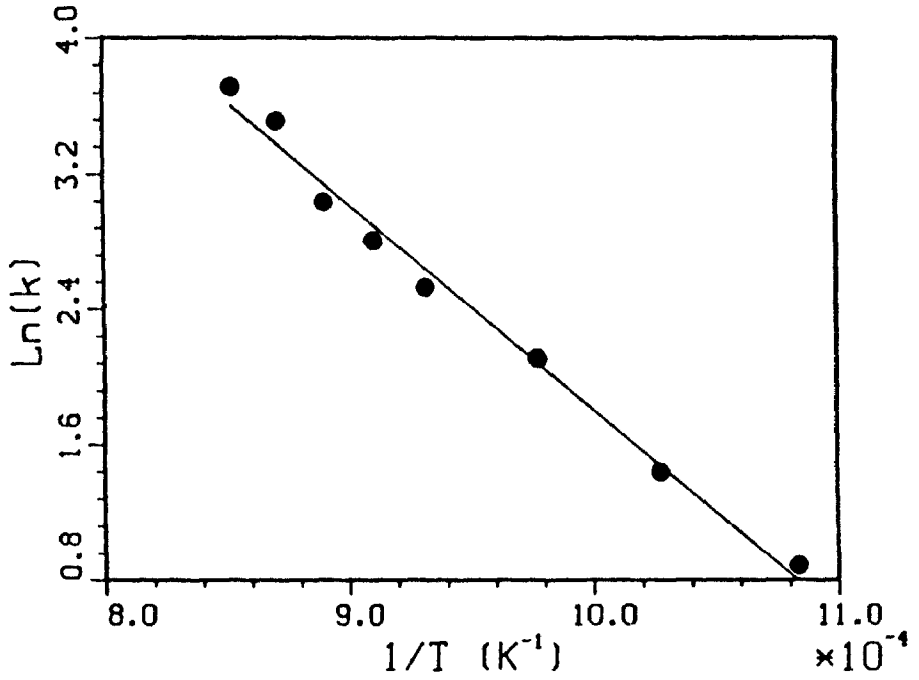

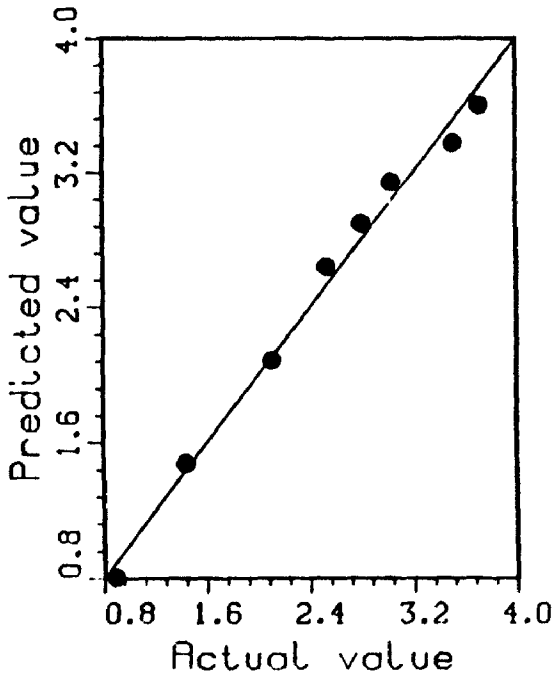

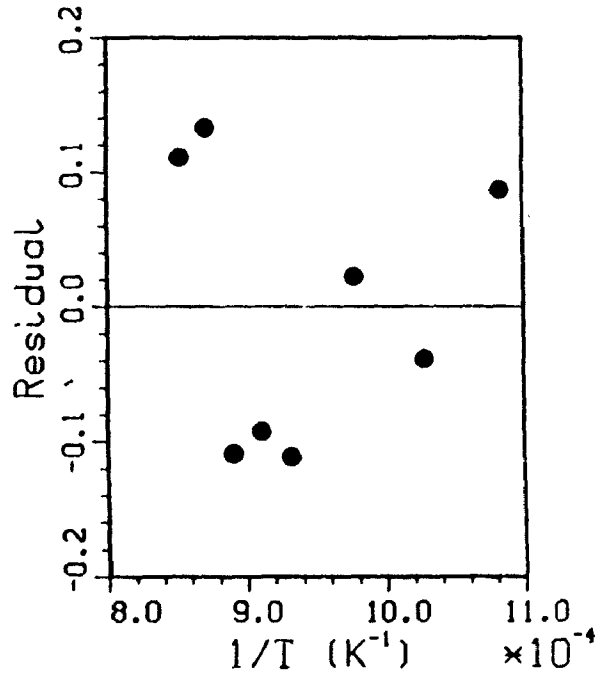

Figure A7.4.1. Prompt Gas Model for Total Gas from Cellulose: Arrhenius Plot

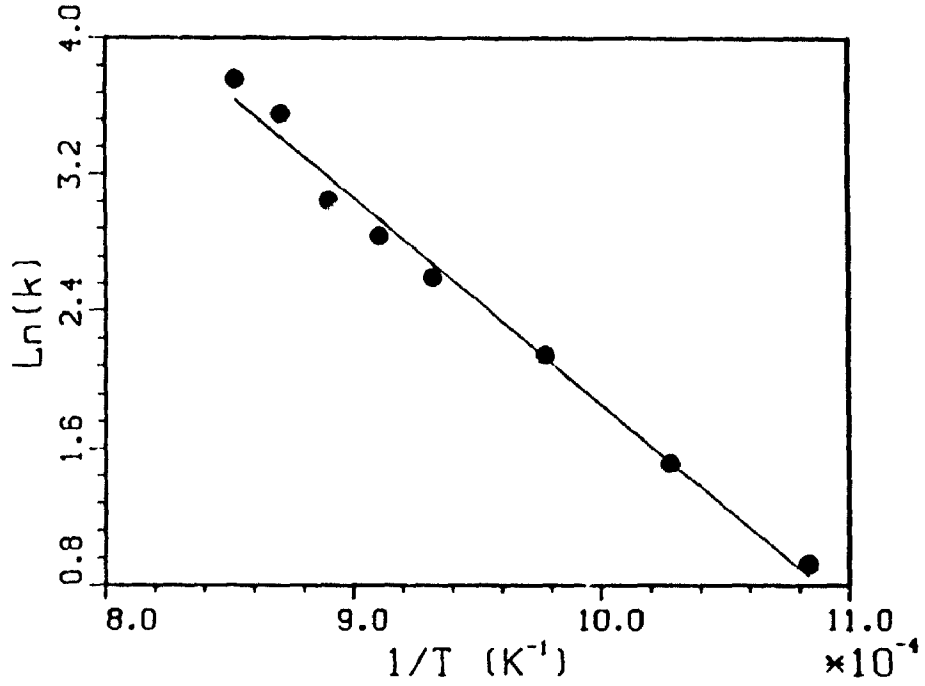

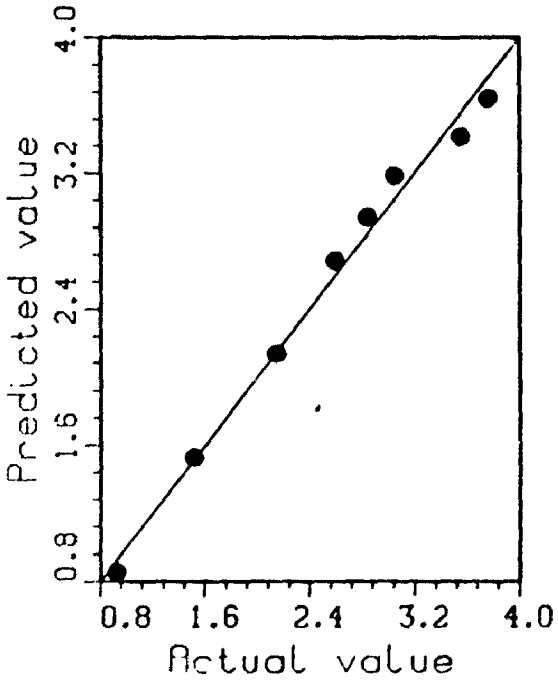

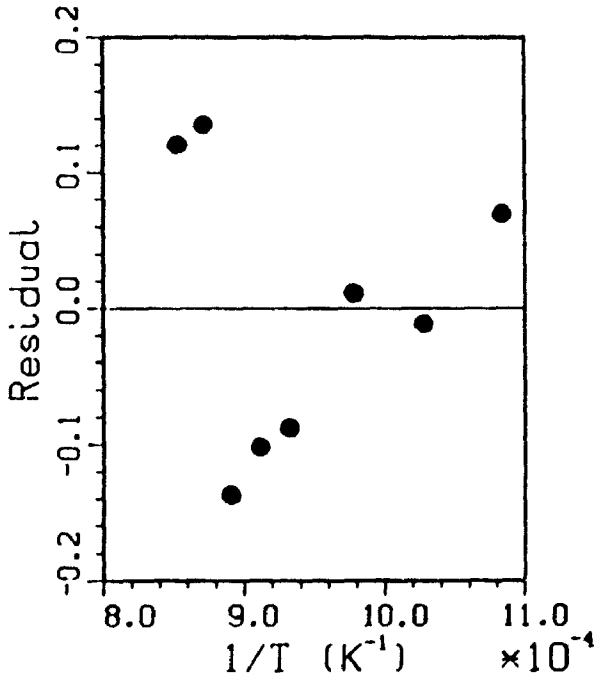

Figure A7.4.2. Prompt Gas Model for CO from Cellulose: Arrhenius Plot

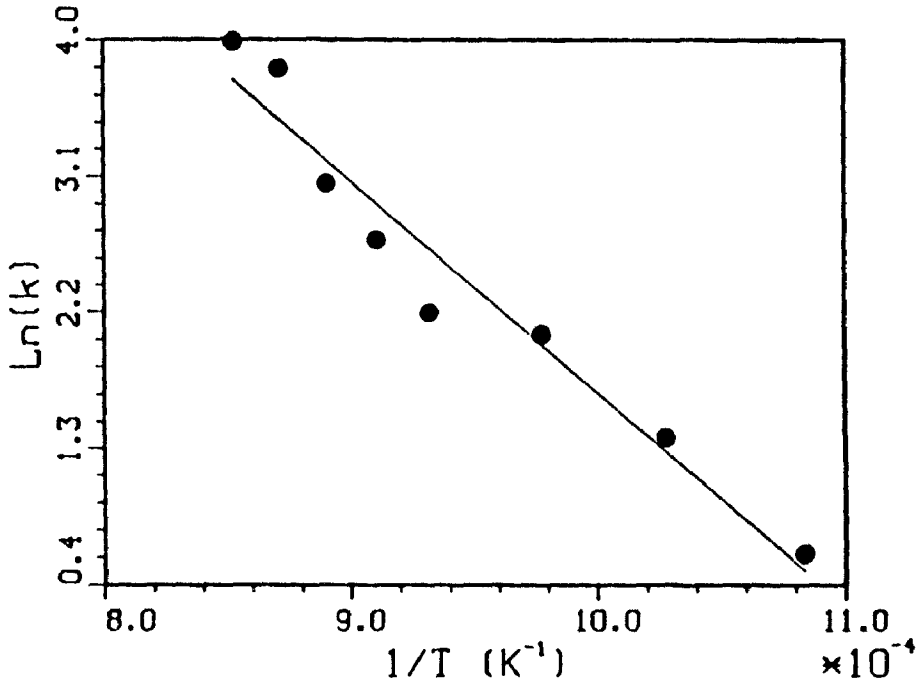

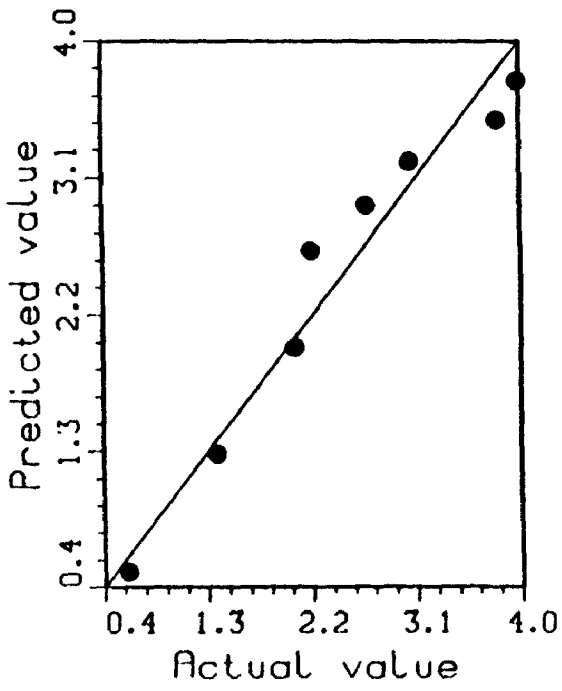

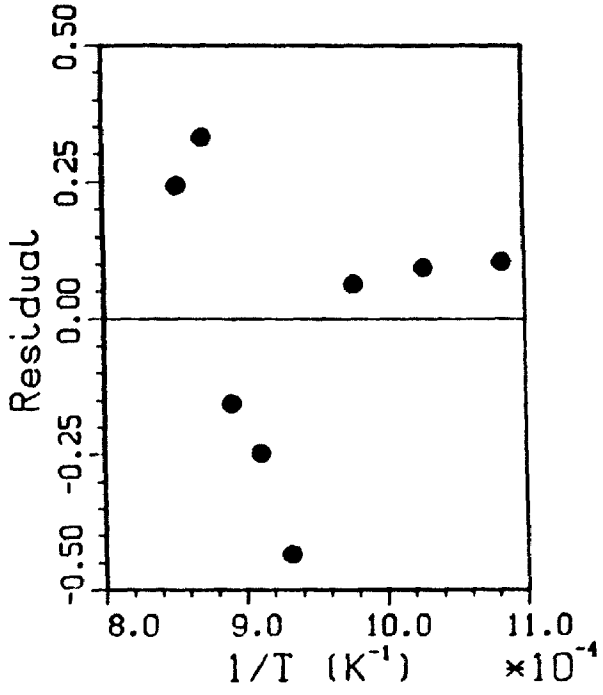

Figure A7.4.3. Prompt Gas Model for CO_2 from Cellulose: Arrhenius Plot

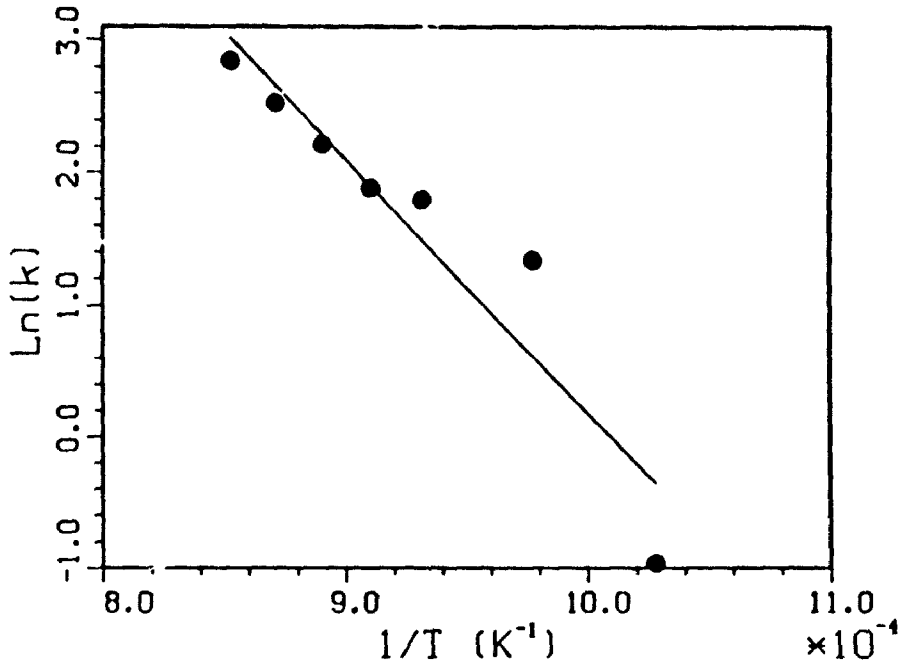

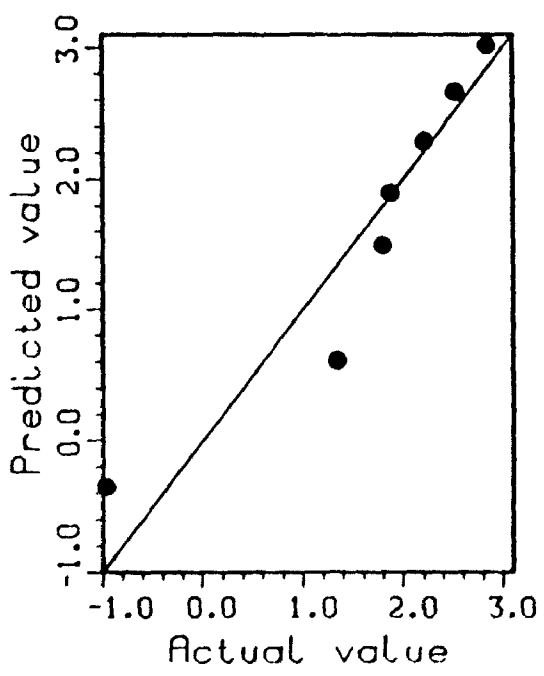

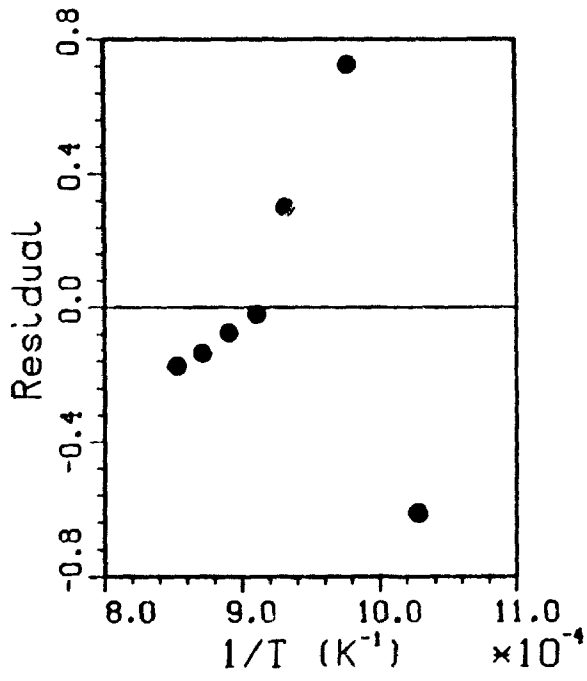

Figure A7.4.4. Prompt Gas Model for CH_4 from Cellulose: Arrhenius Plot

APPENDIX 7.5 WOOD PYROLYSIS REGRESSION CURVES (TOTAL GAS): ZERO-INTECEPT MODEL

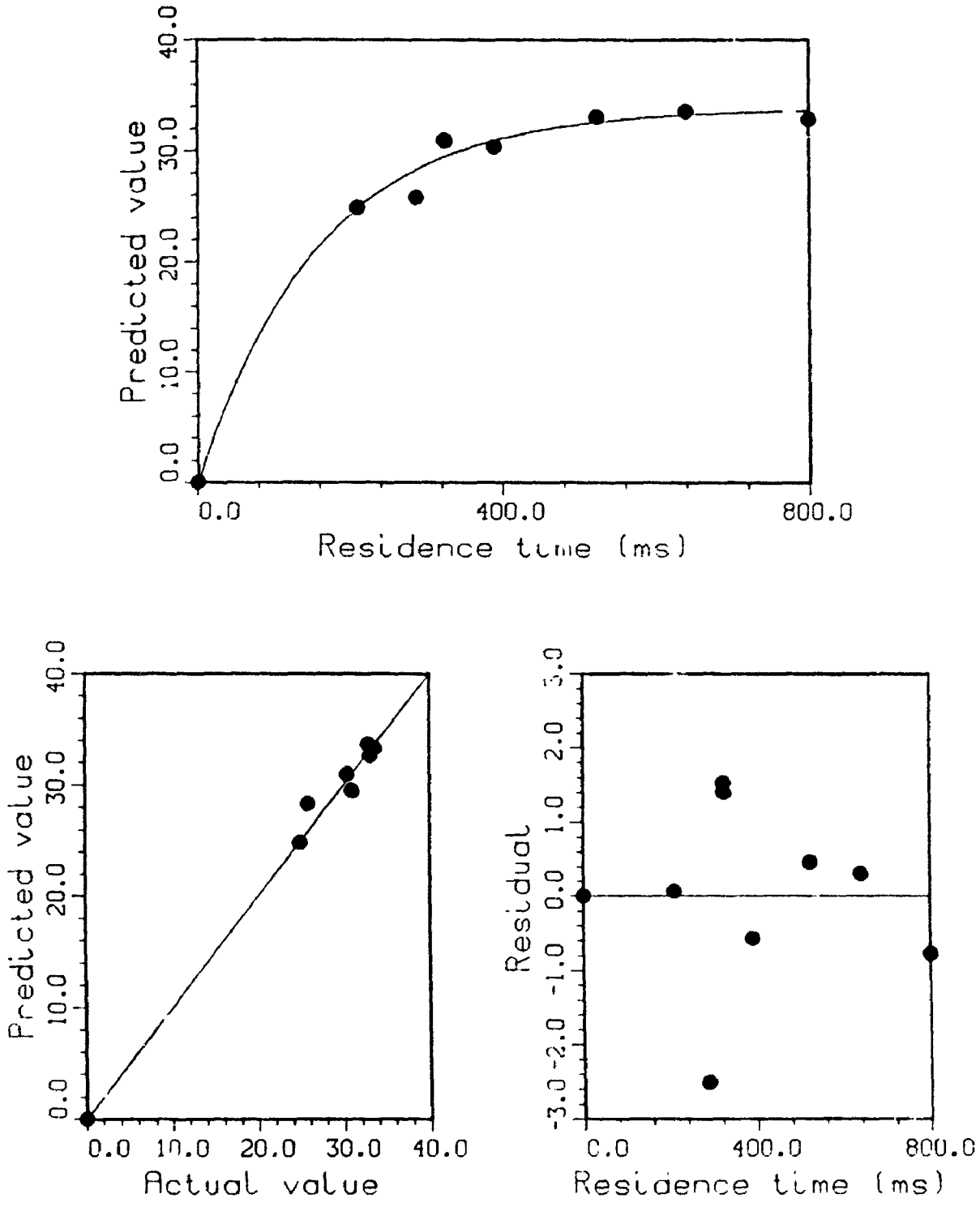

Figure A7.5.1. Zero-Intercept Kinetic Model For Total Gas from Wood: Fast Pyrolysis at 650 °C (Run Numbers and Data in Table 20)

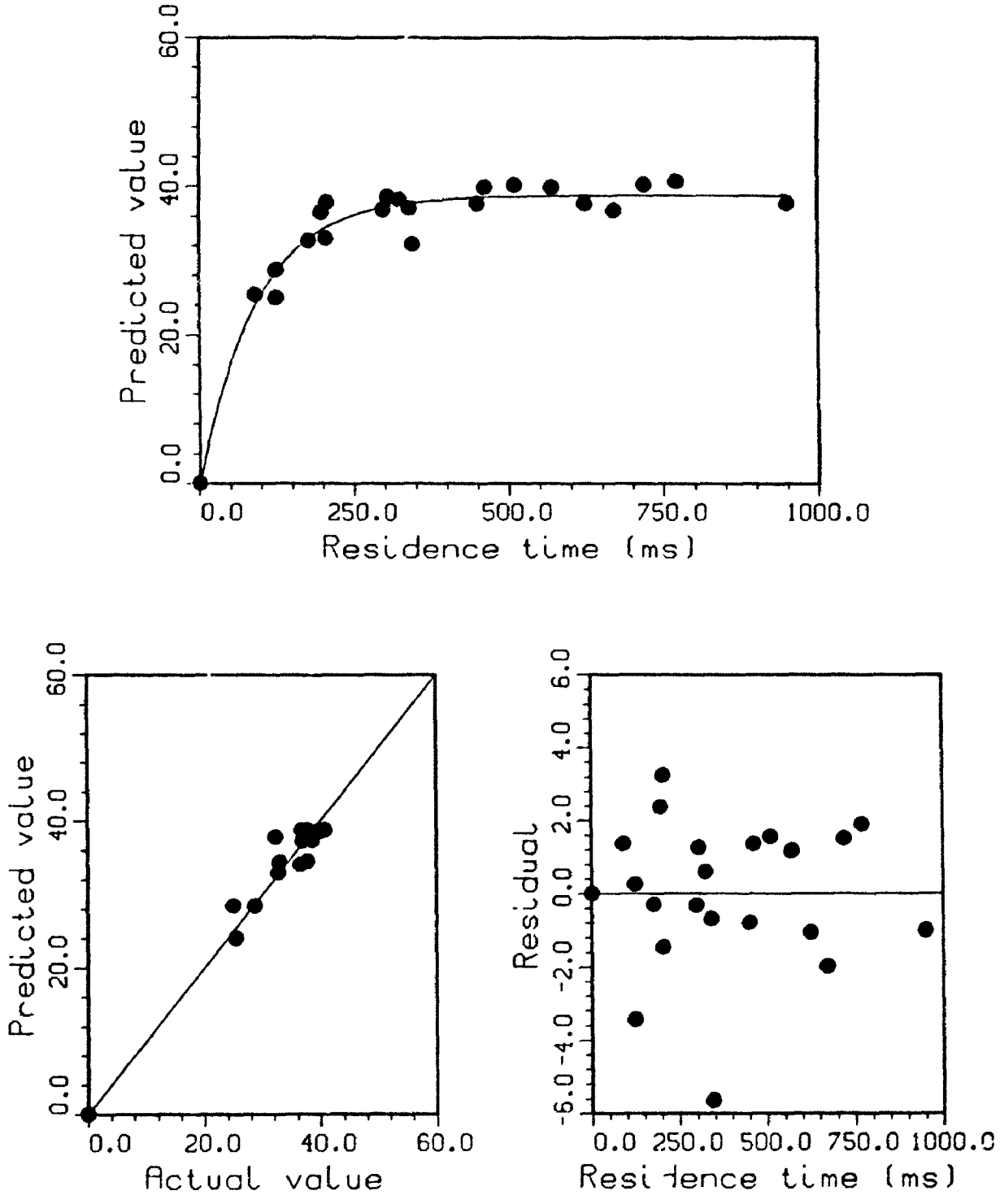

Figure A7.5.2. Zero-Intercept Kinetic Model For Total Gas from Wood: Fast Pyrolysis at 700 °C (Run Numbers and Data in Table 21)

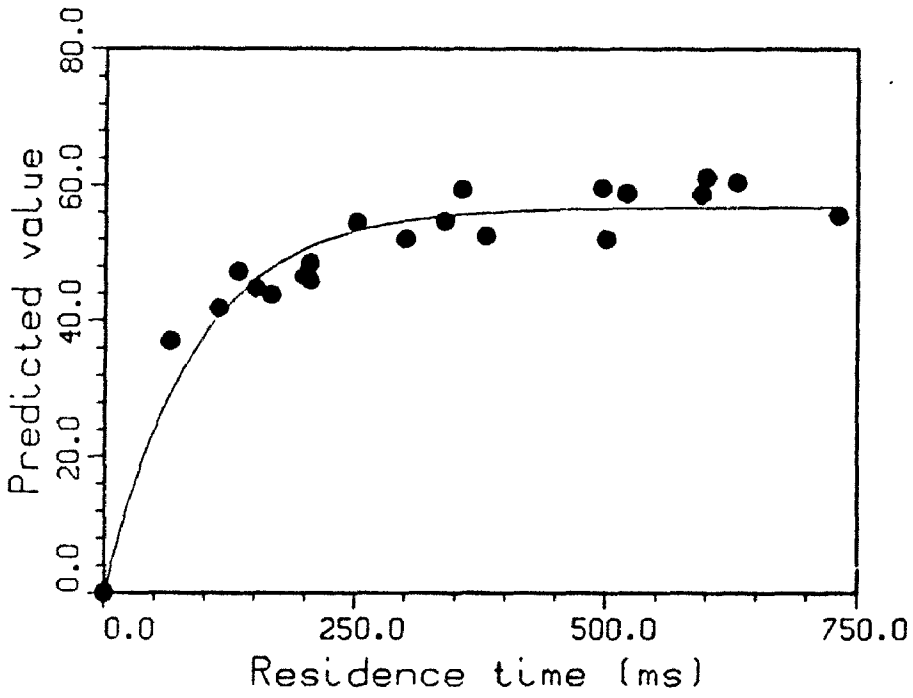

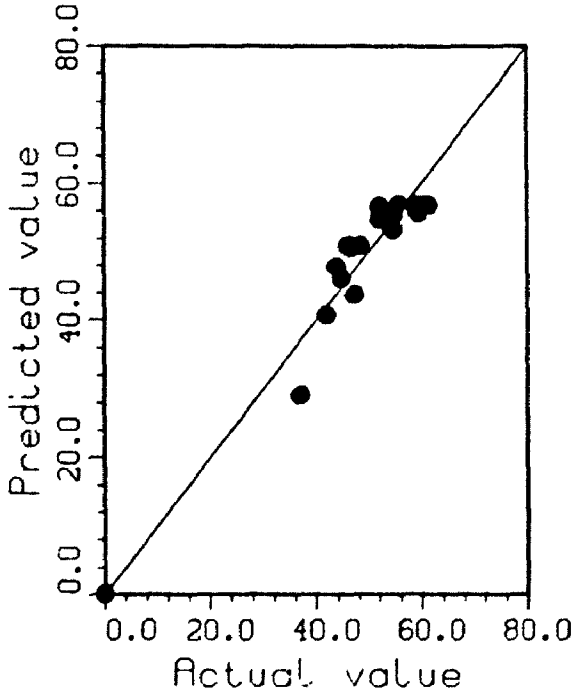

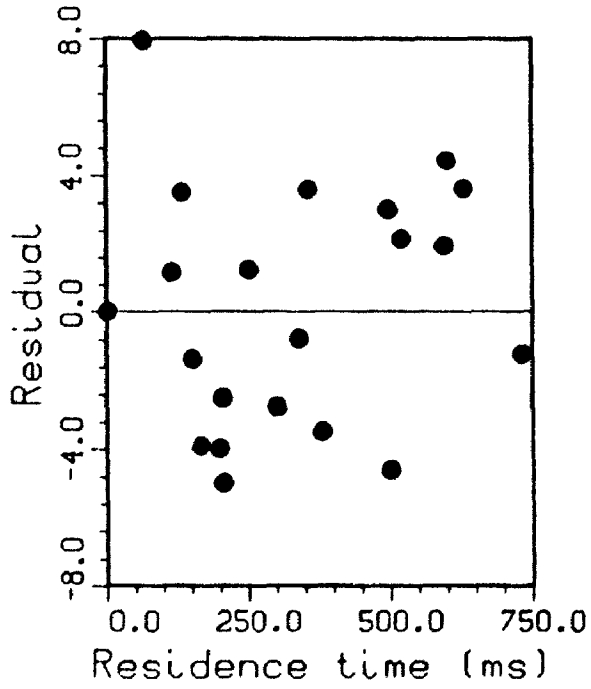

Figure A7.5.3. Zero-Intercept Kinetic Model For Total Gas from Wood: Fast Pyrolysis at 750 °C (Run Numbers and Data in Table 22)

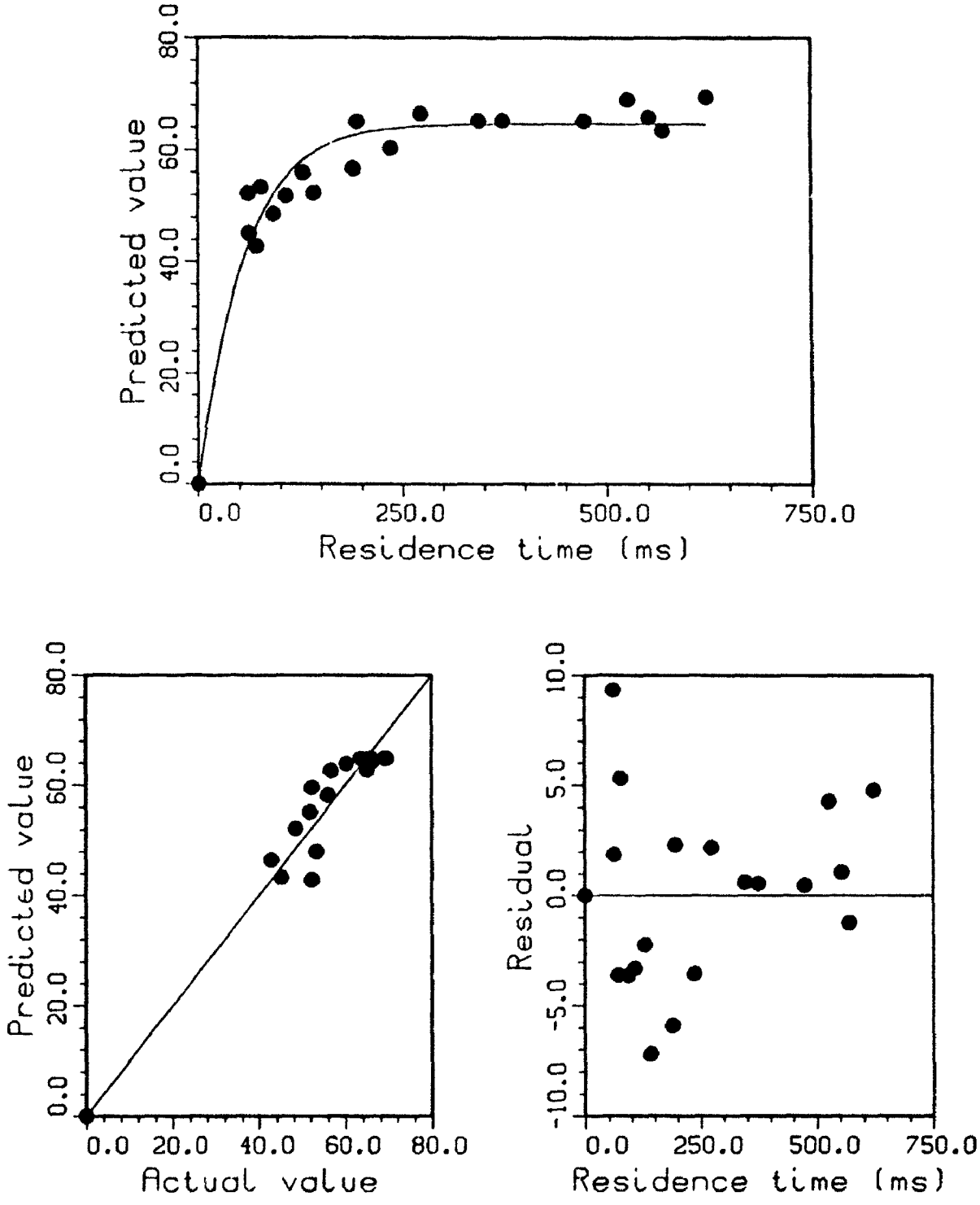

Figure A7.5.4. Zero-Intercept Kinetic Model For Total Gas from Wood: Fast Pyrolysis at 800 °C (Run Numbers and Data in Table 23)

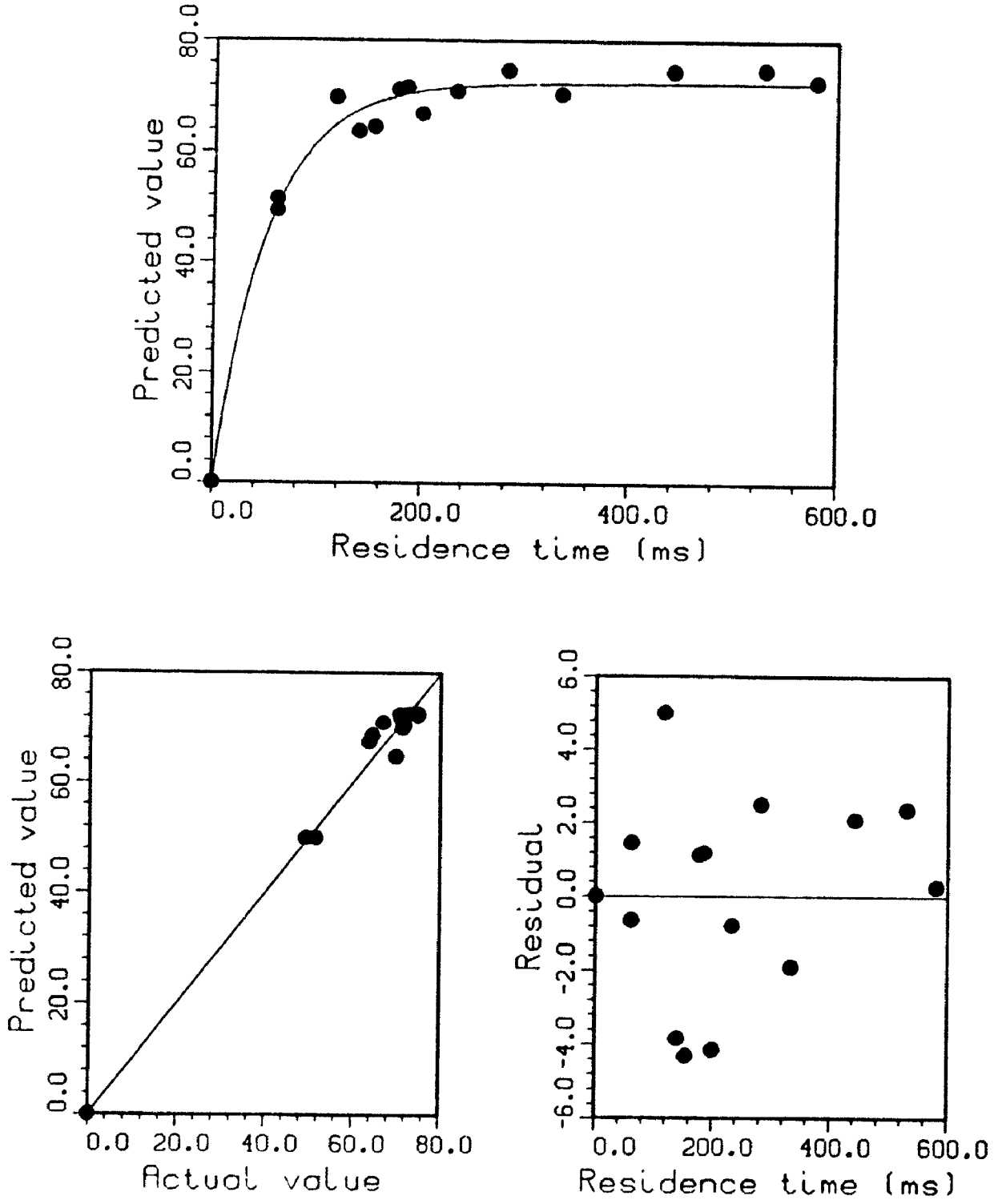

Figure A7.5.5. Zero-Intercept Kinetic Model For Total Gas from Wood: Fast Pyrolysis at 825 °C (Run Numbers and Data in Table 24)

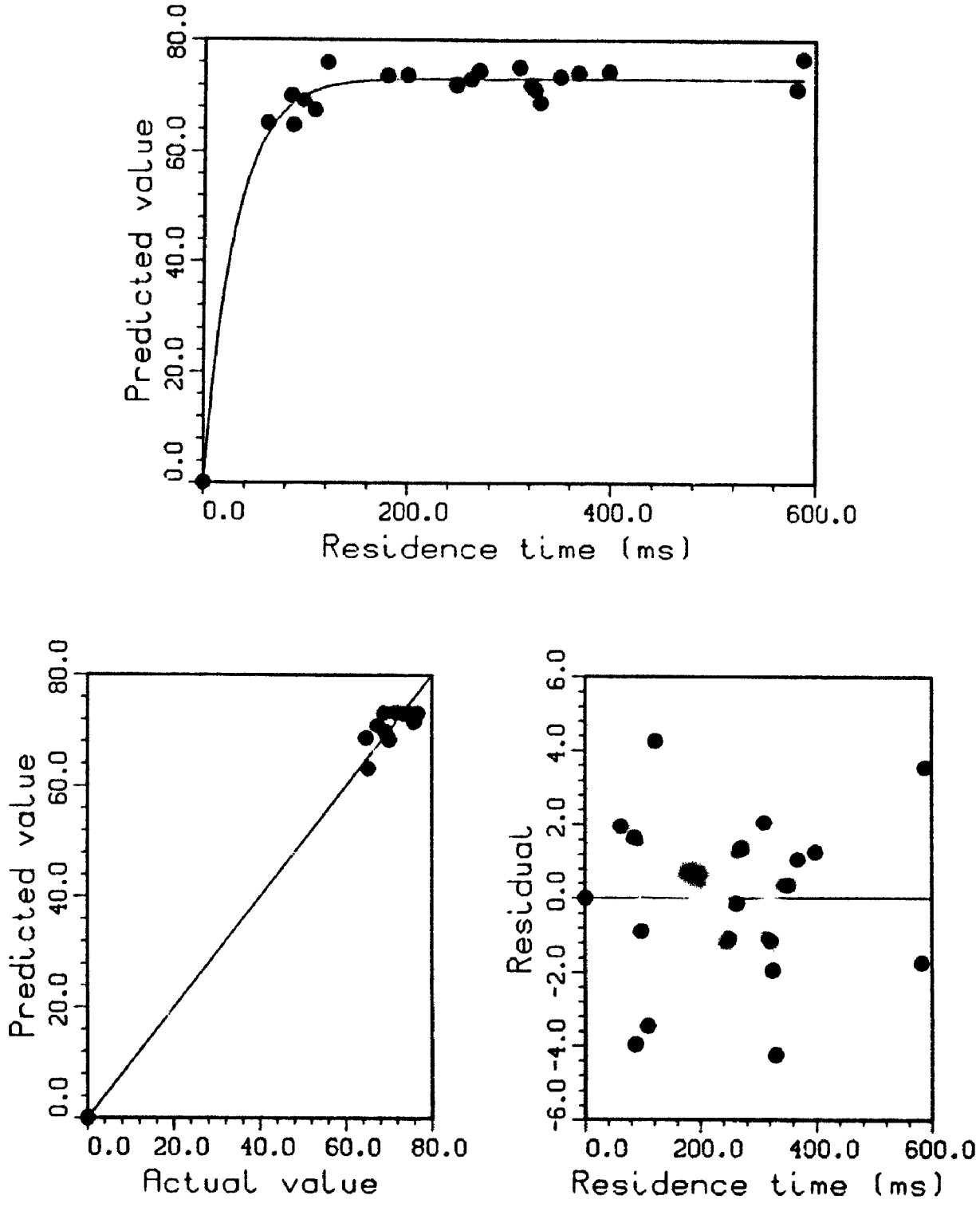

Figure A7.5.6. Zero-Intercept Kinetic Model For Total Gas from Wood: Fast Pyrolysis at 850 °C (Run Numbers and Data in Table 25)

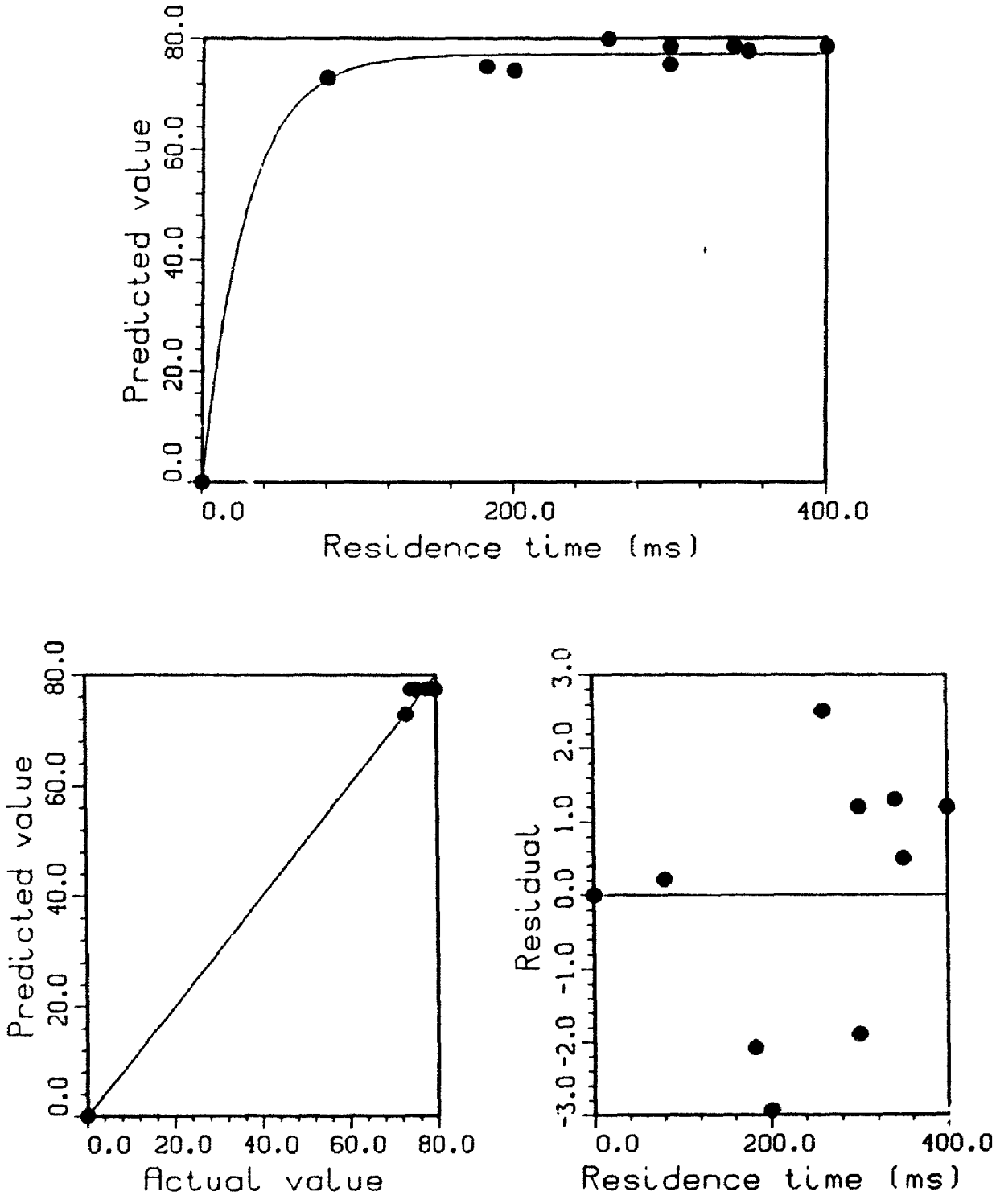

Figure A7.5.7. Zero-Intercept Kinetic Model For Total Gas from Wood: Fast Pyrolysis at 900 °C (Run Numbers and Data in Table 26)

APPENDIX 7.6 WOOD PYROLYSIS REGRESSION CURVES (TOTAL GAS): PROMPT GAS MODEL

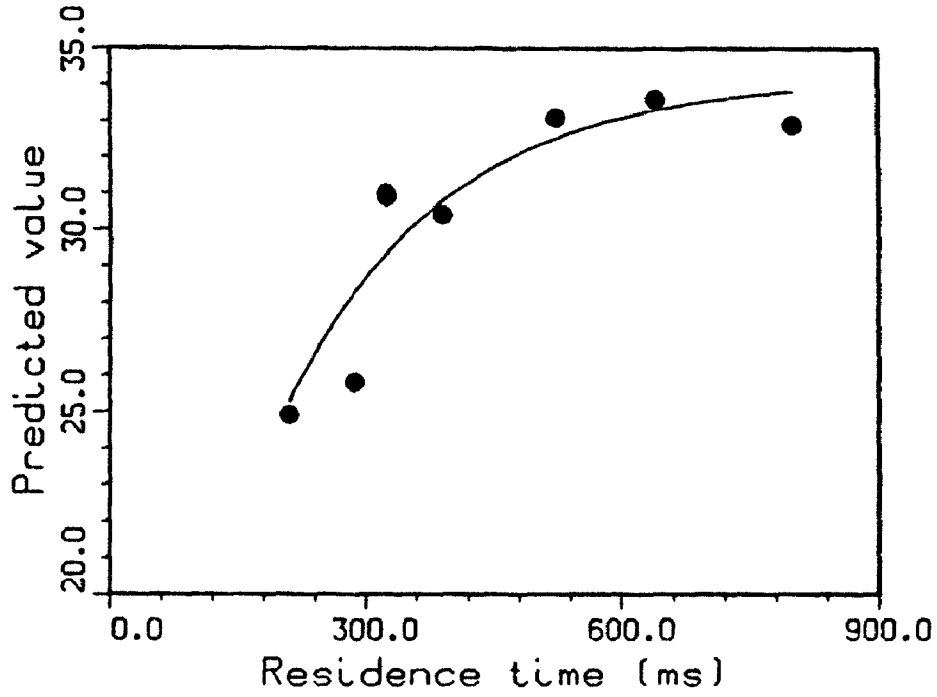

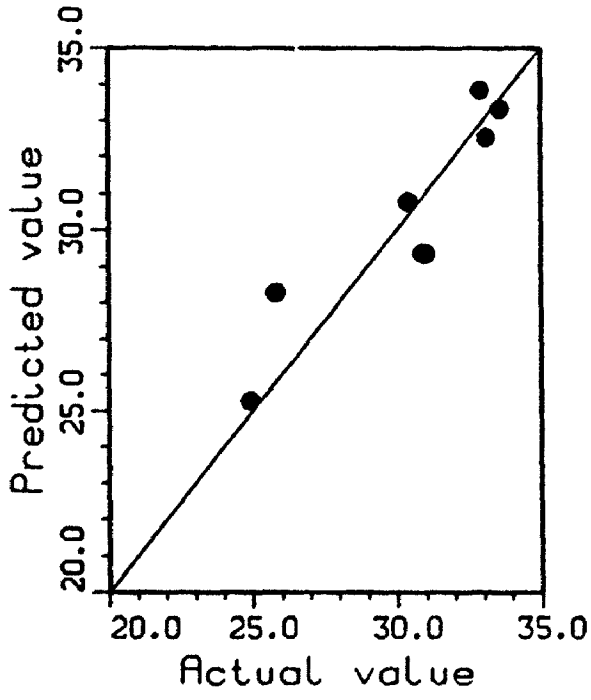

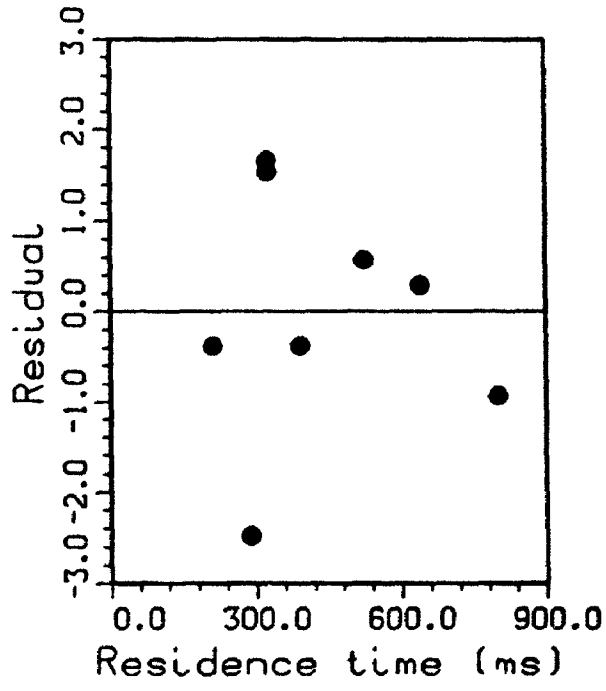

Figure A7.6.1. Prompt Gas Kinetic Model For Total Gas from Wood: Fast Pyrolysis at 650 °C

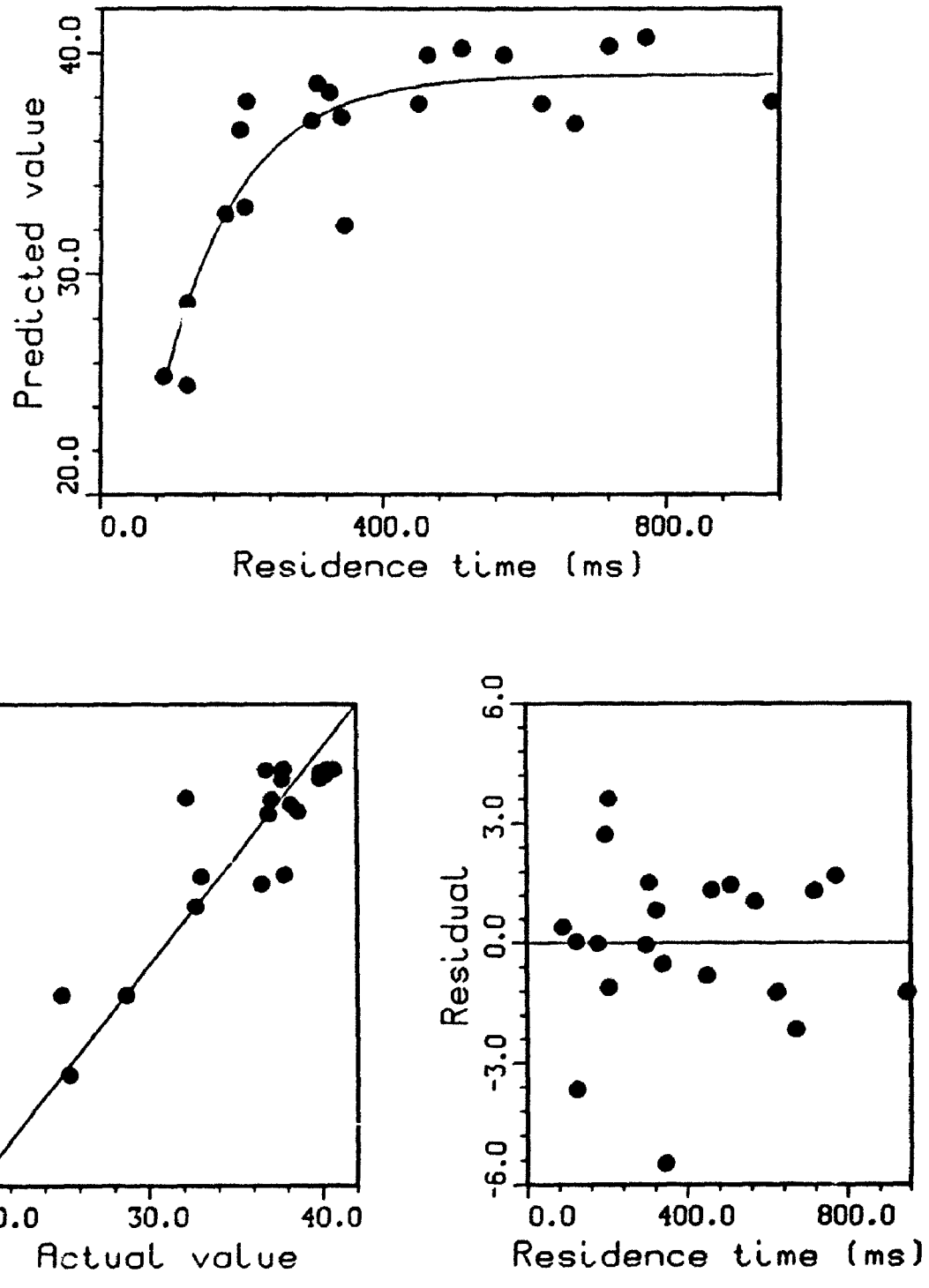

Figure A7.6.2. Prompt Gas Kinetic Model For Total Gas from Wood: Fast Pyrolysis at 700 °C

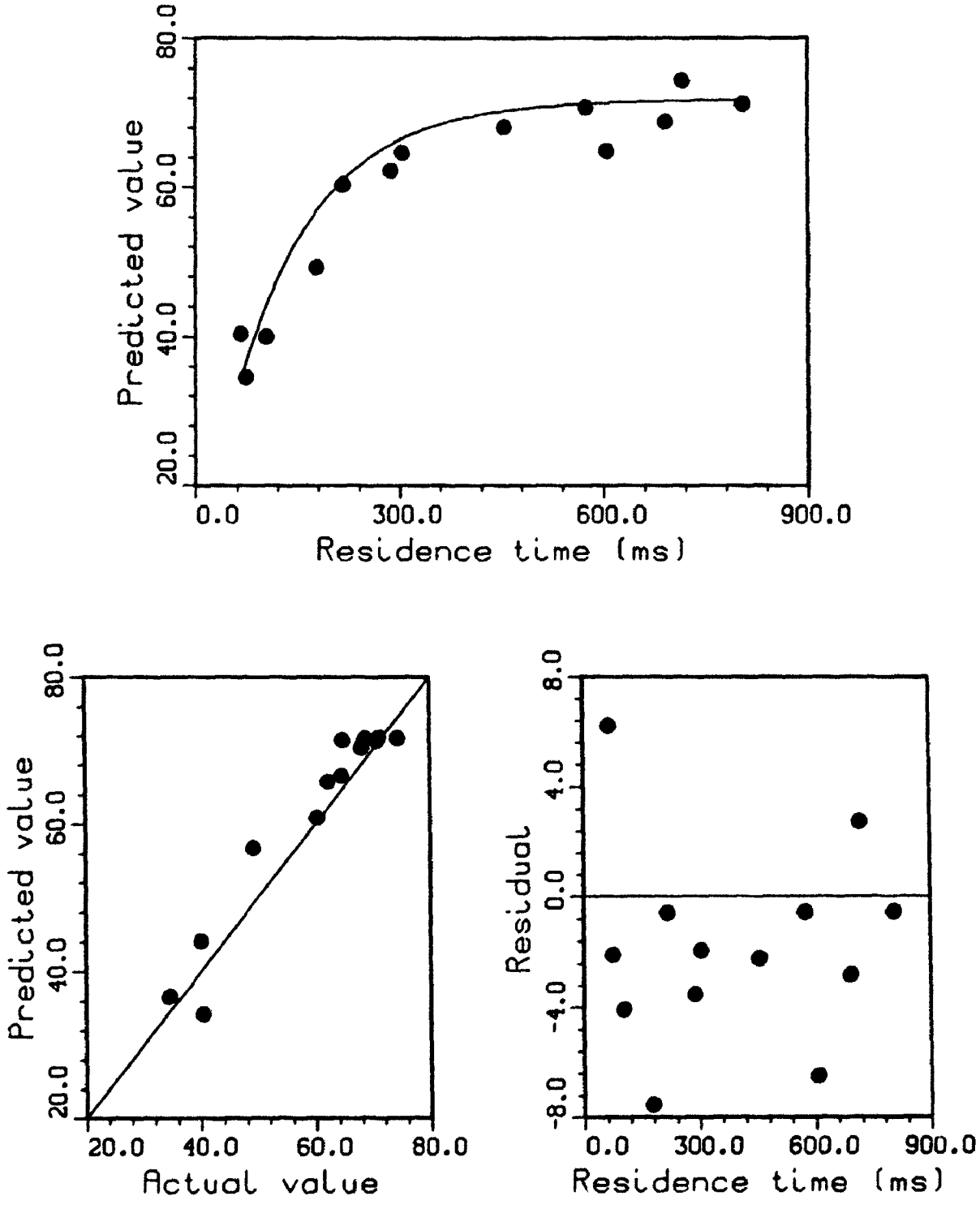

Figure A7.6.3. Prompt Gas Kinetic Model For Total Gas from Wood: Fast Pyrolysis at 750 °C

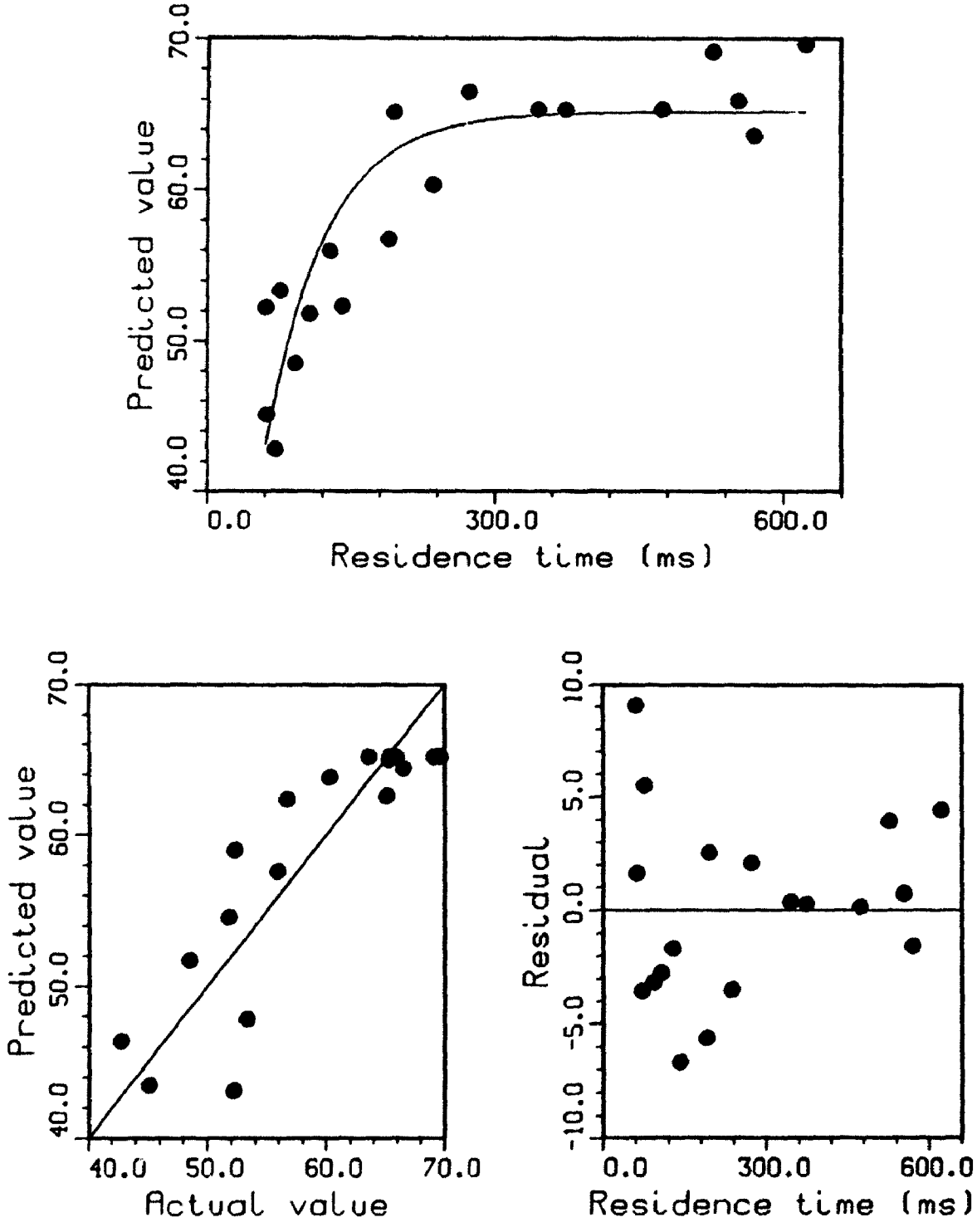

Figure A7.6.4. Prompt Gas Kinetic Model For Total Gas from Wood: Fast Pyrolysis at 800 °C

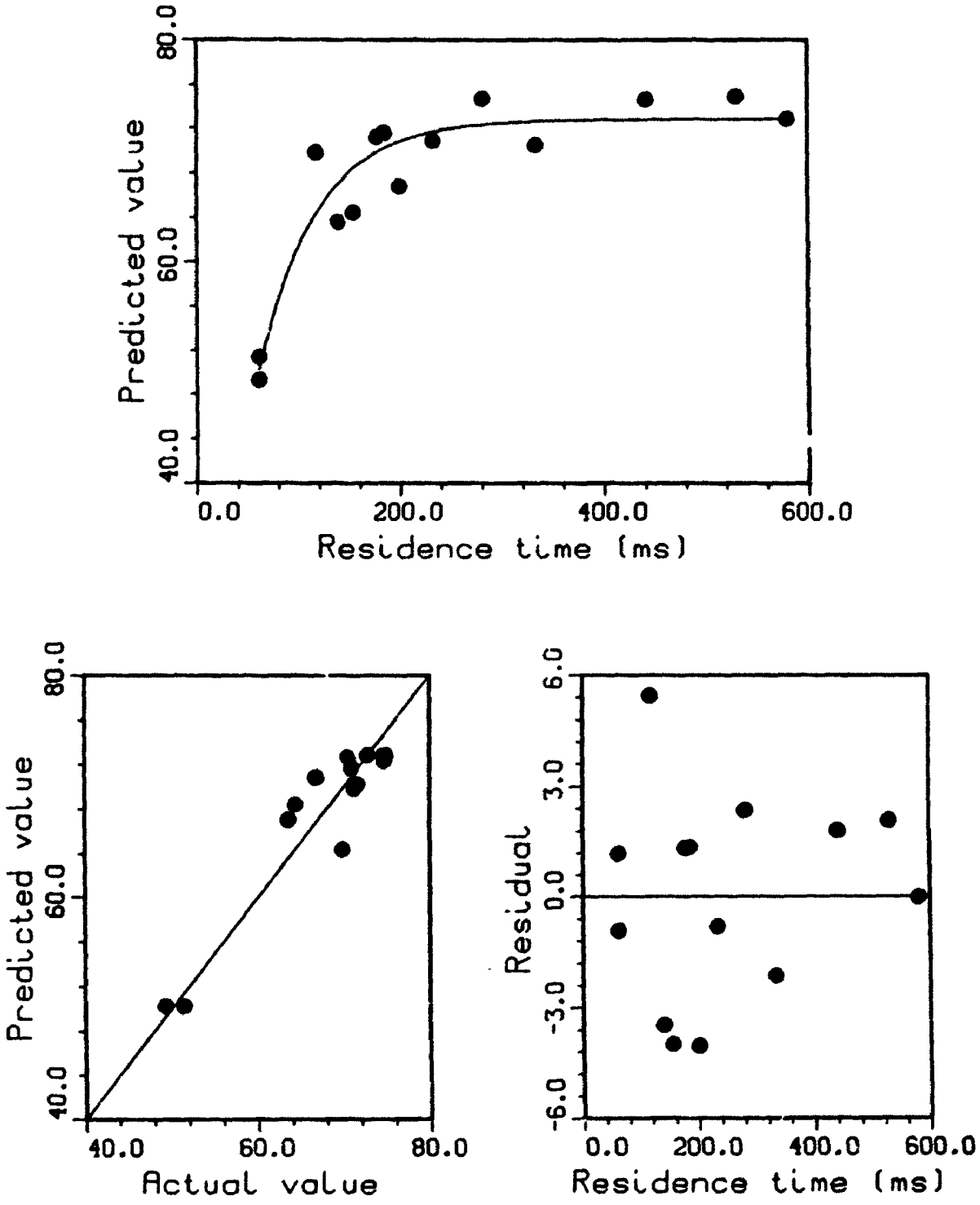

Figure A7.6.5. Prompt Gas Kinetic Model For Total Gas from Wood: Fast Pyrolysis at 825 °C

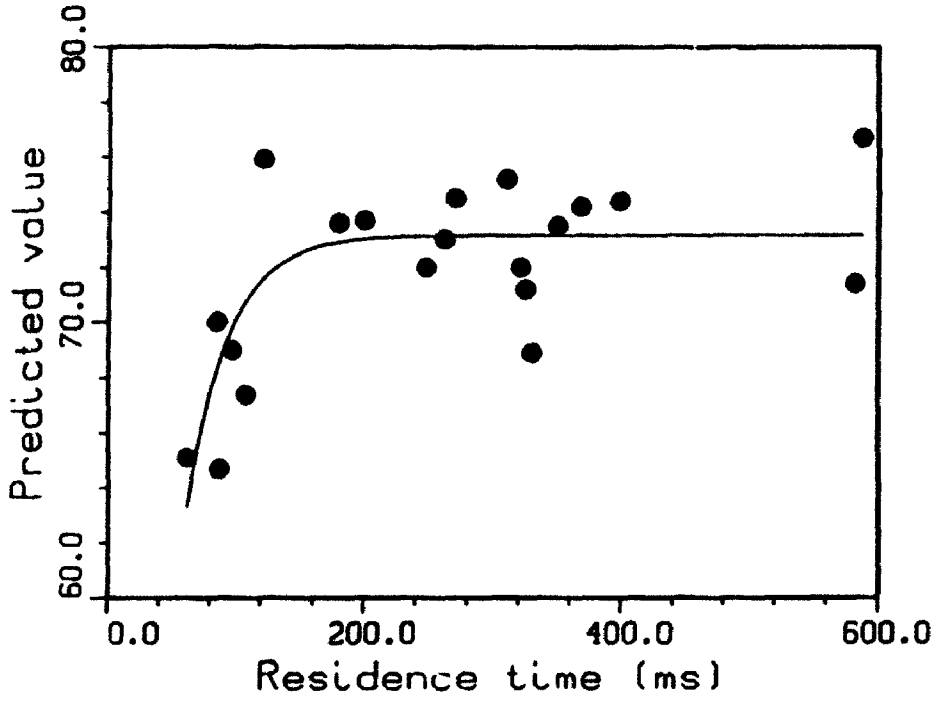

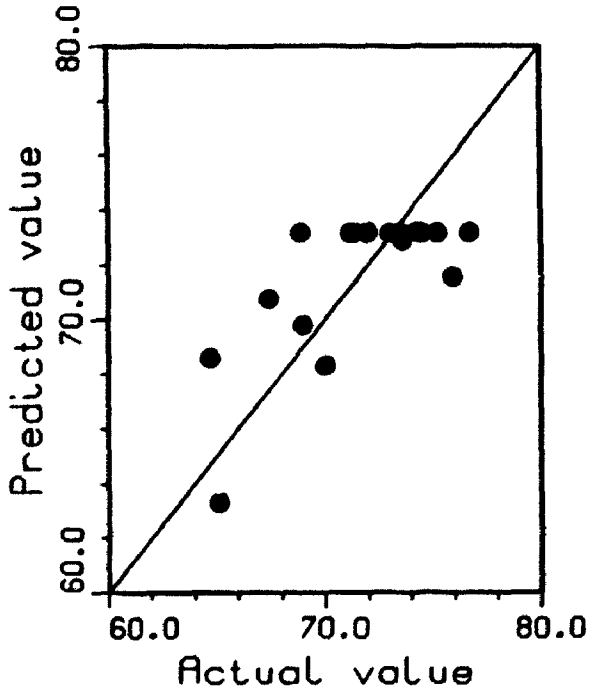

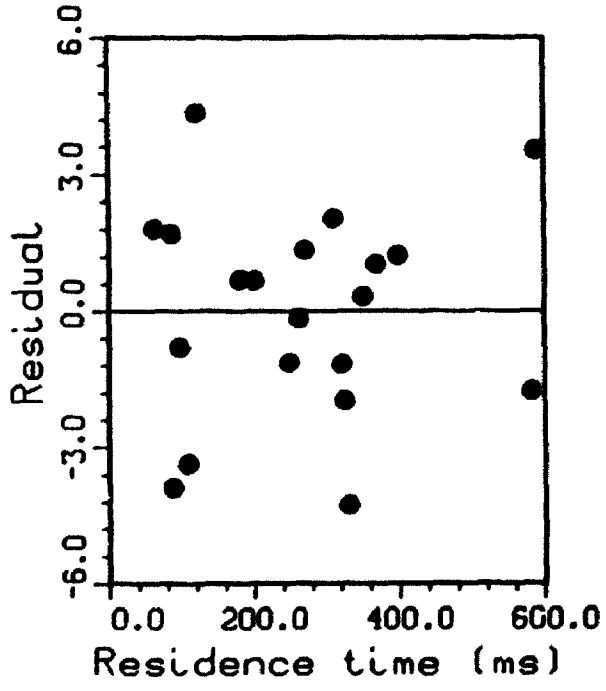

Figure A7.6.6. Prompt Gas Kinetic Model For Total Gas from Wood: Fast Pyrolysis at 850 °C

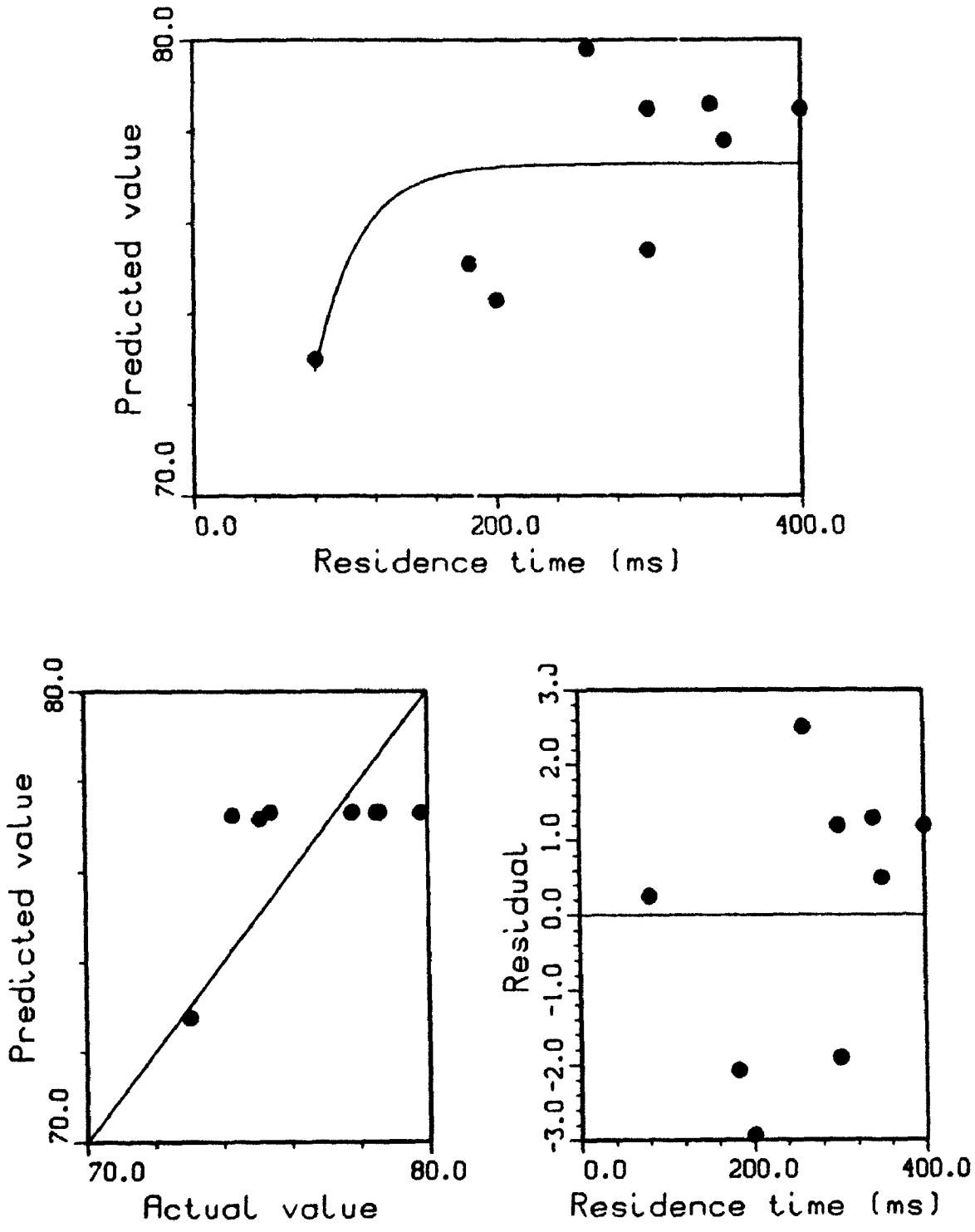

Figure A7.6.7. Prompt Gas Kinetic Model For Total Gas from Wood: Fast Pyrolysis at 900 °C

APPENDIX 8.0 ULTRAPYROLYSIS REACTOR SYSTEM THERMOCOUPLE LOCATIONS

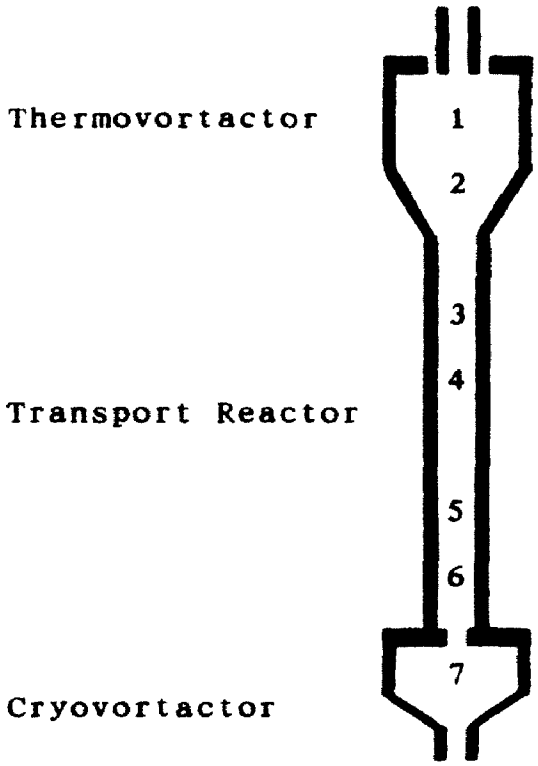

(numbers indicate approximate thermocouple locations)

APPENDIX 9.0 CONFIDENCE INTERVALS FOR CELLULOSE DATA

APPENDIX 9.1 FUNDAMENTALS

$\bar{x}$ sample mean = $\Sigma_{i=1}^{n} (x_i)^2 / n$

s^2 variance = $\Sigma_{i=1}^{n} (x_i - x)^2 / (n-1)$

s (σ) standard deviation/ standard error of the sample mean=s.d. of sampling distribution

s.error = s.d. of subgroup means
= s.e. of the sample mean
s = s.d. of the sample

u population mean

$\frac{s}{x}$ coeff. of variation

Normal = Gaussian

APPENDIX 9.2 CONFIDENCE INTERVALS (C.I.)

C.I. $\pm$ tc $\frac{s}{\sqrt{n}}$

S.E. = $(s/\sqrt{n})$ (s.d. of mean)

s.e. = of sample mean
s = s.d. of sample
n = number of samples
tc = crit. "t" statistic

n	tc	v
2	12.71	1
3	4.30	2
4	3.18	3
5	2.78	4
6	2.57	5
7	2.45	6
8	2.36	7
12	2.20	11
20	2.09	19
infinity	1.96	infinity

v = deg. freedom

APPENDIX 9.3 CELLULOSE DATA

TEMP.[1]	MEAN	S.DEV.	NO.	t_c	S.E.	C.I.
750[2]	69.65	3.20	6	2.57	1.37	±3.36
	(68.1)					
	(71.2)					
	(70.5)					
	(74.4)					
	(64.9)					
	(68.8)					
800[3]	79.80	1.15	4	3.18	0.58	±1.83
	(79.1)					
	(78.6)					
	(80.4)					
	(81.1)					
825	81.73	1.24	4	3.18	0.68	±2.17
	(79.9)					
	(82.5)					
	(82.4)					
850	83.36	0.80	5	2.78	0.36	±0.99
	(82.0)					
	(83.6)					
	(83.6)					
	(83.5)					
	(84.1)					
875	87.15	0.66	4	3.18	0.33	±1.04
	(86.3)					
	(87.2)					
	(87.9)					
	(87.2)					
900	88.85	2.65	6	2.57	1.08	±2.78
	(87.9)					
	(86.2)					
	(92.8)					
	(90.8)					
	(86.1)					
	(89.3)					

1. Below 750 C, all data is in transition region and is therefore residence time-sensitive. All other experiments (i.e., above 750C) were conducted in the constant yield (asymptotic) region and are therefore residence time-insensitive.
2. Some residence time-sensitivity at 750 C.
3. Dedicated replication testing was conducted at 800 C.

C.I. @ 95%; 95% confidence that the true value lies within this interval; 1 in 20 chance it does not!